

SLOPE STABILITY ASSESSMENT OF VARIOUS ROAD CUTS WITH  
EFFECTS OF WEATHERING AT NORTH WEST BLACK SEA REGION  
(TURKEY)

A THESIS SUBMITTED TO  
THE GRADUATE SCHOOL OF NATURAL AND APPLIED SCIENCES  
OF  
MIDDLE EAST TECHNICAL UNIVERSITY

BY

TİMUR ERSÖZ

IN PARTIAL FULFILLMENT OF THE REQUIREMENTS  
FOR  
THE DEGREE OF MASTER OF SCIENCE  
IN  
GEOLOGICAL ENGINEERING

JANUARY 2017



Approval of the thesis:

**SLOPE STABILITY ASSESSMENT OF VARIOUS ROAD CUTS WITH  
EFFECTS OF WEATHERING AT NORTH WEST BLACK SEA REGION  
(TURKEY)**

submitted by **TİMUR ERSÖZ** in partial fulfillment of the requirements for the degree of **Master of Science in Geological Engineering Department, Middle East Technical University** by,

Prof. Dr. Gülbin DURAL  
Dean, Graduate School of **Natural and Applied Sciences**

Prof. Dr. Erdin BOZKURT  
Head of Department, **Geological Engineering**

Prof. Dr. Tamer TOPAL  
Supervisor, **Geological Engineering Dept., METU**

**Examining Committee Members:**

Prof. Dr. Nurkan KARAHANOĞLU  
Geological Engineering Dept., METU

Prof. Dr. Tamer TOPAL  
Geological Engineering Dept., METU

Prof. Dr. Erdal ÇOKÇA  
Civil Engineering Dept., METU

Prof. Dr. Bora ROJAY  
Geological Engineering Dept., METU

Assoc. Prof. Dr. Mutluhan AKIN  
Geological Engineering Dept., Nevşehir HBVU

**Date:** 26.01.2017

**I hereby declare that all information in this document has been obtained and presented in accordance with academic rules and ethical conduct. I also declare that, as required by these rules and conduct, I have fully cited and referenced all material and results that are not original to this work.**

Name, Last Name: Timur ERSÖZ

Signature:

## **ABSTRACT**

### **SLOPE STABILITY ASSESSMENT OF VARIOUS ROAD CUTS WITH EFFECTS OF WEATHERING AT NORTH WEST BLACK SEA REGION (TURKEY)**

ERSÖZ, Timur

M.Sc., Department of Geological Engineering

Supervisor: Prof. Dr. Tamer TOPAL

January 2017, 407 pages

Rocks containing pore spaces, fractures, joints, bedding planes and faults are prone to weathering due to effects of temperature differences, wetting-drying, chemistry of solutions absorbed, and other physical and chemical agents. Especially cut slopes are very sensitive to weathering activities because of disturbed rock mass and topographical condition by excavation. During and right after an excavation process of a cut slope, weathering and erosion may act on this newly exposed rock material. These acting on the material may degrade and change its properties and the stability of the cut slope in its engineering lifetime.

In this study, the effect of physical and chemical weathering agents on shear strength parameters of the rocks are investigated in order to observe the differences between weathered and unweathered rocks. Also, slope stability assessment of twenty cut slopes located at North West Black Sea region of Turkey are studied by the effect of these weathering agents which may alter the parameters like strength, cohesion, internal friction angle, unit weight, water absorption and porosity. In order to compare the condition of the rock materials and analyze the slope stability, the parameters of weathered and relatively fresh rock materials are found with in-situ

tests such as Schmidt hammer and laboratory tests like uniaxial compressive strength, point load and direct shear. In order to reflect the relation between Schmidt rebound values and UCS two new functions are developed. Moreover, slake durability and methylene blue tests are applied to investigate the response of the rock to weathering and presence of clays in rock materials, respectively. In addition to these studies, stability conditions of the road cuts are determined by two empirical systems namely Slope Mass Rating (SMR) and Slope Stability Probability Classification (SSPC). Furthermore, the performances of the weathered and relatively fresh zones of the cut slopes are evaluated and 2-D slope stability and rockfall analysis are modeled. Success rates of empirical solutions and limit equilibrium analyses are compared with field observations, with recommendations for further research for the cut slopes. According to this, SSPC method is found to give results similar to the field performances of the cuts slopes, compared to SMR. It is found that two testing cycles are insufficient to assess the field durability of the rocks based on the slake durability test results. According to field observations and stability analyses, periodic maintenance of the drainage channels is suggested for some road cuts due to surficial failures and degradations.

**Keywords:** Slope Stability, SMR, SSPC, Weathering, North West Black Sea, Turkey

## ÖZ

# KUZEY BATI KARADENİZ BÖLGESİ'NDEKİ (TÜRKİYE) AYRIŞMANIN ETKİSİNDE OLAN ÇEŞİTLİ YOL YARMALARININ ŞEV STABİLİTESİNİN DEĞERLENDİRMESİ

ERSÖZ, Timur

Yüksek Lisans, Jeoloji Mühendisliği Bölümü

Tez Yöneticisi: Prof. Dr. Tamer TOPAL

Ocak 2017, 407 sayfa

Sıcaklık farklılıklarının, ıslanma-kurumanın, kimyasal çözeltilerin emiliminin ve diğer fiziksel ve kimyasal maddelerin etkisinden ötürü, boşluk hacmi, kırık, eklem, tabakalaşma yüzeyi ve fay içeren kayalar ayrışmaya eğilimlidir. Kazıyla örselenmiş kaya kütlesi ve topografik durumundan dolayı özellikle yol yarmaları ayrışmaya karşı oldukça duyarlıdır. Ayrışma ve erozyon, bir yol yarmasının kazı işlemleri sırasında ve hemen sonrasında, kazının etkisiyle yeni ortaya çıkmış bu kaya malzemesine etki edebilir. Mühendislik ömrü boyunca malzemeye etkileyen bu etmenler yol yarmasının özelliklerinin ve duraylılığının bozunmasını ve değişmesini sağlayabilir.

Bu çalışmada, ayrılmış ve ayrılmamış kayaların arasındaki farkları gözlemlemek için fiziksel ve kimyasal ayrışmanın kayaların kesme dayanım parametrelerine etkisi incelenmiştir. Ayrıca, dayanım, kohezyon, içsel sürtünme açısı, birim hacim ağırlık, su emme ve gözeneklilik gibi parametrelerin değişmesine yol açabilen bu ayrışmaların etkisiyle Türkiye'nin Kuzey Batı Karadeniz bölgesinde bulunan 20 yol yarmasının duraylılık değerlendirmesi çalışılmıştır. Kaya malzemelerinin durumunun karşılaştırılması ve şev duraylılığının analizi için, Schmidt çekici gibi yerinde ve tek

eksenli basma dayanımı, nokta yükleme ve direk kesme gibi laboratuvar deneyleriyle ayrıışmış ve taze kaya malzemelerinin parameterleri bulunmuştur. Schmidt geri sekme değeri ve UCS arasındaki ilişkiyi yansıtmak için iki yeni denklem geliştirilmiştir. Buna ek olarak, kayacın ayrıışmaya olan tepkisini incelemek adına suda dağılmaya karşı dayanıklılık deneyi ve kaya malzemesi içindeki killerin mevcudiyetini incelemek için de metilen mavisi deneyi uygulanmıştır. Bu çalışmalara ek olarak, yol yarmalarının duraylılık durumları SMR ve SSPC ampirik sistemleriyle belirlenmiştir. Ayrıca, yol yarmalarının ayrıışmış ve taze bölgelerinin performansları değerlendirilmiş ve 2 boyutlu şev duraylılık ve kaya düşmesi analizleri modellenmiştir. Yol yarmalarının ilerideki araştırmaları için tavsiyelerle birlikte ampirik çözümlerin ve limit denge analizlerinin başarı oranları saha gözlemleriyle karşılaştırılmıştır. Buna göre, SMR metoduna oranla SSPC metodunun yol yarmalarının saha performanslarına daha benzer sonuçlar verdiği bulunmuştur. Suda dağılmaya karşı dayanıklılık deney sonuçları temel alınarak, kayaların saha dayanıklılıklarının değerlendirilmesi için iki deney döngüsünün yetersiz olduğu bulunmuştur. Saha gözlemleri ve duraylılık analizlerine göre, yüzeysel yenilmelerden ve bozunmalardan ötürü bazı yol yarmaları için drenaj kanallarının düzenli bakımı önerilmiştir.

Anahtar Kelimeler: Şev stabilitesi, SMR, SSPC, Ayrıışma, Kuzey Batı Karadeniz, Türkiye

To my Family,  
For [NrM]

## ACKNOWLEDGEMENTS

I would like to express my special thanks to my supervisor Prof. Dr. Tamer Topal for his guidance, technical support, encouragement and patience throughout all process of this thesis. I am very grateful that he taught me how to fish by giving little clues instead of giving me a fish.

I would like to thank Asst. Prof. Dr. Müge Akın for her invaluable technical guidance.

I would like to thank my colleague Yavuz Kaya for his help on laboratory works.

I would like to express my special thanks to Murat Yertutanol for his technical support about laboratory tests.

I would like to thank my dear friend and “ex-project mate” Batuhan Soyugür and, dear friend and “team mate” Serdar Görkem Atasoy for their mental and technical support during this thesis. It would have been impossible to finish field works without their support.

I would like to thank my friends and colleagues Uğur Balcı and Hatice Kılıç for their psychological support during this thesis.

Finally, I would like to state my deepest appreciations to my mother Ayla Ersöz for her love, my father Selçuk Ersöz for his mentoring, my sister İlknur Ersöz Tekeli for her sympathy and my girlfriend Nur Ertaş for her endless love, psychological support, trust and patience throughout all process of this thesis. I would not be able to succeed in this thesis without their endless understanding.

## TABLE OF CONTENTS

ABSTRACT .....	v
ÖZ .....	vii
ACKNOWLEDGEMENTS .....	x
TABLE OF CONTENTS .....	xi
LIST OF TABLES .....	xiv
LIST OF FIGURES .....	xxv
CHAPTERS	
1. INTRODUCTION.....	1
1.1. Purpose and Scope.....	1
1.2. Accessibility and Location .....	2
1.3. Climate and Vegetation .....	4
1.4. Method of Study .....	6
1.5. Previous Studies .....	8
1.5.1. Previous Studies about Geology .....	8
1.5.2. Previous Studies about SSPC.....	11
2. LITERATURE REVIEW ON SLOPE STABILITY, WEATHERING AND SSPC .....	13
2.1. Slope Stability, Weathering and Excavation .....	13
2.1.1. Classification of Slope Movements .....	14
2.1.2. Slope Failure Types .....	15
2.1.3. Rock Strength.....	17
2.1.4. Weathering .....	19
2.1.5. Excavation.....	24
2.2. Slope Stability Probability Classification (SSPC) method.....	25
2.2.1. Exposed Rock Mass (ERM).....	27
2.2.2. Reference Rock Mass (RRM) .....	29
2.2.3. Slope Rock Mass (SRM).....	30
3. GEOLOGY .....	35
3.1. Regional Geology .....	35
3.2. Site Geology .....	36
3.2.1. Yedigöller Formation .....	39
3.2.2. Bolu Granitoid.....	39
3.2.3. Abant Formation .....	40
3.2.4. Akveren Formation .....	40

3.2.5.	Çaycuma Formation .....	41
3.2.6.	Soğanlı Formation .....	41
3.3.	Tectonics and Seismicity .....	42
3.3.1.	Attenuation Relationship.....	42
4.	ENGINEERING GEOLOGICAL PROPERTIES OF ROCKS AT CUT SLOPES .....	45
4.1.	Material Properties of the Rocks at the Cut Slopes .....	46
4.1.1.	Effective Porosity and Unit Weight .....	46
4.1.2.	Uniaxial Compressive Strength.....	48
4.1.3.	Point Load Strength Index.....	50
4.1.4.	Schmidt Rebound Hardness Test .....	53
4.1.5.	Shear Box Test .....	58
4.1.6.	Slake Durability Index Test.....	59
4.1.7.	Methylene Blue Adsorption Test .....	62
4.2.	Mass Properties of the Rocks at the Cut Slopes .....	64
4.3.	Road Cut Characterization.....	69
4.3.1.	Stop 1.....	70
4.3.2.	Stop 2.....	75
4.3.3.	Stop 3.....	79
4.3.4.	Stop 4.....	83
4.3.5.	Stop 5.....	87
4.3.6.	Stop 6.....	90
4.3.7.	Stop 7.....	94
4.3.8.	Stop 8.....	98
4.3.9.	Stop 9.....	102
4.3.10.	Stop 10.....	106
4.3.11.	Stop 11.....	110
4.3.12.	Stop 12.....	113
4.3.13.	Stop 13.....	117
4.3.14.	Stop 14.....	121
4.3.15.	Stop 15.....	125
4.3.16.	Stop 16.....	129
4.3.17.	Stop 17.....	133
4.3.18.	Stop 18.....	137
4.3.19.	Stop 19.....	141
4.3.20.	Stop 20.....	145
5.	SLOPE STABILITY ANALYSES .....	149

5.1.	Kinematic Analyses of the Cut Slopes .....	149
5.2.	Limit Equilibrium Analyses for Discontinuity Controlled Rocks.....	155
5.3.	Limit Equilibrium Analyses for the Rock Mass.....	159
5.4.	Rock Fall Analyses.....	166
5.5.	Slope Mass Rating (SMR).....	173
5.6.	Slope Stability Probability Classification (SSPC).....	176
6.	DISCUSSIONS .....	189
6.1.	Uniaxial Compressive Strength.....	189
6.2.	Weathering .....	192
6.3.	Slope Stability Classification Systems .....	194
6.4.	Effectiveness.....	198
6.5.	Stability .....	200
7.	CONCLUSIONS AND RECOMMENDATIONS .....	203
	REFERENCES.....	207
	APPENDICES .....	217
	APPENDIX A .....	217
	LABORATORY TEST RESULTS .....	217
	APPENDIX B .....	321
	ANALYSES RESULTS .....	321
	SSPC RESULTS .....	341

## LIST OF TABLES

### TABLES

Table 1. Coordinates of the studied cut slopes (Universal Transverse Mercator – Zone: 36T).....	3
Table 2. Meteorological data of Bolu, Karabük and Zonguldak between 1950 and 2014 (DMİ 2015) (Temperature in C° and precipitation in kg/m <sup>2</sup> ).....	5
Table 3. Classification of slope movements (Varnes, 1978).....	14
Table 4. Degrees of rock mass weathering (BS5930, 1981).....	22
Table 5. ME Values for different excavation methods (Hack, 1998) .....	28
Table 6. WE Values for different weathering degrees (Hack, 1998).....	28
Table 7. Estimation of intact rock strength by simple means test (Hack & Huisman, 2002).....	29
Table 8. Distance to NAFZ and PGA values obtained from Idriss (2007) .....	44
Table 9. The parameters for M greater than or equal to 6,75 (Idriss, 2007) .....	44
Table 10. Average values of effective porosity and unit weight of rocks at each road cut.....	47
Table 11. Scale of intact rock strength based on UCS tests (ANON, 1970).....	48
Table 12. Average values of uniaxial compressive strength (UCS) of the rocks at the selected road cuts .....	49
Table 13. Average values of Is <sub>50</sub> of the rocks at each road cut .....	52
Table 14. Average values of Schmidt rebound hardness test of each road cut .....	55
Table 15. Schmidt hammer values converted to UCS according to different studies .....	57
Table 16. Cohesion and internal friction angle values of saw-cut surfaces for peak and residual conditions.....	59
Table 17. Gamble’s slake durability classification .....	60
Table 18. Average values of slake durability test of the rocks at each road cut .....	61
Table 19. Average values of methylene blue adsorption test of the rocks at each road cut.....	64
Table 20. Classification of degree of jointing (Palmstrom, 2005) .....	66
Table 21. Classification of block volume (Palmstrom, 1995).....	66
Table 22. UCS values of the rocks at Stop 1 .....	72
Table 23. Unit weight values of the rocks at Stop 1 .....	73
Table 24. Slake durability and CEC values of the rocks at Stop 1 .....	75

Table 25. UCS and unit weight values of the rocks at Stop 2.....	77
Table 26. Slake durability and methylene blue values of the rocks at Stop 2.....	79
Table 27. UCS and unit weight values of the rocks at Stop 3.....	81
Table 28. Slake durability and methylene blue values of the rocks at Stop 3.....	83
Table 29. UCS and unit weight values of the rocks at Stop 4.....	84
Table 30. Slake durability and methylene blue values of the rock at Stop 4 .....	86
Table 31. UCS and unit weight values of the rocks at Stop 5.....	88
Table 32. Slake durability and methylene blue values of the rocks Stop 5 .....	90
Table 33. UCS and unit weight values of the rocks at Stop 6.....	92
Table 34. Slake durability and methylene blue values of Stop 6 .....	94
Table 35. UCS and unit weight values of the rocks at Stop 7.....	96
Table 36. Slake durability and methylene blue values of Stop 7 .....	98
Table 37. UCS and unit weight values of the rocks at Stop 8.....	100
Table 38. Slake durability and methylene blue values of the rocks at Stop 8.....	102
Table 39. UCS and unit weight values of the rocks at Stop 9.....	104
Table 40. Slake durability and methylene blue values of Stop 9 .....	106
Table 41. UCS and unit weight values of the rocks at Stop 10.....	107
Table 42. Slake durability and methylene blue values of Stop 10 .....	109
Table 43. UCS and unit weight values of the rocks at Stop 11.....	111
Table 44. Slake durability and methylene blue values of Stop 11 .....	113
Table 45. UCS and unit weight values of the rocks at Stop 12.....	115
Table 46. Slake durability and methylene blue values of the rocks at Stop 12.....	117
Table 47. UCS and unit weight values of the rocks at Stop 13.....	119
Table 48. Slake durability and methylene blue values of Stop 13 .....	121
Table 49. UCS values of the rocks at Stop 14 .....	123
Table 50. Unit weight values of the rocks at Stop 14 .....	123
Table 51. Slake durability and methylene blue values of the rocks Stop 14 .....	125
Table 52. UCS values of the rocks at Stop 15 .....	126
Table 53. Unit weight values of the rocks at Stop 15 .....	127
Table 54. Slake durability and methylene blue values of the rocks at Stop 15.....	129
Table 55. UCS values of the sandstone at Stop 16 .....	131
Table 56. Unit weight values of the sandstones at Stop 16.....	131
Table 57. Slake durability and methylene blue values of the sandstone at Stop 16	133

Table 58. UCS values of the rocks at Stop 17 .....	135
Table 59. Unit weight values of the rocks at Stop 17 .....	135
Table 60. Slake durability and methylene blue values of the rock at Stop 17 .....	137
Table 61. UCS and unit weight values of the rocks at Stop 18.....	139
Table 62. Slake durability and methylene blue values of the rocks at Stop 18.....	140
Table 63. UCS values of the rocks at Stop 19.....	142
Table 64. Unit weight values of the rocks at Stop 19 .....	142
Table 65. Slake durability and methylene blue values of the rocks at Stop 19.....	144
Table 66. UCS values of the rocks at Stop 20.....	146
Table 67. Unit weight values of the rocks at Stop 20 .....	146
Table 68. Slake durability and methylene blue values of the rocks at Stop 20.....	148
Table 69. UCS values for fresh and weathered zones of each road cut .....	160
Table 70. GSI values of each road cut .....	160
Table 71. FS results for static and pseudostatic conditions of each road cut.....	162
Table 72. Summary of $R_n$ , $R_t$ and friction angle for the materials encountered .....	167
Table 73. Block volume, unit weight and mass used in rockfall analyses for each road cut.....	168
Table 74. Rating adjustment for joint orientation (Singh & Gahrooei, 1989).....	174
Table 75. $RMR_{basic}$ , SMR and stable probabilities of each road cut .....	175
Table 76. Stability classes as per SMR values (modified from Romana (1985)) ....	176
Table 77. Data collection table of SSPC for a representative slope (Stop 8).....	178
Table 78. Reference rock table of SSPC for a representative slope (Stop 8).....	179
Table 79. Stability table of SSPC for a representative slope (Stop 8) .....	180
Table 80. Stable probabilities of each road cut obtained by using weathered intact rock strength.....	182
Table 81. Internal friction angle ( $\phi$ ) and cohesion (c) values of each road cut obtained by using weathered intact rock strength.....	183
Table 82. Stable probabilities of each road cut obtained by using fresh intact rock strength.....	185
Table 83. Internal friction angle ( $\phi$ ) and cohesion (c) values of each road cut obtained by using fresh intact rock strength .....	186
Table 84. Functions between UCS and Schmidt rebound values and correlation coefficients ( $R^2$ ).....	192

Table 85. Porosity and unit weight of Stop 1 fresh mudstone .....	217
Table 86. Porosity and unit weight of Stop 1 weathered mudstone.....	218
Table 87. Porosity and unit weight of Stop 1 fresh sandstone .....	218
Table 88. Porosity and unit weight of Stop 1 weathered sandstone.....	219
Table 89. Porosity and unit weight of Stop 2 fresh limestone .....	219
Table 90. Porosity and unit weight of Stop 2 weathered limestone.....	220
Table 91. Porosity and unit weight of Stop 3 fresh limestone .....	220
Table 92. Porosity and unit weight of Stop 3 weathered limestone.....	221
Table 93. Porosity and unit weight of Stop 4 fresh granite.....	222
Table 94. Porosity and unit weight of Stop 4 weathered granite .....	222
Table 95. Porosity and unit weight of Stop 5 fresh basalt .....	223
Table 96. Porosity and unit weight of Stop 5 weathered basalt .....	223
Table 97. Porosity and unit weight of Stop 6 weathered granite .....	224
Table 98. Porosity and unit weight of Stop 7 fresh granodiorite .....	224
Table 99. Porosity and unit weight of Stop 7 weathered granodiorite.....	225
Table 100. Porosity and unit weight of Stop 8 fresh sandstone .....	225
Table 101. Porosity and unit weight of Stop 8 weathered sandstone.....	226
Table 102. Porosity and unit weight of Stop 9 fresh limestone .....	226
Table 103. Porosity and unit weight of Stop 9 weathered limestone.....	227
Table 104. Porosity and unit weight of Stop 9 weathered mudstone.....	227
Table 105. Porosity and unit weight of Stop 10 fresh sandstone .....	228
Table 106. Porosity and unit weight of Stop 10 weathered sandstone.....	228
Table 107. Porosity and unit weight of Stop 11 fresh sandstone .....	229
Table 108. Porosity and unit weight of Stop 11 weathered sandstone.....	229
Table 109. Porosity and unit weight of Stop 12 fresh sandstone .....	230
Table 110. Porosity and unit weight of Stop 12 weathered sandstone.....	230
Table 111. Porosity and unit weight of Stop 13 fresh sandstone .....	231
Table 112. Porosity and unit weight of Stop 13 weathered sandstone.....	231
Table 113. Porosity and unit weight of Stop 14 fresh sandstone .....	232
Table 114. Porosity and unit weight of Stop 14 weathered sandstone.....	232
Table 115. Porosity and unit weight of Stop 15 fresh sandstone .....	233
Table 116. Porosity and unit weight of Stop 15 weathered sandstone.....	233
Table 117. Porosity and unit weight of Stop 16 fresh sandstone .....	234

Table 118. Porosity and unit weight of Stop 16 weathered sandstone.....	234
Table 119. Porosity and unit weight of Stop 17 fresh sandstone .....	235
Table 120. Porosity and unit weight of Stop 17 weathered sandstone.....	235
Table 121. Porosity and unit weight of Stop 18 fresh marl.....	236
Table 122. Porosity and unit weight of Stop 18 weathered marl .....	236
Table 123. Porosity and unit weight of Stop 19 fresh marl.....	237
Table 124. Porosity and unit weight of Stop 19 weathered marl .....	237
Table 125. Porosity and unit weight of Stop 20 fresh marl.....	238
Table 126. Porosity and unit weight of Stop 20 weathered marl .....	238
Table 127. UCS of Stop 2 fresh dry limestone .....	239
Table 128. UCS of Stop 2 fresh saturated limestone .....	239
Table 129. UCS of Stop 4 fresh dry/saturated granite .....	239
Table 130. UCS of Stop 8 fresh dry sandstone .....	240
Table 131. UCS of Stop 8 fresh saturated sandstone .....	240
Table 132. Point load strength of Stop 1 fresh dry mudstone in vertical direction..	241
Table 133. Point load strength of Stop 1 fresh dry mudstone in horizontal direction .....	241
Table 134. Point load strength of Stop 1 fresh dry sandstone in vertical direction .	242
Table 135. Point load strength of Stop 1 fresh dry sandstone in horizontal direction .....	242
Table 136. Point load strength of Stop 1 weathered dry mudstone in vertical direction .....	243
Table 137. Point load strength of Stop 1 weathered dry mudstone in horizontal direction.....	243
Table 138. Point load strength of Stop 1 weathered dry sandstone in vertical direction .....	244
Table 139. Point load strength of Stop 1 weathered dry sandstone in horizontal direction.....	244
Table 140. Point load strength of Stop 1 fresh saturated mudstone in vertical direction.....	245
Table 141. Point load strength of Stop 1 fresh saturated mudstone in horizontal direction.....	245

Table 142. Point load strength of Stop 1 fresh saturated sandstone in vertical direction .....	246
Table 143. Point load strength of Stop 1 fresh saturated sandstone in horizontal direction .....	246
Table 144. Point load strength of Stop 1 weathered saturated mudstone in vertical direction .....	247
Table 145. Point load strength of Stop 1 weathered saturated mudstone in horizontal direction .....	247
Table 146. Point load strength of Stop 1 weathered saturated sandstone in vertical direction .....	248
Table 147. Point load strength of Stop 1 weathered saturated sandstone in horizontal direction .....	248
Table 148. Point load strength of Stop 1 failed zone fresh dry mudstone .....	249
Table 149. Point load strength of Stop 1 failed zone weathered dry mudstone .....	249
Table 150. Point load strength of Stop 1 failed zone fresh saturated mudstone .....	250
Table 151. Point load strength of Stop 1 failed zone weathered saturated mudstone .....	250
Table 152. Point load strength of Stop 2 fresh dry limestone .....	251
Table 153. Point load strength of Stop 2 weathered dry limestone .....	251
Table 154. Point load strength of Stop 2 fresh saturated limestone .....	252
Table 155. Point load strength of Stop 2 weathered saturated limestone .....	252
Table 156. Point load strength of Stop 2 failed zone fresh dry limestone .....	253
Table 157. Point load strength of Stop 2 failed zone fresh saturated limestone .....	253
Table 158. Point load strength of Stop 3 fresh dry limestone .....	254
Table 159. Point load strength of Stop 3 weathered dry limestone .....	255
Table 160. Point load strength of Stop 3 fresh saturated limestone .....	256
Table 161. Point load strength of Stop 3 weathered saturated limestone .....	257
Table 162. Point load strength of Stop 4 fresh dry granite .....	258
Table 163. Point load strength of Stop 4 weathered dry granite .....	258
Table 164. Point load strength of Stop 4 fresh saturated granite .....	259
Table 165. Point load strength of Stop 4 weathered saturated granite .....	259
Table 166. Point load strength of Stop 5 fresh dry basalt .....	260
Table 167. Point load strength of Stop 5 fresh saturated basalt .....	260

Table 168. Point load strength of Stop 5 weathered dry basalt.....	261
Table 169. Point load strength of Stop 5 weathered saturated basalt.....	262
Table 170. Point load strength of Stop 6 weathered dry granite .....	263
Table 171. Point load strength of Stop 6 weathered saturated granite .....	263
Table 172. Point load strength of Stop 7 fresh dry granodiorite .....	264
Table 173. Point load strength of Stop 7 weathered dry granodiorite.....	264
Table 174. Point load strength of Stop 7 fresh saturated granodiorite .....	265
Table 175. Point load strength of Stop 7 weathered saturated granodiorite .....	265
Table 176. Point load strength of Stop 8 fresh dry sandstone.....	266
Table 177. Point load strength of Stop 8 weathered dry sandstone .....	266
Table 178. Point load strength of Stop 8 fresh saturated sandstone.....	267
Table 179. Point load strength of Stop 8 weathered saturated sandstone .....	267
Table 180. Point load strength of Stop 9 fresh dry limestone .....	268
Table 181. Point load strength of Stop 9 weathered dry limestone.....	268
Table 182. Point load strength of Stop 9 weathered dry mudstone.....	269
Table 183. Point load strength of Stop 9 fresh saturated limestone .....	269
Table 184. Point load strength of Stop 9 weathered saturated limestone .....	270
Table 185. Point load strength of Stop 9 weathered dry mudstone.....	270
Table 186. Point load strength of Stop 10 fresh dry sandstone.....	271
Table 187. Point load strength of Stop 10 weathered dry sandstone .....	271
Table 188. Point load strength of Stop 10 fresh saturated sandstone.....	272
Table 189. Point load strength of Stop 10 weathered saturated sandstone .....	272
Table 190. Point load strength of Stop 11 fresh dry sandstone.....	273
Table 191. Point load strength of Stop 11 weathered dry sandstone .....	273
Table 192. Point load strength of Stop 11 fresh saturated sandstone.....	274
Table 193. Point load strength of Stop 11 weathered saturated sandstone .....	274
Table 194. Point load strength of Stop 12 fresh dry sandstone.....	275
Table 195. Point load strength of Stop 12 weathered dry sandstone .....	275
Table 196. Point load strength of Stop 12 fresh saturated sandstone.....	276
Table 197. Point load strength of Stop 12 weathered saturated sandstone .....	276
Table 198. Point load strength of Stop 13 fresh dry sandstone.....	277
Table 199. Point load strength of Stop 13 weathered dry sandstone .....	277
Table 200. Point load strength of Stop 13 fresh saturated sandstone.....	278

Table 201. Point load strength of Stop 13 weathered saturated sandstone .....	278
Table 202. Point load strength of Stop 14 fresh dry sandstone in vertical direction	279
Table 203. Point load strength of Stop 14 fresh dry sandstone in horizontal direction .....	279
Table 204. Point load strength of Stop 14 weathered dry sandstone in vertical direction .....	280
Table 205. Point load strength of Stop 14 weathered dry sandstone in horizontal direction .....	280
Table 206. Point load strength of Stop 14 fresh saturated sandstone in vertical direction .....	281
Table 207. Point load strength of Stop 14 fresh saturated sandstone in horizontal direction .....	281
Table 208. Point load strength of Stop 14 weathered saturated sandstone in vertical direction .....	282
Table 209. Point load strength of Stop 14 weathered saturated sandstone in horizontal direction .....	283
Table 210. Point load strength of Stop 15 fresh dry sandstone in vertical direction	284
Table 211. Point load strength of Stop 15 fresh dry sandstone in horizontal direction .....	284
Table 212. Point load strength of Stop 15 weathered dry sandstone in vertical direction .....	285
Table 213. Point load strength of Stop 15 weathered dry sandstone in horizontal direction .....	285
Table 214. Point load strength of Stop 15 fresh saturated sandstone in vertical direction .....	286
Table 215. Point load strength of Stop 15 fresh saturated sandstone in horizontal direction .....	286
Table 216. Point load strength of Stop 15 weathered saturated sandstone in vertical direction .....	287
Table 217. Point load strength of Stop 15 weathered saturated sandstone in horizontal direction .....	287
Table 218. Point load strength of Stop 16 fresh dry sandstone in vertical direction	288

Table 219. Point load strength of Stop 16 fresh dry sandstone in horizontal direction .....	289
Table 220. Point load strength of Stop 16 weathered dry sandstone in vertical direction.....	289
Table 221. Point load strength of Stop 16 weathered dry sandstone in horizontal direction.....	290
Table 222. Point load strength of Stop 16 fresh saturated sandstone in vertical direction.....	290
Table 223. Point load strength of Stop 16 fresh saturated sandstone in horizontal direction.....	291
Table 224. Point load strength of Stop 16 weathered saturated sandstone in vertical direction.....	291
Table 225. Point load strength of Stop 16 weathered saturated sandstone in horizontal direction.....	292
Table 226. Point load strength of Stop 17 fresh dry sandstone in vertical direction	292
Table 227. Point load strength of Stop 17 fresh dry sandstone in horizontal direction .....	293
Table 228. Point load strength of Stop 17 weathered dry sandstone in vertical direction.....	293
Table 229. Point load strength of Stop 17 weathered dry sandstone in horizontal direction.....	294
Table 230. Point load strength of Stop 17 fresh saturated sandstone in vertical direction.....	294
Table 231. Point load strength of Stop 17 fresh saturated sandstone in horizontal direction.....	295
Table 232. Point load strength of Stop 17 weathered saturated sandstone in horizontal direction.....	295
Table 233. Point load strength of Stop 17 weathered saturated sandstone in vertical direction.....	296
Table 234. Point load strength of Stop 18 fresh dry marl .....	296
Table 235. Point load strength of Stop 18 weathered dry marl.....	297
Table 236. Point load strength of Stop 18 fresh saturated marl .....	297
Table 237. Point load strength of Stop 18 weathered saturated marl.....	298

Table 238. Point load strength of Stop 19 fresh dry marl in vertical direction.....	298
Table 239. Point load strength of Stop 19 fresh dry marl in horizontal direction....	299
Table 240. Point load strength of Stop 19 weathered dry marl in vertical direction	299
Table 241. Point load strength of Stop 19 weathered dry marl in horizontal direction .....	300
Table 242. Point load strength of Stop 19 fresh saturated marl in horizontal direction .....	300
Table 243. Point load strength of Stop 19 fresh saturated marl in vertical direction .....	301
Table 244. Point load strength of Stop 19 weathered saturated marl in horizontal direction .....	301
Table 245. Point load strength of Stop 19 weathered saturated marl in vertical direction .....	302
Table 246. Point load strength of Stop 20 fresh dry marl in vertical direction.....	302
Table 247. Point load strength of Stop 20 fresh dry marl in horizontal direction....	303
Table 248. Point load strength of Stop 20 weathered dry marl in vertical direction	303
Table 249. Point load strength of Stop 20 weathered dry marl in horizontal direction .....	304
Table 250. Point load strength of Stop 20 fresh saturated marl in vertical direction .....	304
Table 251. Point load strength of Stop 20 fresh saturated marl in horizontal direction .....	305
Table 252. Point load strength of Stop 20 weathered saturated marl in vertical direction .....	305
Table 253. Point load strength of Stop 20 weathered saturated marl in horizontal direction .....	306
Table 254. Slake durability of Stop 1.....	306
Table 255. Slake durability of Stop 1 failed zone.....	306
Table 256. Slake durability of Stop 2.....	307
Table 257. Slake durability of Stop 3.....	307
Table 258. Slake durability of Stop 4.....	307
Table 259. Slake durability of Stop 5.....	307
Table 260. Slake durability of Stop 6.....	308

Table 261. Slake durability of Stop 7.....	308
Table 262. Slake durability of Stop 8.....	308
Table 263. Slake durability of Stop 9.....	308
Table 264. Slake durability of Stop 10.....	309
Table 265. Slake durability of Stop 11.....	309
Table 266. Slake durability of Stop 12.....	309
Table 267. Slake durability of Stop 13.....	309
Table 268. Slake durability of Stop 14.....	310
Table 269. Slake durability of Stop 15.....	310
Table 270. Slake durability of Stop 16.....	310
Table 271. Slake durability of Stop 17.....	310
Table 272. Slake durability of Stop 18.....	311
Table 273. Slake durability of Stop 19.....	311
Table 274. Slake durability of Stop 20.....	311
Table 275. RMR values of Stop 1, 1-failed, 2, 2-failed, 3 and 4 .....	336
Table 276. RMR values of Stop 5, 6, 7, 8, 9 and 10 .....	337
Table 277. RMR values of Stop 11, 12, 13, 14, 15 and 16 .....	338
Table 278. RMR values of Stop 17, 18, 19 and 20 .....	339

## LIST OF FIGURES

### FIGURES

Figure 1. Location map of the study area.....	2
Figure 2. Plan and related elevation profile view of the study area.....	4
Figure 3. Rock slope failure types (Hoek & Bray, 1981) .....	15
Figure 4. Discontinuity wall weathering (Modified from Huisman (2006)) .....	23
Figure 5. Sketch view of rock masses with various degrees of weathering (Modified from Hack et al. (2002)).....	26
Figure 6. Flow chart of SSPC system (Hack et al. 2002) .....	26
Figure 7. Factor determination chart for spacing parameter (SPA) (Hack, 1998).....	30
Figure 8. Probability of orientation-independent stability (Hack et al. 2002) .....	31
Figure 9. Sliding criterion (Hack et al. 2002) .....	32
Figure 10. Toppling criterion (Hack et al. 2002) .....	33
Figure 11. Location of the study area in İstanbul terrane (Modified from Okay (2008)).....	36
Figure 12. Geological map of study area (Modified from MTA (2002a; 2002b; 2002c)) .....	37
Figure 13. Earthquake zoning map of the study area and its vicinity (GDDA, 1996).....	43
Figure 14. Tested samples in vacuum chamber (left) and air pump (right) system...	46
Figure 15. Compression machine used to determine UCS values of the rocks .....	49
Figure 16. Manual point load device used in this study.....	50
Figure 17. L type Schmidt rebound hammer used in this study.....	54
Figure 18. Slake durability test equipment used in this thesis .....	60
Figure 19. Methylene blue adsorption test equipment used in this thesis.....	63
Figure 20. Profilometer used on discontinuity surfaces.....	67
Figure 21. Undercutting due to differential weathering (sandstone on top, mudstone on bottom) .....	68
Figure 22. Possible evolution of Stop 8 (Akveren FM) after differential weathering.....	69
Figure 23. General view of the cut slope at Stop 1 .....	71
Figure 24. Failed zone of the cut slope at Stop 1 .....	71
Figure 25. Pole (left) and contour (right) diagrams of the discontinuities at Stop 1..	74
Figure 26. Discontinuity spacing frequency histogram of Stop 1.....	74
Figure 27. General view and shear zones (red dashed lines) seen at Stop 2.....	76

Figure 28. Failure of the rock mass at Stop 2.....	76
Figure 29. Pole (left) and contour (right) diagrams of the discontinuities at Stop 2..	78
Figure 30. Discontinuity spacing frequency histogram at Stop 2 .....	78
Figure 31. General view of the cut slope at Stop 3 .....	80
Figure 32. Pole (left) and contour (right) diagrams of the discontinuities at Stop 3..	82
Figure 33. Discontinuity spacing frequency histogram at Stop 3 .....	82
Figure 34. General view of the cut slope at Stop 4 (Failure zone indicated with red dashed line) .....	84
Figure 35. Pole (left) and contour (right) diagrams of the discontinuities at Stop 4..	85
Figure 36. Discontinuity spacing frequency histogram at Stop 4 .....	86
Figure 37. General view and shear zones of Stop 5 (Shear zones indicated with red dashed lines).....	87
Figure 38. Pole (left) and contour (right) diagrams of the discontinuities at Stop 5..	89
Figure 39. Discontinuity spacing frequency histogram at Stop 5 .....	89
Figure 40. General view of the cut slope at Stop 6 .....	91
Figure 41. Pole (left) and contour (right) diagrams of the discontinuities at Stop 6..	93
Figure 42. Discontinuity spacing frequency histogram of Stop 6.....	93
Figure 43. General view of Stop 7 in 2015 (above) and 2016 (below).....	95
Figure 44. Pole (left) and contour (right) diagrams of the discontinuities at Stop 7..	97
Figure 45. Discontinuity spacing frequency histogram of Stop 7 .....	97
Figure 46. General view of the cut slope at Stop 8 .....	99
Figure 47. Fractured mudstone at Stop 8 .....	100
Figure 48. Pole (left) and contour (right) diagrams of the discontinuities at Stop 8	101
Figure 49. Discontinuity spacing frequency histogram of Stop 8.....	101
Figure 50. General view of the cut slope at Stop 9 .....	103
Figure 51. Pole (left) and contour (right) diagrams of the discontinuities at Stop 9	105
Figure 52. Discontinuity spacing frequency histogram at Stop 9 .....	105
Figure 53. General view of the cut slope at Stop 10 .....	107
Figure 54. Pole (left) and contour (right) diagrams of the discontinuities at Stop 10 .....	108
Figure 55. Discontinuity spacing frequency histogram of Stop 10.....	109
Figure 56. General view of the cut slope at Stop 11 .....	110

Figure 57. Pole (left) and contour (right) diagrams of the discontinuities at Stop 11 .....	112
Figure 58. Discontinuity spacing frequency histogram of Stop 11.....	112
Figure 59. General view of the cut slope at Stop 12 .....	114
Figure 60. Pole (left) and contour (right) diagrams of the discontinuities at Stop 12 .....	116
Figure 61. Discontinuity spacing frequency histogram of Stop 12.....	116
Figure 62. General view of the cut slope at Stop 13 .....	118
Figure 63. Pole (left) and contour (right) diagrams of the discontinuities at Stop 13 .....	120
Figure 64. Discontinuity spacing frequency histogram of Stop 13.....	120
Figure 65. General view of the cut slope at Stop 14 .....	122
Figure 66. Pole (left) and contour (right) diagrams of the discontinuities at Stop 14 .....	124
Figure 67. Discontinuity spacing frequency histogram of Stop 14.....	124
Figure 68. General view of the cut slope at Stop 15 .....	126
Figure 69. Pole (left) and contour (right) diagrams of the discontinuities at Stop 15 .....	128
Figure 70. Discontinuity spacing frequency histogram of Stop 15.....	128
Figure 71. General view of the cut slope at Stop 16 .....	130
Figure 72. Pole (left) and contour (right) diagrams of the discontinuities at Stop 16 .....	132
Figure 73. Discontinuity spacing frequency histogram of Stop 16.....	132
Figure 74. General view of the cut slope at Stop 17 .....	134
Figure 75. Pole (left) and contour (right) diagrams of the discontinuities at Stop 17 .....	136
Figure 76. Discontinuity spacing frequency histogram of Stop 17.....	136
Figure 77. General view of the cut slope at Stop 18 .....	138
Figure 78. Pole (left) and contour (right) diagrams of the discontinuities Stop 18 .	139
Figure 79. Discontinuity spacing frequency histogram of Stop 18.....	140
Figure 80. General view and shear zones (red dashed lines) of Stop 19 .....	141
Figure 81. Pole (left) and contour (right) diagrams of the discontinuities at Stop 19 .....	143

Figure 82. Discontinuity spacing frequency histogram of Stop 19 .....	144
Figure 83. General view and shear zones (red dashed lines) of Stop 20.....	145
Figure 84. Pole (left) and contour (right) diagrams of the discontinuities at Stop 20 .....	147
Figure 85. Discontinuity spacing frequency histogram of Stop 20.....	148
Figure 86. Roughness profiles and related JRC values (Barton & Choubey, 1977) .....	151
Figure 87. Cohesion and internal friction angle values of critical slopes .....	152
Figure 88. Kinematic analyses of Stop 8.....	153
Figure 89. Kinematic analyses of Stop 9.....	153
Figure 90. Kinematic analyses of Stop 15.....	154
Figure 91. Kinematic analyses of Stop 19.....	154
Figure 92. Wedge failure analysis of Stop 8 giving FS=5.2 .....	155
Figure 93. Wedge failure analysis of Stop 9 with giving FS=6.8 .....	156
Figure 94. Wedge failure analysis of Stop 15 giving FS=19.4 .....	156
Figure 95. Wedge failure analysis of Stop 19 giving FS=2.4 .....	157
Figure 96. Planar failure analysis of Stop 19 giving FS=0.8 .....	158
Figure 97. Toppling failure analysis of Stop 19 giving FS=2.1 .....	158
Figure 98. Mass failure analysis of Stop 20 after slope flattening .....	163
Figure 99. Mass failure analysis of Stop 1 after slope flattening .....	164
Figure 100. FS results of the failed zone at Stop 1 .....	165
Figure 101. FS results of the failed zone at Stop 2 .....	166
Figure 102. Rockfall analyses of Stops 2, 3, 4 and 5 .....	169
Figure 103. Rockfall analyses of Stop 6, 7 and 8 (Stop 7 w indicates new profile after first investigations).....	170
Figure 104. Rockfall analyses of Stop 9, 10, 11 and 13.....	171
Figure 105. Rockfall analyses of Stop 14, 15, 16 and 18.....	172
Figure 106. Rockfall analyses of Stop 19 and 20.....	173
Figure 107. UCS vs Schmidt rebound value graph according to various researchers and this thesis study.....	191
Figure 108. UCS vs Schmidt rebound value graph according to various researchers and limestone samples of this thesis study .....	191
Figure 109. UCS vs Schmidt rebound value graphs according to various researchers and igneous rock samples of this thesis study .....	192

Figure 110. Dry granite sample from Stop 6.....	193
Figure 111. Distribution of visually estimated stabilities on SMR points .....	196
Figure 112. Results of SSPC and visually estimated stability (using weathered samples directly) .....	197
Figure 113. Results of SSPC and visually estimated stability (using fresh samples directly) .....	197
Figure 114. Factor of safety change against different GSI values for each road cut	199
Figure 115. Factor of safety change against different seismic coefficients for each road cut.....	199
Figure 116. Weaker/Failed zone at Stop 1 divided by red dashed line from stable part .....	201
Figure 117. Failed portion of Stop 19 and shear zones (red dashed lines) .....	202
Figure 118. Methylene blue test results of Stop 1 and Stop 1 failed zone.....	312
Figure 119. Methylene blue test results of Stop 2, 3 and 4.....	313
Figure 120. Methylene blue test results of Stop 5, 6, 7 and 8.....	314
Figure 121. Methylene blue test results of Stop 8, 9 and 10.....	315
Figure 122. Methylene blue test results of Stop 10, 11 and 12.....	316
Figure 123. Methylene blue test results of Stop 12, 13 and 14.....	317
Figure 124. Methylene blue test results of Stop 15, 16 and 17 .....	318
Figure 125. Methylene blue test results of Stop 17, 18, 19 and 20.....	319
Figure 126. Methylene blue test results of Stop 20.....	320
Figure 127. Limit equilibrium analyses of Stop 1 (above) and Stop 1 failed (below) .....	322
Figure 128. Limit equilibrium analyses of Stop 2 (above) and Stop 2 failed (below) .....	323
Figure 129. Limit equilibrium analyses of Stop 3 (above) and Stop 4 (below).....	324
Figure 130. Limit equilibrium analyses of Stop 5 (above) and Stop 6 (below).....	325
Figure 131. Limit equilibrium analyses of Stop 7 (above) and Stop 8 (below).....	326
Figure 132. Limit equilibrium analyses of Stop 9 (above) and Stop 10 (below).....	327
Figure 133. Limit equilibrium analyses of Stop 11 (above) and Stop 12 (below)...	328
Figure 134. Limit equilibrium analyses of Stop 13 (above) and Stop 14 (below)...	329
Figure 135. Limit equilibrium analyses of Stop 15 (above) and Stop 16 (below)...	330
Figure 136. Limit equilibrium analyses of Stop 17 (above) and Stop 18 (below)...	331

Figure 137. Limit equilibrium analyses of Stop 19 (above) and Stop 20 (below)...	332
Figure 138. Rn and Rt values of drainage channel in front of the slopes .....	333
Figure 139. Rn and Rt values of granite.....	333
Figure 140. Rn and Rt values of granodiorite .....	334
Figure 141. Rn and Rt values of limestone .....	334
Figure 142. Rn and Rt values of marl .....	335
Figure 143. Rn and Rt values of sandstone.....	335

## **CHAPTER 1**

### **INTRODUCTION**

#### **1.1. Purpose and Scope**

Rocks contain pore spaces, micro to macro fractures, joints, bedding planes and faults which are prone to weathering due to temperature differences, wetting-drying and chemistry of solutions absorbed. Especially road cuts are very sensitive to weathering activities because of disturbed structure and topographical condition by excavation. Therefore, considering the penetration depth, effects of weathering may decrease strength parameters of rocks and eventually cause of failures. The aim of this study is to investigate road cut slope stabilities with the effects of weathering at North West Black Sea region in Turkey. The slope stability analyses were done by modeling surface of the road cuts as determined depths of weathered rock and considering rest of the slope as relatively fresh rock.

In order to fulfill this study, researches on local geology, literature about methods of slope stability assessment and effects of weathering on rock strength were done. In the field, data were gathered at twenty cut slopes by sample collection, scan-line survey, field observation about weathering degree and excavation type, and in-situ tests like Schmidt rebound hammer. In addition to strength parameter tests on the collected samples, slake durability and methylene blue tests were also applied to the samples in order to investigate the differences in weathering of the rocks. Lastly 2D analyses of the road cuts are carried out according to weathered and relatively fresh strength parameter values of the rocks.

## 1.2. Accessibility and Location

Cut slopes in the study area are located on the Zonguldak-Ankara D750 highway with the city borders of Bolu, Karabük and Zonguldak in Turkey. Their positions are between 10.5 km north of Yeniçağa – Gerede - Mengen Junction and 25 km south of Zonguldak centrum (Figure 1).



Figure 1. Location map of the study area

Coordinates of each cut slope are given in Table 1 according to Universal Transverse Mercator (UTM) as northing and easting. All cut slopes are in the zone of 36 T.

The elevation of the study area is decreasing from south to north direction in a gentle manner (Figure 2). First seven road cut elevations are over 250 m and the rest of them are lower than 250 m above sea level. Especially road cuts 4, 5 and 6 are located in between a deep valley in which they are partly supported by approximately 10 m high stone walls in order to construct the two lane road next to them. Other road cuts are located in a relatively gentler topography.

Table 1. Coordinates of the studied cut slopes (Universal Transverse Mercator – Zone: 36T)

<b>Road Cut</b>	<b>Northing</b>	<b>Easting</b>	<b>Road Cut</b>	<b>Northing</b>	<b>Easting</b>
<b>S1</b>	4522852	421768	<b>S11</b>	4575721	420081
<b>S2</b>	4535346	422464	<b>S12</b>	4576353	419889
<b>S3</b>	4535616	422338	<b>S13</b>	4576481	419803
<b>S4</b>	4543422	422497	<b>S14</b>	4576721	419627
<b>S5</b>	4543261	422400	<b>S15</b>	4577000	419212
<b>S6</b>	4544537	422454	<b>S16</b>	4579728	416799
<b>S7</b>	4554180	414322	<b>S17</b>	4580007	415766
<b>S8</b>	4558052	410276	<b>S18</b>	4581369	412803
<b>S9</b>	4560537	411066	<b>S19</b>	4581303	412625
<b>S10</b>	4575211	420530	<b>S20</b>	4581165	412691

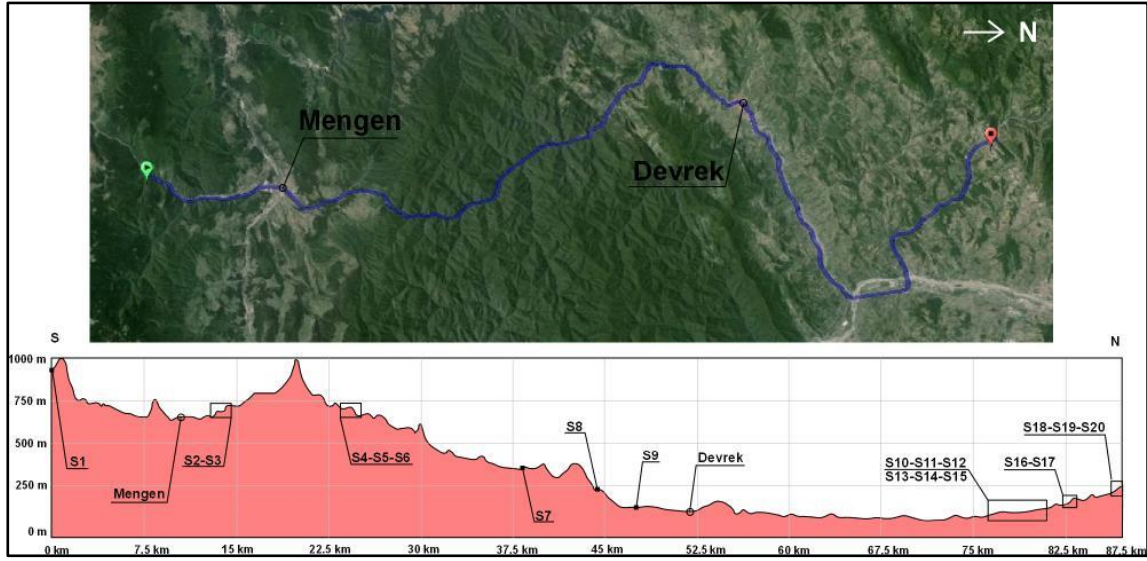


Figure 2. Plan and related elevation profile view of the study area

### 1.3. Climate and Vegetation

Black Sea region climate is effective in the study area. Generally, every season is rainy in these cities. In the Black Sea region, climate is cold in winters and warm in summers. This climate type can be observable in the cities of study area. Natural vegetation is forest for whole Black Sea region.

According to Turkish State Meteorological Service (DMI, 2015) data between the years of 1950-2014, average yearly precipitation of Bolu is  $46 \text{ kg/m}^2$  (Table 2). Highest precipitation is observed in December, lowest one is in August. Average yearly temperature is  $10.5^\circ\text{C}$  for Bolu city. Maximum temperature is observed in August and lowest one is in January (Table 2). Average yearly precipitation of Karabük city is  $35.7 \text{ kg/m}^2$  (Table 2). Different than Bolu, highest precipitation of Karabük is in May, and lowest one is in January. Average yearly temperature for Karabük is  $13.4^\circ\text{C}$ . Similar to Bolu, highest and lowest monthly temperatures are observed in August and January, respectively (Table 2). Average yearly precipitation is  $100.9 \text{ kg/m}^2$  in Zonguldak which is quite higher than Bolu and Karabük (Table 2). Highest monthly precipitation is in December and lowest one is in May for Zonguldak city. Average yearly temperature of Zonguldak is  $13.7^\circ\text{C}$  which is very

similar to Karabük city. Maximum monthly temperature is observed in August and minimum one is in February in Zonguldak (Table 2). Bolu and Karabük are semi-humid to humid while it is very humid for Zonguldak.

Natural vegetation is broad leaf trees for lower elevations. Vegetation changes to composite leaf trees as the elevation rises. Higher elevations are generally dominated by coniferous trees and alpine meadows.

Table 2. Meteorological data of Bolu, Karabük and Zonguldak between 1950 and 2014 (DMİ 2015) (Temperature in C° and precipitation in kg/m<sup>2</sup>)

	Months											
<b>BOLU</b>	<b>1</b>	<b>2</b>	<b>3</b>	<b>4</b>	<b>5</b>	<b>6</b>	<b>7</b>	<b>8</b>	<b>9</b>	<b>10</b>	<b>11</b>	<b>12</b>
Average Temperature	0,9	2	4,9	9,8	14	17,4	19,9	19,8	16,1	11,7	6,9	3
Average Max. Temperature	5,4	7,2	11,1	16,7	21,3	24,7	27,5	27,9	24,4	19,1	13,1	7,5
Average Min. Temperature	-3,2	-2,5	-0,2	4	7,7	10,5	12,7	12,7	9,6	6,2	2,1	-1
Average Precipitation Amount	58,6	46,8	51,7	51,4	59,7	54,8	29,4	23,8	27,6	42,6	44,6	61,3
<b>KARABÜK</b>	<b>1</b>	<b>2</b>	<b>3</b>	<b>4</b>	<b>5</b>	<b>6</b>	<b>7</b>	<b>8</b>	<b>9</b>	<b>10</b>	<b>11</b>	<b>12</b>
Average Temperature	3	4,7	8	12,8	17,4	20,9	23,9	23,6	19,5	14,3	8,3	4,4
Average Max. Temperature	7,4	10,4	14,8	20,3	25,5	29	32,2	32,4	28,3	21,9	14,4	8,8
Average Min. Temperature	-0,5	0,3	2,6	6,8	10,7	13,8	16,4	16,3	12,7	8,7	3,7	0,9
Average Precipitation Amount	18	33,9	41,6	47,3	53,7	42	24,4	23	27	35,5	34	48,2
<b>ZONGULDAK</b>	<b>1</b>	<b>2</b>	<b>3</b>	<b>4</b>	<b>5</b>	<b>6</b>	<b>7</b>	<b>8</b>	<b>9</b>	<b>10</b>	<b>11</b>	<b>12</b>
Average Temperature	6,2	6,2	7,5	11,4	15,5	19,7	21,9	21,9	18,7	15,1	11,6	8,5
Average Max. Temperature	9,2	9,5	10,9	15,1	18,9	23	25,1	25,3	22,4	18,6	15,1	11,6
Average Min. Temperature	3,6	3,4	4,6	8,3	12,2	16	18,2	18,3	15,5	12,3	8,9	5,8
Average Precipitation Amount	136,4	92	96,1	60,9	53,3	72,3	72,5	81,9	108,1	144,1	141,7	152

#### **1.4. Method of Study**

The methodology is divided into four in this thesis. In the first part, literature survey on both rock properties and a new classification system which is SSPC and, geology of study area was conducted. In the second part, field works were done to collect samples from related slopes, and evaluate data on rock classification, rock property, weathering degrees and excavation type of road cuts. In the third part, laboratory tests like Schmidt rebound hammer test, point load test, uniaxial compressive strength (UCS) test, direct shear test along discontinuities were conducted to find strength-related parameters, and slake durability test and methylene blue test to find other rock properties. In the last and fourth part, kinematic, rockfall and limit equilibrium analysis were performed to check the stability of the road cuts.

The first part includes literature survey on weathering and excavation effects on rock strength parameters. As Hack (1998), Miscevic & Roje-Bonacci (2001), Topal and Sozmen (2003), Huisman (2006) and Shrivastava (2014) explain in detail in their studies, weathering affects and most probably decreases rock strength. With the influence of excavation types by disturbing rock mass parameters directly or by working with weathering rock strength can decrease as well. By considering these general information, literature survey was expanded to shear strength parameters like cohesion and internal friction angle used in slope stability analysis. As the main aim of this study is stability analysis of road-cuts, and considering the descent of these rock parameters, possible failure types of road-cuts were surveyed. For the next step at literature survey, Slope Stability Probability Classification (SSPC) developed by (Hack, 1998) was researched in detail with its basic concept and related conclusion. At last, the geology of the study area along the study route was surveyed.

For the second part, field surveys like data collection for rock classification methods, determination of weathering degree and excavation type, sampling for laboratory and in-situ tests were conducted. In order to obtain data for classification methods, scan line surveys were done. Also, discontinuity data as condition, orientation, spacing, aperture, persistence, roughness, wall strength, block size, groundwater inflow and infill material type were collected. In addition to discontinuity data, weathering degree and excavation type were determined in order to observe the effect of them to slope stability. All these data were gathered to obtain rock parameters like cohesion

and internal friction angle by using Geological Strength Index (GSI) (Hoek, 1994), Rock Mass Rating (RMR) (Bieniawski, 1976) and Slope Stability Probability Classification System (SSPC) (Hack, 1998). For GSI system, surface conditions of discontinuities as weathering degree and roughness, and structure of rock mass were considered. Obtained GSI values were used in Hoek-Brown failure criterion (Hoek, et al., 2002) to obtain strength parameters of the rocks. Similar to this system, RMR was used by considering uniaxial compressive strength (UCS) of the rock material, rock quality designation (RQD), groundwater condition and, spacing, condition and orientation of discontinuities. Different than GSI, the RMR system shows rock parameters as ranges rather than showing exact values. In the next step, data collection was completed for SSPC system in order to obtain rock strength parameters for both reference and weathered rocks in the road cuts. Considering these values, probabilistic results of different kind of failure mechanisms (orientation dependent and independent) were obtained. Details of SSPC system are discussed in literature review section, (Chapter 2) of this thesis. By completing field study to collect data for classification systems rock samples were taken for laboratory studies. In the field, in order to compare weathered and relatively fresh rock sample strengths and collect data to obtain UCS values of them, Schmidt hammer test was applied as an in-situ test.

In the third part, laboratory tests were conducted to find strength parameters of both relatively fresh and weathered rocks. In addition, some other tests were also done to detect unit weight, durability against weathering and clay mineral activation of the rocks. Besides Schmidt rebound in-situ test, point load, UCS and direct shear tests were done to obtain rock strength parameters such as cohesion and internal friction angle. Samples were saturated in vacuum chamber and then dried for at least 24 hours to find saturated and dry unit weight of the samples. Slake durability test was conducted to determine the durability of rocks against weathering by simulating wetting and drying. In order to get information about cation exchange capacity and clay content of the samples methylene blue test was done. The main aim of these tests is to determine properties of the rocks to model road cuts against any kind of failure.

In the fourth part, analyses were done on each road cut to observe their state of stability. For discontinuity controlled failures, kinematic analyses were conducted by using Dips (6.0) software (Rocscience, 2013) considering discontinuity data obtained from the field study. Moreover, in order to investigate rockfall risk of road cuts back analysis was done on already fallen rock blocks by RocFall (4.0) program (Rocscience, 2004a). Lastly, limit equilibrium analyses were done by SLIDE (6.0) software (Rocscience, 2011) on each road cut in order to check the overall stability of the slopes. All these analyses were done to assess the stability of each road cut with rock strength properties of the weathered ones on the surface and the relatively fresh ones beyond surface.

## **1.5. Previous Studies**

Previous studies are researched according to geological studies around the study area and SSPC method used in the world.

### **1.5.1. Previous Studies about Geology**

20 different cut slopes are investigated in the study area and they are located in the formations of Yedigöller, Bolu Granitoid, Abant, Akveren, Yığılca, Çaycuma and Soğanlı.

As mentioned in Kaya et al. (1986) Akveren formation consists clayey limestone-marl alternation, tuff, sandstone, claystone and calcareous mudstone. Also, Ozer (1994) investigated the contact between the Hatipler and the overlying Akveren formations near Mengen and he revealed that they are gradational.

Flysch deposits in Çağa Valley, which is located near to one of the investigation areas of this thesis, are consisting of clayey beddings that are producing landslides especially in cut slopes (Yalçiner, 1995). Another study of Yalçiner (1996) claims that valleys containing steep slopes which are composed of impervious Cretaceous and Eocene aged flysch deposits cause failures in Western Black Sea region.

Buzkan (1996) investigated the geology of Devrek-Mengen and Zonguldak area. According to his study, Devrek-Mengen area generally consists of shale, clayey

schist, dolomitic limestone, dolomitic marble, crystalline limestone and granitic rocks are observed. Middle-Lower Eocene aged Çaycuma Formation consisting of sandstone, siltstone, claystone alternation, and agglomerate, tuff, tuffite and marl deposits that are located at the south of Ereğli region (Buzkan, 1996) extends towards east to the study area of this thesis.

Ustaömer (1999) worked on geochemistry of granitoids in Bolu Massif in her study. According to modal analyses, plutons in Bolu Granitoid consist coarse grained tonalite and gabbroic in central part, and rarely granite in some areas. Also, plutons in Bolu Granitoid are cut by numerous lamprophyre and aplite dykes (Ustaömer & Rogers, 1999).

İsmailoğlu et al. (1999) studied landslides occurred in West Black Sea region. Çaycuma formation in this region consists of claystone, mudstone and sandstone alternation and it is showing flysch characteristics. When this formation is considered as a whole it shows weak to moderate strength, however thin and medium bedded claystones and mudstones are weak to very weak in strength. Unstable zones and failures are generally observed between these sandstone and claystone-mudstone bedding planes. According to this report, circular failures are generally observed in completely weathered units which are revealing flysch characteristic. In addition to the circular failures, planar failures are also observed in this region as sliding over saturated and weakened claystones and marls in flysch deposits after heavy rainfalls.

Study of Yiğitbaş et al. (1999) on Western Pontides and geological evolution explains that Akveren formation near Zonguldak region is a typical transgressive sequence resting on various older units.

In the study of seismicity of Abant-Gerede region of North Anatolian Fault Zone (NAFZ), Demirtaş (2000) worked on Bolu Mengen fault and determined its position in Neotectonic time line.

Suzen (2002) studied assessment of landslides by using geographical information systems and remote sensing at Bolu region. In his study Yedigöller and Çaycuma formations are mentioned which are also seen in the study area of this thesis. The main lithologies of Yedigöller formation are amphibolite, gneiss, metadiorite, meta-quartzdiorite and some aplite, andesite, basalt and diabase dikes. According to his

study Çaycuma formation seems like the continuation of Bolu Massif, and consists alternation of turbiditic sandstone and siltstone, calcareous mudstone, mudstone and marl.

Sarı et al. (2004) worked on bituminous shales around Mengen. They observed these shales on Tokmaklar (Soğanlı) formation near to Kıyaslar Village. General rock types of this formation are determined as limestone, marl, claystone, mudstone, siltstone, clayey-sandy limestone, sandstone and conglomerate (Koralay, 2009).

In the study of Göncüoğlu et al. (2008), Soğanlı formation and Arkotdağ mélangé relation is investigated. According to this study Soğanlı formation which consists of sandstones and limestones unconformably overlies the Arkotdağ mélangé.

(Koralay, 2009) studied stratigraphy of Mengen region and introduced the relationship of the formation in this area. According to her study, Fındıklıdere (Akveren) formation consists of sandy limestone, marl and sandstone.

Demirtaş and Ural (2011) published a report about geology and geotechnical properties of Yedigöller formation near Mengen. In this report physical and index properties of soil and mechanical properties of the bedrock are determined. Also, it is classified that Precambrian aged Yedigöller formation is very fractured and may reveal stability problems.

Zonguldak city environmental report prepared by Ministry of Environment and Urbanisation (Yücel et al., 2011) consists of stratigraphic units and their information of Zonguldak and near areas. According to this report, landslides generally occur in Çaycuma formation near Zonguldak. Especially in Devrek region, failure zones of landslides are more than 5 m deep.

Landslide susceptibility map of Devrek area is developed by Yılmaz et al. (2012) by using statistical index (Wi) method which is a bivariate statistical technique utilizing GIS. Landslides are generally observed in Çaycuma formation, consisting alternating sequences of sandstones, siltstones, claystones and volcanoclastic sandstones in the study area. According to this study, landslides occur as rotational and then translational when sliding mass meets with the bedding surfaces. Moreover, it is

indicated that the elevation, lithology, slope, aspect and drainage density are the highest contributing factors of landslide occurrence in the study area.

### **1.5.2. Previous Studies about SSPC**

Slope stability probability classification system, developed by Hack (1998) was firstly used around Falset in northeast Spain, in Tarragona province (Hack et al., 2002). This area is very suitable for this system because of its changing geology, lithology and tectonic environment. Road cuts are also excavated by different techniques and revealing different kinds of weathering degrees. For the development of SSPC system and assessment of stabilities, 184 different slopes were studied. According to this study in Spain, SSPC system gives better correlation results compared to two other classification systems as Haines (Haines and Terbrugge, 1991) and SMR (Romana, 1985).

Another study is conducted by Das et al. (2010) with the comparison of a statistical method and SSPC system in northern Himalayas, India. In this work a road section of 12 km is divided into 32 slopes according to their own homogeneity. As a result of this study, two methods show some differences concerning stability susceptibilities. Comparing two methods; while statistical logistic regression underestimates the results, SSPC reveals more reliable solutions about reflecting the actual ground conditions.

Cabria (2015) worked on 24 different exposures containing andesites, basalts, tuff breccia, tuff lapilli and ignimbrites both in Saint Vincent and Dominica. In this study, average values of internal friction angle and cohesion obtained from Reference Rock Mass (RRM) and Slope Rock Mass (SRM) are compared and differences between them are explained due to weathering conditions of the rocks. In this study, probability of stability classes for each slope are determined.

Li and Xu (2015) studied 10 different excavation slopes in Yunnan province, China. The methods of excavation of these slopes are either machinery excavation or conventional blasting. Also, conditions of discontinuities are changing between moderate to very poor. As a result of this study, actual condition and SSPC results of these slopes are compared. The accuracy of 70 % was achieved with SSPC method

because it is claimed that SSPC emphasizes local effects like weathering and excavation. However its emphasize on intact rock strength is relatively small compared to other classification methods. Therefore it is concluded that in order to overcome the limitations of SSPC method, some corrections should be developed.

## **CHAPTER 2**

### **LITERATURE REVIEW ON SLOPE STABILITY, WEATHERING AND SSPC**

#### **2.1. Slope Stability, Weathering and Excavation**

With the variations of loads acting on slopes and variations of shear strength with time change the factor of safety of the slope (Duncan et al., 2014). The load changes on the slope are due to water and seismic activity as natural occurrences and human activities (Highland & Bobrowsky, 2008). In some rock mass classification systems due to the effect of excavation the rock mass ratings are reduced (Hack, 1998). Also, weathering processes like exerting stress on rocks and direct effect of atmospheric chemicals can break down materials (Gangopadhyay, 2013). Hence, the shear strength parameters can change due to any disturbance of the material with excavation and weathering. As a result of these variations stability of soil or rock slopes becomes an important issue for engineers.

Duncan et al. (2014) divides the causes of slope instability into two as decrease in shear strength and increase in shear stress. Increase in pore pressure, swelling, cyclic loading and weathering can be classified in decrease in shear strength. On the other hand, water pressure in cracks, increase in soil weight due to heavy rain, earthquake shaking and excavation at the bottom of the slope can be included in increase in shear stress. As it is mentioned above, both weathering and excavation can change the factor of safety by decreasing the shear strength and increasing the shear stress.

The effect of weathering and excavation on a rock slope can be simultaneous or weathering can be affected by excavation. Stress relief due to excavation can lead to open new cracks in intact rock and enlarges existing discontinuities (Hack & Price,

1997). This would lead the rock to lose strength and become more deformable (Momeni et al., 2015). Therefore, factor of safety of the rock slope decreases and then loses its stability.

### 2.1.1. Classification of Slope Movements

During or right after human activities, seismic loads, weathering or excavation the stability of the slope would decrease and slope movements can occur. According to Varnes (1978) landslide classification is based on two terms. The first term describes the material type whether it is rock, earth, soil, mud or debris. The second term describes the type of movement which can be fall, topple, slide, spread or flow. Combination of these two terms gives the classification (Table 3).

Table 3. Classification of slope movements (Varnes, 1978)

Type of Movement		Type of Material		
		Bedrock	Engineering Soils	
			Predominantly Coarse	Predominantly Fine
Falls		Rock Fall	Debris Fall	Earth Fall
Topples		Rock Topple	Debris Topple	Earth Topple
Slides	Rotational	Rock Slide	Debris Slide	Earth Slide
	Translational			
Lateral Spreads		Rock Spread	Debris Spread	Earth Spread
Flows		Rock Flow (deep creep)	Debris Flow (soil creep)	Earth Flow (soil creep)
Complex		Combination of two or more principal types of movement		

In addition to type of movement and material, some other descriptors can be used for further classification of the slope movement. They are listed as water condition, rate of movement, style of activity, distribution of activity and state of activity. The type of movement and material are necessary to classify the landslide however; these additional descriptors which were mentioned above can be omitted if they are not relevant (Cruden & VanDine, 2013).

### 2.1.2. Slope Failure Types

Soil or rock slope failures are operated by two types of forces, namely driving and resisting forces. Driving forces are mostly influenced by gravity, and it is one of the major causes which disturb the stability of both natural slopes and excavated slopes (Craig, 2004). When the driving forces exceed the resisting forces, slope failure occurs.

Rock slope failure types are grouped into four categories namely planar, wedge, toppling and circular (Figure 3) according to Hoek & Bray (1981). This categorization is designed as the discontinuity and slope orientations.

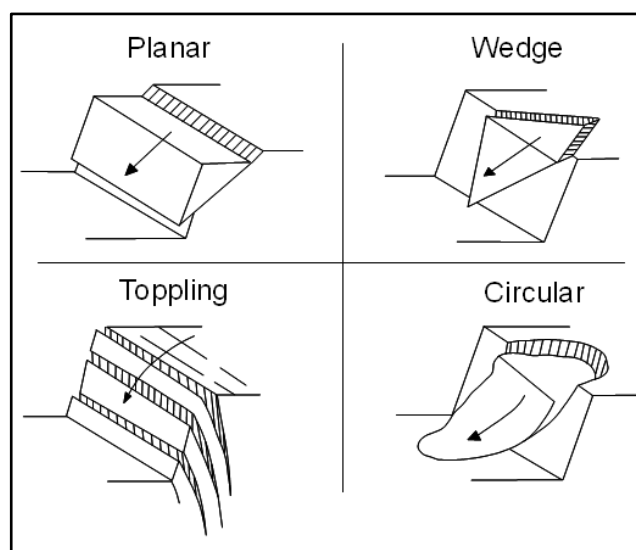


Figure 3. Rock slope failure types (Hoek & Bray, 1981)

#### ***2.1.2.1. Plane Failure***

Plane failure occurs when a discontinuity such as bedding plane, joint, fault etc. which is striking parallel or nearly parallel to the slope face and is dipping with an angle greater than the internal friction angle of the discontinuity (Sharma et al., 1995). In addition to that, the failure plane must “daylight” in slope face which means its dip must be smaller than the dip of the slope face (Hoek & Bray, 1981). Plane failure generally considered with a tension crack either on upper surface or in the face of the slope. After Hoek & Bray (1981), the plane failure analysis is extended to inclined upper slope and non-vertical tension crack by Sharma et al. (1995). Moreover, restraint to sliding has been overcome not only along the surface of sliding but also along the lateral margins of the slide as well. In soft rocks, such as shale, the side restraint can be released by rupture of the rock itself if the base slide inclination is higher than the friction angle. However, in hard rocks the plane sliding occurs only if there are other discontinuities oblique to the crest of the slope (Goodman, 1989).

#### ***2.1.2.2. Wedge Failure***

Wedge failure can be observed when two discontinuities intersect with each other. Based on geometry, there are three general conditions for wedge failure. The first one is that two planes will always intersect in a line. Secondly, the plunge of the line of intersection must be gentler than the dip of slope face and steeper than the average friction angle of the two slide planes. The third and the last condition is that the line of intersection must dip in a direction out of the face for sliding to be feasible (Hoek & Bray, 1981). In other words, dip direction of any plane should not be in between the dip direction of slope face and the line of intersection. Hoek et al. (1973) introduced three different techniques to solve wedge problems which are engineering graphics solutions, using spherical projection and analytical solutions.

#### ***2.1.2.3. Toppling Failure***

Previous two failure modes are related to the sliding of a rock mass. Toppling failure involves pivoting of rock columns, which are slender enough that their center of

gravity falls out of the base, about a fixed point (Hoek & Bray, 1981). Slates, schists and thin bedded sediments which are inclined steeply into the slope face can be given as examples of rock masses which can reveal toppling failure (Goodman, 1989). There are four principle types of toppling failures, which are flexural toppling, block toppling, block flexure toppling and secondary toppling (Goodman & Bray, 1976; Evans, 1981; Hoek & Bray, 1981). Flexural toppling is observed when near vertical discontinuities exist and high columns bend forward in flexure and fail (Evans, 1981). Block toppling occurs when individual columns of hard rock are divided by widely spaced orthogonal discontinuities (Hoek & Bray, 1981). Block flexure toppling is characterized by pseudo-continuous flexure of long columns through accumulated motions along numerous cross joints (Goodman & Bray, 1976). Lastly, the secondary toppling is where failure is initiated by some undercutting agents (Evans, 1981), either by natural agencies such as erosion or weathering or by activities of man (Hoek & Bray, 1981).

#### ***2.1.2.4. Circular Failure***

The previous three failure modes, which are planar, wedge and toppling, are concerned with hard rocks. On the other hand, circular failure occurs in highly jointed or weathered rock (Hoek & Bray, 1981). In planar, wedge and toppling failures, it is assumed that the failure is controlled by geological features such as discontinuities, however circular failure does not takes place on a structural pattern. So that, in circular failure, the individual particles in a soil or rock mass are very small compared to the slope itself and they are not interlocked each other (Hoek & Bray, 1981). So these kind of pervasively fractured rock masses exhibit various types of failure modes therefore slopes in such rock conditions are analyzed using soil mechanics techniques (Hoek & Bray, 1981; Goodman, 1989). In order to determine the factor of safety of a given slope, some circular failure charts are presented by Hoek & Bray (1981).

#### **2.1.3. Rock Strength**

Rock material is defined as polycrystalline solid, consisting of a natural aggregate of minerals. The properties of rock material depend on physical properties of the constituent minerals and their type of bonding to each other. Rock mass, on the other

hand, is separation of intact rocks with discontinuities such as joints, faults, bedding planes or cleavage planes (Deere & Miller, 1966).

Considering the design process of a cut slope, rock strength is one of the most important parameters. The strength of a rock can be evaluated by applying it three stresses which are compressive stress, shear stress and tensile stress. Compressive stress is application of two opposite forces on a rock specimen to decrease the volume of it. Compressive strength is the maximum stress that a loaded specimen can have in order to break down. Shearing is an action caused by two opposite forces as in compressive strength but along a plane of weakness such as fracture, fault or bedding plane inclined at an angle to the forces. Lastly tensile strength is application of two forces directed outwards in opposite action and tends to reduce the volume of the specimen. Laboratory tests like direct pull, bending and “Brazilian” test can be used to determine tensile strength. Also, point load test can be indirectly used to obtain tensile strength (Pariseau, 2012) and provide data to obtain compressive strength by conversion (Gangopadhyay, 2013). Unconfined compressive strength can be determined by uniaxial compression test conducted by taking cylindrical specimen of intact rock (Hudson & Harrison, 2000).

According to Hudson & Harrison (2000) the determination of rock mass properties can be obtained by two approaches. First one is measuring or estimating directly, and the second one is using both intact rock and discontinuity properties. By using intact rock and discontinuity data, various types of rock mass classification can be made which is serving as an index to rock rippability, dredgeability, excavability, cuttability and cavability (Bieniawski, 1989). Rock Quality Designation (RQD) introduced by Deere et al. (1967) and empirical criterion proposed by Hoek & Brown (1980) are one of the commonly used criteria to estimate rock mass strength.

#### ***2.1.3.1. Shear Strength Parameters used in Slope Stability***

Shear failure is very common in cut slopes which consist of weak, soil-like rocks such as highly weathered shales and crushed rock of fault zones (Goodman, 1989). Shear strength of a material can be represented by Mohr-Coulomb equation as given below.

$$\tau = c + \sigma \tan \Phi$$

where  $c$  is cohesion  $\sigma$  is normal stress and  $\Phi$  is internal friction angle. This relationship is assumed at high normal stress values because most of the irregularities could be sheared off (Barton, 1976). On the other hand another equation is developed for irregular rock surfaces and broken rocks when tested at low normal stresses:

$$\tau = c + \sigma \tan (\Phi+i)$$

where  $i$  is the average angle of deviation of particle displacements from the direction of the applied shear stress (Patton, 1966; Barton, 1976).

For the conditions in which the discontinuities are filled with crushed rock material or products of decomposed or weathered material the intact rock surfaces would not touch each other. In this conditions rock mass will have the lowest strength in its joints in other words the shear strength will be lower than the rock itself and have the behavior of infill material (Indraratna et al., 2008). On the other hand, if the discontinuities are planar and unfilled, the cohesion can be assumed as zero as it is shown in below (Barton, 1973; Barton, 1976; Woo et al., 2010).

$$\tau = \sigma \tan [\Phi + \text{JRC} \log (\text{JCS}/\sigma)]$$

The introduced parameters in the equation above are joint roughness coefficient (JRC) and joint wall compressive strength (JCS).

Considering material disturbance, undisturbed peak strength is the strength of a material in the field which is not disturbed (Duncan et al., 2014). When an undisturbed material is sheared and pass the peak value, the residual values are obtained. If a back calculation is needed, the residual values should be used for redesign (Skempton, 1985; Duncan et al., 2014).

#### **2.1.4. Weathering**

There are numerous definitions of weathering in the literature from different point of views of geologists. Fookes et al. (1971) describes weathering as process of alteration of rocks under direct effect of hydrosphere and atmosphere. According to Ollier (1991) weathering is altering and braking down of rocks with the effect of water and air. Weathering definition of Price (1995) for application in geotechnology

is that the irreversible response of soil and rock materials and masses to their natural or artificial exposure to the near surface geomorphological or engineering environment. Weathering is described by Hack (1998) as chemical and physical change in time of rock material and rock mass under influence of atmosphere and hydrosphere. Lastly, weathering can be referred as alteration of rock surfaces which are exposed to atmospheric conditions (Moses et al., 2014).

Conditions controlling weathering in artificial slopes, such as road cuts, fall into three categories as internal, external and geotechnical (Huisman et al., 2006). Internal category includes rock and soil material and mass properties such as porosity, permeability, discontinuities (joint, bedding plane, fracture, fault plane etc.) and material composition. Parameters related to the weathering environment like climate, topography, chemistry of weathering solutions, hydrology and vegetation falls into external category. Lastly, geotechnical one includes slope design parameters which can be aspect, slope angle, height, method of excavation and drainage measures. As Hack (1998), Fookes et al. (1988) and Price (1995) described, weathering is distinguished as two main processes which are physical and chemical weathering.

#### ***2.1.4.1. Types of Weathering***

As it is mentioned above, weathering can be divided into two as physical or mechanical and chemical weathering. Both of them can be observed in most weathering processes however physical weathering occurs near surface while chemical weathering can reach to depths of tens or hundreds of meters below surface (Price, 1995). Biological weathering is less important than these two and it is the combination of biochemical and biophysical effects (Fookes et al., 1971).

Simplest definition of physical weathering is breaking up rocks into small fragments without changing mineral composition of the original rock (Fookes et al., 1971; Fookes et al., 1988; Price, 1995; Hack, 1998; Cabria, 2015). Result of mechanical breakdown of rocks is termed as disintegration. With the effect of temperature differences, application of series of cyclical stresses which can be freeze and thaw and wetting and drying, differential expansion and shrinkage of minerals rock materials and rock mass breaks down (Fookes et al., 1988; Hack, 1998). Another

disintegration of rock material and mass can occur together with pressure release which can be seen after excavation (Huisman et al., 2011; Cabria, 2015).

Other main weathering process is called chemical weathering which is decomposition of minerals (Hack, 1998) to stable or metastable secondary mineral products (Fookes et al., 1988), generally forming clay minerals (ANON, 1977). According to (Loughnan, 1969) the simultaneous chemical weathering processes are the breakdown of the parent material structure, removal of released constituents in solution and reconstitution of the residue with components from atmosphere to form new minerals. Decomposition process has great potential where climatic regime is wet and hot (Saunders & Fookes, 1970). Early stage result of chemical weathering is discoloration of rock material (ANON, 1977), which is caused by dissolved chemical agents in water and groundwater (Hack, 1998).

#### ***2.1.4.2. Weathering Classification***

Classification of weathering is introduced in the literature by many researchers like Moye (1955), Little (1969), Dearman (1976) and Stapledon (1976); working parties as ANON (1977) or as standards which is BS5930 (1981). Each classification shows similarities and the general scheme is formed as term, description and degree or grade. Degrees or grades are generally beginning with I and ends with VI which indicates fresh to residual soil respectively. Grades were designed to assess degree of discoloration, rock to soil ratios and preservation or destruction of original texture. Description of these terms and grades also show similarities but some of them contain subdivisions by using qualifying terms. ANON (1977), for instance, divided grade I into two in order to indicate fresh and faintly weathered rocks and distinguish discoloration whether only on discontinuity surfaces or both on discontinuity surfaces and in all rock material. General terms are given by Dearman (1976) and BS5930 in Table 4.

Table 4. Degrees of rock mass weathering (BS5930, 1981)

<b>Term</b>	<b>Description</b>	<b>Degree</b>
Fresh	No visible sign of rock material weathering; perhaps slight discoloration on major discontinuity surfaces.	I
Slightly Weathered	Discoloration indicates weathering of rock material and discontinuity surfaces. All rock material may be discolored by weathering.	II
Moderately Weathered	Less than half of the rock material is decomposed or disintegrated to a soil. Fresh or discolored rock is present either as a continuous framework or as core stones.	III
Highly Weathered	More than half of the rock material is decomposed or disintegrated to a soil. Fresh or discolored rock is present either as a discontinuous framework or as a core stones.	IV
Completely Weathered	All rock material is decomposed and/or disintegrated to soil. The original mass structure is still largely intact.	V
Residual Soil	All rock material is converted to soil. The mass structure and material fabric is destroyed. There is a large change in volume, but the soil has not been significantly transported.	VI

#### ***2.1.4.3. Effect of Weathering on Rock Strength***

Weathering can influence both intact rock and discontinuities (Hack, 1998), as a result of that whole rock mass can be affected. After wet-dry and freeze-thaw cycles, parameters like unit weight, sonic velocity and uniaxial compressive strength values decline and parameters like effective porosity and water absorption increase. Considering these parameter changes, rock strength starts to decrease. Topal & Sozmen's (2003) work on tuffs reveals the same conclusion about the parameters given above. Miscevic & Roje-Bonacci's (2001) survey on flysch deposits concludes that cyclic wetting-drying is the main cause of degradation of materials in other words loss of rock strength. Another work done by Shrivastava (2014) on basalts

shows that density and compressive strength of fresh rock are higher than the weathered parts at the surface.

Weathering effect can increase with the amount and aperture of the discontinuities. Moreover, weathering can cause to open new discontinuities and enlarges the existing ones. Weathering penetration depth plays an important role in the discontinuities and when it passes the roughness of the discontinuity, the shear strength decreases (Huisman, 2006). Shear strength of a material without weathering is governed by the fresh rock as it is indicated in Figure 4. The upper portion (1) of the figure indicates shear strength of the original rock along dashed line, without any weathering action at the discontinuity (white colored). However at the lower portion (2), the shear strength of the rock along the dashed line is fully determined by weathered part (gray colored), which indicates that weathering is exceeded the discontinuity roughness.

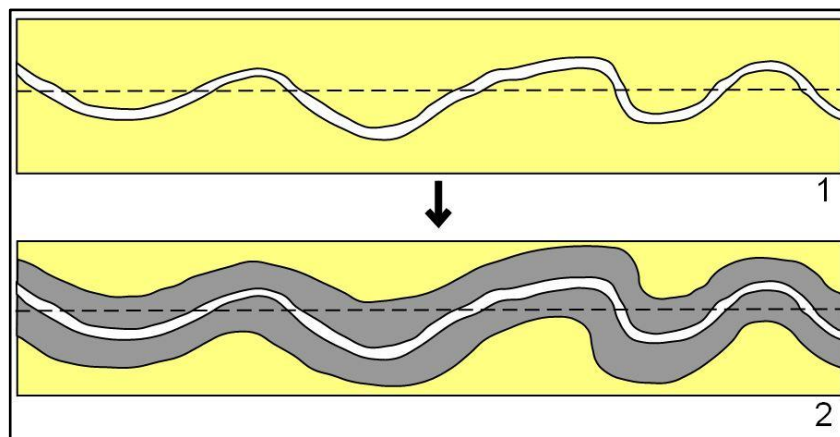


Figure 4. Discontinuity wall weathering (Modified from Huisman (2006))

#### ***2.1.4.4. Weathering in Engineering Time***

Recognition of importance of weathering degrees in time factor generally considered on geologic scale. Weathering models generally describe the evolution of natural slopes in this time span such as thousands of years (Utili, 2004). However, weathering and degrading forces which can reduce the material durability and

strength can be observed in engineering time scale such as tens of years (Fookes et al., 1988). In engineering timescales, decay can severely affect the geotechnical properties of rocks in a rapid way as decreasing the mass strength which results as decrease of slope stability. Most notable rock types which are susceptible to this kind of decay are gypsum and mudstones (Huisman, 2006). Within this engineering time the most relevant chemical weathering process are oxidation reduction and solution, which can be observed in limestones and marbles. Physical weathering and imposed loading are the most aggressive effects on rocks in engineering timescale (Fookes et al., 1988).

According to Huisman (2006) there are three main processes involved in decay of slopes in engineering time:

- 1) Stress relief due to excavation with artificial or natural ways which leads loss of structural integrity.
- 2) Weathering of slope material in-situ by physical and chemical effects leading to weakening of material and mass followed by decrease in block size and increase in discontinuity sets and frequencies.
- 3) Transportation of weathered or unweathered loose particles of a slope by erosion and eventually destroying the fabric of the rock mass structure.

#### **2.1.5. Excavation**

Stress relaxation due to any type of excavation affects the mass strength of the rock. Together with the excavation, the load on the rock is taken away. As a result, expansion of the rock mass takes place. Due to expansion of rocks the contact strength between the particles are reduced, then porosity and permeability increase (Wetzel & Einsele, 1991), which may lead instability of cut slopes. When the Geological Strength Index (GSI), which is developed by (Hoek, 1994) and (Hoek et al., 1995), is used in order to consider entire rock mass. Disturbance factor (D) selection plays an important role on excavations. It is designed both for slopes and tunnels according to their excavation types like blasting, mechanical excavation and hand excavation.

## **2.2. Slope Stability Probability Classification (SSPC) method**

Slope Stability Probability Classification (SSPC) method is developed by Hack (1998), which allows classification of rock mass parameters in rock exposures. This method also supplies information about probability against failure types like planar and toppling considering discontinuity orientations and stability of exposures without considering orientations. Compared to other rock classification systems, SSPC considers local influences like weathering and excavation (Hack et al., 2002). The basic concept of this system can be given as:

- Introducing three step classification systems as “exposure”, “reference” and “slope” rock mass.
- Instead of a single-point rating value, slope stability is evaluated with occurrence of probability of different failure mechanisms.
- Clear and simple procedures in order to collect data in the field (Hack et al., 2002; Li & Xu, 2015).

The three rock masses given above are considered as follows according to SSPC system: The rock mass in the exposure; exposure rock mass (ERM), the rock mass which is an imaginary, unweathered and undisturbed condition prior to excavation; reference rock mass (RRM) and the rock mass where the existing or new slope is to be situated; slope rock mass (SRM) (Figure 5) (Hack et al., 2002). Conversions between these three rock masses can be made by applying parameters which include excavation and weathering type (Figure 6).

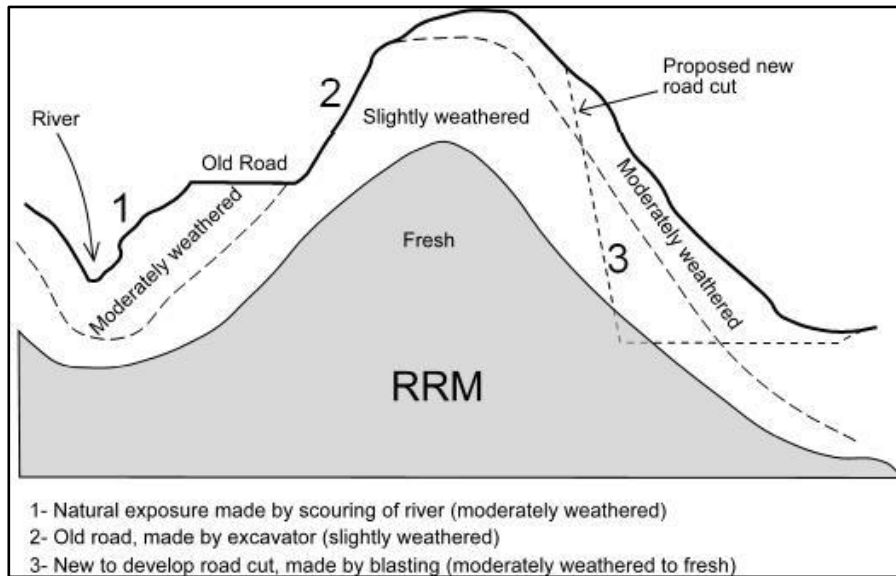


Figure 5. Sketch view of rock masses with various degrees of weathering (Modified from Hack et al. (2002))

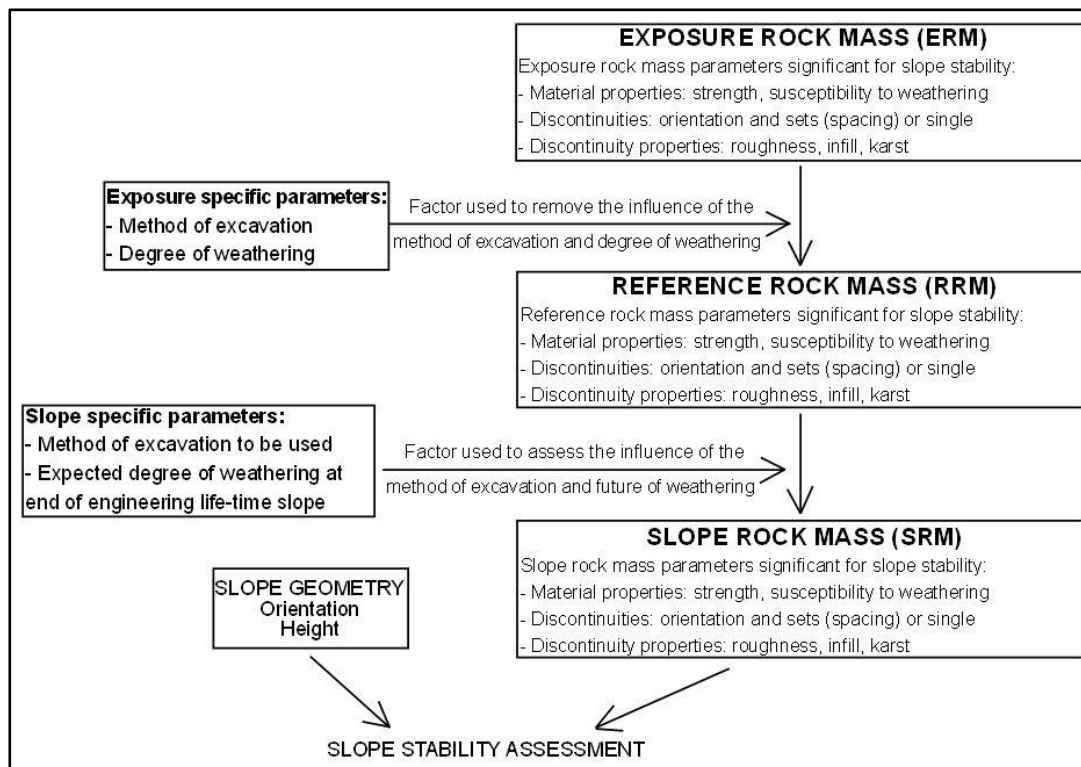


Figure 6. Flow chart of SSPC system (Hack et al. 2002)

According to given flow chart in Figure 6, the difference between exposure rock mass (ERM) and reference rock mass (RRM) is very obvious because of method of excavation and degree of weathering. Therefore with this technique, the parameters of exposure rock mass of the same geotechnical unit which show different degree of weathering and method of excavation can be brought back to reference rock mass parameters which reflect the original geotechnical properties (Hack et al., 2002).

Considering the slope stability assessment, the slope rock mass parameters should be obtained by using slope specific parameters which are dealing with method of excavation to be used in the future and expected degree of weathering at the end of engineering life-time (Hack et al., 2002). In addition to these slope specific parameters, applying slope geometries as orientation and height to the system, the slope stability assessment can be completed. It should be noticed that if an existing slope is examined and future weathering is not the consideration, the slope rock mass (SRM) and exposed rock mass (ERM) will be the same.

### **2.2.1. Exposed Rock Mass (ERM)**

SSPC system makes the slope stability assessment investigations as simple as possible in order to collect data in the field by introducing charts for each rock masses. For exposure rock mass (ERM), the critical rock and field conditions are excavation method (ME), weathering degree (WE), intact rock strength (IRS), visual assessment of slope stability and, condition, spacing and orientation of discontinuities. The method of excavation (ME) in this system is quantified as values equal to one and smaller than one decreasing from handmade excavation to crushed intact rock (Table 5) (Hack, 1998). As method of excavation, weathering degree (WE) is also quantified by this system between one and smaller than one representing the decrease in strength properties (Table 6) (Huisman, 2006). The values given in Table 6 are obtained from the average values of WE cohesion mass and WE  $\Phi$  mass (for orientation independent stability rock mass parameters are influenced by cohesion of the mass and internal friction angle of the mass) (Hack, 1998).

Table 5. ME Values for different excavation methods (Hack, 1998)

<b>Excavation Method</b>	<b>ME Value</b>
Natural/hand made	1.00
Pneumatic hammer excavation	0.76
Pre-splitting/smooth wall blasting	0.99
Conventional blasting with result:	
Good	0.77
Open discontinuities	0.75
Dislodged blocks	0.72
Fractured intact rock	0.67
Crushed intact rock	0.62

Table 6. WE Values for different weathering degrees (Hack, 1998)

<b>Degree of Weathering</b>	<b>WE Value</b>
Fresh	1.00
Slight	0.95
Moderate	0.90
High	0.62
Complete	0.35

The intact rock strength (IRS) is determined by using “simple means” tests with standard hammer (about 1 kg) and hand pressure which is introduced by British Standard (BS5930, 1981) (Table 7) (Hack & Huisman, 2002). Even though these simple mean tests are useful for the field investigations, unconfined compressive strength (UCS) tests should be applied in order to check the accuracy. Visual assessment of slope stability is divided into two as stable and unstable. Further subdivision of unstable part is whether there are large or small problems. The large problems indicate that rock mass as in order of tons in weight, however small problems indicate that rock mass as in order of kilograms in weight (Hack et al., 2002). The condition of discontinuities is assessed according to infill material, karst and roughness. The roughness is evaluated with small scale (0.2m x 0.2m area) and large scale (area between 0.2m x 0.2m and 1.0m x 1.0m).

Table 7. Estimation of intact rock strength by simple means test (Hack & Huisman, 2002)

<b>Intact rock strength</b>	<b>Simple means test</b>
<1.25 MPa	Crumbles in hand
1.25 – 5 MPa	Thin slabs break easily in hand
5 – 12.5 MPa	Thin slabs break by heavy hand pressure
12.5 – 50 MPa	Lumps broken by light hammer blows
50 – 100 MPa	Lumps broken by heavy hammer blows
100 – 200 MPa	Lumps only chip by heavy hammer blows
>200 MPa	Rocks ring on hammer blows. Sparks fly.

### 2.2.2. Reference Rock Mass (RRM)

Through the data obtained for ERM from the field, parameters can be evaluated in order to find cohesion and internal friction angle values for reference rock mass (RRM). Parameters that are needed to find both cohesion and internal friction angle are reference intact rock strength (RIRS), reference rock discontinuity spacing (RSPA) and reference rock discontinuity condition (RCD). As it was mentioned in Figure 6, exposure specific parameters like degree of weathering (WE) and method of excavation (ME) are applied in order to obtain reference rock mass parameters. Therefore, RIRS value is directly calculated by using exposure intact rock strength value and degree of weathering (WE).

Reference rock discontinuity spacing (RSPA) is also calculated by using degree of weathering (WE) and method of excavation (ME). It is important to notice that discontinuity spacing (SPA) parameter which is used to find RSPA is calculated based on discontinuity sets with the smallest spacing according to Figure 7.

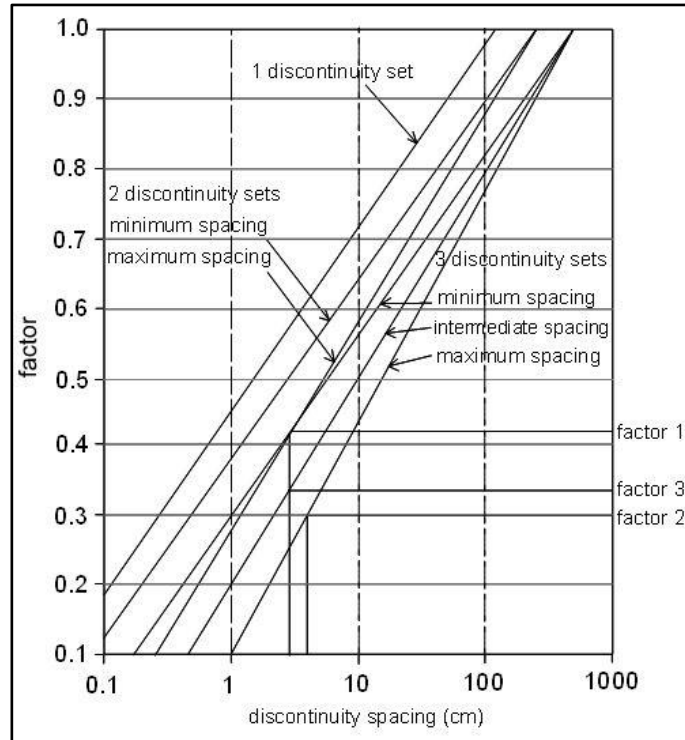


Figure 7. Factor determination chart for spacing parameter (SPA) (Hack, 1998)

In order to obtain reference rock discontinuity condition (RCD), spacing of each discontinuity (DS) obtained from the field and condition factor for a discontinuity (TC) are needed. This condition factor (TC) is calculated by the multiplication of large and small scale roughness, infill material and karst values of each discontinuity.

Combining these three parameters (RIRS, RSPA and RCD) with constants introduced by Hack (1998), internal friction angle and cohesion of reference rock mass can be obtained in terms of degree and Pa respectively.

### 2.2.3. Slope Rock Mass (SRM)

As reference rock mass (RRM) parameters and cohesion-internal friction angle values obtained from exposed rock mass (ERM), parameters of slope rock mass (SRM) and eventually slope stability probabilities for both orientation dependent and orientation independent can be determined by slope specific parameters (Figure 6).

Considering excavation method to be used and expected degree of weathering, with the same logic in reference rock mass (RRM) intact rock strength (SIRS), discontinuity spacing (SSPA) and condition of discontinuities (SCD) can be found. According to these values internal friction angle and cohesion of slope rock mass (SRM) can be calculated with given constants. In addition to reference rock mass (RRM), in slope rock mass (SRM), maximum possible slope height ( $H_{\max}$ ) can be found.

Stability of rock slopes with non-structural control failure depends on factors like the shear strength parameters (cohesion and internal friction angle) of slope rock mass (SRM) and slope height (Li & Xu, 2015). By evaluating the parameters of internal friction angle and maximum slope height found for slope rock mass (SRM) probability of orientation independent stability can be determined (Figure 8).

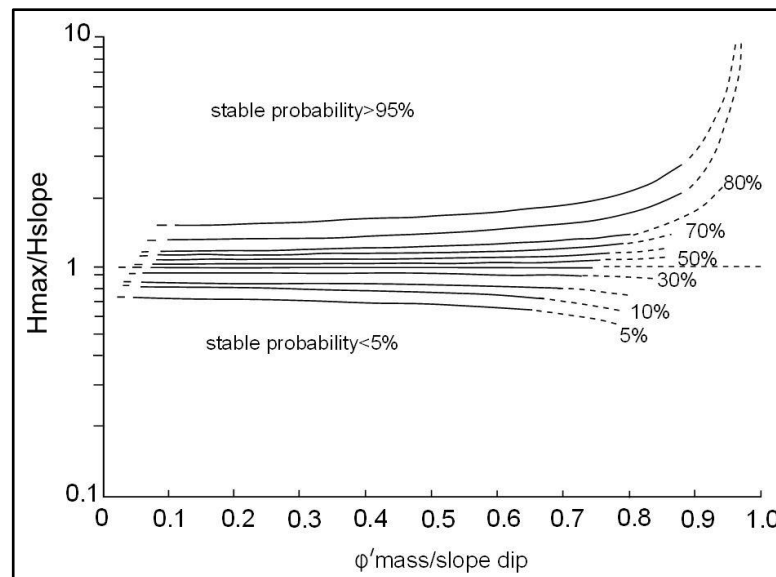


Figure 8. Probability of orientation-independent stability (Hack et al. 2002)

Dashed probability lines in Figure 8 indicate that number of slopes used to develop this chart is not enough to consider them as certain as the lines drawn continuously (Hack et al., 2002).

For orientation dependent stability assessment, SSPC system selects discontinuity condition and relationship between slope orientation and discontinuities. Different failure modes of rock slopes according to sliding and toppling failure criteria are analyzed. The largest possibility of failure is chosen and related failure mode is determined as the stability assessment result (Li & Xu, 2015). There are two graphs related to sliding criterion (Figure 9) and toppling criterion (Figure 10). Considering discontinuity condition factor (TC) and apparent discontinuity dip in direction of slope dip (AP), probability of stability can be determined.

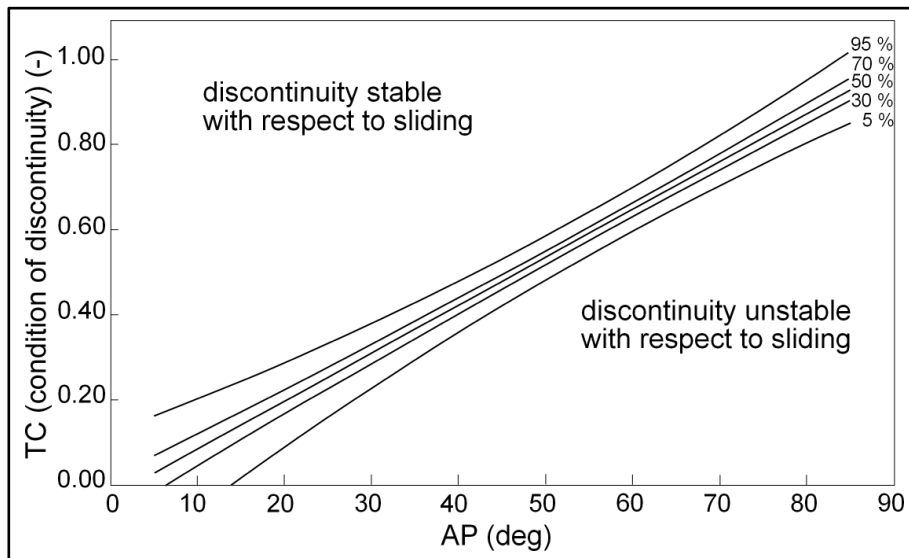


Figure 9. Sliding criterion (Hack et al. 2002)

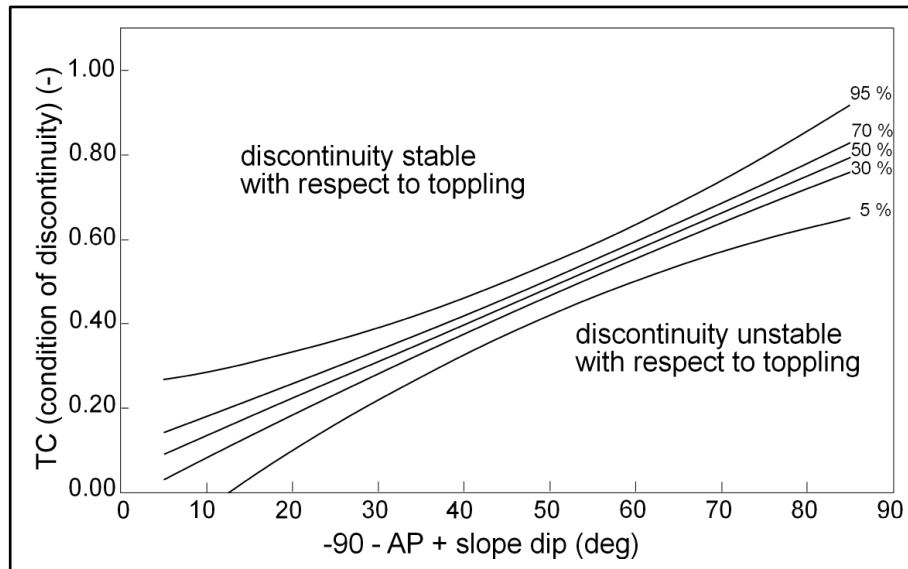


Figure 10. Toppling criterion (Hack et al. 2002)



## CHAPTER 3

### GEOLOGY

#### 3.1. Regional Geology

Turkey is geologically divided into main three tectonic units which are The Pontides, The Anatolides-Taurides and Arabian Platform (Ketin, 1966). The study area, Yeniçağa-Zonguldak part of Ankara Zonguldak highway, is located in the tectonic unit of Pontides. The Pontides show Laurussian continent properties and they can be comparable to the tectonic units of Balkans and Caucasus (Okay, 2008). The three terranes of the Pontides which reveal different geological evolutions are named as Strandja, Sakarya and İstanbul (Okay, 2008) and the study area is located at the eastern part of İstanbul terrane (Figure 11).

The Intra-Pontide suture zone, which is the trace of the Intra-Pontide Ocean, is located at the southern part of the study area (Figure 11). Also, large part of the study area includes Pan-African crystalline basement (Figure 11). This basement consists of Precambrian (Cadomian) age gneisses, amphibolites, metavolcanic rocks, metaophiolite and voluminous granitoids (Ustaömer et al., 2005) unconformably overlain by sedimentary succession of Ordovician to Carboniferous in age (Dean et al., 2000). In the eastern part of the İstanbul terrane, around Zonguldak, shallow marine carbonates are abundant which grade to coal measures (Okay, 2008). The Paleozoic succession, which overlies the basement, is overlain by Middle Devonian to lowermost Carboniferous slope-type and flysch-type sediments of Visean age (Göncüoğlu, 2010). Around Zonguldak area the Middle Devonian and Early Carboniferous succession is mainly made up of shelf carbonates (Göncüoğlu, 2010). Detailed information about the formations which are encountered and seismicity of the study area is given in the following sections.

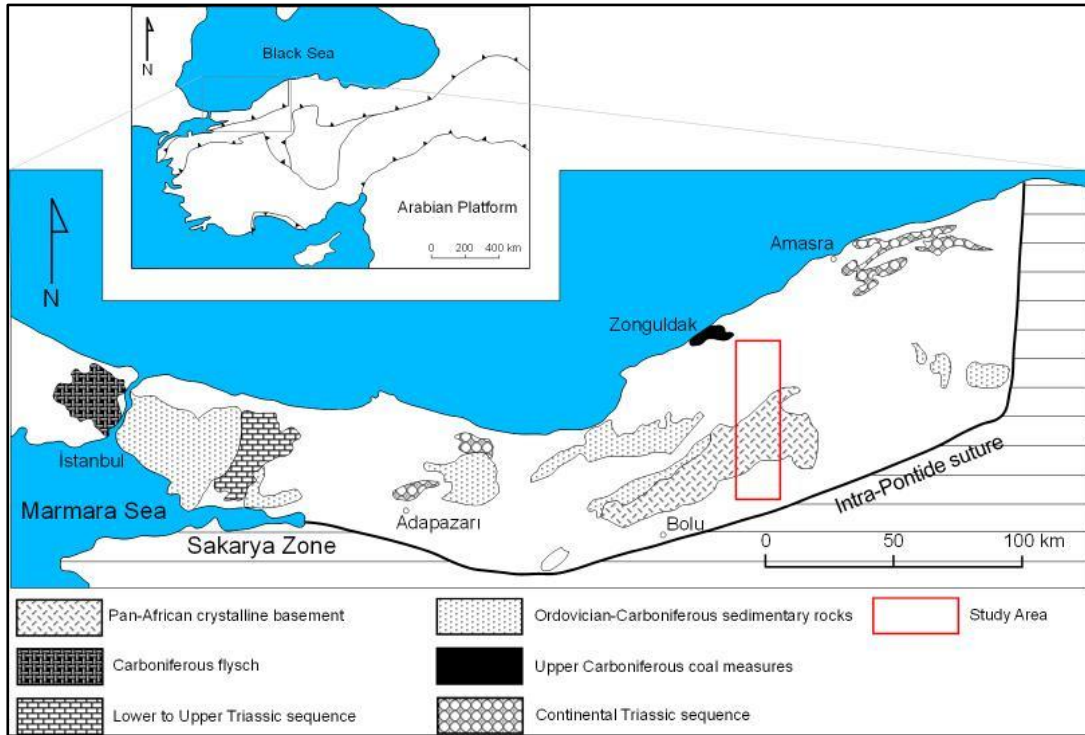


Figure 11. Location of the study area in İstanbul terrane (Modified from Okay (2008))

### 3.2. Site Geology

Even the geological maps modified from MTA 1/100 000 scale geological maps of Turkey (MTA, 2002a; MTA, 2002b; MTA, 2002c) (Figure 12) are including 16 different geological formations, according to studies on rock types in the field for each slope only 6 of them are came across. The obtained data from the field reveal that the formations from older to younger are named as Yedigöller formation, Bolu

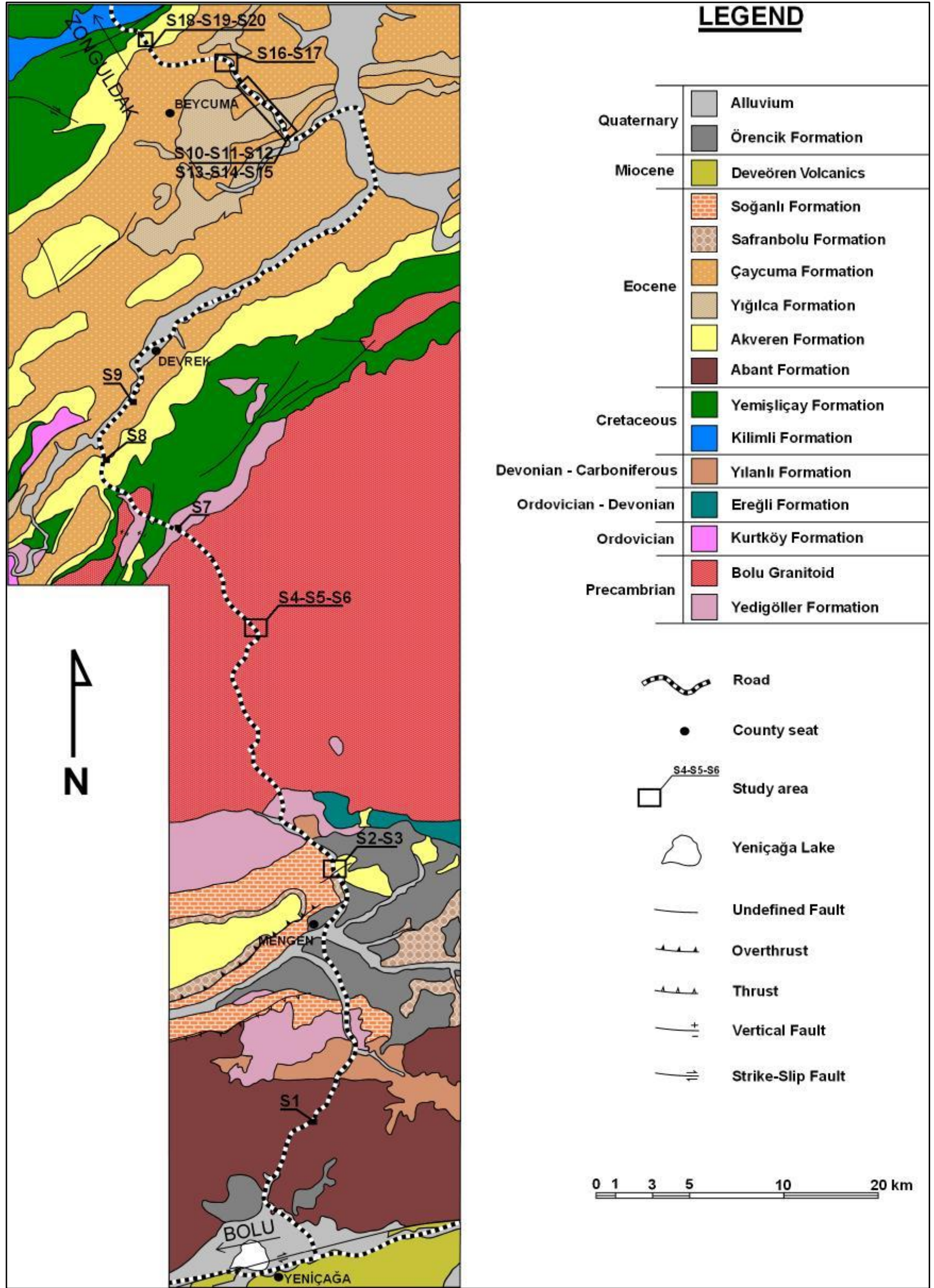


Figure 12. Geological map of study area (Modified from MTA (2002a; 2002b; 2002c))



granitoid, Abant formation, Akveren formation, Çaycuma formation and Soğanlı formation.

### **3.2.1. Yedigöller Formation**

This formation consists of undifferentiated amphibolite, gneiss, migmatite, metagranite, metalava, schist and marble (MTA, 2002a). Precambrian aged Yedigöller formation is conformably overlain by Bolu granitoid in the study area. According to Suzen (2002) some aplite, andesite, basalt and diabase dikes can also be observed in this formation. Physical properties of this formation is determined as very fractured and may cause stability problems (Demirtaş & Ural, 2011). This formation can be observed at the northern part of Mengen Pazarköy zone.

Yedigöller formation is observed in Stop 7 (S7) (Figure 12) and according to field studies general rock type is determined as granodiorite at the studied slope.

### **3.2.2. Bolu Granitoid**

Bolu Granitoid involves granodiorite, tonalite, granite, gabbro, lamprophyre and aplite (MTA, 2002a). As Yedigöller formation, it is also Precambrian in age and overlays it conformably. Bolu granitoid is unconformably overlain by middle Ordovician to lower Devonian aged Ereğli formation in the study area (Figure 12). Plutons in Bolu granitoid consist of coarse grained tonalite, gabbro and granite (Ustaömer, 1999). It is also determined that these plutons are cut by lamprophyre and aplite dykes (Ustaömer & Rogers, 1999). Bolu granitoid and interfingering Yedigöller formation is the basement of the Western Pontides (MTA, 2002a).

In the study area, Stops 4, 5 and 6 (S4-S5-S6) (Figure 12) are observed in Bolu Granitoid. The general rock types in these slopes are determined as moderately weathered granites and basalts.

### **3.2.3. Abant Formation**

Abant formation mainly contains wildflysch, and blocks which are granites and Paleozoic limestones-marbles. This formation is generally formed by yellowish gray, brown, red, purple, light-dark gray, greenish gray flysch deposits and, clastic and carbonate rocks. Also, turbiditic deposits, debris flow deposits, pelagic mudstones, micrites and marls can be observed. Especially in these deposits, flowing and sliding can be encountered (MTA, 2002a).

In the study area, this upper Cretaceous Abant formation is generally observed as flysch deposits of mudstones including limestone blocks where the slopes are failed. Mudstones are generally moderately to highly weathered in this formation which is observed only in Stop 1 (S1) in this thesis (Figure 12).

### **3.2.4. Akveren Formation**

This formation consists of sandy carbonates at the bottom and, clayey limestones, reefal limestones, mudstones and marly turbidities towards upward. Generally hemipelagic limestone, shale, calcarenite, sandstone and conglomerate can be observed as flysch type deposits. Dominant colors in this formation can be observed as yellow, white, cream and grayish green. Beds are thin to medium thick. The unit starts at the bottommost part as sandy limestone and, continues towards upward as clayey limestone-marl and claystone-siltstone alternation (MTA, 2002a). This alternation is mentioned by Kaya et al. (1986) as clayey limestone-marl including tuff, sandstone, claystone and calcareous mudstone. This formation can be correlated with Fındıklidere formation (MTA, 2002a) which contains sandy limestone, marl and sandstone (Koralay, 2009). Thickness of the Akveren formation can be measured up to 400 m.

The Akveren formation can be observed in the study area at Stop 3-8-18-19-20 (S3-S8-S18-S19-S20) (Figure 12) as slightly weathered limestone, sandstone and small quantities of marl.

### **3.2.5. Çaycuma Formation**

Çaycuma formation is generally formed of sandstone, shale and conglomerate. In detail, sandstone, siltstone, claystone alternation and limestone, agglomerate, tuffite and marl interbeddings comprise this formation. Sandstones are classified as yellowish, light green and thin to medium bedded. Siltstones and limestones, on the other hand, are characterized as light greenish, gray and fine to medium grained. The sandstones containing volcanic materials are generally carbonate cemented. The Çaycuma formation overlays the Akveren formation and its thickness is measured as approximately 1200 m (MTA, 2002b). This formation is mapped by Akartuna (1953) as mottled flysch. According to İsmailoğlu et al., (1999), alternation of these deposits shows flysch characteristics.

In the study area the Çaycuma formation is observed at Stop 9-10-11-12-13-14-15-16-17 (S9-S10-S11-S12-S13-S14-S15-S16-S17) (Figure 12) slightly to highly weathered sandstone and mudstone.

### **3.2.6. Soğanlı Formation**

Middle Eocene aged Soğanlı formation is characterized by only limestone. Bottom parts of these deposits are generally composed of detritic limestones and upper parts are gradually becoming micritic limestones. This formation is white, light gray, yellow and medium to thick bedded. Marl interbeddings can be observed between limestone layers. The limestone levels are generally highly jointed with karst. Thickness of this formation can be measured over 200 m. According to rock type properties and fossil contents, it can be stated that this formation is deposited in a shallow shelf environment (MTA, 2002a). According to Göncüoğlu et al. (2008), besides limestone and marl layers, sandstone can also be observed in this formation as well.

The Soğanlı formation can only be observed at Stop 2 (S2) (Figure 12) in the study area. Rock type is determined as light brown, slightly to moderately weathered limestone interbedded with very thin mudstone.

### 3.3. Tectonics and Seismicity

Structural components at the southern parts of the study area are generally aligned NE-SW direction. Therefore, compression in the area is said to be along NW-SE. In the study area, thrust and reverse faults are aligning NE-SW direction. However, strike slip faults are generally aligning NW-SE direction before neotectonic period. Right lateral strike slip faults related to North Anatolian Fault Zone (NAFZ) are generally aligned E-W and SW-NE direction in Late Miocene-Pliocene epoch (MTA, 2002a).

At the northern parts of the study area, back arc products are observed because of subduction of Neotethys. Compressional regime which was started at Upper Cretaceous lasted until Middle Eocene. Due to compressional regime in the northern parts of the study area, NE-SW aligned foldings and small scaled faults can be observed. With the effect of NAFZ, these small scaled faults matching with the main fault are determined (MTA, 2002b).

According to General Directorate of Disaster Affairs' earthquake zoning map of Turkey (GDDA, 1996), the study area is located within the 1<sup>st</sup> and 2<sup>nd</sup> degree earthquake zones (Figure 13). First 9 stops are located in the border of 1<sup>st</sup> degree, and the rests are located in the 2<sup>nd</sup> degree considering the earthquake zones. Peak horizontal ground acceleration (PHGA) values are determined for 1<sup>st</sup> degree as equal or greater than 0.4g and for 2<sup>nd</sup> degree equal or greater than 0.3g and less than 0.4g (GDDA, 1996) (Figure 13).

#### 3.3.1. Attenuation Relationship

Deterministic approach of attenuation relationship presents peak horizontal acceleration (PGA) for certain locations. The next generation attenuation relationship estimates acceleration values for periods ranging between 0,01 and 10 seconds. Idriss (2007) indicates that PGA values are obtained from the exact point of 0,01 second. PGA values obtained from the formula introduced by Idriss (2007) given below:

$$\ln [\text{PGA}(T)] = \alpha_1(T) + \alpha_2(T)M - [\beta_1(T) + \beta_2(T)M] \cdot \ln (R_{\text{ruo}} + 10) + \gamma(T)R_{\text{rup}} + \phi(T)F$$



Figure 13. Earthquake zoning map of the study area and its vicinity (GDDA, 1996)

where  $PGA(T)$  is peak ground acceleration for 0,01 second in g's,  $M$  is moment magnitude which is 7,4 for this thesis according to Bolu-Gerede earthquake taken place in 1944 (Kondo et al., 2005),  $R_{rup}$  is the closest distance to the surface rupture in km (Table 8),  $\gamma(T)$  is distance adjustment factor,  $\phi(T)$  style of faulting factor,  $F$  is source mechanism designator which is 0 for this case because of being strike slip fault and  $\alpha_1(T)$ ,  $\alpha_2(T)$ ,  $\beta_1(T)$ , and  $\beta_2(T)$  are parameters obtained from regressions.

The PGA values calculated by using the formula presented above are given in Table 8. The parameters used for the formula obtained from the regressions are shown in Table 9.

Table 8. Distance to NAFZ and PGA values obtained from Idriss (2007)

<b>Road Cut</b>	<b>Distance to fault-NAFZ (km)</b>	<b>PGA (Idriss, 2007 NGA)</b>	<b>Stop</b>	<b>Distance to fault-NAFZ (km)</b>	<b>PGA (Idriss, 2007 NGA)</b>
<b>S1</b>	10	0,651	<b>S11</b>	60	0,139
<b>S2</b>	20	0,393	<b>S12</b>	61	0,136
<b>S3</b>	21	0,378	<b>S13</b>	60	0,139
<b>S4</b>	28	0,294	<b>S14</b>	61	0,136
<b>S5</b>	28	0,294	<b>S15</b>	62	0,134
<b>S6</b>	29	0,285	<b>S16</b>	65	0,128
<b>S7</b>	41	0,205	<b>S17</b>	67	0,124
<b>S8</b>	46	0,182	<b>S18</b>	67	0,124
<b>S9</b>	48	0,175	<b>S19</b>	67	0,124
<b>S10</b>	59	0,141	<b>S20</b>	67	0,124

Table 9. The parameters for M greater than or equal to 6,75 (Idriss, 2007)

<b>T= 0,01 sec (i.e. PGA)</b>						
<b><math>\alpha_1(T)</math></b>	<b><math>\alpha_2(T)</math></b>	<b><math>\beta_1(T)</math></b>	<b><math>\beta_2(T)</math></b>	<b><math>\gamma(T)</math></b>	<b><math>\phi(T)</math></b>	<b>SE</b>
3,7113	-0,1252	2,9832	-0,2339	0,00047	0,12	0,66

According to these solutions, it is interpreted that PGA values obtained from Idriss (2007) would give more accurate results than GDDA (1996) because of introducing specific fault type and distance to each studied road cut.

## **CHAPTER 4**

### **ENGINEERING GEOLOGICAL PROPERTIES OF ROCKS AT CUT SLOPES**

As it was mentioned in Chapter 3, road cuts consist of various rock types. The material and mass properties of each road cut was determined and evaluated according to field observations, laboratory and in situ tests. For the flysch type deposits, consisting 80% of this thesis area, visual estimation of relatively weaker and stronger portions of the road cut were determined. These observations were also supported by Schmidt rebound hardness test (ISRM, 1981) performed in situ. In the field, it was also observed that each road cut reveals surficial failures (i.e. in this study, the degradation of weathered materials in front of the road cuts), changing in depths, due to variable weathering conditions and highly fractured nature of the rock mass. Due to these conditions, laboratory and in situ tests were applied on each rock type –such as both on sandstone and mudstone- and weathered and relatively fresh rocks (i.e. in this study, relatively fresh is used to distinguish the weathered material in front of the road cuts with the inner parts) to distinguish the material properties. The tests applied on materials were not only focused on the relation of slope stability analysis but also durability and clay content of them which are slake durability (ISRM, 1981) and methylene blue (AFNOR, 1980) tests. In order to determine the rock mass properties, field data gathered from the discontinuities by scan line survey, weathering degree and method of excavation of each road cut were used. Strength of the rock mass of flysch type deposits were calculated by considering weighted percentage of rock types that the road cuts consist of.

#### **4.1. Material Properties of the Rocks at the Cut Slopes**

In this thesis, 7 different type of rocks namely sandstone, mudstone, limestone, marl, granite, granodiorite and basalt were encountered in 20 different road cuts. Laboratory tests were performed in order to determine material properties of each rock at the study area.

##### **4.1.1. Effective Porosity and Unit Weight**

Porosity and unit weight are directly related to the density of rocks which is one of the most important parameter in limit equilibrium methods of slope stability analyses. The effective porosity and unit weight of rock specimens gathered from the field for each road cut was determined according to saturation and buoyancy techniques as indicated in ISRM (1981) by using vacuum chamber (Figure 14).



Figure 14. Tested samples in vacuum chamber (left) and air pump (right) system

Both dry and saturated values of unit weight were calculated according to indicated procedure. Only relatively fresh samples of granite of Stop 6 and mudstone of Stop 9 could not be obtained. Average dry and saturated values of both relatively fresh and weathered specimens of each road cut are given in Table 10. Detailed results of these parameters are given in Appendix A.

Table 10. Average values of effective porosity and unit weight of rocks at each road cut

Road Cut	Rock Type	Fresh			Weathered		
		Dry Unit Weight (kN/m <sup>3</sup> )	Saturated Unit Weight (kN/m <sup>3</sup> )	Porosity (%)	Dry Unit Weight (kN/m <sup>3</sup> )	Saturated Unit Weight (kN/m <sup>3</sup> )	Porosity (%)
1	Mudstone	22,25	25,47	3,93	25,09	25,74	5,32
	Sandstone	25,86	26,19	3,36	25,87	26,21	3,50
2	Limestone	23,60	24,63	9,06	23,74	24,69	11,12
3	Limestone	19,99	21,84	15,13	21,70	23,19	18,80
4	Granite	25,32	25,61	2,69	25,61	25,88	2,94
5	Basalt	24,66	25,94	9,12	25,38	26,28	13,07
6	Granite	-	-	-	24,62	25,33	7,21
7	Granodiorite	25,66	26,22	2,50	26,78	27,03	5,64
8	Sandstone	23,88	24,74	3,27	25,42	25,75	8,76
9	Limestone	24,57	25,08	5,17	24,67	25,18	5,23
	Mudstone	-	-	-	23,29	24,11	8,38
10	Sandstone	23,34	24,40	7,87	24,14	24,91	10,84
11	Sandstone	22,69	24,13	10,47	23,43	24,46	14,67
12	Sandstone	22,92	24,22	11,88	23,40	24,57	13,22
13	Sandstone	21,88	23,62	17,62	21,89	23,73	18,82
14	Sandstone	23,87	24,88	9,32	24,18	25,10	10,31
15	Sandstone	23,74	24,71	7,48	24,41	25,14	9,86
16	Sandstone	22,65	23,92	10,44	23,47	24,50	12,88
17	Sandstone	22,01	23,53	15,42	22,59	24,11	15,49
18	Marl	24,81	25,34	4,94	24,88	25,36	5,39
19	Marl	24,35	25,24	5,70	25,22	25,78	9,08
20	Marl	23,83	24,64	6,09	24,50	25,10	8,26

#### 4.1.2. Uniaxial Compressive Strength

Uniaxial compressive strength (UCS) of rock materials are directly related to the strength parameter of slope stabilization not only in limit equilibrium analysis but also in empirical solutions and rock mass classifications. UCS test is applied in order to classify the strength of the materials. Several classification systems were developed by Coates (1964), Deere & Miller (1966) and Bieniawski (1973) which give very wide range and does not specify lower values in details. However the most detailed range for all type of rocks also indicating soil rock boundary given by ANON (1970) (Table 11). Considering the importance of this parameter uniaxial compressive strength test was applied according to ISRM (1981). The average values of uniaxial compressive strength test results are given in Table 12. Detailed results of them are given in Appendix A.

Table 11. Scale of intact rock strength based on UCS tests (ANON, 1970)

<b>Term</b>	<b>Strength (MPa)</b>
Very weak	<1,25
Weak	1,25 - 5
Moderately weak	5 - 12,5
Moderately strong	12,5 - 50
Strong	50 - 100
Very strong	100 - 200
Extremely strong	>200

Table 12. Average values of uniaxial compressive strength (UCS) of the rocks at the selected road cuts

Road Cut	Rock Type	Sample Type	UCS (MPa)	
			Dry	Saturated
2	Limestone	Fresh	39,8	38,2
4	Granite	Weathered	27,3	5,7
8	Sandstone	Fresh	57,9	35,5

Over 100 samples having dimensions of 50 mm X 50 mm X 50 mm were prepared to apply the tests in laboratory by compression machine (Figure 15) however; samples that contain cracks were excluded by visual examinations. Therefore, UCS tests were done on 39 samples. Moreover, only 3 types of rock over 7 could be investigated by UCS test due to heavy jointing and very low strength for the rest of 4 rock types. Gathered values from uniaxial compressive strength tests indicate that rocks can be classified as moderately weak, moderately strong and strong according to Table 11.



Figure 15. Compression machine used to determine UCS values of the rocks

#### 4.1.3. Point Load Strength Index

Point load strength test is surveyed as an index test in order to obtain information about material strength. Advantageously, it can be correlated with uniaxial tensile and compressive strength (ISRM, 1985). It is a very fast and simple test for even irregular samples; therefore sample preparation process does not take up time. Determination of sizes of irregular samples was calculated cautiously according to test standard. As indicated, for non-parallel sided samples width ( $W$ ) was calculated as the average of the shortest and the longest width. Distance was measured before testing as  $D$  and after failure of the specimen as  $D'$  because platens of the machine may penetrate into the samples. After the testing procedure, the load ( $P$ ) required breaking the specimen applied by hand pressure (Figure 16) was noted as kN. Another important part is that the time spent on test procedure should be between minimum 10 seconds to 60 seconds. Otherwise, the resulting strengths may cause overestimation or underestimation (Topal, 2000).



Figure 16. Manual point load device used in this study

The uncorrected point load strength ( $I_s$ ) was calculated with the measured values of  $(D')^2$  and  $P$ . In order to calculate the corrected point load strength ( $I_{s(50)}$ ) considering the size measurements on irregular samples “the size correction factor  $F$ ” was calculated. Finally, the corrected point load strength ( $I_{s(50)}$ ) of each rock was calculated with multiplication of  $I_s$  and  $F$ . Equations related to these solutions are given below:

$$I_s = P \times (D')^2$$

$$F = (D' / 50)^{0.45}$$

$$I_{s(50)} = F \times I_s$$

Preferably at least 10 specimens should be used for this test, however in some conditions test could not be applied as indicated in the standard, i.e. invalid test, on some rock samples. For this reason, some rock samples in road cuts could not reach desired specimen amount. It is recommended that if specimen amount is at least 10, then higher and lower 2 values of the tests can be ignored to calculate average value. If specimen amount is lower than 10, then the highest and the lowest values should be ignored (Topal, 2000).

The average values of point load strength values of each road cut for both relatively fresh and weathered rocks under dry and saturated conditions are given in Table 13. Rock specimens were tested normal ( $\perp$ ) and parallel ( $\parallel$ ) to the planes of anisotropy, where applicable. The detailed results of each sample are given in Appendix A. As it is mentioned before, correlation between point load results and uniaxial compressive strength (UCS) values is possible and applied in this thesis.

Table 13. Average values of  $I_{s50}$  of the rocks at each road cut

		Is <sub>50</sub> (MPa)				
		Fresh		Weathered		
		Dry	Saturated	Dry	Saturated	
Road Cut	Rock Type	Dry	Saturated	Dry	Saturated	
1- Failed	Mudstone	3,3	0,5	2,8	0,2	
1	Mudstone	5,9	4,5	4,8	2,4	+
	Mudstone	3,7	1,4	3,4	0,9	=
	Sandstone	11,4	6,7	8,9	6,0	+
	Sandstone	6,5	5,1	5,8	3,9	=
2- Failed	Limestone	1,0	0,5	-	-	
2	Limestone	5,5	2,5	4,1	2,3	
3	Limestone	2,1	1,3	0,6	0,5	
4	Granite	5,6	4,8	2,0	1,5	
5	Basalt	2,2	1,6	0,9	0,1	
6	Granite	-	-	0,3	0,03	
7	Granodiorite	7,7	5,9	1,6	0,8	
8	Sandstone	6,9	6,6	3,6	3,3	
9	Limestone	7,4	6,3	5,2	2,8	
	Mudstone	-	-	1,3	0,5	
10	Sandstone	7,2	2,1	3,5	1,4	
11	Sandstone	4,6	4,4	2,1	1,1	
12	Sandstone	2,9	1,8	2,7	1,0	
13	Sandstone	3,5	1,9	1,9	1,1	
14	Sandstone	11,2	4,0	5,9	3,8	+
	Sandstone	3,9	2,8	3,6	2,4	=
15	Sandstone	7,4	5,8	6,7	4,6	+
	Sandstone	6,1	4,3	4,8	2,4	=
16	Sandstone	4,9	2,4	4,0	2,3	+
	Sandstone	2,5	1,7	1,8	1,2	=
17	Sandstone	3,3	2,1	2,2	1,4	+
	Sandstone	1,9	1,5	1,8	1,3	=
18	Marl	6,9	3,8	5,5	3,3	
19	Marl	7,6	5,8	5,2	2,6	+
	Marl	3,5	2,8	3,3	0,9	=
20	Marl	7,9	3,5	4,0	1,8	+
	Marl	4,3	1,4	2,5	0,5	=

The term “Failed” in Table 13 indicates that the samples are taken from the failed zone of that road cut. According to the results, it clearly seems that the relatively fresh samples show higher point load strength index values than the weathered ones. Similarly, the dry samples reveal higher values than the saturated ones. Considering UCS values obtained by uniaxial compressive strength test and corrected point load results, a correlation factor  $k$  value was assigned for the rocks of the selected road cuts. As it was mentioned before, UCS test could only be applied for 3 rock types over 7. According to this,  $k$  values of sandstone, limestone and granite are 5.4, 16.0 and 3.8, respectively. For the rest of the 4 rock types,  $k$  values are assigned according to literature survey. For basalt,  $k$  value is determined as 24 according to (Karaman & Kesimal, 2012). This value is also in the range presented by Bieniawski (1975) and Read et al. (1980). For mudstone,  $k$  value is selected as 8 according to Wilson (1976)’s tests on very weak mudstones. For granodiorite,  $k$  value is determined as 15 according to Durmekova et al. (2014) which is in the range determined for magmatic rocks presented by Hawkins (1998). According to Bowden et al. (1998)’s work on marls,  $k$  value for them is chosen to be 11 to use in the road cuts.

#### **4.1.4. Schmidt Rebound Hardness Test**

Schmidt rebound hardness test is used to determine hardness of rocks. It is generally limited for very soft and very hard rocks (ISRM, 1981). As it is suggested Type L hammer is used for the in-situ tests (Figure 17). The specimens tested by this method should have smooth surfaces and the tested zone should be free from cracks about 6 cm in three dimensions. While conducting the test, hammer was held perpendicular to the investigated surface. At least 10 measurements were taken from the field. These measurements were taken at each rock type, and at weathered and relatively fresh rocks of the road cuts.



Figure 17. L type Schmidt rebound hammer used in this study

This measurement is generally used for comparing the strength of soft and strong rocks in road cuts especially for flysch type deposits. Although this test is available for both laboratory conditions and in-situ, only in-situ test was conducted by this method. Average values of Schmidt rebound hardness test are given in Table 14.

Schmidt rebound hardness test results can be converted into UCS values. In order to convert these values several researchers developed formulas for different type of rocks. Deere & Miller (1966) worked on sandstones, limestones, granites, basalts and other type of rocks different than this study's rock types to develop a formula to convert Schmidt values to compressive strength. Similarly, O'Rourke (1989) worked on sandstones and limestones to develop conversion between Schmidt values and UCS. Study of Katz et al. (2000) containing limestones, sandstones and granites, and other type of igneous rocks reveals an exponential equation to create a relationship between Schmidt values and compressive strength. Also, Sachpazis (1990), Cargill & Shakoor (1990) and Yasar & Erdogan (2004) works on limestones and sandstones present some other formulae for the conversion. For the road cuts containing marl deposits, formula developed by Gokceoglu (1996) can be used. Lastly, for mudstones in flysch type deposits formulae presented by Kidybinski (1980) and Saptono et al. (2013) are considered in this thesis.

Table 14. Average values of Schmidt rebound hardness test of each road cut

Road Cut	Rock Type	Schmidt Value	
		Fresh	Weathered
1	Mudstone	15	13
	Sandstone	40	29
2	Limestone	39	19
3	Limestone	28	15
4	Granite	26	13
5	Basalt	38	21
6	Granite	-	<10
7	Granodiorite	47	23
8	Sandstone	49	32
	Mudstone	-	<10
9	Limestone	48	32
	Mudstone	15	<10
10	Sandstone	36	31
	Mudstone	-	<10
11	Sandstone	36	21
12	Sandstone	30	<10
13	Sandstone	43	24
	Mudstone	-	<10
14	Sandstone	31	27
15	Sandstone	49	36
	Mudstone	-	<10
16	Sandstone	30	12
17	Sandstone	20	13
18	Marl	24	12
19	Marl	39	20
20	Marl	30	25

As indicated above, the Schmidt hammer values are converted to UCS values in Table 15. Also, values obtained from the point load tests are included in Table 15, according to the mentioned k values, for saturated and normal to the plane (⊥) where applicable. 9 different studies and related formulae are considered while calculating the UCS values which are indicated by numbers at the very first row of Table 15. Related study and formula are given below in the order of indicated tables:

[1] (Deere & Miller, 1966)  $\log \sigma_o(ult) = 0,00014 * \gamma * N + 3,16$

[2] (O'Rourke, 1989)  $UCS = 702N - 11040(\text{psi})$

[3] (Katz et al., 2000)  $\ln (UCS) = 0,792 + 0,067 * N \pm 0,231$

[4] (Sachpazis, 1990)  $N = UCS * 0,2329 + 15,7244$

[5] (Cargill & Shakoor, 1990)  $UCS = 4,3 \times 10^2 (N * \gamma) + 1,2$  (Sandstones)

$$UCS = 1,8 \times 10^2 (N * \gamma) + 2,9 \text{ (Carbonates)}$$

[6] (Gokceoglu, 1996)  $UCS = 0,0001 * N^{3,2658}$

[7] (Yasar & Erdogan, 2004)  $UCS = 4 \times 10^{-6} * N^{4,2917}$

[8] (Kidybinski, 1980)  $UCS = 0,447 \exp^{(0,045 * (N+3,5)) + \gamma}$

[9] (Saptono et al., 2013)  $UCS = 0,308 * N^{1,327}$

As it can be analyzed from the tables given below, for some rock types there are several equations to obtain UCS values. The values obtained from each formula are given under related study column; firstly the relatively fresh values on the left and then the weathered values on the right. Comparing these results with the point load (PL in last column) (Table 15) measurements, generally Schmidt hammer conversions are revealed as overestimated results especially for (Deere & Miller, 1966) which is very commonly used for conversions. Also, in some rocks the results are shown as (\*), indicating the values are obtained as negative values which is unacceptable.

Table 15. Schmidt hammer values converted to UCS according to different studies

Road Cut	Rock Type	Schmidt Value		UCS (MPa)				
		Fresh	Weathered	1	2	3	4	5
1	Mudstone	15	13	-	-	-	-	-
	Sandstone	40	29	86-48	117-64	32-15	-	46-34
2	Limestone	39	19	75-26	113-16	30-8	100-14	20-11
3	Limestone	28	16	39-20	59-1,3	14-6	53-1,2	15-9
4	Granite	26	13	40-19	-	13-5	-	-
5	Basalt	38	21	83-31	-	-	-	-
6	Granite	-	<10	--17	-	--4	-	-
7	Granodiorite	47	23	138-34	-	-	-	-
8	Sandstone	49	32	138-52	161-79	59-19	-	55-35
	Mudstone	-	<10	-	-	-	-	-
9	Limestone	48	32	121-55	156-79	55-19	139-70	25-17
	Mudstone	15	<10	-	-	-	-	-
10	Sandstone	36	31	62-48	98-74	25-18	-	40-34
	Mudstone	-	<10	-	-	-	-	-
11	Sandstone	36	21	62-29	98-26	25-9	-	39-23
12	Sandstone	30	<10	45-17	69-*	16-4	-	33-12
13	Sandstone	43	24	86-32	132-40	39-11	-	45-26
	Mudstone	-	<10	-	-	-	-	-
14	Sandstone	31	27	52-41	74-55	18-13	-	35-30
15	Sandstone	49	36	124-62	161-98	59-25	-	54-39
	Mudstone	-	<10	-	-	-	-	-
16	Sandstone	30	12	48-18	69-*	16-5	-	33-13
17	Sandstone	20	13	26-19	21-*	8-6	-	22-14
18	Marl	24	12	-	-	-	-	-
19	Marl	39	20	-	-	-	-	-
20	Marl	30	25	-	-	-	-	-

Table 15. Continued

Stop	Rock Type	Schmidt Value		UCS (MPa)				
		Fresh	Weathered	6	7	8	9	PL
1	Mudstone	15	13	-	-	14-13	11-9	11-7
	Sandstone	40	29	-	30-8	-	41-27	28-21
2	Limestone	39	19	-	27-1	-	-	46-40
3	Limestone	28	16	-	6-1	-	-	21-8
4	Granite	26	13	-	-	-	-	18-5,7
5	Basalt	38	21	-	24-2	-	-	38-2,4
6	Granite	-	<10	-	-	-	-	--1
7	Granodiorite	47	23	-	-	-	-	89-12
8	Sandstone	49	32	-	72-12	-	54-31	36-18
	Mudstone	-	<10	-	-	--9	--6,5	-
9	Limestone	48	32	-	66-12	-	-	100-45
	Mudstone	15	<10	-	-	12-9	11-9	--4
10	Sandstone	36	31	-	19-10	-	36-29	11-8
	Mudstone	-	<10	-	-	--9	--6,5	-
11	Sandstone	36	21	-	19-2	-	36-18	24-6
12	Sandstone	30	<10	-	8-0,1	-	28-6,5	10-5,4
13	Sandstone	43	24	-	41-3	-	45-21	10-6
	Mudstone	-	<10	-	-	--9	--6,5	-
14	Sandstone	31	27	-	10-6	-	29-24	22-20
15	Sandstone	49	36	-	72-19	-	53-36	31-25
	Mudstone	-	<10	-	-	--9	--6,5	-
16	Sandstone	30	12	-	9-0,2	-	28-8,3	13-12
17	Sandstone	20	13	-	2-0,2	-	16-9	11-8
18	Marl	24	12	3,2-0,3	-	-	-	61-42
19	Marl	39	20	16-1,7	-	-	-	64-29
20	Marl	30	25	6,7-3,7	-	-	-	39-20

#### 4.1.5. Shear Box Test

Shear box test by deformation controlled direct shear device was conducted by AKADEMİ Geology and Geotechnics laboratory according to ISRM (2007) for saw-cut samples. In this test, 6cm x 6cm base with 2 cm high 6 specimens (3 on top and 3 on bottom) are loaded under 5, 10 and 20 kg weights. By fixing bottom specimen, shearing was acted on the upper one so that shearing and vertical stresses are obtained. According to 3 different shearing and vertical stresses, cohesion and basic

internal friction angle of each specimen was calculated. According to test results, peak and residual cohesion and basic internal friction angle values of the saw-cut surfaces are presented Table 16.

Table 16. Cohesion and internal friction angle values of saw-cut surfaces for peak and residual conditions

	Peak		Residual	
	c (kPa)	$\phi_b$ (°)	c (kPa)	$\phi_b$ (°)
Limestone	366,84	33,5	202,77	21,4
Sandstone	423,78	41,5	229,98	26,5
Marl	95,64	28,5	42,63	17,8

#### 4.1.6. Slake Durability Index Test

Slake durability index test is applied to the rock samples to determine the resistance to weakening and disintegration by subjecting 2 wetting and drying cycles. According to first and second cycle retaining weights, a slake durability classification is developed by Gamble (1971) (Table 17). This test was applied in the thesis as suggested by ISRM (1981). Approximately 500 g of samples were used for each rock type of each road cut in rotating drums at a speed of 20 rpm for 10 minutes (Figure 18).

Table 17. Gamble's slake durability classification

Group Name	Id(1)	Id(2)
Very High Durability	>99	>98
High Durability	98-99	95-98
Medium High Durability	95-98	85-95
Medium Durability	85-95	60-85
Low Durability	60-85	30-60
Very Low Durability	<60	<30



Figure 18. Slake durability test equipment used in this thesis

Mass weights were recorded before the test, after 1<sup>st</sup> and 2<sup>nd</sup> cycle in order to calculate the first and second slake durability indices. Second slake durability index ( $I_{d2}$ ) is found by the following formula:

$$I_{d2} = (2.C.W / S.W.) * 100$$

where

2 C.W. : 2<sup>nd</sup> cycle retained weight

S.W. : Weight before starting the test.

Average values of the slake durability test results are given in Table 18. Detailed results of slaking durability of rocks at each road cut are given in Appendix A.

“Type” column mentioned in Table 18 is visually estimated according to ASTM D4644-87 (1998) which is related to degradation of the rock samples. As it can be seen from Table 18, durability of the rocks studied in this thesis is in the range of very high to medium durability. In detail, slake durability condition is high and very high, approximately 80 % of the rocks analyzed and the rest is medium and medium high. Decrease of durability of these rocks can be explained by weathering degrees associated with increase of porosity, micro fractures, joints and decrease in grain binding strength (Nickmann et al., 2006).

Table 18. Average values of slake durability test of the rocks at each road cut

Stop	C	Rock Type	Id(1)	Id(2)	Type	Durability
1 - F	F	Mudstone	96,81	<b>95,14</b>	Type II	High
	W	Mudstone	96,88	<b>94,94</b>	Type II	High
1	F	Mudstone	98,98	<b>98,39</b>	Type II	Very High
		Sandstone	99,21	<b>98,67</b>	Type I	Very High
	W	Mudstone	98,55	<b>97,76</b>	Type II	High
		Sandstone	99,04	<b>98,61</b>	Type I	Very High
2	F	Limestone	99,04	<b>98,55</b>	Type I	Very High
	W	Limestone	98,29	<b>97,58</b>	Type I	High
3	F	Limestone	97,79	<b>96,60</b>	Type II	High
	W	Limestone	91,46	<b>85,93</b>	Type II	Medium High
4	F	Granite	99,42	<b>99,19</b>	Type II	Very High
	W	Granite	99,44	<b>98,56</b>	Type II	Very High
5	F	Basalt	98,37	<b>97,39</b>	Type I	High
	W	Basalt	96,56	<b>95,70</b>	Type I	High
6	W	Granite	92,34	<b>89,72</b>	Type III	Medium High
7	F	G.diorite	99,62	<b>99,43</b>	Type I	Very High
	W	G.diorite	99,65	<b>99,48</b>	Type I	Very High
8	F	Sandstone	99,51	<b>99,27</b>	Type I	Very High
	W	Sandstone	99,59	<b>99,35</b>	Type I	Very High

Table 18. Continued

9	F	Limestone	99,49	<b>99,30</b>	Type I	Very High
	W	Limestone	99,24	<b>98,88</b>	Type I	Very High
10	F	Sandstone	97,07	<b>95,56</b>	Type I	High
	W	Sandstone	96,69	<b>95,08</b>	Type I	High
11	F	Sandstone	98,58	<b>97,56</b>	Type II	High
	W	Sandstone	98,65	<b>97,72</b>	Type I	High
12	F	Sandstone	99,66	<b>99,36</b>	Type I	Very High
	W	Sandstone	99,22	<b>98,65</b>	Type I	Very High
13	F	Sandstone	97,36	<b>94,55</b>	Type I	Medium High
	W	Sandstone	96,53	<b>91,80</b>	Type I	Medium High
14	F	Sandstone	98,57	<b>97,55</b>	Type I	High
	W	Sandstone	93,76	<b>89,06</b>	Type I	Medium High
15	F	Sandstone	98,98	<b>98,56</b>	Type I	Very High
	W	Sandstone	98,43	<b>97,81</b>	Type I	High
16	F	Sandstone	98,39	<b>97,36</b>	Type I	High
	W	Sandstone	93,83	<b>91,21</b>	Type I	Medium High
17	F	Sandstone	92,42	<b>88,42</b>	Type II	Medium High
	W	Sandstone	86,33	<b>78,47</b>	Type II	Medium
18	F	Marl	99,36	<b>99,09</b>	Type I	Very High
	W	Marl	99,14	<b>98,64</b>	Type I	Very High
19	F	Marl	98,96	<b>98,48</b>	Type I	Very High
	W	Marl	97,80	<b>96,78</b>	Type I	High
20	F	Marl	99,25	<b>98,56</b>	Type I	Very High
	W	Marl	99,14	<b>98,55</b>	Type I	Very High

\*C: Condition of the rock, F: Relatively Fresh, W: Weathered, 1-F: Stop 1 Failed portion

#### 4.1.7. Methylene Blue Adsorption Test

Methylene blue adsorption test is a very simple test to determine the presence and properties of clay minerals in rocks. If very low amount of methylene is adsorbed by rock, it is either this specimen has very low swelling capacity clay minerals or there are high swelling capacity clay minerals which are in very low amount. Opposite condition of methylene adsorption can be explained with the same logic. In practice, this test can be applied with two ways which are “turbidimetric” and “spot method” (Topal, 1996). In this thesis, spot method is preferred because it is more time conservative than the former one. In this method, methylene blue adsorption (MBA) values, specific surface areas and cation exchange capacity (C.E.C.) can be

determined by simple titration technique. Concentration of methylene blue solution is added to certain amount of specimen powder mixed with distilled water (Figure 19). Strong positive charge of methylene blue ion ( $C_{16}H_{18}N_3SCl$ ) gets rid of the positive ions at the surface of clays. This process goes on until all methylene blue ions attach to the surface of clay minerals. Remaining methylene blue ions stay in the solution mix of water, specimen powder and methylene. C.E.C. can be explained by this maximum adsorption of methylene blue (Topal, 1996).



Figure 19. Methylene blue adsorption test equipment used in this thesis

Methylene blue adsorption test is applied on each rock for all road cuts considered in this thesis. Weathering condition of the rocks, MBA and C.E.C., are determined and average values are given in Table 19. Related photos of the tests are given in Appendix A.

Table 19. Average values of methylene blue adsorption test of the rocks at each road cut

Stop	C	Rock Type	MBA	C.E.C.	Stop	C	Rock Type	MBA	C.E.C.
1-F	F	Mudstone	1,87	4,3	11	F	Sandstone	0,93	2,1
	W	Mudstone	2,13	4,9		W	Sandstone	1,60	3,6
1	F	Mudstone	0,53	1,2	12	W	Mudstone	2,40	5,5
	W	Mudstone	0,93	2,1		F	Sandstone	1,33	3,0
	F	Sandstone	0,40	0,9	13	W	Sandstone	1,33	3,0
	W	Sandstone	0,40	0,9		F	Sandstone	1,07	2,4
2	F	Limestone	0,93	2,1		W	Sandstone	1,20	2,7
	W	Limestone	1,07	2,4		W	Mudstone	2,00	4,6
3	F	Limestone	0,27	0,6	14	F	Sandstone	1,47	3,3
	W	Limestone	0,40	0,9		W	Sandstone	2,27	5,2
4	F	Granite	0,13	0,3	15	F	Sandstone	1,07	2,4
	W	Granite	0,13	0,3		W	Sandstone	1,20	2,7
5	F	Basalt	0,27	0,6		W	Mudstone	2,67	6,1
	W	Basalt	0,93	2,1	16	F	Sandstone	0,93	2,1
6	W	Granite	0,40	0,9		W	Sandstone	0,93	2,1
7	F	Granodiorite	0,67	1,5	17	F	Sandstone	1,33	3,0
	W	Granodiorite	0,67	1,5		W	Sandstone	1,47	3,3
8	F	Sandstone	0,67	1,5	18	F	Marl	1,20	2,7
	W	Sandstone	0,80	1,8		W	Marl	1,33	3,0
	W	Mudstone	1,33	3,0	19	F	Marl	1,20	2,7
9	F	Limestone	0,67	1,5		W	Marl	1,60	3,6
	W	Limestone	0,67	1,5	20	F	Marl	1,33	3,0
	W	Mudstone	2,53	5,8		W	Marl	1,47	3,3
10	F	Sandstone	1,20	2,7					
	W	Sandstone	1,20	2,7					
	W	Mudstone	1,33	3,0					

\*C: Condition of the rock, F: Relatively Fresh, W: Weathered, 1-F: Stop 1 Failed portion, MBA: g/100g, C.E.C.: meq/100g

#### 4.2. Mass Properties of the Rocks at the Cut Slopes

Discontinuities distinguish the rock material from rock mass. The most important features of discontinuities are orientation, spacing, aperture, persistency, roughness, groundwater flow, infill and block size. Because of the importance of these features,

detailed scan line survey is applied in field for each road cut. Other features which controls the rock mass properties are weathering and excavation type, considered in this thesis.

Orientations are extremely important in order to determine the failure type of the road cut. The orientations of discontinuities were noted along the scan line survey by using geological compass. Generally scattered results are obtained on orientation basis.

Not only the orientation of the discontinuities but also spacing and persistency of them are important to determine the slope failure mechanism. Joints are generally bed confined for each road cut. In other words block size generally controlled by bedding thicknesses. Degree of jointing and interrelating block volume were determined according to the data collected from scan line survey to create joint frequency histograms. Degree of jointing ( $J_v$ ) is calculated by considering 3 dominant sets of discontinuities in three dimensions as Palmstrom (1974) suggested, with the given formula below:

$$J_v = 1/S_1 + 1/S_2 + 1/S_3$$

where  $S_1$ ,  $S_2$  and  $S_3$  are spacings for dominant discontinuity sets.

Block volumes are determined by considering joint spacings and angles between them, which are taken as  $90^\circ$  for practical purposes (Palmstrom, 2000). Block volumes ( $V_b$ ) are determined by the given equation below:

$$V_b = \beta \times J_v^{-3}$$

where  $\beta$  is block shape factor and taken as 36 which is suggested for common block shapes (Palmstrom, 2000).

According to these results, degree of jointing is in the range of very high and moderate (Table 20) and block volume is changing between small to moderate (Table 21).

Table 20. Classification of degree of jointing (Palmstrom, 2005)

<b>Degree of Jointing</b>	
<b>Term</b>	<b>J<sub>v</sub></b>
Crushed	>60
Very High	30-60
High	10-30
Moderate	3-10
Low	1-3
Very Low	<1

Table 21. Classification of block volume (Palmstrom, 1995)

<b>Block volume</b>	
<b>Term</b>	<b>V<sub>b</sub> (m<sup>3</sup>)</b>
Very Small	0,00001-0,0002
Small	0,0002-0,01
Moderate	0,01-0,2
Large	0,2-10
Very Large	>10

Roughness and infilling material are also important to determine the rock mass properties. Roughness of discontinuity surfaces were determined according to (ISRM, 1978) and (Hack et al., 2002) which introduce easy data collection to characterize them. Hand profilometer (Figure 20) was used for small scale roughness profiles. Also, infilling materials were determined according to their composition and whether they are cemented, soft sheared or non-softening. In cases like apertures filled with soft sheared materials were investigated on their grain sizes in field.



Figure 20. Profilometer used on discontinuity surfaces

Weathering concept of each road cut was studied for each rock type in field, and weight, porosity, strength, degradation and CEC were compared. Especially flysch type deposits reveal differential weathering due to compositional differences. It is found that due to strength differences, weaker rocks like mudstones were affected more than the sandstones in studied road cuts by both visual estimation and laboratory works. In the study area, weathering degrees are changing between slightly to highly. In the flysch type deposits, while stronger rocks are slightly weathered, weaker rocks –mudstones- are generally moderately weathered. This differential weathering causes undercutting of stronger rocks (Figure 21), changing in depth for each road cut. Possible evolution of a road cut studied in this thesis (Stop 8) is given in Figure 22. In this figure, cross section a-a' is given before differential weathering process on left and after on right which is a very simple example of weathering in the same location under the same conditions affecting different lithologies. This condition is observed for all road cuts with different undercutting depths. While considering the weathering rate of a road cut, worse condition is chosen to be in the safe side. For example, if mudstone is moderately weathered and sandstone is slightly weathered, then entire road cut is chosen to be moderately weathered.



Figure 21. Undercutting due to differential weathering (sandstone on top, mudstone on bottom)

Type of excavation also plays an important role while determining rock mass strength. As it was mentioned in Chapter 2 under excavation subsection before, disturbance factor (D) changes the rock mass properties according to Hoek & Brown (1980) classification. Moreover, excavation type is considered to be one of the most important parameters while determining rock mass properties in SSPC (Hack et al., 2002). In the field, any trace of blasting was not encountered. Furthermore, rocks are mainly in the boundary of moderately strong and strong in which there is no need for blasting to open the road cuts. According to the field investigations, KGM information and considering the strength of the rocks, it is obvious that all road cuts studied in this thesis were created by excavators.

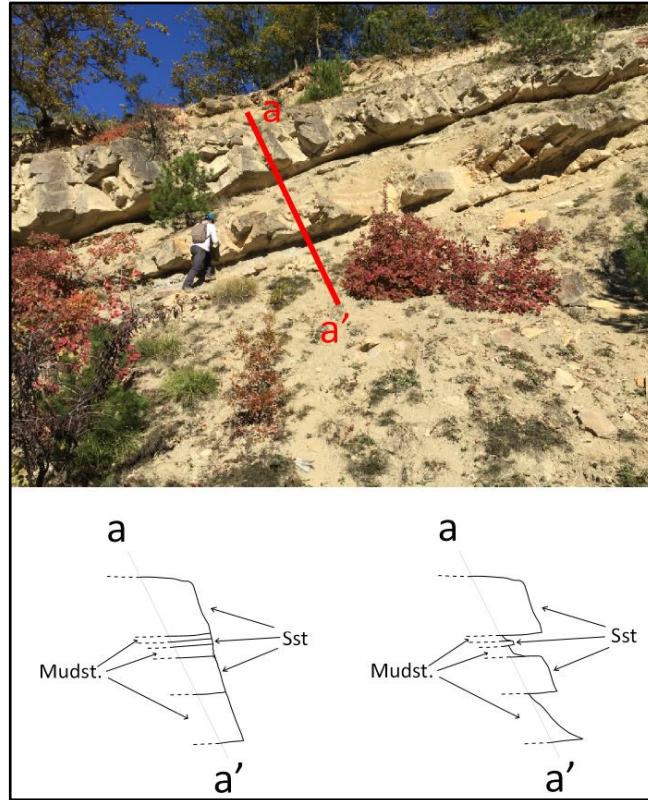


Figure 22. Possible evolution of Stop 8 (Akveren FM) after differential weathering

#### 4.3. Road Cut Characterization

In this thesis 20 different road cuts were studied in detail including their lithological and geometrical description, strength, discontinuity properties, weathering degrees and excavation types. According to personal communication with General Directorate of Highways, studied road cuts were opened between 2008 and 2009 by provincial special administration, however in 2010 they were revised and their slope degrees were reduced. It is known that method of excavation used for all 20 road cuts is mechanical excavation by excavators.

Intact rock strength and unit weight of the flysch type deposits were calculated according to weighted average as introduced by Marinos & Hoek (2001) by visual estimation of percentages of sandstone/limestone/marl to mudstones. Because reliable data can be obtained from the point load test, intact rock strength is used according to these results. As it was mentioned before, the point load tests were

conducted on both the saturated and dry specimens. To be at the safe side, the saturated results are considered for the slope stability analyses not only for the point load test results but also for the unit weight and UCS values.

Desired sized mudstone samples for unit weight were obtained for only Stop 1. Also, some weathered samples could be gathered from Stop 9. Therefore; for flysch type deposits, the unit weight is taken from Stop 1 for the other road cuts (except Stop 9) because mudstone samples could not be obtained because of highly fractured nature of the rock.

Scan line survey was conducted on the road cut to collect data about discontinuity properties such as orientation, persistency, aperture, spacing and infilling. Later this data were used to assess rock mass properties.

In the field, weathering condition and weathering depth was determined visually. Generally surface failures (surficial degradations) were observed because of the weathered zone in front of the relatively fresh original rock. Parameters like unit weight, slake durability and methylene blue values of this weathered zone are taken directly from laboratory results. However for limit equilibrium analysis of the cut slopes, cohesion is taken 0 in order to simulate non-cohesive zone which causes surface failures.

#### **4.3.1. Stop 1**

##### ***Description***

This road cut is located approximately 10 km North of Yeniçağa-Gerede-Mengen Junction in Abant formation. Maximum height of this road cut is about 8 m. Current slope dip is determined as 40°. This road cut consists of 95% of dark gray to black, very thin slabs of mudstone and 5% of light gray, fine to medium grained sandstone. The sandstone blocks are observed generally broken in the matrix of mudstone (Figure 23).

Currently this road cut is partially unstable. As it can be seen from Figure 23, the zone located in the lighter colored portion is failed as circular shape. This zone can be observed clearly from Figure 24.



Figure 23. General view of the cut slope at Stop 1



Figure 24. Failed zone of the cut slope at Stop 1

### ***Strength and Unit Weight***

Saturated UCS values of the mudstone and the sandstone are determined according to related k-values from point load test (Table 22). For the sandstone, related k-value is correlated from UCS test for stable zone however it has not been encountered at the failed zone of this road cut. Mudstone k-value is taken from literature (Wilson 1976) because of the difficulty of obtaining sample size for UCS test. The mudstone is deposited as very thin slabs and under saturated conditions it becomes impossible to saw the material for desired sizes.

Table 22. UCS values of the rocks at Stop 1

		UCS (MPa)				
		Fresh		Weathered		
Stop	Rock Type	Dry	Saturated	Dry	Saturated	
1 - Failed	Mudstone	26,3	4,2	22,8	1,5	
1	Mudstone	47,0	36,3	38,1	19,6	⊥
	Mudstone	29,5	11,1	26,8	6,9	=
	Sandstone	61,8	36,2	48,3	32,4	⊥
	Sandstone	35,3	27,5	31,4	21,5	=

Considering the general orientation of the mudstone slabs and broken sandstone pieces, the UCS values of parallel (=) to bedding plane were taken for the analyses. Therefore using weighted average of these rocks, rock mass strength of the rocks of this road cut is calculated as 12 MPa for the stable zone, and 4 MPa for the unstable zone. As it can be seen from Table 22, dry values are extremely higher than the saturated ones for the failed zone.

Unit weight values of this road cut are summarized in Table 23. As it was mentioned, the weighted average of the saturated unit weight of the mudstone and the sandstone, that is 25,51 kN/m<sup>3</sup> for fresh and 25,76 kN/m<sup>3</sup> for weathered, are calculated and used for the rock mass for both stable and saturated zones.

Table 23. Unit weight values of the rocks at Stop 1

		Unit Weight (kN/m <sup>3</sup> )			
		Fresh		Weathered	
Stop	Rock Type	Dry	Saturated	Dry	Saturated
1	Mudstone	22,25	25,47	25,09	25,74
	Sandstone	25,86	26,19	25,87	26,21

### ***Discontinuity Properties***

Pole plot and contour plot of this road cut are given in Figure 25. As it can be seen, a scattered result is obtained from the orientation data, however the most dominant three discontinuity sets are determined as 69/139, 40/247 and 33/319 as dip/dip direction. Joint spacing frequency is obtained as histogram (Figure 26). Persistence of the joints is coherent with the spacings, and they are mostly bed confined. Apertures can be seen visually and infill material is determined as mostly damp sandy clay. Considering especially the orientation and spacing of discontinuities, it is obvious that this zone is prone to circular failure. Small quantities of rockfall and degradation can be observed. However, the rockfall is not remarkable due to small block volumes.

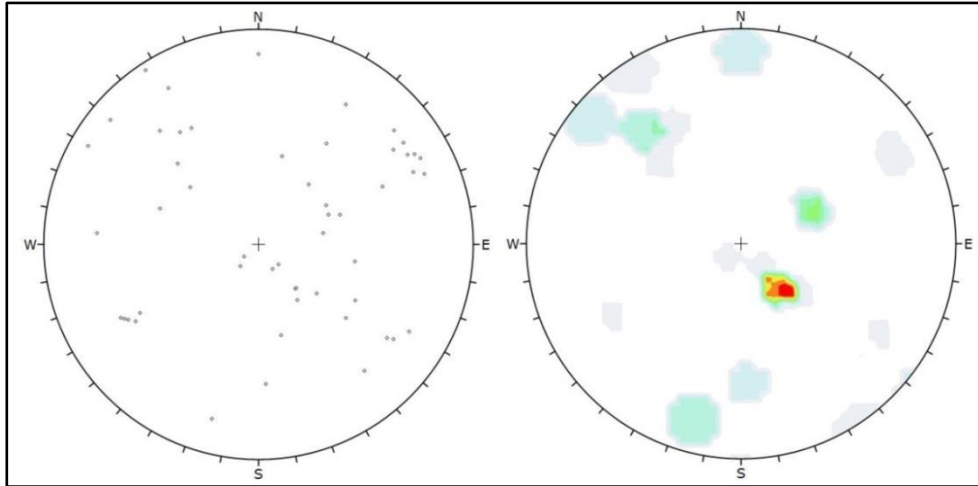


Figure 25. Pole (left) and contour (right) diagrams of the discontinuities at Stop 1

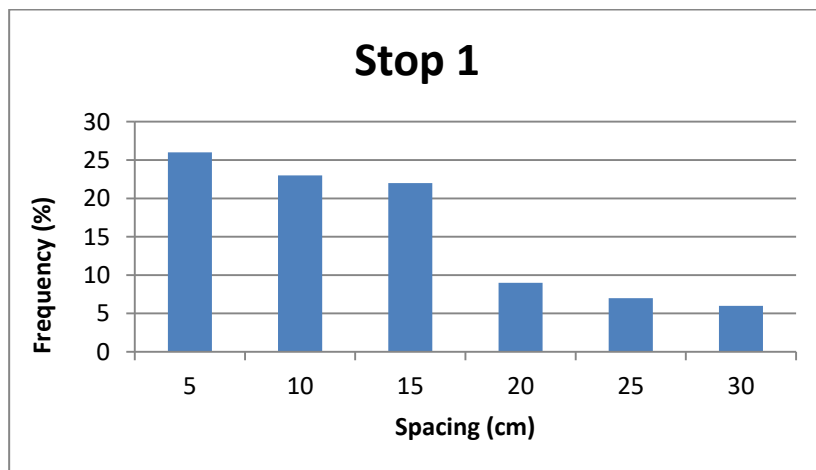


Figure 26. Discontinuity spacing frequency histogram of Stop 1

### ***Weathering and other Properties***

Weathering degree of this road cut is specified as moderately to highly for mudstone, and slightly for sandstone. Because the mudstone is very dominant for this case, weathering of the whole road cut can be assessed as moderately weathered. On the other hand, the failed portion of the road cut is determined as highly weathered.

Thickness of the weathered zone is determined as about 30 cm based on the field study.

Other properties of the rocks which are also used to evaluate slope conditions are slake durability ( $Id_2$ ) and methylene blue values (MBA and CEC) (Table 24). According to these results, rocks at Stop 1 are highly durable against degradation and have very low CEC although mudstone values are more critical than sandstone.

Table 24. Slake durability and CEC values of the rocks at Stop 1

Stop	Rock Type	Fresh			Weathered		
		Slake durability ( $Id_2$ )	MBA (gr/100 g)	CEC (meq/100 g)	Slake durability ( $Id_2$ )	MBA (gr/100 g)	CEC (meq/100 g)
1 - Failed	Mudstone	95,14	1,87	4,30	94,94	2,13	4,90
1	Mudstone	98,39	0,53	1,20	97,76	0,93	2,10
	Sandstone	98,67	0,40	0,90	98,61	0,40	0,90

#### 4.3.2. Stop 2

##### *Description*

This road cut is located about 3.4 km north of Mengen. It is located in Soğanlı formation. Maximum height of this road cut is approximately 10 m. Slope dip amount is determined as  $70^0$ . Lithology at this road cut is yellowish beige crystalline limestone as MTA (2002) report suggested. Approximately 1.5 m thick colluvium is lying unconformably on top of the limestone (Figure 27). This road cut is partially unstable as it can be seen from Figure 28. In the field, shear zones are observed generally in the direction of slope dip (perpendicular to slope orientation), almost parallel to each other with 1 to 2 meters spacing. In Figure 27, they are indicated with red dashed lines. Field observations also revealed that debris accumulations increase right below these shear zones at the bottom of the cut slope. The circular

shaped failure in this road cut is most probably formed due to the frequency increase of these shear zones.



Figure 27. General view and shear zones (red dashed lines) seen at Stop 2

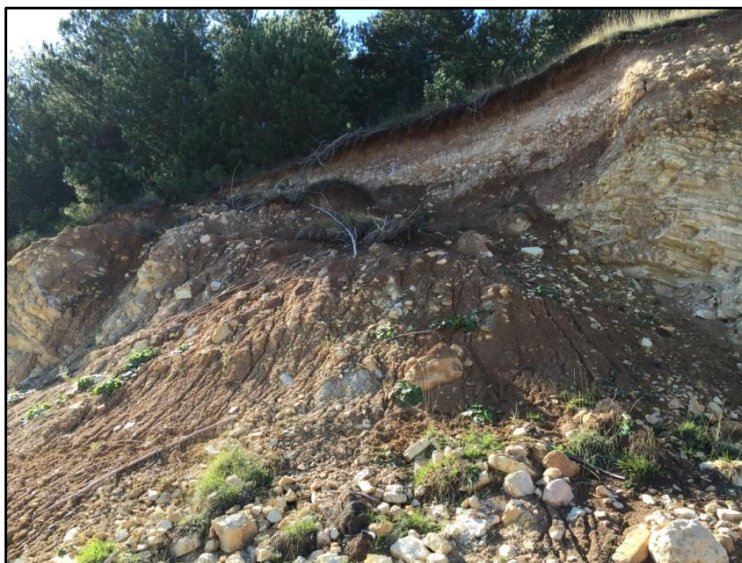


Figure 28. Failure of the rock mass at Stop 2

### ***Strength and Unit Weight***

Fresh and weathered UCS values of the rocks at this road cut are summarized in Table 25. UCS values are directly taken from the UCS test for the relatively fresh limestone. However weathered UCS values are calculated by correlation of the point load tests. UCS value of the failed zone of Stop 2 which is 8 MPa is determined from the point load test by correlation.

Unit weight values of this road cut are summarized in Table 25. For the slope stability analysis, unit weight of this rock is found to be 24,63 kN/m<sup>3</sup> for the fresh limestone, and 24,69 kN/m<sup>3</sup> for the weathered limestone. The unit weight of the soil sample taken from the colluvium is calculated as 12,01 kN/m<sup>3</sup>. The average weight of boulders and gravels in colluvium is estimated as 60% while soil is 40%. Considering the unit weight of the fresh saturated limestone and soil the average unit weight of the colluvium is calculated as 19,62 kN/m<sup>3</sup>.

Table 25. UCS and unit weight values of the rocks at Stop 2

Stop	Rock Type	Fresh		Weathered		Test
		Dry	Saturated	Dry	Saturated	
2	Limestone	38,21	39,82	28,48	15,98	UCS (MPa)
		23,60	24,63	23,74	24,69	Unit Weight (kN/m <sup>3</sup> )

### ***Discontinuity Properties***

Pole and contour plot of the discontinuities at this road cut are shown in Figure 29. A scattered result is obtained from the plots due to the deformation occurred in this road cut. However, there are three dominant discontinuity sets which are 20/270, 69/100 and 75/015 as dip/dip direction. Joint spacing frequency histogram is given in Figure 30. Persistence of the joints is mostly matching with the spacings, and they are mostly bed confined with the only exceptions of shear zones. Discontinuity

apertures do not exceed 5 mm generally and infill material between them is generally medium grained damp clayey sand. Failure type in this road cut is determined as circular with the evidence of already failed portion and scattered data with the shear zones in the stable parts. Because of high degree of jointing, moderate block volumes are calculated which is coherent with small quantities of rockfalls seen in the field.

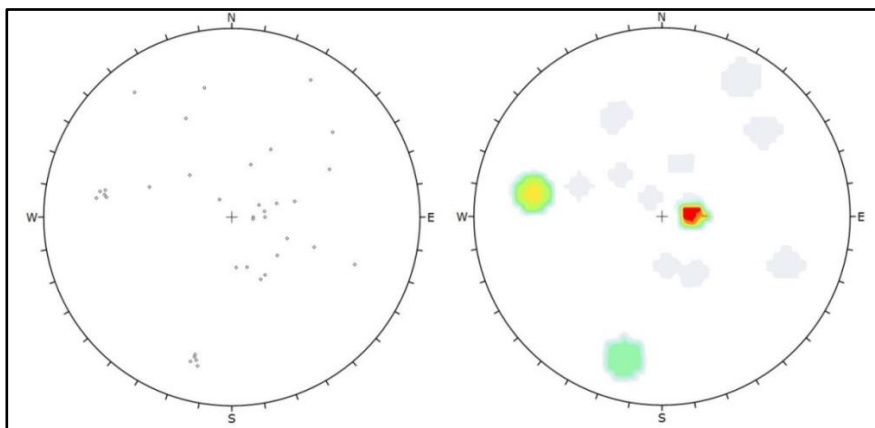


Figure 29. Pole (left) and contour (right) diagrams of the discontinuities at Stop 2

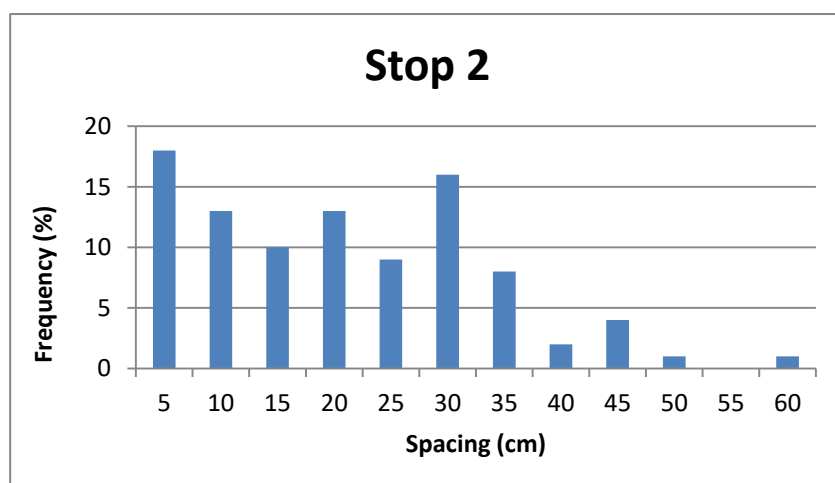


Figure 30. Discontinuity spacing frequency histogram at Stop 2

### ***Weathering and other Properties***

Weathering degree of this road cut is determined as slightly. Only surface staining is observed on the discontinuity walls. Thickness of this weathered zone is determined as 20 cm from the existing surface. Directly proportional with degradation weathering of the rocks increases to moderately at very thick shear zones.

Slake durability ( $Id_2$ ) results given in Table 26 indicate that the rocks at Stop 2 is highly durable against degradation.

Table 26. Slake durability and methylene blue values of the rocks at Stop 2

Stop	Rock Type	Fresh			Weathered		
		Slake durability ( $Id_2$ )	MBA (gr/100 g)	CEC (meq/100 g)	Slake durability ( $Id_2$ )	MBA (gr/100 g)	CEC (meq/100 g)
2	Limestone	98,55	0,93	2,10	97,58	1,07	2,40

### **4.3.3. Stop 3**

#### ***Description***

This road cut is located about 3.7 km north of Mengen, very close to Stop 2, in the Akveren formation. Maximum height of this road cut is about 15 m. Slope dip amount is determined as  $60^0$ . Lithology of this road cut is yellowish beige to white crystalline limestone as the Stop 2 (Figure 31).

This road cut is completely stable but only surficial degradations are observed due to the presence of weathered zone. Surface of this road cut is significantly softer than the relatively fresh original rock that even a light pressure of geological hammer penetrates into the slope (Figure 31).



Figure 31. General view of the cut slope at Stop 3

### ***Strength and Unit Weight***

The UCS values obtained from the rocks at Stop 2 by UCS test are directly used for this road cut because the same lithological properties have been observed in this road cut (Table 27). Therefore, approximately 40 MPa is used for the slope stability analyses (Table 27). Weathered values of UCS (Table 27) however, are obtained by using k value of 16 from the point load index test.

The unit weight values of the rocks at this road cut are summarized in Table 27. For the analysis, the unit weight of this rock is measured as  $21,84 \text{ kN/m}^3$  for the fresh rock, and  $23,19 \text{ kN/m}^3$  for the weathered rock.

Table 27. UCS and unit weight values of the rocks at Stop 3

Stop	Rock Type	Fresh		Weathered		Test
		Dry	Saturated	Dry	Saturated	
3	Limestone	38,21	39,82	9,78	8,25	UCS (MPa)
		19,99	21,84	21,70	23,19	Unit Weight (kN/m <sup>3</sup> )

### ***Discontinuity Properties***

Pole and contour diagrams drawn for this stop are shown Figure 32. Scattered result is obtained from the plots as in Stop 2 and similarly there are three dominant discontinuity sets which are 16/050, 67/180 and 75/255 as dip/dip direction. Surface weathering is quite higher than Stop 2 for this case; therefore joint and bedding plane spacing precision is slightly difficult. Joint spacing frequency histogram reveals a range between 5cm and 60 cm (Figure 33). Joints are generally bed confined and because of that persistency is coherent with joint spacings. As in Stop 2 apertures do not exceed 5 mm and infill material is determined as medium grained damp clayey sand. Failure type in this road cut is most probably circular due to scattered structure. Because of very high degree of jointing, small block volumes are generated. These small blocks produced rockfall and degradation form non-cohesive surfaces due to weathering and they are observed near the bottom of the slope.

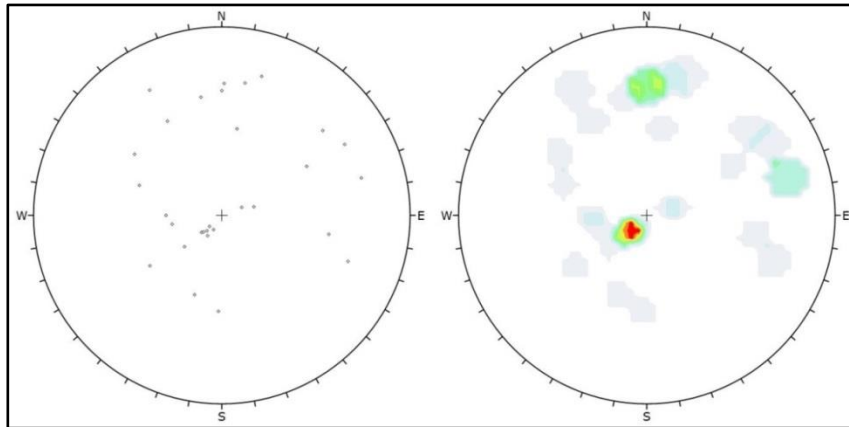


Figure 32. Pole (left) and contour (right) diagrams of the discontinuities at Stop 3

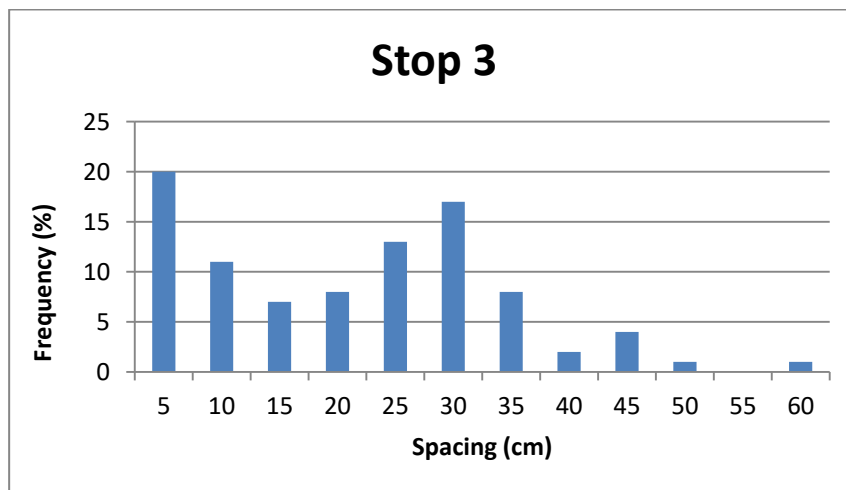


Figure 33. Discontinuity spacing frequency histogram at Stop 3

### ***Weathering and other Properties***

Weathering degree of the rocks at this road cut is determined as moderately. As it was mentioned before, at the surface light pressure of hammer penetrates into weathered zone. Thickness of this weathered zone is measured as 30 cm from the surface.

Slake durability ( $Id_2$ ) and C.E.C. results are given in Table 28. According to these results, even MBA and CEC values do not reveal significant differences between relatively fresh and weathered specimens. Nevertheless, the slake durability is completely different. It is clear that the weathered zone is more prone to degradation.

Table 28. Slake durability and methylene blue values of the rocks at Stop 3

Stop	Rock Type	Fresh			Weathered		
		Slake durability ( $Id_2$ )	MBA (gr/100 g)	CEC (meq/100 g)	Slake durability ( $Id_2$ )	MBA (gr/100 g)	CEC (meq/100 g)
3	Limestone	96,60	0,27	0,60	85,93	0,40	0,90

#### 4.3.4. Stop 4

##### *Description*

This road cut is located approximately 14 km north of Mengen, in the narrow valley section of Bolu Zonguldak motorway, in Bolu Granitoid. Height of this road cut is about 12 meters with 1 bench. Lower section is approximately 8 meters and this portion is chosen to be analyzed. Slope dip amount is determined as  $75^0$ . There is an approximately 10 m high retaining wall made of stones in front of the slope which is nearly vertical. Lithology of this road cut is light brown to gray granite (Figure 34).

This road cut is completely stable but only surface failures are observed due to the weathered zone in the surface as small fragments of rockfall. Also in the surface, a very thin orientation independent failure zone is observed, indicated with red dashed line (Figure 34). This local slope failure was formed most probably due to non-cohesive weathered zone at the surface.



Figure 34. General view of the cut slope at Stop 4 (Failure zone indicated with red dashed line)

### ***Strength and Unit Weight***

For this road cut, the UCS values of the rocks are obtained from the point load values by using related  $k$  value, which is 3,8. According to these approximately 20 MPa is used for the slope stability analyses (Table 29).

The unit weight values of the rocks at Stop 4 are summarized in Table 29. For the analysis, the unit weight of this rock is determined as 25,61 kN/m<sup>3</sup> for the relatively fresh rock, and 25,88 kN/m<sup>3</sup> for the weathered rock.

Table 29. UCS and unit weight values of the rocks at Stop 4

Stop	Rock Type	Fresh		Weathered		Test
		Dry	Saturated	Dry	Saturated	
4	Granite	21,31	18,25	7,74	5,66	UCS (MPa)
		25,32	25,61	25,61	25,88	Unit Weight (kN/m <sup>3</sup> )

### ***Discontinuity Properties***

Pole and contour plots of the discontinuities are shown in Figure 35 for this stop. Intense scattered result is obtained according to the pole plot. The most three dominant joint sets which are 5/090, 65/250 and 64/340 as dip/dip direction are determined in order to use them in the empirical analysis. Joint spacing frequency histogram is shown in Figure 36. Persistence of the joints is generally coherent with joint spacings. Apertures are approximately 5 mm, and infill material is damp sandy clay/silt. Failure type in this road cut is most probably circular due to scattered structure which can be seen from Figure 35. Due to very high joint frequency, small block volumes exist. These small blocks produced local rockfalls and most of them are kept by the stone wall, only very small fragments have fallen near the road. These blocks could not reach the road but accumulated at the drainage channel next to the road.

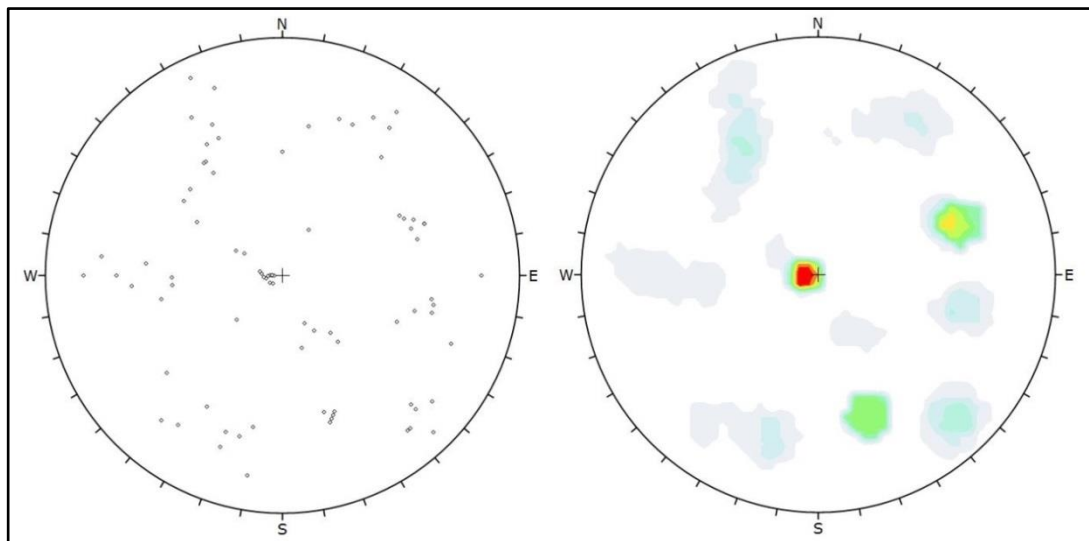


Figure 35. Pole (left) and contour (right) diagrams of the discontinuities at Stop 4

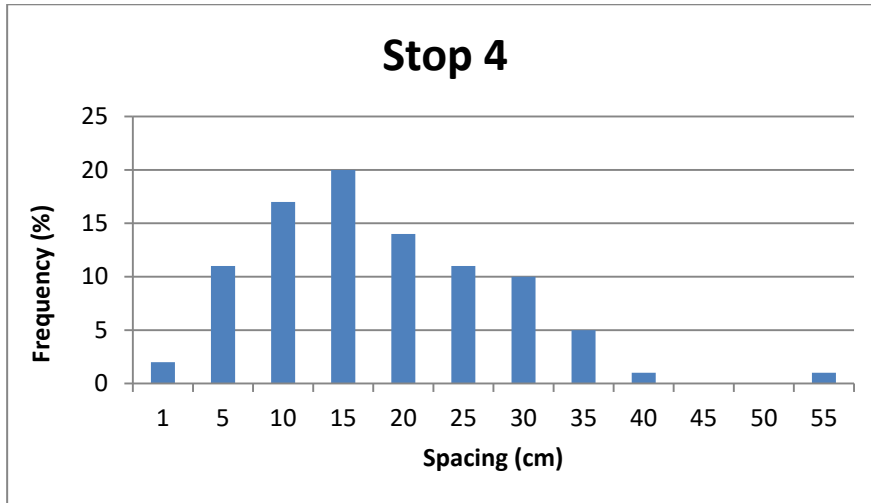


Figure 36. Discontinuity spacing frequency histogram at Stop 4

#### ***Weathering and other Properties***

Surface weathering of this road cut is observed as moderately. Because of extreme jointing in this granite, chemical and physical weathering could easily take place through fractures. Thickness of this weathered zone is determined as 30 cm from the surface.

Slake durability ( $Id_2$ ) and C.E.C. results are given in Table 30. As it can be seen from Table 30, slake durability of this rock is very high. In the tests, it is observed that only the edges of the specimens are broken after second cycle. Also, MBA and CEC values are extremely low.

Table 30. Slake durability and methylene blue values of the rock at Stop 4

Stop	Rock Type	Fresh			Weathered		
		Slake durability ( $Id_2$ )	MBA (gr/100 g)	CEC (meq/100 g)	Slake durability ( $Id_2$ )	MBA (gr/100 g)	CEC (meq/100 g)
4	Granite	99,19	0,13	0,30	98,56	0,13	0,30

#### 4.3.5. Stop 5

##### *Description*

This road cut is located next to Stop 4, in Bolu Granitoid. Height of this road cut is about 20 meters with 1 bench. As in Stop 4 lower section of the slope is chosen to be analyzed. Slope dip amount is determined as  $75^{\circ}$ . There is an approximate 10 m high retaining wall made of stone in front of the slope which is nearly vertical. Lithology of this road cut is reddish brown basalt (Figure 37).

In general, view this road cut is completely stable, however, left part of the slope reveals high frequency of joint spacings probably due to two thick shear zones, shown by red dashed lines in Figure 37. Nevertheless, these zones only produce surface failures and rock fall which do not exceed the wall in front of the slope.



Figure 37. General view and shear zones of Stop 5 (Shear zones indicated with red dashed lines)

### ***Strength and Unit Weight***

For this road cut, the UCS values are obtained from the point load values by using related k value as 24 taken from Read et al. (1980). Any UCS test could not be conducted for basalt because under saturated conditions the samples crumble into pieces. Therefore, desired sizes could be obtained for UCS test. According to these, approximately 38 MPa for relatively fresh saturated basalt is used for the analyses (Table 31). From the results it is observed that saturated values are significantly lower than the dry ones which may cause critical issues after heavy rainfalls.

The unit weight values of the rocks at Stop 5 are summarized in Table 31. The saturated unit weight of the fresh and weathered rocks are calculated as 25,94 and 26,28 kN/m<sup>3</sup>, respectively.

Table 31. UCS and unit weight values of the rocks at Stop 5

Stop	Rock Type	Fresh		Weathered		Test
		Dry	Saturated	Dry	Saturated	
5	Basalt	52,66	38,85	22,24	3,42	UCS (MPa)
		24,66	25,94	25,38	26,28	Unit Weight (kN/m <sup>3</sup> )

### ***Discontinuity Properties***

Pole and contour diagrams of the discontinuities are shown in Figure 38 for this road cut. Scattered result is obtained according to pole plot mostly due to the presence of shear zones. However, three dominant joint sets are determined in order to use them in the empirical analysis which are 62/148, 80/200 and 75/012 as dip/dip direction. Maximum spacing is revealed as 60 cm with minor amount in joint spacing frequency histogram (Figure 39). Persistence of the joints is matching with joint spacings. Apertures are significantly close -less than 1 mm- and infill material is damp sandy clay/silt and some of them are observed as without any infill material.

Failure type in this road cut is most probably circular due to weathering, scattered structure and highly fractured portions with shear zones. Degree of jointing is determined as high so that block volumes are calculated as small. As indicated before, these small blocks produces rockfall and accumulated behind the wall.

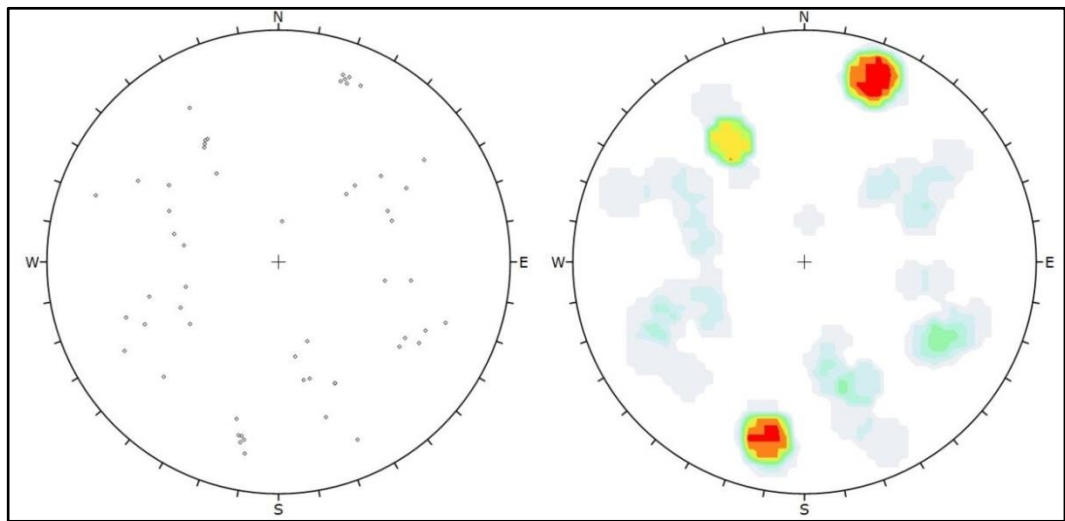


Figure 38. Pole (left) and contour (right) diagrams of the discontinuities at Stop 5

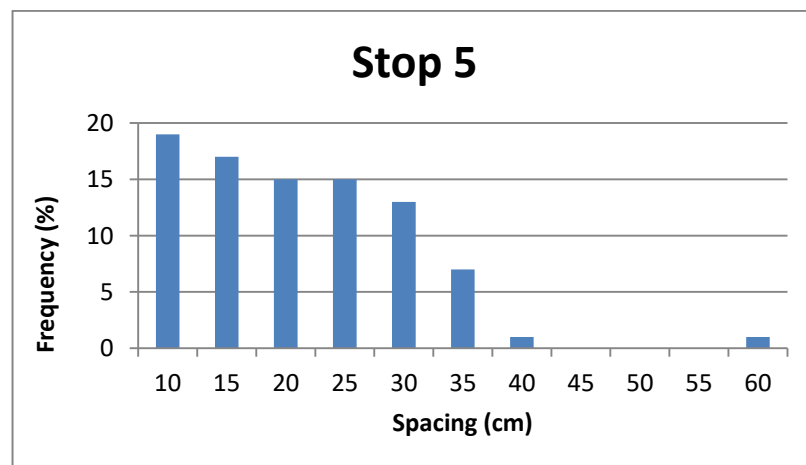


Figure 39. Discontinuity spacing frequency histogram at Stop 5

### ***Weathering and other Properties***

Weathering degree of this road cut is determined as moderately. Due to extreme jointing especially in shear zones, weathering activity increases within the fractures. Thickness of this weathered zone is determined approximately 40 cm from the surface.

Slake durability ( $Id_2$ ) and C.E.C. results are given in Table 32. As it can be seen from Table 32, durability of this rock is high. In detail, weathered specimens reveal higher MBA and CEC values than the relatively fresh ones –nearly 3 times higher- which is coherent with the strength of this material.

Table 32. Slake durability and methylene blue values of the rocks Stop 5

Stop	Rock Type	Fresh			Weathered		
		Slake durability ( $Id_2$ )	MBA (gr/100 g)	CEC (meq/100 g)	Slake durability ( $Id_2$ )	MBA (gr/100 g)	CEC (meq/100 g)
5	Basalt	97,39	0,27	0,60	95,70	0,93	2,10

#### **4.3.6. Stop 6**

##### ***Description***

This road cut is located approximately 1 km north of Stops 4 and 5, in Bolu Granitoid. Height of this road cut is about 10 meters. Slope dip amount is measured as  $65^0$ . There is an approximately 10 m high retaining wall made of stones in front of the slope which is nearly vertical. Lithology of this road cut is light brown to gray granite which is the same rock type as Stop 4 (Figure 40).

In general, this road cut is completely stable. Only surficial failures were observed due to very thick weathering zone. These surficial failures only produced small fragments of rock fall. Already fallen specimens are observed behind the retaining wall.



Figure 40. General view of the cut slope at Stop 6

### ***Strength and Unit Weight***

For this road cut, the fresh UCS and unit weight values are used from fresh results of Stop 4 granite specimens. The reason is that at this road cut the weathered zone is very thick and fractured. Because of this reason, relatively fresh zone behind this thick weathered zone could not be reached. Therefore, saturated fresh strength is taken as 20 MPa for this stop (Table 33), which was already obtained from Stop 4. According to these results, there is an extreme difference between relatively fresh and weathered zones especially for UCS. Very low values of weathered zone indicating soil like material which is also observed in the field that specimens crumbled with very light hand pressures. Many weathered hand specimens were not used while conducting point load test especially in saturated conditions.

Unit weight values of the rocks at Stop 6 are summarized in Table 33. Saturated unit weight of the fresh rock which is taken from Stop 4 as indicated above and the weathered rocks are taken as 25,33 and 25,88 kN/m<sup>3</sup>, respectively.

Table 33. UCS and unit weight values of the rocks at Stop 6

Stop	Rock Type	Fresh		Weathered		Test
		Dry	Saturated	Dry	Saturated	
6	Granite	21,31	18,25	1,10	0,10	UCS (MPa)
		25,32	25,61	24,62	25,33	Unit Weight (kN/m <sup>3</sup> )

### ***Discontinuity Properties***

Pole and contour plots of discontinuities of this road cut are shown in Figure 41. Scattered result is obtained as pole plot indicates. This is because of the highly weathered surface. However the most three dominant joint sets are determined in order to use them in the empirical analysis which are 60/125, 70/025 and 50/245 as dip/dip direction. Joint spacing frequency histogram shows a concentration at 20-30 cm zone (Figure 42). Only a few measurements were taken over 1 m. Persistence of the joints is matching with the joint spacings. A few joints observed over 1 m as spacing frequency indicates however they do not represent the whole road cut. Apertures can be observed visually, which are generally more than 5 mm, however in some cases it is difficult to observe them because of highly weathered structure on the surface. Infill material is damp clay/silt. Failure type in this road cut is most probably circular due to scattered structure, high degree of jointing and soil like material on the surface. Block volumes are small which were calculated from spacing of joints. Some rockfall material is observed detaching from the joints however they do not overtop the retaining wall and create any danger.

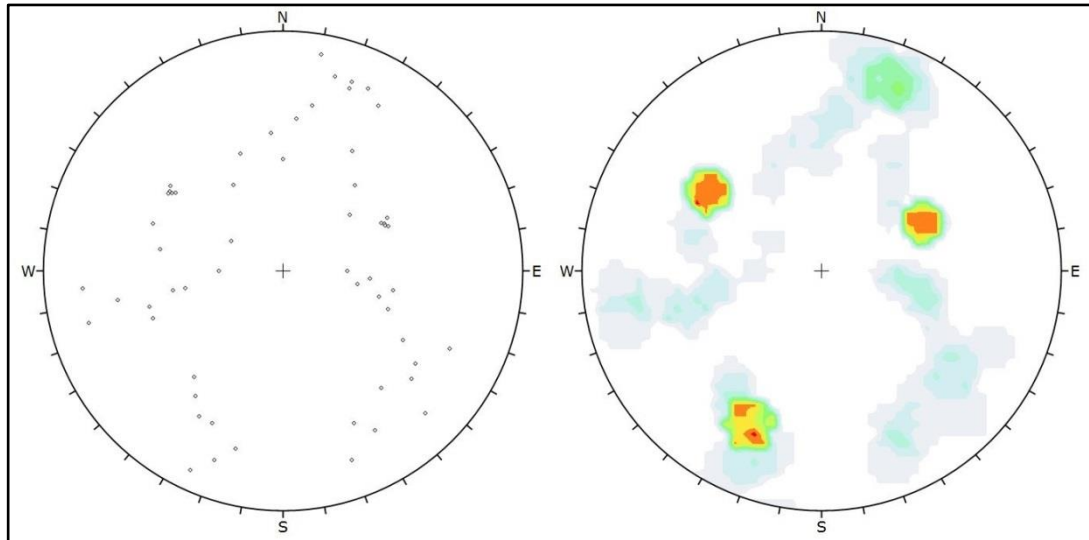


Figure 41. Pole (left) and contour (right) diagrams of the discontinuities at Stop 6

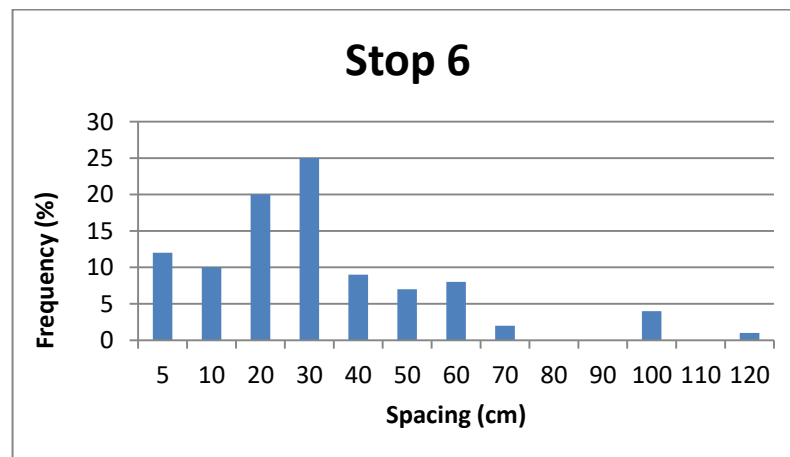


Figure 42. Discontinuity spacing frequency histogram of Stop 6

### ***Weathering and other Properties***

High weathering degree has taken place in this road cut. Due to high weathering some joints are difficult to observe. Thickness of this weathered zone could not be observed clearly, therefore any specimen in the category of relatively fresh could not be taken.

Slake durability ( $Id_2$ ) and C.E.C. results are given in Table 34. Fresh slake durability values are taken from Stop 4, however weathered values are obtained from the materials taken from the surface of this road cut. As it can be seen even surface strength is extremely low, but durability is not as low as strength. Fresh MBA and CEC values are again taken from Stop 4.

Table 34. Slake durability and methylene blue values of Stop 6

Stop	Rock Type	Fresh			Weathered		
		Slake durability ( $Id_2$ )	MBA (gr/100 g)	CEC (meq/100 g)	Slake durability ( $Id_2$ )	MBA (gr/100 g)	CEC (meq/100 g)
6	Granite	99,19	0,13	0,30	89,72	0,40	0,90

#### 4.3.7. Stop 7

##### *Description*

This road cut is located nearly 15 km south of Devrek, in Bolu Granitoid. Apart from Stop 4-5-6 this magmatic section is located northern part of the deep valley, in a gentler place. Height of this road cut is about 15 meters. Slope dip amount is measured as  $75^0$ . This road cut is firstly investigated in October 2015 (Figure 43) and later then it is revisited in June 2016 (Figure 43). As it can be seen from the figure, approximately 7 m high retaining wall is constructed between these dates. Lithology of this road cut is dark green to grayish black granodiorite.

In general, this road cut is completely stable. Only surface failures created some rockfalls in the drainage channel next to the road. Some very small blocks were also observed on the road. The main purpose of this newly constructed wall is possibly to catch these small blocks.



Figure 43. General view of Stop 7 in 2015 (above) and 2016 (below)

### ***Strength and Unit Weight***

UCS values of the rocks at this road cut are obtained from point load results by related  $k$  value which is 15 (Table 35). According to these results, fresh rock is in range of very strong and strong rock; however weathered surface is in moderately strong category. Comparing dry and saturated values of these weathered samples also reveals that after long time connection with water, strength of this material decreases dramatically and can create surficial failures like detachment of small blocks creating rockfall.

Unit weight values of the rocks at this road cut are summarized in Table 35. Saturated unit weight results are considered in analyses for the fresh and weathered rocks which are 26,22 and 27,03 kN/m<sup>3</sup>, respectively.

Table 35. UCS and unit weight values of the rocks at Stop 7

Stop	Rock Type	Fresh		Weathered		Test
		Dry	Saturated	Dry	Saturated	
7	Granodiorite	114,94	88,03	23,67	12,48	UCS (MPa)
		25,66	26,22	26,78	27,03	Unit Weight (kN/m <sup>3</sup> )

### ***Discontinuity Properties***

Pole and contour plots of this road cut are shown in Figure 44. Scattered result obtained as pole plot indicates due to high degree of jointing in different orientations. Three dominant joint sets are obtained in order to use them in the empirical analysis. These are 70/230, 55/340 and 5/020 as dip/dip direction (Figure 44). Maximum joint spacing measured as 90 cm which are very low in amount can be seen in joint spacing frequency histogram (Figure 45). Persistence of the joints is generally matching with joint spacing, however a very long (about 20-25 m) discontinuity is also locally observed, but it does not represent the whole road cut. Apertures are generally narrower than 5 mm and no infill material is observed with some exceptions. These exceptional infill materials are damp clayey/silty sand and clay/silt. Failure type in this road cut is most probably circular due to scattered data and high degree of jointing. Block volumes are categorized as moderate according to joint degree measurements. As mentioned above, some rockfall material is observed that are detached from the joints, however, they do not create any significant danger for the cut slope.

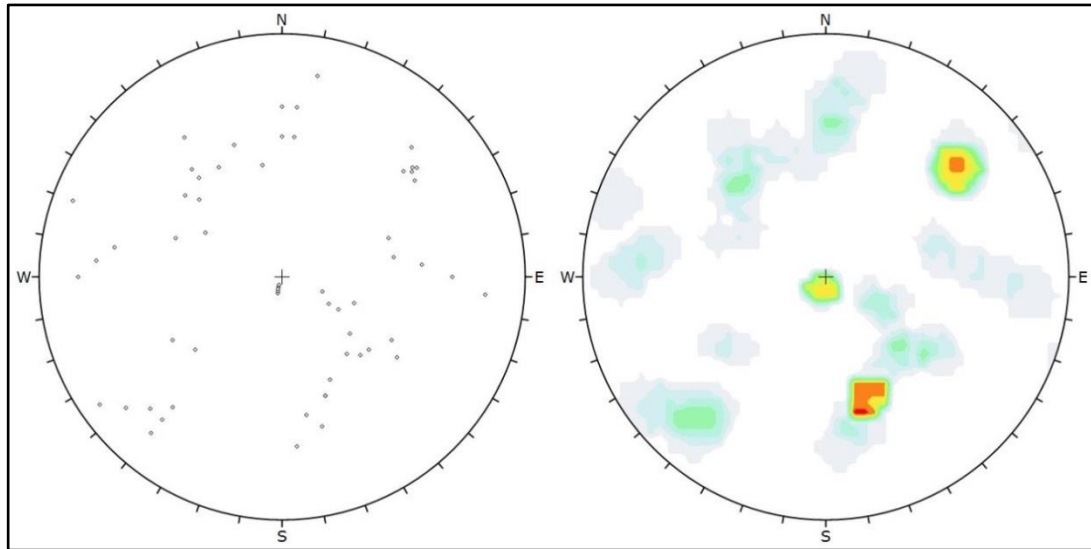


Figure 44. Pole (left) and contour (right) diagrams of the discontinuities at Stop 7

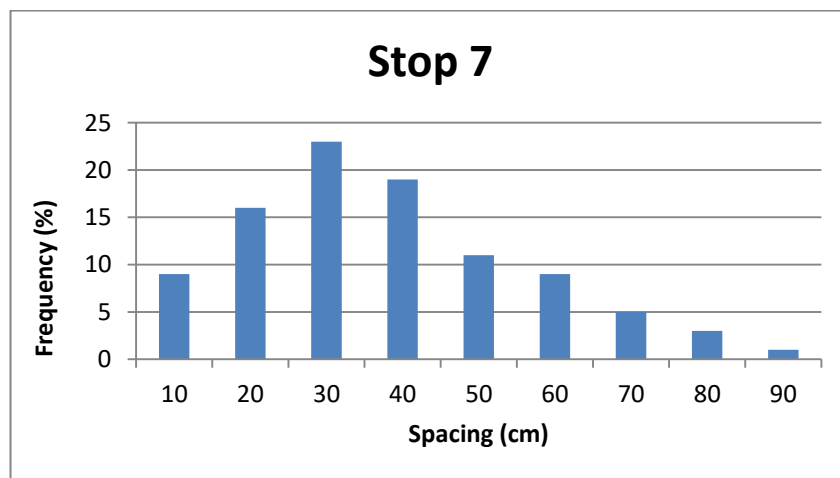


Figure 45. Discontinuity spacing frequency histogram of Stop 7

### ***Weathering and other Properties***

Very thin zone in front of the relatively fresh rock is determined as moderately weathered. However, the weathered zone is mostly in slightly category. This slightly weathered zone is determined as approximately 30 cm.

Slake durability ( $Id_2$ ) and C.E.C. results are given in Table 36. Fresh and weathered slake durability values are very similar to each other in this road cut because of slightly weathering. Moreover, MBA and CEC values are determined as exactly the same for relatively fresh and weathered specimens.

Table 36. Slake durability and methylene blue values of Stop 7

Stop	Rock Type	Fresh			Weathered		
		Slake durability ( $Id_2$ )	MBA (gr/100 g)	CEC (meq/100 g)	Slake durability ( $Id_2$ )	MBA (gr/100 g)	CEC (meq/100 g)
7	Granodiorite	99,43	0,67	1,50	99,48	0,67	1,50

#### 4.3.8. Stop 8

##### *Description*

This road cut is located nearly 7 km south of Devrek, in the Akveren formation. Maximum height of this road cut is about 15 meters. Slope dip amount is measured as  $50^0$ . This road cut consists of 50% of beige, thin to thick bedded of sandstone and 50% of light gray thin to thick bedded mudstone (Figure 46).

Although the slope seems to be generally stable, some moderate size blocks are observed which are already fallen near the slope as warned by a traffic sign at this slope. Fallen blocks are generally sandstone. Mudstones are only observed as disintegrated fragments as surface failures on the slope.



Figure 46. General view of the cut slope at Stop 8

### ***Strength and Unit Weight***

UCS values of the rocks at this road cut are obtained directly from uniaxial compressive strength test on the sandstone (Table 37) and point load values by correlating  $k$  values for the mudstone. The mudstone point load values are used according to Stop 1 –as 11,1 MPa- because in this stop this rock type is completely fractured so that proper sizes could not be obtained for the point load (Figure 47). According to these results, UCS value of the rock is calculated as 23 MPa by using weighted average.

Unit weight values of this road cut are summarized in Table 37. Saturated unit weight results are considered in the analyses for fresh and weathered rocks are determined by weighted average of the sandstone and mudstone, which are 25,12 and 25,75 kN/m<sup>3</sup>, respectively.

Table 37. UCS and unit weight values of the rocks at Stop 8

Stop	Rock Type	Fresh		Weathered		Test
		Dry	Saturated	Dry	Saturated	
8	Sandstone	37,69	35,47	19,53	17,67	UCS (MPa)
		23,88	24,74	25,42	25,75	Unit Weight (kN/m <sup>3</sup> )
1	Mudstone	29,50	11,10	26,80	6,90	UCS (MPa)
		22,25	25,47	25,09	25,74	Unit Weight (kN/m <sup>3</sup> )



Figure 47. Fractured mudstone at Stop 8

### ***Discontinuity Properties***

Pole and contour plots of the discontinuities at this road cut are shown in Figure 48. There are three dominant discontinuity sets which are 30/310, 70/170 and 70/070 as dip/dip direction. Joint spacing frequency histogram is shown in Figure 49. Due to the fact that the mudstone beds are highly fractured, they are not included in this spacing analyses. Persistence of the joints is generally longest for the bedding planes and the rest is matching with the spacings. Joints are generally bed confined. Apertures generally do not exceed 5 mm however some of them are measured as

maximum 2 cm which are prone to produce rockfall. Infill materials can be seen in the narrower apertures as damp clayey/silty sand. Block volumes are categorized as moderate according to joint degree measurements.

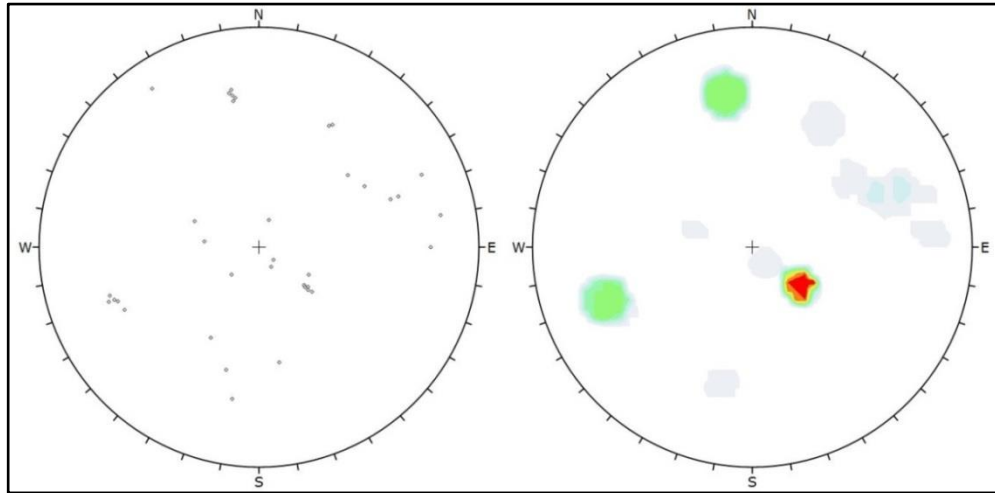


Figure 48. Pole (left) and contour (right) diagrams of the discontinuities at Stop 8

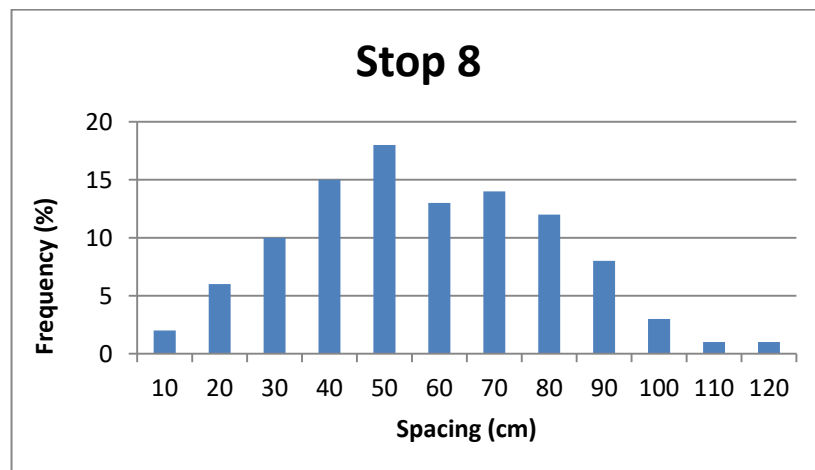


Figure 49. Discontinuity spacing frequency histogram of Stop 8

### ***Weathering and other Properties***

Differential weathering can be observed clearly in this stop because of dramatic strength difference between sandstone and mudstone. While sandstone is slightly weathered, mudstone is in the category of highly weathered. Considering the whole road cut weathering degree is taken as moderately. This weathered zone is 50 cm in average.

Slake durability ( $Id_2$ ) and C.E.C. results are given in Table 38. Fresh and weathered slake durability values are very similar to each other in this road cut because of slightly weathering degree of the sandstone. Due to lack of mudstone sample any slake durability test could not been conducted for the mudstone. However, MBA and CEC values of the weathered mudstone samples could be determined which are nearly 2 times higher than the sandstone values. This result can give a clue about different kinds of weathering degrees in addition to the strength values.

Table 38. Slake durability and methylene blue values of the rocks at Stop 8

Stop	Rock Type	Fresh			Weathered		
		Slake durability ( $Id_2$ )	MBA (gr/100 g)	CEC (meq/100 g)	Slake durability ( $Id_2$ )	MBA (gr/100 g)	CEC (meq/100 g)
8	Sandstone	99,27	0,67	1,50	99,35	0,80	1,80
	Mudstone	-	-	-	-	1,33	3,00

### **4.3.9. Stop 9**

#### ***Description***

This road cut is located about 2 km south of Devrek, in Çaycuma formation. Maximum height of this road cut is about 8 meters. Slope dip amount is measured as  $45^0$ . This road cut consists of nearly 50% of yellowish beige, thick bedded limestone and 50% of light gray thin to thick bedded mudstone (Figure 50).

No slope instability problem affecting the whole slope is seen at the cut slope. However, some small and moderate sized blocks which are already fallen to the toe of the slope and beyond the 2 m high retaining wall made of stones -into the drainage- are observed. Mudstones are only observed as disintegrated fragments as very thin surface failures on the slope.

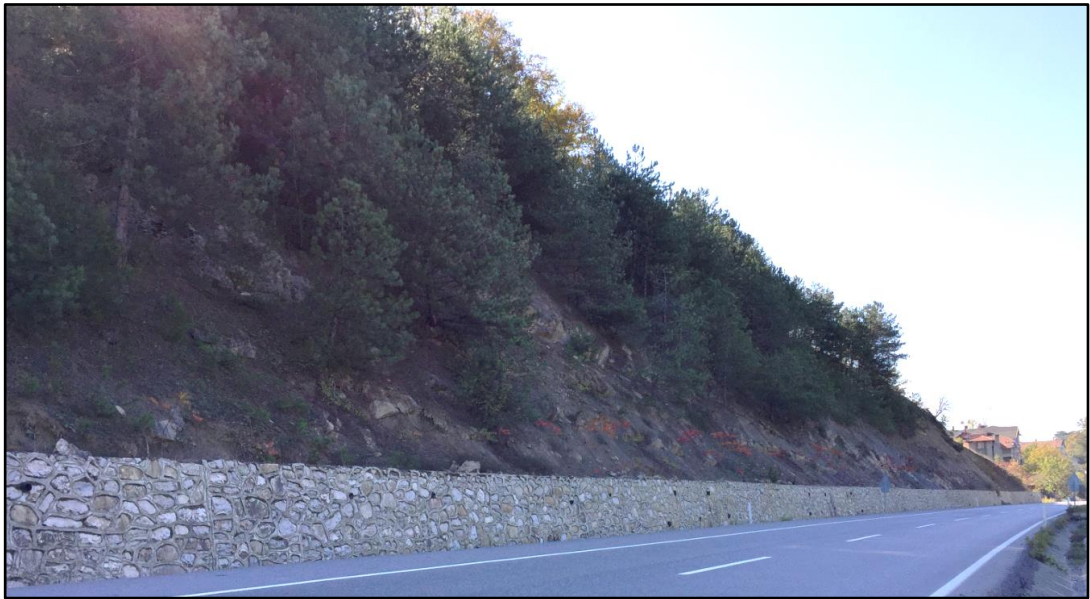


Figure 50. General view of the cut slope at Stop 9

#### ***Strength and Unit Weight***

UCS values of the rocks at this road cut are obtained from point load test for limestone and mudstone (Table 39). In order to convert point load values to UCS, related  $k$  values (16 for limestone and 8 for mudstone) are used. According to these results, the UCS value of the rocks for the whole cut slope is calculated as 55 MPa by using weighted average. Relatively fresh saturated mudstone UCS values are taken from Stop 1 as explained in Stop 8.

Unit weight values of this road cut are summarized in Table 39. Saturated unit weight results are determined by weighted average of the limestone and the mudstone in analyses for fresh and weathered limestone which are 24,60 and 25,46 kN/m<sup>3</sup>, respectively. For the weighted average calculations of unit weight, the fresh mudstone values are taken from Stop 1 because it does not exist in this area. However unit weight of the weathered mudstone could be obtained from this road cut and it is included into the weighted average calculations directly.

Table 39. UCS and unit weight values of the rocks at Stop 9

Stop	Rock Type	Fresh		Weathered		Test
		Dry	Saturated	Dry	Saturated	
9	Limestone	118,40	100,80	83,20	44,80	UCS (MPa)
		24,57	25,08	24,67	25,18	Unit Weight (kN/m <sup>3</sup> )
1	Mudstone	29,50	11,10	10,4	4,00	UCS (MPa)
		22,25	25,47	25,09	25,74	Unit Weight (kN/m <sup>3</sup> )

### ***Discontinuity Properties***

Pole and contour plots of the discontinuities at this road cut are given in Figure 51. Pole plot result does not show a widely scattered structure. Three dominant discontinuity sets are determined as 48/145 for bedding plane, and 66/235 and 30/290 for joints as dip/dip direction. Discontinuity spacing frequency histogram shows that the spacing of discontinuities are mostly concentrated on 20-30-40 cm zone (Figure 52). Only a few spacings are measured wider than 1 m. Persistence of the joints is generally matching with the spacings. Apertures generally measured about 5 mm near the surface, however, only a few of them are filled with damp sandy material. Block volumes are categorized as moderate according to joint degree measurements.

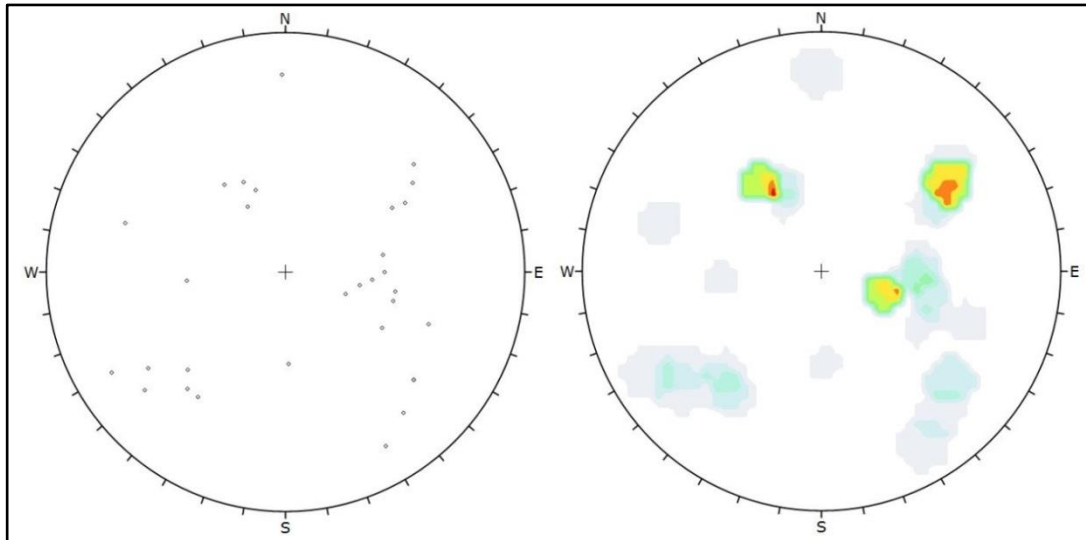


Figure 51. Pole (left) and contour (right) diagrams of the discontinuities at Stop 9

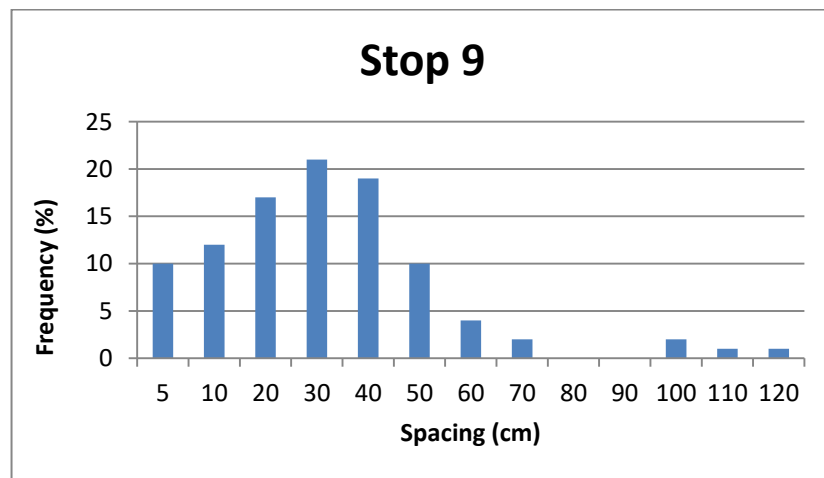


Figure 52. Discontinuity spacing frequency histogram at Stop 9

### ***Weathering and other Properties***

Differential weathering can be observed in this stop because of strength difference between the limestone and the mudstone. While limestone is slightly weathered, mudstone is categorized as highly. Average road cut weathering degree is considered

as moderately. The weathered zone is measured to be 50 cm thick from the cut slope surface.

Slake durability ( $Id_2$ ) and C.E.C. results are given in Table 40. Fresh and weathered slake durability values of the limestone are very similar to each other in this road cut because of slightly weathering degree of limestone. MBA and CEC values of the weathered mudstone samples are determined. These values are significantly higher than MBA and CEC values of the limestone. The difference in the test results indicates that the weathering is slightly effective on the rocks.

Table 40. Slake durability and methylene blue values of Stop 9

Stop	Rock Type	Fresh			Weathered		
		Slake durability ( $Id_2$ )	MBA (gr/100 g)	CEC (meq/100 g)	Slake durability ( $Id_2$ )	MBA (gr/100 g)	CEC (meq/100 g)
9	Limestone	99,30	0,67	1,50	98,88	0,97	1,50
	Mudstone	-	-	-	-	2,53	5,8

#### 4.3.10. Stop 10

##### *Description*

Stop 10 is located about 24 km North of Devrek, in the Çaycuma formation. Maximum height of this road cut is about 8 meters. Slope dip amount is measured as  $50^0$ . This road cut consists of 80% of yellowish beige, coarse grained sandstone and 20% of light gray thin bedded mudstone (Figure 53).

No slope instability problem affecting the whole slope is seen at the cut slope. Some fallen small sized sandstone blocks are observed. Thin bedded mudstone deposits are disintegrated into small fragments due to weathering processes.



Figure 53. General view of the cut slope at Stop 10

#### ***Strength and Unit Weight***

UCS values of the rocks at this road cut are obtained from point load test by using related  $k$  values for each rock type (Table 41). According to these results, UCS value of the rocks is calculated as 17 MPa by using weighted average. Unit weight values of the rocks at this stop are given in Table 41. Saturated unit weight results are determined in analyses by weighted average for fresh and weathered zones which are 24,61 and 25,08  $\text{kN/m}^3$ , respectively.

Table 41. UCS and unit weight values of the rocks at Stop 10

Stop	Rock Type	Fresh		Weathered		Test
		Dry	Saturated	Dry	Saturated	
10	Sandstone	38,78	19,16	11,48	7,50	UCS (MPa)
		23,34	24,40	24,14	24,91	Unit Weight ( $\text{kN/m}^3$ )
1	Mudstone	29,50	11,10	26,80	6,90	UCS (MPa)
		22,25	25,47	25,09	25,74	Unit Weight ( $\text{kN/m}^3$ )

### ***Discontinuity Properties***

Pole and contour plots of the discontinuities at this stop are shown in Figure 54. Pole plot result reveals a scattered structure. Three dominant joint sets are determined among these scattered poles. These are 34/354, 84/226 and 50/160 as dip/dip direction. Joint spacing frequency histogram shows a wide and mostly equally concentrated distribution (Figure 54). All spacings are measured shorter than 1 m. Persistence of the joints are coherent with the spacings. Apertures generally measured less than 5 mm. Infill material between these apertures determined as sandy clay/silt. Block volumes are categorized as moderate according to moderate joint degree measurements.

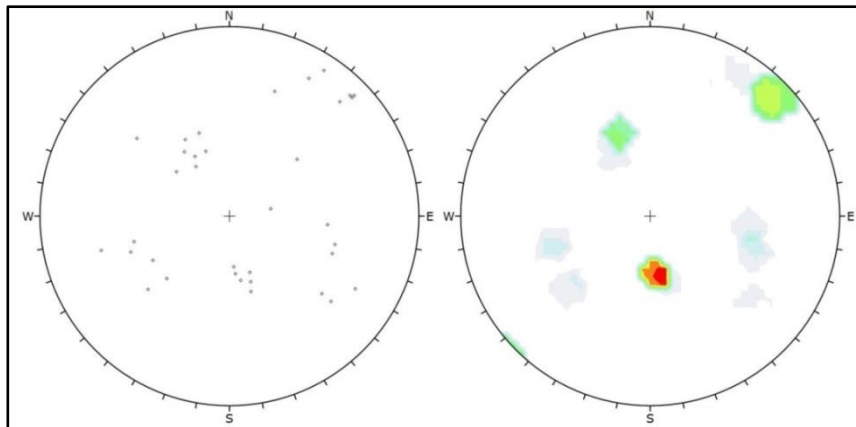


Figure 54. Pole (left) and contour (right) diagrams of the discontinuities at Stop 10

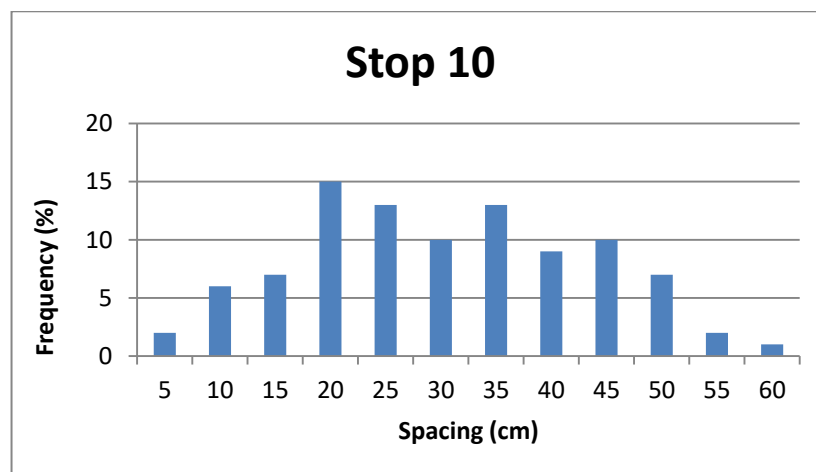


Figure 55. Discontinuity spacing frequency histogram of Stop 10

#### ***Weathering and other Properties***

Differential weathering can be observed in this road cut because of strength difference between sandstone and mudstone. Clearly, due to differential weathering stronger sandstone blocks are hanging over highly weathered mudstone layers. Sandstone layers are determined as slightly weathered. Average road cut weathering degree is considered as moderately. Weathering zone in this road cut is 40 cm from the surface.

Slake durability ( $Id_2$ ) and C.E.C. results are given in Table 42.. MBA and CEC values of the weathered mudstone, however, reveal a bit higher than sandstone.

Table 42. Slake durability and methylene blue values of Stop 10

Stop	Rock Type	Fresh			Weathered		
		Slake durability ( $Id_2$ )	MBA (gr/100 g)	CEC (meq/100 g)	Slake durability ( $Id_2$ )	MBA (gr/100 g)	CEC (meq/100 g)
10	Sandstone	95,56	1,20	2,70	95,08	1,20	2,70
	Mudstone	-	-	-	-	1,33	3,00

#### 4.3.11. Stop 11

##### *Description*

This road cut is located about 0,7 km north of Stop 10, in the Çaycuma formation. Maximum height of this road cut is about 6 meters. Slope dip amount is measured as  $60^{\circ}$ . This road cut consists of 80% of dark brown, coarse grained sandstone and 20% of light brown very thin bedded mudstone (Figure 56). No slope instability problems affecting the whole slope are seen at the cut slope. However, only local surficial degradations are observed.



Figure 56. General view of the cut slope at Stop 11

##### *Strength and Unit Weight*

UCS values of the rocks at this road cut are obtained by the correlation of point load test results (Table 43). According to these results, UCS value of the rock is calculated as 21 MPa by using weighted average of the sandstone from this road cut and the mudstone from Stop 1.

Unit weight values of this stop are given in Table 43. Weighted average unit weight results of the rocks of this road cut are 24,40 and 24,72 kN/m<sup>3</sup>, respectively.

Table 43. UCS and unit weight values of the rocks at Stop 11

Stop	Rock Type	Fresh		Weathered		Test
		Dry	Saturated	Dry	Saturated	
11	Sandstone	25,05	23,72	11,07	6,06	UCS (MPa)
		22,69	24,13	23,43	24,46	Unit Weight (kN/m <sup>3</sup> )
1	Mudstone	29,50	11,10	26,80	6,90	UCS (MPa)
		22,25	25,47	25,09	25,74	Unit Weight (kN/m <sup>3</sup> )

#### ***Discontinuity Properties***

Pole and contour plots of the discontinuities at this stop are shown in Figure 57. Pole plot result reveals an extremely scattered structure. The most three dominant joint sets are determined among these scattered poles. These are 36/336, 60/150 and 87/215 as dip/dip direction. Joint spacing frequency histogram (Figure 58) shows that the maximum spacing is determined as 35 cm. Persistence of the joints is matched with the discontinuity spacings. Apertures are generally measured as less than 5 mm. Infill materials between these apertures meet barely. Infill material – where available- is determined as damp clayey/silty sand. Block volumes are categorized as small according to high joint degree measurements.

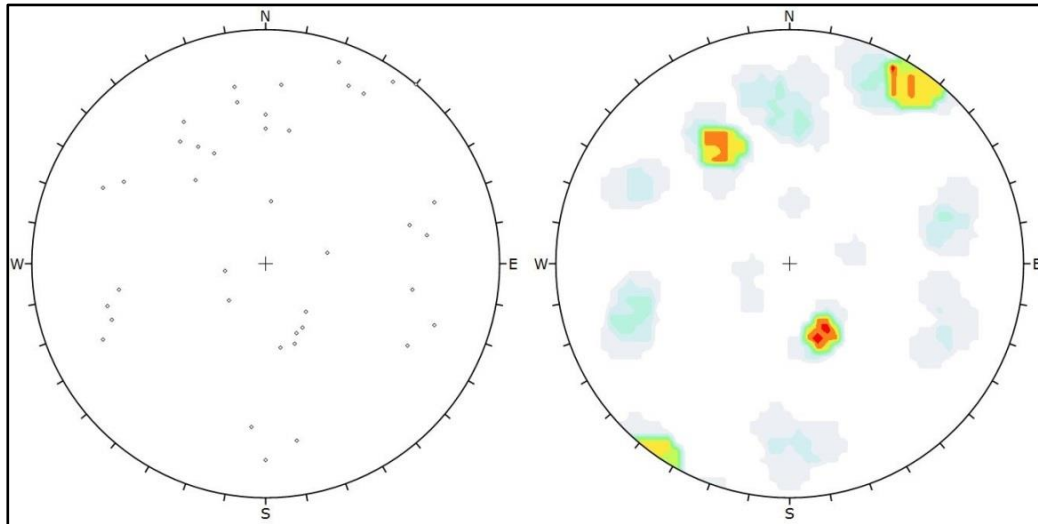


Figure 57. Pole (left) and contour (right) diagrams of the discontinuities at Stop 11

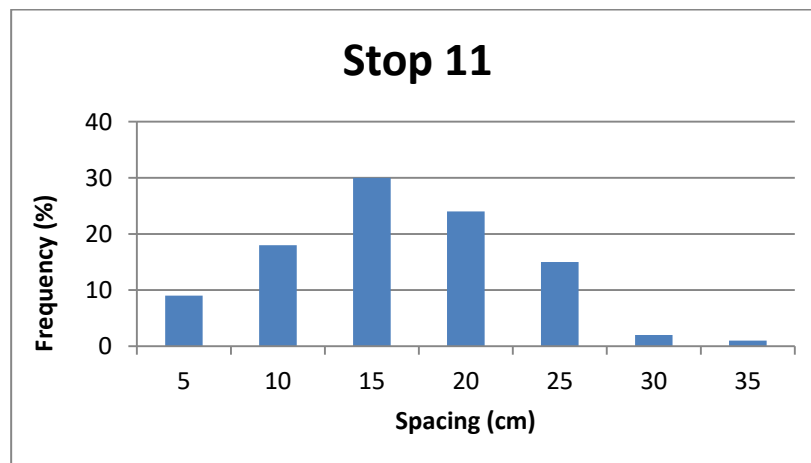


Figure 58. Discontinuity spacing frequency histogram of Stop 11

### ***Weathering and other Properties***

Differential weathering can be observed in this road cut. However, it is not as clear as Stop 8 or 10. The reason is that sandstone layers are as thin as clay layers. In addition, joint degree is high. Where undercutting action take place, small blocks can easily detach from the surface of the slope. Only surface staining is observed on the

sandstone layers which mean that it is slightly weathered. On the other hand in addition to surface staining, the mudstone layers are disintegrated more than the sandstone due to weathering. Considering the whole road cut, weathering degree at this cut slope is taken as moderately. This thin weathered zone is measured as 30 cm from the surface.

Slake durability ( $Id_2$ ) and C.E.C. results are given in Table 44. Fresh and weathered slake durability results are similar to each other for the sandstone. Methylene blue values are higher for the weathered ones. Nevertheless, the weathered mudstone values of methylene blue test are higher than weathered sandstone.

Table 44. Slake durability and methylene blue values of Stop 11

Stop	Rock Type	Fresh			Weathered		
		Slake durability ( $Id_2$ )	MBA (gr/100 g)	CEC (meq/100 g)	Slake durability ( $Id_2$ )	MBA (gr/100 g)	CEC (meq/100 g)
11	Sandstone	97,56	0,93	2,10	97,72	1,60	3,60
	Mudstone	-	-	-	-	2,40	5,50

#### 4.3.12. Stop 12

##### *Description*

This road cut is located about 0,7 km north of Stop 11, in the Çaycuma formation. Maximum height of this road cut is about 6 meters. Slope dip amount is measured as  $50^\circ$ . This road cut consists of 80% of dark brown, coarse grained sandstone and 20% of light brown very thin bedded mudstone (Figure 59). This road cut is very similar to Stop 11 in general except  $10^\circ$  slope difference.

No slope instability problems affecting the whole slope are seen at the cut slope. However, as it be seen in Figure 59, surficial degradations are dominant nearly at one third of the slope. Moreover, any large blocks fallen from the slope are not observed.



Figure 59. General view of the cut slope at Stop 12

### ***Strength and Unit Weight***

UCS values of the rocks at this road cut are obtained by the correlation of point load test results (Table 45). According to these results, UCS value of the rocks is calculated as 10 MPa by using weighted average of the sandstone of this road cut and the mudstone of Stop 1. Increase of surficial degradation and debris amount for this road cut compared to Stop 11 can be explained by the decrease of UCS value by half.

Unit weight values of the rocks at this stop are given in Table 45. Saturated unit weight results of the fresh and weathered rocks of this road cut are determined by weighted average as 24,47 and 24,80 kN/m<sup>3</sup>, respectively which are nearly the same values as Stop 11.

Table 45. UCS and unit weight values of the rocks at Stop 12

Stop	Rock Type	Fresh		Weathered		Test
		Dry	Saturated	Dry	Saturated	
12	Sandstone	15,43	9,94	14,77	5,46	UCS (MPa)
		22,92	24,22	23,40	24,57	Unit Weight (kN/m <sup>3</sup> )
1	Mudstone	29,50	11,10	26,80	6,90	UCS (MPa)
		22,50	25,47	25,09	25,74	Unit Weight (kN/m <sup>3</sup> )

### ***Discontinuity Properties***

Pole and contour plots of the discontinuities at this stop are shown in Figure 60. Pole plot result reveals a scattered structure as in Stop 11. Three dominant discontinuity sets are determined as 35/180, 55/005 and 66/298 in the order of dip/dip direction. Discontinuity spacing frequency histogram (Figure 61) reveals that the maximum spacing is about 35 cm which is very similar to Stop 11. Persistence of the joints is matched with the discontinuity spacings. Apertures are generally measured less than 5 mm, and infill materials between these apertures are determined as damp clayey/silty sand. Block volumes are categorized as small according to high joint degree measurements.

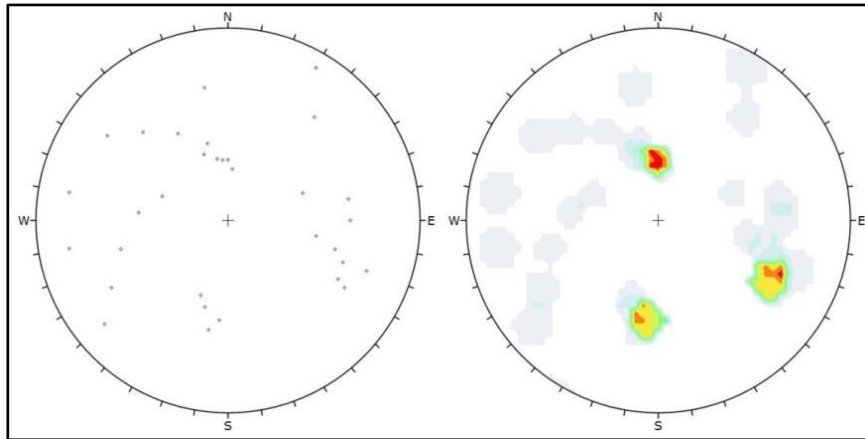


Figure 60. Pole (left) and contour (right) diagrams of the discontinuities at Stop 12

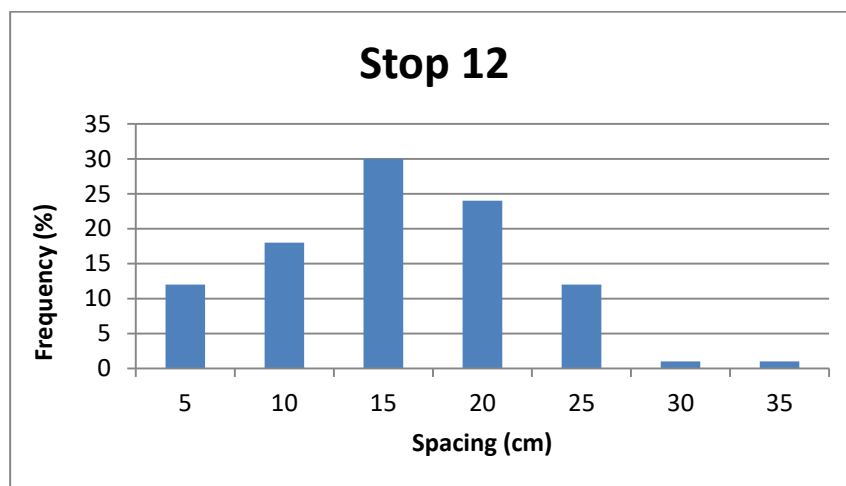


Figure 61. Discontinuity spacing frequency histogram of Stop 12

### ***Weathering and other Properties***

Similar to Stop 11, this road cut also reveals differential weathering due to strength differences between the sandstone and the mudstone. The sandstone is moderately weathered and the mudstone in between them is highly weathered. Considering high amount of surficial degradation due to disintegration and high amount of debris at the toe of the slope, the weathering degree of the road cut is determined as highly. After all, the weathered zone at the surface of this road cut is measured as 30 cm.

Even surface degradation is high, slake durability ( $Id_2$ ) values of the rocks are very high against degradation (Table 46). MBA and CEC values are similar to each other for both relatively fresh and weathered zones (Table 46). All in all, high amount of debris deposit at the toe due to surficial degradation can be explained by very low strength of both the sandstone and the mudstone for this road cut.

Table 46. Slake durability and methylene blue values of the rocks at Stop 12

Stop	Rock Type	Fresh			Weathered		
		Slake durability ( $Id_2$ )	MBA (gr/100 g)	CEC (meq/100 g)	Slake durability ( $Id_2$ )	MBA (gr/100 g)	CEC (meq/100 g)
12	Sandstone	99,36	1,33	3,00	98,65	1,33	3,00

#### 4.3.13. Stop 13

##### *Description*

This stop is located approximately 0,2 km north of Stop 12, in the Çaycuma formation. Total height of this road cut is determined about 20 m with 1 bench, the lower one is about 8 m. Slope dip amount is measured as  $70^0$ . This road cut consists of 70% of dark gray to light brown, coarse to fine grained sandstone and 30% of light gray thin bedded mudstone (Figure 62).

No slope instability problems affecting the whole slope are seen at the cut slope. Only surficial degradations are observed due to weathering. Debris deposits due to surficial degradation are more above the bench compared to lower part. There could be two reasons to explain this; first is that upper part is higher than the lower part of the bench and the failed material could be taken away in the drainage channel.



Figure 62. General view of the cut slope at Stop 13

### ***Strength and Unit Weight***

UCS values of the rocks at this road cut are obtained by the correlation of point load test results (Table 47). According to these results UCS value of the rocks is calculated as 11 MPa by using weighted average. The UCS values are obtained from point load test by applying related  $k$ , which is 5,4.

Unit weight values of this stop are given in Table 47. Saturated unit weight results obtained from weighted average of the sandstone from this road cut and the mudstone from Stop 1 are used in the analyses for the mass. The unit weight values are 24,18 and 24,33 kN/m<sup>3</sup>, respectively.

Table 47. UCS and unit weight values of the rocks at Stop 13

Stop	Rock Type	Fresh		Weathered		Test
		Dry	Saturated	Dry	Saturated	
13	Sandstone	18,83	10,58	10,20	6,10	UCS (MPa)
		21,88	23,62	21,89	23,73	Unit Weight (kN/m <sup>3</sup> )
1	Mudstone	29,50	11,10	26,80	6,90	UCS (MPa)
		22,25	25,47	25,09	25,74	Unit Weight (kN/m <sup>3</sup> )

### *Discontinuity Properties*

Pole and contour plots of the discontinuities at this stop are shown in Figure 63. Pole plot result reveals a scattered structure through East-West direction. Three dominant joint sets are introduced as 45/180, 84/260 and 50/310 as dip/dip direction. Joint spacing frequency histogram reveals that the discontinuity spacings are dominant at smaller than 20 cm zone (Figure 64). Maximum joint spacing is measured as 65 cm only a few times. Persistence of the joints matching with the spacings is generally longer along the bedding planes. The apertures are generally measured as less than 5 mm. Some apertures are lack of infill. On the other hand, the filled apertures are consisting of damp clayey/silty sand. Block volumes are categorized as small according to high joint degree measurements.

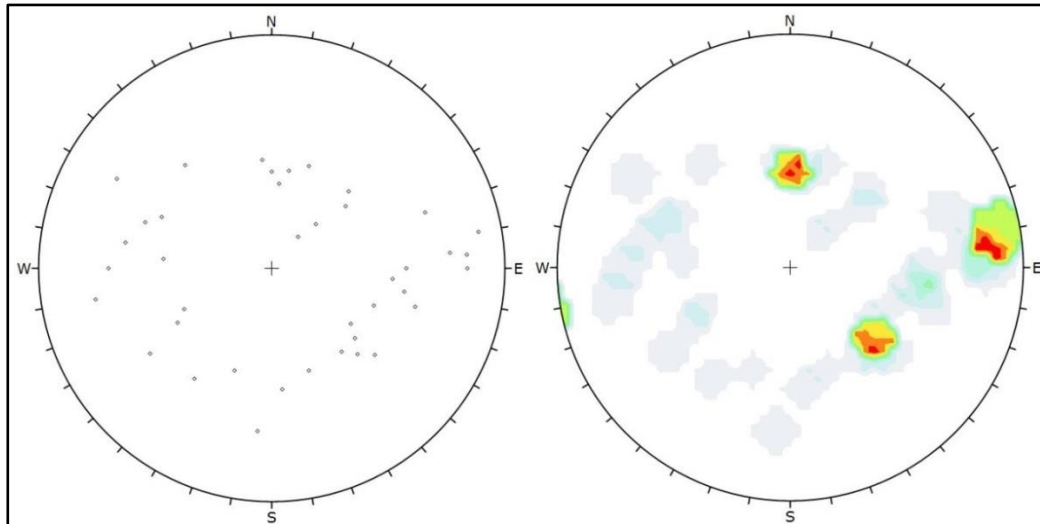


Figure 63. Pole (left) and contour (right) diagrams of the discontinuities at Stop 13

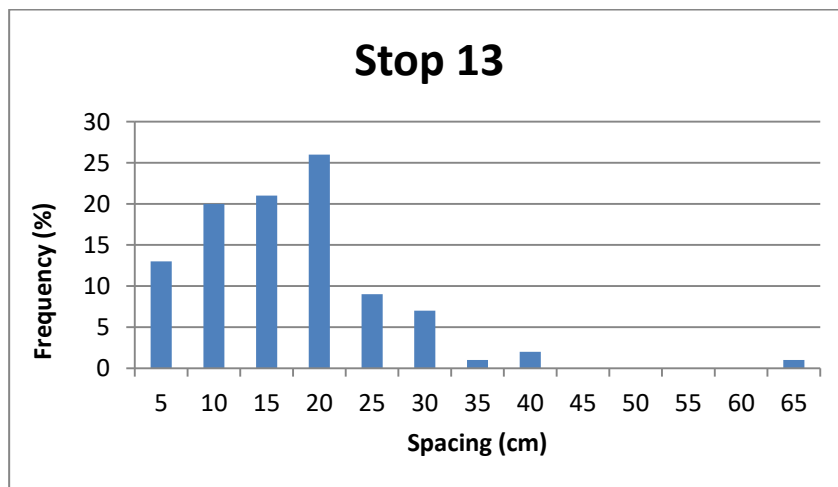


Figure 64. Discontinuity spacing frequency histogram of Stop 13

### ***Weathering and other Properties***

In this road cut, undercutting action is encountered approximately 20 cm in depth because of differential weathering. The sandstone is determined as slightly weathered and mudstone in between them is highly weathered. Whole rock mass is considered

to be moderately weathered in the analyses. Average weathered zone thickness is determined as 45 cm from the surface.

According to the slake durability values, the sandstone has medium high durability which is low if compared with the other sandstones before this road cut (Table 48). MBA and CEC values of fresh and weathered sandstone and weathered mudstone are given in Table 48.

Table 48. Slake durability and methylene blue values of Stop 13

Stop	Rock Type	Fresh			Weathered		
		Slake durability (Id <sub>2</sub> )	MBA (gr/100 g)	CEC (meq/100 g)	Slake durability (Id <sub>2</sub> )	MBA (gr/100 g)	CEC (meq/100 g)
13	Sandstone	94,55	1,07	2,40	91,80	1,20	2,70
	Mudstone	-	-	-	-	2,00	4,60

#### 4.3.14. Stop 14

##### *Description*

This road cut is located approximately 0,3 km north of Stop 13, in the Çaycuma formation. Total height of this road cut is measured about 15 m with 1 bench, the lower one is about 10 m. The slope dip amount is measured as 50°. This road cut consists of 80% of dark brown to light gray, coarse to fine grained sandstone and 20% of light greenish gray thin bedded mudstone (Figure 65). This road cut is completely stable. Surficial degradations due to weathering of mudstone can be observed as deposition at the toe of the slope between sandstone layers (Figure 65).



Figure 65. General view of the cut slope at Stop 14

### ***Strength and Unit Weight***

Considering point load values of the rocks at this road cut, UCS values are determined by correlating k factor which is 5,4 for the sandstone (Table 49). According to these results, the UCS value is calculated as 14 MPa by using weighted average of the sandstone of this road cut and the mudstone of Stop 1. The point load tests are conducted on parallel and normal to the plane of anisotropy. For this road, the cut parallel values are preferred because bedding planes are nearly vertical as it can be seen from Figure 65.

Table 49. UCS values of the rocks at Stop 14

		UCS (MPa)				
		Fresh		Weathered		
Stop	Rock Type	Dry	Saturated	Dry	Saturated	
14	Sandstone	60,71	21,73	31,75	20,78	+
		21,28	15,18	19,61	13,16	=
1	Mudstone	29,50	11,10	26,80	6,90	=

Unit weight values of the sandstone in this road cut are shown in Table 50. The saturated unit weight results of the fresh and weathered rocks at this road cut determined by average weight of the sandstone of this cut slope and mudstone of Stop 1 are 25,00 and 25,23 kN/m<sup>3</sup>, respectively.

Table 50. Unit weight values of the rocks at Stop 14

Stop	Rock Type	Unit Weight (kN/m <sup>3</sup> )			
		Fresh		Weathered	
		Dry	Saturated	Dry	Saturated
14	Sandstone	23,84	24,88	24,18	25,10
1	Mudstone	22,25	25,47	25,09	25,74

### ***Discontinuity Properties***

Pole and contour plots of the discontinuities at this stop are given in Figure 66. Due to highly fractured structure, pole plot reveals a scattered view. Three dominant joint sets are introduced as 75/130, 80/035 and 84/215 in the order of dip/dip direction. Joint spacing frequency histogram is shown in Figure 67. Only a few measurements could be taken over 35 cm spacing between joints. Persistence is generally longer along the bedding planes but they are mostly coherent with the spacing

measurements. Apertures of the joints are not exceeding 5 mm and they are generally filled with damp sandy material. Because fracture frequency is high, block volumes are calculated in the category of small.

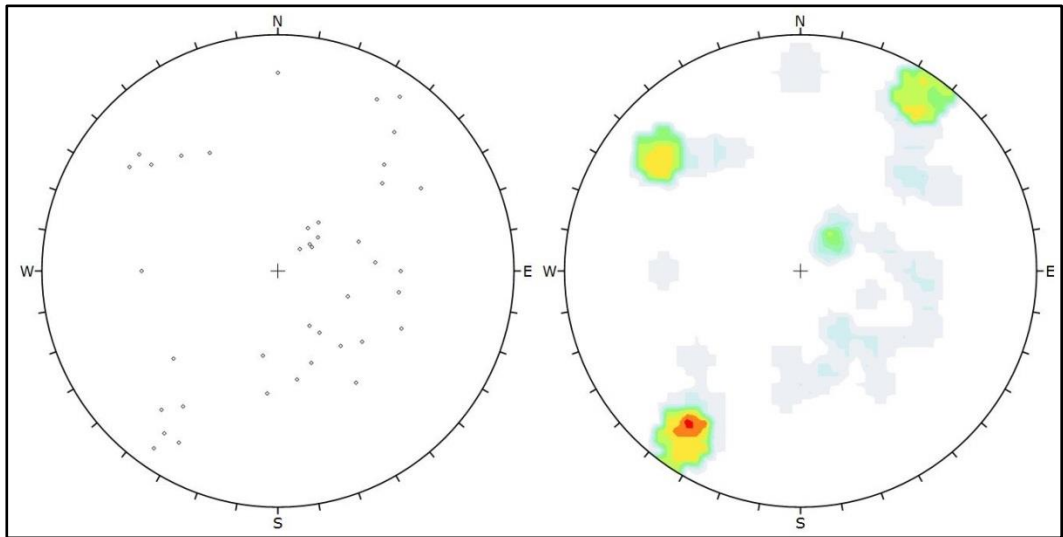


Figure 66. Pole (left) and contour (right) diagrams of the discontinuities at Stop 14

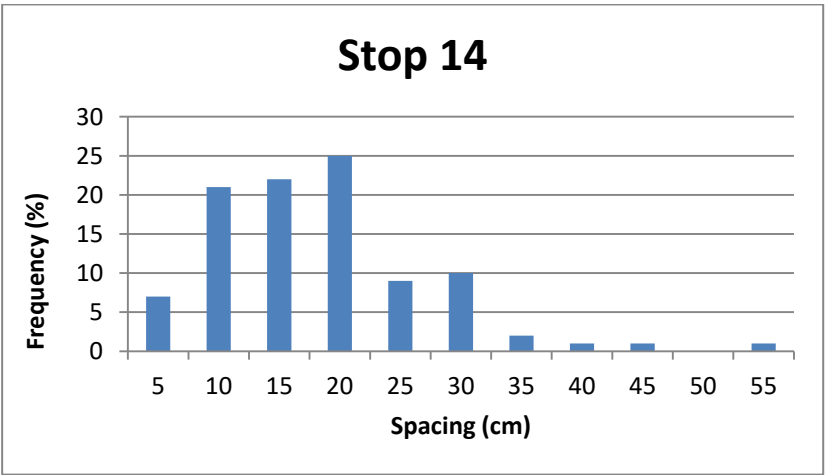


Figure 67. Discontinuity spacing frequency histogram of Stop 14

### ***Weathering and other Properties***

As in Stop 13, undercutting action is taken place in this road cut approximately 20 cm in depth because of differential weathering in other words strength difference between sandstone and mudstone. Highly weathered mudstone between slightly weathered sandstone layers can be determined visually by considering debris deposition at the toe of the slope. This rock mass is considered to be moderately weathered. The weathered zone at the surface is determined as 50 cm thick.

Significant difference between relatively fresh and weathered sandstones with surface degradation is observed for this road cut (Table 51). MBA and CEC values of relatively fresh and weathered sandstone are given in Table 51. Same significant difference can be observed for methylene blue values as well.

Table 51. Slake durability and methylene blue values of the rocks Stop 14

Stop	Rock Type	Fresh			Weathered		
		Slake durability (Id <sub>2</sub> )	MBA (gr/100 g)	CEC (meq/100 g)	Slake durability (Id <sub>2</sub> )	MBA (gr/100 g)	CEC (meq/100 g)
14	Sandstone	97,55	1,47	3,30	89,06	2,27	5,20

### **4.3.15. Stop 15**

#### ***Description***

This road cut is located 0,5 km north of Stop 14, in the Çaycuma formation. Maximum height of this road cut is measured about 15 m. Slope dip amount is measured as 50°. This road cut consists of 80% of light beige to dark brown, fine grained sandstone and 20% of greenish gray mudstone in general (Figure 68). In some parts of this stop especially at the right side, the mudstone and the sandstone percentages are nearly equal. Nevertheless, at the left side of the road cut, thick mudstone layers are interbedded by thin sandstone layers. Surficial degradations of the rocks are observed due to weathering action. It is observed that some degraded rock pieces are deposited at the drainage channel.



Figure 68. General view of the cut slope at Stop 15

### ***Strength and Unit Weight***

UCS values of the rocks at this road cut are determined from the point load values (Table 52). According to these results, the UCS value is calculated as 28 MPa by using weighted average of the sandstone from this road cut and the mudstone from Stop 1. Considering potential failure direction, UCS values obtained from the point load test conducted normal to the plane of anisotropy are used.

Table 52. UCS values of the rocks at Stop 15

		UCS (MPa)				
		Fresh		Weathered		
Stop	Rock Type	Dry	Saturated	Dry	Saturated	
15	Sandstone	40,07	31,58	36,17	24,88	+
		32,85	23,15	26,03	12,98	=
1	Mudstone	29,50	11,10	26,80	6,90	=

Unit weight values of the sandstone in this stop are given in Table 53 which are similar to stop 14. The saturated unit weight results of the relatively fresh and weathered rocks are determined by weighted average of the sandstone from this road cut and the mudstone from Stop 1 are 24,86 and 25,26 kN/m<sup>3</sup>, respectively.

Table 53. Unit weight values of the rocks at Stop 15

		Unit Weight (kN/m <sup>3</sup> )			
		Fresh		Weathered	
Stop	Rock Type	Dry	Saturated	Dry	Saturated
15	Sandstone	23,74	24,71	24,41	25,14
1	Mudstone	22,25	25,47	25,09	25,74

### ***Discontinuity Properties***

Pole and contour plots of the discontinuities at this cut slope are given in Figure 69. Even pole plot reveals a scattered view; it is not as much as stop 14 because of moderate degree of jointing. Three dominant joint sets are clearly visible in the contour plot. They are introduced as 55/330, 49/145 and 78/255 in the order of dip/dip direction. Joint spacing frequency histogram shows a very wide range of measurements (Figure 70). Comparing other stops, discontinuity spacings are a little bit wider for this road cut. Approximately 10% of the measurements reveals that the spacings are between 70 cm to 130 cm. Persistence for bedding planes is generally longer than the other joints which are generally bed confined. Apertures of the joints are similar to stop 14 that are not exceeding 5 mm and they are generally filled with damp clayey/silty sand. Block volumes are determined as moderate due to moderate degree of jointing.

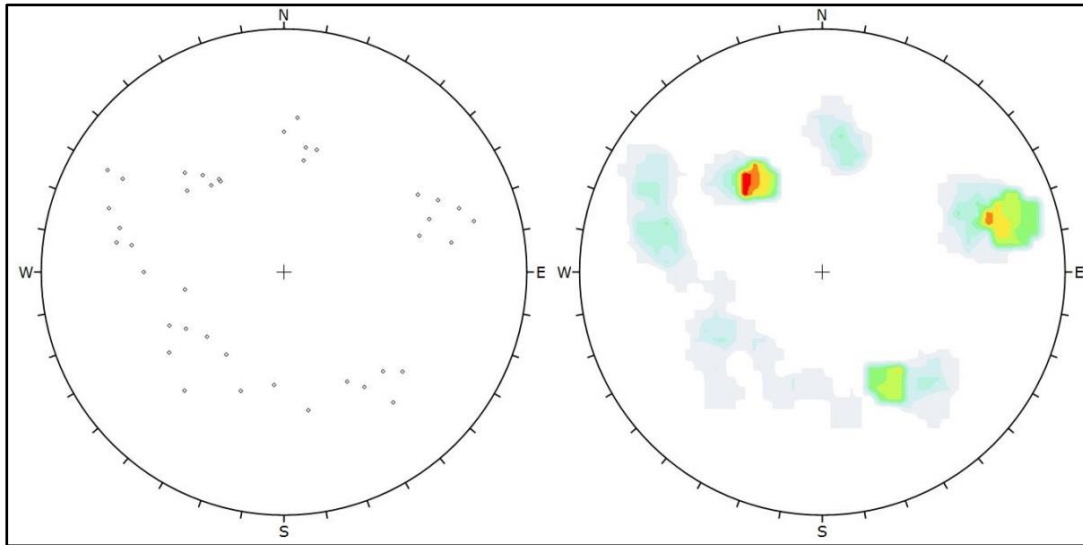


Figure 69. Pole (left) and contour (right) diagrams of the discontinuities at Stop 15

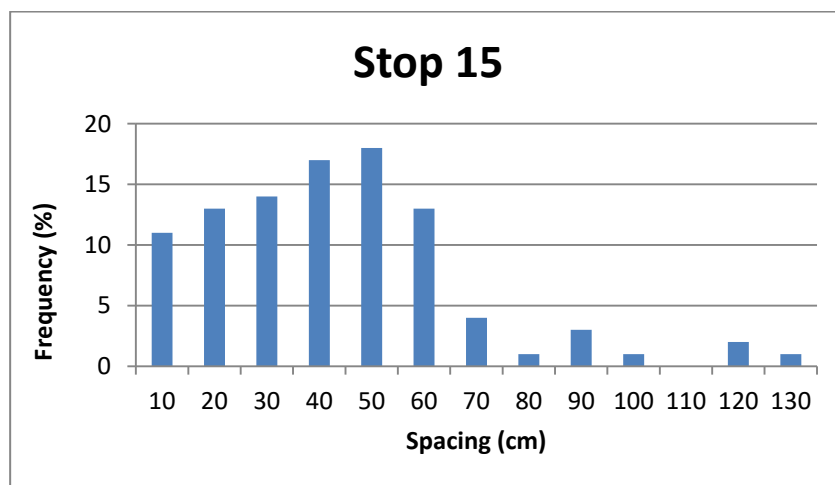


Figure 70. Discontinuity spacing frequency histogram of Stop 15

### ***Weathering and other Properties***

Differential weathering is very obvious and can be determined clearly in field at this cut slope. Especially at the right side of the road cut, shiny and undisturbed sandstone beds are alternating with highly weathered and decomposed mudstones. At the left side, on the other hand, undercutting action can be observed visually.

Because of this undercutting action, relatively larger sandstone blocks fell down compared to the right side. Considering these properties, whole road cut is determined as moderately weathered. This weathering zone at the surface is approximately 30 cm thick.

According to slake durability ( $Id_2$ ), results degradation at this road cut would be very low due to very high durability conditions (Table 54). Highest cation exchange capacity is observed at this road cut among all road cuts and mudstones.

Table 54. Slake durability and methylene blue values of the rocks at Stop 15

Stop	Rock Type	Fresh			Weathered		
		Slake durability ( $Id_2$ )	MBA (gr/100 g)	CEC (meq/100 g)	Slake durability ( $Id_2$ )	MBA (gr/100 g)	CEC (meq/100 g)
15	Sandstone	98,56	1,07	2,40	97,81	1,20	2,70
	Mudstone	-	-	-	-	2,67	6,10

#### 4.3.16. Stop 16

##### *Description*

This stop is located nearly 26 km south of Zonguldak, in the Çaycuma formation. Maximum height of this road cut is determined about 6 m with an approximate 2 m retaining wall in front of it. Slope dip amount is measured as  $55^0$ . This road cut consists of yellowish beige, coarse grained, poorly-lithified sandstone (Figure 71). This road cut is completely stable. Very small blocks are encountered on the wall and some of them are beyond the wall in the drainage channel. This indicates that only surficial degradations took place at this slope.



Figure 71. General view of the cut slope at Stop 16

### ***Strength and Unit Weight***

Because this stop formed by sandstone layers completely, UCS values are determined directly from the point load values of the sandstone (Table 55). Considering failure direction, UCS values obtained from point load test conducted normal to the plane of anisotropy are used. Considering dip directions and amounts of bedding planes normal to the plane (⊥) point load values are chosen to be used. Even fresh and weathered results do not show significant differences, strength of parallel to anisotropy planes are nearly half of normal to the planes. According to these results UCS value of the rock is calculated as 13 MPa.

Unit weight values of sandstone in this slope are given in Table 56. Saturated unit weight results of the fresh and weathered sandstones are 23,92 and 24,50 kN/m<sup>3</sup>, respectively.

Table 55. UCS values of the sandstone at Stop 16

		UCS (MPa)				
		Fresh		Weathered		
Stop	Rock Type	Dry	Saturated	Dry	Saturated	
16	Sandstone	26,93	12,95	21,62	12,65	+
		13,48	9,20	9,93	6,23	=

Table 56. Unit weight values of the sandstones at Stop 16

		Unit Weight (kN/m <sup>3</sup> )			
		Fresh		Weathered	
Stop	Rock Type	Dry	Saturated	Dry	Saturated
16	Sandstone	22,65	23,92	23,47	24,50

### *Discontinuity Properties*

Pole and contour plots are created according to whole road cut are given in Figure 72. Pole plot shows a scattered view mostly in north western, however, some measurements were taken from the other directions as well. Three dominant discontinuity sets are determined as 65/350, 60/080 and 50/165 in the order of dip/dip direction. Joint spacing frequency histogram can be seen in Figure 73. A few measurements could be taken over 1 m. Joints are generally bed confined and persistence is coherent with the discontinuity spacings. Highest persistence is obtained along bedding planes. Apertures of the joints are generally observed as more than 5 mm and they are filled with damp sand and clay sized materials. High degree of jointing at this road cut formed moderate block sizes.

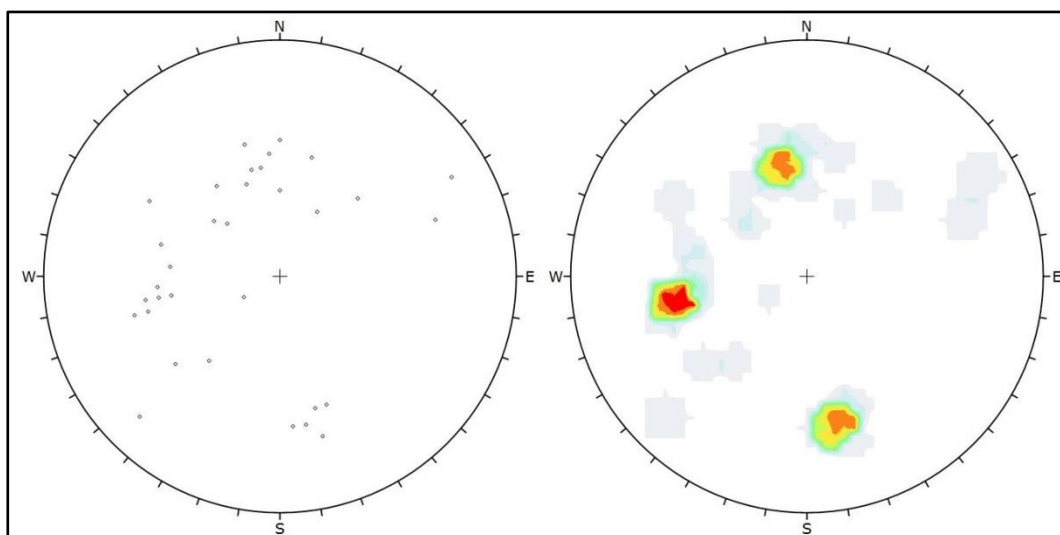


Figure 72. Pole (left) and contour (right) diagrams of the discontinuities at Stop 16

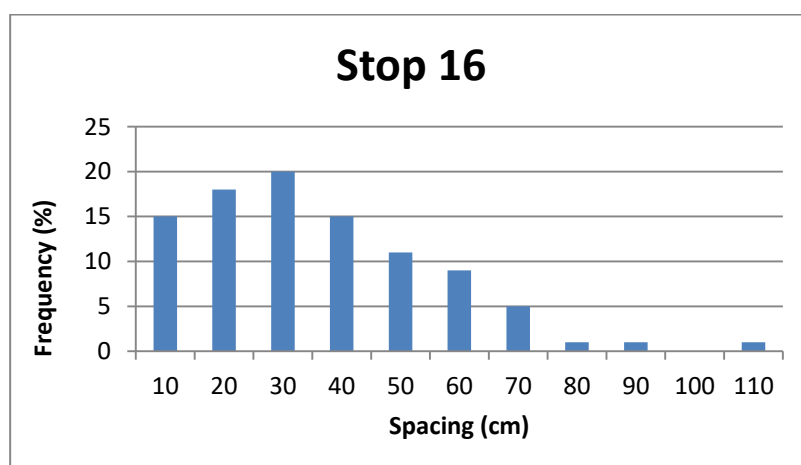


Figure 73. Discontinuity spacing frequency histogram of Stop 16

### ***Weathering and other Properties***

Weathering degree of this road cut is determined as mostly moderately. At some part of the slope, generally thicker sandstone layers show only surface staining along discontinuities. However, in general the sandstone disintegrated into small fragments

which refers moderate weathering category. The weathering zone at the surface is measured as 30 cm thick.

According to slake durability ( $Id_2$ ) results, degradation at this road cut would be low due to high durability conditions (Table 57). The Value differences between relatively fresh and weathered slake durability of the rocks is due to weathering intensity. Despite these differences, methylene blue values (MBA and CEC) are found to be the same for fresh and weathered specimens.

Table 57. Slake durability and methylene blue values of the sandstone at Stop 16

Stop	Rock Type	Fresh			Weathered		
		Slake durability ( $Id_2$ )	MBA (gr/100 g)	CEC (meq/100 g)	Slake durability ( $Id_2$ )	MBA (gr/100 g)	CEC (meq/100 g)
16	Sandstone	97,36	0,93	2,10	91,21	0,93	2,10

#### 4.3.17. Stop 17

##### *Description*

This slope is located 1 km west of Stop 16, in the Çaycuma formation. Maximum height of this road cut is approximately 6 m. Slope dip amount is measured as  $45^0$ . This stop consists of yellowish beige, coarse grained, poorly-lithified sandstone (Figure 74). Only surficial degradations of the rocks from very thin zone due to weathering are observed at this cut slope. Very small detached blocks are deposited at the toe of the slope in the drainage.



Figure 74. General view of the cut slope at Stop 17

### ***Strength and Unit Weight***

This stop consists of only sandstone layers, which are in low strength (Table 58). These UCS values are obtained from the point load tests. According to these results, UCS value of the rock at this road cut is chosen as 11 MPa. This value is chosen by considering failure direction. As it can be seen from the figure, the sandstone layers are nearly parallel to road which concludes that point load values of normal to the plane (+) should be used for stability analyses. Reduction in rock strength can be observed from dry to saturated and relatively fresh to weathered rocks. However, significant differences could not be observed due to anisotropy. The point load tests for some testing samples could not be conducted because of invalid testing.

Unit weight values of the sandstone in this slope are given in Table 59. Saturated unit weight results of the fresh and weathered sandstone are 23,53 and 24,11 kN/m<sup>3</sup>, respectively. These values are very close to stop 16 values.

Table 58. UCS values of the rocks at Stop 17

		UCS (MPa)				
		Fresh		Weathered		
Stop	Rock Type	Dry	Saturated	Dry	Saturated	
17	Sandstone	17,75	11,38	11,62	7,58	+
		10,69	8,32	9,61	6,93	=

Table 59. Unit weight values of the rocks at Stop 17

Stop	Rock Type	Unit Weight (kN/m <sup>3</sup> )			
		Fresh		Weathered	
		Dry	Saturated	Dry	Saturated
17	Sandstone	22,01	23,53	22,59	24,11

### *Discontinuity Properties*

Pole and contour plots of the discontinuities at this road cut are given in Figure 75. Pole plot shows a scattered view and dip amounts generally do not exceed  $60^0$ . Three most dominant discontinuity sets are determined as 50/350, 60/080 and 50/195 in the order of dip/dip direction. According to the field data, joint discontinuity frequency histogram is drawn and it reveals that spacing values do not reach 50 cm (Figure 76). Joints are generally bed confined and persistence is coherent with discontinuity spacings. The joints are generally observed as more than 5 mm and they are filled with damp clay sized materials. Degree of jointing is determined as high and block sizes are calculated as small.

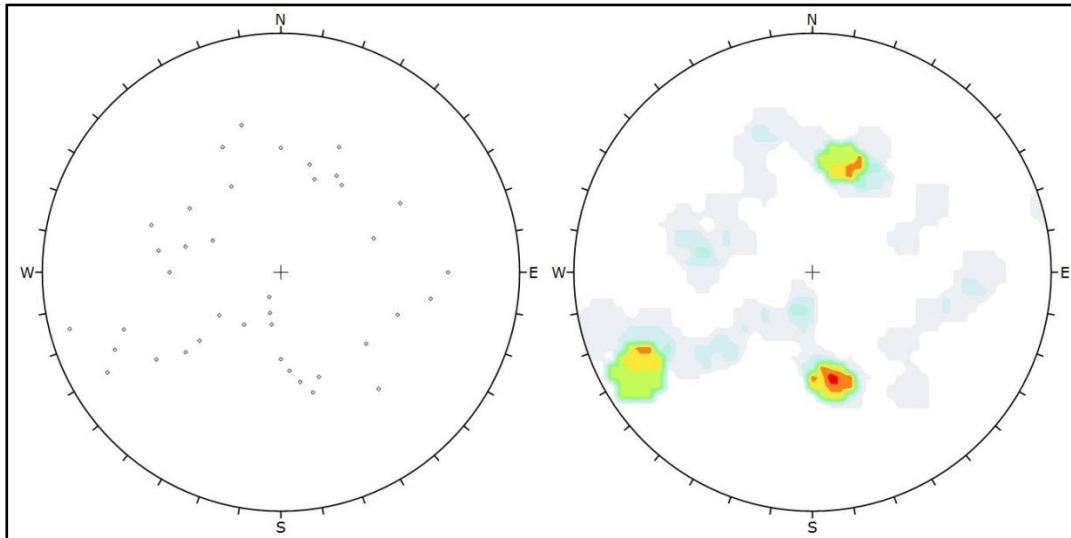


Figure 75. Pole (left) and contour (right) diagrams of the discontinuities at Stop 17

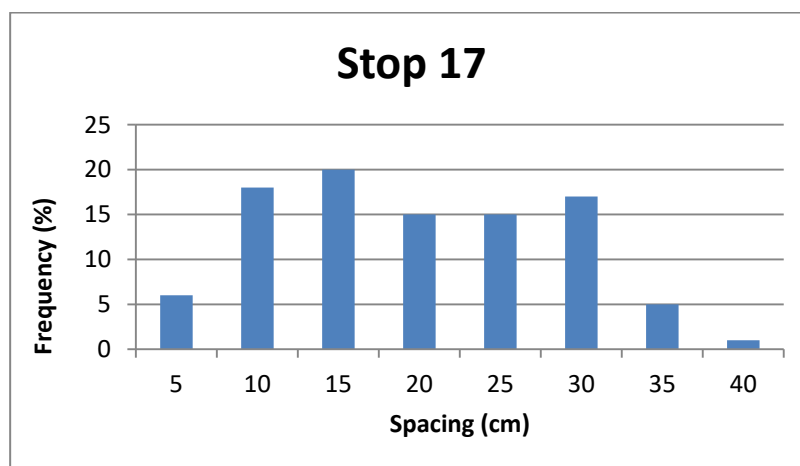


Figure 76. Discontinuity spacing frequency histogram of Stop 17

### ***Weathering and other Properties***

This road cut is determined as moderately weathered. Due to low strength and poorly lithified structure of this sandstone, the weathering causes surficial degradations mainly in the form of soil like material. The weathering zone at the surface is measured as 30 cm thick.

As slake durability test results indicate this stop has medium to medium high slake durability (Table 60). The sandstone has the lowest durability values among all studied road cuts. Especially, the weathered zone is prone to degradation. This explains the low visibility of joints. Despite these differences, methylene blue values (MBA and CEC) are determined to be nearly the same for relatively fresh and weathered rocks at this stop.

Table 60. Slake durability and methylene blue values of the rock at Stop 17

Stop	Rock Type	Fresh			Weathered		
		Slake durability (Id <sub>2</sub> )	MBA (gr/100 g)	CEC (meq/100 g)	Slake durability (Id <sub>2</sub> )	MBA (gr/100 g)	CEC (meq/100 g)
17	Sandstone	88,42	1,33	3,00	78,47	1,47	3,30

#### 4.3.18. Stop 18

##### *Description*

This slope is located about 21 km south of Zonguldak, in the Akveren formation. Maximum height of this road cut is about 10 m. Slope dip amount is measured as 45°. This stop consists of 70% light gray to beige, thin bedded, heavily fractured marl and 30 % dark gray to light brown thin bedded mudstone (Figure 77). Surficial degradations of the rocks due to weathering and erosion are observed at this cut slope. As it can be seen from the figure below, very small fragments –soil like- of mudstone are deposited at the toe of the slope. Some already degraded small marl fragments can also be observed.



Figure 77. General view of the cut slope at Stop 18

### ***Strength and Unit Weight***

UCS values of the rocks at this road cut are determined from the point load test results (Table 61). Correlation factor  $k$  is used as 11 from literature survey and saturated fresh UCS value is calculated as 42 MPa for marl. Using average weighting for strength is resulted as 32 MPa for whole rock slope considering mudstone strength as 10 MPa obtained from Stop 1. Even there are not significant differences between relatively fresh and weathered strength values of marl, saturated values of them are nearly half of the dry ones.

Unit weight values of the marl in this slope are given in Table 61. Saturated unit weight results of fresh and weathered rocks at this cut slope determined by weighted average of the marl from this road cut and mudstone from Stop 1 are 25,38 and 25,47  $\text{kN/m}^3$ , respectively.

Table 61. UCS and unit weight values of the rocks at Stop 18

Stop	Rock Type	Fresh		Weathered		Test
		Dry	Saturated	Dry	Saturated	
18	Marl	75,57	42,06	60,05	36,41	UCS (MPa)
		24,81	25,34	24,88	25,36	Unit Weight (kN/m <sup>3</sup> )
1	Mudstone	29,50	11,10	26,80	6,90	UCS (MPa)
		22,25	25,47	25,09	25,74	Unit Weight (kN/m <sup>3</sup> )

### *Discontinuity Properties*

Pole and contour plots of the discontinuities at this road cut are given in Figure 78. Pole plot does not show an extreme scattered form. Three most dominant joint sets are determined as 75/150, 81/262 and 40/085 as dip/dip direction. Maximum spacing of the discontinuities is measured along bedding planes which is 65 cm (Figure 79). Joints are generally bed confined and persistence is coherent with the spacings. Apertures are mostly less than 5 mm filled with damp clayey/silty sand. High degree of jointing in the rocks implies small sized blocks, which are matched with the already fallen marl fragments.

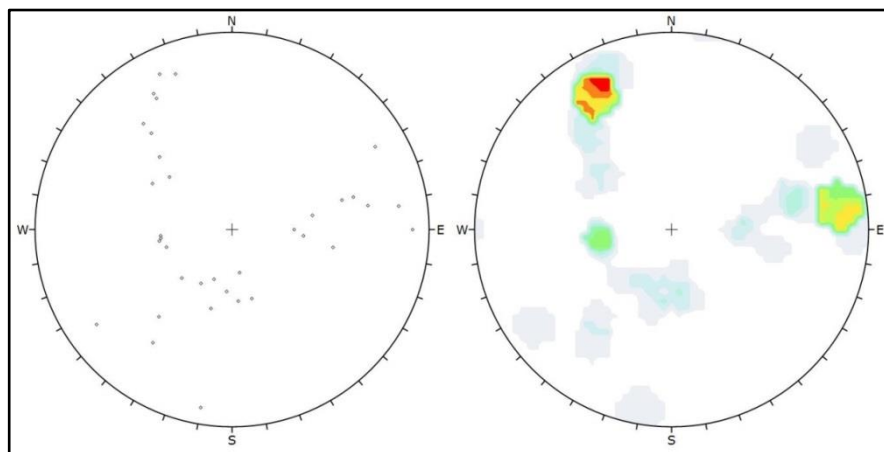


Figure 78. Pole (left) and contour (right) diagrams of the discontinuities Stop 18

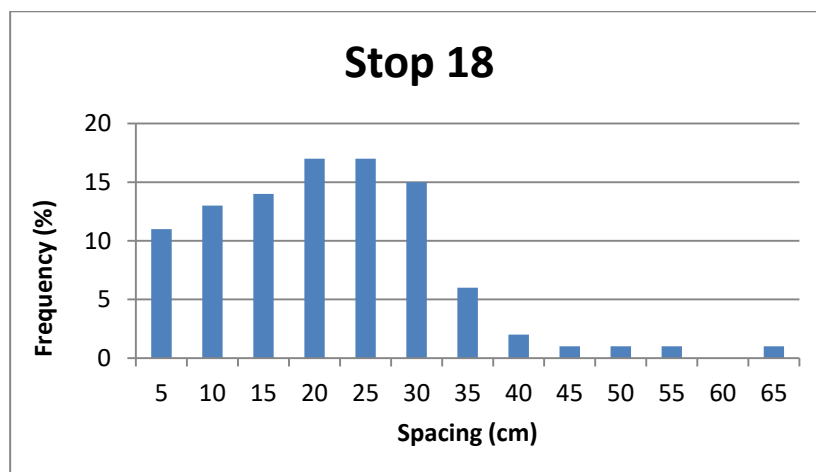


Figure 79. Discontinuity spacing frequency histogram of Stop 18

### ***Weathering and other Properties***

Marl layers are determined as slightly weathered. Whereas mudstone layer in between them are classified as highly weathered. Whole road cut is considered to be moderately weathered. Surficial degradations due to weathered zone are higher along mudstone layers than marl. Average weathered zone is measured as 30 cm for this road cut.

Slake durability and methylene blue test results are given in Table 62. Slake durability of the marl is very high according to the test results.

Table 62. Slake durability and methylene blue values of the rocks at Stop 18

Stop	Rock Type	Fresh			Weathered		
		Slake durability (Id <sub>2</sub> )	MBA (gr/100 g)	CEC (meq/100 g)	Slake durability (Id <sub>2</sub> )	MBA (gr/100 g)	CEC (meq/100 g)
18	Marl	99,09	1,20	2,70	98,64	1,33	3,00

#### 4.3.19. Stop 19

##### *Description*

This road cut is located 0.2 km west of Stop 18, in the Akveren formation. Maximum height of this road cut is about 8 m. Slope dip amount is measured as  $70^{\circ}$ . This stop consists of 80% light gray to beige, thin bedded, heavily fractured marl and 20 % dark to light gray thin bedded mudstone (Figure 80). Currently, no slope failure is observed at this road cut. However, at upper left side of the road cut, a small part of the slope has been failed (Figure 80). Nevertheless, the failed material could not be found near the slope. This failure occurred either on the excavation processes or it was failed after revision of this slope. Nonetheless, some small marl blocks are observed in the drainage channel independent of this failure. Most probably, these fragments are accumulated there due to rock fall. Moreover, weak mudstone layers disintegrated into small fragments and deposited in between strong marl layers. In addition, shear zones are shown by red dashed lines exist at this road cut (Figure 80).

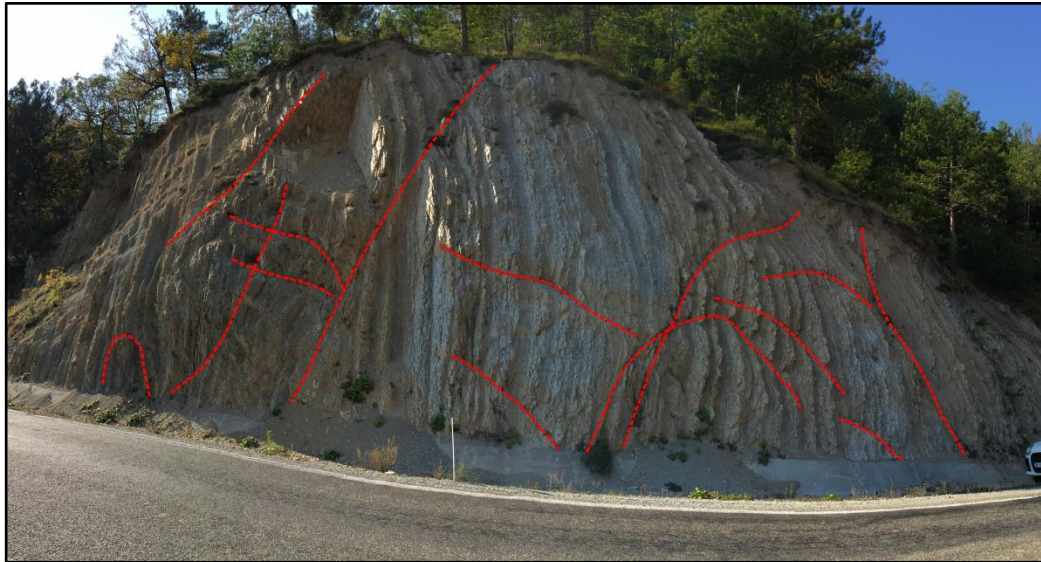


Figure 80. General view and shear zones (red dashed lines) of Stop 19

### ***Strength and Unit Weight***

UCS values of the rocks at this road cut are determined from point load test results (Table 63). Correlation from the point load has been done as in Stop 18, using  $k$  as 11. Considering weighted average of UCS values, the strength of the rocks is calculated as 27 MPa. Mudstone values are taken from Stop 1, whereas marl values are determined from tests applied on parallel to isotropy planes, which is 31 MPa for the relatively fresh saturated samples. The ratio between parallel and perpendicular point load values is about one third to half.

Unit weight values of the marl in this slope are given in Table 64. Saturated unit weight results of the fresh and weathered rocks at this road cut determined by weighted average of the marl from this road cut and the mudstone from Stop 1 are 25,29 and 25,77 kN/m<sup>3</sup>, respectively, which are nearly the same with stop 18.

Table 63. UCS values of the rocks at Stop 19

		UCS (MPa)				
		Fresh		Weathered		
Stop	Rock Type	Dry	Saturated	Dry	Saturated	
19	Marl	84,08	63,69	56,85	28,10	+
		38,20	30,79	36,37	10,41	=
1	Mudstone	29,50	11,10	26,80	6,90	=

Table 64. Unit weight values of the rocks at Stop 19

Stop	Rock Type	Unit Weight (kN/m <sup>3</sup> )			
		Fresh		Weathered	
		Dry	Saturated	Dry	Saturated
19	Marl	24,35	25,24	25,22	25,78
1	Mudstone	22,25	25,47	25,09	25,74

### ***Discontinuity Properties***

Pole and contour plots of the discontinuities at this road cut are shown in Figure 81. An extremely scattered pole plot is obtained at this road cut. However, some concentrations due to bedding planes and joints are determined. Three most dominant discontinuity sets are 75/130, 30/060 and 80/235 as dip/dip direction. Joint spacing frequency histogram is shown in Figure 82. Maximum spacing of the discontinuities is measured along bedding planes and they are approximately 30 to 45 cm. Joints are generally bed confined. Persistence is coherent with the spacings. In addition to these joints, shear zones reveal high persistence, however they do not represent whole road cut. Apertures are mostly less than 5 mm filled with damp sandy silt/clay. Degree of jointing is calculated as high. From this data, block volumes determined as small which are coherent with rock fall samples in drainage channel of the cut slope.

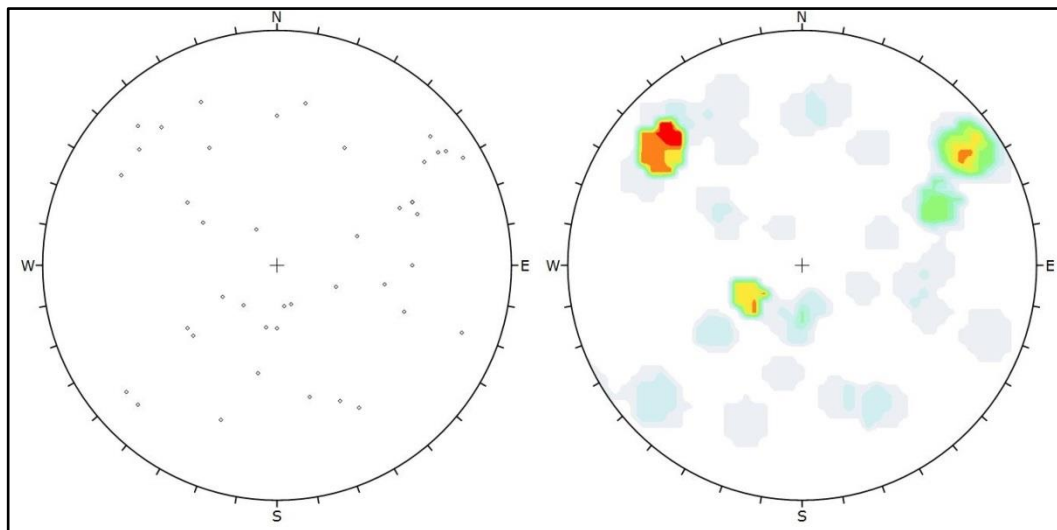


Figure 81. Pole (left) and contour (right) diagrams of the discontinuities at Stop 19

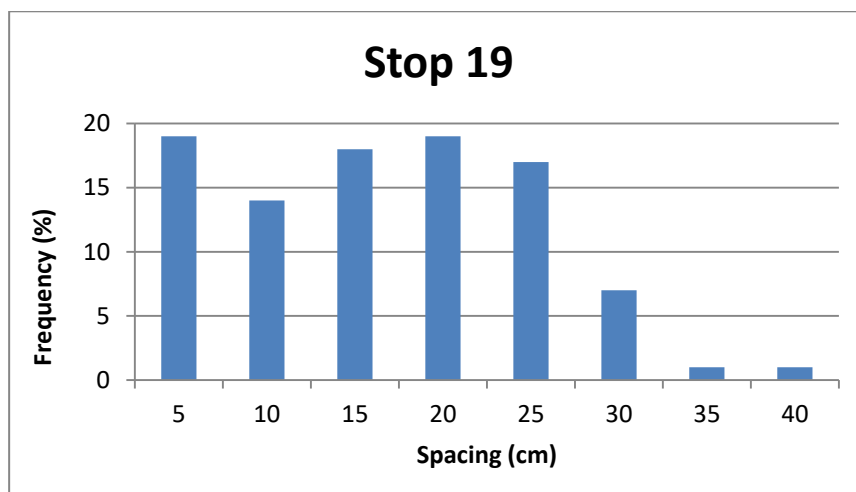


Figure 82. Discontinuity spacing frequency histogram of Stop 19

### ***Weathering and other Properties***

As in stop 18, marly layers are determined to be slightly weathered and mudstones in between them are classified as highly. Weathering degree increases through shear zones. Whole road cut is considered to be moderately weathered based on the field observations. Deposition of small marl fragments and soil like mudstones due to surficial degradations are higher directly under the shear zones. Average weathered zone for this cut slope is determined as 30 cm from the surface.

Slake durability and methylene blue test results are given in Table 65. Durability of the marl is very high for fresh and high for weathered rock according to the test results. The methylene blue tests give low MBA and CEC values.

Table 65. Slake durability and methylene blue values of the rocks at Stop 19

Stop	Rock Type	Fresh			Weathered		
		Slake durability (Id <sub>2</sub> )	MBA (gr/100 g)	CEC (meq/100 g)	Slake durability (Id <sub>2</sub> )	MBA (gr/100 g)	CEC (meq/100 g)
19	Marl	98,48	1,20	2,70	96,78	1,60	3,60

#### 4.3.20. Stop 20

##### *Description*

This road cut is located 0.15 km south of Stop 19, at old Devrek Zonguldak road, in the Akveren formation. Maximum height of this road cut is about 10 m. Slope dip amount is measured as  $75^{\circ}$ . This stop consists of 90% light gray to beige, thin bedded, heavily fractured marl and 10 % dark to light gray thin bedded mudstone (Figure 83). Currently, no slope failure is observed at this road cut. Only small blocks of marl are observed at the drainage channel. These small blocks are mostly concentrated directly below the shear zones which are shown by red dashed lines in Figure 83. Also, some vegetation can be observed where the shear zones are encountered near the toe of the slope. This concentrated vegetation can be explained by water outlet from the shear zones. Especially, at the left part of the slope, water seepage can be seen clearly and vegetation took place both on the shear zone and at the bottom of the slope. At right part of the slope shear zone frequency increases. Therefore, debris deposition is concentrated at the toe of the slope.



Figure 83. General view and shear zones (red dashed lines) of Stop 20

### ***Strength and Unit Weight***

UCS values of this road cut are determined from point load test results (Table 66). Marl values are determined from tests applied on parallel to isotropy planes because bedding planes are perpendicular to the road. These are 15 MPa for relatively fresh saturated samples. Saturated mudstone values are taken from Stop 1. According to weighted average, UCS value of the rocks is calculated as 14 MPa.

Unit weight values of the marl in this slope are given in Table 67. Saturated unit weight results of the fresh and weathered rocks at this road cut determined by weighted average of the marl from this road cut and the mudstone from Stop 1 are 24,72 and 25,16 kN/m<sup>3</sup>, respectively.

Table 66. UCS values of the rocks at Stop 20

		UCS (MPa)				
		Fresh		Weathered		
Stop	Rock Type	Dry	Saturated	Dry	Saturated	
20	Marl	86,49	38,87	44,50	19,27	+
		47,67	15,38	27,77	5,68	=
1	Mudstone	29,50	11,10	26,80	6,90	=

Table 67. Unit weight values of the rocks at Stop 20

		Unit Weight (kN/m <sup>3</sup> )			
		Fresh		Weathered	
Stop	Rock Type	Dry	Saturated	Dry	Saturated
20	Marl	23,83	24,64	24,50	25,10
1	Mudstone	22,25	25,47	25,09	25,74

### ***Discontinuity Properties***

Pole and contour plots of the discontinuities at this road cut are shown in Figure 84. Due to extremely fractured structure, scattered pole plot is obtained. Comparing dominant discontinuity sets with stop 19 would give a very coherent result. Three most dominant discontinuity sets are 70/130, 15/050 and 70/220 as dip/dip direction. Joint spacing frequency histogram reveals that maximum spacing is measured as 45 cm (Figure 85). Maximum persistence is obtained along bedding planes. Joints are generally bed confined however shear zones are exceptional. All in all, discontinuity persistence is coherent with the spacings. Apertures are mostly close or maximum 1 mm at this road cut. Clay/Silt size damp material is observed as infilling. Degree of jointing is determined as high. By this data, block volume at this road cut is calculated as small.

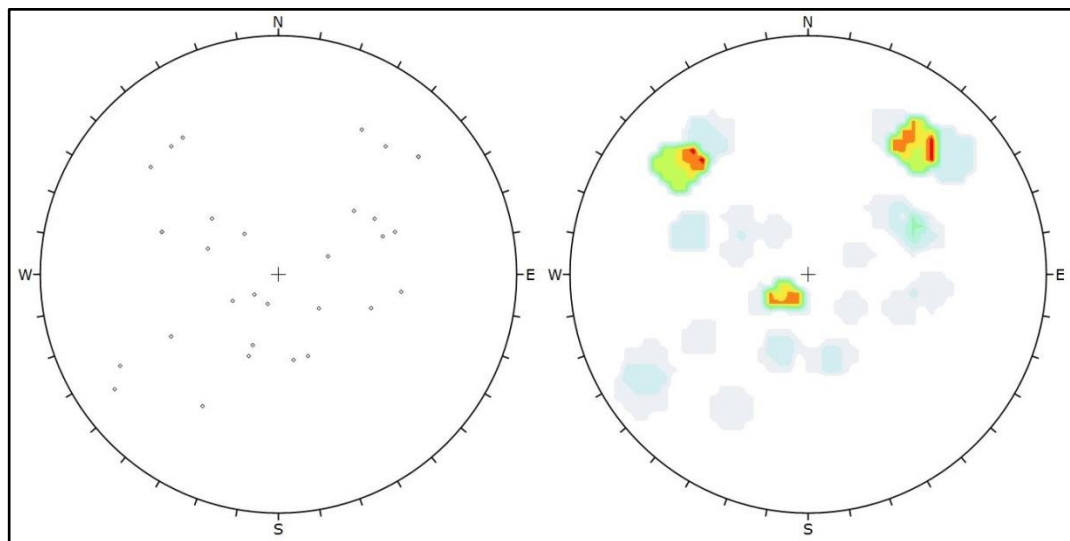


Figure 84. Pole (left) and contour (right) diagrams of the discontinuities at Stop 20

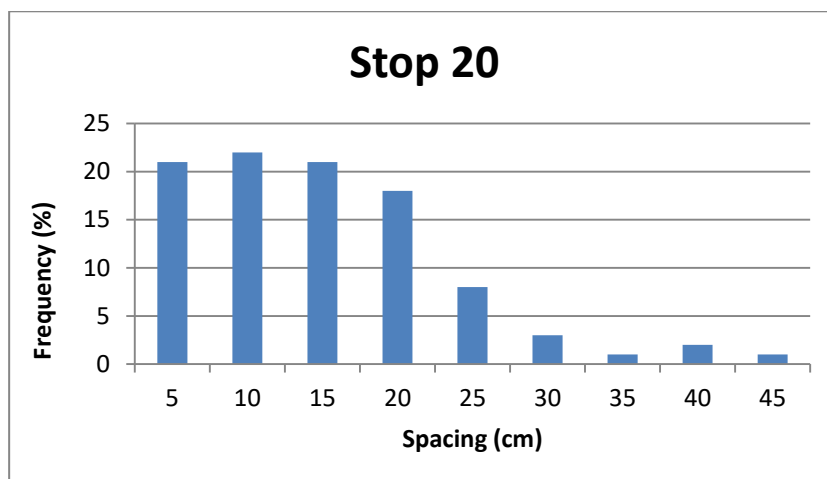


Figure 85. Discontinuity spacing frequency histogram of Stop 20

### ***Weathering and other Properties***

Weathering degree is dominantly slight for marl layers at this slope. However, thin mudstone layers and shear zones are prone to weathering, so that they are determined as highly weathered. Considering the whole road cut, weathering degree is regarded as moderately. This very thin weathered zone is determined as 15 cm from the surface.

Slake durability and methylene blue test results of the rocks seen at the cut slope are given in Table 68. Slake durability of the marl is very high according to test results. MBA and C.E.C. values of the rocks are quite low.

Table 68. Slake durability and methylene blue values of the rocks at Stop 20

Stop	Rock Type	Fresh			Weathered		
		Slake durability (Id <sub>2</sub> )	MBA (gr/100 g)	CEC (meq/100 g)	Slake durability (Id <sub>2</sub> )	MBA (gr/100 g)	CEC (meq/100 g)
20	Marl	98,56	1,33	3,00	98,55	1,47	3,30

## CHAPTER 5

### SLOPE STABILITY ANALYSES

Slope stability analyses were done for each road cut based on according to their characterizations. Stability of these slopes was assessed by considering kinematical and limit equilibrium conditions. Then, rock fall risks were also evaluated according to these results and road cut characteristics. In addition to these assessments, two different empirical methods which are Slope Stability Probability Classification (SSPC) and Slope Mass Rating (SMR) were used to investigate the stability of the road cuts.

#### 5.1. Kinematic Analyses of the Cut Slopes

There are three different failure types that can be determined by applying kinematic analyses which are planar, wedge and toppling. Kinematical analyses are done to determine the failure type by using internal friction angle obtained from shear box test results in Dips software (Rocscience, 2013). For the stereonet, lower hemisphere, Schmidt contour distribution and equal angle projection is used. Under normal circumstances, block sizes larger than moderate ( $0,2 \text{ m}^3$ ) are considered in kinematic analyses. However, in this thesis, block volumes larger than  $0,02 \text{ m}^3$  and discontinuity persistency which is not coherent with the spacings are investigated. Based on these limitations, only 4 stops are considered to be critical in the study area.

Considering Barton & Choubey (1977) equation given below, shear strength parameters of the discontinuities are obtained for each critical cut slope.

$$\tau = \sigma_n \tan[ \varphi + \text{JRC}_n \log_{10}(\text{JCS}_n / \sigma_n) ]$$

the parameter  $\varphi$  can be estimated according to Barton & Choubey (1977) using basic friction angle ( $\varphi_b$ ), which is obtained from the laboratory indicated in Chapter 4 in shear box test subsection. This formula is given as:

$$\varphi = (\varphi_b - 20) + 20(r/R)$$

where  $r$  is Schmidt rebound value for weathered and  $R$  is Schmidt rebound value for relatively fresh surfaces. In addition to friction angle, corrections for scale of the joints are considered by Barton & Bandis (1982) by the formulas given below for JRC (joint roughness coefficient) and JCS (joint wall compressive strength).

$$JRC_n = JRC_0 (L_n / L_0)^{-0.02JRC_0}$$

$$JCS_n = JCS_0 (L_n / L_0)^{-0.03JRC_0}$$

For the compressive strength of the joints (JCS), UCS values are considered to be used which are obtained from Schmidt rebound test by using Deere & Miller (1966). Roughness values are determined from the profiles obtained in the field by using profilometer according to Barton & Choubey (1977) chart (Figure 86).  $L_n$  refers to in situ block size and  $L_0$  refers to 10 cm profilometer length.

According to these equations and laboratory results, three different  $\sigma_n$  (vertical stress) values were assigned for each road cut related to their heights and saturated unit weights. From these values, shear stress versus vertical stress graphs were obtained and, cohesion and internal friction angle values were calculated (Figure 87).

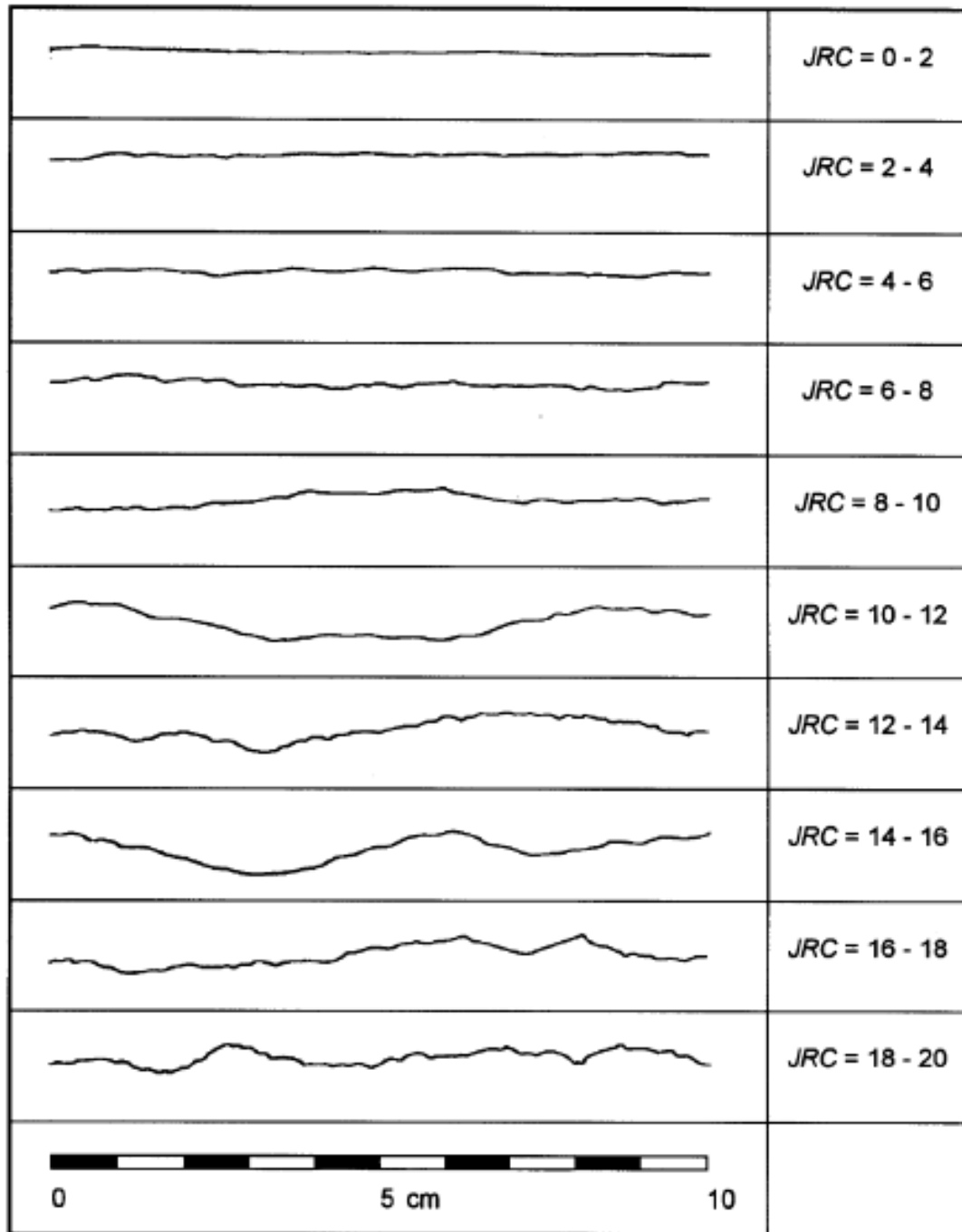


Figure 86. Roughness profiles and related JRC values (Barton & Choubey, 1977)

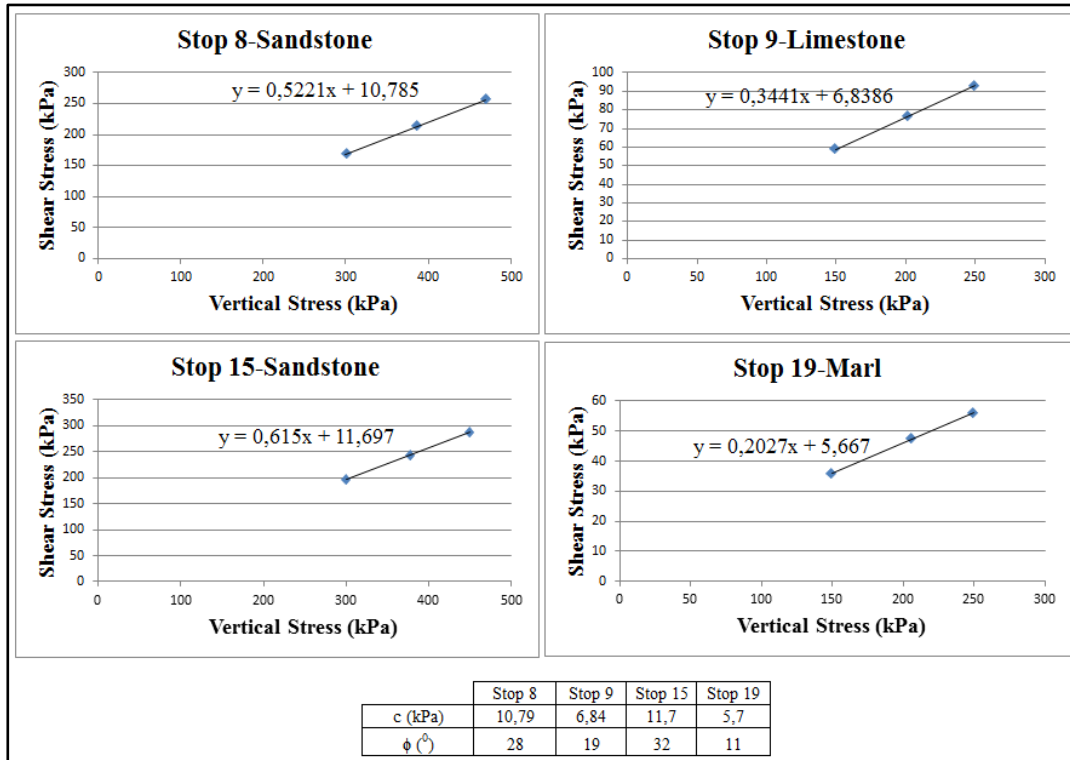


Figure 87. Cohesion and internal friction angle values of critical slopes

Considering internal friction angles for each slope, kinematic analyses of the cut slopes were conducted. For Stop 8, only wedge failure is observed (Figure 88). Kinematic analyses conducted at Stop 9 revealed that only wedge failure is critical due to Joints 1 (66/235) and 2 (30/290) (Figure 89). Similar to Stop 9, Stop 15 reveals only wedge failure according to the kinematic analyses due to Joints 1 (49/145) and 2 (78/255) (Figure 90). The most critical road cut is revealed to be Stop 19 due to extreme scattered discontinuity data. According to the kinematic analyses, there are planar, toppling and wedge failures at this road cut (Figure 91).

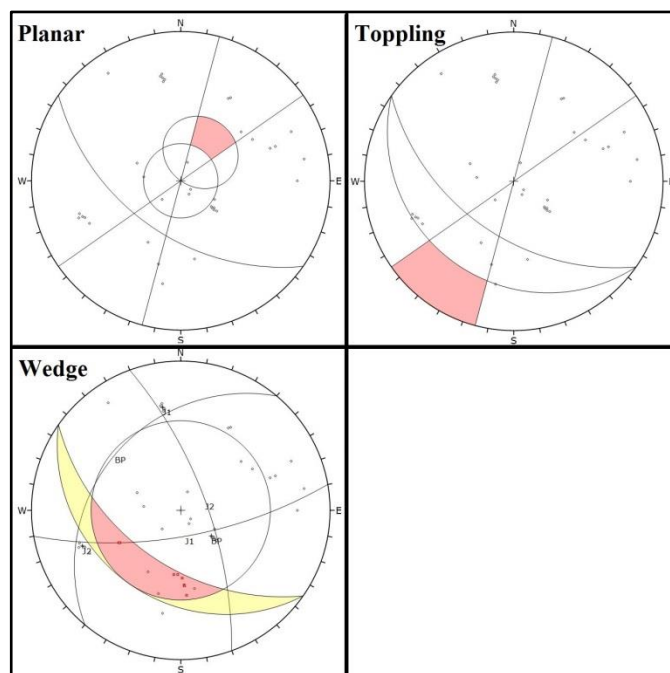


Figure 88. Kinematic analyses of Stop 8

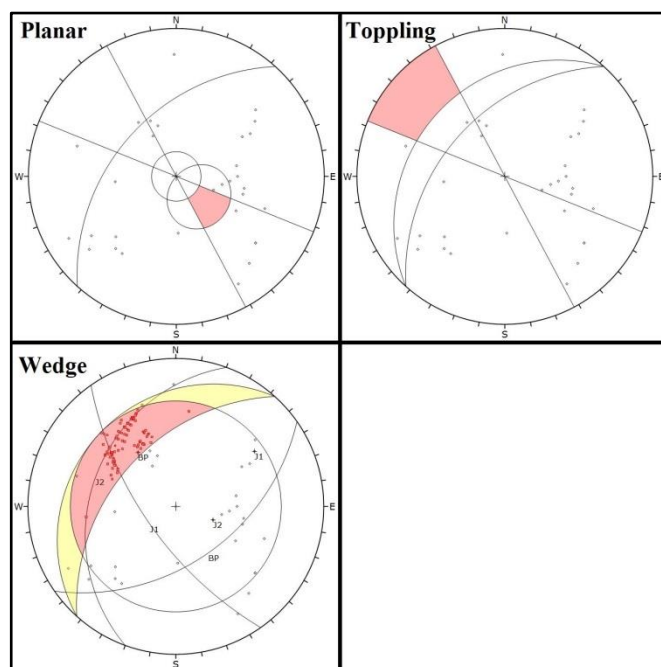


Figure 89. Kinematic analyses of Stop 9

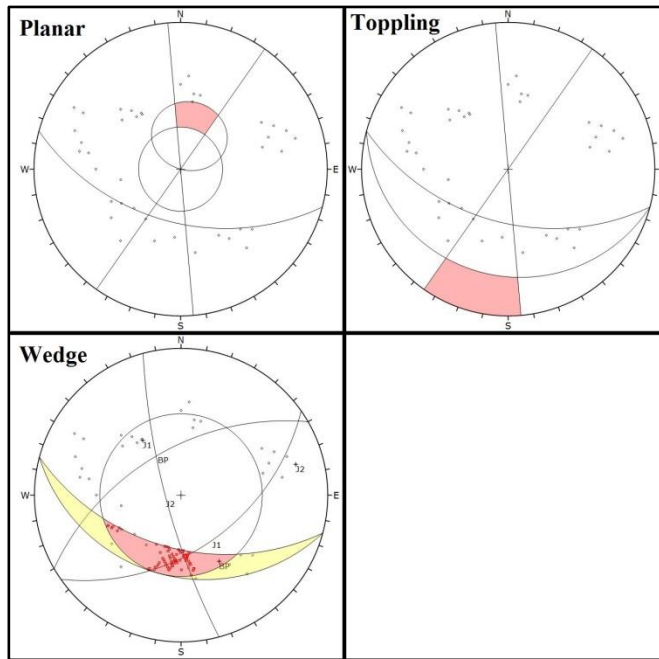


Figure 90. Kinematic analyses of Stop 15

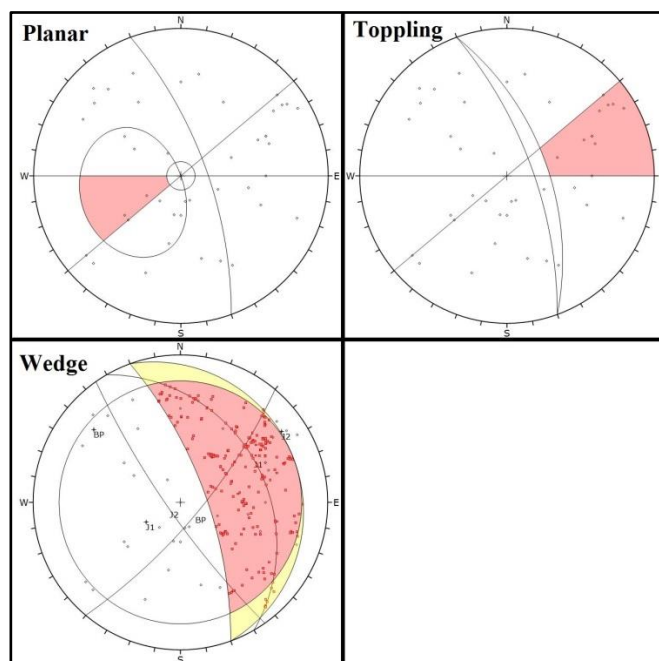


Figure 91. Kinematic analyses of Stop 19

### 5.2.Limit Equilibrium Analyses for Discontinuity Controlled Rocks

Wedge failure encountered at Stop 8, 9, 15 and 19 was investigated through Swedge (4.0) software program (Rocscience, 2004b) which includes parameters like cohesion, unit weight, slope height and seismic load in addition to stereonet analyses. Including cohesion revealed that these cut slopes are stable against wedge failure with very high factor of safeties like 5.2, 6.8, 19.4 and 2.4 for the Stop 8, 9, 15 and 19, respectively (Figures 92-95).

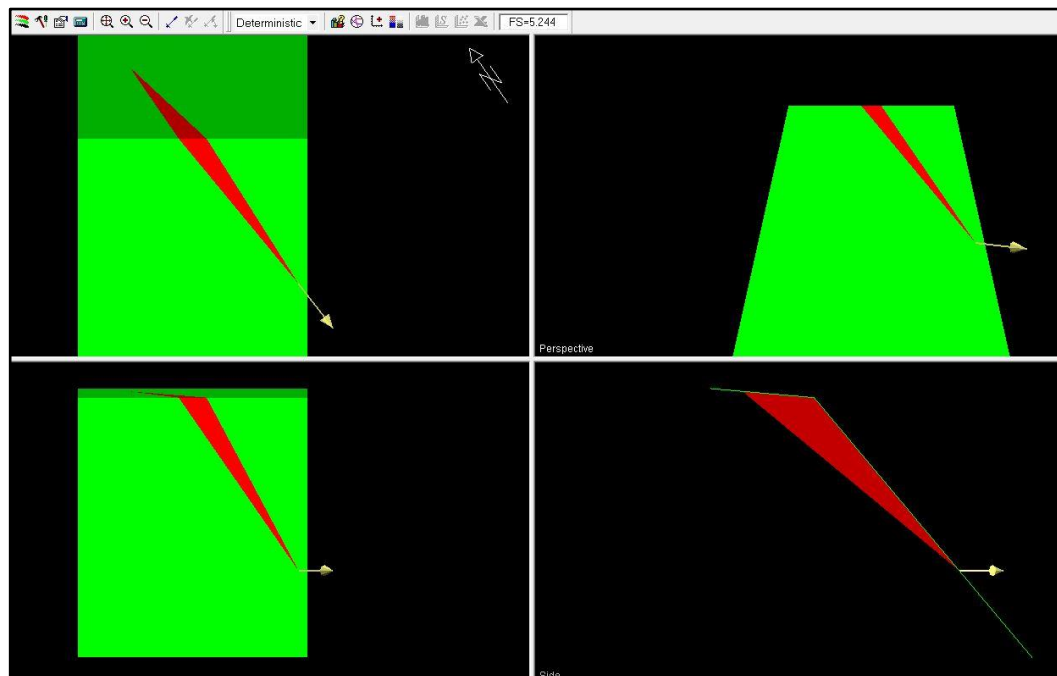


Figure 92. Wedge failure analysis of Stop 8 giving FS=5.2

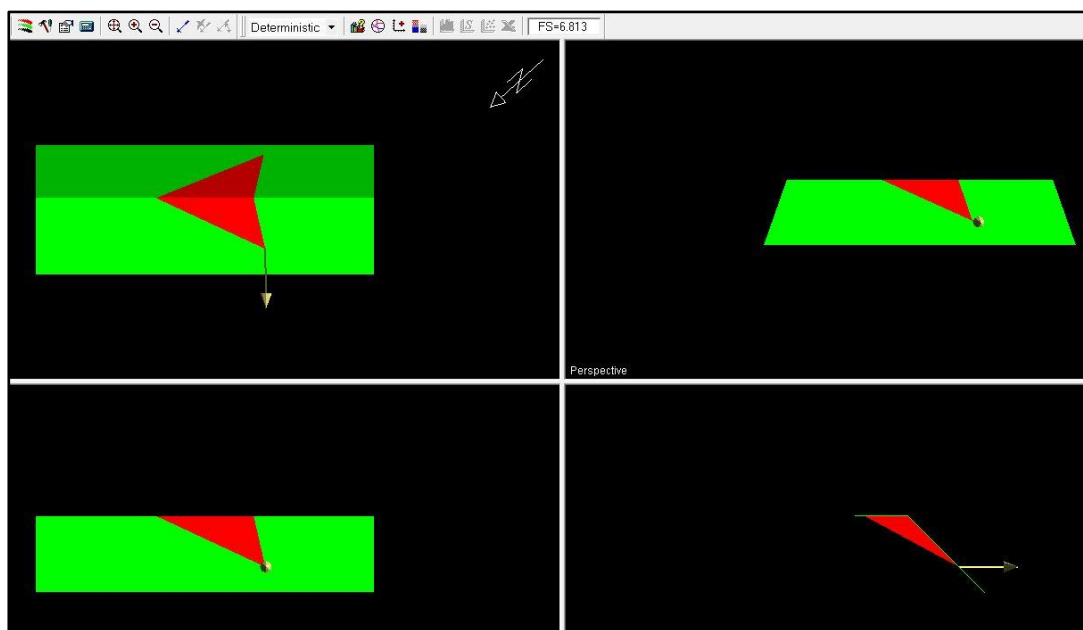


Figure 93. Wedge failure analysis of Stop 9 with giving FS=6.8

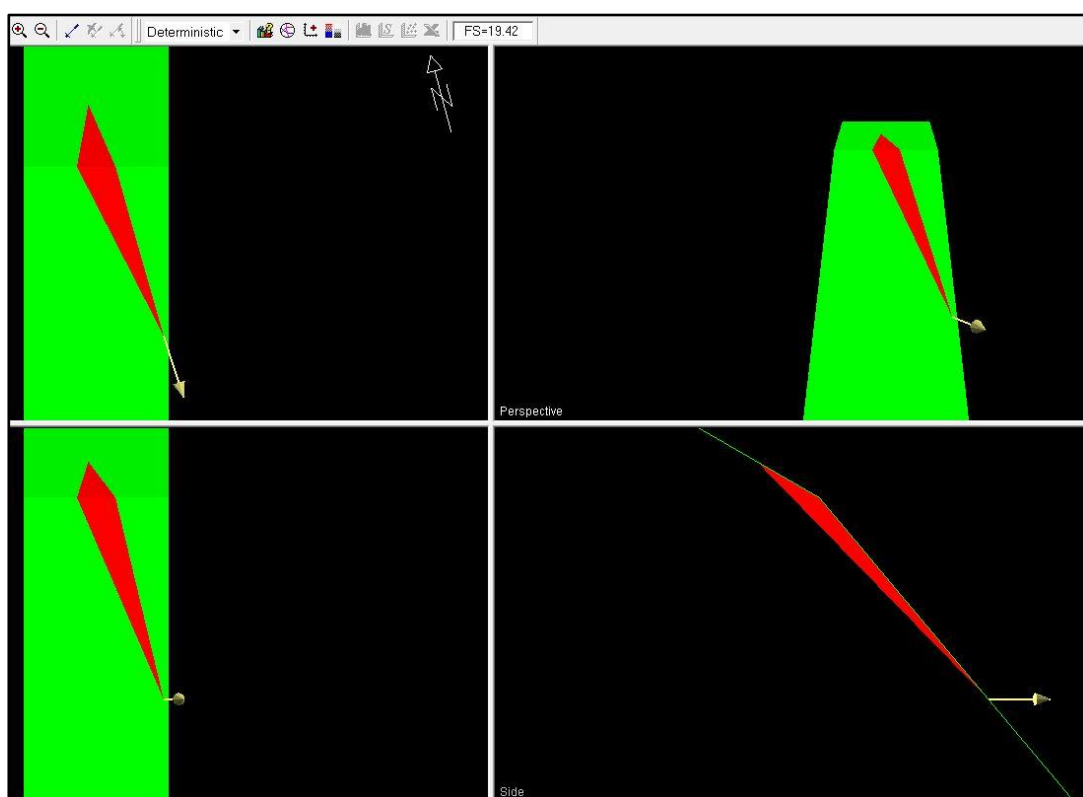


Figure 94. Wedge failure analysis of Stop 15 giving FS=19.4

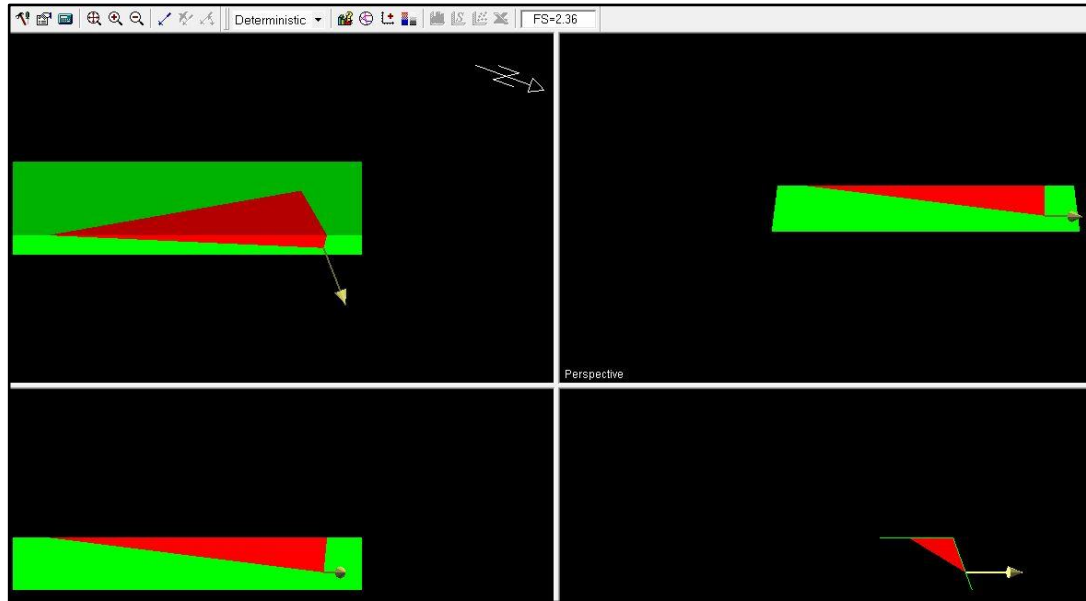


Figure 95. Wedge failure analysis of Stop 19 giving FS=2.4

Planar failure expected to occur based on the kinematic analyses at Stop 19 was investigated by RocPlane (2.0) software program (Rocscience, 2005) including cohesion, unit weight, slope height and seismic load. Joint 1 (30/060) which reveals as the critical discontinuity to create planar failure is assigned into program. Result obtained from the software shows that factor of safety is 0.8 which means unstable (Figure 96).

Toppling failure reached from the kinematic analyses of Stop 19 was investigated by RocTopple (1.0) software program (Rocscience, 2015). Results obtained from this software show that instead of toppling failure, sliding action would take place due to very close spacings of the joints. Despite that, sliding action reveals factor of safety of 2.1 which is significantly stable for this road cut (Figure 97).

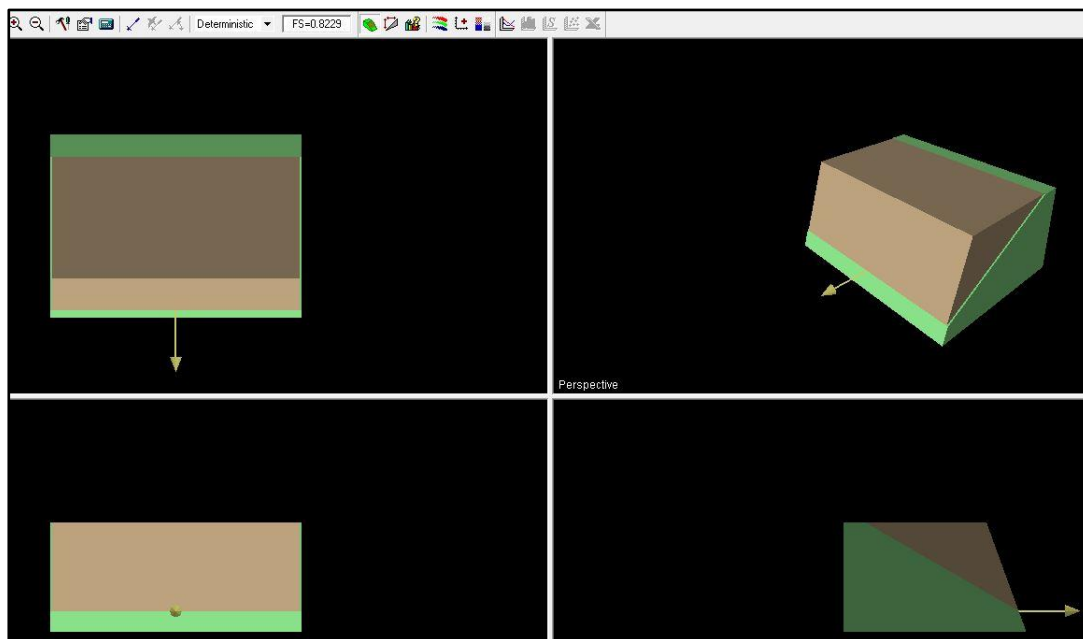


Figure 96. Planar failure analysis of Stop 19 giving  $FS=0.8$

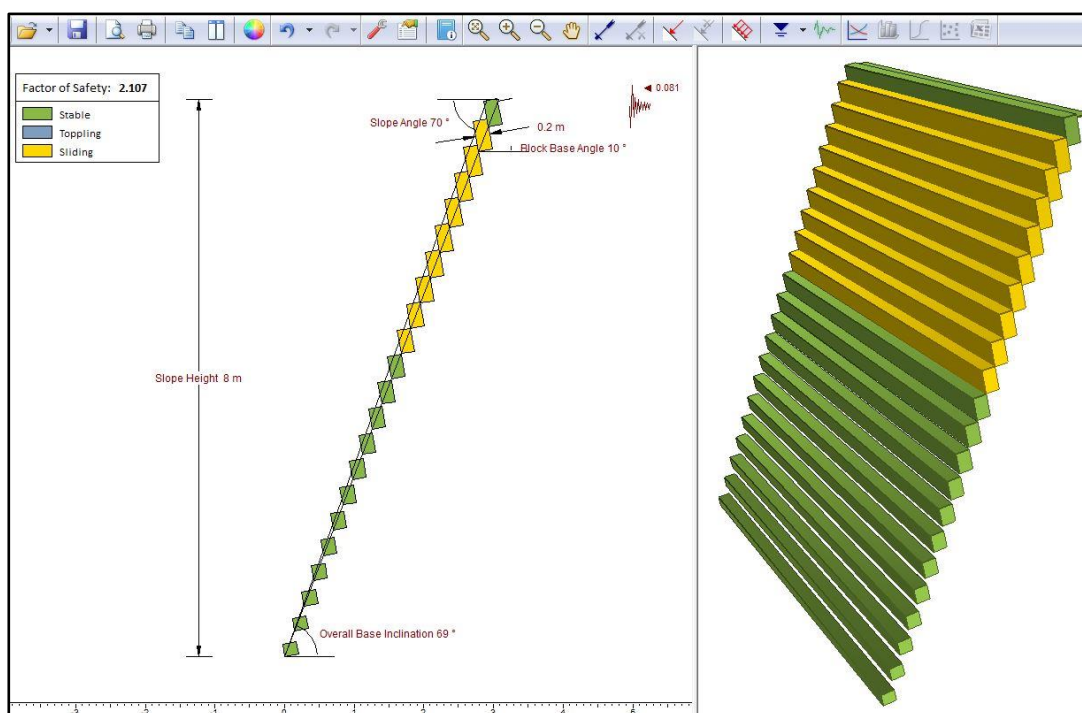


Figure 97. Toppling failure analysis of Stop 19 giving  $FS=2.1$

### **5.3.Limit Equilibrium Analyses for the Rock Mass**

Different from the kinematic analysis, limit equilibrium considers unit weight, cohesion and parameters governing discontinuity conditions. Limit equilibrium analyses were done for each road cut both in static and pseudostatic conditions assigning weathered and relatively fresh rock properties to the related zones. According to the field investigations, the depth and degree of weathered zone was determined. It is observed that because of disintegration and decomposition, this weathered zone reveals surface failures. It is obvious that these surface failures are formed because of detachment of rock fragments from joints. It can be explained that this surface of detachment is cohesionless. In order to simulate that, the cohesion was considered 0 for the weathered zone. Internal friction angle, on the other hand, was determined according to Hoek-Brown classification consisting of UCS, GSI, intact rock constant  $m_i$ , disturbance factor and modulus ratio constant. For the fresh zone, again generalized Hoek-Brown criterion was used. Intact rock strength of each road cut was obtained from the point load data by conversion to the UCS (Table 69). Disturbance factor is the same for all slopes because of the same mechanical excavation method. Intact rock constant  $m_i$  was assigned by considering rock type and average weight method for the flysch type deposits. Distinctly, GSI values (Table 70) are open to interpretation among these parameters. Therefore, limit equilibrium analyses were conducted on these values by considering 5% lower and upper boundaries to observe factor of safety details. In order to investigate mass (circular) failure modes, Spencer method (Spencer, 1967) was preferred because of satisfying conditions of both moments and forces.

Table 69. UCS values for fresh and weathered zones of each road cut

<b>Stop</b>	<b>Fresh (MPa)</b>	<b>Weathered (MPa)</b>	<b>Stop</b>	<b>Fresh (MPa)</b>	<b>Weathered (MPa)</b>
<b>1</b>	12	8	<b>10</b>	17	7
<b>1-F</b>	4,2	1,5	<b>11</b>	21	6
<b>2</b>	40	16	<b>12</b>	10	6
<b>2-F</b>	8	-	<b>13</b>	11	7
<b>3</b>	40	8,5	<b>14</b>	14	12
<b>4</b>	20	6	<b>15</b>	28	21
<b>5</b>	38	4	<b>16</b>	13	12
<b>6</b>	20	0,1	<b>17</b>	11	8
<b>7</b>	88	13	<b>18</b>	32	27
<b>8</b>	23	13	<b>19</b>	27	9,5
<b>9</b>	55	26	<b>20</b>	14	7

Table 70. GSI values of each road cut

<b>Stop</b>	<b>GSI</b>	<b>Stop</b>	<b>GSI</b>
<b>1</b>	20	<b>10</b>	40
<b>1-F</b>	15	<b>11</b>	35
<b>2</b>	40	<b>12</b>	25
<b>2-F</b>	20	<b>13</b>	35
<b>3</b>	30	<b>14</b>	35
<b>4</b>	30	<b>15</b>	40
<b>5</b>	37	<b>16</b>	25
<b>6</b>	28	<b>17</b>	25
<b>7</b>	45	<b>18</b>	35
<b>8</b>	40	<b>19</b>	35
<b>9</b>	36	<b>20</b>	37

For the pseudostatic analyses, PGA values were used according to Idriss (2007). As Kramer (1996) implies that if the slope material was a rigid body, then the internal force applied on a slide would be equal to the product of actual acceleration (horizontally) done by the earthquake. However, slopes are not rigid bodies so that these acceleration values are significantly below the maximum acceleration. There are numerous approaches to reduce the maximum acceleration to an applicable level. In this thesis three different reduction coefficients are used to assess the factor of safety. These reduction coefficients are selected as 0,33 (Marcuson, 1981), 0,5 (Hynes-Griffin & Franklin, 1984) and 0,65 (Bozorgnia & Bertero, 2004).

According to the limit equilibrium results obtained from Slide (6.0) software (Rocscience, 2011), all road cuts are stable for mass (circular) failures, in other words, factor of safety (FS) is over 1,5 for static and 1,1 for pseudostatic conditions (as General Directorate of Highways implies), with some exceptions. These analyses done according to GSI values are given in Table 70. The only failures observed on these analyses occur on the surface. As it was mentioned above, +/- 5 to these GSI values are applied for each road cut to recognize the effect of this parameter. One of the exceptions of the analyses results revealed for Stop 20 (Table 71).

As it can be seen from the Table 71, even FS values are above 1, this slope can be categorized as risky due to General Directorate of Highways restrictions. In order to prevent this failure, slope of the road cut should be decreased to 70<sup>0</sup> (Figure 98). This implies that if the road cut considered to be in the same conditions as in current except slope degree change there is only 1 critical slide (FS=1,204). Except this critical one, all the other slides are above 1,5 shown with green colored arcs.

Table 71. FS results for static and pseudostatic conditions of each road cut

	Static			Pseudostatic		
Stop	(GSI-5)	GSI	(GSI+5)	0,65	0,5	0,33
1	1,9	2,0	2,1	1,0	1,2	1,4
2	2,7	2,9	3,1	2,5	2,7	2,9
3	2,2	2,3	2,4	1,7	1,8	2,0
4	1,7	1,8	1,9	1,4	1,5	1,6
5	2,4	2,6	2,7	2,2	2,4	2,5
6	1,9	2,1	2,2	1,6	1,7	1,8
7	3,9	4,1	4,3	3,6	3,8	4,0
8	2,4	2,6	2,7	2,2	2,3	2,4
9	4,5	4,8	5,1	1,2	1,7	2,2
10	3,1	3,3	3,5	2,9	3,0	3,1
11	2,6	2,8	2,9	2,5	2,6	2,7
12	1,9	2,1	2,2	1,8	1,8	1,9
13	1,5	1,6	1,6	1,3	1,4	1,4
14	2,4	2,6	2,7	2,2	2,3	2,4
15	3,0	3,2	3,3	2,8	2,8	2,9
16	2,0	2,1	2,1	1,8	1,8	1,9
17	2,2	2,4	2,5	2,1	2,1	2,2
18	3,3	3,4	3,5	2,9	3,0	3,1
19	2,0	2,2	2,3	2,1	2,2	2,2
20	1,3	1,4	1,5	1,3	1,4	1,4

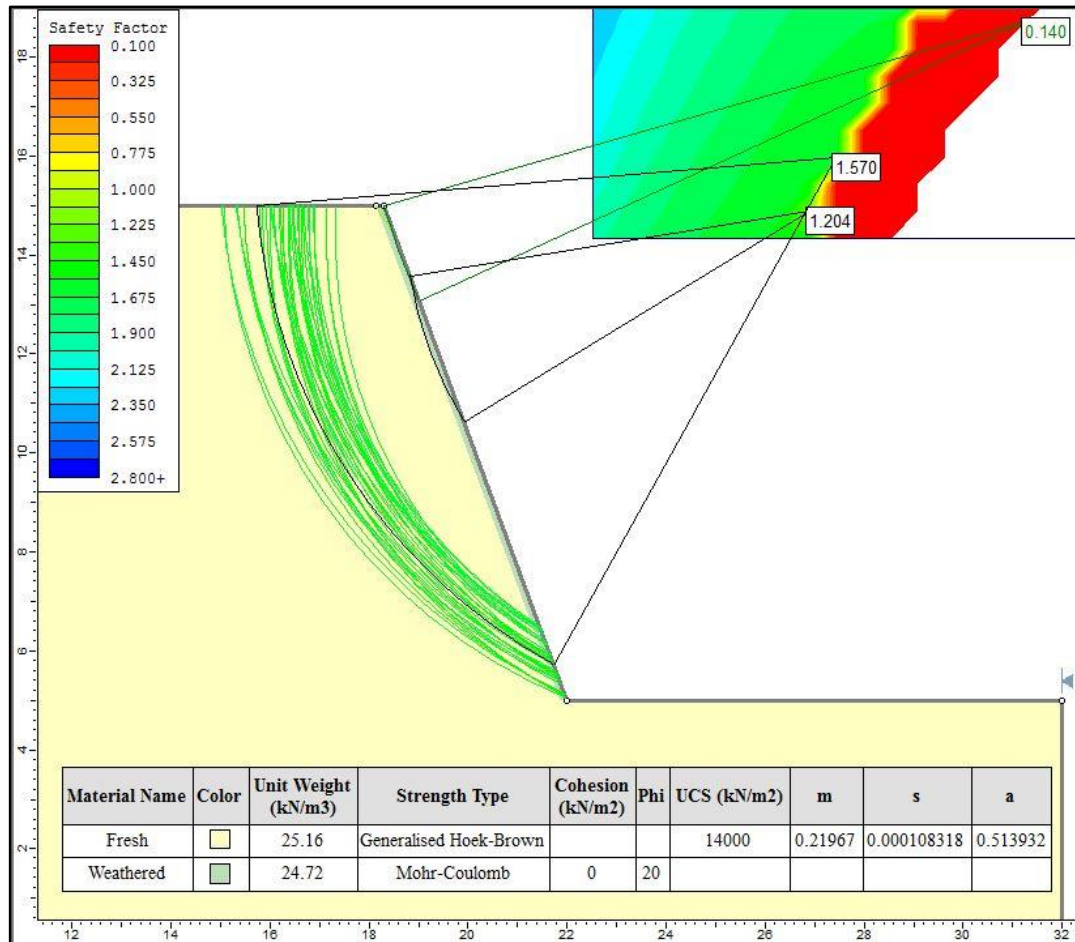


Figure 98. Mass failure analysis of Stop 20 after slope flattening

Another critical condition is obtained for Stop 1 (Table 71). Despite significantly stable condition under static conditions, pseudostatic results show that if seismic coefficient is considered according to Bozorgnia & Bertero (2004), FS value decreases to 1 which is under the threshold value (1.1) for pseudostatic conditions. To avoid this critical condition, slope degree should be decreased to  $35^{\circ}$  (Figure 99). Same scenario is valid for this road cut as in Stop 20. Again FS values below 1 are only revealed on surface and for the rest of the road cut FS values are higher than 1.1 as it is shown Figure 99.

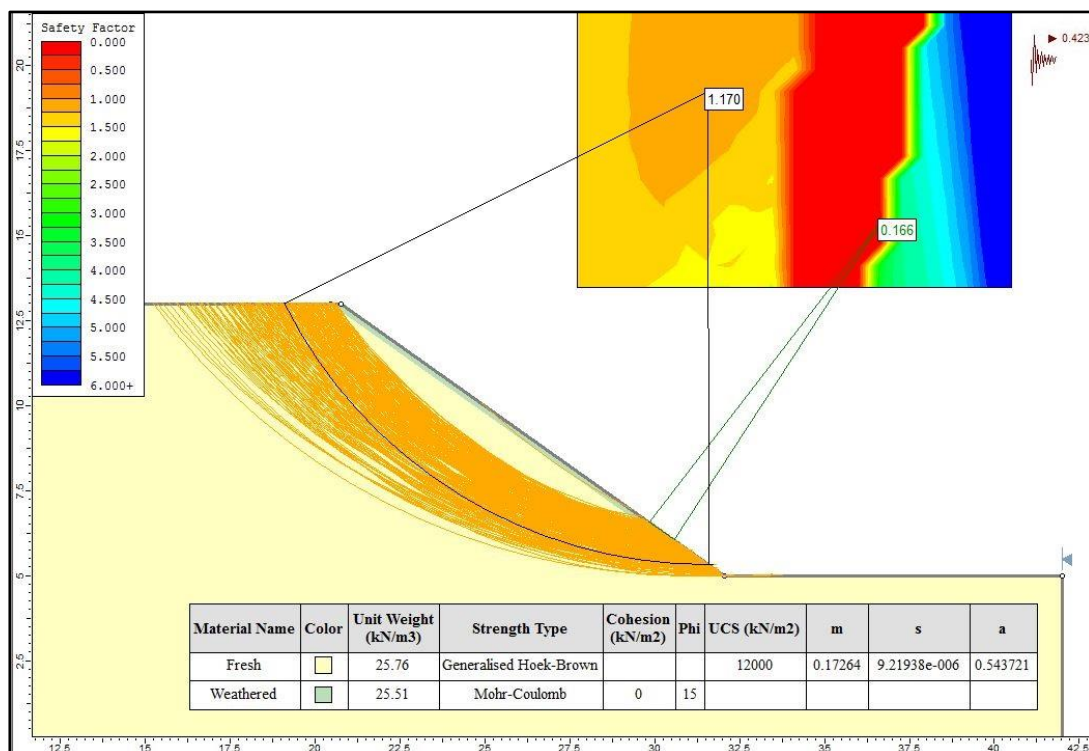


Figure 99. Mass failure analysis of Stop 1 after slope flattening

According to stability analyses, rest of the road cuts are stable and would not show any critical result even under the earthquake forces. All results are coherent with the field observations including already failed cut slopes (Figure 100 and 101).

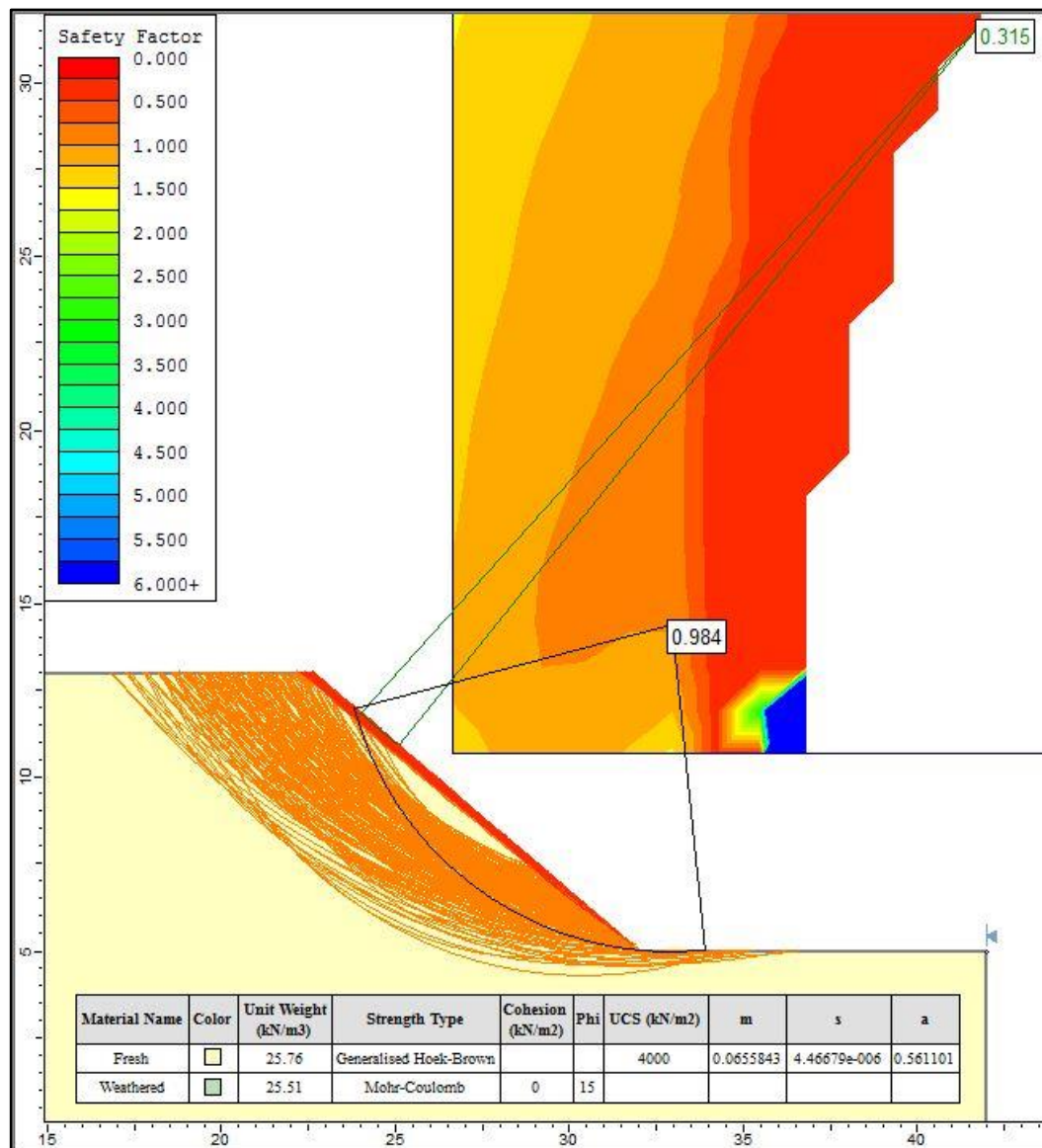


Figure 100. FS results of the failed zone at Stop 1

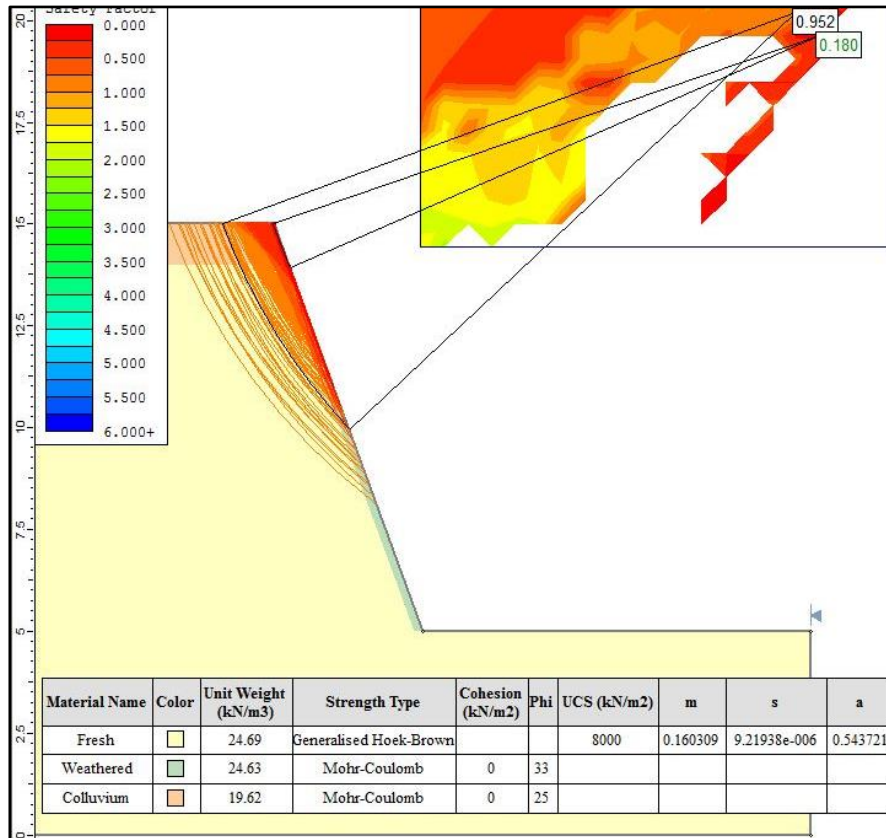


Figure 101. FS results of the failed zone at Stop 2

The details of the analyses under static conditions with average GSI values belonging to each road cut are presented in Appendix B.

#### 5.4. Rock Fall Analyses

As it is mentioned in the kinematic analyses, despite the results show any kind of failure like planar, wedge or toppling, blocks smaller than 0,02 m<sup>3</sup>, in other words medium and small blocks, behave like falling. Moreover very small blocks detached from the surface do not create any significant danger as in Stops 1, 12 and 17. Hence, each slope except the ones which do not reveal any critical disturbance was investigated. In this analysis, RocFall software (4.0) (Rocscience, 2004a) was used. Initial position of the falling rock is chosen from the uppermost part of the slope in order to be on the safe side. Mass of the rocks were directly determined from the multiplication of saturated unit weight and, block sizes were measured from the scan

line survey and already fallen blocks in the field. Normal restitution (Rn), tangential restitution (Rt) and friction angle were assessed determined from the back analysis (Appendix B). These values related to each material are given in Table 72. In this study, basalt was observed in only one slope so that Rn, Rt and friction angle values were taken from Binal and Ercanoğlu (2010). While applying the back analysis, different geometries and weights of the same lithological units were considered. In the software, number of rocks to throw was chosen to be 1000, minimum velocity cut-off was 0,1 m/s, number of horizontal locations to analyze was 100 and horizontal velocity was 1 +/- 0,5 m/s for each road cut.

Table 72. Summary of Rn, Rt and friction angle for the materials encountered

<b>Material</b>	<b>Rn</b>	<b>Rt</b>	<b>φ</b>
Limestone	0,31	0,58	35
Granite	0,38	0,47	48
Basalt	0,22	0,57	34
Granodiorite	0,27	0,51	44
Sandstone	0,50 +/- 0,02	0,58 +/- 0,04	35
Marl	0,27 +/- 0,03	0,62 +/- 0,04	32
Drainage Channel	0,06 +/- 0,02	0,80 +/- 0,06	14

The block volumes were determined according to Palmstrom (2000) for each road cut considering dominant joint sets for each direction. The maximum block volumes, related unit weights and masses are given in Table 73.

Table 73. Block volume, unit weight and mass used in rockfall analyses for each road cut

	<b>Maximum Block Volume (m<sup>3</sup>)</b>	<b>Unit Weight (kN/m<sup>3</sup>)</b>	<b>Mass (kg)</b>
Stop 2	0,0283	24,63	69
Stop 3	0,0004	21,84	1
Stop 4	0,0007	25,61	2
Stop 5	0,0058	25,94	15
Stop 6	0,0058	25,33	15
Stop 7	0,0283	26,22	74
Stop 8	0,1894	24,74	468
Stop 9	0,0283	25,08	71
Stop 10	0,0376	24,40	92
Stop 11	0,0035	24,13	8
Stop 13	0,0035	23,62	8
Stop 14	0,0035	24,88	9
Stop 15	0,0749	24,71	185
Stop 16	0,0127	23,92	30
Stop 18	0,0094	25,34	23
Stop 19	0,0094	25,24	23
Stop 20	0,0035	24,64	9

As it can be seen from Figure 102, any significant danger is not observed at Stop 2 and 3. Despite the already constructed retaining walls made of stones at Stop 4 and 5 (Figure 102) little percentage of the rocks would fall into the drainage channel, which is coherent with the field observations. However, these rocks would not be observed on the road section as it can be seen from the analyses.

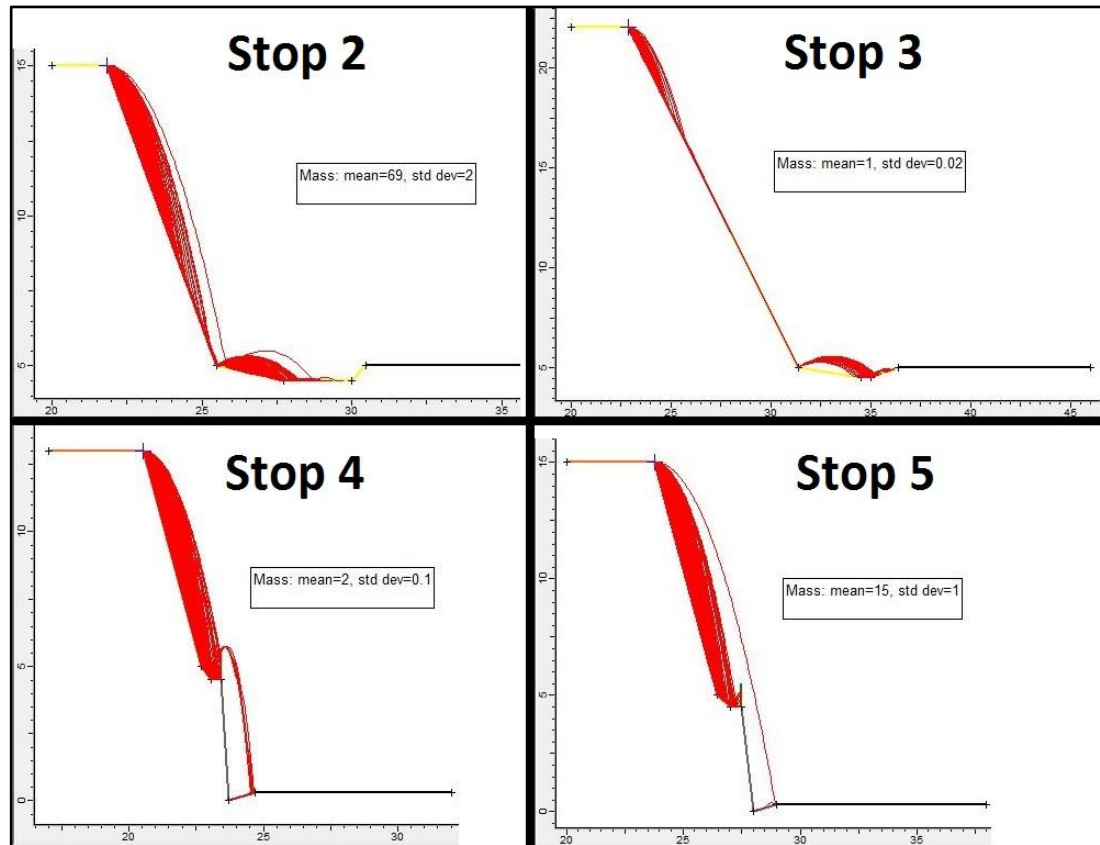


Figure 102. Rockfall analyses of Stops 2, 3, 4 and 5

The already constructed retaining wall made of stones at Stop 6 works perfectly to collect the samples behind itself, unlike Stop 4 and 5 (Figure 103). As it was mentioned in Chapter 4, a retaining wall has been constructed in front of Stop 7 after the first investigations. According to the analysis of this road cut, retaining wall works in high percentage to hold the fallen rocks. Only minor amount of rocks would fall into the drainage channel, after hitting the boulders behind the wall and shattered into pieces. It is observed that even though the rocks have the greatest volume among all studied road cuts, they would only reveal rolling action and accumulate in the ditch next to the road at Stop 8.

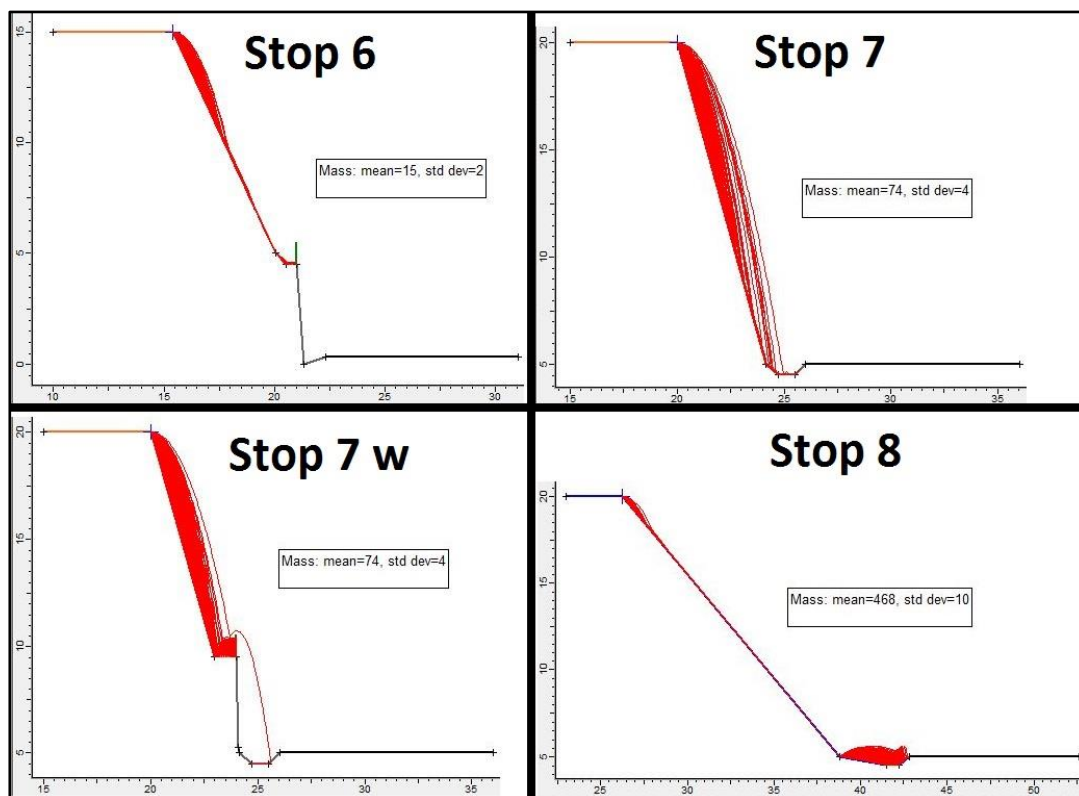


Figure 103. Rockfall analyses of Stop 6, 7 and 8 (Stop 7 w indicates new profile after first investigations)

Analyses done at Stops 9, 10, 11 and 13 show that detached rocks from the surface would accumulate in the drainage channels next to the road (Figure 104). Stops 9, 10 and 11 reveal rolling action along the slope. On the other hand, due to high slope degree, rock fall can be observed at Stop 13. According to this analysis, blocks falling from the upper part of the bench would not reach to the road elevation. The rocks detached from lower part of the bench would accumulate into the drainage channel, however they would not reach to the road.

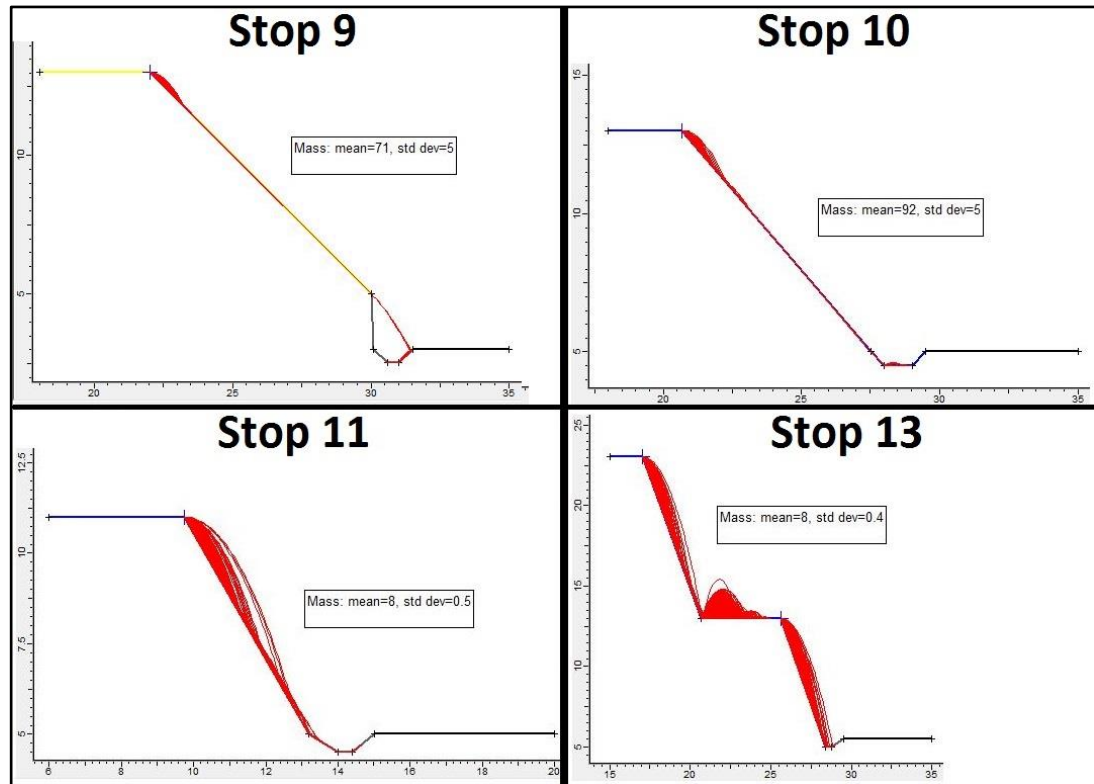


Figure 104. Rockfall analyses of Stop 9, 10, 11 and 13

Analyses done at Stops 14, 15, 16 and 18 show only rolling action due to low slope degrees (Figure 105). Similar to Stop 13, rolling rocks detaching from upper part of the bench accumulate at the bench. Rocks rolling on the surface of the lower part would only reach to the drainage channel. Similar actions can be observed for Stop 15 and 18. Rocks rolling on the surface of Stop 16 bouncing when they reach the retaining wall but shattered pieces would only fall and accumulate in the drainage channel.

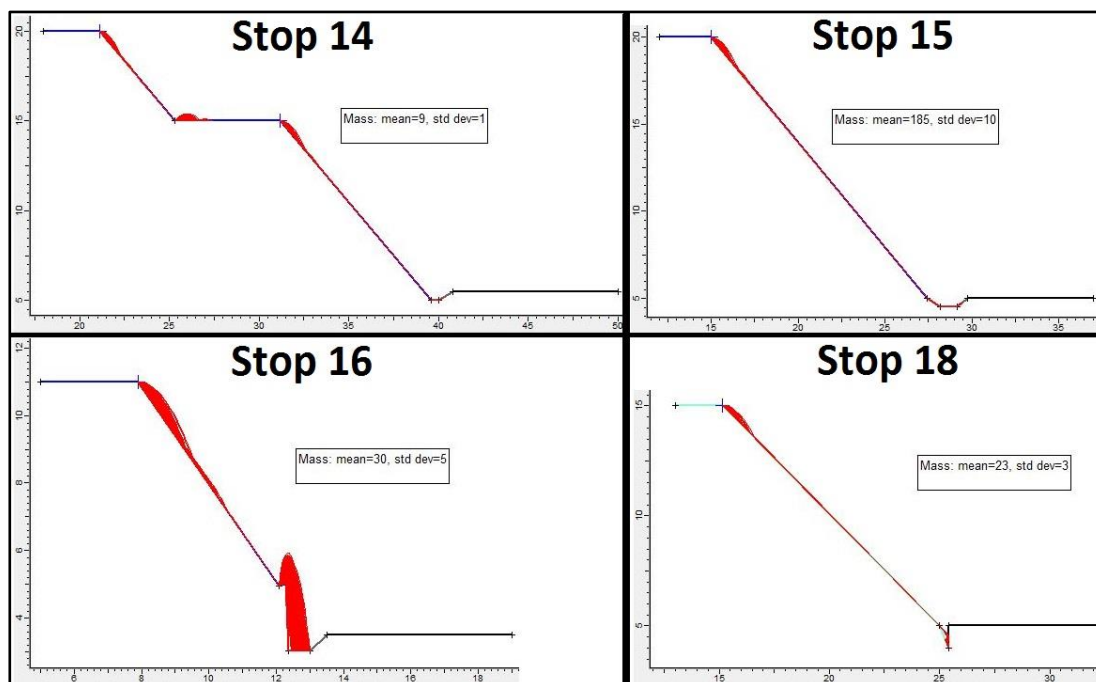


Figure 105. Rockfall analyses of Stop 14, 15, 16 and 18

As analyses indicate that the most intensive falling action is observed at Stop 19 and 20 (Figure 106) without any precaution like retaining walls or steel wire meshes. Despite this, both analyses and field surveys revealed that rocks only accumulate in the drainage channels, in other words, the road would not be endangered due to rockfall.

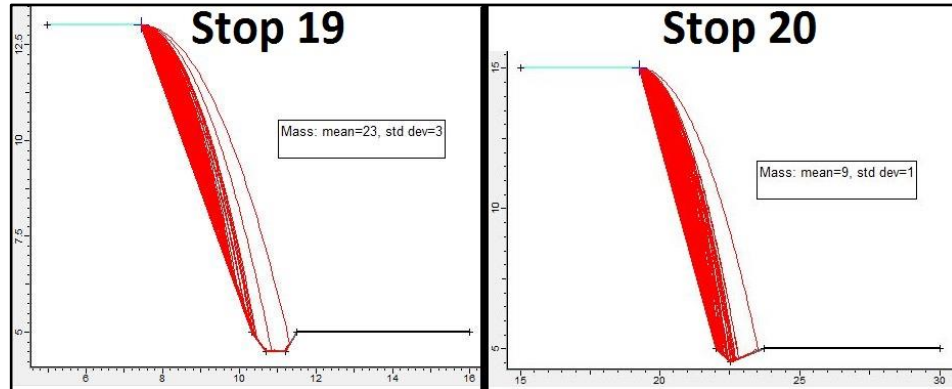


Figure 106. Rockfall analyses of Stop 19 and 20

Neither during the field studies nor in the rockfall analyses, any danger on the road related to rock fall activity is not observed. The only critical circumstance is that some fragments are observed in the drainage channel both in the field and rockfall analyses. In the field, rock fall traffic sign boards are installed next to Stops 8 and 15. Despite these traffic signs, any major rockfall danger on the road was not observed at the field. The rockfall analyses done at these cut slopes are found to be coherent with the observations.

### 5.5.Slope Mass Rating (SMR)

Slope Mass Rating (SMR) system is developed by Romana (1985) which is obtained from Bieniawski's Rock Mass Rating (RMR). This value is obtained by subtracting discontinuity orientation adjustment value from RMR basic evaluated by adding five parameter ratings; strength, RQD, spacing of discontinuities, condition of discontinuities and groundwater condition. Fresh rock strength values (Table 69) were considered and they were assigned from UCS values converted from point load test. For the flysch type deposits, weighted averages of different rock types were used. RQD values were determined by an imaginary borehole drilled vertically from the maximum height of the slope. Exceptions like Stop 14, 18, 19 and 20 where bedding planes are nearly perpendicular to road were drilled with a horizontal imaginary borehole. These imaginary boreholes were designed in order to obtain

most realistic RQD results. Therefore RQD values of these road cuts are not underestimated. Spacing and condition of the discontinuity data were directly collected by scan line survey. Groundwater was considered to be drained from the discontinuity surfaces. Based on conditions of the infill materials, groundwater condition was assigned damp for all slopes. SMR on the other hand deals with the adjustment for joint orientation considering slope dip and dip direction (Table 74). These modes of failures were calculated by adding factors related to joint orientation with respect to slope orientation and method of excavation.

Table 74. Rating adjustment for joint orientation (Singh & Gahrooei, 1989)

<b>Joint Orientation</b>	No mode of failure	One possible mode of failure	One mode of failure	Two mode of failures	Several mode of failures
<b>Rating</b>	0	-5	-25	-50	-60

According to the scan line survey results, it is known that discontinuities mostly reveal scattered distribution. Also, the degree of jointing were calculated in the range of very high to moderate. Taking into account of these results, there should be several mode of failures. According to **Table 74**, rating of several mode of failures were introduced as -60. It means that -60 should be added to  $RMR_{basic}$  values. As it can be seen from **Table 75**, all  $RMR_{basic}$  values in the study area were calculated as maximum 50. This means that adding several mode of failures value concludes negative values of SMR. Obviously, this would not be applicable. Ulusay & Sönmez (2007) suggest that for joint orientation, it should be taken maximum -5 because heavily jointed road cuts would reveal mode of circular failure like in this study. Therefore, considering one possible mode of failure, -5 is added to all  $RMR_{basic}$  values (Table 75). Detailed values of each parameter assigned for related road cut

can be seen in Appendix B. The stability conditions and stable probabilities were assigned according to Romana (1985) (Table 76).

Table 75.  $RMR_{basic}$ , SMR and stable probabilities of each road cut

Stop	$RMR_{basic}$	SMR	Stability	Stable Probability
1-Failed	27	22	Unstable	40%
1	31	26	Unstable	40%
2-Failed	27	22	Unstable	40%
2	45	40	Unstable	40%
3	40	35	Unstable	40%
4	36	31	Unstable	40%
5	43	38	Unstable	40%
6	33	28	Unstable	40%
7	50	45	Partially Stable	60%
8	45	40	Unstable	40%
9	47	42	Partially Stable	60%
10	45	40	Unstable	40%
11	38	33	Unstable	40%
12	35	30	Unstable	40%
13	38	33	Unstable	40%
14	38	33	Unstable	40%
15	45	40	Unstable	40%
16	35	30	Unstable	40%
17	35	30	Unstable	40%
18	40	35	Unstable	40%
19	40	35	Unstable	40%
20	43	38	Unstable	40%

Table 76. Stability classes as per SMR values (modified from Romana (1985))

<b>SMR value</b>	0-20	21-40	41-60	61-80	81-100
<b>Stability</b>	Completely unstable	Unstable	Partially stable	Stable	Completely stable
<b>Stable probability</b>	10%	40%	60%	80%	100%

According to the SMR results, almost all slopes are under risk of instability. Considering mostly weak and moderately strong rock mass, low RQD values, very high to moderate jointing degree, SMR values mostly coherent with the field observations in terms of surficial failures. Two partially stable results belonging to Stop 7 and 9 are obtained because of relatively stronger rock mass results and higher RQD values than the others.

#### **5.6.Slope Stability Probability Classification (SSPC)**

Another empirical method used in thesis is Slope Stability Probability Classification (SSPC) system which is developed by Hack (1998). SSPC introduces very simple data collection and most importantly includes weathering and excavation effects on slope stability. Following excavation method, intact rock strength, weathering degree and discontinuity properties like orientation, spacing, roughness and infill material, SSPC brings out internal friction angle and cohesion for reference and slope rock mass. It is acceptable that reference rock reflects relatively fresh rock mass behind the slope rock mass which is the weathered and disturbed zone. Using empirical formulae introduced by SSPC, orientation independent and orientation dependent probabilistic slope stability results can be obtained. Important factors governing orientation independent stability are dip amount and maximum height of the slope in addition to cohesion and internal friction angle. On the other hand slope orientation plays an important role for orientation dependent stability in addition to discontinuity conditions. Monte Carlo probabilistic approach is applied by Hack (1998) to eliminate the errors like parameter variation at rock mass and measuring rock mass

parameters while collecting data. In the light of this information, SSPC system was applied and stability results were obtained for each road cut. These stable probabilities were obtained by directly using the Reference Intact Rock Strength (RIRS) computed by weathered rock mass strength.

An example solution is introduced by using Stop 8 “weighted average” weathered intact rock strength which is calculated as 13 MPa (IRS) (Table 69) and estimated weathering degree parameter as 0,9 (WE) (Table 77). Therefore, RIRS is calculated by using these values according to formula below:

$$\text{RIRS} = \text{IRS} / \text{WE} \Rightarrow \text{RIRS} = 13 / 0,9$$

The resultant RIRS value is obtained as 14,4 (Table 78). Then this value is used to obtain reference/fresh rock friction angle ( $\phi$ ) and cohesion (c) including discontinuity spacing (RSPA) corrected by weathering and excavation, and condition of discontinuities (RCD) corrected by weathering, according to formulae below:

$$\phi = \text{RIRS} * 0,2417 + \text{RSPA} * 52,12 + \text{RCD} * 5,779 \Rightarrow \phi = 34,53^0$$

$$c = \text{RIRS} * 94,27 + \text{RSPA} * 28629 + \text{RCD} * 3593 \Rightarrow c = 18,7 \text{ kPa}$$

After generating reference/fresh rock parameters, same excavation method and weathering degree were applied to obtain weathered/disturbed friction angle and cohesion which are  $25,08^0$  and 13,5 kPa (Table 79). Details of these calculation steps for all road cuts can be seen in Appendix B.

Table 77. Data collection table of SSPC for a representative slope (Stop 8)

DATA COLLECTION TABLE								
Excavation Method (ME)			Intact Rock Strength (IRS)					
Natural/hand-made		1,00	<1.25 MPa		Crumbles in hand			
Pneumatic hammer excavation		0,76	1.25-5 MPa		Thin slabs break easy in hand			
Pre-splitting/smooth wall blasting		0,99	5-12.5 MPa		Thin slabs broken by heavy hand pressure			
Conventional blasting with result:			12.5-50 MPa		Lumps broken by light hammer blows			
Good		0,77	50-100 MPa		Lumps broken by heavy hammer blows			
Open discontinuities		0,75	100-200 MPa		Lumps only chip by heavy hammer blows			
Dislodged blocks		0,72	>200 MPa		Rocks ring on hammer blows			
Fractured intact rock		0,67	Weathering degree (WE)		Unweathered		1,00	
Crushed intact rock		0,62			Slightly		0,95	
Lithology					Moderately		0,90	
50% Sandstone / 50% Mudstone					Highly		0,62	
					Completely		0,35	
Discontinuities (B: Bedding; J: Joint)			B	J1	J2	Slope		
Dip direction (degrees)			310	170	70	Dip direction (degrees)	215	
Dip (degrees)			30	70	70	Dip (degrees)	50	
Spacing (DS) (cm)			50	80	40	Slope height (m)	15	
Condition of discontinuities						Slope Stability		
Large scale roughness (RL)	Wavy		1,00				Stable	1
	Slightly wavy		0,95			X	Small problem	2
	Curved		0,85	X	X		Large problem	3
	Slightly curved		0,80				Notes: 1) For infill "gouge>irregularities" and "flowing material" small scale roughness= 0,55 2) If roughness is anisotropic (e.g. Ripple marks, striation, etc.) roughness should be assessed perpendicular and parallel to the roughness and directions noted on this form 3) Non-fitting of discontinuities should be marked in roughness columns.	
	Straight		0,75					
Small scale roughness (RS)	Rough stepped		0,95					
	Smooth stepped		0,90	X	X	X		
	Polished stepped		0,85					
	Rough undulating		0,80					
	Smooth undulating		0,75					
	Polished undulating		0,70					
	Rough planar		0,65					
	Smooth planar		0,60					
Polished planar		0,55						
Infill material (IM)	Cemented / cemented infill		1,07					
	No infill - surface staining		1,00					
	Non-softening & sheared material	Coarse	0,95					
		Medium	0,90					
		Fine	0,85					
	Soft sheared material	Coarse	0,75					
		Medium	0,65	X	X	X		
		Fine	0,55					
	Gouge < irregularities		0,42					
	Gouge > irregularities		0,17					
Flowing material		0,05						
Karst (KA)	None		1,00	X	X	X		
	Karst		0,92					

Table 78. Reference rock table of SSPC for a representative slope (Stop 8)

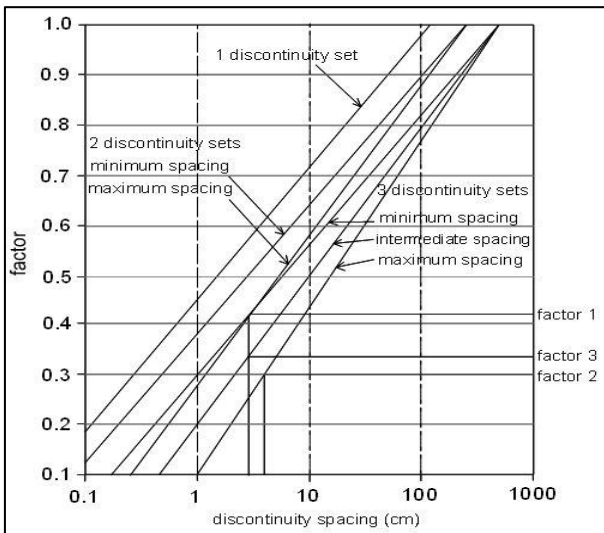
REFERENCE ROCK TABLE						
Intact Rock Strength (RIRS)						
RIRS = IRS / WE = 13 / 0,90					14,444	
Discontinuity Spacing (SPA)						
Discontinuities	B	J1	J2	SPA = factor 1 x factor 2 x factor 3	0,531	
Dip direction (degrees)	310	170	70			
Dip (degrees)	30	70	70			
Spacing (m)	50	80	40			
The spacing parameter (SPA) is calculated based on the three discontinuity sets with the smallest spacings in following figure:				SPA = 0,71 x 0,70 x 0,73 = 0,363		
				Corrected for weathering and method of excavation:		
				RSPA = SPA / (WE x ME)		
				RSPA = 0,363 / (0,90 x 0,76)		
Condition of discontinuities						
Discontinuities	B	J1	J2	RTC is the discontinuity condition of a single discontinuity (set) in the reference rock mass corrected for discontinuity weathering. $RTC = TC / \sqrt{1,452 - 1,220 * e^{(-WE)}}$		
Large scale roughness (RI)	0,85	0,85	0,95			
Small scale roughness (Rs)	0,90	0,90	0,90			
Infill material (Im)	0,65	0,65	0,65			
Karst (Ka)	1,00	1,00	1,00			
TC = RI x Rs x Im x Ka	0,497	0,497	0,556			
RTC	0,509	0,509	0,568			
Weighted by spacing: $CD = \frac{\frac{TC_1}{DS_1} + \frac{TC_2}{DS_2} + \frac{TC_3}{DS_3}}{\frac{1}{DS_1} + \frac{1}{DS_2} + \frac{1}{DS_3}} =$					0,523	
Corrected by weathering: RCD (with a maximum of 1.0165) = CD/WE =				0,523 / 0,90 =	0,581	
Reference unit friction and cohesion (RFRI & FCOH)						
$\phi(RRM) = RIRS * 0,2417 + RSPA * 52,12 + RCD * 5,779 =$ (If RIRS > 132 MPa, then RIRS = 132)					34,53°	
coh(RRM) = RIRS * 94,27 + RSPA * 28629 + RCD * 3593 = (If RIRS > 132 MPa, then RIRS = 132)					18,7 kPa	

Table 79. Stability table of SSPC for a representative slope (Stop 8)

STABILITY TABLE							
Method of Excavation (SME)			Weathering (SWE)				
Natural/hand-made		1,00	Unweathered	1,00			
Pneumatic hammer excavation		0,76	Slightly	0,95			
Pre-splitting/smooth wall blasting		0,99	Moderately	0,90			
Conventional blasting with result:			Highly	0,62			
Good		0,77	Completely	0,35			
Open discontinuities		0,75	Slope geometry features				
Dislodged blocks		0,72	Slope dip direction (degrees)	215			
Fractured intact rock		0,67	Slope dip (degrees)	50			
Crushed intact rock		0,62	Height (m)	15			
Orientation-independent stability							
Intact Rock Strength (SIRS)							
SIRS = RIRS (from reference rock mass) x SWE (weathering slope) =			14,444 x 0,90	13 MPa			
Discontinuity spacing (SSPA)							
SSPA = RSPA x SWE x SME			0,531x0,90x0,76	0,363			
Condition of discontinuity (SCD)							
SCD = RCD x SWE =			0,581 x 0,90	0,523			
Slope unit friction and cohesion (SFRI & SCOH)							
SFRI = SIRS * 0,2417 + SSPA * 52,12 + SCD * 5,779 =				25,08°			
(If RIRS > 132 Mpa, then RIRS =132)							
SCOH = SIRS * 94,27 + SSPA * 28629 + SCD * 3593 =				13,5 kPa			
(If RIRS > 132 Mpa, then RIRS =132)							
If SFRI < slope dip, maximum possible height (Hmax):				16,1 m			
Hmax = (1,6x10 <sup>-4</sup> x SCOH) x sin(slopedip) x cos(SFRI) / (1 - cos(slopedip - SFRI)) =							
Ratios	SFRI / Slope dip			0,502			
	Hmax/ Hslope			1,073			
Stable probability: if SFRI > slope dip, probability = % 100, else use the figure for orientation-independent stability:				50%			
Orientation-dependent stability							
Discontinuities		B	J1	J2			
Dip direction (degrees)		310	170	70			
Dip (degrees)		30	70	70			
With, Against, Vertical or Equal		A	W	A			
AP (degrees)		-3	63	-66			
RTC		0,509	0,509	0,568			
STC = RTC x sqrt(1,452 - 1,220 x e <sup>(-SWE)</sup> )		0,497	0,497	0,556			
Stable probability:	Sliding	100%	100%	100%			
	Toppling	100%	100%	>95%			
Stable probability:		>95%					
Determine orientation stability:							
Calculate AP: β = discontinuity dip, σ = slope dip direction, τ= discontinuity dip direction, δ = σ - τ, AP= arctan(cosδ x tanβ)							
Stability		Sliding	Toppling	Stability	Sliding	Toppling	
AP>84°or AP<-84°	Vertical	100%	100%	AP<0° and (-90°<AP+slope dip)<0°	Against	100%	100%
(slope dip + 5°) < AP < 84°	With	100%	100%	AP<0° and (-90°<AP+slope dip)>0°	Against	100%	Use graph toppling
(slope dip - 5°) < AP < (slope dip + 5°)	Equal	100%	100%				
0°< AP < (slope dip - 5°)	With	Use graph sliding	100%				
Slope final stable probability		50%					

As it was discussed before, depth of weathered/disturbed zone in front of the relatively fresh rock is determined by visual estimation and in-situ test like Schmidt rebound and “simple means”. As mentioned in the rockfall analyses, block volumes in the study area are too small to create any danger like sliding, toppling or wedge but only creating rock fall hazards. These sliding and toppling risks on slope rock mass (weathered/disturbed zone in this case) (Table 80) should be taken into consideration of small rock fall hazards. Evaluating this way, almost all road cuts except Stop 9 are concordant with the field observations which reveal surface failure problems (Table 80). The details of each slope consisting data collection table, reference rock table and stability table can be seen in Appendix B. On these tables, highlighted sections indicate decided data in the field for the related road cut. These results reflect the original method introduced by SSPC.

Table 80. Stable probabilities of each road cut obtained by using weathered intact  
rock strength

	<b>Mass</b>	<b>Sliding/Toppling</b>
<b>Stop 1</b>	5%	95%
<b>Stop 1 F</b>	5%	95%
<b>Stop 2</b>	5%	100%
<b>Stop 2 F</b>	5%	100%
<b>Stop 3</b>	5%	95%
<b>Stop 4</b>	5%	5%
<b>Stop 5</b>	5%	50%
<b>Stop 6</b>	5%	5%
<b>Stop 7</b>	5%	95%
<b>Stop 8</b>	50%	95%
<b>Stop 9</b>	95%	95%
<b>Stop 10</b>	40%	5%
<b>Stop 11</b>	5%	95%
<b>Stop 12</b>	5%	95%
<b>Stop 13</b>	5%	80%
<b>Stop 14</b>	5%	95%
<b>Stop 15</b>	20%	15%
<b>Stop 16</b>	20%	5%
<b>Stop 17</b>	30%	80%
<b>Stop 18</b>	50%	95%
<b>Stop 19</b>	5%	5%
<b>Stop 20</b>	5%	5%

The internal friction angle and cohesion values obtained from SSPC are summarized in Table 81.

Table 81. Internal friction angle ( $\phi$ ) and cohesion (c) values of each road cut obtained by using weathered intact rock strength

	Reference/Fresh		Slope/Weathered		Weathering Degree
	$\phi$ °	c (kPa)	$\phi$ °	c (kPa)	
<b>Stop 1</b>	14,26	7,7	10,89	5,9	Moderately
<b>Stop 1 F</b>	18,40	10,3	9,40	5,3	Highly
<b>Stop 2</b>	25,64	13,5	18,91	9,9	Moderately
<b>Stop 2 F</b>	32,95	18,0	16,25	8,9	Highly
<b>Stop 3</b>	21,33	11,5	15,51	8,3	Moderately
<b>Stop 4</b>	17,04	9,3	12,65	6,9	Moderately
<b>Stop 5</b>	18,60	10,2	13,53	7,5	Moderately
<b>Stop 6</b>	25,47	14,3	12,58	7,1	Highly
<b>Stop 7</b>	25,97	14,1	20,56	11,1	Slightly
<b>Stop 8</b>	34,53	18,7	25,08	13,5	Moderately
<b>Stop 9</b>	29,91	15,3	22,60	11,6	Moderately
<b>Stop 10</b>	25,54	13,9	18,39	10,0	Moderately
<b>Stop 11</b>	20,40	11,2	15,00	8,2	Moderately
<b>Stop 12</b>	24,95	13,7	12,79	7,0	Highly
<b>Stop 13</b>	16,72	9,1	12,46	6,8	Moderately
<b>Stop 14</b>	17,98	9,5	13,50	7,1	Moderately
<b>Stop 15</b>	31,14	16,3	22,93	11,9	Moderately
<b>Stop 16</b>	22,03	11,7	16,22	8,6	Moderately
<b>Stop 17</b>	18,14	9,8	13,30	7,2	Moderately
<b>Stop 18</b>	25,11	12,8	19,34	9,8	Moderately
<b>Stop 19</b>	20,36	11,0	15,00	8,0	Moderately
<b>Stop 20</b>	16,47	8,9	12,19	6,6	Moderately

It can be observed that reference/fresh rock mass friction angle and cohesion values do not exceed  $35^{\circ}$  and 20 kPa, respectively. Similarly slope/weathered rock mass values do not exceed  $25^{\circ}$  and 15 kPa. Analyses reveal that fresh values are decreasing for the weathered rock in the same ratio for both internal friction angle and cohesion. Also, it is calculated that there is an agreement within the weathering categories about decreasing ratios. As it can be seen from Table 81, the decrease rate of  $\phi$  and  $c$  for highly weathered rock values nearly 50%, moderately weathered rocks about 75% and slightly weathered rocks approximately 85%, from fresh rock to weathered rock.

In order to check the success rate change, same parameter generation is made by directly applying fresh intact rock strength values obtained from the point load test to Reference Intact Rock Strength (RIRS) without any weathering correction. Again using the same road cut example (Stop 8), the RIRS value is used as 23 MPa (Table 69). It should be noted that this value is not obtained from any weathering correction because it reflects the fresh rock value already. Again using the same steps of formulae fresh rock friction angle and cohesion are obtained. From these fresh rock parameters, weathered rock friction angle and cohesion are calculated by applying weathering and excavation corrections. Following same condition for all slopes in the study area, weathered rock stable probabilities were calculated (Table 82). As Table 82 indicates, most of the road cuts are determined correctly with respect to field observations with some exceptions shown by red color. For the stable probability of Stop 10 (mentioned with asterisks (\*)) even mass failure percentage reveal partially stable, orientation dependent percentage show significant danger.

Table 82. Stable probabilities of each road cut obtained by using fresh intact rock strength

	<b>Mass</b>	<b>Sliding/Toppling</b>
<b>Stop 1</b>	5%	95%
<b>Stop 1 F</b>	5%	95%
<b>Stop 2</b>	5%	100%
<b>Stop 2 F</b>	5%	100%
<b>Stop 3</b>	5%	95%
<b>Stop 4</b>	5%	5%
<b>Stop 5</b>	5%	50%
<b>Stop 6</b>	5%	5%
<b>Stop 7</b>	5%	95%
<b>Stop 8</b>	80%	95%
<b>Stop 9</b>	95%	95%
<b>Stop 10</b>	70%*	5%*
<b>Stop 11</b>	20%	95%
<b>Stop 12</b>	10%	95%
<b>Stop 13</b>	5%	80%
<b>Stop 14</b>	5%	95%
<b>Stop 15</b>	40%	15%
<b>Stop 16</b>	10%	5%
<b>Stop 17</b>	40%	80%
<b>Stop 18</b>	70%	95%
<b>Stop 19</b>	5%	5%
<b>Stop 20</b>	5%	5%

The friction angle and cohesion values obtained from the fresh rock UCS values are summarized in Table 83.

Table 83. Internal friction angle ( $\phi$ ) and cohesion (c) values of each road cut obtained by using fresh intact rock strength

	Reference/Fresh		Slope/Weathered		Weathering Degree
	$\phi$ °	c (kPa)	$\phi$ °	c (kPa)	
<b>Stop 1</b>	15,00	8,0	11,55	6,1	Moderately
<b>Stop 1 F</b>	18,63	10,4	9,57	5,3	Highly
<b>Stop 2</b>	25,64	13,5	23,74	11,8	Moderately
<b>Stop 2 F</b>	32,95	18,0	16,25	8,9	Highly
<b>Stop 3</b>	28,72	14,4	22,28	11,0	Moderately
<b>Stop 4</b>	20,26	10,6	15,55	8,0	Moderately
<b>Stop 5</b>	26,71	13,4	20,83	10,3	Moderately
<b>Stop 6</b>	30,26	16,1	15,55	8,2	Highly
<b>Stop 7</b>	43,94	21,1	37,63	17,8	Slightly
<b>Stop 8</b>	36,59	19,5	26,95	14,2	Moderately
<b>Stop 9</b>	36,22	18,0	28,28	13,8	Moderately
<b>Stop 10</b>	27,77	14,8	20,40	10,8	Moderately
<b>Stop 11</b>	23,87	12,5	18,11	9,4	Moderately
<b>Stop 12</b>	25,03	13,7	12,83	7,0	Highly
<b>Stop 13</b>	17,50	9,4	13,19	7,0	Moderately
<b>Stop 14</b>	18,14	9,6	13,74	7,2	Moderately
<b>Stop 15</b>	32,26	16,8	23,94	12,3	Moderately
<b>Stop 16</b>	21,95	11,7	16,22	8,6	Moderately
<b>Stop 17</b>	18,64	9,9	13,81	7,3	Moderately
<b>Stop 18</b>	25,60	13,0	19,82	9,9	Moderately
<b>Stop 19</b>	24,33	12,5	18,57	9,4	Moderately
<b>Stop 20</b>	17,98	9,5	13,64	7,1	Moderately

The same ratio differences for different weathering degrees are valid for these parameters as in the previous ones. Different than the parameters obtained from weathered UCS values (Table 81) these parameters are higher in terms of both fresh - weathered conditions and  $(\phi)$  -  $(c)$  conditions. This variation occurs due to fresh-weathered rock UCS value differences.

Comparing these two stable probability results, the parameters governed from weathered rock are executing weathered/disturbed zone with a great success (with only exception of Stop 9) (Table 80). Results governed by using relatively fresh rock sample strength, on the other hand, reveal approximately 85% success rate, which is lower than the original method.



## CHAPTER 6

### DISCUSSIONS

#### 6.1. Uniaxial Compressive Strength

Point load test average values shown in Table 13 indicate that saturated values are lower than the dry values. According to the results, it is estimated that values decrease about 40% for the relatively fresh and nearly 50% for the weathered rocks. Maximum decrease is observed for the failed zone of Stop 1 mudstone specimens nearly 85% and 90% for the relatively fresh and the weathered samples, respectively. It can be stated that strength reduction difference between fresh and weathered zones can be attributed to micro fractures. UCS values of the mudstone layers at flysch unit are correlated from Stop 1, which has the most suitable mudstone specimens to conduct the point load test. The mudstone layers at rest of the road cuts are intensely fractured and their intact rock sizes do not match with the desired test specifications. In addition, even weathered samples could be conducted by point load test; relatively fresh specimens could not be reached because of deep weathering zone at Stop 9. Taking into account all of these, the most reliable data for mudstone is determined from Stop 1. Comparing intact rock strength of the flysch unit studied in this thesis, for some road cuts (Stops 11, 12, 13 and 20) mudstone values are nearly 1 MPa higher than the sandstone and marl specimens. For Stop 11 and 12, it could be acceptable by considering nearly the same weathering rates, decomposition and very thin undercutting action under the sandstone layers. Despite that, all these 4 road cuts reveal contradiction because field observations indicate weaker mudstone layers than the sandstone or marl. This can be explained by the invisible micro fractures in these sandstones or marl. While conducting point load test, the samples could be failed through these fractures which cannot be realized.

Uniaxial compressive strength determination from the Schmidt rebound test (Table 15) could not be conducted for all rock layers. For Schmidt rebound test, the desired mudstone samples could not be reached in the field due to the same reasons explained for point load test. In specifications of this test, it is indicated that at least 10 cm intact rock without any fractures should be used. Again, due to deep weathering zones, relatively fresh samples could not be obtained to conduct this test. In addition to this, comparison is done between point load test and Schmidt rebound hammer conversions. As it can be seen from Table 15, UCS values of the rocks obtained from Schmidt rebound test results mostly higher than the UCS values converted from the point load test. On the other hand, equation developed by Yasar & Erdogan (2004) reveals dramatic underestimation of the weathered values compared to the point load test results. Also, equation developed for marls by Gokceoglu (1996) shows extreme underestimation for both weathered and relatively fresh samples. Despite Deere & Miller (1966) equation reveal overestimation on Schmidt rebound test results compared to point load test results, Barton & Bandis (1982) suggest to use this to determine joint wall compressive strength. In this thesis, including all available data for both fresh and weathered zones of the rocks, a scattered result is obtained (Figure 107). The equation for the scattered data and  $R^2$  value is shown in Figure 107 belonging to this thesis study. It is observed that  $R^2$  value is very low (0.35) to define a correct equation to obtain UCS from Schmidt hammer rebound values. Nearly the same  $R^2$  results are obtained for the road cuts including marls and sandstones which are 0.44 and 0.53, respectively. On the other hand, the  $R^2$  values obtained for the road cuts including limestones (0.84) and igneous rocks (granite, basalt and granodiorite) (0.99) are significantly high (Figures 108 and 109). It should be noted that these values are obtained including both fresh and weathered rock samples. Therefore, equations given for the limestones and igneous rocks can be used to determine UCS from Schmidt hammer rebound values for both fresh and weathered samples (Table 84).

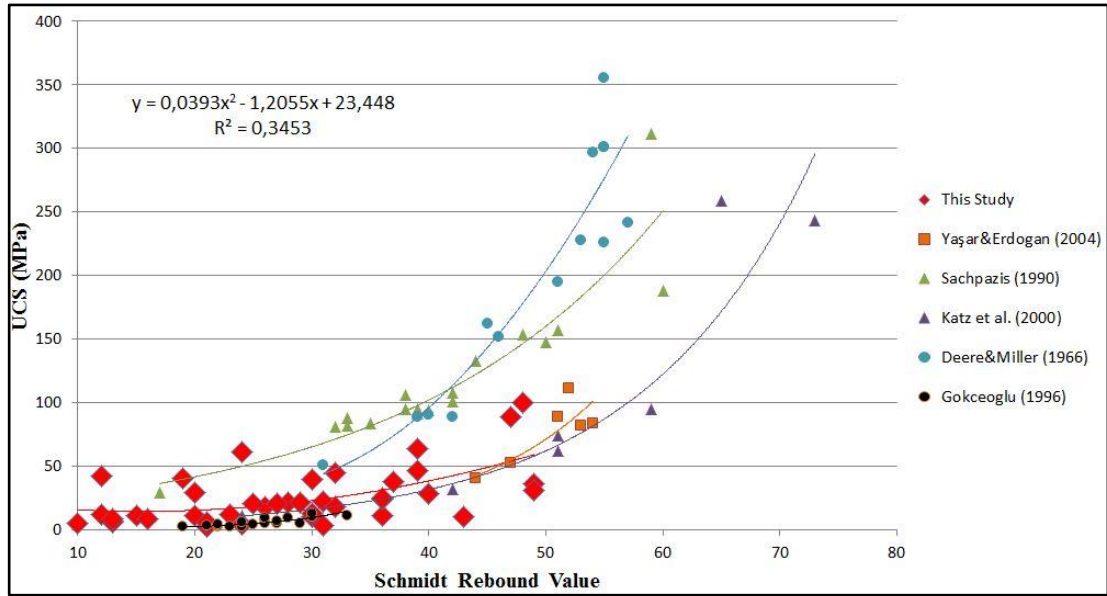


Figure 107. UCS vs Schmidt rebound value graph according to various researchers and this thesis study

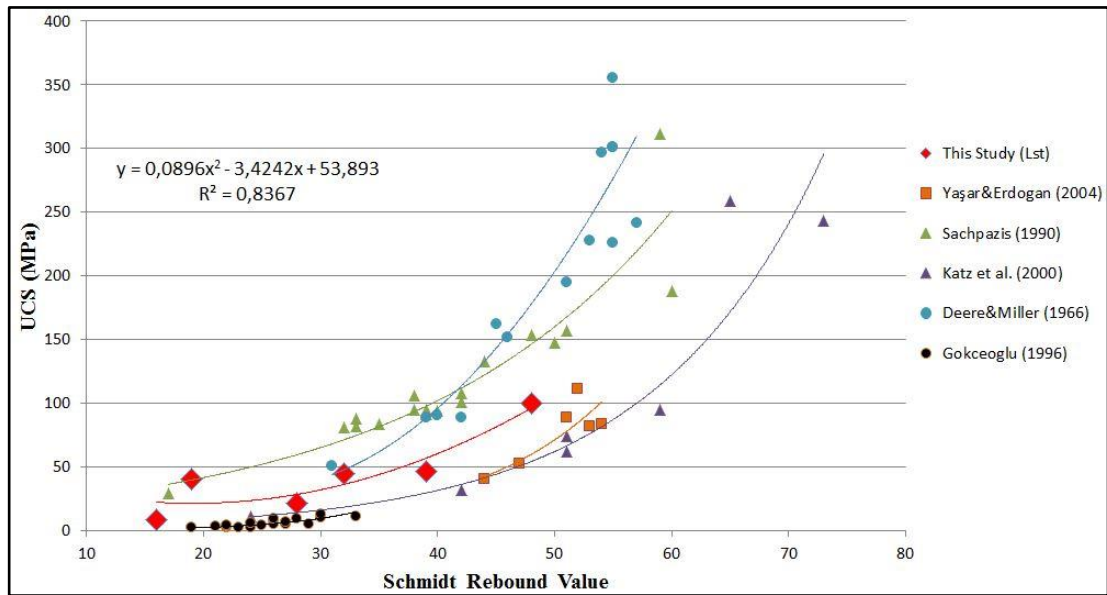


Figure 108. UCS vs Schmidt rebound value graph according to various researchers and limestone samples of this thesis study

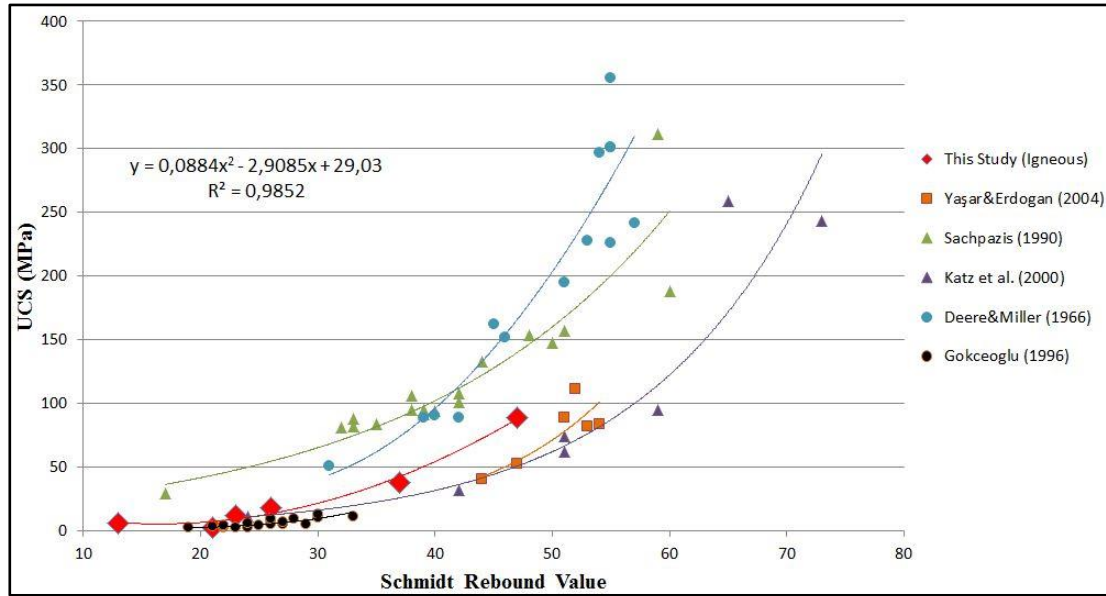


Figure 109. UCS vs Schmidt rebound value graphs according to various researchers and igneous rock samples of this thesis study

Table 84. Functions between UCS and Schmidt rebound values and correlation coefficients ( $R^2$ )

Rock Type	Function	Correlation Coefficient ( $R^2$ )
Limestone	$UCS=0,0896(L^2)-3,4242(L)+53,893$	0,8367
Igneous	$UCS=0,0884(L^2)-2,9085(L)+29,030$	0,9852

\*UCS in terms of MPa, L: Schmidt rebound value (applied perpendicular to the surface)

## 6.2.Weathering

In this thesis, weathering concerns with engineering time span which is tens of years. Weathering in engineering time affects mostly the weak rocks such as gypsum, claystone or mudstone. In study the area, it is very clear that the mudstone layers are affected by weathering in engineering timescale considering that the road cuts are reconstructed in 2010. In addition to the mudstone layers, the rocks in between them such as sandstone, marl and limestone are also affected by weathering mostly along the discontinuities. Similar to the flysch unit, the igneous rocks in the study area are affected by weathering around both discontinuities and shear zones. It is observed

that from 2010 to present (2016), the most effected rock type is the mudstone according to the field observations. The mudstone layers on the surface are broken into small pieces (maximum 3 cm in length) due to weathering. Also, comparing to accompanying layer in flysch unit weathering effect is both deeper and higher in the mudstones for all studied road cuts. In addition to the mudstone, the granite at Stop 6 is highly weathered on the surface. The weathered zone on the surface of this granite was significantly deep. At this zone granite is very weak that crumbles in hand (Figure 110). Especially saturated samples revealed much weaker intact rock strength. It is observed that braking takes place on dark colored zones in granite particles. Due to this intense weathering action, locations of discontinuities are hard to define.



Figure 110. Dry granite sample from Stop 6

Despite the adverse effects of weathering on the mudstones and granite at Stop 6, the durability results from slake durability test reveal medium high for granite and high for mudstone samples taken from Stop 1. According to the field observations and

laboratory strength tests, it is expected that durability should be lower for these rocks. This can be explained by two reasons. First of all, according to ASTM D4644-87 (1998) the degradation types of mudstone and granite are type II and III, respectively (Table 18). This explains their highly fractured texture on the surface. Secondly,  $Id_2$  would not be enough to explain the real durability condition of these rocks. Further investigation on this test would reveal more coherent results about durability of the samples.

Methylene Blue Adsorption (MBA) test results show that the relatively fresh sample values are nearly half of the weathered ones. These differences would not reflect any significance because their values are in the same mineral range. For example, Cation Exchange Capacity (CEC) results reveal that the values of all stops including both fresh and weathered samples are changing between 0,3 and 6,1 which means they are in the range of kaolinite mineral. On the other hand, Methylene Blue Adsorption (MBA) values of all stops including fresh and weathered samples are in the range of 0,13 to 2,67. This means that possible minerals can be biotite, chlorite, illite and kaolinite at the study area. Despite very vast range of minerals any of them are not prone to swelling action. From different standpoint, it is known that MBA test results may reveal the amount of clay minerals if only one clay mineral type exists. Therefore even there are high swelling capacity minerals in the samples, because of tiny amount, they would not show remarkable swelling action.

### **6.3. Slope Stability Classification Systems**

Two different classification systems namely, SMR and SSPC, are used in this thesis to determine the stable probabilities of the road cuts. Both of them are based on empirical solutions to introduce shear strength parameters and probabilities against slope failures.

SMR results summarized in Table 75 are nearly similar to GSI values (Table 70) which are evaluated independently to avoid bias. It is suggested that in order to find GSI values, RMR values are decreased by 5 (Hoek & Brown, 1997). In this case, these values are significantly coherent. On the other hand, SMR results reflects unstable and partially unstable results according to Romana (1985). Single

probability numbers are assigned for very wide ranges. For example Stop 1 is in the same category with Stop 8 which has very different results like 26 and 40, respectively. Moreover, SMR value of the failed zone of Stop 1 is determined as 22 by following suggestions of Ulusay & Sönmez (2007). According to Romana (1985), this slope is in the category of unstable with 40% stable probability. However this zone is already failed which means that it should be named as completely unstable. Therefore, rather than following -5 rating for one possible mode of failure (Singh & Gahrooe, 1989) for all road cuts having heavily jointed textures, one mode of failure which has -25 rating should be applied. With this solution, SMR values of the failed zones of Stop 1 and 3 decrease to 2 which is in the category of completely unstable and 10% stable probability according to Romana (1985).

Another contradiction for the SMR system is that the ratings are assigned according to the saturated relatively fresh rock samples. This means that results are reflecting stability of fresh zone behind the estimated weathered zone. According to the field observations, all road cuts are stable with minor exceptions, and excluding failed zones of Stop 1 and 2. These exceptions are due to shear zones as in Stop 4, 5 and 19 which are independent from discontinuity sets used to evaluate the classification systems. However, the results reveal that most of the road cuts are categorized as unstable, in other words stable probabilities are lower than 50%, except Stop 7 and 9. These results could be useful for the weathered zones which show surficial failures (surficial degradations), but would not give true solutions for the fresh zones (whole cut slope) of the road cuts.

Distribution of stable and unstable slopes according to the field observations on SMR points can be seen in Figure 111. As it was mentioned above, two unstable zones at Stops 1 and 2 are located in the unstable zone. However, if -25 rating is applied at these zones, they will automatically shift to the completely unstable category, mentioned by red color in Figure 111. Despite most of the road cuts are stable in the study area with very small surficial failures, SMR results show exact opposite condition. Except already failed zones, any distinctive results about stable slopes could not be obtained by the SMR method.

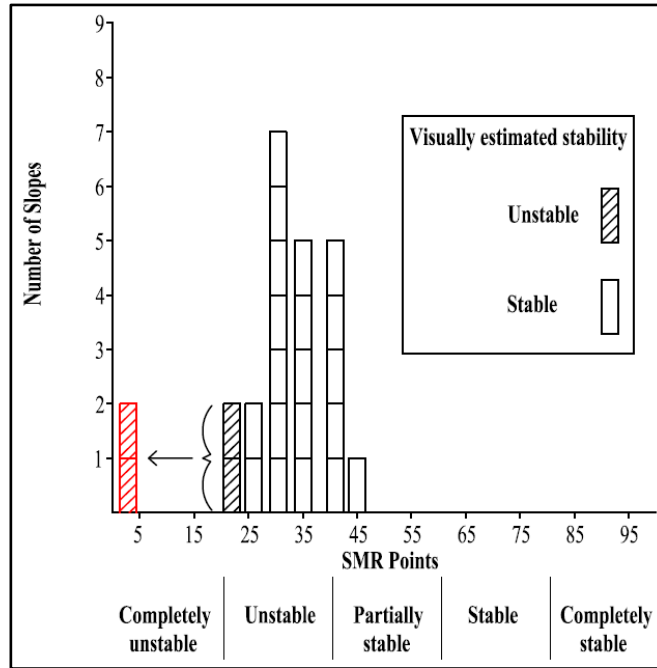


Figure 111. Distribution of visually estimated stabilities on SMR points

Basically original method of SSPC system suggests collecting examples and obtaining data from the surface of the slope, which is weathered and disturbed zone most cases. From this data relatively fresh rock properties can be evaluated. In this thesis, advantageously both weathered/disturbed and relatively fresh data were collected. Considering this, in addition to the original method, data obtained from directly relatively fresh zone was used. According to this, 2 different probabilistic results are obtained (Tables 80 and 82). The original method (using weathered samples directly) reveals 95% success considering the field observations for the surficial degradations (Figure 112). Conversion of fresh zone strength data directly, on the other hand, reveals 85% success (Figure 113).

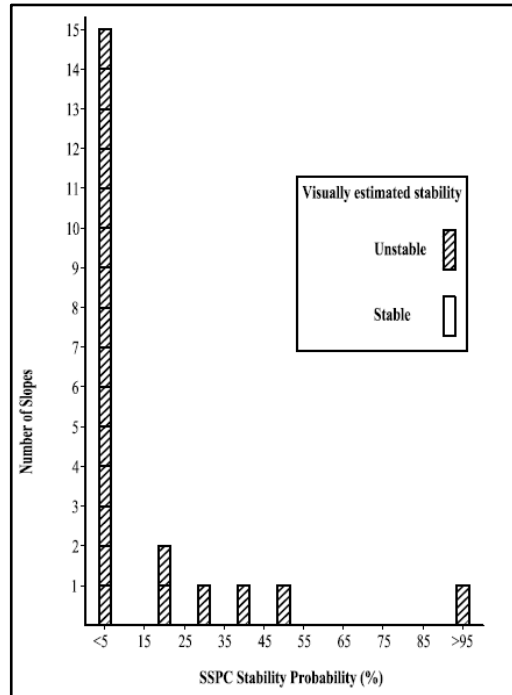


Figure 112. Results of SSPC and visually estimated stability (using weathered samples directly)

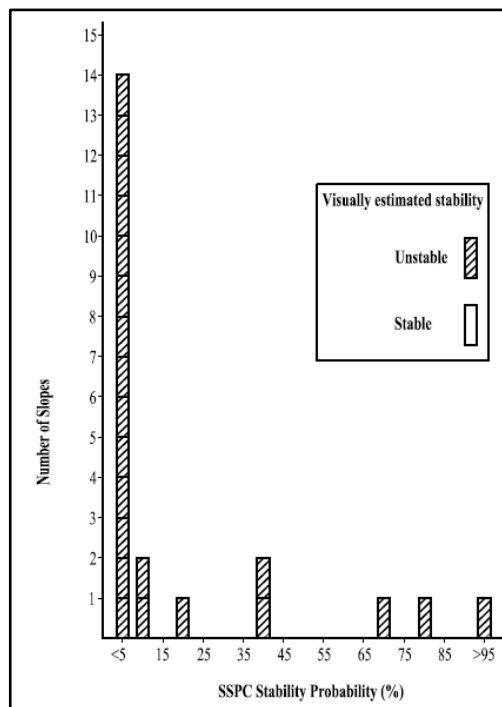


Figure 113. Results of SSPC and visually estimated stability (using fresh samples directly)

These results show that success rate of the SSPC method is very high if samples are directly collected from the weathered/disturbed zone (Figure 112). Nevertheless, accuracy decreases if samples are collected from relatively fresh zone and apply strength values of these relatively fresh samples (Figure 113). It is determined that in order to obtain more successful results, it is better to use weathered/disturbed data in the SSPC method.

These two classification systems (SMR and SSPC) are developed to decide general condition of the slopes. Data collection is easy and fast which can introduce immediate idea about the road cuts. It is known that these solutions are governed by regressions using back analysis therefore they are not final. Considering the surface failures of the road cuts, good results can be obtained from both methods. However, for the entire stability of a slope, it would be better to do further research like limit equilibrium analyses.

#### **6.4.Effectiveness**

In this thesis, to be on the safe side and investigate the effect of GSI and pseudostatic values on slope stability, some effectiveness works were done. As it can be seen from Table 71, for both static and dynamic conditions, the effectiveness against factor of safety is researched by changing GSI values  $\pm 5$  and coefficients of seismic force (Figures 114 and 115).

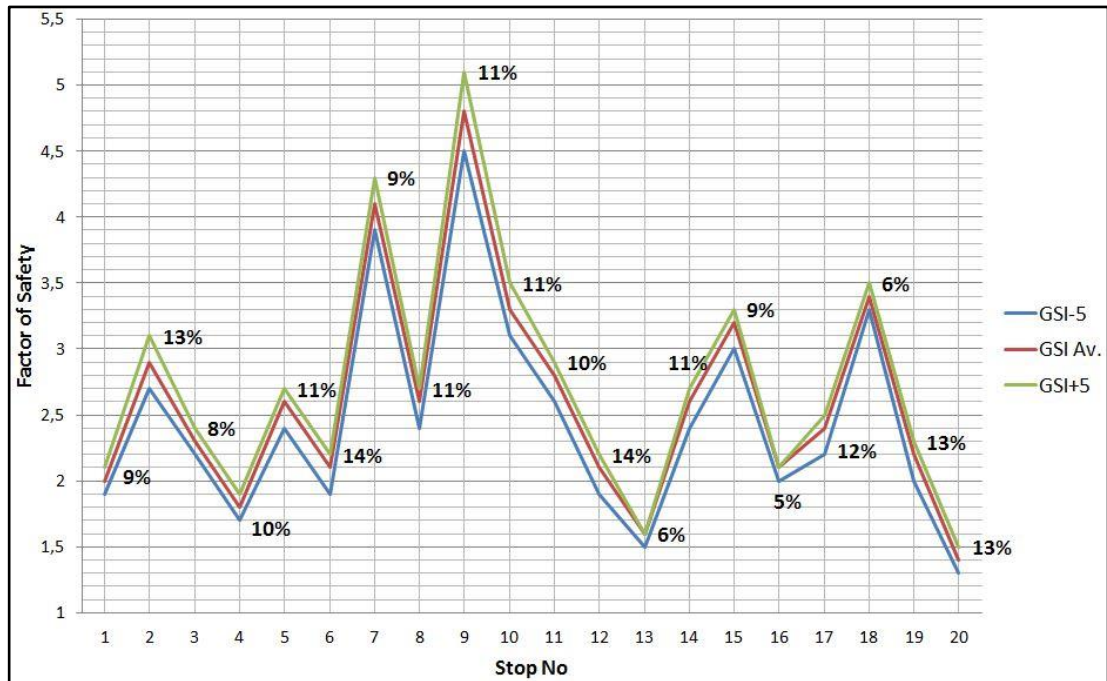


Figure 114. Factor of safety change against different GSI values for each road cut

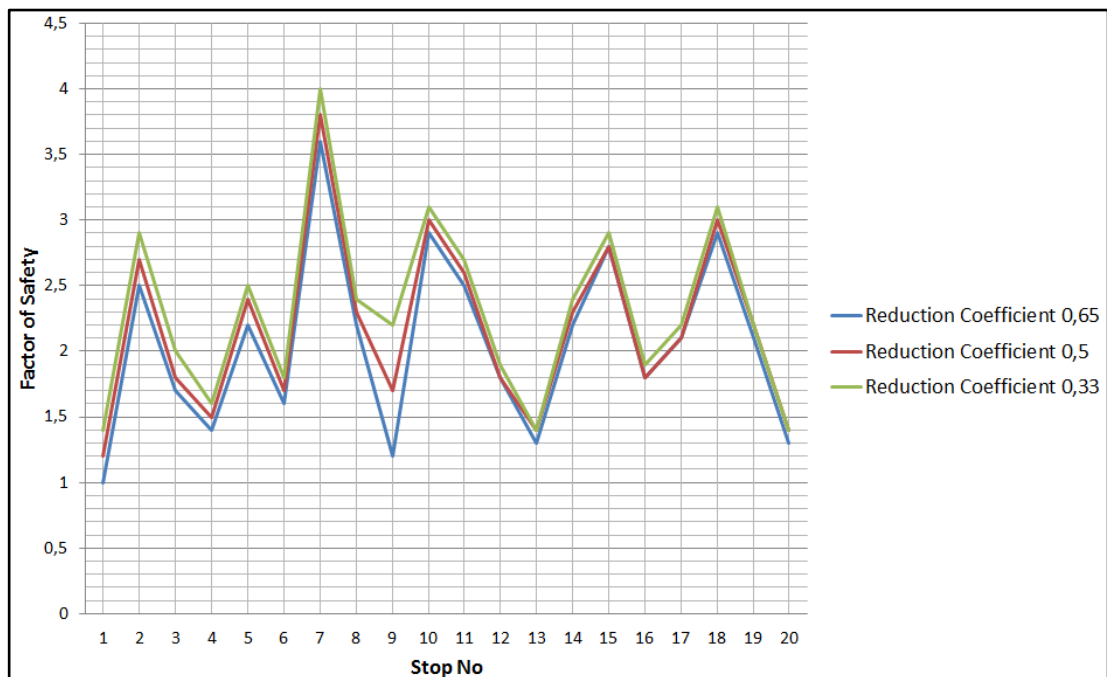


Figure 115. Factor of safety change against different seismic coefficients for each road cut

GSI values imply maximum 14% change of the safety factor (Figure 114). Over 20 different road cuts average change is found to be 10%. This means that variations of GSI values in 10 rating points range affect significant changes in factor of safety for instance at Stop 9 (Figure 114). Therefore, if factor of safety value is on the edge of failure as in Stop 20, GSI determination should be done carefully because even 10 rating points would change the stability condition of the slope. In this thesis, it can be stated that GSI values are assigned correctly by checking these solutions.

Analyses on GSI values reveal that among  $s$ ,  $a$  and  $m$  coefficients of Hoek Brown equation, the most sensitive constant is  $s$ , followed by  $m$ . Constant  $s$  is a measure of how fractured the rock is and  $m$  is related to mineral composition of the rock. These results show the importance of fracture frequency of the rock mass.

Dynamic analyses were done according to the recommendations by three researchers (Marcuson 1981; Hynes-Griffin & Franklin 1984; Bozorgnia & Bertero 2004). In these analyses, average GSI values were used, and all the other parameters were fixed by only changing seismic coefficients. Results reveal that maximum average reduction on factor of safety is 20%, according to Bozorgnia & Bertero's (2004) suggestion. On the other hand, if seismic reduction factor is applied as 0,33 as Marcuson (1981) suggested, average reduction of safety factor is determined as 10%. The only failure condition for dynamic condition is observed at Stop 1 with Bozorgnia & Bertero (2004), which may explain the failed zone of this slope. However, according to Disaster and Emergency Management Presidency, any earthquake over 4  $M_w$  was not detected between 2010 and 2015 (AFAD, 2015) near the study area.

### **6.5.Stability**

In this thesis, two already failed zones were observed at Stops 1 and 2. In addition, at Stop 19 some critical shear zones were determined, which may cause small failures. It is known that these slopes were reconstructed in 2010 in the thesis area. This means that failures probably took place in between 2010 and 2015. As it was discussed in the before, the failure at Stop 1 would not be explained by earthquake action due to low seismic action between these dates.

Despite having same composition of rocks this weaker zone has lower strength values compared to the stable part (Figure 116). The failed zone at Stop 2, on the other hand, is not as huge as in Stop 1. Also, this failed zone is explained by a different mechanism. As it was mentioned in road cut characterization, there are several shear zones located on this road cut. These shear zones are generally perpendicular to slope which means that they would not create significant discontinuity-controlled danger. On the other hand some of them are located diagonally on the slope. The failed zone at Stop 2 can be explained by increasing the frequency of these diagonally located shear zones.



Figure 116. Weaker/Failed zone at Stop 1 divided by red dashed line from stable part

Nearly the same scenario is observed at Stop 19. According to kinematic analyses, planar failure would take place at this slope. However it is known that spacings are very close to each other and this planar failure will only create small surficial failures as rock falls. Nevertheless, a small portion of this slope (Figure 117) is observed to be failed like a planar failure. This portion can be explained by intersection of a horizontal shear zone and bedding plane, both of them having longer persistence

compared to other joint sets. However, the shear zone located horizontally could not be observed clearly because of the debris and shown as question marks in Figure 117.

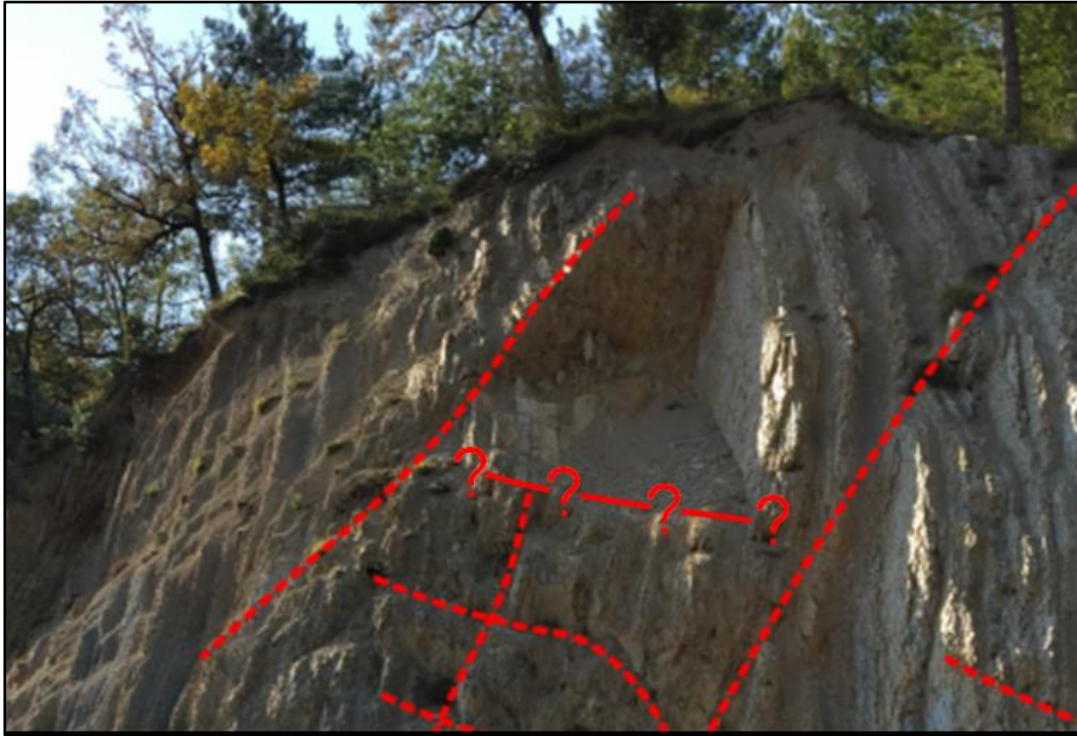


Figure 117. Failed portion of Stop 19 and shear zones (red dashed lines)

## CHAPTER 7

### CONCLUSIONS AND RECOMMENDATIONS

Stability of twenty different road cuts located between Bolu Zonguldak highway was researched in this thesis. Seven different rock types namely, mudstone, limestone, granite, basalt, granodiorite, sandstone and marl exposed where the cut slopes are located. Depth of weathered/disturbed zone in front of each road cut was measured in the field and properties were assigned separately. Differential weathering and undercutting action were investigated for the alternating rocks.

Based on the field study, block volumes are found to be lower than  $0,2 \text{ m}^3$  (moderate and small block) due to high frequency of discontinuity sets. Considering this data, kinematic analyses are done only for the critical slopes. According to these analyses, wedge, planar and toppling failures are found for these critical slopes. Limit equilibrium analyses performed on these slopes revealed that only planar failure can occur for Stop 19 ( $FS=0.8$ ), which is coherent with the field observations. For the rest of the slopes, rockfall analyses are performed. Any rockfall hazards which can affect the road were not encountered on these analyses. It is observed that only minor amount of rock can reach the drainage channels next to road which is matching with the field observations. Limit equilibrium analyses are also done according to circular failure conditions due to highly fractured texture of road cuts. Stability of each road cut is investigated under static and pseudostatic conditions. In order to determine seismic forces attenuation relationship is used. In these analyses, GSI values of the rock masses are taken  $\pm 5$  rating to investigate the effect of this parameter. Also, peak ground acceleration reduction factors are applied using the formula by three different researchers. Factor of safety results are changing between 1.3 and 5.1 for static conditions under different GSI values. These results are coherent with the field

observations for the stable road cuts. Factor of safety values are found to be less than 1.0 for the unstable cut slopes, which are again matching with the field observations. The range of the safety factor of the slopes is found between 1.0 and 4.0 under pseudostatic conditions for three different reduction coefficients. Slope flattening to  $70^{\circ}$  for Stop 20 and  $35^{\circ}$  for Stop 1 is found to be the solution under both static and pseudostatic conditions.

Two different empirical methods namely SMR and SSPC are used to determine strength parameters and stable probabilities in this study. It is observed that SMR could not reveal significant distinctive results based on the field observations. While nearly all road cuts are stable, SMR shows unstable conditions. SSPC reveals more reliable data for the surface conditions of the slopes. According to these analyses, SSPC revealed 95% success for the surficial failures using original method. Rock mass shear strength parameters obtained from SSPC method is changing between  $9-25^{\circ}$  ( $\phi$ ) and 5-14 kPa (c) for the weathered surfaces, and  $15-44^{\circ}$  ( $\phi$ ) and 8-21 kPa (c) for the relatively fresh zones.

According to the field surveys, laboratory data and stability analyses, the failure at Stop 1 occurred due to weak rock mass. However, failures at Stop 2 and Stop 19 could be due to shear zone and joint. For all the other road cuts, only surficial degradation is observed. As laboratory tests like unit weight, point load, slake durability and methylene blue adsorption, and in situ test Schmidt rebound hammer imply, weathered rock values are always lower than the fresh ones. This can be explained by the weathering and excavation actions on the surface of the road cuts. Considering all these laboratory data and field observations, it is not expected to have any significant instability problem for the road cuts. Nevertheless, surficial failures of the cut slopes can be observed in the future because of ongoing atmospheric conditions.

Due to low strength and highly fractured condition of the rock mass, samples for the UCS tests cannot be taken for all rock types. Correlation factor k between point load and UCS test may be used for only granite, sandstone and limestone. For the rest of the rocks in the field, correlation factor is taken from the literature. Relation between Schmidt rebound hammer and UCS is also investigated, and for the igneous rocks and the limestones two functions are developed. These functions with high

correlation coefficients ( $R^2$ ) can be used to determine UCS of the rocks directly from the Schmidt rebound values. In the study area, methylene blue adsorption test revealed that the clay minerals do not show any significant swelling action or clay minerals with high swelling capacity are in tiny amount. The durability of the rocks in the study area is changing between medium and very high according to slake durability tests.

According to these results, following recommendations can be given:

- RMR/SMR and SSPC methods can be applicable for the surface of the road cuts however some further investigations and analyses need to be done for relatively fresh/undisturbed zones of the cut slopes.
- Even though the degradation differences are observed easily in field, slake durability test results do not reflect these observations. In order to overcome this, slake durability test cycles should be extended.
- Before the point load test conducted, the properties of the samples should be investigated carefully. Tiny fractures on the samples should be determined and these samples should not be used to obtain accurate results. Also, the weathering penetration depth should be defined especially for the weak rocks.
- In order to obtain accurate results for the Schmidt rebound hammer test, spaces behind the sample rocks should be avoided in the field.
- The drainage channels in front of the slopes, especially for the Stops 4, 5, 7, 8, 9, 10, 11, 13, 14, 15, 16, 18, 19 and 20 should be maintained periodically due to debris accumulation caused by the surface failures and rockfalls.



## REFERENCES

- AFAD, 2015. 1900-20xx Earthquake Catalogue. Available at: <http://www.deprem.gov.tr/tr/depremkatalogu>.
- AFNOR, 1980. Essai au bleu de methylene. *AFNOR 80181, Paris La Defence*, pp.18–592.
- Akartuna, M., 1953. *Report on Çaycuma-Devrek-Yenice-Kozcağız zone geology*, MTA Report.
- ANON, 1977. The description of rock masses for engineering purposes - Report by Geological Society Engineering Group Working Party. *Quarterly Journal of Engineering Geology and Hydrogeology*, 10, pp.355–388.
- ANON, 1970. The logging of rock cores for engineering purposes. *Quarterly Journal of Engineering Geology*, 3, pp.1–24.
- ASTM D4644-87, 1998. Standard test method for slake durability of shales and similar weak rocks. *Annual book of ASTM standards*, 14.02.
- Barton, N., 1973. Review of a new shear strength criterion for rock joints. *Engineering Geology*, 7, pp.287–332.
- Barton, N., 1976. The Shear Strength of Rock and Rock Joints. *International Journal of rock mechanics and mining sciences & Geomechanics abstracts*, 9, pp.255–279.
- Barton, N. & Bandis, S.C., 1982. Effects of block size on the shear behaviour of jointed rock. In *23rd U.S. symp. on rock mechanics*. Berkeley, pp. 739–760.
- Barton, N. & Choubey, V., 1977. The shear strength of rock joints in theory and practice. *Rock Mech.*, 10, pp.1–54.
- Bieniawski, Z.T., 1973. Engineering classification of jointed rock masses. *Trans. S. Afr. Inst. Civ. Eng.*, 15, pp.335–344.
- Bieniawski, Z.T., 1989. *Engineering Rock Mass Classification-A complete manual for engineers and geologists in mining, civil and petroleum engineering*, Wiley.
- Bieniawski, Z.T., 1976. Exploration for rock engineering. In *proceedings of the Symposium on Exploration for Rock Engineering*. Johannesburg: AA Balkema.
- Bieniawski, Z.T., 1975. The point-load test in geotechnical practice. *Engineering Geology*, 9, pp.1–11.
- Binal, A. & Ercanoğlu, M., 2010. Assessment of rockfall potential in the Kula (Manisa,Turkey) Geopark Region. *Environmental Earth Sciences*, 61, pp.1361–1373.

- Bowden, A.J., Lamom-Blick, J. & Ulhutt, S., 1998. Point load testing of weak rocks with particular reference to chalk. *Quarterly Journal of Engineering Geology*, 11, pp.95–103.
- Bozorgnia, Y. & Bertero, V.V., 2004. *Earthquake Engineering: from engineering seismology to performance-based engineering*, Boca Raton, Florida, USA: ICC-CRC Press.
- BS5930, 1981. *Code of practice for ground investigations*, London: British Standards Institute.
- Buzkan, İ., 1996. Investigation of the sand-gravel-crashed stone deposits in the Zonguldak Region. *National Crashed Stone Symposium*, pp.69–83.
- Cabria, X.A., 2015. *Effects of weathering in the rock and rock mass properties and the influence of salts in the coastal roadcuts in Saint Vincent and Dominica*. University of Twente.
- Cargill, J.S. & Shakoor, A., 1990. Evaluation of empirical methods for measuring the uniaxial compressive strength of rock. *International Journal of rock mechanics and mining sciences & Geomechanics abstracts*, 27, pp.495–503.
- Coates, D.F., 1964. Classification of rock for rock mechanics. *Int. J. Rock Mech. Min. Sci.*, 1, pp.421–429.
- Craig, R.F., 2004. *Craig's Soil Mechanics* 7th ed., CRC Press.
- Cruden, D. & VanDine, D.F., 2013. Classification, Description, Causes and Indirect Effects - Canadian Technical Guidelines and Best Practices related to Landslides: a national initiative for loss reduction. *Geological Survey of Canada*, Open File(7359), p.22.
- Das, I., Sahoo, S., van Westen, C., Stein, A. & Hack, R., 2010. Landslide susceptibility assessment using logistic regression and its comparison with a rock mass classification system, along a road section in the northern Himalayas (India). *Geomorphology*, 114, pp.627–637.
- Dean, W.T., Monod, O., Rickards, R., Demir, O. & Bultynck, P., 2000. Lower Paleozoic stratigraphy and paleontology, Karadere-Zirze area, Pontus Mountains, northern Turkey. *Geological Magazine*, 137, pp.555–582.
- Dearman, W.R., 1976. Weathering classification in the characterisation of rock: a revision. *Bulletin of the International Association of Engineering Geology*, 13, pp.123–127.
- Deere, D.U., Hendron, F., Patton, F.D. & Cording, E.J., 1967. *Design of surface and near surface constructions in rock*, SME/AIME, NY.
- Deere, D.U. & Miller, R.P., 1966. *Engineering Classification and Index Properties for intact rock*, Illinois Univ at Urbana Dept of Civil Engineering.
- Demirtaş, R., 2000. *Paleoseismicity and neotectonics of the Abant-Gerede Region of the North Anatolian Fault Zone*. Ankara University.

- Demirtaş, R. & Ural, B., 2011. *Bolu ili, Mengen İlçesi, Kayabükü Köyü G27-b-05-d-4-a Pafta, 153 Ada, 1-20 nolu Parsellere ait Mevzi İmar Planına Esas Jeolojik-Jeoteknik Etüt Raporu*,
- DMİ, 2015. Devlet Meteoroloji İşleri Genel Müdürlüğü. Available at: <http://www.mgm.gov.tr/veridegerlendirme/il-ve-ilceler-istatistik.aspx?m> [Accessed December 1, 2015].
- Duncan, J.M., Wright, S.G. & Brandon, T.L., 2014. *Soil strength and slope stability* 2nd ed., New Jersey: Wiley.
- Durmekova, T., Frankovska, J. & Kopecky, M., 2014. Correlation between point load index and uniaxial compressive strength for soft and weak rocks. *Acta Geologica Slovaca*, 6, pp.61–69.
- Evans, R.S., 1981. An analysis of secondary toppling rock failures-the stress redistribution method. *Quarterly Journal of Engineering Geology and Hydrogeology*, 14, pp.77–86.
- Fookes, P.G., Dearman, W.R. & Franklin, J.A., 1971. Some engineering aspects of rock weathering with field examples from Dartmoor and elsewhere. *Quarterly Journal of Engineering Geology and Hydrogeology*, 4, pp.139–185.
- Fookes, P.G., Gourley, C.S. & Ohikere, C., 1988. Rock weathering in engineering time. *Quarterly Journal of Engineering Geology and Hydrogeology*, 21(1), pp.33–57. Available at: <http://qjehg.lyellcollection.org/content/21/1/33.short> [Accessed October 6, 2015].
- Gamble, J.C., 1971. *Durability-plasticity classification of shales and other argillaceous rocks*. Ph.D. thesis, University of Illinois.
- Gangopadhyay, S., 2013. *Engineering Geology*, New Delhi, India: Oxford University Press.
- GDDA, 1996. *Earthquake zoning map of Turkey*, Earthquake research department, General Directorate of Disaster Affairs, Ministry of Reconstruction and Resettlement of Turkey.
- Gokceoglu, C., 1996. Schmidt sertlik çekici kullanılarak tahmin edilen tek eskenli sıkışma dayanımı verilerinin güvenilirliği üzerine bir değerlendirme. *Jeoloji Mühendisliği*, 48, pp.78–81.
- Goodman, R.E., 1989. *Introduction to rock mechanics* 2nd ed., Wiley.
- Goodman, R.E. & Bray, J.W., 1976. Toppling of Rock Slopes. *Proc. Specialty Conference on Rock Engineering for Foundations and Slopes. Boulder, Colorado, ASCE, Vol. 2*, pp.201–234.
- Göncüoğlu, M.C., 2010. *Introduction to the geology of Turkey: Geodynamic evolution of the Pre-Alpine and Alpine terranes*, Ankara: MTA.
- Göncüoğlu, M.C., Gürsu, S., Tekin, U.K. & Köksal, S., 2008. New data on the evolution of the Neotethyan oceanic branches in Turkey: Late Jurassic ridge

- spreading in the Intra-Pontide branch. *Ophioliti*, 33(2), pp.153–164.
- Hack, R., 1998. *Slope Stability Probability Classification; SSPC; 2nd version*. University of Technology Delft; International Institute for Aerospace Survey and Earth Sciences; ITC, Delft, Enschede, The Netherlands.
- Hack, R. & Huisman, M., 2002. Estimating the intact rock strength of a rock mass by simple means. In J. L. van Rooy & C. A. Jermy, eds. *Engineering Geology for Developing Countries - Proceedings of 9th Congress of the International Association for Engineering Geology and the Environment*. Durban, South Africa.
- Hack, R. & Price, D., 1997. Quantification of Weathering. *Proc. Engineering geology and the environment*, pp.145–150.
- Hack, R., Price, D. & Rengers, N., 2002. A new approach to rock slope stability - a probability classification (SSPC). *Bulletin of Engineering Geology and the Environment*. Springer Verlag., 62.
- Haines, A. & Terbrugge, P.J., 1991. Preliminary estimation of rock slope stability using rock mass classification systems. In W. Wittke, ed. *Proc. 7th Congr. on Rock Mechanics 2, ISRM*. Aachen, Germany. Balkema, Rotterdam, pp. 887–892.
- Hawkins, A.B., 1998. Aspects of rock strength. *Bulletin of engineering geology and the environment*, 1, pp.17–30.
- Highland, L. & Bobrowsky, P.T., 2008. *The Landslide Handbook-A Guide to Understanding Landslides*, Reston, VA, USA: US Geological Survey.
- Hoek, E., Torres, C.C. & Corkum, B., 2002. Hoek-Brown Failure Criterion - 2002 Edition. In *Proc. NARMS-TAC Conference*. Toronto, pp. 267–273.
- Hoek, E., 1994. Strength of rock and rock masses. *ISRM New Journal*, 2, pp.4–16.
- Hoek, E. & Bray, J., 1981. *Rock Slope Engineering*, CRC Press.
- Hoek, E., Bray, J.W. & Boyd, J.M., 1973. The stability of a rock slope containing a wedge resting on two intersecting discontinuities. *Quarterly Journal of Engineering Geology and Hydrogeology*, 6, pp.1–55.
- Hoek, E. & Brown, E.T., 1980. Empirical Strength Criterion for Rock Masses. *J. Geotech. Eng. ASCE*, 106(GT9), pp.1013–1035.
- Hoek, E. & Brown, E.T., 1997. Practical estimates of rock mass strength. *International Journal of rock mechanics and mining sciences*, 34(8), pp.1165–1186.
- Hoek, E., Kaiser, P.K. & Bawden, W.F., 1995. *Support of underground excavations in hard rock*, Balkema, Rotterdam.
- Hudson, J.A. & Harrison, J.P., 2000. *Engineering Rock Mechanics-An Introduction to the Principles*, Elsevier.

- Huisman, M., 2006. *Assessment of rock mass decay in artificial slopes*. International Institute for Aeroscape Survey and Earth Sciences (ITC).
- Huisman, M., Hack, H.R.G.K. & Nieuwenhuis, J.D., 2006. Predicting Rock Mass Decay in Engineering Lifetimes: The Influence of Slope Aspect and Climate. *Environmental & Engineering Geoscience*, 12, pp.39–51.
- Huisman, M., Nieuwenhuis, J.D. & Hack, H.R.G.K., 2011. Numerical modelling of combined erosion and weathering of slopes in weak rock. *Earth Surface Processes and Landforms*, 36(13), pp.1705–1714.
- Hynes-Griffin, M.E. & Franklin, A.G., 1984. *Rationalizing the seismic coefficient method*, Vicksburg, Mississippi, Miscellaneous Paper GL-84-13, 21 pp.
- Idriss, I.M., 2007. *Empirical model for estimating the average horizontal values of pseudo-absolute spectral accelerations generated by crustal earthquakes*, PEER Report draft, Pacific earthquake engineering research center, Berkeley, CA, pp 76.
- Indraratna, B., Jayanathan, M. & Brown, T., 2008. Shear Strength Model for Overconsolidated Clay-Infilled Idealised Rock Joints. *Geotechnique*, 58(1), pp.55–65.
- İsmailoğlu, Ş., Özcan, Ü., Küçük, İ., Çağlan, D. & Bayrak, D., 1999. *Report related to floods and landslides in Lower Filyos valley, Bartın, Karabük, Alaplı regions (West BlackSea)*, Ankara.
- ISRM, 1978. Commission on standardization of laboratory and field tests: suggested methods for the quantitative description of discontinuities in rock masses. *International Journal of rock mechanics and mining sciences & Geomechanics abstracts*, 15, pp.319–368.
- ISRM, 1985. Suggested method for determining point load strength. *International Journal of rock mechanics and mining sciences & Geomechanics abstracts*, 22, pp.51–60.
- ISRM, 1981. Suggested methods for determining hardness and abrasiveness of rocks. Rock characterization, testing and monitoring: ISRM suggested Methods. *OXford: Pergamon*, pp.95–96.
- ISRM, 2007. The complete ISRM suggested methods for rock characterization, testing and monitoring: 1976-2006. *Suggested methods prepared by the Commision on Testing Methods, ISRM*.
- Karaman, K. & Kesimal, A., 2012. Evaluation of point load test methods and porosity for estimation the uniaxial compressive strength of rocks. *Madencilik*, 51, pp.3–14.
- Katz, O., Reches, Z. & Roegiers, J.C., 2000. Evaluation of mechanical rock properties using a Schmidt Hammer. *International Journal of rock mechanics and mining sciences*, 37, pp.723–728.
- Kaya, O., Dizer, A., Tansel, I. & Özer, S., 1986. Stratigraphy of the Upper

- Cretaceous and Paleogene in Yığılca-Bolu (NW Turkey). *Bull. Min. Res. Expl.*, 107, pp.1–20.
- Ketin, İ., 1966. Tectonic units of Anatolia. *Maden Tetkik ve Arama Bulletin*, 66, pp.23–34.
- Kidybinski, A., 1980. Bursting liability indices of coal. *Int. J. Rock Mech. Min. Sci. Geomech. Abstr.*, 17, pp.167–171.
- Kondo, H., Awata, Y., Emre, Ö., Doğan, A., Özalp, S., Tokay, F., Yıldırım, C., Yoshioka, T. & Okumura, K., 2005. Slip distribution, fault geometry, and fault segmentation of the 1944 Bolu-Gerede earthquake rupture, North Anatolian Fault, Turkey. *Bulletin of seismological society of America*, 95, pp.1234–1249.
- Koralay, D.B., 2009. *Investigation of hydrocarbon potential and trace element distribution of Eocene bituminous shales in Bolu Basin*. Ankara University.
- Kramer, S.L., 1996. *Geotechnical earthquake engineering*, New Jersey: PrenticeHall, Upper Saddle River.
- Li, X.Z. & Xu, Q., 2015. Application of the SSPC method in the stability assessment of highway rock slopes in the Yunnan province of China. *Bulletin of Engineering Geology and the Environment*.
- Little, A.L., 1969. Engineering classification of residual tropical soils. *Proceeding of the 7th International Conference on Soil Mechanics and Foundation Engineering Mexico*, 1, pp.1–10.
- Loughnan, F.C., 1969. *Chemical weathering of the silicate minerals*, New York: Elsevier.
- Marcuson, W.F., 1981. Moderator's report for session on "Earth dams and stability of slopes under dynamic loads." In *Proceedings, International conference on recent advances in geotechnical earthquake engineering and soil dynamics*. St. Louis, Missouri, p. Vol. 3, p. 1175.
- Marinos, P. & Hoek, E., 2001. Estimating the geotechnical properties of heterogeneous rock masses such as Flysch. *Bulletin of engineering geology and the environment*, 60, pp.85–92.
- Miscevic, P. & Roje-Bonacci, T., 2001. Weathering process in eocene flysch in region of Split (Croatia). *Rudarsko-geolosko-naftni zbornik*, 13, pp.47–55.
- Momeni, A.A., Khanlari, G.R., Heidari, M., Sephai, A.A. & Bazvand, E., 2015. New engineering geological weathering classification for granitoid rocks. *Engineering Geology*, 185, pp.43–51.
- Moses, C., Robinson, D. & Barlow, J., 2014. Methods for measuring rock surface weathering and erosion: A critical review. *Earth-Science Reviews*, 135, pp.141–161.
- Moye, D.G., 1955. Engineering geology of the Snowy Mountains scheme. *Journal of the Institution of Engineers of Australia*, 27, pp.281–299.

- MTA, 2002a. *1/100 000 scale geological maps of Turkey, Bolu-G28 Quadrangle*, MTA Publications: Ankara.
- MTA, 2002b. *1/100 000 scale geological maps of Turkey, Zonguldak-E27-F27 Quadrangle*, MTA Publications: Ankara.
- MTA, 2002c. *1/100 000 scale geological maps of Turkey, Zonguldak-F28 Quadrangle*, MTA Publications: Ankara.
- Nickmann, M., Spaun, G. & Thuro, K., 2006. Engineering geological classification of weak rocks. *The geological society of London*, pp.1–9.
- O'Rourke, J.E., 1989. Rock index properties for geoengineering in underground development. *Min. Eng.*, pp.106–110.
- Okay, A.I., 2008. Geology of Turkey: A Synopsis. *Anschnitt*, 21, pp.19–42.
- Ollier, C., 1991. *Ancient Landforms*, Belhaven Press.
- Ozer, S., 1994. New Species of radiolitidae from the Bolu Area (W. Black-Sea) and Kocaeli Peninsula. *Mineral Res. Expl. Bull.*, 116, pp.1–8.
- Palmstrom, A., 2000. Block size and block size distribution. *Workshop on "Reliability of classification systems" in connection with the GeoEng 2000 conference, Melbourne*, p.12 p.
- Palmstrom, A., 1974. *Characterization of jointing density and the quality of rock masses*, Norway.
- Palmstrom, A., 2005. Measurements of and correlations between block size and rock quality designation (RQD). *Tunneling and Underground Space Technology*, 20, pp.362–377.
- Palmstrom, A., 1995. RMi - a rock mass characterization system for rock engineering purposes. *PhD thesis, University of Oslo, Department of Geology*, p.400.
- Pariseau, G.W., 2012. *Design Analysis in Rock Mechanics*, CRC Press.
- Patton, F.D., 1966. *Multiple Modes of Shear Failure in Rock and Related Materials*. Thesis, University of Ill.
- Price, D.G., 1995. Weathering and weathering processes. *Quarterly Journal of Engineering Geology and Hydrogeology*, 28, pp.243–252.
- Read, J.R.J., Thornton, P.N. & Regan, W.M., 1980. A rational approach to the point load test. In *Proceedings 3rd., Australian and New Zealand Conference on Geomechanics, Wellington*. pp. 35–39.
- Rocscience, 2004a. Rocfall 4.0.3.9-Scientific software-Statistical analysis of rockfalls.
- Rocscience, 2004b. Swedge 4.078 wedge analysis.

- Rocscience, 2005. RocPlane 2.032 planar failure analysis.
- Rocscience, 2011. Slide 6.009-2D limit equilibrium slope stability analysis.
- Rocscience, 2013. Dips 6.008 - Data interpretation package using stereographic projection.
- Rocscience, 2015. RocTopple toppling failure analysis.
- Romana, M., 1985. New adjustment rating for application of the Bieniawski classification to slopes. In *Proc. Int. Symp. on Rock Mechanics, Mining Civ Works, ISRM*. Zacatecas, Mexico, pp. 59–63.
- Sachpazis, C.I., 1990. Correlating Schmidt hardness with compressive strength and Young's modulus of carbonate rocks. *Bulletin of the International Association of Engineering Geology*, 42, pp.75–83.
- Saptono, S., Kramadibrata, S. & Sulistianto, B., 2013. Using the Schmidt hammer on rock mass characteristic in sedimentary rock at Tutupan coal mine. *Procedia Earth and Planetary Science*, 6, pp.390–395.
- Sarı, A., Üzmez, B. & Aliyev, S.A., 2004. Hydrocarbon potential of the bituminous shales around Mengen (Bolu). *İstanbul Üniv. Müh. Fak. Yerbilimleri Dergisi*, 2, pp.91–102.
- Saunders, M.K. & Fookes, P.G., 1970. A review of the relationship of rock weathering and climate and its significance to foundation engineering. *Engineering Geology*, 4(4), pp.289–325.
- Sharma, S., Raghuvanshi, T.K. & Anbalagan, R., 1995. Plane failure analysis of rock slopes. *Geotechnical and Geological Engineering*, 13, pp.105–111.
- Shrivastava, G., 2014. Influence of weathering on the engineering properties of basalt near Indore, Madhya Pradesh. *IOSR Journal of Mechanical and Civil Engineering*, pp.18–22.
- Singh, R.N. & Gahrooee, D.R., 1989. Application of rock mass weakening coefficient for stability assessment of slopes in heavily jointed rock mass. *International journal of surface mining*, 3, pp.207–219.
- Skempton, A.W., 1985. Residual Strength of Clays in Landslides, Folded Strata and the Laboratory. *Geotechnique*, 35(1), pp.3–18.
- Spencer, E., 1967. A method of analysis of the stability of embankments assuming parallel inter-slice forces. *Geotechnique*, 17, pp.11–26.
- Stapledon, D.H., 1976. Geological hazards and water storage. *Bulletin of the International Association of Engineering Geology*, 14, pp.249–262.
- Suzen, M.L., 2002. *Data driven landslide hazard assessment using geographical information systems and remote sensing*. Middle East Technical University.
- Topal, T., 2000. Problems faced in the application of the point load index test. *Geological Engineering*, 24, pp.73–86.

- Topal, T., 1996. The use of methylene blue adsorption test to assess the clay content of the Cappadocian Tuff. In *International congress on deterioration and conservation of stone*. pp. 791–799.
- Topal, T. & Sozmen, B., 2003. Deterioration mechanisms of tuffs in Midas monument. *Engineering Geology*, 68, pp.201–223.
- Ulusay, R. & Sönmez, H., 2007. *Kaya kütlelerinin mühendislik özellikleri* 2nd ed., Ankara: TMMOB Jeoloji Mühendisleri Odası.
- Ustaömer, P.A., 1999. Pre-Early Ordovician Cadomian arc-type granitoids, the Bolu Massif, West Pontides, northern Turkey: geochemical evidence. *Int. Journ. Earth Sciences*, 88, pp.2–12.
- Ustaömer, P.A., Mundil, R. & Renne, P.R., 2005. U/Pb and Pb/Pb zircon ages for arc-related intrusions of the Bolu Massif (W Pontides, NW Turkey): evidence for Late Precambrian (Cadomian) age. *Terra Nova*, 17, pp.215–223.
- Ustaömer, P.A. & Rogers, G., 1999. The Bolu Massif: remnant of a pre-Early Ordovician active margin in the west Pontides, northern Turkey. *Geol. Mag.*, 136 (5), pp.579–592.
- Utili, S., 2004. *Evolution of natural slopes subject to weathering: an analytical and numerical study*. Politecnico di Milano.
- Wetzel, A. & Einsele, G., 1991. On the physical weathering of various mudrocks. *Bulletin of the International Association of Engineering Geology*, 44, pp.89–99.
- Wilson, L.C., 1976. Tests of bored and driven piles in Cretaceous mudstone at Port Elizabeth, South Africa. *Geotechnique*, 26, pp.5–12.
- Woo, I., Fleurisson, J.A. & Park, H.J., 2010. Influence of weathering on shear strength of joints in a porphyritic granite rock mass in Jechon area, South Korea. *Geosciences Journal*, 14, pp.289–299.
- Yalçiner, N.P., 1996. Kardeniz bölgesi heyelanlari ve önlenmesi yolunda önerilerimiz. *Coğrafya Dergisi*, (4). Available at: <http://www.journals.istanbul.edu.tr/iucografya/article/view/1023016614> [Accessed January 27, 2016].
- Yalçiner, N.P., 1995. Yeniçağa depresyonunun (Bolu) jeomorfolojik oluşum ve gelişimi. *Coğrafya Dergisi*, (4). Available at: <http://www.journals.istanbul.edu.tr/iucografya/article/view/1023016612> [Accessed January 27, 2016].
- Yasar, E. & Erdogan, Y., 2004. Estimation of rock physicommechanical properties using hardness methods. *Engineering Geology*, 71, pp.281–288.
- Yiğitbaş, E., Elmas, A. & Yılmaz, Y., 1999. Pre-Cenozoic tectono-stratigraphic components of the Western Pontides and their geological evolution. *Geological Journal*, 34, pp.55–74.
- Yılmaz, Ç., Topal, T. & Suzen, M.L., 2012. GIS-based landslide susceptibility

mapping using bivariate statistical analysis in Devrek (Zonguldak-Turkey).  
*Environmental Earth Sciences*, 65, pp.2161–2178.

Yücel, Ş., Aydın, M., Kuvvetli, E. & Güneş, H., 2011. *Zonguldak İl Çevre Durum Raporu*, Zonguldak.

## APPENDICES

### APPENDIX A

#### LABORATORY TEST RESULTS

Table 85. Porosity and unit weight of Stop 1 fresh mudstone

Sample No	Msat (gr)	Msub (gr)	Mdry (gr)	Vv (cm3)	V (cm3)	Porosity (%)	Dry Unit W. (kN/m3)	Sat. Unit W. (kN/m3)
1	406,38	253,96	400,33	6,05	152,42	3,97	25,77	26,16
2	354,56	220,55	344,59	9,97	134,01	7,44	25,23	25,96
3	375,50	231,94	364,24	11,26	143,56	7,84	24,89	25,66
4	447,77	275,47	431,42	16,35	172,30	9,49	24,56	25,49
5	320,22	195,46	315,88	4,34	124,76	3,48	24,84	25,18
6	512,18	315,13	508,47	3,71	197,05	1,88	25,31	25,50
7	342,89	210,41	340,77	2,12	132,48	1,60	25,23	25,39
8	223,41	138,79	218,45	4,96	84,62	5,86	25,32	25,90
9	265,31	165,44	258,16	7,15	99,87	7,16	25,36	26,06
10	222,96	139,15	219,17	3,79	83,81	4,52	25,65	26,10

Table 86. Porosity and unit weight of Stop 1 weathered mudstone

<b>Sample No</b>	<b>Msat (gr)</b>	<b>Msub (gr)</b>	<b>Mdry (gr)</b>	<b>Vv (cm3)</b>	<b>V (cm3)</b>	<b>Porosity (%)</b>	<b>Dry Unit W. (kN/m3)</b>	<b>Sat. Unit W. (kN/m3)</b>
<b>1</b>	182,17	111,46	174,35	7,82	70,71	11,06	24,19	25,27
<b>2</b>	386,77	240,49	379,59	7,18	146,28	4,91	25,46	25,94
<b>3</b>	332,25	206,91	327,17	5,08	125,34	4,05	25,61	26,00
<b>4</b>	256,15	155,88	254,11	2,04	100,27	2,03	24,86	25,06
<b>5</b>	321,14	197,41	319,42	1,72	123,73	1,39	25,33	25,46
<b>6</b>	305,49	188,44	302,79	2,70	117,05	2,31	25,38	25,60
<b>7</b>	259,47	160,71	254,15	5,32	98,76	5,39	25,25	25,77
<b>8</b>	255,89	155,96	250,46	5,43	99,93	5,43	24,59	25,12
<b>9</b>	312,46	190,12	311,43	1,03	122,34	0,84	24,97	25,06
<b>10</b>	296,74	182,25	294,58	2,16	114,49	1,89	25,24	25,43

Table 87. Porosity and unit weight of Stop 1 fresh sandstone

<b>Sample No</b>	<b>Msat (gr)</b>	<b>Msub (gr)</b>	<b>Mdry (gr)</b>	<b>Vv (cm3)</b>	<b>V (cm3)</b>	<b>Porosity (%)</b>	<b>Dry Unit W. (kN/m3)</b>	<b>Sat. Unit W. (kN/m3)</b>
<b>1</b>	193,18	121,12	191,30	1,88	72,06	2,61	26,04	26,30
<b>2</b>	587,07	366,94	580,05	7,02	220,13	3,19	25,85	26,16
<b>3</b>	787,08	493,38	780,51	6,57	293,70	2,24	26,07	26,29
<b>4</b>	530,02	331,19	520,62	9,40	198,83	4,73	25,69	26,15
<b>5</b>	344,76	215,11	338,35	6,41	129,65	4,94	25,60	26,09
<b>6</b>	178,80	112,18	174,68	4,12	66,62	6,18	25,72	26,33
<b>7</b>	288,19	180,42	286,11	2,08	107,77	1,93	26,04	26,23
<b>8</b>	334,46	210,85	330,39	4,07	123,61	3,29	26,22	26,54
<b>9</b>	259,84	161,88	256,15	3,69	97,96	3,77	25,65	26,02
<b>10</b>	306,54	190,91	304,12	2,42	115,63	2,09	25,80	26,01

Table 88. Porosity and unit weight of Stop 1 weathered sandstone

<b>Sample No</b>	<b>Msat (gr)</b>	<b>Msub (gr)</b>	<b>Mdry (gr)</b>	<b>Vv (cm3)</b>	<b>V (cm3)</b>	<b>Porosity (%)</b>	<b>Dry Unit W. (kN/m3)</b>	<b>Sat. Unit W. (kN/m3)</b>
<b>1</b>	179,40	111,78	176,26	3,14	67,62	4,64	25,57	26,03
<b>2</b>	336,41	210,25	330,04	6,37	126,16	5,05	25,66	26,16
<b>3</b>	312,20	196,28	310,92	1,28	115,92	1,10	26,31	26,42
<b>4</b>	272,95	170,99	270,01	2,94	101,96	2,88	25,98	26,26
<b>5</b>	701,74	438,13	692,32	9,42	263,61	3,57	25,76	26,11
<b>6</b>	671,40	421,68	662,46	8,94	249,72	3,58	26,02	26,38
<b>7</b>	255,94	160,10	253,03	2,91	95,84	3,04	25,90	26,20
<b>8</b>	242,89	152,33	240,84	2,05	90,56	2,26	26,09	26,31
<b>9</b>	401,33	250,48	394,03	7,30	150,85	4,84	25,62	26,10
<b>10</b>	394,51	245,44	390,58	3,93	149,07	2,64	25,70	25,96

Table 89. Porosity and unit weight of Stop 2 fresh limestone

<b>Sample No</b>	<b>Msat (gr)</b>	<b>Msub (gr)</b>	<b>Mdry (gr)</b>	<b>Vv (cm3)</b>	<b>V (cm3)</b>	<b>Porosity (%)</b>	<b>Dry Unit W. (kN/m3)</b>	<b>Sat. Unit W. (kN/m3)</b>
<b>1</b>	118,59	71,73	114,17	4,42	46,86	9,43	23,90	24,83
<b>2</b>	130,10	78,02	124,42	5,68	52,08	10,91	23,44	24,51
<b>3</b>	359,07	215,84	343,19	15,88	143,23	11,09	23,51	24,59
<b>4</b>	362,35	219,29	349,26	13,09	143,06	9,15	23,95	24,85
<b>5</b>	290,55	175,90	279,83	10,72	114,65	9,35	23,94	24,86
<b>6</b>	180,62	107,82	172,12	8,50	72,80	11,68	23,19	24,34
<b>7</b>	177,97	107,22	170,84	7,13	70,75	10,08	23,69	24,68
<b>8</b>	135,48	82,13	129,22	6,26	53,35	11,73	23,76	24,91
<b>9</b>	370,36	224,13	350,11	20,25	146,23	13,85	23,49	24,85
<b>10</b>	178,13	106,79	168,19	9,94	71,34	13,93	23,13	24,49

Table 90. Porosity and unit weight of Stop 2 weathered limestone

<b>Sample No</b>	<b>Msat (gr)</b>	<b>Msub (gr)</b>	<b>Mdry (gr)</b>	<b>Vv (cm3)</b>	<b>V (cm3)</b>	<b>Porosity (%)</b>	<b>Dry Unit W. (kN/m3)</b>	<b>Sat. Unit W. (kN/m3)</b>
<b>1</b>	153,26	92,02	146,98	6,28	61,24	10,25	23,54	24,55
<b>2</b>	354,69	214,89	342,72	11,97	139,80	8,56	24,05	24,89
<b>3</b>	330,15	198,75	317,03	13,12	131,40	9,98	23,67	24,65
<b>4</b>	365,27	220,18	351,84	13,43	145,09	9,26	23,79	24,70
<b>5</b>	481,09	293,85	467,52	13,57	187,24	7,25	24,49	25,21
<b>6</b>	627,70	379,54	605,72	21,98	248,16	8,86	23,94	24,81
<b>7</b>	588,66	355,90	566,60	22,06	232,76	9,48	23,88	24,81
<b>8</b>	620,19	360,19	610,11	10,08	260,00	3,88	23,02	23,40
<b>9</b>	482,11	290,74	455,16	26,95	191,37	14,08	23,33	24,71
<b>10</b>	350,77	210,79	338,13	12,64	139,98	9,03	23,70	24,58

Table 91. Porosity and unit weight of Stop 3 fresh limestone

<b>Sample No</b>	<b>Msat (gr)</b>	<b>Msub (gr)</b>	<b>Mdry (gr)</b>	<b>Vv (cm3)</b>	<b>V (cm3)</b>	<b>Porosity (%)</b>	<b>Dry Unit W. (kN/m3)</b>	<b>Sat. Unit W. (kN/m3)</b>
<b>1</b>	137,38	78,91	127,32	10,06	58,47	17,21	21,36	23,05
<b>2</b>	159,36	92,12	149,26	10,10	67,24	15,02	21,78	23,25
<b>3</b>	303,13	176,27	284,45	18,68	126,86	14,72	22,00	23,44
<b>4</b>	182,51	103,66	166,52	15,99	78,85	20,28	20,72	22,71
<b>5</b>	409,35	237,09	381,55	27,80	172,26	16,14	21,73	23,31
<b>6</b>	554,73	318,57	515,62	39,11	236,16	16,56	21,42	23,04
<b>7</b>	633,53	368,85	594,44	39,09	264,68	14,77	22,03	23,48
<b>8</b>	501,44	290,94	492,76	8,68	210,50	4,12	22,96	23,37
<b>9</b>	256,94	148,71	240,87	16,07	108,23	14,85	21,83	23,29
<b>10</b>	307,15	180,94	290,13	17,02	126,21	13,49	22,55	23,87
<b>11</b>	319,11	183,75	296,24	22,87	135,36	16,90	21,47	23,13
<b>12</b>	315,17	181,00	292,61	22,56	134,17	16,81	21,39	23,04
<b>13</b>	300,46	175,61	280,13	20,33	124,85	16,28	22,01	23,61
<b>14</b>	290,74	165,44	270,16	20,58	125,30	16,42	21,15	22,76
<b>15</b>	330,55	190,98	305,42	25,13	139,57	18,01	21,47	23,23
<b>16</b>	326,94	186,15	316,54	10,40	140,79	7,39	22,06	22,78
<b>17</b>	331,57	190,41	317,17	14,40	141,16	10,20	22,04	23,04
<b>18</b>	280,46	160,69	260,87	19,59	119,77	16,36	21,37	22,97
<b>19</b>	210,78	122,18	195,41	15,37	88,60	17,35	21,64	23,34
<b>20</b>	305,90	175,45	280,13	25,77	130,45	19,75	21,07	23,00

Table 92. Porosity and unit weight of Stop 3 weathered limestone

<b>Sample No</b>	<b>Msat (gr)</b>	<b>Msub (gr)</b>	<b>Mdry (gr)</b>	<b>Vv (cm3)</b>	<b>V (cm3)</b>	<b>Porosity (%)</b>	<b>Dry Unit W. (kN/m3)</b>	<b>Sat. Unit W. (kN/m3)</b>
<b>1</b>	281,81	159,96	260,13	21,68	121,85	17,79	20,94	22,69
<b>2</b>	286,27	158,80	261,28	24,99	127,47	19,60	20,11	22,03
<b>3</b>	224,94	127,47	207,41	17,53	97,47	17,99	20,88	22,64
<b>4</b>	252,99	139,91	230,50	22,49	113,08	19,89	20,00	21,95
<b>5</b>	310,48	170,43	297,31	13,17	140,05	9,40	20,83	21,75
<b>6</b>	254,71	140,25	244,05	10,66	114,46	9,31	20,92	21,83
<b>7</b>	296,34	165,47	277,77	18,57	130,87	14,19	20,82	22,21
<b>8</b>	264,05	151,65	232,15	31,90	112,40	28,38	20,26	23,05
<b>9</b>	304,12	170,48	275,79	28,33	133,64	21,20	20,24	22,32
<b>10</b>	287,26	162,71	265,71	21,55	124,55	17,30	20,93	22,63
<b>11</b>	438,77	234,14	389,92	48,85	204,63	23,87	18,69	21,03
<b>12</b>	348,79	191,57	317,79	31,00	157,22	19,72	19,83	21,76
<b>13</b>	209,04	114,68	189,36	19,68	94,36	20,86	19,69	21,73
<b>14</b>	311,49	170,41	285,48	26,01	141,08	18,44	19,85	21,66
<b>15</b>	287,28	155,97	261,15	26,13	131,31	19,90	19,51	21,46
<b>16</b>	305,13	164,71	274,59	30,54	140,42	21,75	19,18	21,32
<b>17</b>	299,35	159,94	269,56	29,79	139,41	21,37	18,97	21,06
<b>18</b>	260,95	141,47	241,47	19,48	119,48	16,30	19,83	21,43
<b>19</b>	320,18	170,56	295,44	24,74	149,62	16,54	19,37	20,99
<b>20</b>	225,88	121,25	202,69	23,19	104,63	22,16	19,00	21,18

Table 93. Porosity and unit weight of Stop 4 fresh granite

<b>Sample No</b>	<b>Msat (gr)</b>	<b>Msub (gr)</b>	<b>Mdry (gr)</b>	<b>Vv (cm3)</b>	<b>V (cm3)</b>	<b>Porosity (%)</b>	<b>Dry Unit W. (kN/m3)</b>	<b>Sat. Unit W. (kN/m3)</b>
<b>1</b>	137,01	85,03	136,11	0,90	51,98	1,73	25,69	25,86
<b>2</b>	158,75	98,63	157,80	0,95	60,12	1,58	25,75	25,90
<b>3</b>	208,64	129,59	207,33	1,31	79,05	1,66	25,73	25,89
<b>4</b>	257,89	160,06	255,87	2,02	97,83	2,06	25,66	25,86
<b>5</b>	178,30	110,64	176,89	1,41	67,66	2,08	25,65	25,85
<b>6</b>	189,66	117,58	188,13	1,53	72,08	2,12	25,60	25,81
<b>7</b>	183,76	114,02	182,49	1,27	69,74	1,82	25,67	25,85
<b>8</b>	210,18	130,88	203,71	6,47	79,30	8,16	25,20	26,00
<b>9</b>	260,43	161,05	256,18	4,25	99,38	4,28	25,29	25,71
<b>10</b>	190,13	118,47	189,13	1,00	71,66	1,40	25,89	26,03

Table 94. Porosity and unit weight of Stop 4 weathered granite

<b>Sample No</b>	<b>Msat (gr)</b>	<b>Msub (gr)</b>	<b>Mdry (gr)</b>	<b>Vv (cm3)</b>	<b>V (cm3)</b>	<b>Porosity (%)</b>	<b>Dry Unit W. (kN/m3)</b>	<b>Sat. Unit W. (kN/m3)</b>
<b>1</b>	525,43	324,86	520,08	5,35	200,57	2,67	25,44	25,70
<b>2</b>	205,46	126,53	202,96	2,50	78,93	3,17	25,23	25,54
<b>3</b>	169,27	104,86	167,82	1,45	64,41	2,25	25,56	25,78
<b>4</b>	440,18	273,45	432,18	8,00	166,73	4,80	25,43	25,90
<b>5</b>	210,41	129,71	207,41	3,00	80,70	3,72	25,21	25,58
<b>6</b>	520,88	321,78	514,82	6,06	199,10	3,04	25,37	25,66
<b>7</b>	418,22	258,99	411,07	7,15	159,23	4,49	25,33	25,77
<b>8</b>	170,90	105,91	168,41	2,49	64,99	3,83	25,42	25,80
<b>9</b>	490,51	299,94	488,90	1,61	190,57	0,84	25,17	25,25
<b>10</b>	200,89	122,46	200,45	0,44	78,43	0,56	25,07	25,13

Table 95. Porosity and unit weight of Stop 5 fresh basalt

<b>Sample No</b>	<b>Msat (gr)</b>	<b>Msub (gr)</b>	<b>Mdry (gr)</b>	<b>Vv (cm3)</b>	<b>V (cm3)</b>	<b>Porosity (%)</b>	<b>Dry Unit W. (kN/m3)</b>	<b>Sat. Unit W. (kN/m3)</b>
<b>1</b>	246,13	156,15	235,13	11,00	89,98	12,22	25,63	26,83
<b>2</b>	421,16	259,41	415,12	6,04	161,75	3,73	25,18	25,54
<b>3</b>	105,54	65,99	101,88	3,66	39,55	9,25	25,27	26,18
<b>4</b>	337,13	210,70	325,18	11,95	126,43	9,45	25,23	26,16
<b>5</b>	156,83	98,48	153,15	3,68	58,35	6,31	25,75	26,37
<b>6</b>	175,18	110,41	168,47	6,71	64,77	10,36	25,52	26,53
<b>7</b>	147,84	92,43	141,21	6,63	55,41	11,97	25,00	26,17
<b>8</b>	204,18	128,49	198,41	5,77	75,69	7,62	25,72	26,46
<b>9</b>	103,98	65,84	98,71	5,27	38,14	13,82	25,39	26,74
<b>10</b>	108,11	66,95	105,44	2,67	41,16	6,49	25,13	25,77

Table 96. Porosity and unit weight of Stop 5 weathered basalt

<b>Sample No</b>	<b>Msat (gr)</b>	<b>Msub (gr)</b>	<b>Mdry (gr)</b>	<b>Vv (cm3)</b>	<b>V (cm3)</b>	<b>Porosity (%)</b>	<b>Dry Unit W. (kN/m3)</b>	<b>Sat. Unit W. (kN/m3)</b>
<b>1</b>	179,26	114,00	174,00	5,26	65,26	8,06	26,16	26,95
<b>2</b>	329,71	210,43	320,54	9,17	119,28	7,69	26,36	27,12
<b>3</b>	96,88	57,29	88,08	8,80	39,59	22,23	21,83	24,01
<b>4</b>	238,71	144,12	222,90	15,81	94,59	16,71	23,12	24,76
<b>5</b>	170,04	107,78	163,63	6,41	62,26	10,30	25,78	26,79
<b>6</b>	277,15	171,10	261,99	15,16	106,05	14,30	24,24	25,64
<b>7</b>	176,05	111,87	170,68	5,37	64,18	8,37	26,09	26,91
<b>8</b>	103,90	63,86	97,63	6,27	40,04	15,66	23,92	25,46
<b>9</b>	183,92	113,17	173,15	10,77	70,75	15,22	24,01	25,50
<b>10</b>	98,00	61,47	93,54	4,46	36,53	12,21	25,12	26,32

Table 97. Porosity and unit weight of Stop 6 weathered granite

<b>Sample No</b>	<b>Msat (gr)</b>	<b>Msub (gr)</b>	<b>Mdry (gr)</b>	<b>Vv (cm3)</b>	<b>V (cm3)</b>	<b>Porosity (%)</b>	<b>Dry Unit W. (kN/m3)</b>	<b>Sat. Unit W. (kN/m3)</b>
<b>1</b>	126,35	76,73	121,56	4,79	49,62	9,65	24,03	24,98
<b>2</b>	175,29	106,86	169,90	5,39	68,43	7,88	24,36	25,13
<b>3</b>	231,14	140,74	223,75	7,39	90,40	8,17	24,28	25,08
<b>4</b>	266,00	163,81	260,30	5,70	102,19	5,58	24,99	25,54
<b>5</b>	113,89	69,90	111,01	2,88	43,99	6,55	24,76	25,40
<b>6</b>	180,91	111,17	176,59	4,32	69,74	6,19	24,84	25,45
<b>7</b>	115,05	71,53	113,43	1,62	43,52	3,72	25,57	25,93
<b>8</b>	200,13	122,16	191,84	8,29	77,97	10,63	24,14	25,18
<b>9</b>	199,10	121,70	193,39	5,71	77,40	7,38	24,51	25,23
<b>10</b>	347,64	213,30	339,12	8,52	134,34	6,34	24,76	25,39

Table 98. Porosity and unit weight of Stop 7 fresh granodiorite

<b>Sample No</b>	<b>Msat (gr)</b>	<b>Msub (gr)</b>	<b>Mdry (gr)</b>	<b>Vv (cm3)</b>	<b>V (cm3)</b>	<b>Porosity (%)</b>	<b>Dry Unit W. (kN/m3)</b>	<b>Sat. Unit W. (kN/m3)</b>
<b>1</b>	320,86	210,30	319,87	0,99	110,56	0,90	28,38	28,47
<b>2</b>	379,93	240,32	377,73	2,20	139,61	1,58	26,54	26,70
<b>3</b>	236,45	149,76	235,17	1,28	86,69	1,48	26,61	26,76
<b>4</b>	132,33	83,44	131,17	1,16	48,89	2,37	26,32	26,55
<b>5</b>	100,51	63,30	99,54	0,97	37,21	2,61	26,24	26,50
<b>6</b>	266,26	169,00	265,24	1,02	97,26	1,05	26,75	26,86
<b>7</b>	380,41	241,16	373,46	6,95	139,25	4,99	26,31	26,80
<b>8</b>	330,47	214,65	323,55	6,92	115,82	5,97	27,40	27,99
<b>9</b>	250,71	160,44	248,00	2,71	90,27	3,00	26,95	27,25
<b>10</b>	230,44	144,89	229,55	0,89	85,55	1,04	26,32	26,42

Table 99. Porosity and unit weight of Stop 7 weathered granodiorite

<b>Sample No</b>	<b>Msat (gr)</b>	<b>Msub (gr)</b>	<b>Mdry (gr)</b>	<b>Vv (cm3)</b>	<b>V (cm3)</b>	<b>Porosity (%)</b>	<b>Dry Unit W. (kN/m3)</b>	<b>Sat. Unit W. (kN/m3)</b>
<b>1</b>	242,70	152,10	239,94	2,76	90,60	3,05	25,98	26,28
<b>2</b>	342,89	214,13	333,46	9,43	128,76	7,32	25,41	26,12
<b>3</b>	76,56	47,88	74,30	2,26	28,68	7,88	25,41	26,19
<b>4</b>	228,48	143,50	226,12	2,36	84,98	2,78	26,10	26,38
<b>5</b>	110,46	69,46	105,47	4,99	41,00	12,17	25,24	26,43
<b>6</b>	350,18	227,35	339,41	10,77	122,83	8,77	27,11	27,97
<b>7</b>	190,56	115,25	188,49	2,07	75,31	2,75	24,55	24,82
<b>8</b>	90,44	55,48	88,03	2,41	34,96	6,89	24,70	25,38
<b>9</b>	131,71	82,44	130,93	0,78	49,27	1,58	26,07	26,22
<b>10</b>	250,69	157,48	247,71	2,98	93,21	3,20	26,07	26,38

Table 100. Porosity and unit weight of Stop 8 fresh sandstone

<b>Sample No</b>	<b>Msat (gr)</b>	<b>Msub (gr)</b>	<b>Mdry (gr)</b>	<b>Vv (cm3)</b>	<b>V (cm3)</b>	<b>Porosity (%)</b>	<b>Dry Unit W. (kN/m3)</b>	<b>Sat. Unit W. (kN/m3)</b>
<b>1</b>	156,63	96,88	154,30	2,33	59,75	3,90	25,33	25,72
<b>2</b>	165,12	102,21	162,29	2,83	62,91	4,50	25,31	25,75
<b>3</b>	240,11	148,29	236,68	3,43	91,82	3,74	25,29	25,65
<b>4</b>	484,04	300,42	478,12	5,92	183,62	3,22	25,54	25,86
<b>5</b>	398,80	247,15	392,92	5,88	151,65	3,88	25,42	25,80
<b>6</b>	668,25	413,72	658,96	9,29	254,53	3,65	25,40	25,76
<b>7</b>	543,11	336,19	538,13	4,98	206,92	2,41	25,51	25,75
<b>8</b>	480,44	297,13	476,99	3,45	183,31	1,88	25,53	25,71
<b>9</b>	331,79	205,13	327,88	3,91	126,66	3,09	25,39	25,70
<b>10</b>	401,98	248,91	398,22	3,76	153,07	2,46	25,52	25,76

Table 101. Porosity and unit weight of Stop 8 weathered sandstone

<b>Sample No</b>	<b>Msat (gr)</b>	<b>Msub (gr)</b>	<b>Mdry (gr)</b>	<b>Vv (cm3)</b>	<b>V (cm3)</b>	<b>Porosity (%)</b>	<b>Dry Unit W. (kN/m3)</b>	<b>Sat. Unit W. (kN/m3)</b>
<b>1</b>	200,12	120,92	193,64	6,48	79,20	8,18	23,98	24,79
<b>2</b>	170,40	103,24	164,98	5,42	67,16	8,07	24,10	24,89
<b>3</b>	127,80	76,71	122,68	5,12	51,09	10,02	23,56	24,54
<b>4</b>	197,96	119,05	190,52	7,44	78,91	9,43	23,69	24,61
<b>5</b>	192,22	116,11	185,17	7,05	76,11	9,26	23,87	24,78
<b>6</b>	210,48	126,99	203,47	7,01	83,49	8,40	23,91	24,73
<b>7</b>	180,41	108,59	173,63	6,78	71,82	9,44	23,72	24,64
<b>8</b>	220,58	132,91	214,22	6,36	87,67	7,25	23,97	24,68
<b>9</b>	290,71	175,99	281,03	9,68	114,72	8,44	24,03	24,86
<b>10</b>	188,75	114,32	181,95	6,80	74,43	9,14	23,98	24,88

Table 102. Porosity and unit weight of Stop 9 fresh limestone

<b>Sample No</b>	<b>Msat (gr)</b>	<b>Msub (gr)</b>	<b>Mdry (gr)</b>	<b>Vv (cm3)</b>	<b>V (cm3)</b>	<b>Porosity (%)</b>	<b>Dry Unit W. (kN/m3)</b>	<b>Sat. Unit W. (kN/m3)</b>
<b>1</b>	439,92	270,20	433,01	6,91	169,72	4,07	25,03	25,43
<b>2</b>	291,10	177,59	287,76	3,34	113,51	2,94	24,87	25,16
<b>3</b>	127,13	76,95	123,46	3,67	50,18	7,31	24,14	24,85
<b>4</b>	350,41	210,15	340,58	9,83	140,26	7,01	23,82	24,51
<b>5</b>	221,81	133,13	218,55	3,26	88,68	3,68	24,18	24,54
<b>6</b>	313,54	190,19	310,54	3,00	123,35	2,43	24,70	24,94
<b>7</b>	291,42	180,41	288,56	2,86	111,01	2,58	25,50	25,75
<b>8</b>	321,63	195,39	318,17	3,46	126,24	2,74	24,72	24,99
<b>9</b>	223,11	137,78	221,18	1,93	85,33	2,26	25,43	25,65
<b>10</b>	250,41	155,89	234,10	16,31	94,52	17,26	24,30	25,99

Table 103. Porosity and unit weight of Stop 9 weathered limestone

<b>Sample No</b>	<b>Msat (gr)</b>	<b>Msub (gr)</b>	<b>Mdry (gr)</b>	<b>Vv (cm3)</b>	<b>V (cm3)</b>	<b>Porosity (%)</b>	<b>Dry Unit W. (kN/m3)</b>	<b>Sat. Unit W. (kN/m3)</b>
<b>1</b>	188,78	115,54	185,72	3,06	73,24	4,18	24,88	25,29
<b>2</b>	198,64	120,18	195,31	3,33	78,46	4,24	24,42	24,84
<b>3</b>	187,61	113,78	184,18	3,43	73,83	4,65	24,47	24,93
<b>4</b>	109,84	67,08	108,38	1,46	42,76	3,41	24,86	25,20
<b>5</b>	365,85	226,94	362,87	2,98	138,91	2,15	25,63	25,84
<b>6</b>	355,44	216,94	350,15	5,29	138,50	3,82	24,80	25,18
<b>7</b>	212,18	130,48	195,18	17,00	81,70	20,81	23,44	25,48
<b>8</b>	311,41	184,13	308,17	3,24	127,28	2,55	23,75	24,00
<b>9</b>	305,64	185,47	301,49	4,15	120,17	3,45	24,61	24,95
<b>10</b>	209,13	127,46	207,13	2,00	81,67	2,45	24,88	25,12

Table 104. Porosity and unit weight of Stop 9 weathered mudstone

<b>Sample No</b>	<b>Msat (gr)</b>	<b>Msub (gr)</b>	<b>Mdry (gr)</b>	<b>Vv (cm3)</b>	<b>V (cm3)</b>	<b>Porosity (%)</b>	<b>Dry Unit W. (kN/m3)</b>	<b>Sat. Unit W. (kN/m3)</b>
<b>1</b>	186,84	110,09	179,47	7,37	76,75	9,60	22,94	23,88
<b>2</b>	86,87	51,87	83,79	3,08	35,00	8,80	23,49	24,35
<b>3</b>	127,73	75,87	123,53	4,20	51,86	8,10	23,37	24,16
<b>4</b>	154,53	91,65	149,41	5,12	62,88	8,14	23,31	24,11
<b>5</b>	93,81	55,55	91,14	2,67	38,26	6,98	23,37	24,05
<b>6</b>	131,15	77,69	126,19	4,96	53,46	9,28	23,16	24,07
<b>7</b>	89,02	52,74	86,32	2,70	36,28	7,44	23,34	24,07
<b>8</b>	120,81	70,82	115,30	5,51	49,99	11,02	22,63	23,71
<b>9</b>	280,34	165,77	271,24	9,10	114,57	7,94	23,22	24,00
<b>10</b>	229,18	138,32	223,29	5,89	90,86	6,48	24,11	24,74

Table 105. Porosity and unit weight of Stop 10 fresh sandstone

<b>Sample No</b>	<b>Msat (gr)</b>	<b>Msub (gr)</b>	<b>Mdry (gr)</b>	<b>Vv (cm3)</b>	<b>V (cm3)</b>	<b>Porosity (%)</b>	<b>Dry Unit W. (kN/m3)</b>	<b>Sat. Unit W. (kN/m3)</b>
<b>1</b>	179,96	109,00	173,88	6,08	70,96	8,57	24,04	24,88
<b>2</b>	415,52	250,96	398,96	16,56	164,56	10,06	23,78	24,77
<b>3</b>	318,20	192,94	307,80	10,40	125,26	8,30	24,11	24,92
<b>4</b>	204,93	123,86	197,57	7,36	81,07	9,08	23,91	24,80
<b>5</b>	534,30	325,43	518,87	15,43	208,87	7,39	24,37	25,09
<b>6</b>	250,12	151,97	242,14	7,98	98,15	8,13	24,20	25,00
<b>7</b>	330,54	200,54	321,36	9,18	130,00	7,06	24,25	24,94
<b>8</b>	401,59	243,18	391,12	10,47	158,41	6,61	24,22	24,87
<b>9</b>	350,81	212,11	342,18	8,63	138,70	6,22	24,20	24,81
<b>10</b>	260,33	158,11	252,94	7,39	102,22	7,23	24,27	24,98

Table 106. Porosity and unit weight of Stop 10 weathered sandstone

<b>Sample No</b>	<b>Msat (gr)</b>	<b>Msub (gr)</b>	<b>Mdry (gr)</b>	<b>Vv (cm3)</b>	<b>V (cm3)</b>	<b>Porosity (%)</b>	<b>Dry Unit W. (kN/m3)</b>	<b>Sat. Unit W. (kN/m3)</b>
<b>1</b>	353,58	209,89	335,31	18,27	143,69	12,71	22,89	24,14
<b>2</b>	336,55	199,55	316,65	19,90	137,00	14,53	22,67	24,10
<b>3</b>	209,62	125,85	200,05	9,57	83,77	11,42	23,43	24,55
<b>4</b>	413,75	249,16	396,10	17,65	164,59	10,72	23,61	24,66
<b>5</b>	246,48	148,36	235,60	10,88	98,12	11,09	23,56	24,64
<b>6</b>	342,18	205,18	330,55	11,63	137,00	8,49	23,67	24,50
<b>7</b>	420,46	251,58	402,18	18,28	168,88	10,82	23,36	24,42
<b>8</b>	250,91	151,05	241,09	9,82	99,86	9,83	23,68	24,65
<b>9</b>	350,88	208,53	336,46	14,42	142,35	10,13	23,19	24,18
<b>10</b>	205,46	122,17	198,22	7,24	83,29	8,69	23,35	24,20

Table 107. Porosity and unit weight of Stop 11 fresh sandstone

<b>Sample No</b>	<b>Msat (gr)</b>	<b>Msub (gr)</b>	<b>Mdry (gr)</b>	<b>Vv (cm3)</b>	<b>V (cm3)</b>	<b>Porosity (%)</b>	<b>Dry Unit W. (kN/m3)</b>	<b>Sat. Unit W. (kN/m3)</b>
<b>1</b>	210,34	126,29	201,95	8,39	84,05	9,98	23,57	24,55
<b>2</b>	280,11	167,50	268,27	11,84	112,61	10,51	23,37	24,40
<b>3</b>	171,03	102,69	164,35	6,68	68,34	9,77	23,59	24,55
<b>4</b>	228,76	137,07	219,27	9,49	91,69	10,35	23,46	24,48
<b>5</b>	155,24	93,36	149,36	5,88	61,88	9,50	23,68	24,61
<b>6</b>	182,09	109,16	174,39	7,70	72,93	10,56	23,46	24,49
<b>7</b>	254,10	151,54	242,24	11,86	102,56	11,56	23,17	24,31
<b>8</b>	263,66	157,58	252,35	11,31	106,08	10,66	23,34	24,38
<b>9</b>	324,33	193,86	310,22	14,11	130,47	10,81	23,33	24,39
<b>10</b>	194,72	116,42	186,11	8,61	78,30	11,00	23,32	24,40

Table 108. Porosity and unit weight of Stop 11 weathered sandstone

<b>Sample No</b>	<b>Msat (gr)</b>	<b>Msub (gr)</b>	<b>Mdry (gr)</b>	<b>Vv (cm3)</b>	<b>V (cm3)</b>	<b>Porosity (%)</b>	<b>Dry Unit W. (kN/m3)</b>	<b>Sat. Unit W. (kN/m3)</b>
<b>1</b>	224,58	131,35	206,55	18,03	93,23	19,34	21,73	23,63
<b>2</b>	138,33	80,64	127,86	10,47	57,69	18,15	21,74	23,52
<b>3</b>	252,63	148,16	236,45	16,18	104,47	15,49	22,20	23,72
<b>4</b>	215,37	128,77	204,05	11,32	86,60	13,07	23,11	24,40
<b>5</b>	169,52	101,50	160,79	8,73	68,02	12,83	23,19	24,45
<b>6</b>	216,70	129,27	204,49	12,21	87,43	13,97	22,94	24,31
<b>7</b>	207,39	122,26	194,20	13,19	85,13	15,49	22,38	23,90
<b>8</b>	233,68	139,90	221,83	11,85	93,78	12,64	23,20	24,44
<b>9</b>	188,08	112,90	178,48	9,60	75,18	12,77	23,29	24,54
<b>10</b>	314,17	187,55	297,74	16,43	126,62	12,98	23,07	24,34

Table 109. Porosity and unit weight of Stop 12 fresh sandstone

<b>Sample No</b>	<b>Msat (gr)</b>	<b>Msub (gr)</b>	<b>Mdry (gr)</b>	<b>Vv (cm3)</b>	<b>V (cm3)</b>	<b>Porosity (%)</b>	<b>Dry Unit W. (kN/m3)</b>	<b>Sat. Unit W. (kN/m3)</b>
<b>1</b>	126,00	75,20	118,40	7,60	50,80	14,96	22,86	24,33
<b>2</b>	332,76	200,85	316,98	15,78	131,91	11,96	23,57	24,75
<b>3</b>	213,29	128,49	204,45	8,84	84,80	10,42	23,65	24,67
<b>4</b>	300,58	180,79	286,56	14,02	119,79	11,70	23,47	24,62
<b>5</b>	175,40	105,58	167,88	7,52	69,82	10,77	23,59	24,64
<b>6</b>	270,78	161,00	254,52	16,26	109,78	14,81	22,74	24,20
<b>7</b>	292,08	174,26	275,35	16,73	117,82	14,20	22,93	24,32
<b>8</b>	296,47	179,10	285,13	11,34	117,37	9,66	23,83	24,78
<b>9</b>	204,87	123,22	196,16	8,71	81,65	10,67	23,57	24,61
<b>10</b>	144,76	87,41	139,23	5,53	57,35	9,64	23,82	24,76

Table 110. Porosity and unit weight of Stop 12 weathered sandstone

<b>Sample No</b>	<b>Msat (gr)</b>	<b>Msub (gr)</b>	<b>Mdry (gr)</b>	<b>Vv (cm3)</b>	<b>V (cm3)</b>	<b>Porosity (%)</b>	<b>Dry Unit W. (kN/m3)</b>	<b>Sat. Unit W. (kN/m3)</b>
<b>1</b>	155,88	89,90	142,33	13,55	65,98	20,54	21,16	23,18
<b>2</b>	167,79	101,05	159,92	7,87	66,74	11,79	23,51	24,66
<b>3</b>	94,24	56,16	88,64	5,60	38,08	14,71	22,84	24,28
<b>4</b>	122,71	73,42	116,20	6,51	49,29	13,21	23,13	24,42
<b>5</b>	142,54	84,97	134,57	7,97	57,57	13,84	22,93	24,29
<b>6</b>	60,77	36,07	57,16	3,61	24,70	14,62	22,70	24,14
<b>7</b>	142,97	86,07	135,95	7,02	56,90	12,34	23,44	24,65
<b>8</b>	295,56	176,72	281,07	14,49	118,84	12,19	23,20	24,40
<b>9</b>	110,88	65,56	106,71	4,17	45,32	9,20	23,10	24,00
<b>10</b>	160,46	95,44	153,49	6,97	65,02	10,72	23,16	24,21

Table 111. Porosity and unit weight of Stop 13 fresh sandstone

<b>Sample No</b>	<b>Msat (gr)</b>	<b>Msub (gr)</b>	<b>Mdry (gr)</b>	<b>Vv (cm3)</b>	<b>V (cm3)</b>	<b>Porosity (%)</b>	<b>Dry Unit W. (kN/m3)</b>	<b>Sat. Unit W. (kN/m3)</b>
<b>1</b>	78,44	45,92	72,08	6,36	32,52	19,56	21,74	23,66
<b>2</b>	227,48	137,32	218,58	8,90	90,16	9,87	23,78	24,75
<b>3</b>	103,07	59,97	94,09	8,98	43,10	20,84	21,42	23,46
<b>4</b>	87,25	51,01	80,22	7,03	36,24	19,40	21,72	23,62
<b>5</b>	95,26	55,75	87,52	7,74	39,51	19,59	21,73	23,65
<b>6</b>	78,25	45,91	72,14	6,11	32,34	18,89	21,88	23,74
<b>7</b>	222,56	131,05	205,69	16,87	91,51	18,44	22,05	23,86
<b>8</b>	210,75	123,30	193,37	17,38	87,45	19,87	21,69	23,64
<b>9</b>	334,99	195,22	306,44	28,55	139,77	20,43	21,51	23,51
<b>10</b>	210,48	122,27	191,67	18,81	88,21	21,32	21,32	23,41

Table 112. Porosity and unit weight of Stop 13 weathered sandstone

<b>Sample No</b>	<b>Msat (gr)</b>	<b>Msub (gr)</b>	<b>Mdry (gr)</b>	<b>Vv (cm3)</b>	<b>V (cm3)</b>	<b>Porosity (%)</b>	<b>Dry Unit W. (kN/m3)</b>	<b>Sat. Unit W. (kN/m3)</b>
<b>1</b>	133,55	77,03	121,50	12,05	56,52	21,32	21,09	23,18
<b>2</b>	158,22	94,79	151,92	6,30	63,43	9,93	23,50	24,47
<b>3</b>	170,12	98,81	155,54	14,58	71,31	20,45	21,40	23,40
<b>4</b>	209,14	121,73	192,04	17,10	87,41	19,56	21,55	23,47
<b>5</b>	149,59	87,82	139,24	10,35	61,77	16,76	22,11	23,76
<b>6</b>	162,62	94,00	148,23	14,39	68,62	20,97	21,19	23,25
<b>7</b>	218,94	130,29	206,48	12,46	88,65	14,06	22,85	24,23
<b>8</b>	361,68	210,09	331,93	29,75	151,59	19,63	21,48	23,41
<b>9</b>	176,03	102,34	164,99	11,04	73,69	14,98	21,96	23,43
<b>10</b>	369,47	215,70	340,98	28,49	153,77	18,53	21,75	23,57

Table 113. Porosity and unit weight of Stop 14 fresh sandstone

<b>Sample No</b>	<b>Msat (gr)</b>	<b>Msub (gr)</b>	<b>Mdry (gr)</b>	<b>Vv (cm3)</b>	<b>V (cm3)</b>	<b>Porosity (%)</b>	<b>Dry Unit W. (kN/m3)</b>	<b>Sat. Unit W. (kN/m3)</b>
<b>1</b>	60,87	37,08	58,70	2,17	23,79	9,12	24,21	25,10
<b>2</b>	73,18	44,53	70,36	2,82	28,65	9,84	24,09	25,06
<b>3</b>	158,11	96,13	151,81	6,30	61,98	10,16	24,03	25,03
<b>4</b>	100,41	61,00	96,46	3,95	39,41	10,02	24,01	24,99
<b>5</b>	142,39	86,70	136,22	6,17	55,69	11,08	24,00	25,08
<b>6</b>	123,88	75,22	117,94	5,94	48,66	12,21	23,78	24,97
<b>7</b>	147,85	90,21	143,13	4,72	57,64	8,19	24,36	25,16
<b>8</b>	54,19	33,12	52,54	1,65	21,07	7,83	24,46	25,23
<b>9</b>	120,84	73,86	118,46	2,38	46,98	5,07	24,74	25,23
<b>10</b>	144,59	88,11	139,11	5,48	56,48	9,70	24,16	25,11

Table 114. Porosity and unit weight of Stop 14 weathered sandstone

<b>Sample No</b>	<b>Msat (gr)</b>	<b>Msub (gr)</b>	<b>Mdry (gr)</b>	<b>Vv (cm3)</b>	<b>V (cm3)</b>	<b>Porosity (%)</b>	<b>Dry Unit W. (kN/m3)</b>	<b>Sat. Unit W. (kN/m3)</b>
<b>1</b>	152,08	90,92	144,90	7,18	61,16	11,74	23,24	24,39
<b>2</b>	290,61	178,09	282,27	8,34	112,52	7,41	24,61	25,34
<b>3</b>	187,59	106,97	167,52	20,07	80,62	24,89	20,38	22,83
<b>4</b>	92,77	56,02	88,46	4,31	36,75	11,73	23,61	24,76
<b>5</b>	425,03	257,18	406,59	18,44	167,85	10,99	23,76	24,84
<b>6</b>	485,84	292,87	463,00	22,84	192,97	11,84	23,54	24,70
<b>7</b>	174,00	106,70	169,41	4,59	67,30	6,82	24,69	25,36
<b>8</b>	161,62	99,28	157,62	4,00	62,34	6,42	24,80	25,43
<b>9</b>	227,29	140,09	222,42	4,87	87,20	5,58	25,02	25,57
<b>10</b>	125,25	77,19	122,54	2,71	48,06	5,64	25,01	25,57

Table 115. Porosity and unit weight of Stop 15 fresh sandstone

Sample No	Msat (gr)	Msub (gr)	Mdry (gr)	Vv (cm3)	V (cm3)	Porosity (%)	Dry Unit W. (kN/m3)	Sat. Unit W. (kN/m3)
1	326,21	198,75	316,60	9,61	127,46	7,54	24,37	25,11
2	296,27	181,29	288,23	8,04	114,98	6,99	24,59	25,28
3	250,20	152,53	242,18	8,02	97,67	8,21	24,32	25,13
4	255,61	156,10	249,03	6,58	99,51	6,61	24,55	25,20
5	245,03	149,89	238,13	6,90	95,14	7,25	24,55	25,27
6	306,33	187,00	296,04	10,29	119,33	8,62	24,34	25,18
7	125,72	77,12	122,93	2,79	48,60	5,74	24,81	25,38
8	333,84	200,38	321,22	12,62	133,46	9,46	23,61	24,54
9	276,58	168,82	268,65	7,93	107,76	7,36	24,46	25,18
10	461,95	281,79	449,39	12,56	180,16	6,97	24,47	25,15

Table 116. Porosity and unit weight of Stop 15 weathered sandstone

Sample No	Msat (gr)	Msub (gr)	Mdry (gr)	Vv (cm3)	V (cm3)	Porosity (%)	Dry Unit W. (kN/m3)	Sat. Unit W. (kN/m3)
1	254,92	155,27	249,03	5,89	99,65	5,91	24,52	25,10
2	118,21	71,63	113,90	4,31	46,58	9,25	23,99	24,90
3	183,28	108,85	172,35	10,93	74,43	14,68	22,72	24,16
4	387,85	235,70	375,23	12,62	152,15	8,29	24,19	25,01
5	389,98	235,83	376,75	13,23	154,15	8,58	23,98	24,82
6	203,69	123,83	198,97	4,72	79,86	5,91	24,44	25,02
7	289,32	174,38	277,39	11,93	114,94	10,38	23,67	24,69
8	244,93	146,22	232,30	12,63	98,71	12,80	23,09	24,34
9	174,91	104,60	165,54	9,37	70,31	13,33	23,10	24,40
10	208,84	125,64	200,94	7,90	83,20	9,50	23,69	24,62

Table 117. Porosity and unit weight of Stop 16 fresh sandstone

<b>Sample No</b>	<b>Msat (gr)</b>	<b>Msub (gr)</b>	<b>Mdry (gr)</b>	<b>Vv (cm3)</b>	<b>V (cm3)</b>	<b>Porosity (%)</b>	<b>Dry Unit W. (kN/m3)</b>	<b>Sat. Unit W. (kN/m3)</b>
<b>1</b>	217,55	131,06	208,77	8,78	86,49	10,15	23,68	24,68
<b>2</b>	201,03	117,92	189,46	11,57	83,11	13,92	22,36	23,73
<b>3</b>	342,29	205,39	328,37	13,92	136,90	10,17	23,53	24,53
<b>4</b>	257,27	153,96	246,03	11,24	103,31	10,88	23,36	24,43
<b>5</b>	259,85	157,47	250,88	8,97	102,38	8,76	24,04	24,90
<b>6</b>	148,63	90,62	144,31	4,32	58,01	7,45	24,40	25,13
<b>7</b>	140,08	82,87	132,89	7,19	57,21	12,57	22,79	24,02
<b>8</b>	207,37	124,23	198,43	8,94	83,14	10,75	23,41	24,47
<b>9</b>	168,59	99,57	160,12	8,47	69,02	12,27	22,76	23,96
<b>10</b>	190,89	116,33	185,35	5,54	74,56	7,43	24,39	25,12

Table 118. Porosity and unit weight of Stop 16 weathered sandstone

<b>Sample No</b>	<b>Msat (gr)</b>	<b>Msub (gr)</b>	<b>Mdry (gr)</b>	<b>Vv (cm3)</b>	<b>V (cm3)</b>	<b>Porosity (%)</b>	<b>Dry Unit W. (kN/m3)</b>	<b>Sat. Unit W. (kN/m3)</b>
<b>1</b>	165,44	100,74	160,38	5,06	64,70	7,82	24,32	25,08
<b>2</b>	76,13	41,16	67,55	8,58	34,97	24,54	18,95	21,36
<b>3</b>	124,87	74,96	119,73	5,14	49,91	10,30	23,53	24,54
<b>4</b>	107,98	63,19	102,00	5,98	44,79	13,35	22,34	23,65
<b>5</b>	170,70	94,81	154,60	16,10	75,89	21,21	19,98	22,07
<b>6</b>	184,96	111,12	177,57	7,39	73,84	10,01	23,59	24,57
<b>7</b>	136,39	81,78	130,82	5,57	54,61	10,20	23,50	24,50
<b>8</b>	108,93	64,80	104,12	4,81	44,13	10,90	23,15	24,21
<b>9</b>	241,71	145,63	232,20	9,51	96,08	9,90	23,71	24,68
<b>10</b>	171,30	102,72	164,07	7,23	68,58	10,54	23,47	24,50

Table 119. Porosity and unit weight of Stop 17 fresh sandstone

Sample No	Msat (gr)	Msub (gr)	Mdry (gr)	Vv (cm3)	V (cm3)	Porosity (%)	Dry Unit W. (kN/m3)	Sat. Unit W. (kN/m3)
1	126,59	74,90	118,38	8,21	51,69	15,88	22,47	24,02
2	242,66	142,94	226,05	16,61	99,72	16,66	22,24	23,87
3	170,95	101,59	160,40	10,55	69,36	15,21	22,69	24,18
4	174,40	103,25	163,34	11,06	71,15	15,54	22,52	24,05
5	150,09	89,53	141,67	8,42	60,56	13,90	22,95	24,31
6	240,18	142,85	220,47	19,71	97,33	20,25	22,22	24,21
7	165,99	97,74	155,16	10,83	68,25	15,87	22,30	23,86
8	210,46	125,58	195,12	15,34	84,88	18,07	22,55	24,32
9	221,48	131,46	210,96	10,52	90,02	11,69	22,99	24,14
10	290,63	172,55	276,63	14,00	118,08	11,86	22,98	24,15

Table 120. Porosity and unit weight of Stop 17 weathered sandstone

Sample No	Msat (gr)	Msub (gr)	Mdry (gr)	Vv (cm3)	V (cm3)	Porosity (%)	Dry Unit W. (kN/m3)	Sat. Unit W. (kN/m3)
1	108,54	62,91	98,56	9,98	45,63	21,87	21,19	23,34
2	268,26	157,82	247,18	21,08	110,44	19,09	21,96	23,83
3	94,90	55,74	88,16	6,74	39,16	17,21	22,09	23,77
4	255,18	147,86	250,44	4,74	107,32	4,42	22,89	23,33
5	128,79	75,48	118,24	10,55	53,31	19,79	21,76	23,70
6	95,88	55,70	90,63	5,25	40,18	13,07	22,13	23,41
7	111,46	64,93	104,56	6,90	46,53	14,83	22,04	23,50
8	220,18	127,41	205,44	14,74	92,77	15,89	21,72	23,28
9	89,55	52,71	80,94	8,61	36,84	23,37	21,55	23,85
10	101,58	58,74	99,58	2,00	42,84	4,67	22,80	23,26

Table 121. Porosity and unit weight of Stop 18 fresh marl

<b>Sample No</b>	<b>Msat (gr)</b>	<b>Msub (gr)</b>	<b>Mdry (gr)</b>	<b>Vv (cm3)</b>	<b>V (cm3)</b>	<b>Porosity (%)</b>	<b>Dry Unit W. (kN/m3)</b>	<b>Sat. Unit W. (kN/m3)</b>
<b>1</b>	226,02	138,65	221,85	4,17	87,37	4,77	24,91	25,38
<b>2</b>	171,82	105,69	169,29	2,53	66,13	3,83	25,11	25,49
<b>3</b>	182,30	112,05	179,30	3,00	70,25	4,27	25,04	25,46
<b>4</b>	181,50	111,29	178,37	3,13	70,21	4,46	24,92	25,36
<b>5</b>	67,83	41,41	66,25	1,58	26,42	5,98	24,60	25,19
<b>6</b>	74,55	45,78	73,14	1,41	28,77	4,90	24,94	25,42
<b>7</b>	74,87	45,84	73,27	1,60	29,03	5,51	24,76	25,30
<b>8</b>	118,33	72,68	116,19	2,14	45,65	4,69	24,97	25,43
<b>9</b>	160,67	98,68	158,00	2,67	61,99	4,31	25,00	25,43
<b>10</b>	245,33	149,83	238,92	6,41	95,50	6,71	24,54	25,20

Table 122. Porosity and unit weight of Stop 18 weathered marl

<b>Sample No</b>	<b>Msat (gr)</b>	<b>Msub (gr)</b>	<b>Mdry (gr)</b>	<b>Vv (cm3)</b>	<b>V (cm3)</b>	<b>Porosity (%)</b>	<b>Dry Unit W. (kN/m3)</b>	<b>Sat. Unit W. (kN/m3)</b>
<b>1</b>	136,51	83,59	133,40	3,11	52,92	5,88	24,73	25,31
<b>2</b>	122,42	75,10	120,09	2,33	47,32	4,92	24,90	25,38
<b>3</b>	198,45	122,14	194,77	3,68	76,31	4,82	25,04	25,51
<b>4</b>	100,17	61,41	98,00	2,17	38,76	5,60	24,80	25,35
<b>5</b>	154,45	94,80	151,12	3,33	59,65	5,58	24,85	25,40
<b>6</b>	252,75	155,02	246,99	5,76	97,73	5,89	24,79	25,37
<b>7</b>	110,83	67,88	108,30	2,53	42,95	5,89	24,74	25,31
<b>8</b>	142,95	87,82	139,67	3,28	55,13	5,95	24,85	25,44
<b>9</b>	131,11	80,78	128,50	2,61	50,33	5,19	25,05	25,56
<b>10</b>	120,46	72,75	118,46	2,00	47,71	4,19	24,36	24,77

Table 123. Porosity and unit weight of Stop 19 fresh marl

<b>Sample No</b>	<b>Msat (gr)</b>	<b>Msub (gr)</b>	<b>Mdry (gr)</b>	<b>Vv (cm3)</b>	<b>V (cm3)</b>	<b>Porosity (%)</b>	<b>Dry Unit W. (kN/m3)</b>	<b>Sat. Unit W. (kN/m3)</b>
<b>1</b>	163,68	101,66	160,67	3,01	62,02	4,85	25,41	25,89
<b>2</b>	309,91	191,98	303,34	6,57	117,93	5,57	25,23	25,78
<b>3</b>	419,79	259,95	411,09	8,70	159,84	5,44	25,23	25,76
<b>4</b>	193,64	119,89	189,49	4,15	73,75	5,63	25,21	25,76
<b>5</b>	173,41	107,79	170,23	3,18	65,62	4,85	25,45	25,92
<b>6</b>	236,80	146,11	230,75	6,05	90,69	6,67	24,96	25,61
<b>7</b>	116,05	71,40	112,34	3,71	44,65	8,31	24,68	25,50
<b>8</b>	169,12	104,49	164,96	4,16	64,63	6,44	25,04	25,67
<b>9</b>	227,63	141,59	223,49	4,14	86,04	4,81	25,48	25,95
<b>10</b>	194,72	121,18	191,43	3,29	73,54	4,47	25,54	25,98

Table 124. Porosity and unit weight of Stop 19 weathered marl

<b>Sample No</b>	<b>Msat (gr)</b>	<b>Msub (gr)</b>	<b>Mdry (gr)</b>	<b>Vv (cm3)</b>	<b>V (cm3)</b>	<b>Porosity (%)</b>	<b>Dry Unit W. (kN/m3)</b>	<b>Sat. Unit W. (kN/m3)</b>
<b>1</b>	100,38	61,48	96,98	3,40	38,90	8,74	24,46	25,31
<b>2</b>	245,92	151,55	239,22	6,70	94,37	7,10	24,87	25,56
<b>3</b>	187,44	114,31	180,38	7,06	73,13	9,65	24,20	25,14
<b>4</b>	236,36	145,14	229,23	7,13	91,22	7,82	24,65	25,42
<b>5</b>	124,52	76,32	120,34	4,18	48,20	8,67	24,49	25,34
<b>6</b>	193,60	117,99	186,38	7,22	75,61	9,55	24,18	25,12
<b>7</b>	136,48	82,12	129,60	6,88	54,36	12,66	23,39	24,63
<b>8</b>	123,60	75,65	119,30	4,30	47,95	8,97	24,41	25,29
<b>9</b>	104,60	64,22	101,32	3,28	40,38	8,12	24,61	25,41
<b>10</b>	83,82	51,17	80,71	3,11	32,65	9,53	24,25	25,18

Table 125. Porosity and unit weight of Stop 20 fresh marl

<b>Sample No</b>	<b>Msat (gr)</b>	<b>Msub (gr)</b>	<b>Mdry (gr)</b>	<b>Vv (cm3)</b>	<b>V (cm3)</b>	<b>Porosity (%)</b>	<b>Dry Unit W. (kN/m3)</b>	<b>Sat. Unit W. (kN/m3)</b>
<b>1</b>	210,00	128,49	205,60	4,40	81,51	5,40	24,74	25,27
<b>2</b>	115,64	70,56	113,18	2,46	45,08	5,46	24,63	25,16
<b>3</b>	73,37	44,55	71,39	1,98	28,82	6,87	24,30	24,97
<b>4</b>	177,33	107,55	172,34	4,99	69,78	7,15	24,23	24,93
<b>5</b>	262,69	160,30	256,70	5,99	102,39	5,85	24,59	25,17
<b>6</b>	167,66	102,04	164,19	3,47	65,62	5,29	24,55	25,06
<b>7</b>	163,23	99,19	159,08	4,15	64,04	6,48	24,37	25,00
<b>8</b>	196,97	119,92	192,02	4,95	77,05	6,42	24,45	25,08
<b>9</b>	261,46	159,18	257,18	4,28	102,28	4,18	24,67	25,08
<b>10</b>	121,22	74,18	117,55	3,67	47,04	7,80	24,51	25,28

Table 126. Porosity and unit weight of Stop 20 weathered marl

<b>Sample No</b>	<b>Msat (gr)</b>	<b>Msub (gr)</b>	<b>Mdry (gr)</b>	<b>Vv (cm3)</b>	<b>V (cm3)</b>	<b>Porosity (%)</b>	<b>Dry Unit W. (kN/m3)</b>	<b>Sat. Unit W. (kN/m3)</b>
<b>1</b>	238,81	144,53	230,11	8,70	94,28	9,23	23,94	24,85
<b>2</b>	127,96	77,39	123,40	4,56	50,57	9,02	23,94	24,82
<b>3</b>	250,47	150,14	240,84	9,63	100,33	9,60	23,55	24,49
<b>4</b>	128,16	77,18	120,01	8,15	50,98	15,99	23,09	24,66
<b>5</b>	301,43	182,46	293,54	7,89	118,97	6,63	24,20	24,86
<b>6</b>	259,81	155,44	255,74	4,07	104,37	3,90	24,04	24,42
<b>7</b>	331,47	200,99	318,56	12,91	130,48	9,89	23,95	24,92
<b>8</b>	234,56	140,41	230,13	4,43	94,15	4,71	23,98	24,44
<b>9</b>	258,19	153,55	252,18	6,01	104,64	5,74	23,64	24,21
<b>10</b>	237,84	143,43	230,41	7,43	94,41	7,87	23,94	24,71

Table 127. UCS of Stop 2 fresh dry limestone

Sample	Area (cm <sup>2</sup> )	F (Kgf)	F/A (Kgf/cm <sup>2</sup> )	F/A (MPa)
F1	25,66	12533	488,43	47,90
F2	25,47	4708	184,84	18,13
F3	25,32	8586	339,10	33,25
F4	25,83	2890	111,89	10,97
F5	25,96	15370	592,06	58,06
F6	25,80	8862	343,49	33,68
F7	25,64	21336	832,14	81,60

Table 128. UCS of Stop 2 fresh saturated limestone

Sample	Area (cm <sup>2</sup> )	F (Kgf)	F/A (Kgf/cm <sup>2</sup> )	F/A (MPa)
F1	25,45	12533	492,46	48,29
F2	25,62	4708	183,76	18,02
F3	25,58	8586	335,65	32,92
F4	25,88	2890	111,67	10,95
F5	25,81	15370	595,51	58,40
F6	25,82	8862	343,22	33,66
F7	25,59	21336	833,76	81,76
F8	25,48	12375	485,68	47,63

Table 129. UCS of Stop 4 fresh dry/saturated granite

	Sample	Area (cm <sup>2</sup> )	F (Kgf)	F/A (Kgf/cm <sup>2</sup> )	F/A (MPa)
DRY	W1	24,62	4890	198,62	19,48
DRY	W2	24,88	8927	358,80	35,19
SAT.	W1	25,59	1614	63,07	6,19
SAT.	W2	24,78	1320	53,27	5,22

Table 130. UCS of Stop 8 fresh dry sandstone

<b>Sample</b>	<b>Area (cm<sup>2</sup>)</b>	<b>F (Kgf)</b>	<b>F/A (Kgf/cm<sup>2</sup>)</b>	<b>F/A (MPa)</b>
F1	25,59	20504	801,25	78,58
F2	25,63	14012	546,70	53,61
F3	25,55	14041	549,55	53,89
F4	25,56	15137	592,21	58,08
F5	25,71	15080	586,54	57,52
F6	25,67	17296	673,78	66,08
F7	25,57	17787	695,62	68,22
F8	25,71	13986	543,99	53,35
F9	25,49	12974	508,98	49,91
F10	25,67	13790	537,20	52,68

Table 131. UCS of Stop 8 fresh saturated sandstone

<b>Sample</b>	<b>Area (cm<sup>2</sup>)</b>	<b>F (Kgf)</b>	<b>F/A (Kgf/cm<sup>2</sup>)</b>	<b>F/A (MPa)</b>
F1	25,60	10013	391,13	38,36
F2	25,43	9540	375,15	36,79
F3	25,47	12596	494,54	48,50
F4	25,34	6600	260,46	25,54
F5	25,49	13109	514,28	50,43
F6	25,50	12274	481,33	47,20
F7	24,47	7715	315,28	30,92
F8	25,70	6761	263,07	25,80
F9	25,65	8128	316,88	31,08
F10	25,61	5902	230,46	22,60

Table 132. Point load strength of Stop 1 fresh dry mudstone in vertical direction

<b>Sample No</b>	<b>W (mm)</b>	<b>D (mm)</b>	<b>D' (mm)</b>	<b>P (kN)</b>	<b>De2 (mm2)</b>	<b>De (mm)</b>	<b>Is (MPa)</b>	<b>F</b>	<b>Is(50) (MPa)</b>
F1	75,73	33,31	25,87	13,0	2495,71	49,96	5,2089	0,9996	5,2067
F2	60,91	28,10	28,10	10,0	2180,35	46,69	4,5864	0,9664	4,4322
F3	50,85	16,15	11,79	4,7	763,72	27,64	6,1541	0,7434	4,5752
F4	33,30	20,95	10,22	2,6	433,54	20,82	5,9972	0,6453	3,8701
F5	51,00	16,95	8,77	5,5	569,77	23,87	9,6530	0,6909	6,6696
F6	23,32	16,18	10,75	4,8	319,35	17,87	15,0305	0,5978	8,9858
F7	47,07	11,84	6,54	4,7	392,15	19,80	11,9852	0,6293	7,5426
F8	43,09	29,15	25,46	9,6	1397,54	37,38	6,8692	0,8647	5,9397
F9	49,89	30,46	19,63	5,5	1247,57	35,32	4,4086	0,8405	3,7054
F10	39,78	17,96	11,44	7,3	579,72	24,08	12,5922	0,6939	8,7382

Table 133. Point load strength of Stop 1 fresh dry mudstone in horizontal direction

<b>Sample No</b>	<b>W (mm)</b>	<b>D (mm)</b>	<b>D' (mm)</b>	<b>P (kN)</b>	<b>De2 (mm2)</b>	<b>De (mm)</b>	<b>Is (MPa)</b>	<b>F</b>	<b>Is(50) (MPa)</b>
F1	77,52	17,95	9,75	4,6	962,83	31,03	4,7776	0,7878	3,7637
F2	41,09	22,15	14,29	3,6	748,00	27,35	4,8129	0,7396	3,5595
F3	51,81	19,05	16,10	3,7	1062,60	32,60	3,4820	0,8074	2,8115
F4	47,17	18,25	15,42	3,7	926,58	30,44	3,9932	0,7803	3,1157
F5	18,83	20,32	10,51	4,8	252,11	15,88	19,0396	0,5635	10,7292
F6	16,47	13,81	11,15	2,2	233,94	15,29	9,4042	0,5531	5,2013
F7	16,73	46,58	41,61	1,2	886,80	29,78	1,3532	0,7717	1,0443

Table 134. Point load strength of Stop 1 fresh dry sandstone in vertical direction

<b>Sample No</b>	<b>W (mm)</b>	<b>D (mm)</b>	<b>D' (mm)</b>	<b>P (kN)</b>	<b>De2 (mm<sup>2</sup>)</b>	<b>De (mm)</b>	<b>Is (MPa)</b>	<b>F</b>	<b>Is(50) (MPa)</b>
F1	46,22	20,74	13,48	12,0	793,69	28,17	15,1193	0,7506	11,3490
F2	65,14	36,20	25,87	21,0	2146,72	46,33	9,7824	0,9626	9,4168
F3	42,50	29,75	20,95	14,0	1134,24	33,68	12,3431	0,8207	10,1301
F4	40,42	23,34	15,12	20,0	778,54	27,90	25,6893	0,7470	19,1905
F5	30,36	20,09	10,74	9,0	415,37	20,38	21,6674	0,6384	13,8334
F6	52,68	25,35	9,07	14,0	608,67	24,67	23,0009	0,7024	16,1568
F7	38,47	25,40	17,97	12,0	880,64	29,68	13,6264	0,7704	10,4977
F8	28,75	21,38	11,76	5,6	430,70	20,75	13,0021	0,6443	8,3767
F9	34,44	30,79	25,11	15,9	1101,64	33,19	14,4330	0,8148	11,7593
F10	39,43	35,03	23,47	9,5	1178,88	34,33	8,0585	0,8287	6,6778

Table 135. Point load strength of Stop 1 fresh dry sandstone in horizontal direction

<b>Sample No</b>	<b>W (mm)</b>	<b>D (mm)</b>	<b>D' (mm)</b>	<b>P (kN)</b>	<b>De2 (mm<sup>2</sup>)</b>	<b>De (mm)</b>	<b>Is (MPa)</b>	<b>F</b>	<b>Is(50) (MPa)</b>
F1	53,70	19,21	13,66	8,0	934,45	30,57	8,5612	0,7819	6,6940
F2	43,49	21,06	16,18	8,0	896,39	29,94	8,9247	0,7738	6,9061
F3	47,87	29,52	18,96	11,0	1156,20	34,00	9,5139	0,8247	7,8457
F4	44,41	34,75	25,58	9,0	1447,14	38,04	6,2191	0,8723	5,4247
F5	39,73	36,64	26,85	11,0	1358,92	36,86	8,0947	0,8586	6,9504
F6	34,03	27,75	18,53	5,6	803,28	28,34	6,9714	0,7529	5,2487
F7	32,74	36,65	26,96	9,0	1124,42	33,53	8,0041	0,8189	6,5548

Table 136. Point load strength of Stop 1 weathered dry mudstone in vertical direction

Sample No	W (mm)	D (mm)	D' (mm)	P (kN)	De2 (mm <sup>2</sup> )	De (mm)	Is (MPa)	F	Is(50) (MPa)
W1	48,05	13,13	9,59	4,3	587,01	24,23	7,3253	0,6961	5,0992
W2	30,73	28,89	23,15	6,0	906,24	30,10	6,6208	0,7759	5,1373
W3	41,19	25,83	15,48	2,3	812,26	28,50	2,8316	0,7550	2,1378
W4	39,46	29,18	25,87	5,5	1300,42	36,06	4,2294	0,8493	3,5918
W5	35,18	30,15	23,47	5,8	1051,81	32,43	5,5143	0,8054	4,4411
W6	40,78	35,78	30,93	6,9	1606,78	40,08	4,2943	0,8954	3,8450
W7	35,96	30,43	24,71	7,8	1131,94	33,64	6,8908	0,8203	5,6525
W8	37,00	30,33	22,19	6,9	1045,90	32,34	6,5972	0,8042	5,3058
W9	29,58	25,99	21,43	6,1	807,52	28,42	7,5540	0,7539	5,6948
W10	35,35	30,46	25,35	7,0	1141,56	33,79	6,1320	0,8220	5,0407

Table 137. Point load strength of Stop 1 weathered dry mudstone in horizontal direction

Sample No	W (mm)	D (mm)	D' (mm)	P (kN)	De2 (mm <sup>2</sup> )	De (mm)	Is (MPa)	F	Is(50) (MPa)
W1	62,92	44,55	39,47	9,0	3163,63	56,25	2,8448	1,0606	3,0173
W2	55,78	35,18	30,55	5,9	2170,80	46,59	2,7179	0,9653	2,6236
W3	35,13	30,44	23,88	6,3	1068,67	32,69	5,8952	0,8086	4,7668
W4	44,59	40,99	31,71	5,9	1801,21	42,44	3,2756	0,9213	3,0178
W5	65,18	20,46	15,63	4,7	1297,79	36,02	3,6215	0,8488	3,0740
W6	36,55	30,55	19,41	5,1	903,74	30,06	5,6432	0,7754	4,3758
W7	34,78	30,43	20,41	2,7	904,28	30,07	2,9858	0,7755	2,3155
W8	33,44	30,11	23,74	5,1	1011,29	31,80	5,0430	0,7975	4,0219

Table 138. Point load strength of Stop 1 weathered dry sandstone in vertical direction

Sample No	W (mm)	D (mm)	D' (mm)	P (kN)	De2 (mm <sup>2</sup> )	De (mm)	Is (MPa)	F	Is(50) (MPa)
W1	32,66	15,96	14,90	6,0	619,92	24,90	9,6787	0,7057	6,8299
W2	40,44	30,14	21,82	11,0	1124,08	33,53	9,7858	0,8189	8,0133
W3	32,33	12,05	6,20	4,8	255,35	15,98	18,7981	0,5653	10,6270
W4	45,32	18,31	11,76	12,0	678,93	26,06	17,6748	0,7219	12,7593
W5	44,59	22,18	18,46	6,7	1048,58	32,38	6,3896	0,8048	5,1421
W6	39,46	17,46	15,73	12,9	790,71	28,12	16,3145	0,7499	12,2347
W7	33,96	17,96	13,49	9,7	583,59	24,16	16,6212	0,6951	11,5533
W8	35,23	18,36	15,99	6,3	717,61	26,79	8,7791	0,7320	6,4259
W9	44,13	25,18	18,46	9,7	1037,76	32,21	9,3471	0,8027	7,5027
W10	35,18	30,86	18,91	9,4	847,46	29,11	11,0920	0,7630	8,4636

Table 139. Point load strength of Stop 1 weathered dry sandstone in horizontal direction

Sample No	W (mm)	D (mm)	D' (mm)	P (kN)	De2 (mm <sup>2</sup> )	De (mm)	Is (MPa)	F	Is(50) (MPa)
W1	53,18	20,95	20,95	11,0	1419,26	37,67	7,7505	0,8680	6,7276
W2	31,70	44,19	42,15	2,1	1702,11	41,26	1,2338	0,9084	1,1207
W3	20,08	25,71	24,15	5,6	617,75	24,85	9,0652	0,7050	6,3914
W4	33,49	19,26	15,46	5,5	659,56	25,68	8,3389	0,7167	5,9764
W5	29,78	20,46	17,89	6,8	678,68	26,05	10,0194	0,7218	7,2323
W6	41,43	35,89	29,71	9,1	1568,01	39,60	5,8035	0,8899	5,1647
W7	44,18	34,71	27,43	9,7	1543,77	39,29	6,2833	0,8865	5,5699
W8	45,56	39,67	33,24	10,5	1929,19	43,92	5,4427	0,9373	5,1012

Table 140. Point load strength of Stop 1 fresh saturated mudstone in vertical direction

Sample No	W (mm)	D (mm)	D' (mm)	P (kN)	De2 (mm <sup>2</sup> )	De (mm)	Is (MPa)	F	Is(50) (MPa)
F1	39,92	22,46	10,26	4,8	521,76	22,84	9,1997	0,6759	6,2181
F2	58,38	36,93	26,42	7,2	1964,84	44,33	3,6644	0,9416	3,4503
F3	24,28	13,44	9,32	1,7	288,27	16,98	5,8973	0,5827	3,4365
F4	50,17	23,07	15,78	4,9	1008,51	31,76	4,8586	0,7970	3,8721
F5	46,18	23,18	12,19	5,1	717,11	26,78	7,1118	0,7318	5,2047
F6	22,13	20,79	13,46	4,3	379,45	19,48	11,3321	0,6242	7,0732
F7	43,58	21,46	17,46	2,8	969,31	31,13	2,8887	0,7891	2,2794
F8	26,19	23,64	15,13	5,3	504,78	22,47	10,4996	0,6703	7,0382
F9	34,55	31,73	25,98	4,9	1143,45	33,81	4,2853	0,8224	3,5241
F10	35,61	29,43	22,46	4,5	1018,85	31,92	4,4167	0,7990	3,5289

Table 141. Point load strength of Stop 1 fresh saturated mudstone in horizontal direction

Sample No	W (mm)	D (mm)	D' (mm)	P (kN)	De2 (mm <sup>2</sup> )	De (mm)	Is (MPa)	F	Is(50) (MPa)
F1	55,07	25,63	20,76	0,8	1456,37	38,16	0,5493	0,8736	0,4799
F2	32,34	20,71	14,53	2,5	598,60	24,47	4,1764	0,6995	2,9215
F3	44,10	44,64	40,13	2,3	2254,44	47,48	1,0202	0,9745	0,9942
F4	41,05	35,18	30,18	1,7	1578,20	39,73	1,0772	0,8914	0,9602
F5	38,96	33,77	28,46	2,9	1412,49	37,58	2,0531	0,8670	1,7800
F6	25,79	21,46	15,88	1,8	521,71	22,84	3,4502	0,6759	2,3319
F7	43,48	25,69	20,93	0,3	1159,28	34,05	0,2588	0,8252	0,2135
F8	46,53	40,56	30,79	0,9	1825,04	42,72	0,4931	0,9243	0,4558
F9	26,93	22,87	11,47	1,7	393,49	19,84	4,3203	0,6299	2,7212

Table 142. Point load strength of Stop 1 fresh saturated sandstone in vertical direction

Sample No	W (mm)	D (mm)	D' (mm)	P (kN)	De2 (mm <sup>2</sup> )	De (mm)	Is (MPa)	F	Is(50) (MPa)
F1	37,54	14,57	9,66	6,1	461,96	21,49	13,2047	0,6556	8,6575
F2	50,16	37,09	13,65	8,0	872,21	29,53	9,1721	0,7685	7,0492
F3	33,51	26,96	12,99	5,3	554,52	23,55	9,5579	0,6863	6,5593
F4	35,46	33,43	28,59	6,4	1291,47	35,94	4,9556	0,8478	4,2013
F5	23,47	21,78	15,13	5,8	452,36	21,27	12,8217	0,6522	8,3624
F6	41,56	29,52	24,43	7,9	1293,39	35,96	6,1080	0,8481	5,1802
F7	38,99	35,96	29,78	7,8	1479,14	38,46	5,2733	0,8770	4,6249
F8	25,41	21,43	15,97	10,6	516,94	22,74	20,5053	0,6743	13,8274
F9	29,79	25,98	19,53	9,1	741,14	27,22	12,2783	0,7379	9,0600
F10	49,86	46,13	40,87	9,6	2595,90	50,95	3,6981	1,0095	3,7331

Table 143. Point load strength of Stop 1 fresh saturated sandstone in horizontal direction

Sample No	W (mm)	D (mm)	D' (mm)	P (kN)	De2 (mm <sup>2</sup> )	De (mm)	Is (MPa)	F	Is(50) (MPa)
F1	50,57	16,50	10,00	3,2	644,20	25,38	4,9674	0,7125	3,5391
F2	89,86	39,09	24,34	13,0	2786,23	52,78	4,6658	1,0275	4,7940
F3	87,73	25,62	13,02	6,1	1455,09	38,15	4,1922	0,8734	3,6617
F4	18,32	41,59	35,61	5,4	831,05	28,83	6,4978	0,7593	4,9339
F5	33,06	27,97	22,13	14,0	932,00	30,53	15,0215	0,7814	11,7377
F6	32,16	20,16	14,46	6,6	592,40	24,34	11,1411	0,6977	7,7732
F7	25,78	24,13	20,15	5,2	661,74	25,72	7,8581	0,7173	5,6364
F8	19,5	18,1	12,79	2,8	317,06	17,81	8,8311	0,5968	5,2701
F9	42,1	21,5	15,43	3,5	827,72	28,77	4,2285	0,7586	3,2075

Table 144. Point load strength of Stop 1 weathered saturated mudstone in vertical direction

Sample No	W (mm)	D (mm)	D' (mm)	P (kN)	De2 (mm <sup>2</sup> )	De (mm)	Is (MPa)	F	Is(50) (MPa)
W1	57,52	16,74	10,48	1,3	767,91	27,71	1,6929	0,7445	1,2603
W2	42,53	15,29	8,91	2,4	482,73	21,97	4,9717	0,6629	3,2957
W3	41,61	29,54	20,00	12,0	1060,13	32,56	11,3194	0,8070	9,1344
W4	82,06	40,02	20,99	13,0	2194,19	46,84	5,9247	0,9679	5,7346
W5	74,19	24,86	15,69	2,4	1482,85	38,51	1,6185	0,8776	1,4204
W6	59,14	25,89	18,71	2,1	1409,57	37,54	1,4898	0,8665	1,2910
W7	51,17	19,73	15,68	2,0	1022,10	31,97	1,9568	0,7996	1,5647
W8	49,27	21,33	15,46	1,7	970,34	31,15	1,7520	0,7893	1,3828

Table 145. Point load strength of Stop 1 weathered saturated mudstone in horizontal direction

Sample No	W (mm)	D (mm)	D' (mm)	P (kN)	De2 (mm <sup>2</sup> )	De (mm)	Is (MPa)	F	Is(50) (MPa)
W1	59,65	16,50	12,28	0,6	933,12	30,55	0,6430	0,7816	0,5026
W2	57,19	24,26	12,85	1,4	936,17	30,60	1,4955	0,7823	1,1698
W3	19,03	40,31	35,56	0,8	862,05	29,36	0,9280	0,7663	0,7111
W4	24,12	35,08	28,66	1,1	880,61	29,68	1,2491	0,7704	0,9623
W5	41,21	23,58	20,41	1,0	1071,46	32,73	0,9333	0,8091	0,7551
W6	58,15	15,78	11,87	1,3	879,29	29,65	1,4785	0,7701	1,1386
W7	56,23	28,13	23,79	1,0	1704,09	41,28	0,5868	0,9086	0,5332
W8	20,68	15,42	11,73	0,5	309,01	17,58	1,6180	0,5929	0,9594
W9	40,13	25,33	21,65	1,1	1106,77	33,27	0,9939	0,8157	0,8107
W10	25,77	20,46	17,81	0,9	584,67	24,18	1,5393	0,6954	1,0705

Table 146. Point load strength of Stop 1 weathered saturated sandstone in vertical direction

<b>Sample No</b>	<b>W (mm)</b>	<b>D (mm)</b>	<b>D' (mm)</b>	<b>P (kN)</b>	<b>De2 (mm2)</b>	<b>De (mm)</b>	<b>Is (MPa)</b>	<b>F</b>	<b>Is(50) (MPa)</b>
W1	34,81	18,77	10,95	4,5	485,57	22,04	9,2675	0,6639	6,1524
W2	35,43	17,18	11,46	4,1	517,23	22,74	7,9268	0,6744	5,3461
W3	22,18	11,46	7,13	2,1	201,46	14,19	10,4241	0,5328	5,5539
W4	25,19	22,49	15,99	5,5	513,11	22,65	10,7190	0,6731	7,2148
W4	44,13	23,15	18,73	9,1	1052,94	32,45	8,6425	0,8056	6,9623
W6	25,79	24,43	18,44	10,1	605,82	24,61	16,6717	0,7016	11,6971
W7	26,43	20,48	13,82	3,4	465,30	21,57	7,3071	0,6568	4,7995
W8	27,13	26,46	13,63	3,1	471,06	21,70	6,5809	0,6588	4,3358

Table 147. Point load strength of Stop 1 weathered saturated sandstone in horizontal direction

<b>Sample No</b>	<b>W (mm)</b>	<b>D (mm)</b>	<b>D' (mm)</b>	<b>P (kN)</b>	<b>De2 (mm2)</b>	<b>De (mm)</b>	<b>Is (MPa)</b>	<b>F</b>	<b>Is(50) (MPa)</b>
W1	62,84	24,50	19,70	10,0	1577,00	39,71	6,3411	0,8912	5,6512
W2	44,41	15,61	7,33	2,4	414,68	20,36	5,7876	0,6382	3,6935
W3	52,96	41,96	30,45	10,0	2054,31	45,32	4,8678	0,9521	4,6346
W4	75,70	27,70	20,93	2,2	2018,35	44,93	1,0652	0,9479	1,0097
W5	53,27	15,43	9,84	3,3	667,74	25,84	4,9420	0,7189	3,5528
W6	34,34	20,73	17,81	2,8	779,10	27,91	3,5939	0,7472	2,6852
W7	35,53	30,43	23,58	7,0	1067,26	32,67	6,5589	0,8083	5,3016

Table 148. Point load strength of Stop 1 failed zone fresh dry mudstone

Sample No	W (mm)	D (mm)	D' (mm)	P (kN)	De2 (mm <sup>2</sup> )	De (mm)	Is (MPa)	F	Is(50) (MPa)
F1	35,88	15,06	9,54	1,6	436,04	20,88	3,6693	0,6462	2,3713
F2	53,88	15,83	8,15	4,9	559,39	23,65	8,7595	0,6878	6,0245
F3	41,69	11,34	8,74	3,6	464,17	21,54	7,7558	0,6564	5,0911
F4	42,00	12,83	7,28	4,2	389,50	19,74	10,7830	0,6283	6,7746
F5	32,83	12,17	9,77	3,4	408,60	20,21	8,3211	0,6358	5,2908
F6	44,18	17,58	15,13	1,0	851,52	29,18	1,1744	0,7639	0,8972
F7	42,42	19,94	16,43	3,1	887,85	29,80	3,4916	0,7720	2,6954
F8	43,88	23,59	17,42	3,0	973,74	31,20	3,0809	0,7900	2,4339
F9	47,83	22,84	19,83	1,0	1208,24	34,76	0,8276	0,8338	0,6901
F10	33,08	27,49	24,11	1,9	1016,00	31,87	1,8701	0,7984	1,4931

Table 149. Point load strength of Stop 1 failed zone weathered dry mudstone

Sample No	W (mm)	D (mm)	D' (mm)	P (kN)	De2 (mm <sup>2</sup> )	De (mm)	Is (MPa)	F	Is(50) (MPa)
W1	35,84	14,93	8,80	2,2	401,77	20,04	5,4757	0,6332	3,4670
W2	30,32	15,23	10,65	1,5	411,35	20,28	3,6465	0,6369	2,3225
W3	22,96	13,69	11,63	1,9	340,16	18,44	5,5856	0,6073	3,3924
W4	22,03	30,24	25,18	3,2	706,64	26,58	4,5284	0,7291	3,3019
W5	30,80	23,18	18,51	2,6	726,25	26,95	3,5800	0,7342	2,6283
W6	33,94	19,91	15,42	2,4	666,69	25,82	3,5999	0,7186	2,5869
W7	29,77	39,85	29,32	3,5	1111,92	33,35	3,1477	0,8166	2,5706
W8	45,48	31,45	24,67	5,5	1429,29	37,81	3,8481	0,8696	3,3461
W9	37,11	26,64	23,16	2,6	1094,86	33,09	2,3747	0,8135	1,9318
W10	35,28	29,30	26,93	2,4	1210,31	34,79	1,9830	0,8341	1,6541

Table 150. Point load strength of Stop 1 failed zone fresh saturated mudstone

Sample No	W (mm)	D (mm)	D' (mm)	P (kN)	De2 (mm)2	De (mm)	Is (MPa)	F	Is(50) (MPa)
F1	36,33	38,42	31,29	0,6	1448,11	38,05	0,4143	0,8724	0,3615
F2	51,37	17,80	13,43	0,8	878,85	29,65	0,9103	0,7700	0,7009
F3	38,44	20,18	15,37	1,0	752,64	27,43	1,3287	0,7407	0,9842
F4	45,46	35,85	28,69	0,6	1661,46	40,76	0,3611	0,9029	0,3261
F5	34,82	30,59	25,20	0,8	1117,79	33,43	0,7157	0,8177	0,5852
F6	35,50	24,10	17,11	0,7	773,76	27,82	0,9047	0,7459	0,6748
F7	45,78	17,52	12,67	0,3	738,90	27,18	0,4060	0,7373	0,2994
F8	40,39	19,32	16,61	0,3	854,62	29,23	0,3510	0,7646	0,2684
F9	37,28	21,34	12,93	0,8	614,05	24,78	1,3028	0,7040	0,9172
F10	52,17	36,44	33,51	0,8	2227,03	47,19	0,3592	0,9715	0,3490

Table 151. Point load strength of Stop 1 failed zone weathered saturated mudstone

Sample No	W (mm)	D (mm)	D' (mm)	P (kN)	De2 (mm)2	De (mm)	Is (MPa)	F	Is(50) (MPa)
W1	33,87	19,11	16,02	0,1	691,21	26,29	0,1447	0,7251	0,1049
W2	41,89	20,58	19,55	0,1	1043,25	32,30	0,0959	0,8037	0,0770
W3	31,07	15,00	14,50	0,1	573,90	23,96	0,1742	0,6922	0,1206
W4	46,83	14,41	8,40	0,1	501,11	22,39	0,1996	0,6691	0,1335
W5	31,92	29,85	23,86	0,3	970,21	31,15	0,3092	0,7893	0,2441
W6	33,49	11,56	7,05	0,1	300,77	17,34	0,3325	0,5889	0,1958
W7	27,30	19,01	16,43	0,2	571,39	23,90	0,3500	0,6914	0,2420
W8	26,90	28,13	27,54	0,5	943,73	30,72	0,5298	0,7838	0,4153
W9	39,03	14,63	10,14	0,2	504,16	22,45	0,3967	0,6701	0,2658
W10	26,22	16,18	13,65	0,1	455,93	21,35	0,2193	0,6535	0,1433

Table 152. Point load strength of Stop 2 fresh dry limestone

Sample No	W (mm)	D (mm)	D' (mm)	P (kN)	De2 (mm <sup>2</sup> )	De (mm)	Is (MPa)	F	Is(50) (MPa)
F1	30,33	27,38	17,18	5,4	663,78	25,76	8,1352	0,7178	5,8397
F2	35,30	24,58	19,83	5,2	891,72	29,86	5,7754	0,7728	4,4633
F3	43,90	39,23	35,02	5,4	1958,44	44,25	2,7573	0,9408	2,5940
F4	29,91	27,20	19,24	5,5	733,08	27,08	7,5026	0,7359	5,5210
F5	51,80	45,78	34,05	12,0	2246,87	47,40	5,3408	0,9737	5,2001
F6	49,86	24,44	23,83	10,0	1513,58	38,90	6,6068	0,8821	5,8279
F7	19,55	17,99	11,66	4,9	290,39	17,04	16,8741	0,5838	9,8510
F8	35,21	30,90	24,96	10,0	1119,54	33,46	8,9322	0,8180	7,3069
F9	51,04	46,64	32,72	10,0	2127,43	46,12	4,7005	0,9605	4,5147
F10	30,09	18,89	14,53	4,0	556,95	23,60	7,1819	0,6870	4,9341

Table 153. Point load strength of Stop 2 weathered dry limestone

Sample No	W (mm)	D (mm)	D' (mm)	P (kN)	De2 (mm <sup>2</sup> )	De (mm)	Is (MPa)	F	Is(50) (MPa)
W1	32,72	21,51	16,56	4,2	690,25	26,27	6,0848	0,7249	4,4107
W2	44,46	20,84	13,52	4,7	765,73	27,67	6,1379	0,7439	4,5662
W3	37,56	24,68	20,01	3,0	957,42	30,94	3,1334	0,7867	2,4650
W4	45,62	16,02	8,79	1,6	510,83	22,60	3,1322	0,6723	2,1059
W5	38,01	27,23	19,31	5,6	935,00	30,58	5,9893	0,7820	4,6838
W6	39,24	23,62	18,88	4,7	943,76	30,72	4,9801	0,7838	3,9036
W7	38,17	26,82	21,63	4,6	1051,74	32,43	4,3737	0,8054	3,5224
W8	32,78	25,51	22,45	6,0	937,47	30,62	6,4002	0,7825	5,0084
W9	42,17	38,79	26,82	10,5	1440,76	37,96	7,2878	0,8713	6,3498
W10	41,89	35,72	27,68	7,5	1477,09	38,43	5,0776	0,8767	4,4517

Table 154. Point load strength of Stop 2 fresh saturated limestone

Sample No	W (mm)	D (mm)	D' (mm)	P (kN)	De2 (mm)2	De (mm)	Is (MPa)	F	Is(50) (MPa)
F1	49,78	32,23	21,72	4,1	1377,35	37,11	2,9767	0,8615	2,5646
F2	25,64	24,11	14,81	3,2	483,73	21,99	6,6153	0,6632	4,3875
F3	50,71	23,71	10,79	2,5	697,02	26,40	3,5867	0,7267	2,6063
F4	47,61	27,37	17,86	2,8	1083,20	32,91	2,5849	0,8113	2,0972
F5	60,09	49,11	43,53	5,6	3332,12	57,72	1,6806	1,0745	1,8058
F6	40,62	32,20	20,33	4,5	1051,98	32,43	4,2776	0,8054	3,4453
F7	44,28	39,57	17,85	4,1	1006,88	31,73	4,0720	0,7966	3,2439
F8	43,97	18,44	13,42	2,1	751,69	27,42	2,7937	0,7405	2,0687
F9	34,47	32,11	22,14	2,5	972,19	31,18	2,5715	0,7897	2,0307
F10	41,88	31,65	19,53	2,4	1041,93	32,28	2,3034	0,8035	1,8507

Table 155. Point load strength of Stop 2 weathered saturated limestone

Sample No	W (mm)	D (mm)	D' (mm)	P (kN)	De2 (mm)2	De (mm)	Is (MPa)	F	Is(50) (MPa)
W1	35,62	22,25	17,61	2,4	799,07	28,27	3,0035	0,7519	2,2583
W2	50,27	35,03	27,18	5,5	1740,56	41,72	3,1599	0,9135	2,8864
W3	35,65	22,41	15,42	1,6	700,28	26,46	2,2848	0,7275	1,6622
W4	43,65	35,89	25,85	3,3	1437,39	37,91	2,2958	0,8708	1,9992
W5	43,29	31,36	23,14	4,1	1276,09	35,72	3,2129	0,8453	2,7157
W6	51,75	28,72	16,14	2,5	1064,01	32,62	2,3496	0,8077	1,8978
W7	62,16	43,36	40,72	5,4	3224,40	56,78	1,6747	1,0657	1,7847
W8	38,06	16,75	13,98	1,9	677,81	26,03	2,8032	0,7216	2,0227
W9	31,40	28,46	18,59	2,7	743,60	27,27	3,6310	0,7385	2,6815
W10	36,91	22,36	14,85	3,4	698,23	26,42	4,8694	0,7270	3,5399

Table 156. Point load strength of Stop 2 failed zone fresh dry limestone

Sample No	W (mm)	D (mm)	D' (mm)	P (kN)	De2 (mm <sup>2</sup> )	De (mm)	Is (MPa)	F	Is(50) (MPa)
F1	31,03	25,07	24,89	1,2	983,87	31,37	1,2197	0,7920	0,9660
F2	41,72	23,23	22,55	1,2	1198,45	34,62	1,0013	0,8321	0,8332
F3	25,15	17,90	16,43	0,7	526,39	22,94	1,3298	0,6774	0,9008
F4	42,50	27,79	26,13	1,4	1414,68	37,61	0,9896	0,8673	0,8583
F5	39,03	29,92	28,45	0,7	1414,53	37,61	0,4949	0,8673	0,4292
F6	29,15	20,98	19,99	1,2	742,30	27,25	1,6166	0,7382	1,1933
F7	17,05	16,78	16,43	1,5	356,86	18,89	4,2034	0,6147	2,5837
F8	36,42	23,00	21,85	1,5	1013,73	31,84	1,4797	0,7980	1,1808
F9	29,74	19,81	18,11	1,1	686,10	26,19	1,6033	0,7238	1,1604
F10	29,25	25,47	24,13	1,0	899,11	29,99	1,1122	0,7744	0,8613

Table 157. Point load strength of Stop 2 failed zone fresh saturated limestone

Sample No	W (mm)	D (mm)	D' (mm)	P (kN)	De2 (mm <sup>2</sup> )	De (mm)	Is (MPa)	F	Is(50) (MPa)
F1	29,91	16,83	15,44	0,4	588,29	24,25	0,6799	0,6965	0,4736
F2	23,36	14,03	12,98	0,3	386,26	19,65	0,7767	0,6270	0,4869
F3	25,50	14,79	13,74	0,4	446,33	21,13	0,8962	0,6500	0,5825
F4	25,67	16,40	15,33	0,4	501,30	22,39	0,7979	0,6692	0,5340
F5	19,83	17,45	16,47	0,2	416,05	20,40	0,4807	0,6387	0,3070
F6	28,27	15,80	14,11	0,1	508,14	22,54	0,1968	0,6714	0,1321
F7	24,92	13,37	12,36	0,5	392,37	19,81	1,2743	0,6294	0,8021
F8	37,61	22,31	20,94	0,9	1003,25	31,67	0,8971	0,7959	0,7140
F9	30,20	22,57	21,55	0,1	829,06	28,79	0,1206	0,7589	0,0915
F10	22,04	12,72	11,23	0,5	315,30	17,76	1,5858	0,5959	0,9450

Table 158. Point load strength of Stop 3 fresh dry limestone

Sample No	W (mm)	D (mm)	D' (mm)	P (kN)	De2 (mm <sup>2</sup> )	De (mm)	Is (MPa)	F	Is(50) (MPa)
F1	55,07	21,74	14,57	4,6	1022,13	31,97	4,5004	0,7996	3,5987
F2	38,25	29,92	25,15	3,5	1225,46	35,01	2,8561	0,8367	2,3898
F3	38,19	34,97	26,80	3,5	1303,81	36,11	2,6844	0,8498	2,2812
F4	36,25	34,92	17,52	3,8	809,04	28,44	4,6969	0,7542	3,5426
F5	38,67	28,01	21,43	0,8	1055,67	32,49	0,7578	0,8061	0,6109
F6	49,64	26,31	16,86	2,6	1066,15	32,65	2,4387	0,8081	1,9707
F7	57,60	32,59	24,32	2,1	1784,50	42,24	1,1768	0,9192	1,0817
F8	34,75	29,62	23,42	2,3	1036,75	32,20	2,2185	0,8025	1,7803
F9	38,89	24,80	11,20	2,3	554,86	23,56	4,1452	0,6864	2,8451
F10	40,61	20,32	14,24	3,0	736,67	27,14	4,0724	0,7368	3,0004
F11	37,94	31,30	31,15	0,8	1505,52	38,80	0,5314	0,8809	0,4681
F12	52,33	17,43	10,16	2,5	677,29	26,02	3,6912	0,7215	2,6630
F13	42,08	37,79	22,37	3,3	1199,15	34,63	2,7520	0,8322	2,2902
F14	45,55	32,65	27,35	2,1	1587,00	39,84	1,3233	0,8926	1,1811
F15	43,55	40,35	31,56	4,4	1750,88	41,84	2,5130	0,9148	2,2989
F16	39,75	37,24	31,43	3,7	1591,52	39,89	2,3248	0,8932	2,0766
F17	45,70	43,71	31,09	2,6	1809,95	42,54	1,4365	0,9224	1,3251
F18	45,61	41,53	40,65	5,4	2361,84	48,60	2,2864	0,9859	2,2541
F19	44,13	30,27	25,99	2,3	1461,07	38,22	1,5742	0,8743	1,3764
F20	45,79	35,19	30,48	3,9	1777,94	42,17	2,1936	0,9183	2,0144

Table 159. Point load strength of Stop 3 weathered dry limestone

Sample No	W (mm)	D (mm)	D' (mm)	P (kN)	De2 (mm <sup>2</sup> )	De (mm)	Is (MPa)	F	Is(50) (MPa)
W1	48,78	22,90	18,02	0,7	1119,77	33,46	0,5805	0,8181	0,4749
W2	28,14	22,18	17,86	0,3	640,23	25,30	0,4686	0,7114	0,3333
W3	34,45	30,81	25,04	0,4	1098,89	33,15	0,3640	0,8142	0,2964
W4	60,01	45,24	43,10	1,5	3294,82	57,40	0,4553	1,0715	0,4878
W5	68,75	56,73	43,59	0,8	3817,60	61,79	0,2096	1,1116	0,2329
W6	59,8	30,5	35,8	0,9	2724,14	52,19	0,3304	1,0217	0,3375
W7	62,5	35,4	30,2	1,1	2404,51	49,04	0,4575	0,9903	0,4530
W8	37,1	20,2	13,7	0,9	650,07	25,50	1,3845	0,7141	0,9886
W9	30,8	20,7	14,9	0,3	583,26	24,15	0,5144	0,6950	0,3575
W10	46	30,1	16	0,6	934,42	30,57	0,6421	0,7819	0,5021
W11	29,67	21,68	16,73	0,7	632,33	25,15	1,1070	0,7092	0,7851
W12	45,49	18,75	11,55	1,1	669,31	25,87	1,6435	0,7193	1,1822
W13	66,72	36,28	28,92	1,8	2458,02	49,58	0,7120	0,9958	0,7089
W14	60,49	32,28	22,04	2,1	1698,34	41,21	1,2365	0,9079	1,1226
W15	82,79	39,50	31,69	2,0	3342,18	57,81	0,5984	1,0753	0,6435
W16	31,8	22,8	15,8	0,9	639,04	25,28	1,4084	0,7110	1,0014
W17	44,6	20,5	17,4	1,1	989,97	31,46	1,1111	0,7933	0,8814
W18	61,1	30,6	23,4	0,9	1818,33	42,64	0,4950	0,9235	0,4571
W19	37,5	20,9	13,4	0,9	640,26	25,30	1,4057	0,7114	1,0000
W20	80	35,4	30,8	1,1	3135,40	55,99	0,3508	1,0583	0,3713

Table 160. Point load strength of Stop 3 fresh saturated limestone

Sample No	W (mm)	D (mm)	D' (mm)	P (kN)	De2 (mm <sup>2</sup> )	De (mm)	Is (MPa)	F	Is(50) (MPa)
F1	44,60	39,65	31,09	2,9	1766,39	42,03	1,6418	0,9168	1,5052
F2	67,63	48,73	37,58	3,5	3237,62	56,90	1,0810	1,0668	1,1532
F3	46,79	23,86	17,55	1,7	1046,07	32,34	1,6251	0,8043	1,3071
F4	49,31	33,65	24,73	3,9	1553,42	39,41	2,5106	0,8878	2,2290
F5	32,52	21,55	19,75	0,2	818,18	28,60	0,2444	0,7564	0,1849
F6	61,85	41,09	36,68	1,5	2890,01	53,76	0,5190	1,0369	0,5382
F7	46,19	44,15	38,42	1,1	2260,66	47,55	0,4866	0,9752	0,4745
F8	34,57	11,01	4,92	0,9	216,67	14,72	4,1538	0,5426	2,2538
F9	30,60	19,66	10,55	0,6	411,25	20,28	1,4590	0,6369	0,9292
F10	32,17	16,04	9,60	1,6	393,42	19,83	4,0669	0,6298	2,5615
F11	29,09	15,25	9,12	1,0	337,96	18,38	2,9589	0,6064	1,7942
F12	40,58	13,49	7,48	1,0	386,67	19,66	2,5862	0,6271	1,6218
F13	36,77	20,89	14,94	1,6	699,80	26,45	2,2149	0,7274	1,6111
F14	46,98	20,58	15,92	1,3	952,77	30,87	1,3644	0,7857	1,0721
F15	41,90	24,67	16,11	2,1	859,88	29,32	2,4422	0,7658	1,8703
F16	29,68	24,94	24,14	0,4	912,71	30,21	0,4383	0,7773	0,3407
F17	37,26	18,95	13,57	1,1	644,10	25,38	1,7078	0,7124	1,2167
F18	36,90	20,08	13,47	1,3	633,18	25,16	2,0531	0,7094	1,4565
F19	37,49	20,54	15,56	1,2	743,11	27,26	1,6148	0,7384	1,1924
F20	47,25	14,10	13,50	0,2	812,58	28,51	0,2461	0,7551	0,1858

Table 161. Point load strength of Stop 3 weathered saturated limestone

Sample No	W (mm)	D (mm)	D' (mm)	P (kN)	De2 (mm <sup>2</sup> )	De (mm)	Is (MPa)	F	Is(50) (MPa)
W1	35,82	17,68	15,33	0,1	699,52	26,45	0,1430	0,7273	0,1040
W2	34,27	25,36	18,02	0,4	786,68	28,05	0,5085	0,7490	0,3808
W3	38,78	27,47	19,72	0,2	974,19	31,21	0,2053	0,7901	0,1622
W4	25,77	18,72	15,23	0,3	499,97	22,36	0,6000	0,6687	0,4013
W5	62,78	28,68	12,09	0,7	966,89	31,09	0,7240	0,7886	0,5709
W6	47,78	41,18	29,45	0,3	1792,51	42,34	0,1674	0,9202	0,1540
W7	44,9	41	30,5	0,5	1743,17	41,75	0,2868	0,9138	0,2621
W8	57,2	45,2	31,5	0,3	2292,55	47,88	0,1309	0,9786	0,1281
W9	27,1	20,1	15,8	0,4	545,71	23,36	0,7330	0,6835	0,5010
W10	44	35,2	30,4	0,9	1705,80	41,30	0,5276	0,9089	0,4795
W11	36,51	28,33	15,47	0,7	719,50	26,82	0,9729	0,7324	0,7126
W12	37,92	17,40	8,08	0,4	390,31	19,76	1,0248	0,6286	0,6442
W13	52,00	39,14	21,68	1,6	1436,13	37,90	1,1141	0,8706	0,9699
W14	36,65	20,91	10,97	0,5	512,17	22,63	0,9762	0,6728	0,6568
W15	39,46	35,46	30,88	1,1	1552,26	39,40	0,7086	0,8877	0,6290
W16	35,18	30,61	24,13	1,5	1081,39	32,88	1,3871	0,8110	1,1249
W17	49,55	40,31	30,77	1,3	1942,23	44,07	0,6693	0,9388	0,6284
W18	43,1	39	31,9	0,9	1753,22	41,87	0,5133	0,9151	0,4698
W19	22,5	20,4	18,8	1,1	538,33	23,20	2,0434	0,6812	1,3919
W20	25,1	22,2	17,2	0,5	549,02	23,43	0,9107	0,6846	0,6234

Table 162. Point load strength of Stop 4 fresh dry granite

Sample No	W (mm)	D (mm)	D' (mm)	P (kN)	De2 (mm <sup>2</sup> )	De (mm)	Is (MPa)	F	Is(50) (MPa)
F1	26,16	15,70	13,08	5,5	435,89	20,88	12,6179	0,6462	8,1535
F2	29,21	20,25	19,47	3,3	724,48	26,92	4,5550	0,7337	3,3420
F3	39,55	19,60	9,58	7,0	482,66	21,97	14,5029	0,6629	9,6135
F4	35,15	23,46	13,00	7,0	582,10	24,13	12,0254	0,6946	8,3534
F5	32,80	32,68	24,59	3,9	1027,45	32,05	3,7958	0,8007	3,0392
F6	38,62	29,29	20,37	8,0	1002,15	31,66	7,9828	0,7957	6,3519
F7	31,29	18,69	15,42	2,9	614,64	24,79	4,7182	0,7042	3,3224
F8	35,07	15,45	13,63	4,2	608,92	24,68	6,8974	0,7025	4,8455
F9	38,74	27,13	21,13	5,7	1042,77	32,29	5,4662	0,8036	4,3929
F10	37,89	25,44	20,09	7,5	969,69	31,14	7,7344	0,7892	6,1038

Table 163. Point load strength of Stop 4 weathered dry granite

Sample No	W (mm)	D (mm)	D' (mm)	P (kN)	De2 (mm <sup>2</sup> )	De (mm)	Is (MPa)	F	Is(50) (MPa)
W1	23,80	16,25	16,20	1,1	491,16	22,16	2,2396	0,6658	1,4910
W2	34,21	25,08	25,00	3,0	1089,49	33,01	2,7536	0,8125	2,2373
W3	27,79	22,13	19,63	2,7	694,93	26,36	3,8853	0,7261	2,8211
W4	28,59	24,37	24,15	2,5	879,55	29,66	2,8424	0,7702	2,1891
W5	33,27	27,72	24,81	1,9	1051,50	32,43	1,8069	0,8053	1,4552
W6	31,08	22,65	22,46	3,2	889,24	29,82	3,5986	0,7723	2,7791
W7	27,05	22,67	22,36	1,9	770,49	27,76	2,4659	0,7451	1,8373
W8	48,18	21,61	18,65	1,9	1144,66	33,83	1,6599	0,8226	1,3654
W9	31,5	23,4	19,9	2,5	797,23	28,24	3,1359	0,7515	2,3565
W10	29,8	26	21,4	2,1	812,16	28,50	2,5857	0,7550	1,9521

Table 164. Point load strength of Stop 4 fresh saturated granite

Sample No	W (mm)	D (mm)	D' (mm)	P (kN)	De2 (mm <sup>2</sup> )	De (mm)	Is (MPa)	F	Is(50) (MPa)
F1	30,98	24,19	18,40	8,0	726,16	26,95	11,0169	0,7341	8,0878
F2	35,52	19,38	15,27	5,5	690,94	26,29	7,9601	0,7251	5,7716
F3	41,94	20,78	12,55	5,0	670,51	25,89	7,4571	0,7196	5,3664
F4	33,16	27,46	25,68	4,5	1084,78	32,94	4,1483	0,8116	3,3668
F5	32,98	17,75	15,51	4,5	651,62	25,53	6,9059	0,7145	4,9344
F6	30,45	27,27	28,32	4,4	1098,53	33,14	4,0054	0,8142	3,2611
F7	22,30	22,10	22,00	4,7	624,97	25,00	7,5204	0,7071	5,3176
F8	40,41	17,12	13,52	3,8	695,98	26,38	5,4599	0,7264	3,9660
F9	38,46	25,77	20,99	5,0	1028,38	32,07	4,8620	0,8009	3,8938
F10	42,11	27,18	21,04	8,0	1128,66	33,60	7,0881	0,8197	5,8101

Table 165. Point load strength of Stop 4 weathered saturated granite

Sample No	W (mm)	D (mm)	D' (mm)	P (kN)	De2 (mm <sup>2</sup> )	De (mm)	Is (MPa)	F	Is(50) (MPa)
W1	33,90	21,13	18,45	1,9	796,76	28,23	2,3847	0,7514	1,7917
W2	29,49	24,72	15,00	1,1	563,50	23,74	1,9521	0,6890	1,3450
W3	27,25	27,13	22,15	1,3	768,90	27,73	1,6907	0,7447	1,2591
W4	36,01	22,05	19,52	1,1	895,43	29,92	1,2285	0,7736	0,9503
W5	22,57	20,52	19,79	0,6	568,99	23,85	1,0545	0,6907	0,7283
W6	34,30	9,50	8,30	1,7	362,66	19,04	4,6876	0,6171	2,8929
W7	35,88	30,98	22,70	1,9	1037,55	32,21	1,8312	0,8026	1,4698
W8	41,25	25,89	23,22	3,1	1220,16	34,93	2,5407	0,8358	2,1236

Table 166. Point load strength of Stop 5 fresh dry basalt

Sample No	W (mm)	D (mm)	D' (mm)	P (kN)	De2 (mm2)	De (mm)	Is (MPa)	F	Is(50) (MPa)
F1	25,18	16,48	13,44	2,1	431,11	20,76	4,8712	0,6444	3,1390
F2	33,46	27,13	25,18	3,2	1073,28	32,76	2,9815	0,8095	2,4134
F3	29,44	17,69	15,44	1,9	579,05	24,06	3,2812	0,6937	2,2763
F4	36,13	27,18	24,18	2,2	1112,90	33,36	1,9768	0,8168	1,6147
F5	44,13	21,48	15,33	2,4	861,80	29,36	2,7849	0,7662	2,1339
F6	25,56	23,11	23,18	2,3	754,75	27,47	3,0474	0,7413	2,2589
F7	42,13	26,39	23,11	3,1	1240,29	35,22	2,4994	0,8393	2,0977
F8	28,46	27,13	25,98	2,5	941,90	30,69	2,6542	0,7835	2,0795
F9	45,13	39,84	35,96	3,4	2067,36	45,47	1,6446	0,9536	1,5683
F10	22,39	21,13	19,87	2,2	566,74	23,81	3,8819	0,6900	2,6786

Table 167. Point load strength of Stop 5 fresh saturated basalt

Sample No	W (mm)	D (mm)	D' (mm)	P (kN)	De2 (mm2)	De (mm)	Is (MPa)	F	Is(50) (MPa)
F1	39,41	23,18	21,99	2,1	1103,98	33,23	1,9022	0,8152	1,5506
F2	25,13	17,88	15,71	2,2	502,92	22,43	4,3745	0,6697	2,9296
F3	38,99	21,04	19,88	1,5	987,42	31,42	1,5191	0,7928	1,2043
F4	27,84	22,44	19,14	1,9	678,80	26,05	2,7991	0,7219	2,0205
F5	21,13	13,45	11,96	1,1	321,93	17,94	3,4169	0,5990	2,0469
F6	25,49	21,48	18,74	1,5	608,51	24,67	2,4650	0,7024	1,7314
F7	33,19	21,87	17,96	1,1	759,35	27,56	1,4486	0,7424	1,0754
F8	28,47	16,84	24,13	1,2	875,14	29,58	1,3712	0,7692	1,0547
F9	18,99	13,27	11,44	0,8	276,75	16,64	2,8907	0,5768	1,6674
F10	35,99	18,76	14,13	1,5	647,82	25,45	2,3155	0,7135	1,6520

Table 168. Point load strength of Stop 5 weathered dry basalt

Sample No	W (mm)	D (mm)	D' (mm)	P (kN)	De2 (mm <sup>2</sup> )	De (mm)	Is (MPa)	F	Is(50) (MPa)
W1	24,04	14,46	12,63	1,2	386,78	19,67	3,1025	0,6272	1,9458
W2	30,05	24,78	22,57	2,3	863,99	29,39	2,6621	0,7667	2,0411
W3	31,59	19,68	17,40	1,8	700,21	26,46	2,5707	0,7275	1,8701
W4	26,98	15,50	14,14	1,3	485,98	22,05	2,6750	0,6640	1,7762
W5	42,60	19,45	13,31	1,7	722,30	26,88	2,3536	0,7332	1,7255
W6	38,48	24,94	24,32	1,0	1192,14	34,53	0,8388	0,8310	0,6971
W7	35,35	18,98	15,86	0,6	714,21	26,72	0,8401	0,7311	0,6142
W8	36,83	21,37	20,13	0,1	944,44	30,73	0,1059	0,7840	0,0830
W9	33,44	27,45	21,83	1,0	929,93	30,49	1,0753	0,7810	0,8398
W10	37,89	28,72	25,69	1,1	1239,99	35,21	0,8871	0,8392	0,7445
W11	27,33	13,58	12,61	0,3	439,02	20,95	0,6833	0,6473	0,4424
W12	25,92	19,99	18,56	0,9	612,83	24,76	1,4686	0,7036	1,0334
W13	24,45	15,51	11,21	0,6	349,15	18,69	1,7184	0,6113	1,0505
W14	29,10	28,75	23,29	0,7	863,36	29,38	0,8108	0,7666	0,6215
W15	35,64	27,79	22,86	0,6	1037,87	32,22	0,5781	0,8027	0,4640
W16	28,30	23,66	21,63	1,2	779,78	27,92	1,5389	0,7473	1,1500
W17	34,23	19,11	17,86	0,4	778,79	27,91	0,5136	0,7471	0,3837
W18	32,73	27,70	19,24	0,8	802,20	28,32	0,9973	0,7526	0,7506
W19	35,25	19,01	13,02	0,4	584,66	24,18	0,6842	0,6954	0,4758
W20	23,90	22,43	20,41	0,5	621,40	24,93	0,8046	0,7061	0,5681

Table 169. Point load strength of Stop 5 weathered saturated basalt

Sample No	W (mm)	D (mm)	D' (mm)	P (kN)	De2 (mm <sup>2</sup> )	De (mm)	Is (MPa)	F	Is(50) (MPa)
W1	31,37	20,75	18,68	0,6	746,49	27,32	0,8038	0,7392	0,5942
W2	22,49	15,98	14,92	0,2	427,45	20,67	0,4679	0,6430	0,3009
W3	35,86	23,52	21,48	0,5	981,24	31,32	0,5096	0,7915	0,4033
W4	25,26	21,51	20,53	0,3	660,62	25,70	0,4541	0,7170	0,3256
W5	29,51	21,01	20,13	0,2	756,73	27,51	0,2643	0,7417	0,1960
W6	28,21	19,38	20,14	0,1	723,76	26,90	0,1382	0,7335	0,1013
W7	28,64	22,23	20,53	0,1	749,02	27,37	0,1335	0,7398	0,0988
W8	37,35	32,12	29,98	0,2	1426,44	37,77	0,1402	0,8691	0,1219
W9	35,42	28,56	27,95	0,1	1261,13	35,51	0,0793	0,8428	0,0668
W10	33,86	15,09	15,00	0,1	647,01	25,44	0,1546	0,7133	0,1102
W11	38,65	29,33	28,56	0,1	1406,17	37,50	0,0711	0,8660	0,0616
W12	41,55	29,58	29,01	0,1	1535,50	39,19	0,0651	0,8853	0,0577
W13	52,22	39,90	28,91	0,2	1923,16	43,85	0,1040	0,9365	0,0974
W14	36,21	21,69	20,98	0,1	967,75	31,11	0,1033	0,7888	0,0815
W15	23,31	12,62	11,65	0,1	345,94	18,60	0,2891	0,6099	0,1763
W16	38,95	23,78	22,11	0,1	1097,05	33,12	0,0912	0,8139	0,0742
W17	31,93	18,39	17,51	0,1	712,22	26,69	0,1404	0,7306	0,1026
W18	27,24	15,99	15,25	0,1	529,18	23,00	0,1890	0,6783	0,1282
W19	16,29	16,04	15,43	0,1	320,20	17,89	0,3123	0,5982	0,1868
W20	32,04	16,69	15,78	0,1	644,07	25,38	0,1553	0,7124	0,1106

Table 170. Point load strength of Stop 6 weathered dry granite

Sample No	W (mm)	D (mm)	D' (mm)	P (kN)	De2 (mm <sup>2</sup> )	De (mm)	Is (MPa)	F	Is(50) (MPa)
W1	35,70	28,82	26,13	0,1	1188,33	34,47	0,0842	0,8303	0,0699
W2	38,82	37,79	22,18	0,4	1096,85	33,12	0,3647	0,8139	0,2968
W3	39,37	24,11	18,25	0,5	915,29	30,25	0,5463	0,7779	0,4249
W4	31,94	30,12	22,31	0,2	907,75	30,13	0,2203	0,7763	0,1710
W5	37,83	25,31	17,55	2,1	845,75	29,08	2,4830	0,7627	1,8937
W6	31,06	24,69	15,90	0,1	629,11	25,08	0,1590	0,7083	0,1126
W7	35,33	28,05	18,72	0,5	842,52	29,03	0,5935	0,7619	0,4522
W8	35,36	22,73	16,23	0,1	731,07	27,04	0,1368	0,7354	0,1006
W9	25,80	19,70	13,62	0,6	447,64	21,16	1,3404	0,6505	0,8719
W10	37,97	26,32	19,15	0,7	926,27	30,43	0,7557	0,7802	0,5896
W11	36,47	26,48	19,95	0,2	926,85	30,44	0,2158	0,7803	0,1684
W12	40,37	26,38	18,89	0,1	971,45	31,17	0,1029	0,7895	0,0813
W13	26,50	25,27	20,85	0,4	703,85	26,53	0,5683	0,7284	0,4140
W14	34,36	26,03	14,48	0,2	633,80	25,18	0,3156	0,7096	0,2239
W15	29,36	24,26	17,69	0,1	661,63	25,72	0,1511	0,7172	0,1084

Table 171. Point load strength of Stop 6 weathered saturated granite

Sample No	W (mm)	D (mm)	D' (mm)	P (kN)	De2 (mm <sup>2</sup> )	De (mm)	Is (MPa)	F	Is(50) (MPa)
W1	28,90	25,77	25,13	0,0	925,17	30,42	0,0000	0,7800	0,0000
W2	28,86	21,90	20,45	0,0	751,83	27,42	0,0000	0,7405	0,0000
W3	30,25	19,85	18,33	0,1	706,35	26,58	0,1416	0,7291	0,1032
W4	24,81	12,71	11,95	0,1	377,68	19,43	0,2648	0,6234	0,1651
W5	28,31	19,07	18,55	0,0	668,98	25,86	0,0000	0,7192	0,0000
W6	36,67	25,95	24,13	0,0	1127,19	33,57	0,0000	0,8194	0,0000
W7	32,82	18,77	17,93	0,0	749,63	27,38	0,0000	0,7400	0,0000
W8	30,12	14,46	14,23	0,1	546,00	23,37	0,1832	0,6836	0,1252
W9	27,87	21,24	20,98	0,0	744,86	27,29	0,0000	0,7388	0,0000
W10	34,62	19,21	18,23	1,5	803,98	28,35	1,8657	0,7531	1,4050
W11	37,06	18,50	18,25	0,0	861,59	29,35	0,0000	0,7662	0,0000
W12	30,29	17,51	16,29	0,0	628,57	25,07	0,0000	0,7081	0,0000
W13	30,61	25,38	24,33	0,0	948,72	30,80	0,0000	0,7849	0,0000
W14	20,68	17,20	16,75	0,1	441,26	21,01	0,2266	0,6482	0,1469
W15	26,54	21,52	20,18	0,0	682,26	26,12	0,0000	0,7228	0,0000

Table 172. Point load strength of Stop 7 fresh dry granodiorite

Sample No	W (mm)	D (mm)	D' (mm)	P (kN)	De2 (mm <sup>2</sup> )	De (mm)	Is (MPa)	F	Is(50) (MPa)
F1	39,59	24,93	19,01	7,0	958,73	30,96	7,3013	0,7869	5,7457
F2	24,02	23,65	21,64	4,3	662,16	25,73	6,4939	0,7174	4,6587
F3	50,12	30,13	29,22	15,0	1865,61	43,19	8,0403	0,9294	7,4729
F4	39,28	32,79	27,01	12,0	1351,53	36,76	8,8788	0,8575	7,6134
F5	36,39	31,59	27,12	10,0	1257,19	35,46	7,9542	0,8421	6,6983
F6	25,21	18,64	16,60	12,0	533,10	23,09	22,5097	0,6795	15,2963
F7	42,82	29,31	28,53	14,0	1556,25	39,45	8,9960	0,8882	7,9907
F8	30,56	29,13	24,60	9,0	957,68	30,95	9,3977	0,7867	7,3934
F9	27,86	17,98	14,61	8,0	518,52	22,77	15,4287	0,6748	10,4120
F10	28,96	18,45	17,43	7,2	643,02	25,36	11,1971	0,7122	7,9740

Table 173. Point load strength of Stop 7 weathered dry granodiorite

Sample No	W (mm)	D (mm)	D' (mm)	P (kN)	De2 (mm <sup>2</sup> )	De (mm)	Is (MPa)	F	Is(50) (MPa)
W1	43,55	27,39	23,88	2,1	1324,81	36,40	1,5851	0,8532	1,3524
W2	44,22	38,51	35,23	3,1	1984,55	44,55	1,5621	0,9439	1,4745
W3	29,37	20,94	13,82	1,8	517,06	22,74	3,4812	0,6744	2,3476
W4	30,67	12,22	11,43	0,8	446,57	21,13	1,7914	0,6501	1,1646
W5	26,04	22,01	20,13	0,4	667,75	25,84	0,5990	0,7189	0,4306
W6	31,99	28,44	27,93	5,3	1138,19	33,74	4,6565	0,8214	3,8250
W7	31,52	28,13	26,22	2,8	1052,81	32,45	2,6596	0,8056	2,1425
W8	28,89	18,04	15,13	0,8	556,82	23,60	1,4367	0,6870	0,9870

Table 174. Point load strength of Stop 7 fresh saturated granodiorite

Sample No	W (mm)	D (mm)	D' (mm)	P (kN)	De2 (mm <sup>2</sup> )	De (mm)	Is (MPa)	F	Is(50) (MPa)
F1	16,11	10,44	9,55	2,0	195,99	14,00	10,2047	0,5291	5,3997
F2	38,04	22,39	18,75	8,5	908,60	30,14	9,3551	0,7764	7,2636
F3	41,28	29,87	24,34	5,5	1279,94	35,78	4,2971	0,8459	3,6348
F4	48,87	25,10	24,60	20,0	1531,47	39,13	13,0594	0,8847	11,5535
F5	23,35	12,98	11,55	3,7	343,56	18,54	10,7697	0,6089	6,5572
F6	23,48	19,31	17,30	2,1	517,46	22,75	4,0583	0,6745	2,7373
F7	24,47	19,84	18,50	5,4	576,68	24,01	9,3639	0,6930	6,4894

Table 175. Point load strength of Stop 7 weathered saturated granodiorite

Sample No	W (mm)	D (mm)	D' (mm)	P (kN)	De2 (mm <sup>2</sup> )	De (mm)	Is (MPa)	F	Is(50) (MPa)
W1	30,64	23,41	22,11	0,1	862,99	29,38	0,1159	0,7665	0,0888
W2	34,27	25,60	18,97	1,3	828,16	28,78	1,5698	0,7587	1,1909
W3	19,46	16,17	11,80	0,7	292,52	17,10	2,3930	0,5849	1,3996
W4	34,80	26,25	25,13	2,6	1114,04	33,38	2,3338	0,8170	1,9068
W5	34,08	19,31	16,30	0,4	707,65	26,60	0,5653	0,7294	0,4123
W6	32,14	14,09	13,53	0,6	553,95	23,54	1,0831	0,6861	0,7431
W7	25,37	19,55	18,50	0,6	597,89	24,45	1,0035	0,6993	0,7018
W8	33,43	23,82	21,23	0,1	904,10	30,07	0,1106	0,7755	0,0858
W9	25,55	12,37	10,33	0,3	336,22	18,34	0,8923	0,6056	0,5403
W10	29,27	19,88	10,73	1,0	400,09	20,00	2,4995	0,6325	1,5809

Table 176. Point load strength of Stop 8 fresh dry sandstone

Sample No	W (mm)	D (mm)	D' (mm)	P (kN)	De2 (mm <sup>2</sup> )	De (mm)	Is (MPa)	F	Is(50) (MPa)
F1	39,68	16,65	10,71	4,6	541,37	23,27	8,4970	0,6822	5,7963
F2	34,77	19,15	10,28	4,1	455,33	21,34	9,0044	0,6533	5,8824
F3	24,56	17,46	9,46	4,7	295,97	17,20	15,8799	0,5866	9,3148
F4	31,58	15,61	9,99	4,7	401,89	20,05	11,6947	0,6332	7,4051
F5	39,93	25,68	14,57	10,0	741,12	27,22	13,4931	0,7379	9,9563
F6	37,51	25,03	19,37	3,8	925,57	30,42	4,1056	0,7800	3,2025
F7	43,23	24,26	19,30	8,0	1062,85	32,60	7,5269	0,8075	6,0779
F8	39,00	19,26	13,21	5,5	656,29	25,62	8,3804	0,7158	5,9987
F9	40,39	21,96	12,19	9,0	627,20	25,04	14,3494	0,7077	10,1555
F10	40,42	30,27	20,17	7,0	1038,56	32,23	6,7401	0,8028	5,4111

Table 177. Point load strength of Stop 8 weathered dry sandstone

Sample No	W (mm)	D (mm)	D' (mm)	P (kN)	De2 (mm <sup>2</sup> )	De (mm)	Is (MPa)	F	Is(50) (MPa)
W1	36,78	16,54	8,97	2,8	420,28	20,50	6,6623	0,6403	4,2660
W2	28,67	27,57	18,44	4,3	673,47	25,95	6,3848	0,7204	4,5999
W3	30,87	21,79	16,86	3,3	663,02	25,75	4,9772	0,7176	3,5718
W4	40,72	30,24	14,78	4,5	766,68	27,69	5,8695	0,7442	4,3679
W5	35,59	19,15	15,08	1,6	683,69	26,15	2,3402	0,7232	1,6924
W6	45,99	33,26	27,03	9,0	1583,58	39,79	5,6833	0,8921	5,0702
W7	27,33	17,77	11,40	1,9	396,89	19,92	4,7872	0,6312	3,0218
W8	30,54	11,62	11,33	0,1	440,79	20,99	0,2269	0,6480	0,1470
W9	31,36	22,10	23,64	4,2	944,40	30,73	4,4473	0,7840	3,4866
W10	41,38	36,59	30,27	7,0	1595,63	39,95	4,3870	0,8938	3,9211

Table 178. Point load strength of Stop 8 fresh saturated sandstone

Sample No	W (mm)	D (mm)	D' (mm)	P (kN)	De2 (mm <sup>2</sup> )	De (mm)	Is (MPa)	F	Is(50) (MPa)
F1	38,15	27,17	17,89	9,0	869,43	29,49	10,3516	0,7679	7,9493
F2	36,52	21,26	15,31	5,1	712,26	26,69	7,1603	0,7306	5,2313
F3	37,00	34,80	24,90	8,0	1173,63	34,26	6,8165	0,8277	5,6423
F4	32,86	15,59	9,14	3,6	382,60	19,56	9,4093	0,6255	5,8852
F5	40,79	28,77	20,51	10,0	1065,74	32,65	9,3832	0,8080	7,5819
F6	27,38	25,78	15,93	10,0	555,62	23,57	17,9978	0,6866	12,3575
F7	39,59	38,92	32,07	12,0	1617,39	40,22	7,4194	0,8968	6,6540
F8	24,15	22,77	18,35	4,9	564,53	23,76	8,6799	0,6893	5,9834
F9	37,55	33,98	26,80	10,0	1281,96	35,80	7,8005	0,8462	6,6010
F10	40,88	17,37	11,36	5,3	591,59	24,32	8,9589	0,6975	6,2485

Table 179. Point load strength of Stop 8 weathered saturated sandstone

Sample No	W (mm)	D (mm)	D' (mm)	P (kN)	De2 (mm <sup>2</sup> )	De (mm)	Is (MPa)	F	Is(50) (MPa)
W1	32,12	22,59	19,62	5,2	802,80	28,33	6,4774	0,7528	4,8760
W2	34,65	24,30	19,11	2,7	843,52	29,04	3,2009	0,7621	2,4395
W3	49,65	19,68	10,38	1,5	656,52	25,62	2,2848	0,7159	1,6356
W4	44,37	40,03	39,96	3,9	2258,63	47,53	1,7267	0,9749	1,6834
W5	32,62	24,25	22,08	5,0	917,52	30,29	5,4495	0,7783	4,2416
W6	44,25	22,55	15,59	4,2	878,80	29,64	4,7792	0,7700	3,6800
W7	37,40	27,08	19,20	3,9	914,75	30,24	4,2635	0,7778	3,3159
W8	32,71	28,50	20,91	5,4	871,29	29,52	6,1977	0,7683	4,7620
W9	47,98	38,79	29,78	4,2	1820,18	42,66	2,3075	0,9237	2,1315
W10	51,16	34,82	24,48	7,0	1595,41	39,94	4,3876	0,8938	3,9216

Table 180. Point load strength of Stop 9 fresh dry limestone

Sample No	W (mm)	D (mm)	D' (mm)	P (kN)	De2 (mm <sup>2</sup> )	De (mm)	Is (MPa)	F	Is(50) (MPa)
F1	21,90	21,72	15,55	5,1	433,82	20,83	11,7562	0,6454	7,5876
F2	35,63	25,25	20,55	9,0	932,73	30,54	9,6490	0,7815	7,5412
F3	29,12	24,36	17,24	9,0	639,53	25,29	14,0729	0,7112	10,0084
F4	35,80	34,94	28,91	4,3	1318,44	36,31	3,2614	0,8522	2,7793
F5	23,63	22,40	10,59	2,0	318,78	17,85	6,2739	0,5976	3,7491
F6	29,14	17,80	10,43	5,6	387,17	19,68	14,4638	0,6273	9,0735
F7	34,13	17,58	15,44	7,0	671,30	25,91	10,4276	0,7199	7,5063
F8	34,79	21,97	14,16	8,0	627,55	25,05	12,7480	0,7078	9,0234
F9	30,72	19,90	12,23	10,0	478,61	21,88	20,8940	0,6615	13,8207
F10	41,27	31,18	28,17	8,0	1480,99	38,48	5,4018	0,8773	4,7390

Table 181. Point load strength of Stop 9 weathered dry limestone

Sample No	W (mm)	D (mm)	D' (mm)	P (kN)	De2 (mm <sup>2</sup> )	De (mm)	Is (MPa)	F	Is(50) (MPa)
W1	43,35	18,56	16,38	5,3	904,55	30,08	5,8593	0,7756	4,5443
W2	43,87	14,08	9,69	5,6	541,53	23,27	10,3411	0,6822	7,0548
W3	33,35	22,21	16,47	5,5	699,71	26,45	7,8604	0,7274	5,7173
W4	38,93	10,15	7,76	4,3	384,84	19,62	11,1736	0,6264	6,9988
W5	35,53	10,17	6,24	3,0	282,43	16,81	10,6221	0,5798	6,1582
W6	27,33	20,45	15,75	4,2	548,34	23,42	7,6595	0,6843	5,2418
W7	35,16	32,02	25,53	5,4	1143,48	33,82	4,7224	0,8224	3,8836
W8	39,37	23,83	17,29	5,5	867,14	29,45	6,3427	0,7674	4,8675
W9	37,08	28,88	16,24	3,8	767,11	27,70	4,9537	0,7443	3,6869
W10	29,28	24,60	21,32	4,2	795,22	28,20	5,2815	0,7510	3,9664

Table 182. Point load strength of Stop 9 weathered dry mudstone

Sample No	W (mm)	D (mm)	D' (mm)	P (kN)	De2 (mm <sup>2</sup> )	De (mm)	Is (MPa)	F	Is(50) (MPa)
W1	26,18	13,41	9,55	0,9	318,50	17,85	2,8258	0,5974	1,6882
W2	20,98	15,14	11,14	0,7	297,73	17,25	2,3511	0,5874	1,3812
W3	25,22	19,52	13,48	0,5	433,08	20,81	1,1545	0,6451	0,7448
W4	23,13	20,71	13,34	0,9	393,06	19,83	2,2897	0,6297	1,4418
W5	20,98	16,82	12,91	1,2	345,03	18,58	3,4779	0,6095	2,1198
W6	22,05	19,54	13,73	0,5	385,66	19,64	1,2965	0,6267	0,8125

Table 183. Point load strength of Stop 9 fresh saturated limestone

Sample No	W (mm)	D (mm)	D' (mm)	P (kN)	De2 (mm <sup>2</sup> )	De (mm)	Is (MPa)	F	Is(50) (MPa)
F1	37,28	20,86	15,28	3,8	725,65	26,94	5,2367	0,7340	3,8437
F2	37,09	29,04	25,43	8,0	1201,53	34,66	6,6582	0,8326	5,5438
F3	29,09	20,98	11,36	10,0	420,97	20,52	23,7546	0,6406	15,2169
F4	54,46	27,79	14,80	10,0	1026,76	32,04	9,7394	0,8005	7,7967
F5	41,40	17,37	13,11	5,3	691,41	26,29	7,6655	0,7252	5,5589
F6	35,87	23,07	19,53	4,1	892,41	29,87	4,5943	0,7730	3,5512
F7	49,32	31,21	17,23	10,0	1082,53	32,90	9,2376	0,8112	7,4935
F8	40,20	20,34	14,37	4,5	735,89	27,13	6,1150	0,7366	4,5042
F9	27,01	26,70	22,32	8,0	767,98	27,71	10,4170	0,7445	7,7552
F10	48,12	24,61	19,17	11,0	1175,11	34,28	9,3608	0,8280	7,7508

Table 184. Point load strength of Stop 9 weathered saturated limestone

Sample No	W (mm)	D (mm)	D' (mm)	P (kN)	De2 (mm <sup>2</sup> )	De (mm)	Is (MPa)	F	Is(50) (MPa)
W1	35,84	31,40	23,34	8,0	1065,61	32,64	7,5074	0,8080	6,0660
W2	38,10	26,80	15,92	5,6	772,68	27,80	7,2475	0,7456	5,4039
W3	25,14	10,49	6,52	1,7	208,81	14,45	8,1415	0,5376	4,3768
W4	45,58	17,73	9,54	3,2	553,93	23,54	5,7769	0,6861	3,9635
W5	44,41	22,86	13,55	8,0	766,57	27,69	10,4361	0,7441	7,7659
W6	40,17	31,23	24,02	0,3	1229,15	35,06	0,2441	0,8374	0,2044
W7	40,49	38,13	34,08	3,4	1757,83	41,93	1,9342	0,9157	1,7712
W8	29,26	22,75	16,77	0,5	625,08	25,00	0,7999	0,7071	0,5656
W9	28,50	28,29	25,13	0,3	912,36	30,21	0,3288	0,7772	0,2556
W10	50,90	25,75	21,18	0,1	1373,33	37,06	0,0728	0,8609	0,0627

Table 185. Point load strength of Stop 9 weathered dry mudstone

Sample No	W (mm)	D (mm)	D' (mm)	P (kN)	De2 (mm <sup>2</sup> )	De (mm)	Is (MPa)	F	Is(50) (MPa)
W1	21,33	15,41	12,81	0,0	348,07	18,66	0,0000	0,6108	0,0000
W2	20,46	17,23	14,99	0,4	390,69	19,77	1,0238	0,6287	0,6437
W3	18,71	15,88	11,46	0,1	273,14	16,53	0,3661	0,5749	0,2105
W4	23,56	20,41	13,47	0,3	404,27	20,11	0,7421	0,6341	0,4706
W5	22,81	19,84	13,53	0,5	393,15	19,83	1,2718	0,6297	0,8009
W6	25,94	20,77	12,58	0,5	415,70	20,39	1,2028	0,6386	0,7681
W7	26,17	20,05	12,00	0,1	400,05	20,00	0,2500	0,6325	0,1581

Table 186. Point load strength of Stop 10 fresh dry sandstone

Sample No	W (mm)	D (mm)	D' (mm)	P (kN)	De2 (mm <sup>2</sup> )	De (mm)	Is (MPa)	F	Is(50) (MPa)
F1	36,35	27,82	20,38	10,0	943,71	30,72	10,5965	0,7838	8,3059
F2	43,35	23,35	12,92	10,0	713,48	26,71	14,0158	0,7309	10,2442
F3	46,75	18,72	10,98	9,0	653,90	25,57	13,7635	0,7151	9,8429
F4	42,53	18,88	13,01	5,1	704,86	26,55	7,2355	0,7287	5,2724
F5	53,19	19,73	12,40	10,0	840,20	28,99	11,9019	0,7614	9,0621
F6	46,26	42,25	20,29	5,3	1195,69	34,58	4,4326	0,8316	3,6862
F7	32,39	24,41	16,28	3,8	671,73	25,92	5,6570	0,7200	4,0729
F8	44,78	24,13	20,18	10,0	1151,16	33,93	8,6869	0,8238	7,1559
F9	43,26	19,71	11,46	5,4	631,54	25,13	8,5505	0,7089	6,0619
F10	51,09	17,55	10,98	7,5	714,61	26,73	10,4952	0,7312	7,6741

Table 187. Point load strength of Stop 10 weathered dry sandstone

Sample No	W (mm)	D (mm)	D' (mm)	P (kN)	De2 (mm <sup>2</sup> )	De (mm)	Is (MPa)	F	Is(50) (MPa)
W1	39,97	36,80	30,27	3,4	1541,26	39,26	2,1735	0,8861	1,9260
W2	58,65	26,97	20,52	3,4	1533,12	39,16	2,2177	0,8849	1,9625
W3	47,97	36,87	28,71	5,5	1754,42	41,89	3,1349	0,9153	2,8693
W4	36,15	32,32	26,35	4,5	1213,44	34,83	3,7085	0,8347	3,0954
W5	48,65	18,17	10,69	4,0	662,51	25,74	6,0377	0,7175	4,3319
W6	44,18	11,63	7,10	2,6	399,59	19,99	6,5067	0,6323	4,1141
W7	31,83	14,08	8,35	1,9	338,57	18,40	5,6118	0,6066	3,4043
W8	33,37	25,75	16,57	4,6	704,38	26,54	6,5305	0,7286	4,7579
W9	40,87	35,47	27,09	4,9	1410,41	37,56	3,4742	0,8667	3,0109
W10	38,96	28,01	20,13	3,6	999,06	31,61	3,6034	0,7951	2,8650
W11	52,56	28,63	20,21	7,0	1353,17	36,79	5,1730	0,8577	4,4371
W12	39,39	19,51	18,87	5,3	946,87	30,77	5,5974	0,7845	4,3911
W13	44,63	26,80	20,37	5,4	1158,11	34,03	4,6628	0,8250	3,8468

Table 188. Point load strength of Stop 10 fresh saturated sandstone

Sample No	W (mm)	D (mm)	D' (mm)	P (kN)	De2 (mm2)	De (mm)	Is (MPa)	F	Is(50) (MPa)
F1	46,97	18,83	13,24	1,5	792,21	28,15	1,8934	0,7503	1,4206
F2	26,84	26,94	21,24	1,1	726,22	26,95	1,5147	0,7341	1,1120
F3	36,47	31,43	21,64	1,4	1005,36	31,71	1,3925	0,7963	1,1089
F4	32,46	31,23	21,54	1,7	890,69	29,84	1,9086	0,7726	1,4746
F5	34,23	33,20	17,82	4,5	777,04	27,88	5,7912	0,7467	4,3241
F6	41,38	34,93	10,92	3,7	575,63	23,99	6,4277	0,6927	4,4526
F7	33,84	32,92	23,07	2,9	994,51	31,54	2,9160	0,7942	2,3158
F8	56,94	23,45	14,32	3,2	1038,70	32,23	3,0808	0,8029	2,4734
F9	43,52	35,42	16,36	3,1	906,99	30,12	3,4179	0,7761	2,6526
F10	50,19	24,95	12,42	1,3	794,09	28,18	1,6371	0,7507	1,2290

Table 189. Point load strength of Stop 10 weathered saturated sandstone

Sample No	W (mm)	D (mm)	D' (mm)	P (kN)	De2 (mm2)	De (mm)	Is (MPa)	F	Is(50) (MPa)
W1	53,64	34,91	29,68	3,2	2028,07	45,03	1,5779	0,9490	1,4975
W2	55,48	18,90	11,99	1,5	847,40	29,11	1,7701	0,7630	1,3506
W3	41,09	18,69	12,69	1,2	664,24	25,77	1,8066	0,7180	1,2970
W4	41,20	11,44	10,05	1,4	527,46	22,97	2,6542	0,6777	1,7989
W5	39,54	24,44	18,42	1,2	927,80	30,46	1,2934	0,7805	1,0095
W6	38,01	13,72	6,39	1,6	309,41	17,59	5,1712	0,5931	3,0672
W7	30,25	18,82	15,43	1,4	594,60	24,38	2,3545	0,6983	1,6443
W8	46,02	42,82	40,61	1,2	2380,73	48,79	0,5040	0,9879	0,4979
W9	41,64	35,41	32,14	2,4	1704,85	41,29	1,4077	0,9087	1,2793
W10	52,21	34,72	27,03	2,4	1797,75	42,40	1,3350	0,9209	1,2294

Table 190. Point load strength of Stop 11 fresh dry sandstone

Sample No	W (mm)	D (mm)	D' (mm)	P (kN)	De2 (mm <sup>2</sup> )	De (mm)	Is (MPa)	F	Is(50) (MPa)
F1	56,52	29,00	19,76	10,0	1422,72	37,72	7,0288	0,8686	6,1049
F2	50,56	30,29	22,61	5,6	1456,26	38,16	3,8455	0,8736	3,3595
F3	53,71	15,51	9,60	2,1	656,84	25,63	3,1971	0,7159	2,2890
F4	33,83	27,74	20,35	4,2	876,99	29,61	4,7891	0,7696	3,6857
F5	39,15	27,45	20,68	5,5	1031,37	32,11	5,3327	0,8014	4,2738
F6	33,33	26,28	20,54	5,5	872,10	29,53	6,3066	0,7685	4,8468
F7	39,60	28,20	22,05	9,0	1112,33	33,35	8,0911	0,8167	6,6082
F8	28,28	26,02	19,40	5,6	698,89	26,44	8,0127	0,7271	5,8263
F9	38,82	28,25	20,42	5,5	1009,81	31,78	5,4465	0,7972	4,3421
F10	41,85	29,91	23,74	7,0	1265,63	35,58	5,5308	0,8435	4,6653

Table 191. Point load strength of Stop 11 weathered dry sandstone

Sample No	W (mm)	D (mm)	D' (mm)	P (kN)	De2 (mm <sup>2</sup> )	De (mm)	Is (MPa)	F	Is(50) (MPa)
W1	36,76	25,38	24,13	0,2	1129,96	33,61	0,1770	0,8199	0,1451
W2	31,36	20,93	19,18	1,9	766,22	27,68	2,4797	0,7441	1,8450
W3	26,78	24,02	23,15	0,6	789,75	28,10	0,7597	0,7497	0,5696
W4	18,66	16,95	15,13	1,8	359,65	18,96	5,0049	0,6159	3,0823
W5	27,51	18,09	15,19	2,4	532,33	23,07	4,5085	0,6793	3,0626
W6	20,46	24,16	11,07	2,1	288,53	16,99	7,2784	0,5829	4,2423
W7	30,98	18,92	15,23	0,5	601,05	24,52	0,8319	0,7002	0,5825
W8	29,70	18,96	15,33	5,2	580,00	24,08	8,9655	0,6940	6,2222
W9	61,44	22,85	16,33	2,0	1278,11	35,75	1,5648	0,8456	1,3232
W10	49,27	45,37	44,28	4,6	2779,20	52,72	1,6551	1,0268	1,6995

Table 192. Point load strength of Stop 11 fresh saturated sandstone

Sample No	W (mm)	D (mm)	D' (mm)	P (kN)	De2 (mm <sup>2</sup> )	De (mm)	Is (MPa)	F	Is(50) (MPa)
F1	29,70	29,44	27,15	0,9	1027,20	32,05	0,8762	0,8006	0,7015
F2	39,06	28,84	15,66	5,2	779,21	27,91	6,6734	0,7472	4,9863
F3	40,67	28,05	23,90	2,5	1238,23	35,19	2,0190	0,8389	1,6938
F4	30,76	26,41	16,81	5,3	658,70	25,67	8,0462	0,7165	5,7647
F5	27,95	18,31	13,97	4,9	497,40	22,30	9,8512	0,6679	6,5793
F6	44,62	27,01	18,01	5,5	1023,70	32,00	5,3727	0,7999	4,2978
F7	26,32	25,83	23,21	2,4	778,20	27,90	3,0840	0,7469	2,3036
F8	40,81	26,52	19,99	5,4	1039,23	32,24	5,1962	0,8030	4,1723
F9	44,50	29,45	13,21	8,0	748,85	27,37	10,6831	0,7398	7,9033
F10	38,15	28,75	13,87	5,0	674,06	25,96	7,4177	0,7206	5,3451

Table 193. Point load strength of Stop 11 weathered saturated sandstone

Sample No	W (mm)	D (mm)	D' (mm)	P (kN)	De2 (mm <sup>2</sup> )	De (mm)	Is (MPa)	F	Is(50) (MPa)
W1	65,18	23,46	21,16	0,7	1756,95	41,92	0,3984	0,9156	0,3648
W2	40,09	28,11	25,13	0,7	1283,39	35,82	0,5454	0,8465	0,4617
W3	27,37	19,67	14,65	2,8	510,79	22,60	5,4817	0,6723	3,6855
W4	32,86	27,41	16,44	4,9	688,18	26,23	7,1203	0,7243	5,1575
W5	30,83	19,67	15,67	0,3	615,42	24,81	0,4875	0,7044	0,3434
W6	53,77	20,63	18,73	0,1	1282,95	35,82	0,0779	0,8464	0,0660
W7	23,48	21,61	19,56	0,2	585,06	24,19	0,3418	0,6955	0,2378
W8	29,00	28,12	26,55	2,9	980,83	31,32	2,9567	0,7914	2,3400
W9	39,48	19,80	19,33	0,7	972,16	31,18	0,7200	0,7897	0,5686
W10	34,58	21,88	19,43	1,1	855,91	29,26	1,2852	0,7649	0,9831

Table 194. Point load strength of Stop 12 fresh dry sandstone

Sample No	W (mm)	D (mm)	D' (mm)	P (kN)	De2 (mm <sup>2</sup> )	De (mm)	Is (MPa)	F	Is(50) (MPa)
F1	38,90	26,42	23,86	2,3	1182,36	34,39	1,9453	0,8293	1,6132
F2	50,13	42,09	30,78	5,7	1965,61	44,34	2,8999	0,9416	2,7307
F3	40,44	32,49	31,66	2,4	1630,99	40,39	1,4715	0,8987	1,3225
F4	36,26	32,22	22,04	3,2	1018,05	31,91	3,1433	0,7988	2,5109
F5	44,23	21,34	17,45	5,5	983,20	31,36	5,5940	0,7919	4,4299
F6	33,92	31,72	20,44	9,0	883,22	29,72	10,1900	0,7710	7,8561
F7	38,05	29,26	25,92	2,4	1256,38	35,45	1,9103	0,8420	1,6084
F8	43,18	37,01	24,39	11,0	1341,61	36,63	8,1991	0,8559	7,0176
F9	35,40	19,30	18,63	1,8	840,13	28,98	2,1425	0,7614	1,6313
F10	47,10	30,47	27,88	1,1	1672,80	40,90	0,6576	0,9044	0,5947

Table 195. Point load strength of Stop 12 weathered dry sandstone

Sample No	W (mm)	D (mm)	D' (mm)	P (kN)	De2 (mm <sup>2</sup> )	De (mm)	Is (MPa)	F	Is(50) (MPa)
W1	32,77	26,29	23,36	2,1	975,17	31,23	2,1535	0,7903	1,7019
W2	40,27	30,08	24,55	4,7	1259,40	35,49	3,7319	0,8425	3,1441
W3	29,55	21,95	17,29	4,9	650,85	25,51	7,5286	0,7143	5,3777
W4	24,63	19,95	17,84	1,8	559,74	23,66	3,2158	0,6879	2,2121
W5	35,64	19,03	13,33	2,6	605,20	24,60	4,2961	0,7014	3,0135
W6	22,24	18,28	14,77	2,3	418,45	20,46	5,4964	0,6396	3,5157
W7	22,22	19,58	16,51	0,7	467,33	21,62	1,4979	0,6575	0,9849
W8	24,96	20,15	15,45	2,2	491,25	22,16	4,4784	0,6658	2,9817
W9	31,52	18,95	16,73	3,7	671,76	25,92	5,5079	0,7200	3,9656
W10	34,42	16,33	14,33	1,2	628,33	25,07	1,9098	0,7080	1,3522

Table 196. Point load strength of Stop 12 fresh saturated sandstone

Sample No	W (mm)	D (mm)	D' (mm)	P (kN)	De2 (mm2)	De (mm)	Is (MPa)	F	Is(50) (MPa)
F1	35,93	17,31	13,05	2,7	597,31	24,44	4,5203	0,6991	3,1603
F2	31,16	30,86	26,11	1,1	1036,42	32,19	1,0613	0,8024	0,8516
F3	24,02	18,55	17,06	0,2	522,01	22,85	0,3831	0,6760	0,2590
F4	27,70	23,09	17,02	4,3	600,58	24,51	7,1598	0,7001	5,0125
F5	36,82	29,78	19,40	1,1	909,95	30,17	1,2089	0,7767	0,9390
F6	25,62	17,10	15,73	1,7	513,38	22,66	3,3114	0,6732	2,2291
F7	28,82	19,55	18,42	2,5	676,26	26,01	3,6968	0,7212	2,6661
F8	37,29	21,63	18,55	1,2	881,18	29,68	1,3618	0,7705	1,0493
F9	27,29	17,61	15,73	1,2	546,84	23,38	2,1944	0,6839	1,5007
F10	22,99	19,23	15,23	1,6	446,04	21,12	3,5872	0,6499	2,3314

Table 197. Point load strength of Stop 12 weathered saturated sandstone

Sample No	W (mm)	D (mm)	D' (mm)	P (kN)	De2 (mm2)	De (mm)	Is (MPa)	F	Is(50) (MPa)
W1	31,29	18,98	15,26	5,6	608,26	24,66	9,2066	0,7023	6,4660
W2	36,69	26,95	25,13	0,9	1174,55	34,27	0,7663	0,8279	0,6344
W3	39,06	29,21	26,13	1,5	1300,18	36,06	1,1537	0,8492	0,9797
W4	32,56	22,01	17,15	0,8	711,34	26,67	1,1246	0,7304	0,8214
W5	34,07	21,80	13,56	1,7	588,52	24,26	2,8886	0,6966	2,0121
W6	29,83	20,06	13,48	0,9	512,24	22,63	1,7570	0,6728	1,1821
W7	26,86	31,84	21,35	0,6	730,52	27,03	0,8213	0,7352	0,6039
W8	25,88	18,62	14,66	0,4	483,31	21,98	0,8276	0,6631	0,5488
W9	30,07	27,47	19,33	0,8	740,45	27,21	1,0804	0,7377	0,7970
W10	29,02	24,92	16,13	0,9	596,30	24,42	1,5093	0,6988	1,0548

Table 198. Point load strength of Stop 13 fresh dry sandstone

<b>Sample No</b>	<b>W (mm)</b>	<b>D (mm)</b>	<b>D' (mm)</b>	<b>P (kN)</b>	<b>De2 (mm2)</b>	<b>De (mm)</b>	<b>Is (MPa)</b>	<b>F</b>	<b>Is(50) (MPa)</b>
F1	40,55	27,47	24,66	2,1	1273,84	35,69	1,6486	0,8449	1,3928
F2	34,51	21,41	16,35	2,5	718,78	26,81	3,4781	0,7323	2,5469
F3	27,93	22,04	14,56	2,4	518,04	22,76	4,6329	0,6747	3,1258
F4	26,15	15,52	13,10	1,2	436,39	20,89	2,7498	0,6464	1,7774
F5	29,51	14,64	10,67	1,7	401,11	20,03	4,2382	0,6329	2,6824
F6	27,13	16,58	14,01	2,1	484,19	22,00	4,3371	0,6634	2,8772
F7	31,08	14,42	10,29	3,9	407,41	20,18	9,5728	0,6354	6,0822
F8	43,47	16,71	11,94	5,5	661,19	25,71	8,3184	0,7171	5,9653
F9	27,09	20,08	15,23	2,2	525,58	22,93	4,1858	0,6771	2,8344
F10	39,68	19,96	10,73	10,0	542,38	23,29	18,4373	0,6825	12,5831

Table 199. Point load strength of Stop 13 weathered dry sandstone

<b>Sample No</b>	<b>W (mm)</b>	<b>D (mm)</b>	<b>D' (mm)</b>	<b>P (kN)</b>	<b>De2 (mm2)</b>	<b>De (mm)</b>	<b>Is (MPa)</b>	<b>F</b>	<b>Is(50) (MPa)</b>
W1	37,21	31,41	26,15	1,2	1239,54	35,21	0,9681	0,8391	0,8124
W2	36,48	32,75	32,45	2,5	1507,99	38,83	1,6578	0,8813	1,4610
W3	33,30	33,10	22,42	0,9	951,06	30,84	0,9463	0,7854	0,7432
W4	38,91	20,43	18,67	3,4	925,41	30,42	3,6740	0,7800	2,8658
W5	43,39	30,22	25,40	1,5	1403,96	37,47	1,0684	0,8657	0,9249
W6	26,46	26,32	13,48	0,5	454,37	21,32	1,1004	0,6529	0,7185
W7	22,81	18,45	15,23	1,6	442,54	21,04	3,6155	0,6486	2,3451
W8	42,25	35,64	30,56	2,8	1644,79	40,56	1,7023	0,9006	1,5332
W9	24,21	19,65	10,45	1,8	322,29	17,95	5,5851	0,5992	3,3466
W10	45,32	23,97	17,46	5,5	1008,01	31,75	5,4563	0,7969	4,3479

Table 200. Point load strength of Stop 13 fresh saturated sandstone

Sample No	W (mm)	D (mm)	D' (mm)	P (kN)	De2 (mm2)	De (mm)	Is (MPa)	F	Is(50) (MPa)
F1	27,05	15,15	11,47	1,1	395,24	19,88	2,7831	0,6306	1,7549
F2	29,28	13,95	9,21	1,2	343,53	18,53	3,4932	0,6088	2,1268
F3	33,67	27,28	17,99	0,4	771,62	27,78	0,5184	0,7454	0,3864
F4	39,06	32,94	30,19	8,0	1502,19	38,76	5,3255	0,8804	4,6888
F5	35,65	26,38	22,51	0,3	1022,27	31,97	0,2935	0,7997	0,2347
F6	32,84	21,66	14,04	0,2	587,35	24,24	0,3405	0,6962	0,2371
F7	26,58	16,04	10,94	1,2	370,43	19,25	3,2395	0,6204	2,0099
F8	33,10	17,37	9,92	1,9	418,28	20,45	4,5424	0,6396	2,9051
F9	30,37	13,09	7,92	2,1	306,41	17,50	6,8536	0,5917	4,0552
F10	30,67	24,73	20,12	0,5	786,09	28,04	0,6361	0,7488	0,4763

Table 201. Point load strength of Stop 13 weathered saturated sandstone

Sample No	W (mm)	D (mm)	D' (mm)	P (kN)	De2 (mm2)	De (mm)	Is (MPa)	F	Is(50) (MPa)
W1	38,56	19,39	14,81	3,8	727,48	26,97	5,2235	0,7345	3,8365
W2	20,58	29,44	25,18	3,6	660,13	25,69	5,4534	0,7168	3,9093
W3	40,68	23,56	21,13	1,0	1094,99	33,09	0,9132	0,8135	0,7429
W4	36,30	34,79	31,46	1,1	1454,77	38,14	0,7561	0,8734	0,6604
W5	40,05	26,44	22,62	1,0	1154,05	33,97	0,8665	0,8243	0,7142
W6	27,29	25,18	23,11	0,9	803,40	28,34	1,1202	0,7529	0,8434
W7	37,61	34,56	33,51	1,2	1605,49	40,07	0,7474	0,8952	0,6691
W8	34,21	26,35	21,82	0,1	950,91	30,84	0,1052	0,7853	0,0826
W9	36,14	25,48	24,26	1,0	1116,89	33,42	0,8953	0,8176	0,7320
W10	28,71	25,01	22,33	0,9	816,68	28,58	1,1020	0,7560	0,8331

Table 202. Point load strength of Stop 14 fresh dry sandstone in vertical direction

<b>Sample No</b>	<b>W (mm)</b>	<b>D (mm)</b>	<b>D' (mm)</b>	<b>P (kN)</b>	<b>De2 (mm<sup>2</sup>)</b>	<b>De (mm)</b>	<b>Is (MPa)</b>	<b>F</b>	<b>Is(50) (MPa)</b>
F1	24,02	21,33	15,66	9,0	479,18	21,89	18,7822	0,6617	12,4276
F2	22,51	21,37	11,77	10,0	337,51	18,37	29,6290	0,6062	17,9599
F3	29,33	17,48	12,02	5,4	449,10	21,19	12,0239	0,6510	7,8280
F4	33,17	12,28	6,45	4,3	272,54	16,51	15,7773	0,5746	9,0658
F5	34,06	16,38	12,25	11,0	531,51	23,05	20,6958	0,6790	14,0532
F6	25,23	22,2	17,6	9,0	564,06	23,75	15,9558	0,6892	10,9967
F7	32,15	18,5	13,5	8,3	552,49	23,51	15,0229	0,6856	10,3003
F8	31,1	19,2	12,3	7,3	487,70	22,08	14,9684	0,6646	9,9478
F9	33,49	13,8	9,45	4,9	403,16	20,08	12,1540	0,6337	7,7020
F10	27,59	16	10,5	9,1	367,98	19,18	24,7293	0,6194	15,3174

Table 203. Point load strength of Stop 14 fresh dry sandstone in horizontal direction

<b>Sample No</b>	<b>W (mm)</b>	<b>D (mm)</b>	<b>D' (mm)</b>	<b>P (kN)</b>	<b>De2 (mm<sup>2</sup>)</b>	<b>De (mm)</b>	<b>Is (MPa)</b>	<b>F</b>	<b>Is(50) (MPa)</b>
F1	32,17	27,60	22,75	5,3	932,32	30,53	5,6848	0,7815	4,4424
F2	21,21	18,90	17,44	0,5	471,21	21,71	1,0611	0,6589	0,6992
F3	30,79	36,98	29,71	3,6	1165,31	34,14	3,0893	0,8263	2,5526
F4	28,48	24,44	16,75	3,3	607,69	24,65	5,4304	0,7022	3,8130
F5	30,69	19,14	12,25	4,7	478,92	21,88	9,8137	0,6616	6,4926
F6	25,18	22,49	18,15	1,9	582,19	24,13	3,2636	0,6947	2,2671
F7	31,46	23,16	19,79	2,5	793,11	28,16	3,1521	0,7505	2,3657
F8	29,56	27,48	22,56	4,9	849,52	29,15	5,7680	0,7635	4,4038
F9	22,79	20,73	13,97	6,1	405,57	20,14	15,0404	0,6346	9,5453
F10	29,13	25,74	20,43	5,3	758,12	27,53	6,9910	0,7421	5,1878

Table 204. Point load strength of Stop 14 weathered dry sandstone in vertical direction

Sample No	W (mm)	D (mm)	D' (mm)	P (kN)	De2 (mm <sup>2</sup> )	De (mm)	Is (MPa)	F	Is(50) (MPa)
W1	28,49	25,59	16,02	5,5	581,41	24,11	9,4597	0,6944	6,5692
W2	25,08	16,20	11,18	3,7	357,19	18,90	10,3586	0,6148	6,3686
W3	28,37	27,57	25,13	2,2	908,20	30,14	2,4224	0,7764	1,8806
W4	27,98	25,55	15,48	5,0	551,76	23,49	9,0619	0,6854	6,2112
W5	26,15	26,13	20,18	6,0	672,24	25,93	8,9254	0,7201	6,4272
W6	29,13	28,18	22,78	6,9	845,33	29,07	8,1625	0,7626	6,2244
W7	30,41	29,55	23,15	5,1	896,80	29,95	5,6869	0,7739	4,4011
W8	27,65	25,15	18,56	4,0	653,74	25,57	6,1187	0,7151	4,3754
W9	26,13	16,48	13,7	4,5	454,36	21,32	9,9040	0,6529	6,4666
W10	25,58	18,66	12,15	4,3	395,92	19,90	10,8608	0,6308	6,8514

Table 205. Point load strength of Stop 14 weathered dry sandstone in horizontal direction

Sample No	W (mm)	D (mm)	D' (mm)	P (kN)	De2 (mm <sup>2</sup> )	De (mm)	Is (MPa)	F	Is(50) (MPa)
W1	22,50	25,22	19,85	2,5	568,95	23,85	4,3941	0,6907	3,0349
W2	27,88	9,97	6,51	0,9	231,21	15,21	3,8926	0,5515	2,1466
W3	24,86	25,77	14,01	3,3	443,68	21,06	7,4378	0,6491	4,8275
W4	28,38	13,64	11,19	1,5	404,55	20,11	3,7078	0,6342	2,3517
W5	15,18	13,2	9,08	2,1	175,59	13,25	11,9600	0,5148	6,1570
W6	23,25	20,6	14,2	1,6	419,09	20,47	3,8178	0,6399	2,4429
W7	26,98	26	23,5	2,5	806,99	28,41	3,0979	0,7538	2,3351
W8	23,49	19,2	15	3,4	449,15	21,19	7,5698	0,6510	4,9283
W9	27,18	23,2	18,2	5,3	628,43	25,07	8,4337	0,7081	5,9717
W10	25,55	22,5	17,4	2,6	567,31	23,82	4,5831	0,6902	3,1632

Table 206. Point load strength of Stop 14 fresh saturated sandstone in vertical direction

Sample No	W (mm)	D (mm)	D' (mm)	P (kN)	De2 (mm <sup>2</sup> )	De (mm)	Is (MPa)	F	Is(50) (MPa)
F1	31,38	27,86	18,90	3,0	755,52	27,49	3,9708	0,7414	2,9441
F2	25,66	25,02	14,81	2,7	484,11	22,00	5,5773	0,6634	3,6997
F3	24,58	21,73	11,96	2,3	374,49	19,35	6,1416	0,6221	3,8209
F4	20,74	14,06	9,54	2,7	252,05	15,88	10,7121	0,5635	6,0362
F5	20,64	14,72	12,15	0,5	319,46	17,87	1,5651	0,5979	0,9358
F6	26,26	18,73	14,01	2,7	468,67	21,65	5,7610	0,6580	3,7908
F7	20,10	15,02	10,58	3,7	270,90	16,46	13,6581	0,5737	7,8362
F8	18,23	18,37	13,43	3,0	311,88	17,66	9,6190	0,5943	5,7166
F9	17,24	18,54	13,12	1,7	288,14	16,97	5,8999	0,5827	3,4377
F10	15,13	23,60	18,55	1,6	357,53	18,91	4,4751	0,6150	2,7520

Table 207. Point load strength of Stop 14 fresh saturated sandstone in horizontal direction

Sample No	W (mm)	D (mm)	D' (mm)	P (kN)	De2 (mm <sup>2</sup> )	De (mm)	Is (MPa)	F	Is(50) (MPa)
F1	21,71	21,24	14,89	2,7	411,80	20,29	6,5566	0,6371	4,1770
F2	28,92	29,06	21,61	1,2	796,13	28,22	1,5073	0,7512	1,1323
F3	30,72	25,68	19,71	2,8	771,33	27,77	3,6301	0,7453	2,7055
F4	25,37	13,23	11,43	2,1	369,40	19,22	5,6849	0,6200	3,5246
F5	18,80	14,01	10,55	2,7	252,66	15,90	10,6862	0,5638	6,0252
F6	19,21	19,85	15,82	1,5	387,14	19,68	3,8746	0,6273	2,4306
F7	27,69	9,99	7,12	0,1	251,15	15,85	0,3982	0,5630	0,2242
F8	28,27	20,92	15,16	2,1	545,95	23,37	3,8465	0,6836	2,6295
F9	26,56	19,09	17,19	1,7	581,61	24,12	2,9229	0,6945	2,0300
F10	23,12	19,14	14,03	2,5	413,21	20,33	6,0501	0,6376	3,8577

Table 208. Point load strength of Stop 14 weathered saturated sandstone in vertical direction

Sample No	W (mm)	D (mm)	D' (mm)	P (kN)	De2 (mm <sup>2</sup> )	De (mm)	Is (MPa)	F	Is(50) (MPa)
W1	26,26	20,39	16,63	0,8	556,31	23,59	1,4380	0,6868	0,9877
W2	41,62	18,83	13,32	3,4	706,21	26,57	4,8144	0,7290	3,5099
W3	36,53	16,16	8,63	4,0	401,60	20,04	9,9602	0,6331	6,3057
W4	37,48	27,26	18,63	1,8	889,49	29,82	2,0236	0,7723	1,5629
W5	27,35	20,55	12,54	5,6	436,90	20,90	12,8175	0,6466	8,2873
W6	31,25	21,67	15,32	5,3	609,87	24,70	8,6903	0,7028	6,1075
W7	39,46	20,21	12,26	5,3	616,28	24,82	8,6000	0,7046	6,0598
W8	26,06	16,62	8,63	0,2	286,49	16,93	0,6981	0,5818	0,4062
W9	45,23	12,14	9,50	0,3	547,37	23,40	0,5481	0,6840	0,3749
W10	13,25	12,35	10,15	1,8	171,32	13,09	10,5066	0,5116	5,3756
W11	25,87	11,67	6,50	1,4	214,21	14,64	6,5356	0,5410	3,5360
W12	20,89	8,68	4,91	0,3	130,66	11,43	2,2960	0,4781	1,0978
W13	30,87	18,00	13,07	3,0	513,98	22,67	5,8369	0,6734	3,9303
W14	27,96	12,18	7,68	3,7	273,54	16,54	13,5261	0,5751	7,7794
W15	27,26	19,81	14,31	2,8	496,93	22,29	5,6346	0,6677	3,7623
W16	21,06	19,90	10,97	0,7	294,30	17,16	2,3785	0,5858	1,3932
W17	22,84	14,19	8,92	0,6	259,53	16,11	2,3119	0,5676	1,3123
W18	18,81	16,89	13,92	1,0	333,55	18,26	2,9981	0,6044	1,8120
W19	19,94	14,76	10,10	0,4	256,55	16,02	1,5591	0,5660	0,8825
W20	23,49	10,10	5,13	3,0	153,51	12,39	19,5430	0,4978	9,7283
W21	20,52	9,40	5,78	2,5	151,09	12,29	16,5464	0,4958	8,2041
W22	20,14	10,19	5,81	1,7	149,06	12,21	11,4047	0,4941	5,6356

Table 209. Point load strength of Stop 14 weathered saturated sandstone in horizontal direction

Sample No	W (mm)	D (mm)	D' (mm)	P (kN)	De2 (mm <sup>2</sup> )	De (mm)	Is (MPa)	F	Is(50) (MPa)
W1	26,40	25,54	17,97	1,2	604,34	24,58	1,9856	0,7012	1,3923
W2	34,15	26,83	22,44	1,1	976,21	31,24	1,1268	0,7905	0,8907
W3	31,14	20,18	17,50	0,2	694,20	26,35	0,2881	0,7259	0,2091
W4	15,99	13,75	11,63	0,4	236,90	15,39	1,6885	0,5548	0,9368
W5	18,60	26,06	21,28	1,0	504,21	22,45	1,9833	0,6701	1,3291
W6	18,07	20,60	13,33	0,9	306,84	17,52	2,9331	0,5919	1,7361
W7	17,91	15,00	11,57	2,4	263,97	16,25	9,0918	0,5700	5,1827
W8	12,25	16,41	13,65	0,8	213,01	14,59	3,7557	0,5403	2,0291
W9	23,34	13,76	9,28	1,3	275,92	16,61	4,7116	0,5764	2,7157
W10	15,82	14,98	8,37	2,1	168,68	12,99	12,4496	0,5097	6,3451
W11	17,29	23,02	19,14	0,4	421,57	20,53	0,9488	0,6408	0,6080
W12	30,16	16,48	13,55	1,1	520,60	22,82	2,1130	0,6755	1,4274
W13	25,61	16,17	9,62	0,5	313,84	17,72	1,5931	0,5952	0,9483
W14	19,71	13,89	8,54	1,0	214,42	14,64	4,6636	0,5412	2,5238
W15	28,19	23,67	19,26	4,4	691,64	26,30	6,3617	0,7252	4,6138
W16	18,47	21,00	14,75	3,1	347,05	18,63	8,9325	0,6104	5,4524
W17	22,28	16,29	12,75	4,5	361,87	19,02	12,4353	0,6168	7,6703
W18	18,59	13,98	10,47	1,1	247,95	15,75	4,4365	0,5612	2,4897
W19	19,21	40,98	35,39	2,3	866,04	29,43	2,6558	0,7672	2,0375
W20	17,40	19,01	16,38	1,2	363,07	19,05	3,3051	0,6173	2,0403
W21	13,13	15,05	10,95	1,3	183,15	13,53	7,0980	0,5203	3,6928

Table 210. Point load strength of Stop 15 fresh dry sandstone in vertical direction

Sample No	W (mm)	D (mm)	D' (mm)	P (kN)	De2 (mm <sup>2</sup> )	De (mm)	Is (MPa)	F	Is(50) (MPa)
F1	30,77	23,84	17,16	5,3	672,63	25,94	7,8795	0,7202	5,6749
F2	47,79	28,86	22,94	7,0	1396,56	37,37	5,0123	0,8645	4,3333
F3	39,05	22,06	13,70	5,6	681,51	26,11	8,2171	0,7226	5,9374
F4	44,93	21,03	10,77	9,0	616,43	24,83	14,6002	0,7047	10,2883
F5	33,71	26,81	18,99	13,0	815,48	28,56	15,9415	0,7557	12,0475
F6	23,99	19,53	11,55	3,7	352,97	18,79	10,4824	0,6130	6,4255
F7	31,55	24,89	19,55	7,1	785,74	28,03	9,0361	0,7487	6,7658
F8	45,85	20,13	15,47	6,9	903,57	30,06	7,6364	0,7754	5,9210
F9	21,59	17,55	12,63	6,1	347,37	18,64	17,5608	0,6105	10,7215
F10	41,05	25,13	21,58	10,5	1128,48	33,59	9,3045	0,8197	7,6266

Table 211. Point load strength of Stop 15 fresh dry sandstone in horizontal direction

Sample No	W (mm)	D (mm)	D' (mm)	P (kN)	De2 (mm <sup>2</sup> )	De (mm)	Is (MPa)	F	Is(50) (MPa)
F1	39,75	27,08	17,29	5,4	875,51	29,59	6,1678	0,7693	4,7447
F2	32,77	13,75	8,15	3,5	340,22	18,45	10,2874	0,6074	6,2483
F3	27,07	22,35	17,79	4,5	613,47	24,77	7,3353	0,7038	5,1628
F4	31,10	35,19	27,53	11,0	1090,68	33,03	10,0855	0,8127	8,1966
F5	38,10	36,38	24,58	10,0	1192,99	34,54	8,3823	0,8311	6,9669
F6	42,39	19,50	14,07	2,4	759,78	27,56	3,1588	0,7425	2,3454
F7	42,49	33,25	23,79	12,0	1287,69	35,88	9,3190	0,8472	7,8947
F8	44,10	26,66	19,70	8,0	1106,71	33,27	7,2286	0,8157	5,8963
F9	25,18	20,66	15,73	5,0	504,56	22,46	9,9096	0,6703	6,6420
F10	38,46	26,41	16,58	5,5	812,31	28,50	6,7708	0,7550	5,1119

Table 212. Point load strength of Stop 15 weathered dry sandstone in vertical direction

Sample No	W (mm)	D (mm)	D' (mm)	P (kN)	De2 (mm <sup>2</sup> )	De (mm)	Is (MPa)	F	Is(50) (MPa)
W1	42,39	12,47	5,15	3,7	278,10	16,68	13,3046	0,5775	7,6836
W2	42,52	41,97	30,07	14,0	1628,76	40,36	8,5955	0,8984	7,7224
W3	41,59	40,15	31,46	10,1	1666,78	40,83	6,0596	0,9036	5,4756
W4	40,95	39,79	32,79	9,2	1710,51	41,36	5,3785	0,9095	4,8917
W5	39,29	35,78	28,91	11,2	1446,97	38,04	7,7403	0,8722	6,7513
W6	38,23	29,19	22,45	13,4	1093,33	33,07	12,2561	0,8132	9,9668
W7	44,58	40,72	32,74	12,3	1859,30	43,12	6,6154	0,9287	6,1434
W8	41,78	39,46	33,51	9,8	1783,50	42,23	5,4948	0,9190	5,0499
W9	42,19	40,17	34,71	11,9	1865,50	43,19	6,3790	0,9294	5,9288
W10	37,46	35,38	29,11	14,2	1389,12	37,27	10,2223	0,8634	8,8257

Table 213. Point load strength of Stop 15 weathered dry sandstone in horizontal direction

Sample No	W (mm)	D (mm)	D' (mm)	P (kN)	De2 (mm <sup>2</sup> )	De (mm)	Is (MPa)	F	Is(50) (MPa)
W1	18,27	45,97	40,28	5,5	937,47	30,62	5,8668	0,7825	4,5910
W2	34,14	19,86	14,69	3,4	638,87	25,28	5,3219	0,7110	3,7838
W3	30,17	27,92	22,60	5,5	868,59	29,47	6,3321	0,7677	4,8615
W4	25,04	19,94	12,33	2,8	393,30	19,83	7,1192	0,6298	4,4836
W5	24,19	18,46	13,59	3,2	418,78	20,46	7,6412	0,6398	4,8885
W6	36,15	21,99	16,74	5,1	770,89	27,76	6,6157	0,7452	4,9299
W7	20,46	43,15	39,46	6,3	1028,47	32,07	6,1256	0,8009	4,9058
W8	33,15	30,49	25,41	9,7	1073,05	32,76	9,0397	0,8094	7,3168
W9	52,18	43,56	38,96	2,6	2589,72	50,89	1,0040	1,0089	1,0129
W10	25,78	21,49	16,22	4,8	532,68	23,08	9,0111	0,6794	6,1222

Table 214. Point load strength of Stop 15 fresh saturated sandstone in vertical direction

Sample No	W (mm)	D (mm)	D' (mm)	P (kN)	De2 (mm2)	De (mm)	Is (MPa)	F	Is(50) (MPa)
F1	37,47	15,62	9,12	1,1	435,32	20,86	2,5269	0,6460	1,6323
F2	27,86	28,35	19,55	5,1	693,84	26,34	7,3504	0,7258	5,3351
F3	40,42	8,74	4,37	1,8	225,01	15,00	7,9995	0,5477	4,3816
F4	36,02	12,49	8,51	3,5	390,48	19,76	8,9632	0,6287	5,6348
F5	34,70	20,59	14,24	2,8	629,46	25,09	4,4482	0,7084	3,1510
F6	34,92	20,51	13,41	10,0	596,53	24,42	16,7636	0,6989	11,7163
F7	29,81	29,28	19,86	5,4	754,17	27,46	7,1602	0,7411	5,3065
F8	39,62	13,44	7,79	3,9	393,17	19,83	9,9193	0,6297	6,2466
F9	17,31	17,07	12,75	3,8	281,15	16,77	13,5159	0,5791	7,8270
F10	22,94	15,93	9,99	0,5	291,94	17,09	1,7127	0,5846	1,0012
F11	14,67	13,24	8,66	3,7	161,84	12,72	22,8625	0,5044	11,5321
F12	15,20	14,22	9,20	1,0	178,14	13,35	5,6136	0,5167	2,9003
F13	24,82	8,45	4,61	1,9	145,76	12,07	13,0353	0,4914	6,4054
F14	14,82	13,00	5,56	1,3	104,97	10,25	12,3848	0,4527	5,6062
F15	19,78	10,08	5,18	3,7	130,52	11,42	28,3475	0,4780	13,5504

Table 215. Point load strength of Stop 15 fresh saturated sandstone in horizontal direction

Sample No	W (mm)	D (mm)	D' (mm)	P (kN)	De2 (mm2)	De (mm)	Is (MPa)	F	Is(50) (MPa)
F1	32,37	16,70	11,39	2,7	469,67	21,67	5,7487	0,6584	3,7847
F2	26,04	13,17	8,48	2,2	281,30	16,77	7,8209	0,5792	4,5296
F3	15,62	20,34	14,30	4,3	284,54	16,87	15,1120	0,5808	8,7775
F4	15,24	14,27	12,55	3,7	243,65	15,61	15,1860	0,5587	8,4849
F5	19,21	17,62	12,50	0,4	305,89	17,49	1,3077	0,5914	0,7734
F6	15,84	14,67	8,24	0,5	166,27	12,89	3,0072	0,5078	1,5271
F7	26,25	14,74	12,64	0,6	422,68	20,56	1,4195	0,6412	0,9103
F8	25,33	14,56	9,51	1,6	306,86	17,52	5,2140	0,5919	3,0862
F9	19,20	11,80	6,41	1,0	156,78	12,52	6,3784	0,5004	3,1919
F10	19,84	20,01	14,12	5,6	356,87	18,89	15,6921	0,6147	9,6455

Table 216. Point load strength of Stop 15 weathered saturated sandstone in vertical direction

Sample No	W (mm)	D (mm)	D' (mm)	P (kN)	De2 (mm2)	De (mm)	Is (MPa)	F	Is(50) (MPa)
W1	43,54	39,24	29,00	7,0	1608,48	40,11	4,3519	0,8956	3,8976
W2	44,15	38,96	19,58	4,3	1101,22	33,18	3,9048	0,8147	3,1811
W3	38,84	23,77	15,50	5,6	766,90	27,69	7,3021	0,7442	5,4343
W4	24,82	24,49	14,57	4,9	460,67	21,46	10,6366	0,6552	6,9689
W5	23,79	13,53	8,47	3,3	256,69	16,02	12,8560	0,5661	7,2773
W6	35,24	24,85	15,96	5,6	716,47	26,77	7,8161	0,7317	5,7188
W7	37,45	19,77	11,83	1,2	564,37	23,76	2,1263	0,6893	1,4656
W8	44,15	43,55	38,13	9,3	2144,51	46,31	4,3367	0,9624	4,1735
W9	39,15	35,13	31,89	5,1	1590,44	39,88	3,2067	0,8931	2,8638
W10	38,79	31,55	27,46	7,3	1356,91	36,84	5,3799	0,8583	4,6177

Table 217. Point load strength of Stop 15 weathered saturated sandstone in horizontal direction

Sample No	W (mm)	D (mm)	D' (mm)	P (kN)	De2 (mm2)	De (mm)	Is (MPa)	F	Is(50) (MPa)
W1	37,04	37,87	16,73	2,9	789,40	28,10	3,6737	0,7496	2,7538
W2	44,31	36,42	25,27	4,1	1426,39	37,77	2,8744	0,8691	2,4982
W3	46,27	19,48	13,70	3,0	807,51	28,42	3,7151	0,7539	2,8007
W4	25,44	13,93	13,58	0,5	440,10	20,98	1,1361	0,6477	0,7359
W5	38,95	15,08	11,63	1,2	577,06	24,02	2,0795	0,6931	1,4414
W6	25,18	16,38	9,94	0,8	318,84	17,86	2,5091	0,5976	1,4994
W7	36,96	13,13	9,06	1,5	426,57	20,65	3,5164	0,6427	2,2600
W8	44,42	28,07	25,58	3,5	1447,47	38,05	2,4180	0,8723	2,1092
W9	36,08	25,74	15,72	1,8	722,52	26,88	2,4913	0,7332	1,8266
W10	23,60	18,63	13,71	1,0	412,17	20,30	2,4262	0,6372	1,5460
W11	31,68	27,98	20,10	3,5	811,17	28,48	4,3148	0,7547	3,2565
W12	28,94	19,46	13,78	3,9	508,02	22,54	7,6769	0,6714	5,1543
W13	22,73	20,18	13,93	4,5	403,35	20,08	11,1566	0,6338	7,0708
W14	24,44	16,66	12,65	3,3	393,84	19,85	8,3790	0,6300	5,2788
W15	23,89	17,90	11,95	1,0	363,68	19,07	2,7497	0,6176	1,6982
W16	25,94	25,00	20,16	1,0	666,18	25,81	1,5011	0,7185	1,0785

Table 218. Point load strength of Stop 16 fresh dry sandstone in vertical direction

<b>Sample No</b>	<b>W (mm)</b>	<b>D (mm)</b>	<b>D' (mm)</b>	<b>P (kN)</b>	<b>De2 (mm)<sup>2</sup></b>	<b>De (mm)</b>	<b>Is (MPa)</b>	<b>F</b>	<b>Is(50) (MPa)</b>
F1	34,85	25,79	18,53	5,6	822,64	28,68	6,8074	0,7574	5,1558
F2	38,50	15,92	12,08	5,0	592,46	24,34	8,4394	0,6977	5,8883
F3	25,09	17,27	12,76	2,8	407,83	20,19	6,8656	0,6355	4,3633
F4	35,33	24,08	17,76	3,4	799,31	28,27	4,2537	0,7520	3,1986
F5	28,13	26,85	19,50	5,7	698,77	26,43	8,1572	0,7271	5,9311
F6	34,69	24,82	16,93	9,0	748,16	27,35	12,0296	0,7396	8,8974
F7	28,04	20,84	15,58	2,9	556,51	23,59	5,2110	0,6869	3,5794
F8	24,41	21,15	20,45	2,4	635,90	25,22	3,7742	0,7102	2,6803
F9	30,03	30,01	24,40	4,0	933,42	30,55	4,2853	0,7817	3,3498
F10	23,67	21,28	18,19	2,6	548,48	23,42	4,7404	0,6844	3,2443
F11	30,47	12,32	7,34	4,1	284,90	16,88	14,3908	0,5810	8,3613
F12	40,98	14,68	9,96	3,1	519,95	22,80	5,9621	0,6753	4,0263
F13	28,57	19,55	12,86	4,6	468,04	21,63	9,8283	0,6578	6,4649
F14	26,30	15,38	10,19	3,5	341,40	18,48	10,2520	0,6079	6,2321
F15	26,26	12,03	8,60	3,2	287,69	16,96	11,1231	0,5824	6,4785
F16	29,53	20,48	17,76	5,3	668,09	25,85	7,9330	0,7190	5,7038

Table 219. Point load strength of Stop 16 fresh dry sandstone in horizontal direction

Sample No	W (mm)	D (mm)	D' (mm)	P (kN)	De2 (mm) <sup>2</sup>	De (mm)	Is (MPa)	F	Is(50) (MPa)
F1	26,51	24,48	20,31	1,5	685,88	26,19	2,1870	0,7237	1,5828
F2	43,49	39,52	28,77	2,2	1593,89	39,92	1,3803	0,8936	1,2334
F3	28,54	28,03	24,16	3,5	878,38	29,64	3,9846	0,7699	3,0678
F4	26,37	26,80	22,00	5,1	739,03	27,19	6,9009	0,7374	5,0885
F5	23,03	14,86	10,35	1,2	303,64	17,43	3,9520	0,5903	2,3330
F6	23,68	23,89	21,08	2,1	635,89	25,22	3,3025	0,7102	2,3453
F7	28,20	19,08	17,25	1,4	619,68	24,89	2,2592	0,7056	1,5941
F8	31,19	9,06	4,93	0,7	195,88	14,00	3,5736	0,5291	1,8907
F9	27,15	23,43	19,25	0,4	665,78	25,80	0,6008	0,7184	0,4316
F10	34,29	26,76	19,03	0,6	831,26	28,83	0,7218	0,7594	0,5481
F11	25,62	30,52	23,36	5,3	762,40	27,61	6,9517	0,7431	5,1660
F12	23,40	12,01	7,28	1,7	217,01	14,73	7,8338	0,5428	4,2521
F13	24,73	19,30	15,26	3,0	480,74	21,93	6,2404	0,6622	4,1324
F14	21,34	20,49	13,46	1,5	365,91	19,13	4,0994	0,6185	2,5356

Table 220. Point load strength of Stop 16 weathered dry sandstone in vertical direction

Sample No	W (mm)	D (mm)	D' (mm)	P (kN)	De2 (mm) <sup>2</sup>	De (mm)	Is (MPa)	F	Is(50) (MPa)
W1	39,72	11,15	5,87	4,0	297,01	17,23	13,4674	0,5871	7,9066
W2	32,79	26,48	25,29	0,7	1056,38	32,50	0,6626	0,8063	0,5343
W3	43,55	14,25	7,78	1,2	431,62	20,78	2,7802	0,6446	1,7921
W4	35,61	13,45	7,59	2,1	344,31	18,56	6,0992	0,6092	3,7156
W5	37,16	12,39	8,82	3,6	417,52	20,43	8,6224	0,6393	5,5120
W6	46,18	26,38	20,24	9,0	1190,68	34,51	7,5587	0,8307	6,2793
W7	37,48	34,51	28,45	5,5	1358,35	36,86	4,0490	0,8586	3,4763
W8	37,52	30,84	23,62	5,5	1128,95	33,60	4,8718	0,8198	3,9937
W9	40,17	23,35	19,62	5,4	1003,99	31,69	5,3785	0,7961	4,2816
W10	39,12	17,71	15,90	2,9	792,37	28,15	3,6599	0,7503	2,7461
W11	33,75	9,42	5,78	2,2	248,50	15,76	8,8530	0,5615	4,9709
W12	19,93	20,76	16,50	2,0	418,91	20,47	4,7743	0,6398	3,0546
W13	30,37	10,02	6,44	1,9	249,15	15,78	7,6259	0,5619	4,2847

Table 221. Point load strength of Stop 16 weathered dry sandstone in horizontal direction

Sample No	W (mm)	D (mm)	D' (mm)	P (kN)	De2 (mm) <sup>2</sup>	De (mm)	Is (MPa)	F	Is(50) (MPa)
W1	32,67	34,35	27,75	3,3	1154,89	33,98	2,8574	0,8244	2,3557
W2	25,64	28,76	17,08	2,3	557,87	23,62	4,1228	0,6873	2,8336
W3	49,73	19,08	14,02	0,3	888,17	29,80	0,3378	0,7720	0,2608
W4	46,83	23,44	22,73	0,3	1355,98	36,82	0,2212	0,8582	0,1899
W5	33,82	29,43	26,99	3,2	1162,80	34,10	2,7520	0,8258	2,2727
W6	32,49	24,58	17,03	1,1	704,85	26,55	1,5606	0,7287	1,1372
W7	25,40	19,51	16,35	2,9	529,03	23,00	5,4817	0,6782	3,7179
W8	26,61	24,90	22,61	0,2	766,44	27,68	0,2609	0,7441	0,1942
W9	32,92	22,63	16,61	3,0	696,56	26,39	4,3069	0,7265	3,1291
W10	25,35	30,10	27,37	3,5	883,86	29,73	3,9599	0,7711	3,0535
W11	33,37	26,60	23,27	3,4	989,20	31,45	3,4371	0,7931	2,7260
W12	29,31	20,19	15,25	2,3	569,40	23,86	4,0394	0,6908	2,7905
W13	40,33	38,47	36,13	1,9	1856,21	43,08	1,0236	0,9283	0,9502

Table 222. Point load strength of Stop 16 fresh saturated sandstone in vertical direction

Sample No	W (mm)	D (mm)	D' (mm)	P (kN)	De2 (mm) <sup>2</sup>	De (mm)	Is (MPa)	F	Is(50) (MPa)
F1	47,51	22,29	11,72	2,7	709,32	26,63	3,8065	0,7298	2,7781
F2	28,66	24,62	14,95	1,7	545,82	23,36	3,1146	0,6836	2,1290
F3	35,74	19,48	13,56	1,3	617,37	24,85	2,1057	0,7049	1,4844
F4	40,07	29,13	24,58	3,6	1254,68	35,42	2,8693	0,8417	2,4150
F5	40,78	21,15	13,69	2,3	711,18	26,67	3,2341	0,7303	2,3619
F6	43,19	27,19	23,20	1,3	1276,44	35,73	1,0185	0,8453	0,8609
F7	22,72	24,73	15,48	1,7	448,03	21,17	3,7944	0,6506	2,4688
F8	38,08	23,38	13,59	2,7	659,24	25,68	4,0956	0,7166	2,9349
F9	38,89	24,60	16,33	2,7	809,01	28,44	3,3374	0,7542	2,5172
F10	25,76	10,15	6,78	1,2	222,49	14,92	5,3936	0,5462	2,9459
F11	27,69	13,23	7,69	1,0	271,26	16,47	3,6866	0,5739	2,1158

Table 223. Point load strength of Stop 16 fresh saturated sandstone in horizontal direction

Sample No	W (mm)	D (mm)	D' (mm)	P (kN)	De2 (mm) <sup>2</sup>	De (mm)	Is (MPa)	F	Is(50) (MPa)
F1	25,75	43,79	35,88	1,2	1176,96	34,31	1,0196	0,8283	0,8446
F2	21,88	25,36	21,48	0,7	598,70	24,47	1,1692	0,6995	0,8179
F3	23,57	23,47	18,81	0,9	564,78	23,77	1,5935	0,6894	1,0986
F4	26,77	33,78	15,00	1,6	511,53	22,62	3,1279	0,6726	2,1037
F5	23,85	37,50	33,33	2,6	1012,64	31,82	2,5676	0,7978	2,0483
F6	27,65	25,67	15,52	1,4	546,66	23,38	2,5610	0,6838	1,7513
F7	25,42	19,82	15,01	1,4	486,06	22,05	2,8803	0,6640	1,9126
F8	22,31	22,56	17,86	1,2	507,59	22,53	2,3641	0,6713	1,5869
F9	28,15	23,09	15,14	3,1	542,92	23,30	5,7099	0,6827	3,8979
F10	20,61	23,43	12,98	0,8	340,79	18,46	2,3475	0,6076	1,4264
F11	26,80	22,12	15,47	2,0	528,15	22,98	3,7868	0,6780	2,5673

Table 224. Point load strength of Stop 16 weathered saturated sandstone in vertical direction

Sample No	W (mm)	D (mm)	D' (mm)	P (kN)	De2 (mm) <sup>2</sup>	De (mm)	Is (MPa)	F	Is(50) (MPa)
W1	44,65	26,86	20,21	4,0	1149,52	33,90	3,4797	0,8235	2,8654
W2	35,32	28,60	20,64	1,9	928,67	30,47	2,0459	0,7807	1,5973
W3	32,92	25,44	17,70	3,5	742,27	27,24	4,7152	0,7382	3,4807
W4	38,80	22,10	14,50	2,9	716,69	26,77	4,0464	0,7317	2,9608
W5	44,66	27,99	21,64	3,3	1231,14	35,09	2,6804	0,8377	2,2454
W6	44,12	23,82	15,21	4,1	854,86	29,24	4,7961	0,7647	3,6676
W7	43,07	20,40	12,49	2,0	685,28	26,18	2,9185	0,7236	2,1118
W8	37,50	16,15	10,61	1,5	506,85	22,51	2,9595	0,6710	1,9859
W9	38,86	28,20	24,18	1,8	1196,99	34,60	1,5038	0,8318	1,2509
W10	52,65	17,19	15,40	1,9	1032,88	32,14	1,8395	0,8017	1,4748
W11	35,30	35,77	31,54	2,5	1418,30	37,66	1,7627	0,8679	1,5298
W12	35,71	9,82	5,89	0,9	267,94	16,37	3,3590	0,5722	1,9219
W13	27,55	16,21	6,86	1,1	240,76	15,52	4,5690	0,5571	2,5452
W14	25,19	13,94	9,08	1,5	291,37	17,07	5,1481	0,5843	3,0080

Table 225. Point load strength of Stop 16 weathered saturated sandstone in horizontal direction

Sample No	W (mm)	D (mm)	D' (mm)	P (kN)	De2 (mm)2	De (mm)	Is (MPa)	F	Is(50) (MPa)
W1	38,77	39,60	32,56	2,3	1608,09	40,10	1,4303	0,8956	1,2809
W2	20,71	32,73	31,15	0,0	821,80	28,67	0,0000	0,7572	0,0000
W3	35,70	46,74	37,80	4,8	1719,06	41,46	2,7922	0,9106	2,5427
W4	47,73	22,09	19,68	1,1	1196,59	34,59	0,9193	0,8318	0,7646
W5	26,82	27,60	26,75	0,7	913,93	30,23	0,7659	0,7776	0,5956
W6	26,75	20,43	15,25	0,7	519,67	22,80	1,3470	0,6752	0,9095
W7	23,79	18,86	19,64	1,0	595,20	24,40	1,6801	0,6985	1,1736
W8	17,46	20,06	15,80	1,4	351,42	18,75	3,9838	0,6123	2,4393
W9	24,84	23,58	17,55	1,0	555,34	23,57	1,8007	0,6865	1,2362
W10	20,86	25,64	19,60	0,4	520,84	22,82	0,7680	0,6756	0,5189
W11	27,05	20,02	13,55	1,5	466,91	21,61	3,2126	0,6574	2,1119

Table 226. Point load strength of Stop 17 fresh dry sandstone in vertical direction

Sample No	W (mm)	D (mm)	D' (mm)	P (kN)	De2 (mm)2	De (mm)	Is (Mpa)	F	Is(50) (Mpa)
F1	15,16	15,08	11,21	1,6	216,49	14,71	7,3907	0,5425	4,0092
F2	21,30	19,88	17,86	2,1	484,61	22,01	4,3334	0,6635	2,8754
F3	26,07	8,06	5,95	1,8	197,60	14,06	9,1093	0,5302	4,8300
F4	21,08	39,83	17,28	1,9	464,03	21,54	4,0946	0,6564	2,6876
F5	30,01	25,92	17,13	1,8	654,87	25,59	2,7486	0,7154	1,9664
F6	32,36	21,47	16,23	2,1	669,05	25,87	3,1388	0,7192	2,2576
F7	30,42	13,14	9,64	2,1	373,57	19,33	5,6215	0,6217	3,4951
F8	22,90	18,46	11,29	1,4	329,35	18,15	4,2508	0,6025	2,5609
F9	22,06	16,24	16,18	1,8	454,69	21,32	3,9588	0,6530	2,5852
F10	15,40	18,42	12,96	1,6	254,25	15,95	6,2931	0,5647	3,5538
F11	24,59	14,44	9,67	2,0	302,91	17,40	6,6026	0,5900	3,8955

Table 227. Point load strength of Stop 17 fresh dry sandstone in horizontal direction

<b>Sample No</b>	<b>W (mm)</b>	<b>D (mm)</b>	<b>D' (mm)</b>	<b>P (kN)</b>	<b>De2 (mm2)</b>	<b>De (mm)</b>	<b>Is (Mpa)</b>	<b>F</b>	<b>Is(50) (Mpa)</b>
F1	28,88	14,17	10,85	0,8	399,17	19,98	2,0042	0,6321	1,2669
F2	24,21	18,17	16,15	0,9	498,08	22,32	1,8069	0,6681	1,2072
F3	36,62	19,97	15,17	1,1	707,68	26,60	1,5544	0,7294	1,1338
F4	17,94	12,46	11,18	1,0	255,50	15,98	3,9139	0,5654	2,2129
F5	23,82	10,92	7,85	0,9	238,20	15,43	3,7783	0,5556	2,0992
F6	19,55	20,37	17,90	2,3	445,79	21,11	5,1594	0,6498	3,3527
F7	30,84	17,67	10,39	2,0	408,19	20,20	4,8997	0,6357	3,1146

Table 228. Point load strength of Stop 17 weathered dry sandstone in vertical direction

<b>Sample No</b>	<b>W (mm)</b>	<b>D (mm)</b>	<b>D' (mm)</b>	<b>P (kN)</b>	<b>De2 (mm2)</b>	<b>De (mm)</b>	<b>Is (Mpa)</b>	<b>F</b>	<b>Is(50) (Mpa)</b>
W1	33,32	28,82	18,24	1,7	774,21	27,82	2,1958	0,7460	1,6380
W2	29,15	24,10	19,77	1,4	734,13	27,09	1,9070	0,7361	1,4038
W3	21,70	20,98	18,84	1,8	520,80	22,82	3,4562	0,6756	2,3350
W4	24,87	19,43	15,33	1,5	485,68	22,04	3,0885	0,6639	2,0504
W5	34,08	9,03	8,17	1,3	354,69	18,83	3,6651	0,6137	2,2494
W6	38,68	17,20	10,87	1,4	535,61	23,14	2,6139	0,6803	1,7783
W7	19,58	17,68	15,13	1,4	377,38	19,43	3,7098	0,6233	2,3124
W8	27,03	23,87	15,97	1,9	549,90	23,45	3,4552	0,6848	2,3662
W9	32,69	32,02	27,56	1,6	1147,69	33,88	1,3941	0,8231	1,1475
W10	20,66	18,46	11,84	1,3	311,61	17,65	4,1719	0,5942	2,4788

Table 229. Point load strength of Stop 17 weathered dry sandstone in horizontal direction

Sample No	W (mm)	D (mm)	D' (mm)	P (kN)	De2 (mm <sup>2</sup> )	De (mm)	Is (Mpa)	F	Is(50) (Mpa)
W1	30,41	19,92	14,66	0,9	567,91	23,83	1,5848	0,6904	1,0941
W2	28,93	12,80	8,19	1,1	301,83	17,37	3,6444	0,5895	2,1483
W3	22,28	17,91	16,15	0,8	458,37	21,41	1,7453	0,6544	1,1421
W4	21,96	19,13	18,59	1,1	520,05	22,80	2,1152	0,6753	1,4285
W5	15,23	16,49	15,11	1,2	293,15	17,12	4,0934	0,5852	2,3954
W6	150,50	14,09	11,37	1,4	2179,85	46,69	0,6422	0,9663	0,6206
W7	15,33	10,88	9,95	1,1	194,31	13,94	5,6611	0,5280	2,9891
W8	15,12	18,66	15,38	1,5	296,24	17,21	5,0635	0,5867	2,9708

Table 230. Point load strength of Stop 17 fresh saturated sandstone in vertical direction

Sample No	W (mm)	D (mm)	D' (mm)	P (kN)	De2 (mm <sup>2</sup> )	De (mm)	Is (Mpa)	F	Is(50) (Mpa)
F1	42,03	20,07	19,55	1,4	1046,73	32,35	1,3375	0,8044	1,0759
F2	26,32	20,19	16,36	1,2	548,53	23,42	2,1877	0,6844	1,4973
F3	26,88	28,63	23,18	2,2	793,73	28,17	2,7717	0,7506	2,0806
F4	25,37	15,12	9,99	1,4	322,86	17,97	4,3362	0,5995	2,5994
F5	30,55	20,95	16,46	1,3	640,58	25,31	2,0294	0,7115	1,4439
F6	23,22	20,00	12,68	1,5	375,07	19,37	3,9993	0,6224	2,4890
F7	29,45	14,43	10,93	1,3	410,05	20,25	3,1704	0,6364	2,0176
F8	24,65	14,91	11,00	1,4	345,41	18,59	4,0531	0,6097	2,4711
F9	30,75	21,06	15,24	1,7	596,98	24,43	2,8477	0,6990	1,9906
F10	25,64	19,55	12,04	1,4	393,26	19,83	3,5600	0,6298	2,2420
F11	29,76	21,37	12,91	1,4	489,43	22,12	2,8605	0,6652	1,9027
F12	21,40	21,32	12,78	1,2	348,40	18,67	3,4443	0,6110	2,1045
F13	28,79	22,42	17,06	1,6	625,68	25,01	2,5572	0,7073	1,8087
F14	26,32	21,06	13,29	1,9	445,60	21,11	4,2640	0,6498	2,7705

Table 231. Point load strength of Stop 17 fresh saturated sandstone in horizontal direction

Sample No	W (mm)	D (mm)	D' (mm)	P (kN)	De2 (mm <sup>2</sup> )	De (mm)	Is (Mpa)	F	Is(50) (Mpa)
F1	34,89	30,85	24,75	1,6	1100,04	33,17	1,4545	0,8145	1,1846
F2	30,00	26,75	26,34	1,6	1006,62	31,73	1,5895	0,7966	1,2661
F3	27,93	14,34	10,29	1,7	366,11	19,13	4,6434	0,6186	2,8724
F4	29,08	21,07	17,26	1,4	639,39	25,29	2,1896	0,7111	1,5571
F5	22,78	19,33	14,13	1,4	410,04	20,25	3,4143	0,6364	2,1728
F6	29,82	24,80	16,74	1,4	635,91	25,22	2,2016	0,7102	1,5635
F7	28,95	15,39	12,18	1,3	449,19	21,19	2,8941	0,6511	1,8843
F8	31,11	27,58	25,13	1,5	995,92	31,56	1,5062	0,7945	1,1966
F9	33	28,1	27	1,6	1132,89	33,66	1,4123	0,8205	1,1588

Table 232. Point load strength of Stop 17 weathered saturated sandstone in horizontal direction

Sample No	W (mm)	D (mm)	D' (mm)	P (kN)	De2 (mm <sup>2</sup> )	De (mm)	Is (Mpa)	F	Is(50) (Mpa)
W1	24,00	10,60	7,89	0,9	241,22	15,53	3,7310	0,5573	2,0794
W2	35,53	12,05	12,00	0,9	543,13	23,31	1,6571	0,6827	1,1313
W3	35,63	31,21	25,18	1,2	1142,88	33,81	1,0500	0,8223	0,8634
W4	24,04	19,15	19,10	0,9	584,92	24,19	1,5387	0,6955	1,0701
W5	31,79	16,29	15,71	0,8	636,20	25,22	1,2575	0,7103	0,8931
W6	19,69	13,03	13,00	0,9	326,08	18,06	2,7601	0,6010	1,6587
W7	25,60	16,36	12,66	0,9	412,86	20,32	2,1799	0,6375	1,3896
W8	19,05	12,31	12,15	1,0	294,85	17,17	3,3916	0,5860	1,9875
W9	20,50	21,48	17,89	0,9	467,19	21,61	1,9264	0,6575	1,2666
W10	25,56	19,65	11,53	0,9	375,42	19,38	2,3973	0,6225	1,4923

Table 233. Point load strength of Stop 17 weathered saturated sandstone in vertical direction

Sample No	W (mm)	D (mm)	D' (mm)	P (kN)	De2 (mm <sup>2</sup> )	De (mm)	Is (Mpa)	F	Is(50) (Mpa)
W1	31,96	23,90	21,10	1,5	859,05	29,31	1,7461	0,7656	1,3369
W2	35,84	20,05	15,72	1,5	717,71	26,79	2,0900	0,7320	1,5298
W3	24,63	25,17	19,35	1,5	607,12	24,64	2,4707	0,7020	1,7344
W4	29,58	38,13	35,96	1,6	1355,03	36,81	1,1808	0,8580	1,0132
W5	32,15	31,19	25,25	1,4	1034,12	32,16	1,3538	0,8020	1,0857
W6	27,66	21,78	12,21	1,5	430,23	20,74	3,4865	0,6441	2,2456

Table 234. Point load strength of Stop 18 fresh dry marl

Sample No	W (mm)	D (mm)	D' (mm)	P (kN)	De2 (mm <sup>2</sup> )	De (mm)	Is (MPa)	F	Is(50) (MPa)
F1	22,42	25,05	18,87	9,0	538,94	23,22	16,6995	0,6814	11,3790
F2	46,99	25,01	16,27	8,0	973,92	31,21	8,2142	0,7900	6,4895
F3	42,22	10,26	7,18	3,9	386,17	19,65	10,0993	0,6269	6,3314
F4	20,41	16,44	13,87	3,6	360,62	18,99	9,9828	0,6163	6,1522
F5	53,61	21,66	16,23	5,5	1108,40	33,29	4,9621	0,8160	4,0491
F6	20,95	17,27	11,30	5,1	301,57	17,37	16,9113	0,5893	9,9665
F7	28,14	25,48	23,48	7,0	841,69	29,01	8,3166	0,7617	6,3350
F8	47,55	13,87	7,42	5,0	449,45	21,20	11,1246	0,6512	7,2439
F9	32,09	18,07	11,37	4,5	464,79	21,56	9,6817	0,6566	6,3574
F10	25,21	10,78	8,79	3,9	282,29	16,80	13,8157	0,5797	8,0087
F11	24,47	21,27	17,22	5,1	536,78	23,17	9,5011	0,6807	6,4675
F12	52,05	28,87	19,98	12,0	1324,79	36,40	9,0580	0,8532	7,7283

Table 235. Point load strength of Stop 18 weathered dry marl

Sample No	W (mm)	D (mm)	D' (mm)	P (kN)	De2 (mm <sup>2</sup> )	De (mm)	Is (MPa)	F	Is(50) (MPa)
W1	29,18	21,27	17,20	2,8	639,36	25,29	4,3794	0,7111	3,1143
W2	34,37	32,66	28,48	4,4	1246,95	35,31	3,5286	0,8404	2,9654
W3	32,62	24,46	21,48	5,5	892,58	29,88	6,1619	0,7730	4,7631
W4	31,13	33,91	22,08	5,3	875,61	29,59	6,0530	0,7693	4,6565
W5	28,70	12,09	8,15	3,1	297,97	17,26	10,4038	0,5876	6,1129
W6	25,69	14,80	10,62	3,9	347,55	18,64	11,2214	0,6106	6,8520
W7	29,27	26,86	23,61	5,4	880,34	29,67	6,1340	0,7703	4,7252
W8	31,35	12,50	9,01	2,8	359,83	18,97	7,7815	0,6159	4,7930
W9	30,74	16,02	10,48	4,7	410,39	20,26	11,4526	0,6365	7,2898
W10	31,50	15,99	12,64	4,9	507,21	22,52	9,6607	0,6711	6,4837
W11	25,38	11,69	10,25	1,9	331,39	18,20	5,7333	0,6034	3,4595
W12	33,94	7,96	5,39	4,0	233,04	15,27	17,1644	0,5526	9,4842
W13	30,34	13,04	9,30	4,5	359,44	18,96	12,5194	0,6158	7,7091

Table 236. Point load strength of Stop 18 fresh saturated marl

Sample No	W (mm)	D (mm)	D' (mm)	P (kN)	De2 (mm <sup>2</sup> )	De (mm)	Is (MPa)	F	Is(50) (MPa)
F1	41,33	28,40	14,46	4,8	761,31	27,59	6,3049	0,7429	4,6836
F2	34,29	14,92	12,40	4,0	541,65	23,27	7,3848	0,6823	5,0383
F3	34,49	10,64	9,34	1,5	410,37	20,26	3,6553	0,6365	2,3266
F4	32,44	17,22	14,77	2,8	610,37	24,71	4,5874	0,7029	3,2246
F5	27,56	14,19	12,46	0,3	437,45	20,92	0,6858	0,6468	0,4435
F6	34,89	27,54	18,03	4,9	801,36	28,31	6,1146	0,7524	4,6009
F7	30,35	29,63	22,06	4,3	852,89	29,20	5,0417	0,7643	3,8531
F8	35,79	27,68	23,02	4,5	1049,54	32,40	4,2876	0,8049	3,4513
F9	38,55	22,84	14,10	4,2	692,43	26,31	6,0656	0,7255	4,4003
F10	32,14	12,60	10,10	2,1	413,52	20,34	5,0783	0,6377	3,2386
F11	38,10	29,00	25,45	3,8	1235,22	35,15	3,0764	0,8384	2,5792
F12	44,32	18,80	13,12	4,4	740,74	27,22	5,9400	0,7378	4,3825
F13	37,78	25,86	18,51	5,4	890,84	29,85	6,0617	0,7726	4,6834

Table 237. Point load strength of Stop 18 weathered saturated marl

Sample No	W (mm)	D (mm)	D' (mm)	P (kN)	De2 (mm <sup>2</sup> )	De (mm)	Is (MPa)	F	Is(50) (MPa)
W1	46,31	32,84	14,50	3,9	855,41	29,25	4,5592	0,7648	3,4870
W2	36,65	13,05	9,84	3,7	459,41	21,43	8,0538	0,6547	5,2731
W3	20,40	27,41	18,67	3,3	485,18	22,03	6,8016	0,6637	4,5144
W4	49,34	28,23	13,89	5,1	873,04	29,55	5,8417	0,7687	4,4907
W5	35,51	27,92	21,43	4,0	969,40	31,14	4,1263	0,7891	3,2561
W6	21,21	15,99	12,37	0,7	334,23	18,28	2,0944	0,6047	1,2664
W7	27,95	16,07	13,01	2,4	463,22	21,52	5,1811	0,6561	3,3993
W8	37,65	27,30	24,15	1,1	1158,28	34,03	0,9497	0,8250	0,7835
W9	32,95	20,19	14,22	2,1	596,88	24,43	3,5183	0,6990	2,4593
W10	30,95	10,96	6,92	2,3	272,83	16,52	8,4301	0,5748	4,8453
W11	28,47	28,13	25,29	1,8	917,21	30,29	1,9625	0,7783	1,5273
W12	38,15	24,54	19,58	1,7	951,56	30,85	1,7865	0,7855	1,4033
W13	40,95	21,73	14,93	5,3	778,83	27,91	6,8051	0,7471	5,0840
W14	38,82	10,23	6,99	1,1	345,67	18,59	3,1822	0,6098	1,9405
W15	16,76	13,81	7,58	2,3	161,84	12,72	14,2120	0,5044	7,1687

Table 238. Point load strength of Stop 19 fresh dry marl in vertical direction

Sample No	W (mm)	D (mm)	D' (mm)	P (kN)	De2 (mm <sup>2</sup> )	De (mm)	Is (MPa)	F	Is(50) (MPa)
F1	46,92	31,06	21,18	10,0	1265,94	35,58	7,8992	0,8436	6,6635
F2	53,47	46,78	19,82	10,0	1350,03	36,74	7,4072	0,8572	6,3498
F3	51,01	35,68	16,33	9,0	1061,14	32,58	8,4815	0,8072	6,8459
F4	37,86	26,21	20,01	7,0	965,07	31,07	7,2534	0,7882	5,7173
F5	45,11	34,76	11,61	9,0	667,17	25,83	13,4898	0,7187	9,6957
F6	35,55	18,64	16,51	5,4	747,68	27,34	7,2223	0,7395	5,3410
F7	35,73	33,13	13,23	5,5	602,18	24,54	9,1335	0,7006	6,3986
F8	42,05	40,80	10,36	5,1	554,95	23,56	9,1900	0,6864	6,3080
F9	35,52	31,13	9,26	6,5	419,00	20,47	15,5131	0,6398	9,9258
F10	32,25	33,94	26,47	12,0	1087,46	32,98	11,0349	0,8121	8,9616
F11	44,46	20,30	11,96	12,0	677,38	26,03	17,7154	0,7215	12,7812
F12	30,01	22,07	12,98	10,0	496,22	22,28	20,1525	0,6675	13,4512

Table 239. Point load strength of Stop 19 fresh dry marl in horizontal direction

Sample No	W (mm)	D (mm)	D' (mm)	P (kN)	De2 (mm <sup>2</sup> )	De (mm)	Is (MPa)	F	Is(50) (MPa)
F1	55,57	47,38	18,08	4,7	1279,88	35,78	3,6722	0,8459	3,1062
F2	30,41	28,79	23,19	4,0	898,35	29,97	4,4526	0,7742	3,4474
F3	25,72	25,48	23,55	2,3	771,60	27,78	2,9808	0,7454	2,2218
F4	25,19	21,17	15,94	2,7	511,50	22,62	5,2786	0,6726	3,5501
F5	32,62	31,41	24,45	5,5	1016,00	31,87	5,4134	0,7984	4,3222
F6	34,98	38,28	30,58	2,7	1362,66	36,91	1,9814	0,8592	1,7025
F7	35,5	33,5	31,4	4,1	1420,10	37,68	2,8871	0,8682	2,5064
F8	38	35,6	33,9	5,4	1639,14	40,49	3,2944	0,8998	2,9645
F9	29	27,9	25,4	6,8	940,01	30,66	7,2340	0,7831	5,6647
F10	24,4	23,5	21,1	5,4	655,37	25,60	8,2397	0,7155	5,8958

Table 240. Point load strength of Stop 19 weathered dry marl in vertical direction

Sample No	W (mm)	D (mm)	D' (mm)	P (kN)	De2 (mm <sup>2</sup> )	De (mm)	Is (MPa)	F	Is(50) (MPa)
W1	70,91	32,45	28,96	11,0	2615,99	51,15	4,2049	1,0114	4,2529
W2	65,04	23,21	21,05	10,0	1744,07	41,76	5,7337	0,9139	5,2401
W3	37,66	21,94	21,07	11,0	1010,82	31,79	10,8822	0,7974	8,6776
W4	53,81	29,38	27,00	13,0	1850,79	43,02	7,0240	0,9276	6,5154
W5	39,30	20,19	12,79	4,4	640,31	25,30	6,8716	0,7114	4,8885
W6	48,26	38,46	34,93	10,0	2147,42	46,34	4,6568	0,9627	4,4831
W7	55,16	32,29	24,96	8,0	1753,88	41,88	4,5613	0,9152	4,1745
W8	28,48	32,33	20,37	5,5	739,03	27,19	7,4422	0,7374	5,4876
W9	28,53	30,19	28,15	4,5	1023,08	31,99	4,3985	0,7998	3,5180
W10	39,89	19,22	11,52	7,0	585,39	24,19	11,9578	0,6956	8,3182
W11	41,01	28,73	15,13	4,7	790,42	28,11	5,9462	0,7499	4,4588
W12	36,54	21,92	16,98	4,0	790,38	28,11	5,0608	0,7498	3,7949
W13	31,55	27,76	21,84	8,0	877,77	29,63	9,1140	0,7698	7,0157

Table 241. Point load strength of Stop 19 weathered dry marl in horizontal direction

Sample No	W (mm)	D (mm)	D' (mm)	P (kN)	De2 (mm <sup>2</sup> )	De (mm)	Is (MPa)	F	Is(50) (MPa)
W1	39,73	27,33	22,93	5,1	1160,52	34,07	4,3946	0,8254	3,6274
W2	65,89	41,05	38,12	10,0	3199,65	56,57	3,1253	1,0636	3,3242
W3	38,92	24,93	23,53	2,9	1166,61	34,16	2,4858	0,8265	2,0546
W4	45,86	38,44	32,44	7,0	1895,16	43,53	3,6936	0,9331	3,4465
W5	24,64	21,93	16,73	4,9	525,13	22,92	9,3310	0,6770	6,3170
W6	21,18	20,11	18,20	0,8	491,05	22,16	1,6292	0,6657	1,0846
W7	25,48	24,13	22,84	4,5	741,35	27,23	6,0700	0,7379	4,4793
W8	22,15	20,46	19,13	2,3	539,78	23,23	4,2610	0,6817	2,9045

Table 242. Point load strength of Stop 19 fresh saturated marl in horizontal direction

Sample No	W (mm)	D (mm)	D' (mm)	P (kN)	De2 (mm <sup>2</sup> )	De (mm)	Is (MPa)	F	Is(50) (MPa)
F1	59,45	57,31	50,00	14,0	3786,62	61,54	3,6972	1,1094	4,1016
F2	48,01	12,15	7,43	2,6	454,41	21,32	5,7217	0,6529	3,7359
F3	50,23	16,96	10,15	1,9	649,47	25,48	2,9255	0,7139	2,0886
F4	50,67	18,91	13,62	3,7	879,14	29,65	4,2087	0,7701	3,2410
F5	39,78	30,09	25,01	2,3	1267,39	35,60	1,7753	0,8438	1,4980
F6	32,40	25,93	24,03	4,7	991,81	31,49	4,7388	0,7936	3,7609
F7	41,47	37,36	29,64	4,0	1565,82	39,57	2,5546	0,8896	2,2726
F8	36,17	30,46	25,78	3,2	1187,85	34,47	2,6939	0,8302	2,2366
F9	33,64	32,34	32,20	5,3	1379,88	37,15	3,8409	0,8619	3,3106
F10	28,06	28,46	19,87	1,7	710,26	26,65	2,3935	0,7301	1,7474
F11	20,52	15,94	11,45	4,4	299,30	17,30	14,7007	0,5882	8,6473
F12	21,46	26,06	22,32	4,7	610,17	24,70	7,7027	0,7029	5,4140
F13	24,13	19,74	16,14	0,9	496,13	22,27	1,8141	0,6674	1,2108
F14	27,90	20,63	16,20	0,4	575,77	24,00	0,6947	0,6928	0,4813

Table 243. Point load strength of Stop 19 fresh saturated marl in vertical direction

Sample No	W (mm)	D (mm)	D' (mm)	P (kN)	De2 (mm <sup>2</sup> )	De (mm)	Is (MPa)	F	Is(50) (MPa)
F1	47,63	26,35	22,13	7,0	1342,74	36,64	5,2132	0,8561	4,4629
F2	44,91	31,65	20,30	12,0	1161,37	34,08	10,3327	0,8256	8,5304
F3	55,05	35,59	19,77	12,0	1386,42	37,23	8,6554	0,8630	7,4692
F4	60,74	22,60	14,83	7,0	1147,48	33,87	6,1003	0,8231	5,0212
F5	38,88	26,73	18,91	4,1	936,59	30,60	4,3776	0,7824	3,4248
F6	32,60	24,90	17,29	5,0	718,03	26,80	6,9635	0,7321	5,0977
F7	49,74	25,55	10,64	8,0	674,18	25,97	11,8662	0,7206	8,5511
F8	32,08	18,28	11,82	3,0	483,04	21,98	6,2107	0,6630	4,1177
F9	27,36	17,68	14,10	4,1	491,43	22,17	8,3429	0,6659	5,5552
F10	36,85	15,57	8,45	4,6	396,67	19,92	11,5967	0,6311	7,3190
F11	36,40	22,00	13,65	5,0	632,94	25,16	7,8996	0,7093	5,6035

Table 244. Point load strength of Stop 19 weathered saturated marl in horizontal direction

Sample No	W (mm)	D (mm)	D' (mm)	P (kN)	De2 (mm <sup>2</sup> )	De (mm)	Is (MPa)	F	Is(50) (MPa)
W1	60,19	34,60	23,92	3,2	1834,07	42,83	1,7448	0,9255	1,6147
W2	51,31	16,01	7,93	1,0	518,33	22,77	1,9293	0,6748	1,3018
W3	50,71	15,12	11,22	0,9	724,80	26,92	1,2417	0,7338	0,9112
W4	70,87	19,99	13,68	1,9	1235,03	35,14	1,5384	0,8384	1,2898
W5	41,65	21,95	13,79	1,0	731,66	27,05	1,3668	0,7355	1,0053
W6	32,59	33,50	32,91	0,7	1366,29	36,96	0,5123	0,8598	0,4405
W7	33,10	22,00	14,62	1,4	616,46	24,83	2,2710	0,7047	1,6003
W8	21,46	31,52	26,83	0,4	733,47	27,08	0,5454	0,7360	0,4014
W9	20,59	31,45	27,15	0,6	712,13	26,69	0,8425	0,7306	0,6155
W10	19,82	18,18	13,62	0,6	343,88	18,54	1,7448	0,6090	1,0626
W11	21,41	23,06	20,22	0,3	551,48	23,48	0,5440	0,6853	0,3728

Table 245. Point load strength of Stop 19 weathered saturated marl in vertical direction

Sample No	W (mm)	D (mm)	D' (mm)	P (kN)	De2 (mm <sup>2</sup> )	De (mm)	Is (MPa)	F	Is(50) (MPa)
W1	45,58	22,18	13,08	2,7	759,47	27,56	3,5551	0,7424	2,6393
W2	53,05	24,98	15,50	3,2	1047,48	32,36	3,0549	0,8045	2,4578
W3	53,93	19,48	6,18	2,3	424,57	20,61	5,4172	0,6420	3,4776
W4	47,91	23,43	12,17	2,6	742,76	27,25	3,5005	0,7383	2,5844
W5	47,43	20,19	9,98	2,3	603,00	24,56	3,8143	0,7008	2,6731
W6	31,75	20,00	15,32	1,7	619,63	24,89	2,7436	0,7056	1,9358
W7	43,61	23,51	16,80	1,7	933,31	30,55	1,8215	0,7817	1,4238
W8	29,04	22,34	13,72	1,6	507,55	22,53	3,1524	0,6713	2,1160
W9	35,12	19,70	11,89	2,8	531,94	23,06	5,2637	0,6792	3,5750

Table 246. Point load strength of Stop 20 fresh dry marl in vertical direction

Sample No	W (mm)	D (mm)	D' (mm)	P (kN)	De2 (mm <sup>2</sup> )	De (mm)	Is (MPa)	F	Is(50) (MPa)
F1	30,59	10,94	5,92	4,0	230,69	15,19	17,3392	0,5512	9,5566
F2	36,80	16,86	11,97	5,1	561,14	23,69	9,0886	0,6883	6,2558
F3	20,58	32,81	12,08	5,5	316,70	17,80	17,3668	0,5966	10,3609
F4	27,85	12,22	7,03	3,1	249,41	15,79	12,4294	0,5620	6,9854
F5	27,60	19,65	11,65	5,6	409,61	20,24	13,6717	0,6362	8,6982
F6	42,59	19,06	11,51	5,5	624,47	24,99	8,8074	0,7070	6,2265
F7	37,26	12,17	6,15	4,3	291,91	17,09	14,7306	0,5846	8,6109
F8	28,77	14,37	8,56	4,5	313,72	17,71	14,3439	0,5952	8,5373
F9	30,65	16,89	12,31	4,4	480,64	21,92	9,1545	0,6622	6,0618
F10	25,98	16,49	12,15	5,1	402,11	20,05	12,6831	0,6333	8,0320

Table 247. Point load strength of Stop 20 fresh dry marl in horizontal direction

Sample No	W (mm)	D (mm)	D' (mm)	P (kN)	De2 (mm <sup>2</sup> )	De (mm)	Is (MPa)	F	Is(50) (MPa)
F1	41,11	49,78	44,93	9,0	2352,96	48,51	3,8250	0,9850	3,7674
F2	18,15	20,81	17,04	2,6	393,98	19,85	6,5993	0,6301	4,1580
F3	16,51	24,46	19,93	3,3	419,16	20,47	7,8728	0,6399	5,0378
F4	45,99	22,15	17,15	4,1	1004,75	31,70	4,0806	0,7962	3,2490
F5	17,18	15,48	12,11	2,3	265,03	16,28	8,6782	0,5706	4,9519
F6	18,74	12,13	9,48	4,4	226,31	15,04	19,4422	0,5485	10,6644
F7	21,42	18,41	12,73	2,1	347,36	18,64	6,0456	0,6105	3,6911
F8	37,55	30,46	23,41	3,3	1119,80	33,46	2,9469	0,8181	2,4109
F9	23,4	21,2	16	4,5	477,26	21,85	9,4289	0,6610	6,2325
F10	36,9	30,2	23,1	4,8	1087,49	32,98	4,4138	0,8121	3,5846

Table 248. Point load strength of Stop 20 weathered dry marl in vertical direction

Sample No	W (mm)	D (mm)	D' (mm)	P (kN)	De2 (mm <sup>2</sup> )	De (mm)	Is (MPa)	F	Is(50) (MPa)
W1	48,80	21,31	19,48	5,4	1210,99	34,80	4,4592	0,8343	3,7201
W2	52,77	22,58	14,69	2,1	987,50	31,42	2,1266	0,7928	1,6859
W3	50,74	16,57	10,45	5,4	675,46	25,99	7,9946	0,7210	5,7638
W4	47,13	25,99	20,15	5,5	1209,77	34,78	4,5463	0,8340	3,7918
W5	35,08	30,48	23,88	6,8	1067,15	32,67	6,3721	0,8083	5,1506
W6	38,46	35,99	27,46	2,1	1345,37	36,68	1,5609	0,8565	1,3369
W7	36,25	30,60	21,94	5,4	1013,15	31,83	5,3299	0,7979	4,2526
W8	44,17	35,74	27,18	4,1	1529,35	39,11	2,6809	0,8844	2,3709
W9	31,71	25,82	18,55	5,7	749,33	27,37	7,6068	0,7399	5,6284
W10	42,56	25,18	19,43	9,1	1053,43	32,46	8,6385	0,8057	6,9599

Table 249. Point load strength of Stop 20 weathered dry marl in horizontal direction

Sample No	W (mm)	D (mm)	D' (mm)	P (kN)	De2 (mm <sup>2</sup> )	De (mm)	Is (MPa)	F	Is(50) (MPa)
W1	25,55	50,50	48,29	5,5	1571,73	39,65	3,4993	0,8905	3,1160
W2	52,15	30,46	29,19	3,8	1939,18	44,04	1,9596	0,9385	1,8390
W3	17,87	21,20	19,04	2,0	433,43	20,82	4,6143	0,6453	2,9775
W4	19,58	21,87	19,65	1,5	490,12	22,14	3,0605	0,6654	2,0365
W5	41,9	36	34,2	4,3	1823,51	42,70	2,3581	0,9241	2,1792
W6	18,9	15,2	13,6	5,1	329,10	18,14	15,4969	0,6023	9,3345
W7	26,4	30,4	28,6	3,8	961,58	31,01	3,9518	0,7875	3,1121
W8	21,8	19,6	17,4	2,1	480,99	21,93	4,3660	0,6623	2,8915
W9	25,7	23,1	20,4	1,9	667,16	25,83	2,8479	0,7187	2,0469
W10	43,5	41	38,7	3,5	2148,71	46,35	1,6289	0,9629	1,5684

Table 250. Point load strength of Stop 20 fresh saturated marl in vertical direction

Sample No	W (mm)	D (mm)	D' (mm)	P (kN)	De2 (mm <sup>2</sup> )	De (mm)	Is (MPa)	F	Is(50) (MPa)
F1	30,24	14,60	10,24	2,3	394,47	19,86	5,8306	0,6303	3,6748
F2	43,67	23,19	18,28	4,0	1016,93	31,89	3,9334	0,7986	3,1413
F3	34,51	15,53	8,31	2,1	365,32	19,11	5,7483	0,6183	3,5541
F4	40,70	20,28	10,79	2,1	559,43	23,65	3,7538	0,6878	2,5818
F5	55,40	25,64	9,13	2,0	644,33	25,38	3,1040	0,7125	2,2116
F6	46,70	14,82	9,28	2,3	552,07	23,50	4,1661	0,6855	2,8559
F7	29,06	16,14	9,29	1,5	343,91	18,54	4,3616	0,6090	2,6563
F8	33,14	15,31	10,32	2,6	435,67	20,87	5,9678	0,6461	3,8558
F9	27,65	17,60	11,74	1,9	413,52	20,34	4,5947	0,6377	2,9302
F10	28,14	18,68	10,08	3,0	361,34	19,01	8,3025	0,6166	5,1192
F11	24,93	18,20	10,74	3,3	341,08	18,47	9,6751	0,6078	5,8801
F12	24,01	28,39	16,69	2,9	510,48	22,59	5,6809	0,6722	3,8188
F13	29,83	15,67	12,16	2,3	462,08	21,50	4,9775	0,6557	3,2637
F14	27,68	16,23	8,90	3,2	313,82	17,72	10,1968	0,5952	6,0695
F15	25,90	15,80	11,38	2,8	375,47	19,38	7,4574	0,6225	4,6424
F16	20,52	15,69	10,71	1,4	279,96	16,73	5,0007	0,5785	2,8928

Table 251. Point load strength of Stop 20 fresh saturated marl in horizontal direction

Sample No	W (mm)	D (mm)	D' (mm)	P (kN)	De2 (mm <sup>2</sup> )	De (mm)	Is (MPa)	F	Is(50) (MPa)
F1	31,11	27,68	17,30	1,1	685,61	26,18	1,6044	0,7237	1,1610
F2	17,50	36,06	29,16	1,5	650,06	25,50	2,3075	0,7141	1,6477
F3	21,30	26,37	18,14	0,9	492,21	22,19	1,8285	0,6661	1,2180
F4	25,88	20,95	19,03	1,4	627,38	25,05	2,2315	0,7078	1,5794
F5	34,44	35,42	33,42	1,2	1466,22	38,29	0,8184	0,8751	0,7162
F6	25,95	23,55	20,55	2,1	679,33	26,06	3,0913	0,7220	2,2319
F7	31,11	30,48	28,94	1,3	1146,91	33,87	1,1335	0,8230	0,9328
F8	35,64	30,55	27,13	2,4	1231,74	35,10	1,9485	0,8378	1,6324
F9	33,48	25,89	22,81	2,2	972,84	31,19	2,2614	0,7898	1,7861
F10	37,00	30,50	28,00	1,9	1317,49	36,30	1,4421	0,8520	1,2287

Table 252. Point load strength of Stop 20 weathered saturated marl in vertical direction

Sample No	W (mm)	D (mm)	D' (mm)	P (kN)	De2 (mm <sup>2</sup> )	De (mm)	Is (MPa)	F	Is(50) (MPa)
W1	26,42	15,40	9,31	1,0	313,34	17,70	3,1914	0,5950	1,8989
W2	33,86	18,65	15,29	1,6	659,52	25,68	2,4260	0,7167	1,7387
W3	29,89	16,88	11,13	0,9	423,79	20,59	2,1237	0,6417	1,3627
W4	29,47	18,07	10,23	1,1	384,05	19,60	2,8642	0,6261	1,7932
W5	24,88	19,97	12,65	1,1	400,93	20,02	2,7436	0,6328	1,7362
W6	35,11	30,05	24,61	1,5	1100,71	33,18	1,3628	0,8146	1,1101
W7	28,44	27,84	23,84	2,1	863,71	29,39	2,4314	0,7667	1,8641
W8	31,44	25,96	21,96	2,0	879,52	29,66	2,2740	0,7702	1,7513
W9	32,55	30,41	23,44	2,3	971,94	31,18	2,3664	0,7896	1,8686
W10	41,95	35,71	29,51	4,1	1577,00	39,71	2,5999	0,8912	2,3170

Table 253. Point load strength of Stop 20 weathered saturated marl in horizontal direction

Sample No	W (mm)	D (mm)	D' (mm)	P (kN)	De2 (mm <sup>2</sup> )	De (mm)	Is (MPa)	F	Is(50) (MPa)
W1	19,01	27,93	25,26	0,3	611,71	24,73	0,4904	0,7033	0,3449
W2	32,36	35,18	24,47	1,1	1008,73	31,76	1,0905	0,7970	0,8691
W3	54,10	28,59	21,90	1,3	1509,29	38,85	0,8613	0,8815	0,7592
W4	30,29	37,82	23,75	1,1	916,42	30,27	1,2003	0,7781	0,9340
W5	20,92	39,80	38,15	0,1	1016,69	31,89	0,0984	0,7986	0,0785
W6	30,86	25,18	23,08	0,8	907,32	30,12	0,8817	0,7762	0,6844
W7	30,00	32,85	30,15	0,2	1152,23	33,94	0,1736	0,8239	0,1430
W8	25,15	27,35	27,01	0,4	865,35	29,42	0,4622	0,7670	0,3546
W9	29,76	23,35	21,66	0,5	821,15	28,66	0,6089	0,7570	0,4610
W10	49,01	38,70	36,15	0,3	2256,96	47,51	0,1329	0,9748	0,1296
W11	19,95	29,86	24,61	0,8	625,44	25,01	1,2791	0,7072	0,9046

Table 254. Slake durability of Stop 1

		Start W. (g)	1st Cycle W. (g)	Id(1)	2nd Cycle W. (g)	Id(2)	Type	Durability
F	Mudstone	484,90	479,94	98,98	477,09	<b>98,39</b>	Type II	Very High
	Sandstone	520,10	515,97	99,21	513,20	<b>98,67</b>	Type I	Very High
W	Mudstone	501,61	494,32	98,55	490,38	<b>97,76</b>	Type II	High
	Sandstone	528,26	523,19	99,04	520,91	<b>98,61</b>	Type I	Very High

Table 255. Slake durability of Stop 1 failed zone

		Start W. (g)	1st Cycle W. (g)	Id(1)	2nd Cycle W. (g)	Id(2)	Type	Durability
F	Mudstone	470,17	455,17	96,81	447,30	<b>95,14</b>	Type II	High
W	Mudstone	506,48	490,70	96,88	480,84	<b>94,94</b>	Type II	High

Table 256. Slake durability of Stop 2

		<b>Start W. (g)</b>	<b>1st Cycle W. (g)</b>	<b>Id(1)</b>	<b>2nd Cycle W. (g)</b>	<b>Id(2)</b>	<b>Type</b>	<b>Durability</b>
F	Limestone	502,91	498,06	99,04	495,62	<b>98,55</b>	Type I	Very High
W	Limestone	472,06	464,01	98,29	460,65	<b>97,58</b>	Type I	High

Table 257. Slake durability of Stop 3

		<b>Start W. (g)</b>	<b>1st Cycle W. (g)</b>	<b>Id(1)</b>	<b>2nd Cycle W. (g)</b>	<b>Id(2)</b>	<b>Type</b>	<b>Durability</b>
F	Limestone	545,44	533,39	97,79	526,90	<b>96,60</b>	Type II	High
W	Limestone	508,17	464,79	91,46	436,65	<b>85,93</b>	Type II	Medium High

Table 258. Slake durability of Stop 4

		<b>Start W. (g)</b>	<b>1st Cycle W. (g)</b>	<b>Id(1)</b>	<b>2nd Cycle W. (g)</b>	<b>Id(2)</b>	<b>Type</b>	<b>Durability</b>
F	Granite	508,74	505,77	99,42	504,62	<b>99,19</b>	Type II	Very High
W	Granite	510,5	507,6	99,44	503,13	<b>98,56</b>	Type II	Very High

Table 259. Slake durability of Stop 5

		<b>Start W. (g)</b>	<b>1st Cycle W. (g)</b>	<b>Id(1)</b>	<b>2nd Cycle W. (g)</b>	<b>Id(2)</b>	<b>Type</b>	<b>Durability</b>
F	Basalt	498,11	489,97	98,37	485,13	<b>97,39</b>	Type I	High
W	Basalt	456,91	441,18	96,56	437,26	<b>95,70</b>	Type I	High

Table 260. Slake durability of Stop 6

		<b>Start W. (g)</b>	<b>1st Cycle W. (g)</b>	<b>Id(1)</b>	<b>2nd Cycle W. (g)</b>	<b>Id(2)</b>	<b>Type</b>	<b>Durability</b>
W	Granite	464,63	429,06	92,34	416,86	<b>89,72</b>	Type III	Medium High

Table 261. Slake durability of Stop 7

		<b>Start W. (g)</b>	<b>1st Cycle W. (g)</b>	<b>Id(1)</b>	<b>2nd Cycle W. (g)</b>	<b>Id(2)</b>	<b>Type</b>	<b>Durability</b>
F	G.diorite	521,61	519,63	99,62	518,64	<b>99,43</b>	Type I	Very High
W	G.diorite	440,66	439,12	99,65	438,35	<b>99,48</b>	Type I	Very High

Table 262. Slake durability of Stop 8

		<b>Start W. (g)</b>	<b>1st Cycle W. (g)</b>	<b>Id(1)</b>	<b>2nd Cycle W. (g)</b>	<b>Id(2)</b>	<b>Type</b>	<b>Durability</b>
F	Sandstone	501,72	499,25	99,51	498,07	<b>99,27</b>	Type I	Very High
W	Sandstone	496,27	494,24	99,59	493,03	<b>99,35</b>	Type I	Very High

Table 263. Slake durability of Stop 9

		<b>Start W. (g)</b>	<b>1st Cycle W. (g)</b>	<b>Id(1)</b>	<b>2nd Cycle W. (g)</b>	<b>Id(2)</b>	<b>Type</b>	<b>Durability</b>
F	Limestone	472,56	470,16	99,49	469,26	<b>99,30</b>	Type I	Very High
W	Limestone	447,94	444,55	99,24	442,94	<b>98,88</b>	Type I	Very High

Table 264. Slake durability of Stop 10

		<b>Start W. (g)</b>	<b>1st Cycle W. (g)</b>	<b>Id(1)</b>	<b>2nd Cycle W. (g)</b>	<b>Id(2)</b>	<b>Type</b>	<b>Durability</b>
F	Sandstone	538,38	522,59	97,07	514,47	<b>95,56</b>	Type I	High
W	Sandstone	535,14	517,42	96,69	508,81	<b>95,08</b>	Type I	High

Table 265. Slake durability of Stop 11

		<b>Start W. (g)</b>	<b>1st Cycle W. (g)</b>	<b>Id(1)</b>	<b>2nd Cycle W. (g)</b>	<b>Id(2)</b>	<b>Type</b>	<b>Durability</b>
F	Sandstone	475,34	468,57	98,58	463,76	<b>97,56</b>	Type II	High
W	Sandstone	496,09	489,38	98,65	484,78	<b>97,72</b>	Type I	High

Table 266. Slake durability of Stop 12

		<b>Start W. (g)</b>	<b>1st Cycle W. (g)</b>	<b>Id(1)</b>	<b>2nd Cycle W. (g)</b>	<b>Id(2)</b>	<b>Type</b>	<b>Durability</b>
F	Sandstone	300,16	299,15	99,66	298,23	<b>99,36</b>	Type I	Very High
W	Sandstone	522,94	518,88	99,22	515,87	<b>98,65</b>	Type I	Very High

Table 267. Slake durability of Stop 13

		<b>Start W. (g)</b>	<b>1st Cycle W. (g)</b>	<b>Id(1)</b>	<b>2nd Cycle W. (g)</b>	<b>Id(2)</b>	<b>Type</b>	<b>Durability</b>
F	Sandstone	358,07	348,61	97,36	338,54	<b>94,55</b>	Type I	Medium High
W	Sandstone	440,33	425,06	96,53	404,23	<b>91,80</b>	Type I	Medium High

Table 268. Slake durability of Stop 14

		<b>Start W. (g)</b>	<b>1st Cycle W. (g)</b>	<b>Id(1)</b>	<b>2nd Cycle W. (g)</b>	<b>Id(2)</b>	<b>Type</b>	<b>Durability</b>
F	Sandstone	254,52	250,87	98,57	248,29	<b>97,55</b>	Type I	High
W	Sandstone	459,03	430,37	93,76	408,83	<b>89,06</b>	Type I	Medium High

Table 269. Slake durability of Stop 15

		<b>Start W. (g)</b>	<b>1st Cycle W. (g)</b>	<b>Id(1)</b>	<b>2nd Cycle W. (g)</b>	<b>Id(2)</b>	<b>Type</b>	<b>Durability</b>
F	Sandstone	387,83	383,87	98,98	382,24	<b>98,56</b>	Type I	Very High
W	Sandstone	459,66	452,44	98,43	449,61	<b>97,81</b>	Type I	High

Table 270. Slake durability of Stop 16

		<b>Start W. (g)</b>	<b>1st Cycle W. (g)</b>	<b>Id(1)</b>	<b>2nd Cycle W. (g)</b>	<b>Id(2)</b>	<b>Type</b>	<b>Durability</b>
F	Sandstone	428,75	421,83	98,39	417,43	<b>97,36</b>	Type I	High
W	Sandstone	489,50	459,31	93,83	446,46	<b>91,21</b>	Type I	Medium High

Table 271. Slake durability of Stop 17

		<b>Start W. (g)</b>	<b>1st Cycle W. (g)</b>	<b>Id(1)</b>	<b>2nd Cycle W. (g)</b>	<b>Id(2)</b>	<b>Type</b>	<b>Durability</b>
F	Sandstone	261,90	242,06	92,42	231,56	<b>88,42</b>	Type II	Medium High
W	Sandstone	209,94	181,25	86,33	164,73	<b>78,47</b>	Type II	Medium

Table 272. Slake durability of Stop 18

		<b>Start W. (g)</b>	<b>1st Cycle W. (g)</b>	<b>Id(1)</b>	<b>2nd Cycle W. (g)</b>	<b>Id(2)</b>	<b>Type</b>	<b>Durability</b>
F	Marl	399,04	396,48	99,36	395,39	<b>99,09</b>	Type I	Very High
W	Marl	485,61	481,45	99,14	479,02	<b>98,64</b>	Type I	Very High

Table 273. Slake durability of Stop 19

		<b>Start W. (g)</b>	<b>1st Cycle W. (g)</b>	<b>Id(1)</b>	<b>2nd Cycle W. (g)</b>	<b>Id(2)</b>	<b>Type</b>	<b>Durability</b>
F	Marl	474,32	469,37	98,96	467,09	<b>98,48</b>	Type I	Very High
W	Marl	489,86	479,10	97,80	474,08	<b>96,78</b>	Type I	High

Table 274. Slake durability of Stop 20

		<b>Start W. (g)</b>	<b>1st Cycle W. (g)</b>	<b>Id(1)</b>	<b>2nd Cycle W. (g)</b>	<b>Id(2)</b>	<b>Type</b>	<b>Durability</b>
F	Marl	442,50	439,16	99,25	436,15	<b>98,56</b>	Type I	Very High
W	Marl	484,76	480,60	99,14	477,72	<b>98,55</b>	Type I	Very High

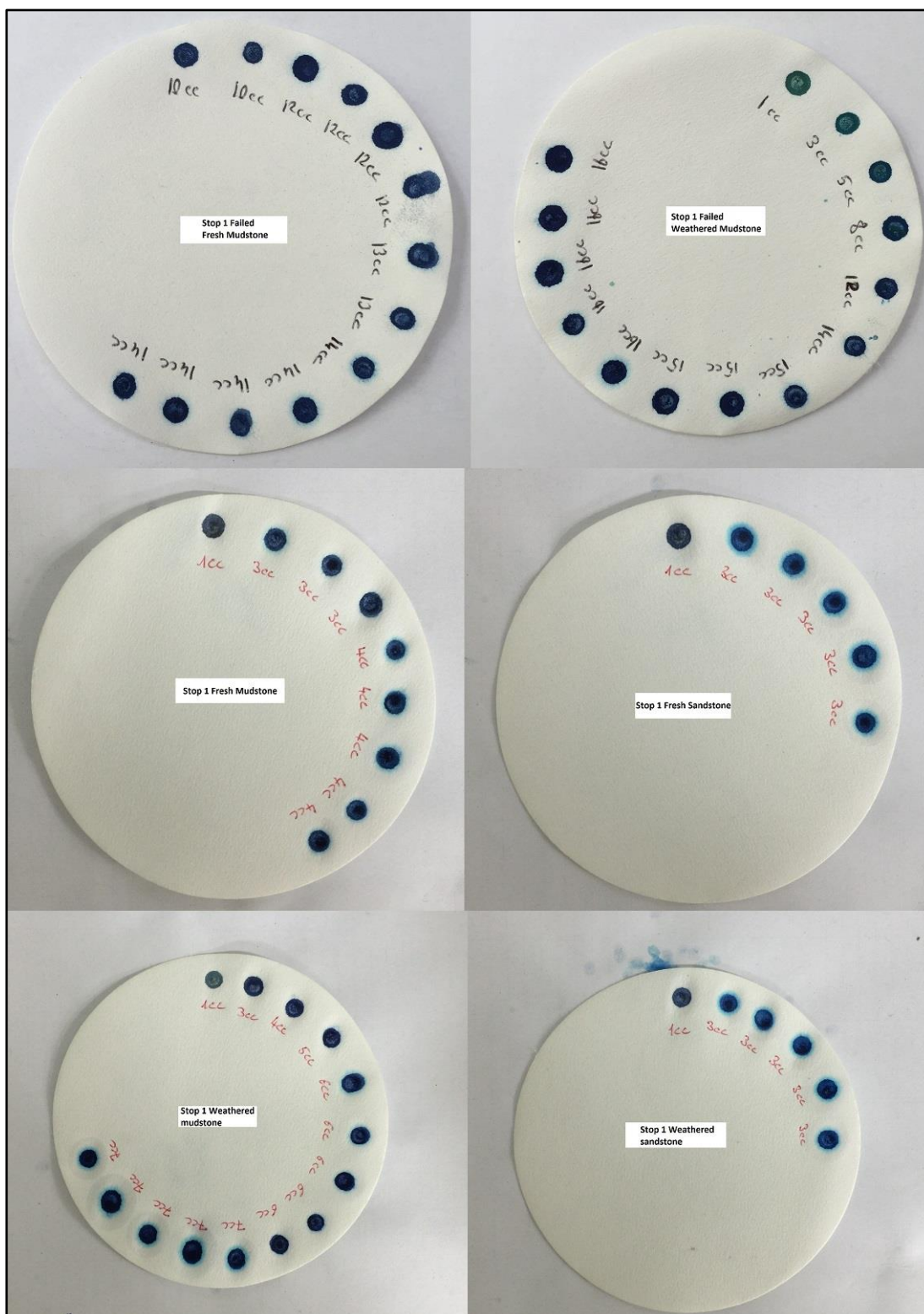


Figure 118. Methylene blue test results of Stop 1 and Stop 1 failed zone

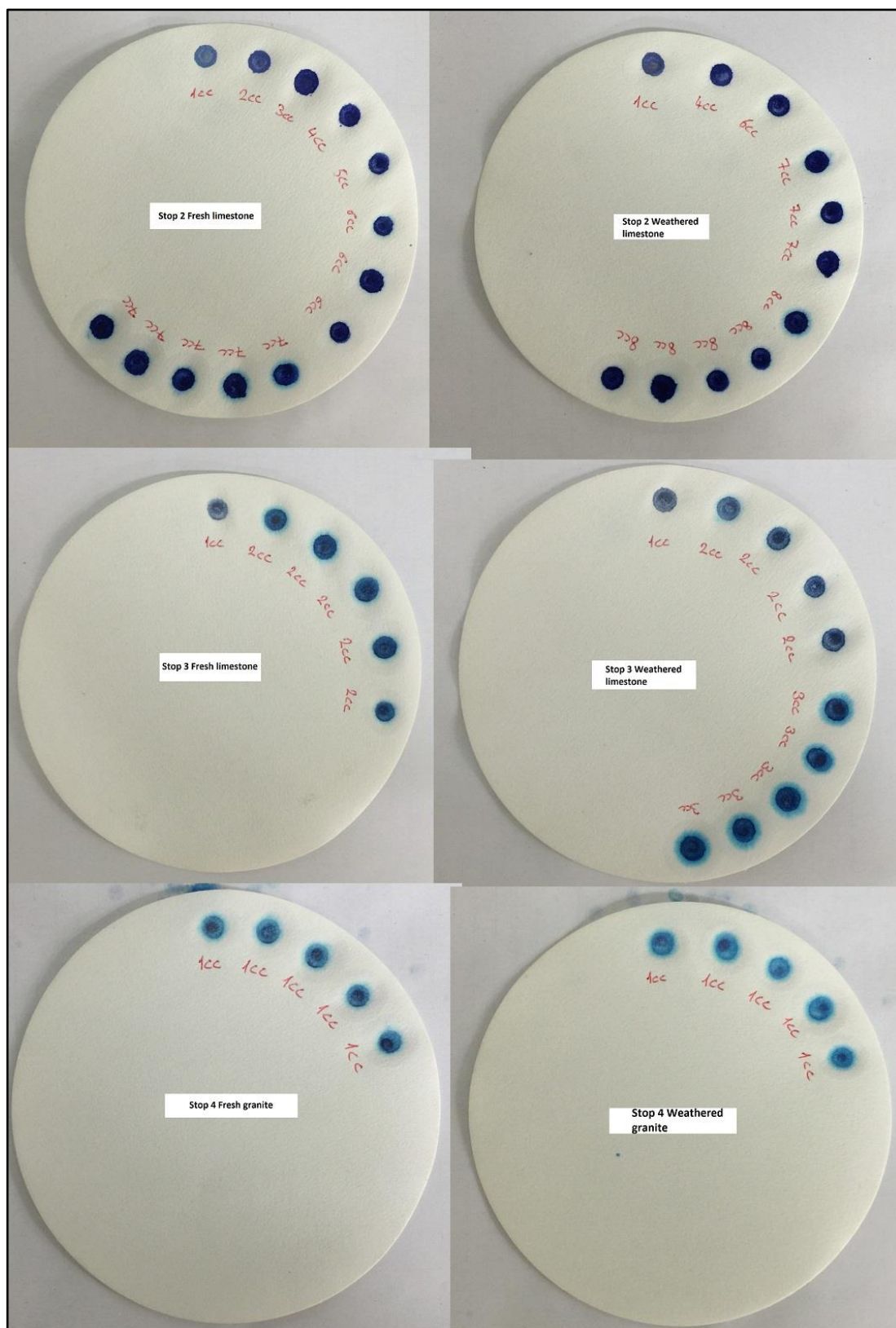


Figure 119. Methylene blue test results of Stop 2, 3 and 4

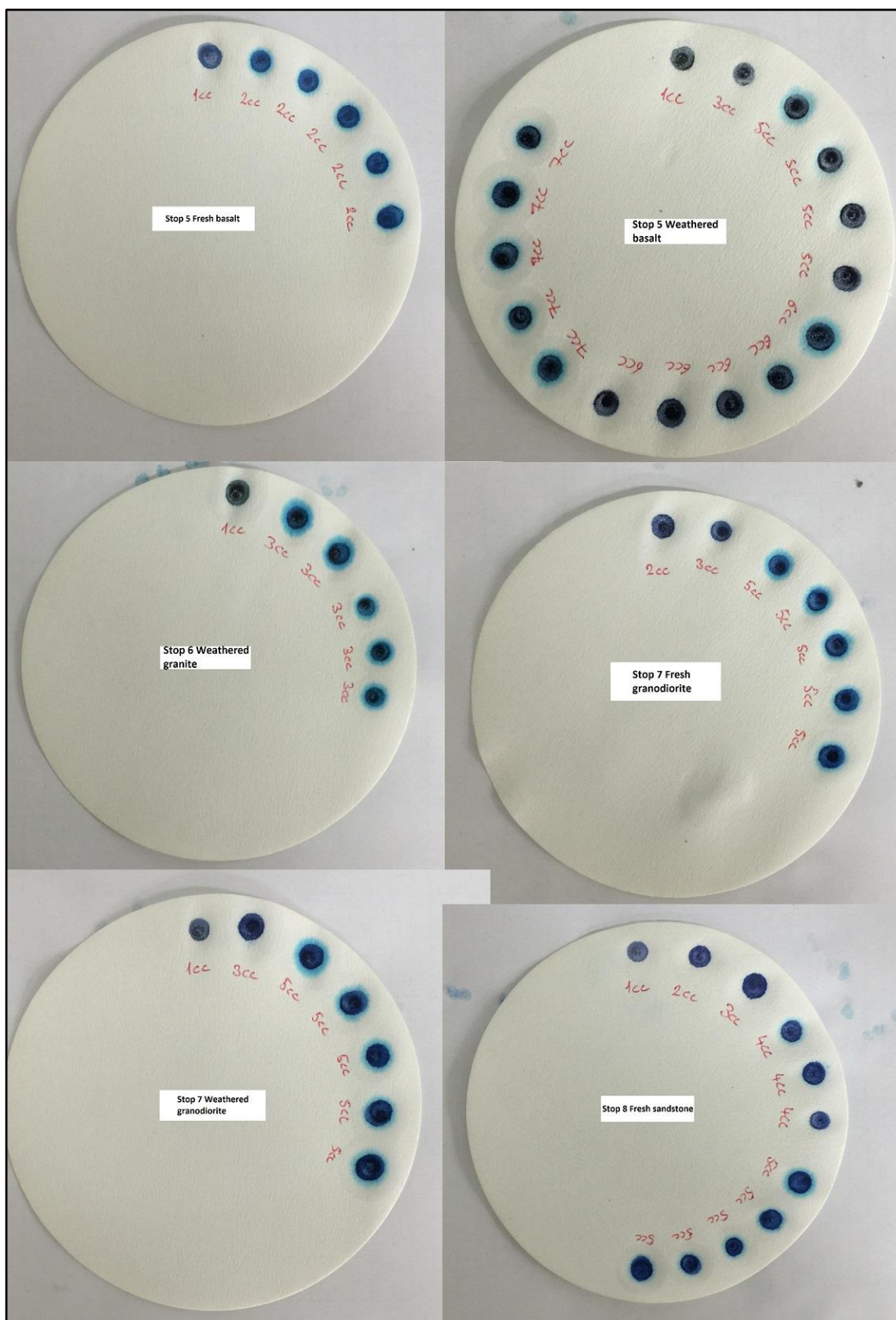


Figure 120. Methylene blue test results of Stop 5, 6, 7 and 8



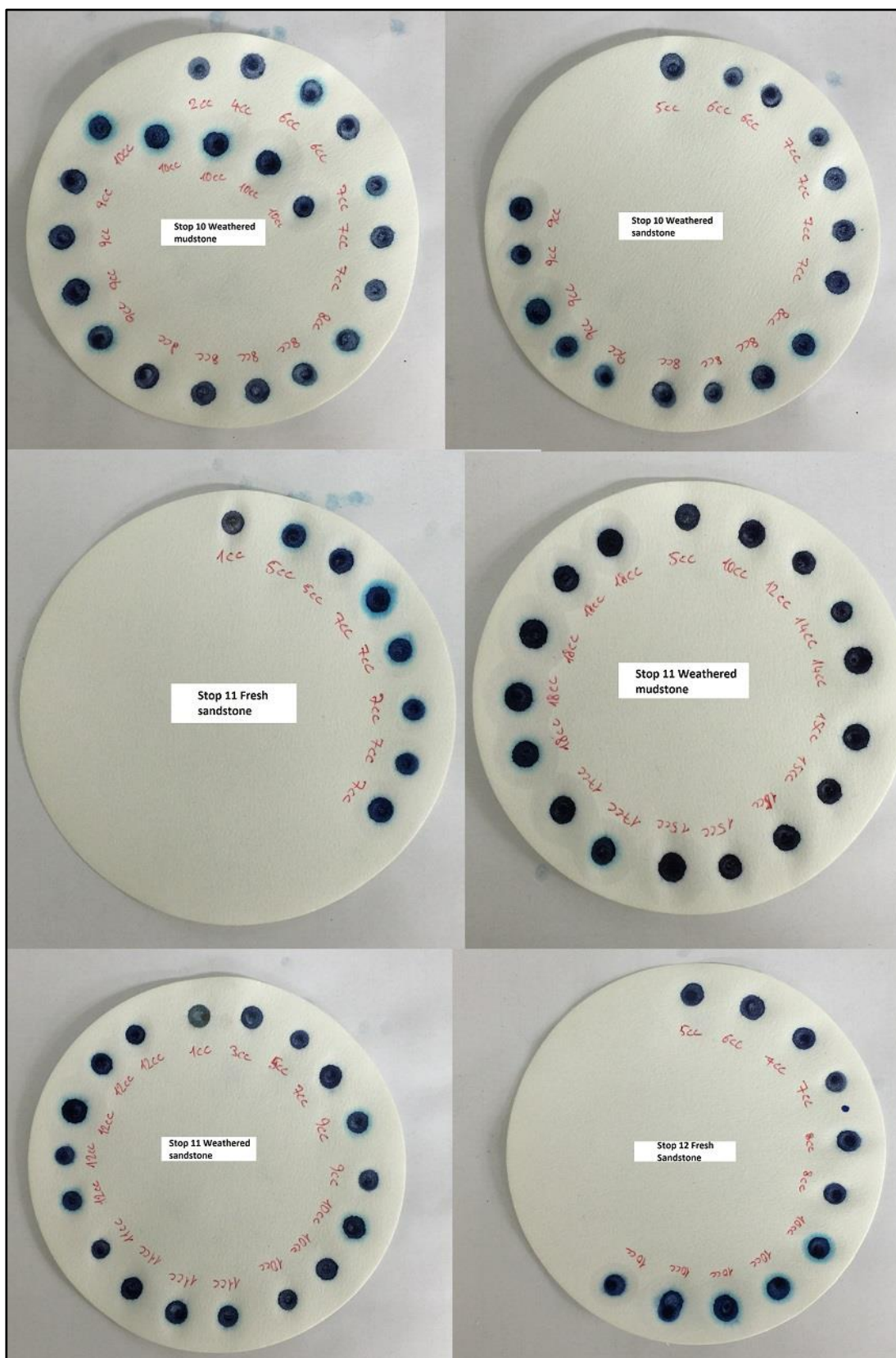


Figure 122. Methylene blue test results of Stop 10, 11 and 12

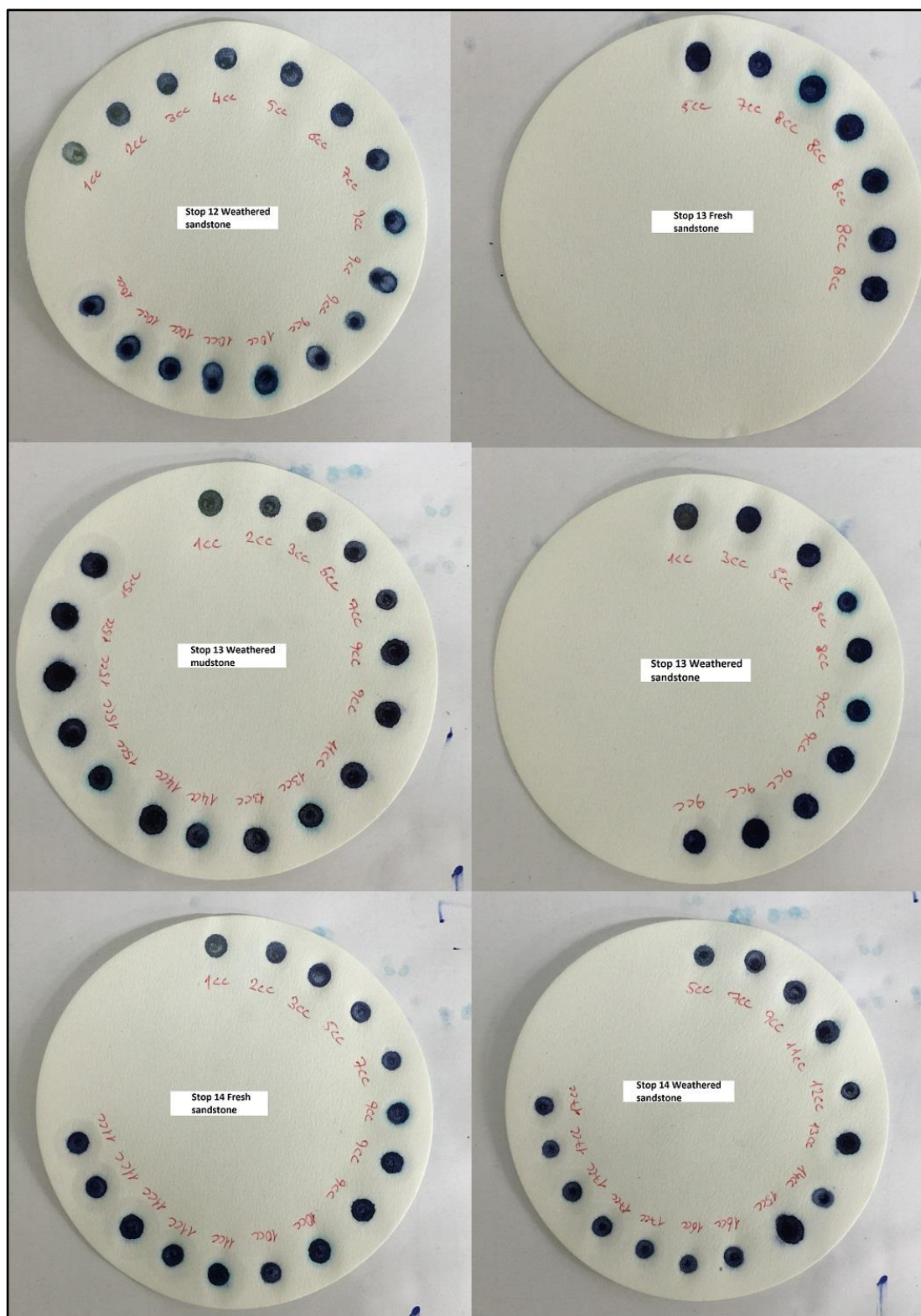


Figure 123. Methylene blue test results of Stop 12, 13 and 14

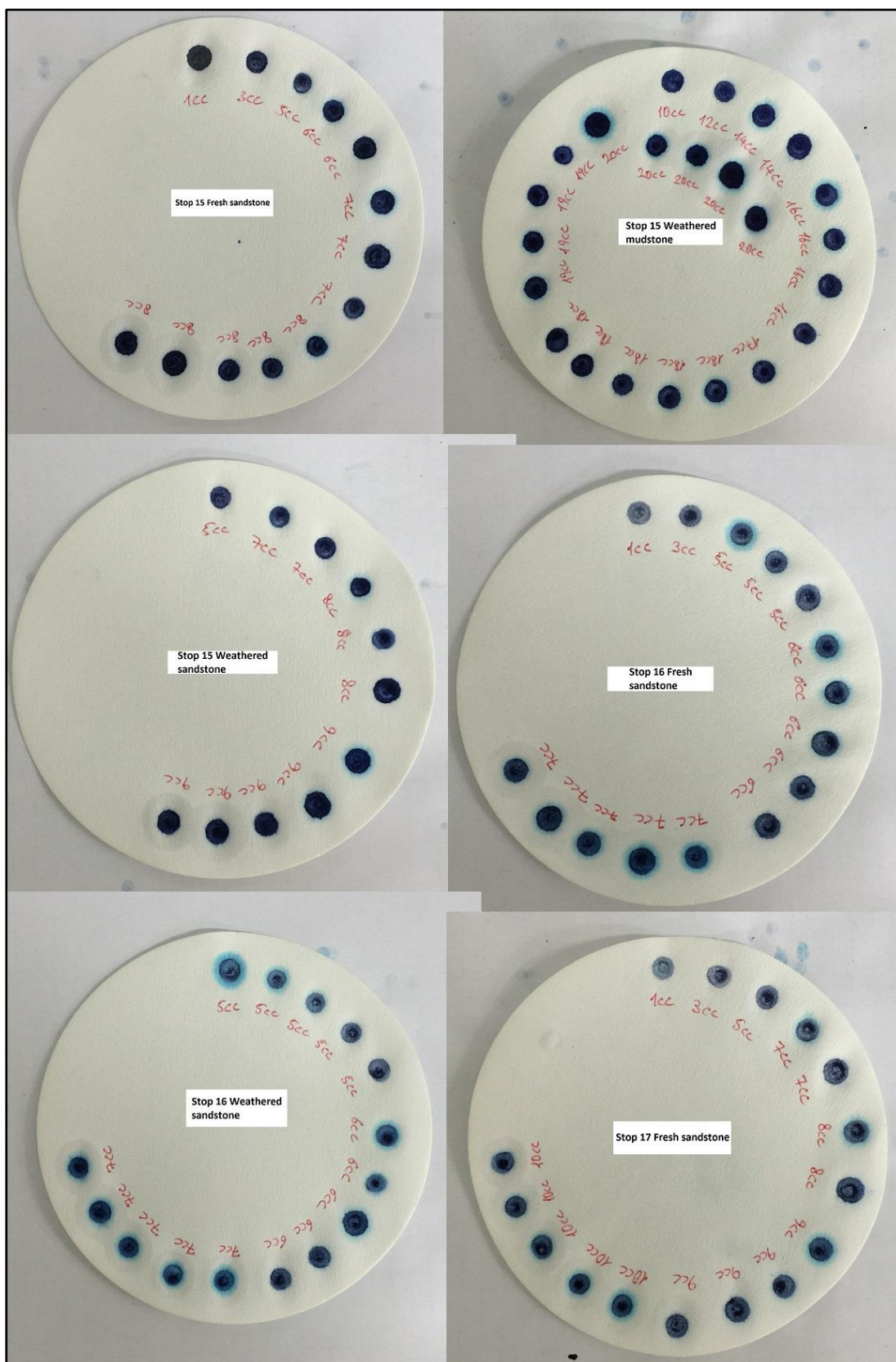


Figure 124. Methylene blue test results of Stop 15, 16 and 17

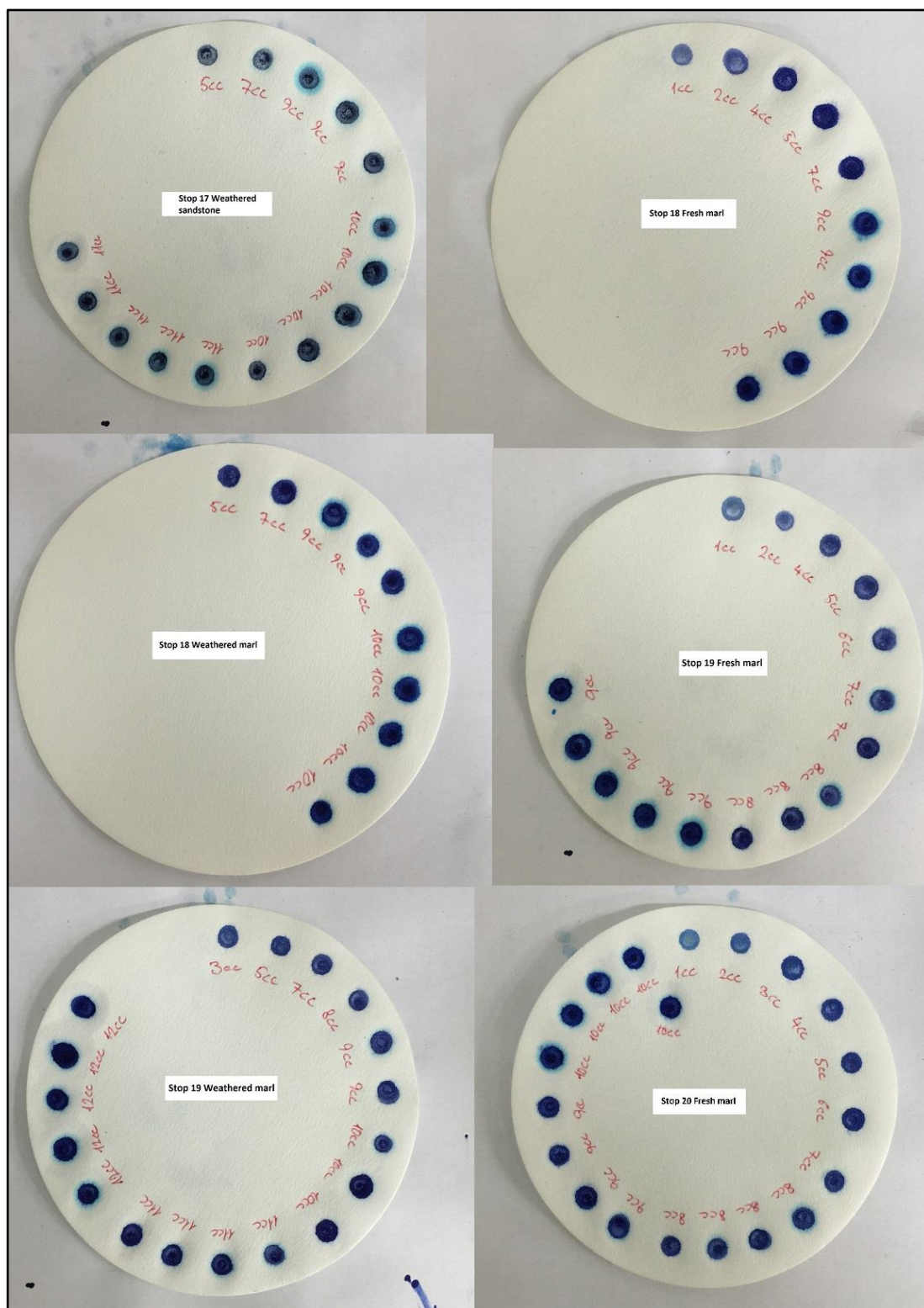


Figure 125. Methylene blue test results of Stop 17, 18, 19 and 20

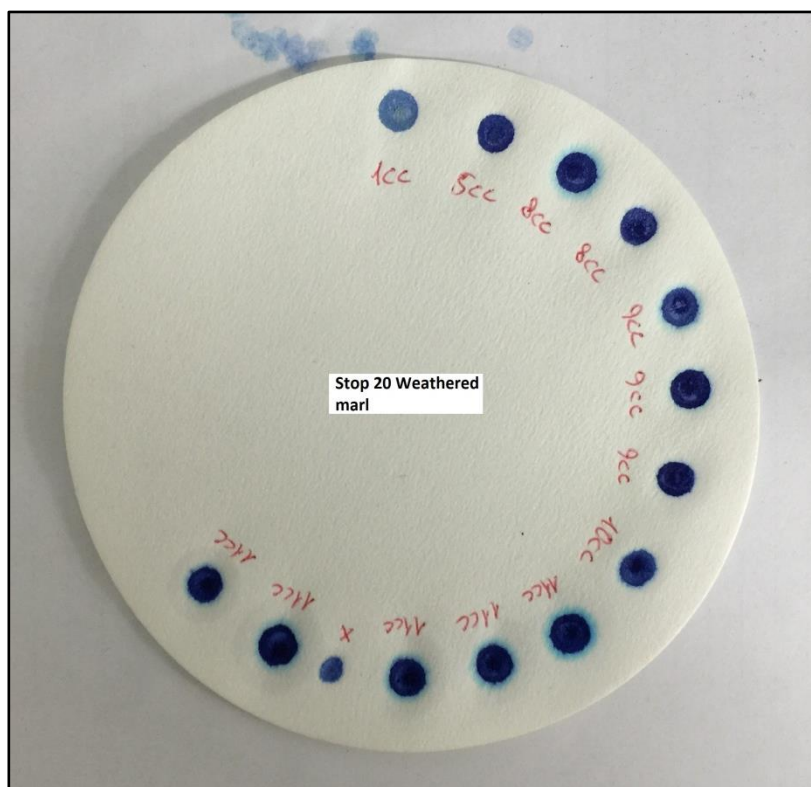


Figure 126. Methylene blue test results of Stop 20

## **APPENDIX B**

### **ANALYSES RESULTS**

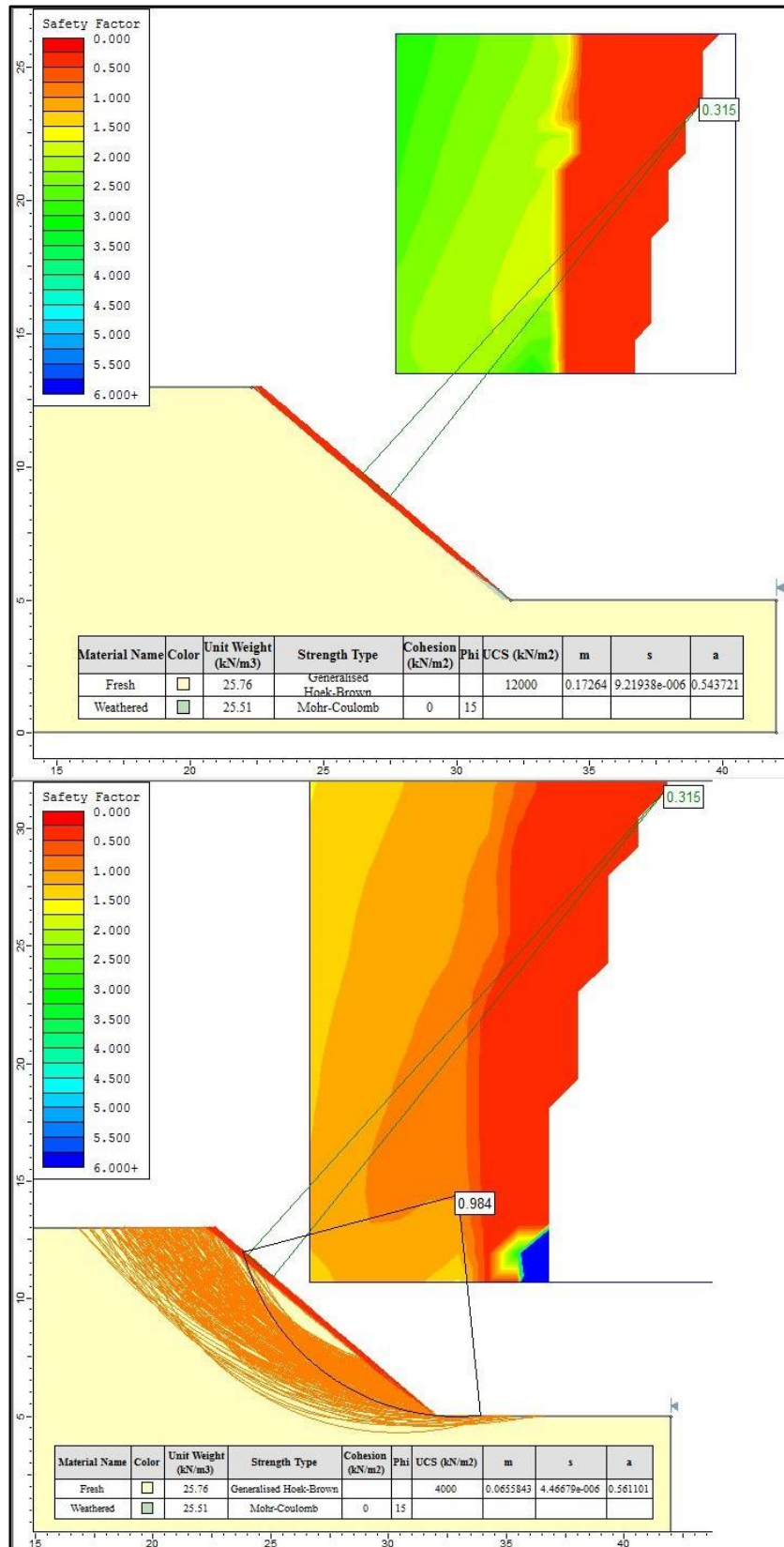


Figure 127. Limit equilibrium analyses of Stop 1 (above) and Stop 1 failed (below)

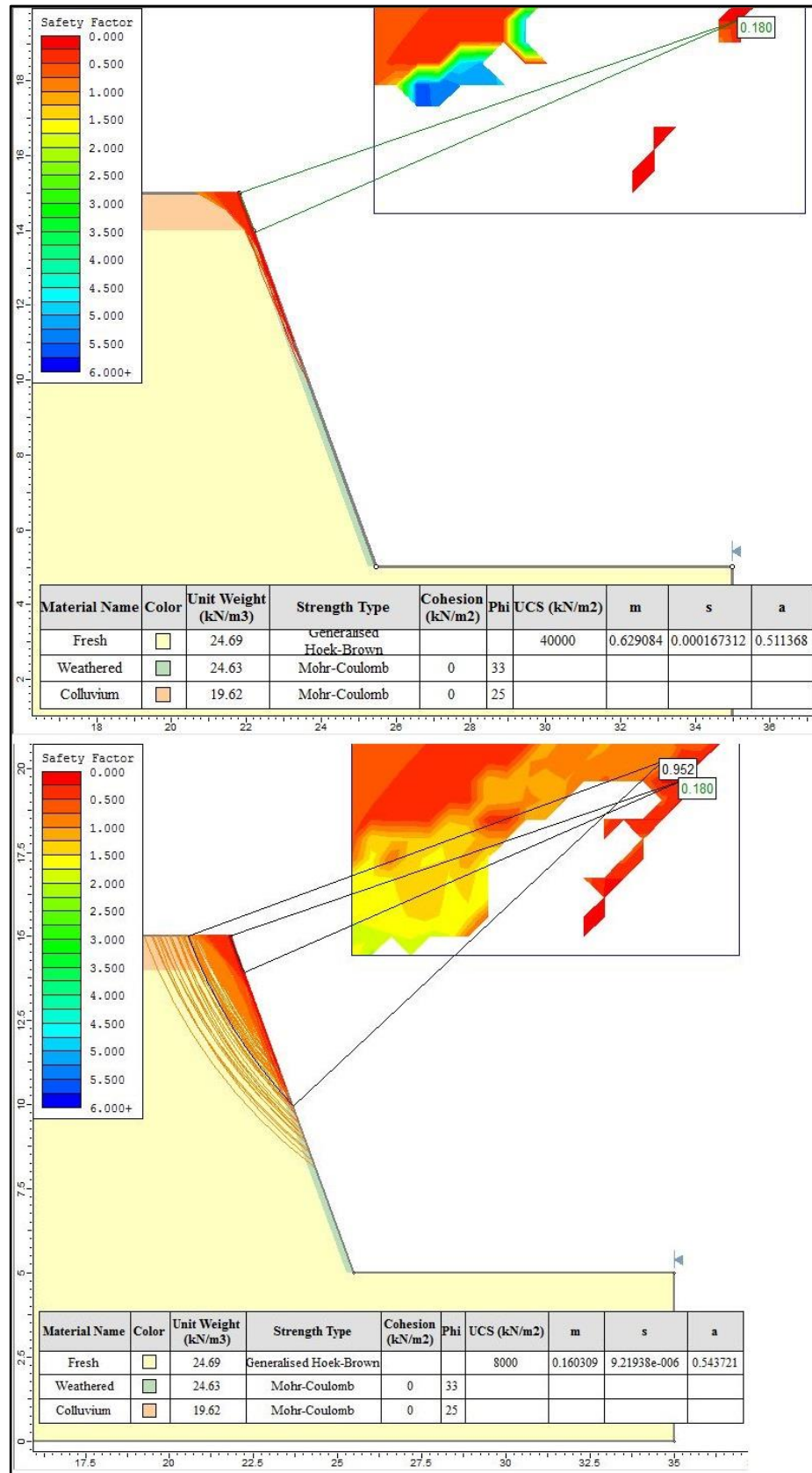


Figure 128. Limit equilibrium analyses of Stop 2 (above) and Stop 2 failed (below)

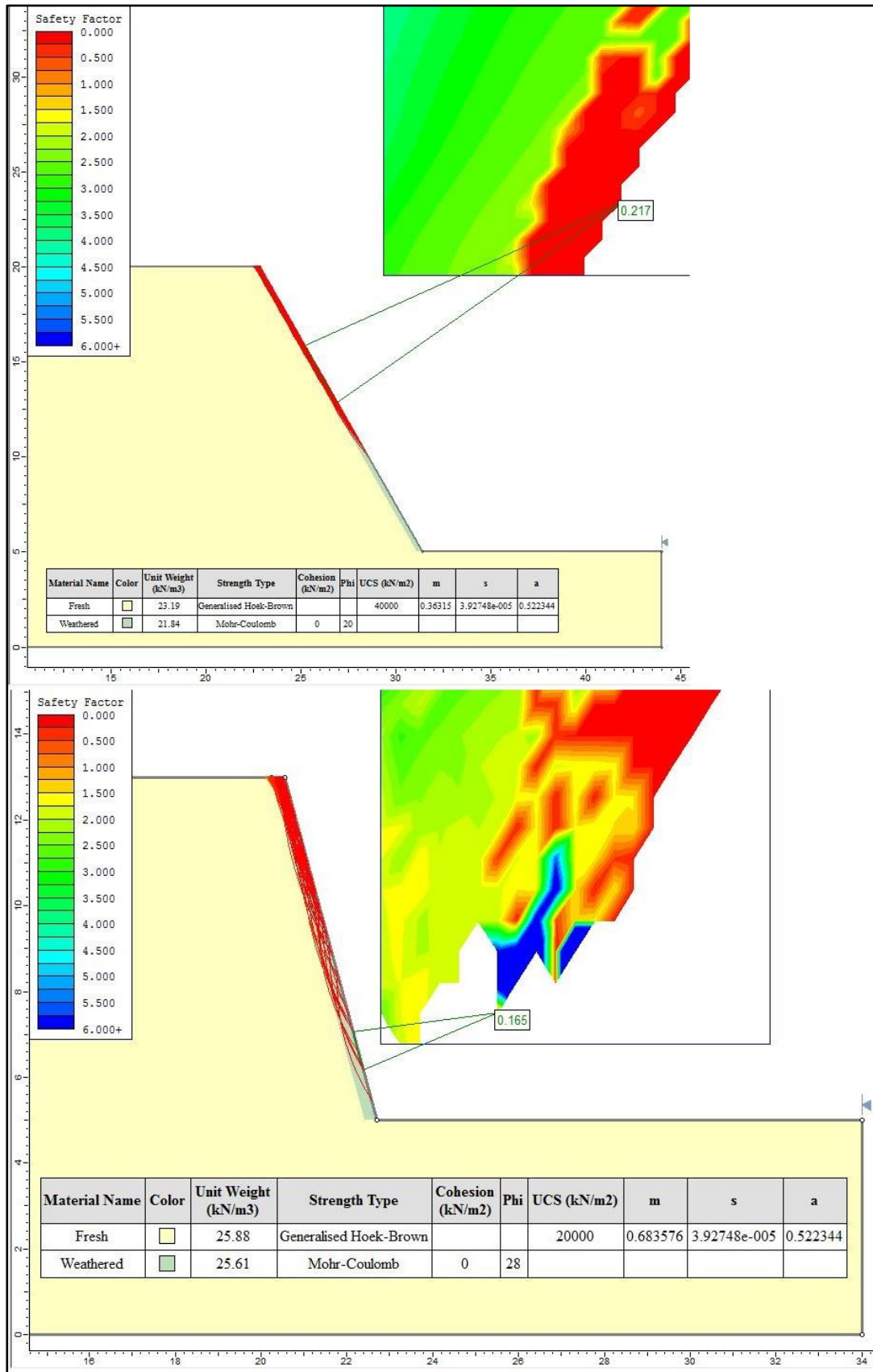


Figure 129. Limit equilibrium analyses of Stop 3 (above) and Stop 4 (below)

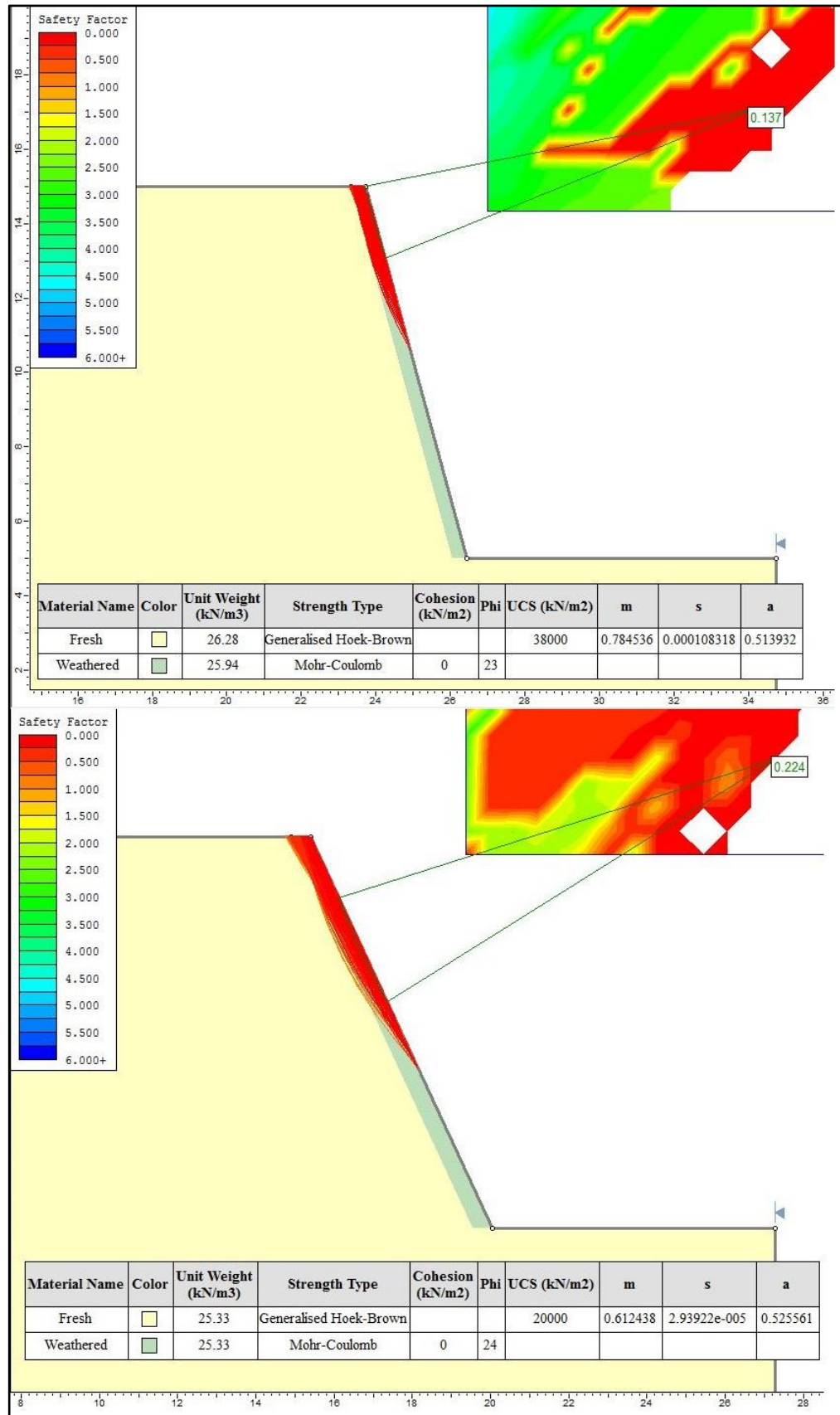


Figure 130. Limit equilibrium analyses of Stop 5 (above) and Stop 6 (below)

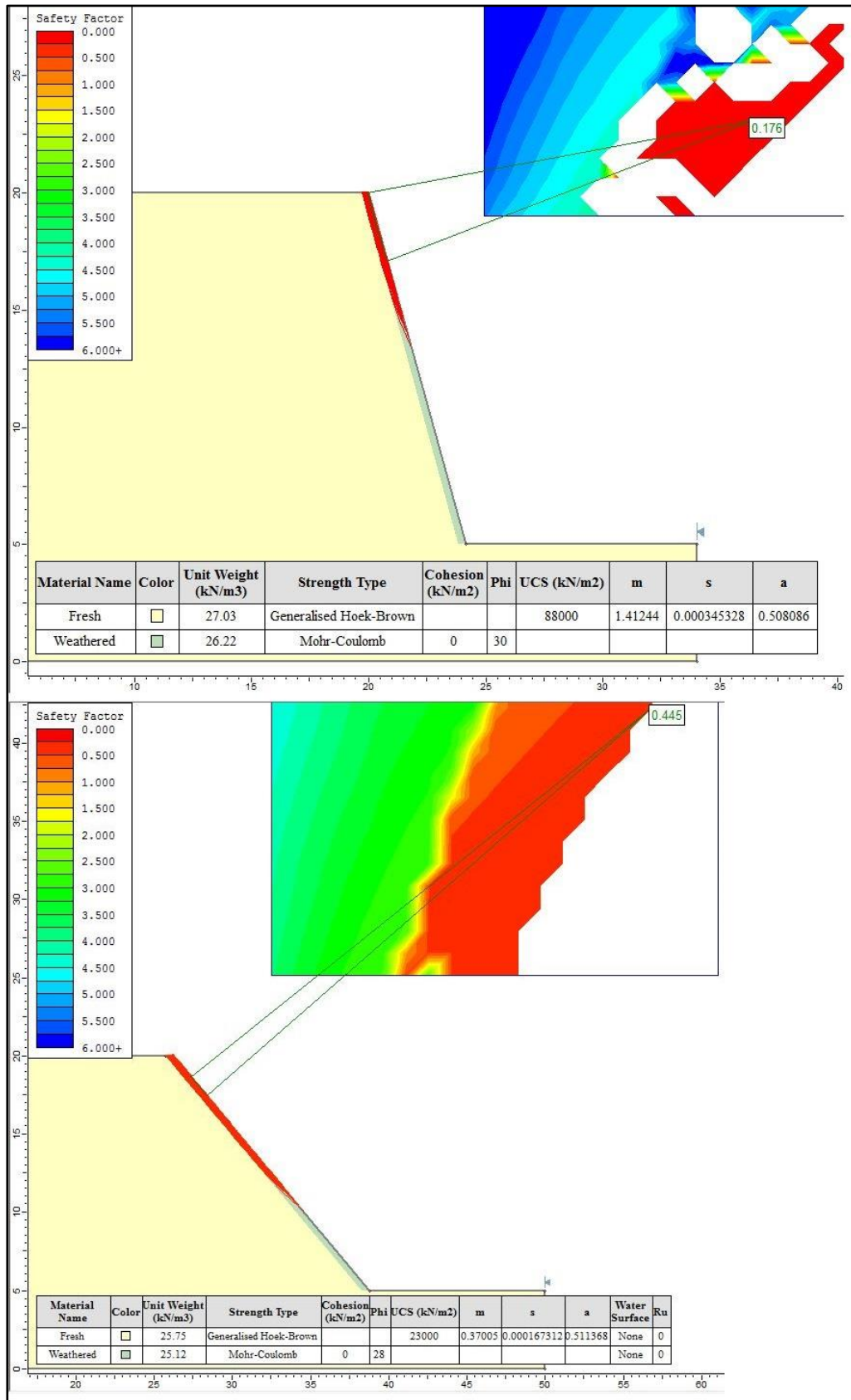


Figure 131. Limit equilibrium analyses of Stop 7 (above) and Stop 8 (below)

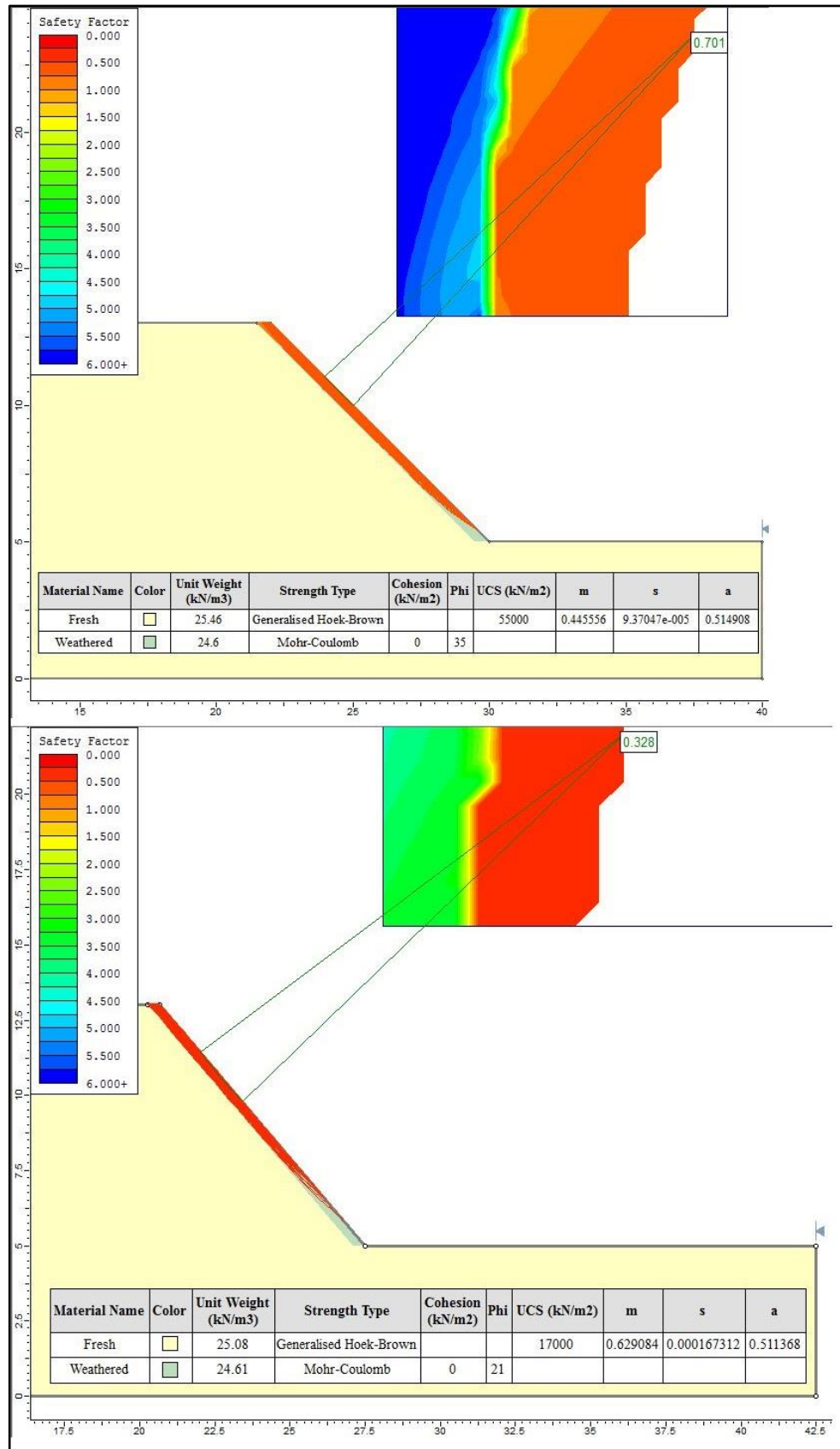


Figure 132. Limit equilibrium analyses of Stop 9 (above) and Stop 10 (below)

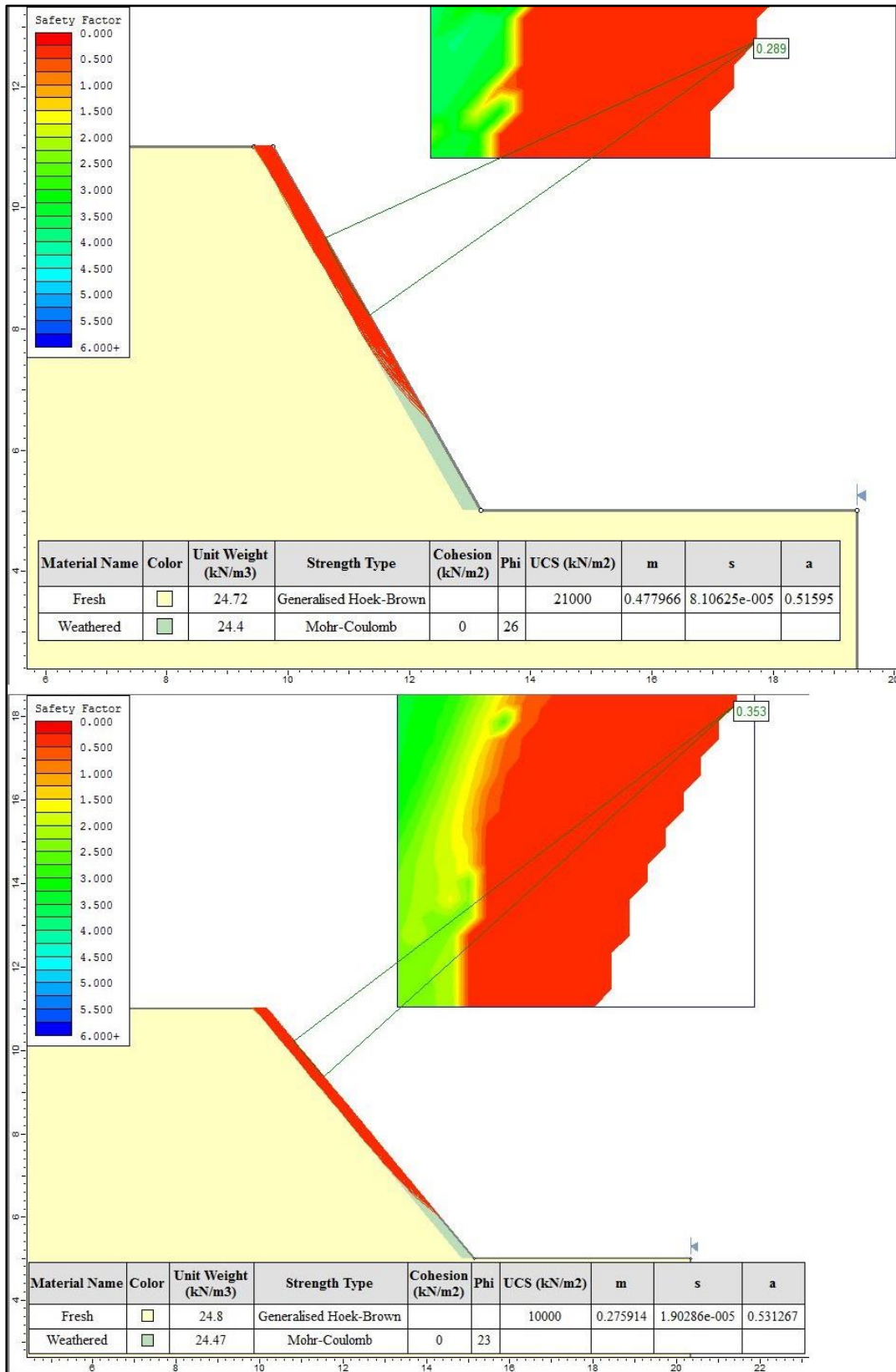


Figure 133. Limit equilibrium analyses of Stop 11 (above) and Stop 12 (below)

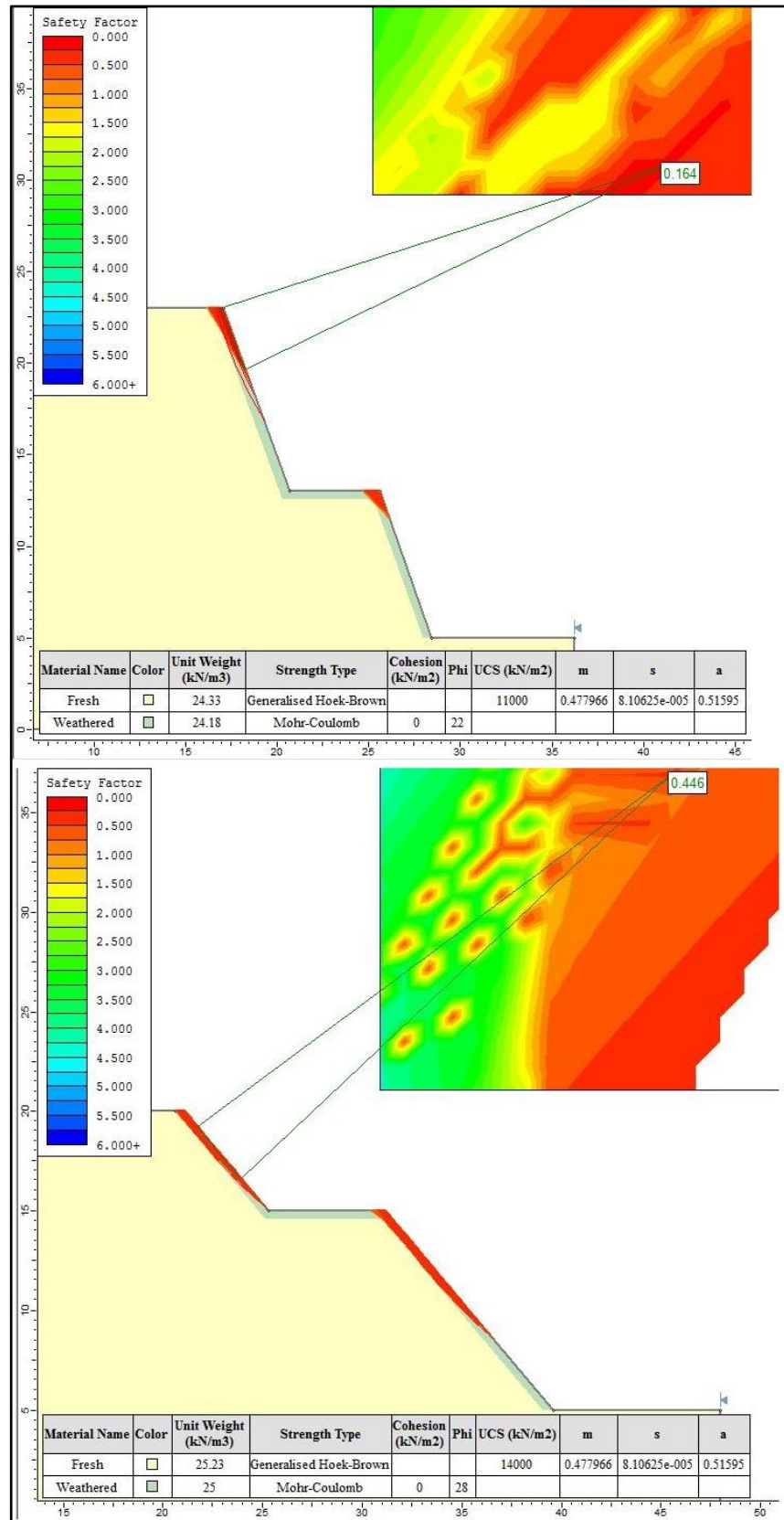


Figure 134. Limit equilibrium analyses of Stop 13 (above) and Stop 14 (below)

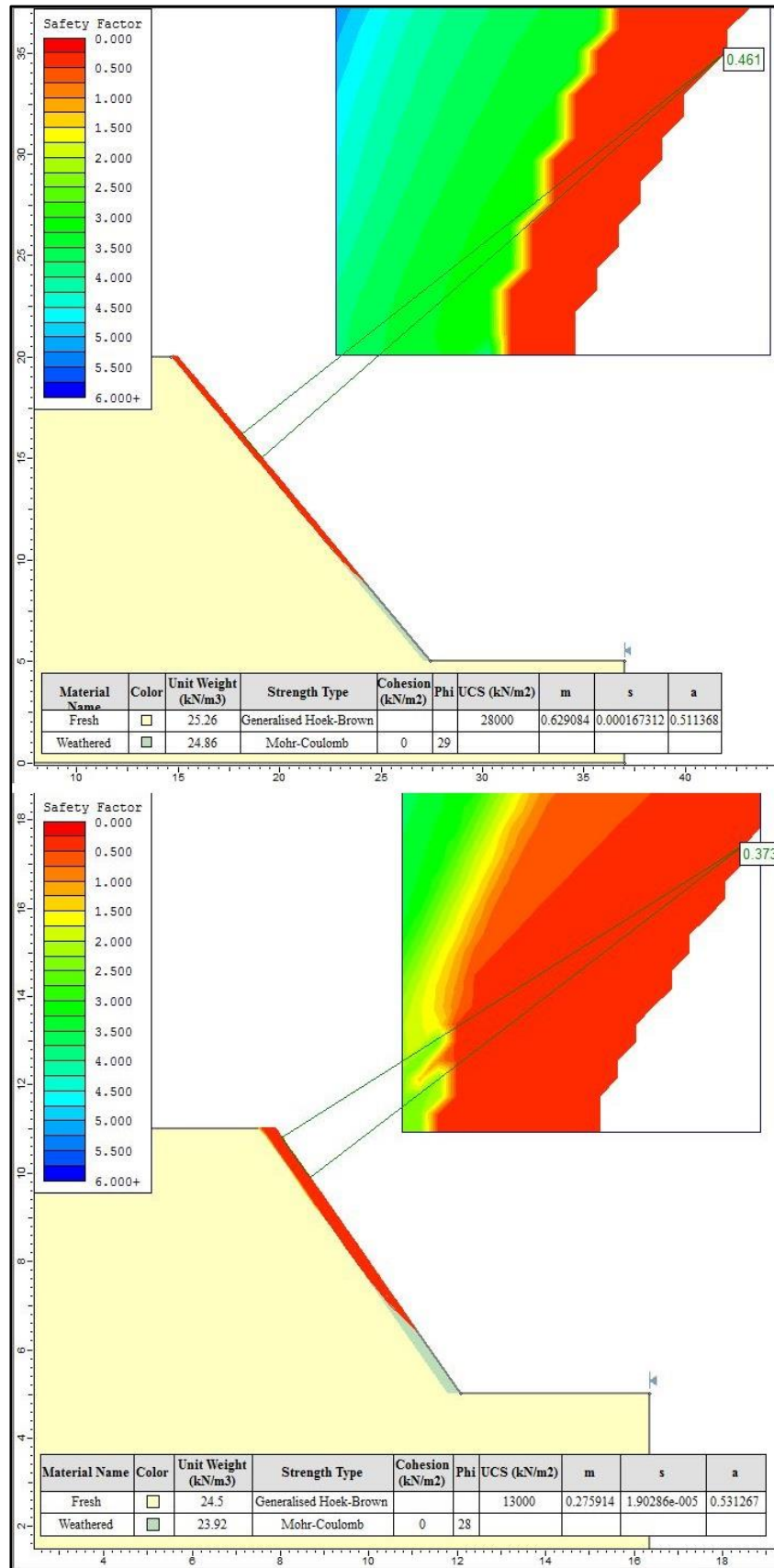


Figure 135. Limit equilibrium analyses of Stop 15 (above) and Stop 16 (below)

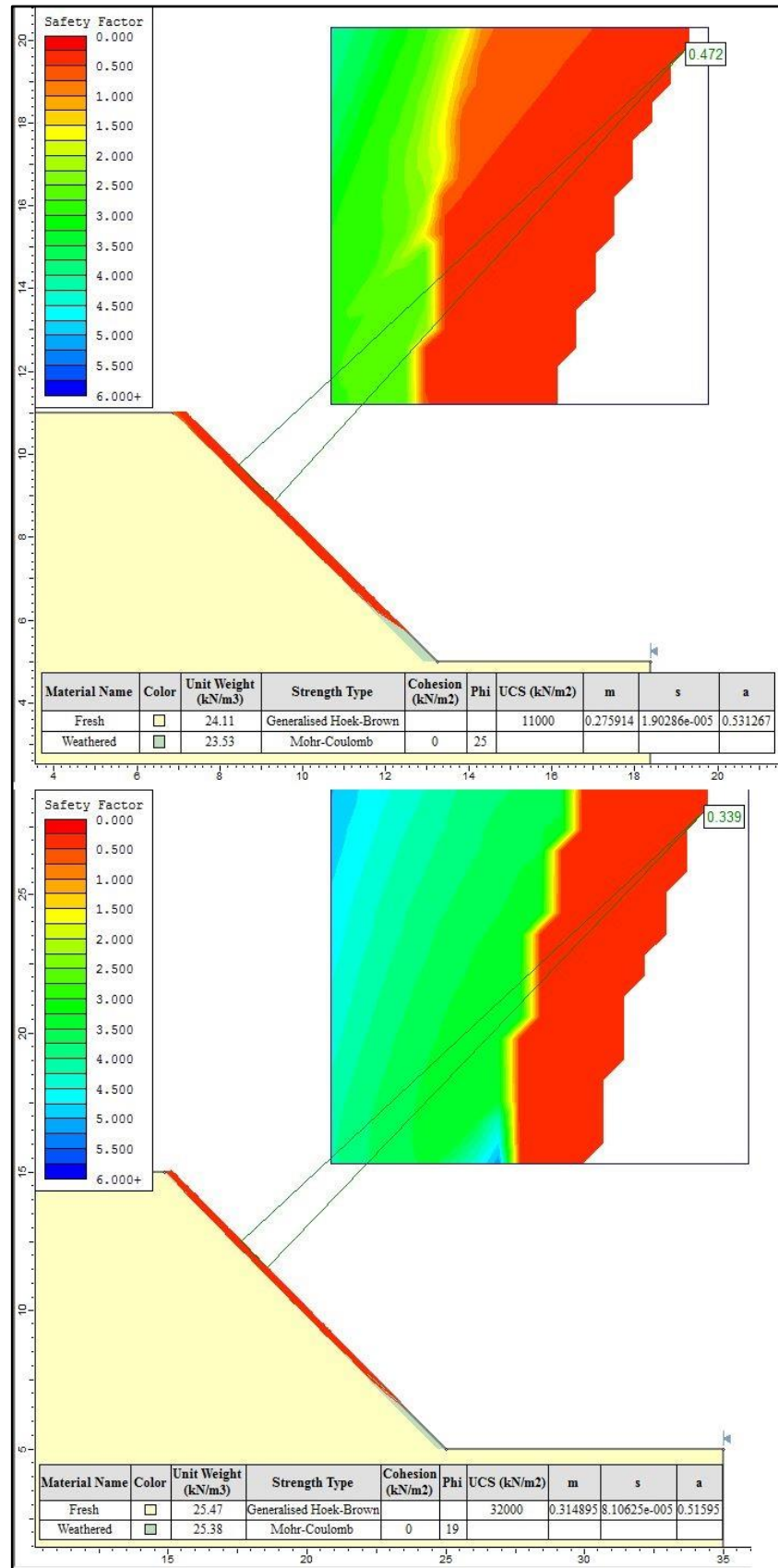


Figure 136. Limit equilibrium analyses of Stop 17 (above) and Stop 18 (below)

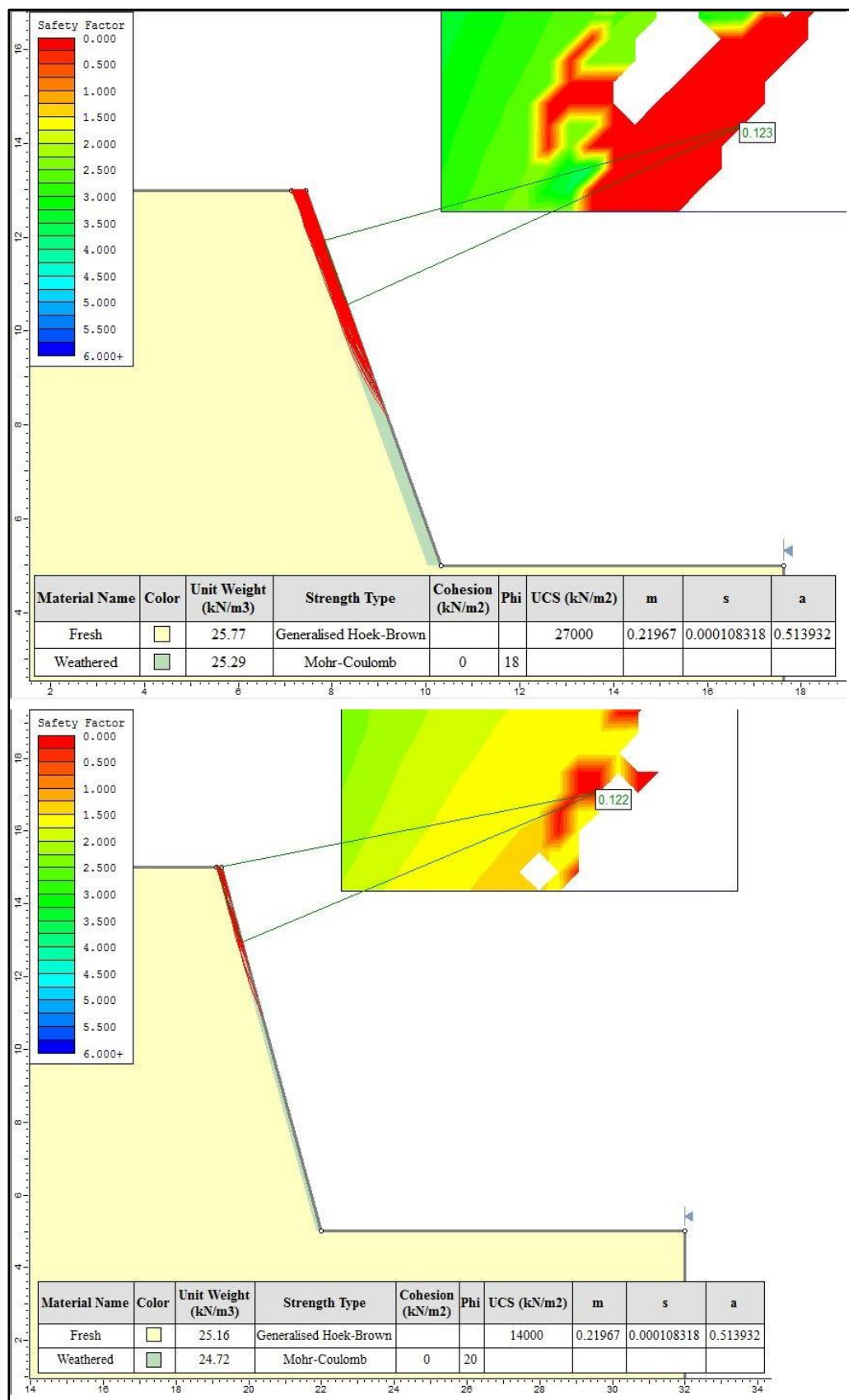


Figure 137. Limit equilibrium analyses of Stop 19 (above) and Stop 20 (below)

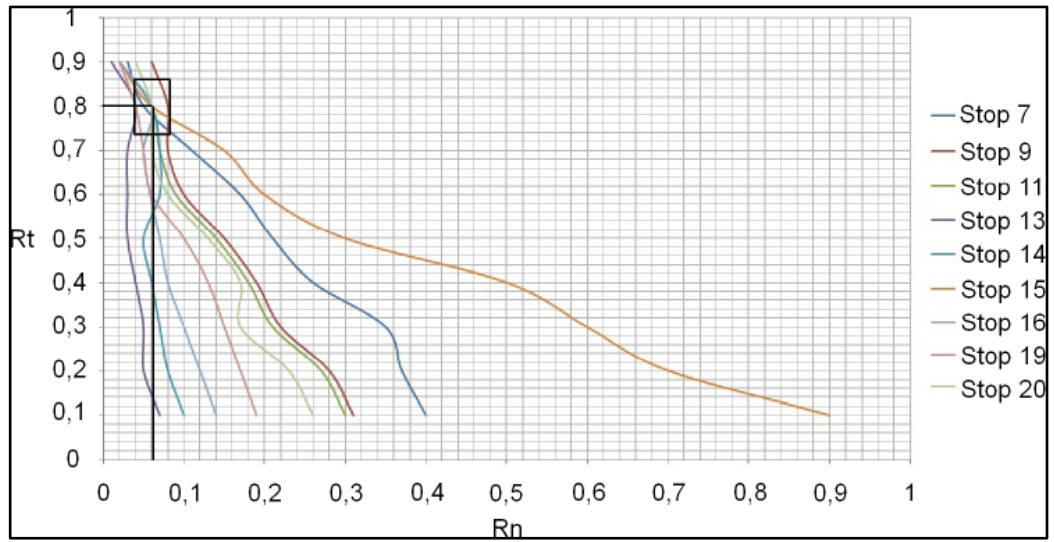


Figure 138.  $R_n$  and  $R_t$  values of drainage channel in front of the slopes

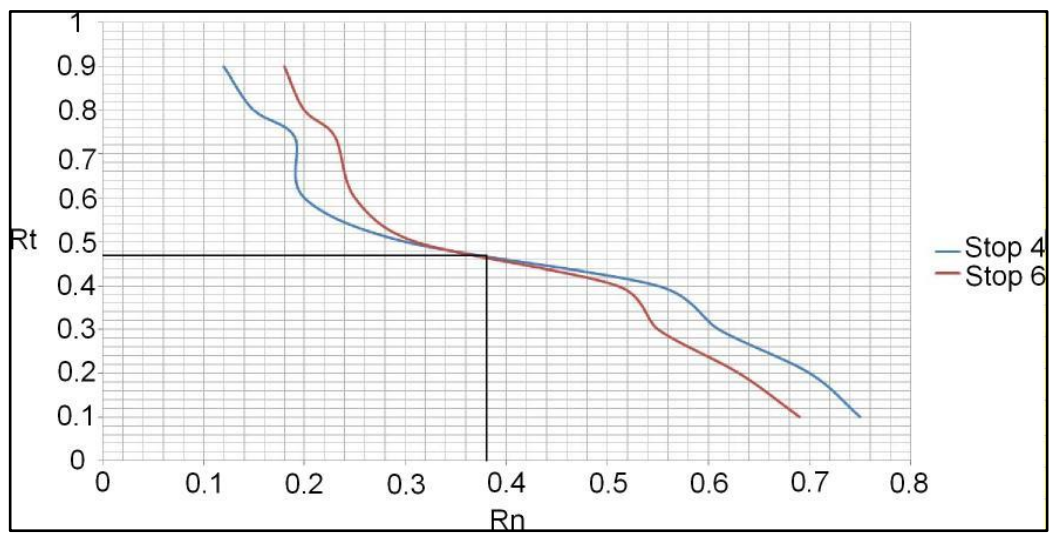


Figure 139.  $R_n$  and  $R_t$  values of granite

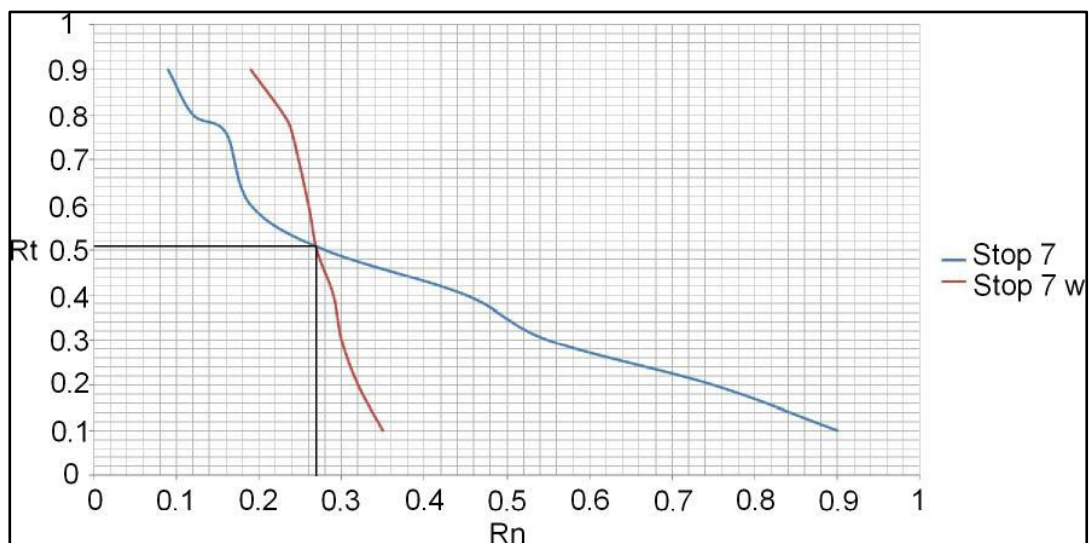


Figure 140.  $R_n$  and  $R_t$  values of granodiorite

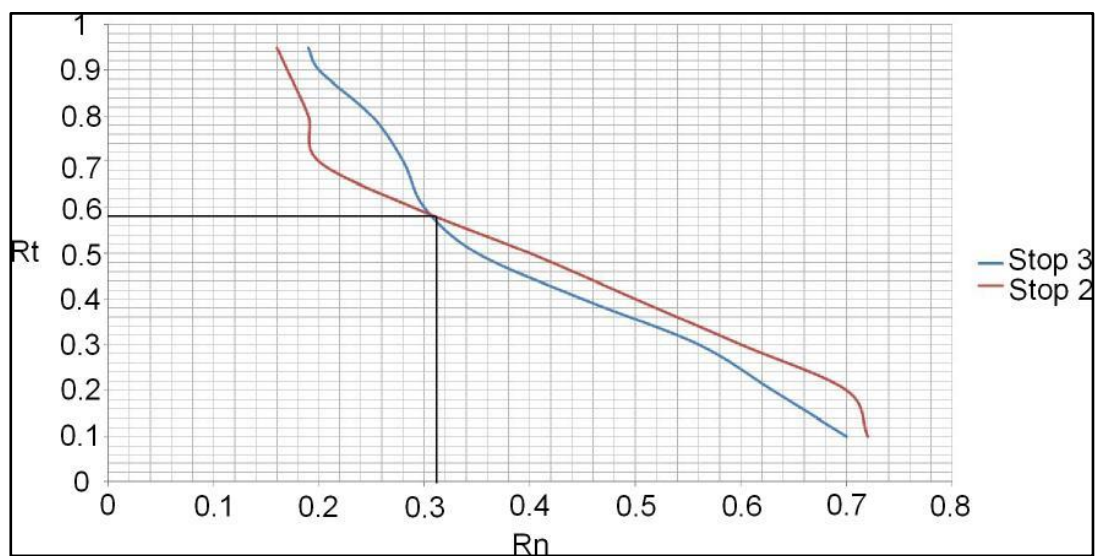


Figure 141.  $R_n$  and  $R_t$  values of limestone

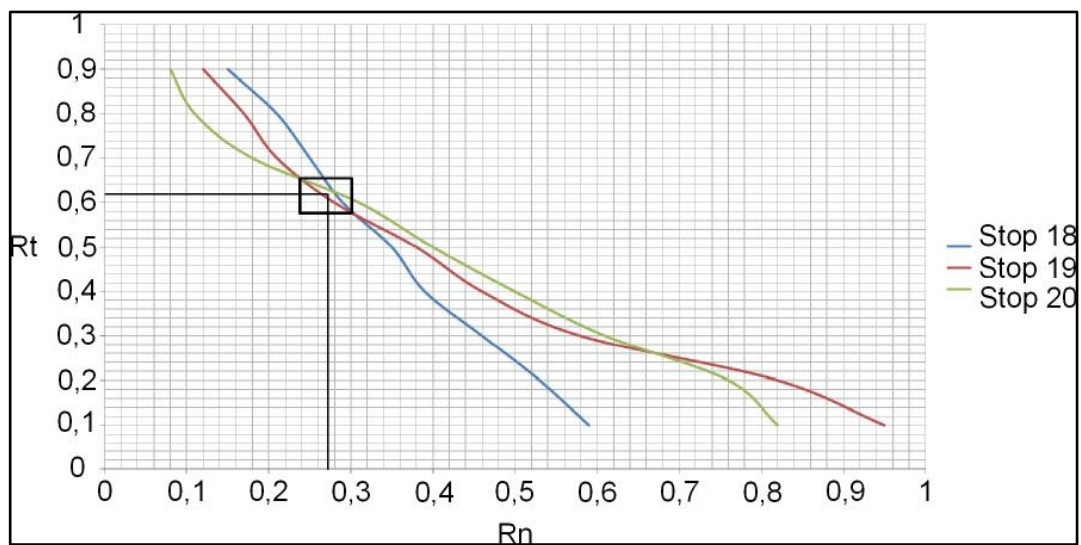


Figure 142.  $R_n$  and  $R_t$  values of marl

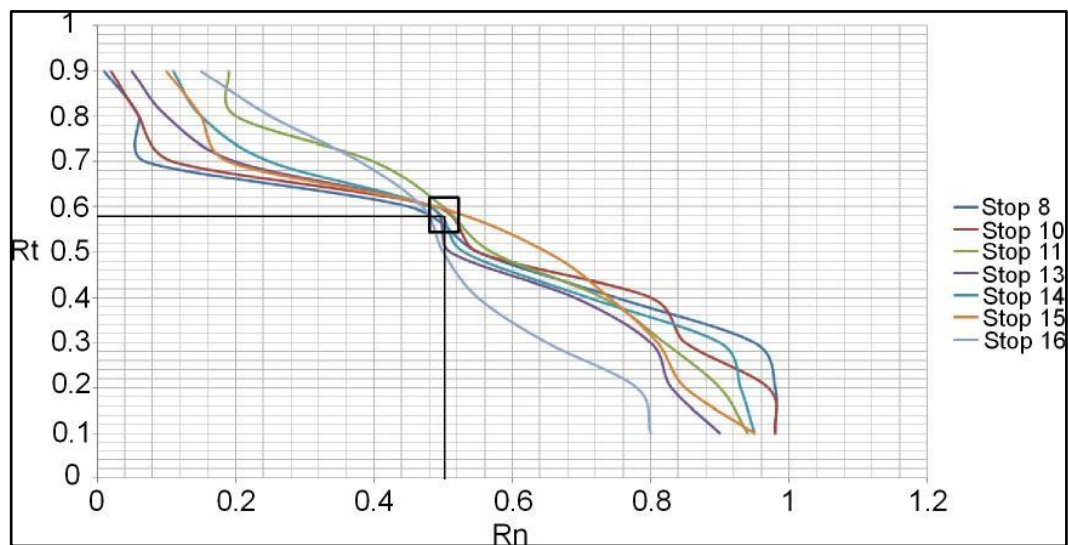


Figure 143.  $R_n$  and  $R_t$  values of sandstone

Table 275. RMR values of Stop 1, 1-failed, 2, 2-failed, 3 and 4

Stop 1		Value	Stop 1-Failed		Value
Strength		2	Strength		1
RQD		3	RQD		3
Spacing of Discontinuity		8	Spacing of Discontinuity		5
Condition of Disc.	Persistency	6	Condition of Disc.	Persistency	6
	Aperture	0		Aperture	0
	Roughness	1		Roughness	1
	Infilling	0		Infilling	0
	Weathering	1		Weathering	1
Groundwater Condition		10	Groundwater		10
<b>RMR basic</b>		<b>31</b>	<b>RMR basic</b>		<b>27</b>
Disc. Orientation Adjustment		-5	Disc. Orientation Adjustment		-5
<b>Total</b>		<b>26</b>	<b>Total</b>		<b>22</b>
Stop 2		Value	Stop 2-Failed		Value
Strength		4	Strength		1
RQD		8	RQD		3
Spacing of Discontinuity		10	Spacing of Discontinuity		5
Condition of Disc.	Persistency	6	Condition of Disc.	Persistency	6
	Aperture	1		Aperture	0
	Roughness	1		Roughness	1
	Infilling	2		Infilling	0
	Weathering	3		Weathering	1
Groundwater		10	Groundwater		10
<b>RMR basic</b>		<b>45</b>	<b>RMR basic</b>		<b>27</b>
Disc. Orientation Adjustment		-5	Disc. Orientation Adjustment		-5
<b>Total</b>		<b>40</b>	<b>Total</b>		<b>22</b>
Stop 3		Value	Stop 4		Value
Strength		4	Strength		2
RQD		3	RQD		3
Spacing of Discontinuity		8	Spacing of Discontinuity		8
Condition of Disc.	Persistency	6	Condition of Disc.	Persistency	6
	Aperture	1		Aperture	1
	Roughness	3		Roughness	1
	Infilling	2		Infilling	2
	Weathering	3		Weathering	3
Groundwater		10	Groundwater		10
<b>RMR basic</b>		<b>40</b>	<b>RMR basic</b>		<b>36</b>
Disc. Orientation Adjustment		-5	Disc. Orientation Adjustment		-5
<b>Total</b>		<b>35</b>	<b>Total</b>		<b>31</b>

Table 276. RMR values of Stop 5, 6, 7, 8, 9 and 10

Stop 5		Value	Stop 6		Value
Strength		4	Strength		2
RQD		3	RQD		3
Spacing of Discontinuity		8	Spacing of Discontinuity		8
Condition of Disc.	Persistence	6	Condition of Disc.	Persistence	6
	Aperture	4		Aperture	0
	Roughness	3		Roughness	3
	Infilling	2		Infilling	0
	Weathering	3		Weathering	1
Groundwater		10	Groundwater		10
<b>RMR basic</b>		<b>43</b>	<b>RMR basic</b>		<b>33</b>
Disc. Orientation Adjustment		-5	Disc. Orientation Adjustment		-5
<b>Total</b>		<b>38</b>	<b>Total</b>		<b>28</b>
Stop 7		Value	Stop 8		Value
Strength		7	Strength		2
RQD		8	RQD		8
Spacing of Discontinuity		8	Spacing of Discontinuity		10
Condition of Disc.	Persistence	6	Condition of Disc.	Persistence	6
	Aperture	1		Aperture	1
	Roughness	3		Roughness	3
	Infilling	2		Infilling	2
	Weathering	5		Weathering	3
Groundwater		10	Groundwater		10
<b>RMR basic</b>		<b>50</b>	<b>RMR basic</b>		<b>45</b>
Disc. Orientation Adjustment		-5	Disc. Orientation Adjustment		-5
<b>Total</b>		<b>45</b>	<b>Total</b>		<b>40</b>
Stop 9		Value	Stop 10		Value
Strength		7	Strength		2
RQD		8	RQD		8
Spacing of Discontinuity		8	Spacing of Discontinuity		10
Condition of Disc.	Persistence	6	Condition of Disc.	Persistence	6
	Aperture	0		Aperture	1
	Roughness	3		Roughness	3
	Infilling	2		Infilling	2
	Weathering	3		Weathering	3
Groundwater		10	Groundwater		10
<b>RMR basic</b>		<b>47</b>	<b>RMR basic</b>		<b>45</b>
Disc. Orientation Adjustment		-5	Disc. Orientation Adjustment		-5
<b>Total</b>		<b>42</b>	<b>Total</b>		<b>40</b>

Table 277. RMR values of Stop 11, 12, 13, 14, 15 and 16

Stop 11		Value	Stop 12		Value
Strength		2	Strength		2
RQD		3	RQD		3
Spacing of Discontinuity		8	Spacing of Discontinuity		8
Condition of Disc.	Persistency	6	Condition of Disc.	Persistency	6
	Aperture	1		Aperture	0
	Roughness	3		Roughness	3
	Infilling	2		Infilling	0
	Weathering	3		Weathering	3
Groundwater		10	Groundwater		10
<b>RMR basic</b>		<b>38</b>	<b>RMR basic</b>		<b>35</b>
Disc. Orientation Adjustment		-5	Disc. Orientation Adjustment		-5
<b>Total</b>		<b>33</b>	<b>Total</b>		<b>30</b>
Stop 13		Value	Stop 14		Value
Strength		2	Strength		2
RQD		3	RQD		3
Spacing of Discontinuity		8	Spacing of Discontinuity		8
Condition of Disc.	Persistency	6	Condition of Disc.	Persistency	6
	Aperture	1		Aperture	1
	Roughness	3		Roughness	3
	Infilling	2		Infilling	2
	Weathering	3		Weathering	3
Groundwater		10	Groundwater		10
<b>RMR basic</b>		<b>38</b>	<b>RMR basic</b>		<b>38</b>
Disc. Orientation Adjustment		-5	Disc. Orientation Adjustment		-5
<b>Total</b>		<b>33</b>	<b>Total</b>		<b>33</b>
Stop 15		Value	Stop 16		Value
Strength		4	Strength		2
RQD		8	RQD		3
Spacing of Discontinuity		10	Spacing of Discontinuity		8
Condition of Disc.	Persistency	4	Condition of Disc.	Persistency	6
	Aperture	1		Aperture	0
	Roughness	3		Roughness	3
	Infilling	2		Infilling	0
	Weathering	3		Weathering	3
Groundwater		10	Groundwater		10
<b>RMR basic</b>		<b>45</b>	<b>RMR basic</b>		<b>35</b>
Disc. Orientation Adjustment		-5	Disc. Orientation Adjustment		-5
<b>Total</b>		<b>40</b>	<b>Total</b>		<b>30</b>

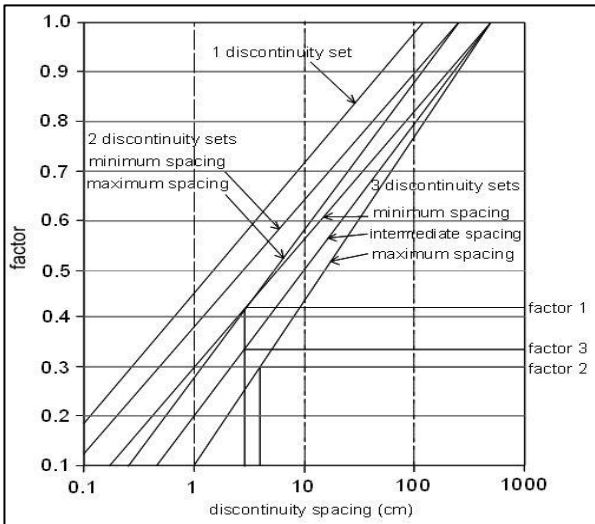
Table 278. RMR values of Stop 17, 18, 19 and 20

Stop 17		Value	Stop 18		Value
Strength		2	Strength		4
RQD		3	RQD		3
Spacing of Discontinuity		8	Spacing of Discontinuity		8
Condition of Disc.	Persistence	6	Condition of Disc.	Persistence	6
	Aperture	0		Aperture	1
	Roughness	3		Roughness	3
	Infilling	0		Infilling	2
	Weathering	3		Weathering	3
Groundwater		10	Groundwater		10
<b>RMR basic</b>		<b>35</b>	<b>RMR basic</b>		<b>40</b>
Disc. Orientation Adjustment		-5	Disc. Orientation Adjustment		-5
<b>Total</b>		<b>30</b>	<b>Total</b>		<b>35</b>
Stop 19		Value	Stop 20		Value
Strength		4	Strength		2
RQD		3	RQD		3
Spacing of Discontinuity		8	Spacing of Discontinuity		8
Condition of Disc.	Persistence	6	Condition of Disc.	Persistence	6
	Aperture	1		Aperture	4
	Roughness	3		Roughness	3
	Infilling	2		Infilling	2
	Weathering	3		Weathering	5
Groundwater		10	Groundwater		10
<b>RMR basic</b>		<b>40</b>	<b>RMR basic</b>		<b>43</b>
Disc. Orientation Adjustment		-5	Disc. Orientation Adjustment		-5
<b>Total</b>		<b>35</b>	<b>Total</b>		<b>38</b>



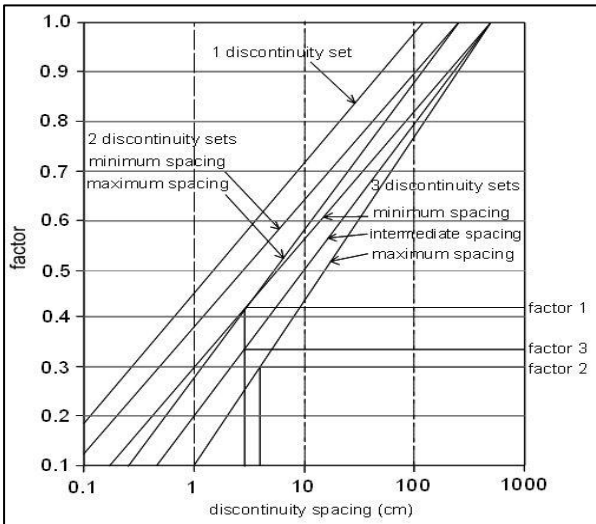
## **SSPC RESULTS**

STOP 1 - DATA COLLECTION TABLE								
Excavation Method (ME)			Intact Rock Strength (IRS)					
Natural/hand-made	1,00	<1.25 MPa			Crumbles in hand			
Pneumatic hammer excavation*	0,76	1.25-5 MPa			Thin slabs break easy in hand			
Pre-splitting/smooth wall blasting	0,99	5-12.5 MPa			Thin slabs broken by heavy hand pressure*			
Conventional blasting with result:		12.5-50 MPa			Lumps broken by light hammer blows			
Good	0,77	50-100 MPa			Lumps broken by heavy hammer blows			
Open discontinuities	0,75	100-200 MPa			Lumps only chip by heavy hammer blows			
Dislodged blocks	0,72	>200 MPa			Rocks ring on hammer blows			
Fractured intact rock	0,67	Weathering degree (WE)			Unweathered		1,00	
Crushed intact rock	0,62				Slightly		0,95	
Lithology					Moderately*		0,90	
95% Mudstone / 5% Sandstone					Highly		0,62	
					Completely		0,35	
Discontinuities (B: Bedding; J: Joint)				B	J1	J2	Slope	
Dip direction (degrees)				139	247	319	Dip direction (degrees)	310
Dip (degrees)				69	40	33	Dip (degrees)	40
Spacing (DS) (cm)				5	15	10	Slope height (m)	8
Condition of discontinuities						Slope Stability		
Large scale roughness (RL)	Wavy		1,00	X			Stable	1
	Slightly wavy		0,95				Small problem*	2
	Curved		0,85				Large problem	3
	Slightly curved		0,80		X	X	Notes: 1) For infill "gouge">irregularities" and "flowing material" small scale roughness= 0,55 2) If roughness is anisotropic (e.g. Ripple marks, striation, etc.) roughness should be assessed perpendicular and parallel to the roughness and directions noted on this form 3) Non-fitting of discontinuities should be marked in roughness columns.	
	Straight		0,75					
Small scale roughness (RS)	Rough stepped		0,95	X				
	Smooth stepped		0,90		X	X		
	Polished stepped		0,85					
	Rough undulating		0,80					
	Smooth undulating		0,75					
	Polished undulating		0,70					
	Rough planar		0,65					
	Smooth planar		0,60					
	Polished planar		0,55					
Infill material (IM)	Cemented / cemented infill		1,07					
	No infill - surface staining		1,00					
	Non-softening & sheared material	Coarse	0,95					
		Medium	0,90					
		Fine	0,85					
	Soft sheared material	Coarse	0,75					
		Medium	0,65					
		Fine	0,55	X	X	X		
	Gouge < irregularities		0,42					
	Gouge > irregularities		0,17					
Flowing material		0,05						
Karst (KA)	None		1,00	X	X	X		
	Karst		0,92					

STOP 1 - REFERENCE ROCK TABLE				
Intact Rock Strength (RIRS)				
RIRS = IRS / WE = 8 / 0,90				8,889
Discontinuity Spacing (SPA)				
Discontinuities	B	J1	J2	SPA = factor 1 x factor 2 x factor 3
Dip direction (degrees)	139	247	319	
Dip (degrees)	69	40	33	
Spacing (m)	5	15	10	
The spacing parameter (SPA) is calculated based on the three discontinuity sets with the smallest spacings in following figure:				SPA = 0,50 x 0,50 x 0,48 = 0,120
				
Corrected for weathering and method of excavation:				
RSPA = SPA / (WE x ME)				
RSPA = 0,120 / (0,90 x 0,76)				
				0,175
Condition of discontinuities				
Discontinuities	B	J1	J2	RTC is the discontinuity condition of a single discontinuity (set) in the reference rock mass corrected for discontinuity weathering. $RTC = TC / \sqrt{1,452 - 1,220 * e^{(-WE)}}$
Large scale roughness (Rl)	1,00	0,80	0,80	
Small scale roughness (Rs)	0,95	0,90	0,90	
Infill material (Im)	0,55	0,55	0,55	
Karst (Ka)	1,00	1,00	1,00	
TC = Rl x Rs x Im x Ka	0,523	0,396	0,396	
RTC	0,534	0,405	0,405	
Weighted by spacing: $CD = \frac{\frac{TC_1}{DS_1} + \frac{TC_2}{DS_2} + \frac{TC_3}{DS_3}}{\frac{1}{DS_1} + \frac{1}{DS_2} + \frac{1}{DS_3}} =$				0,465
Corrected by weathering: RCD (with a maximum of 1.0165) = CD/WE =				0,465 / 0,90 = 0,517
Reference unit friction and cohesion (RFRI & FCOH)				
$\phi(RRM) = RIRS * 0,2417 + RSPA * 52,12 + RCD * 5,779 =$ (If RIRS > 132 MPa, then RIRS = 132)				14,26°
$coh(RRM) = RIRS * 94,27 + RSPA * 28629 + RCD * 3593 =$ (If RIRS > 132 MPa, then RIRS = 132)				7,7 kPa

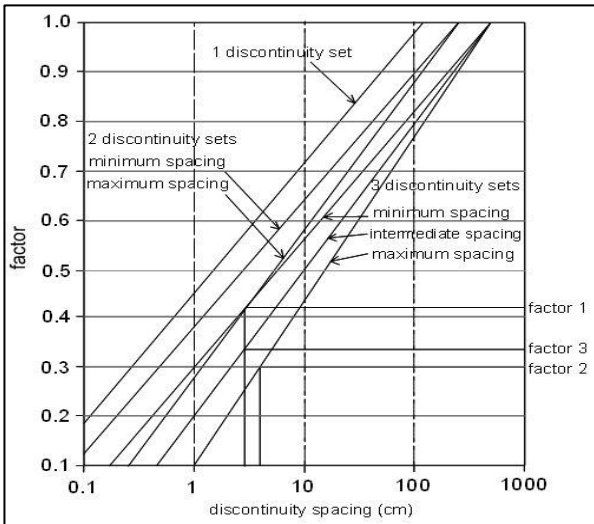
STOP 1 - STABILITY TABLE							
Method of Excavation (SME)				Weathering (SWE)			
Natural/hand-made		1,00		Unweathered		1,00	
Pneumatic hammer excavation*		0,76		Slightly		0,95	
Pre-splitting/smooth wall blasting		0,99		Moderately*		0,90	
Conventional blasting with result:				Highly		0,62	
Good		0,77		Completely		0,35	
Open discontinuities		0,75		Slope geometry features			
Dislodged blocks		0,72		Slope dip direction (degrees)		310	
Fractured intact rock		0,67		Slope dip (degrees)		40	
Crushed intact rock		0,62		Height (m)		8	
Orientation-independent stability							
Intact Rock Strength (SIRS)							
SIRS = RIRS (from reference rock mass) x SWE (weathering slope) =				8,889 x 0,9		8 MPa	
Discontinuity spacing (SSPA)							
SSPA = RSPA x SWE x SME				0,175x0,90x0,76		0,120	
Condition of discontinuity (SCD)							
SCD = RCD x SWE =				0,517 x 0,9		0,4653	
Slope unit friction and cohesion (SFRI & SCOH)							
SFRI = SIRS * 0,2417 + SSPA * 52,12 + SCD * 5,779 =						10,89°	
(If RIRS > 132 Mpa, then RIRS =132)							
SCOH = SIRS * 94,27 + SSPA * 28629 + SCD * 3593 =						5,9 kPa	
(If RIRS > 132 Mpa, then RIRS =132)							
If SFRI < slope dip, maximum possible height (Hmax):						4,7 m	
Hmax = (1,6x10 <sup>-4</sup> x SCOH) x sin(slopedip) x cos(SFRI) / (1 - cos(slopedip - SFRI)) =							
Ratios	SFRI / Slope dip					0,27	
	Hmax / Hslope					0,5875	
Stable probability: if SFRI > slope dip, probability = % 100, else use the figure for orientation-independent stability:						<5%	
Orientation-dependent stability							
Discontinuities		B		J1	J2		
Dip direction (degrees)		139		247	319		
Dip (degrees)		69		40	33		
With, Against, Vertical or Equal		A		W	W		
AP (degrees)		-68		21	32		
RTC		0,534		0,405	0,405		
STC = RTC x sqrt(1,452 - 1,220 x e <sup>(-SWE)</sup> )		0,523		0,396	0,396		
Stable probability:	Sliding		100%	>95%	95%		
	Toppling		>95%	100%	100%		
Stable probability:		95%					
Determine orientation stability:							
Calculate AP: β = discontinuity dip, σ = slope dip direction, τ= discontinuity dip direction, δ = σ - τ, AP= arctan(cosδ x tanβ)							
Stability		Sliding	Toppling	Stability		Sliding	Toppling
AP>84°or AP<-84°	Vertical	100%	100%	AP<0° and (-90° AP+slope dip)<0°	Against	100%	100%
(slope dip + 5°) < AP < 84°	With	100%	100%	AP<0° and (-90° AP+slope dip)>0°	Against	100%	Use graph toppling
(slope dip - 5°) < AP < (slope dip + 5°	Equal	100%	100%				
0°< AP < (slope dip - 5°	With	Use graph sliding	100%				
Slope final stable probability		<5%					

STOP 1 FAILED ZONE - DATA COLLECTION TABLE								
Excavation Method (ME)			Intact Rock Strength (IRS)					
Natural/hand-made		1,00	<1.25 MPa			Crumbles in hand		
Pneumatic hammer excavation*		0,76	1.25-5 MPa			Thin slabs break easy in hand		
Pre-splitting/smooth wall blasting		0,99	5-12.5 MPa			Thin slabs broken by heavy hand pressure*		
Conventional blasting with result:			12.5-50 MPa			Lumps broken by light hammer blows		
Good		0,77	50-100 MPa			Lumps broken by heavy hammer blows		
Open discontinuities		0,75	100-200 MPa			Lumps only chip by heavy hammer blows		
Dislodged blocks		0,72	>200 MPa			Rocks ring on hammer blows		
Fractured intact rock		0,67	Weathering degree (WE)			Unweathered		1,00
Crushed intact rock		0,62				Slightly		0,95
Lithology						Moderately*		0,90
95% Mudstone / 5% Sandstone						Highly		0,62
						Completely		0,35
Discontinuities (B: Bedding; J: Joint)				B	J1	J2	Slope	
Dip direction (degrees)				138	236	320	Dip direction (degrees)	310
Dip (degrees)				74	38	27	Dip (degrees)	40
Spacing (DS) (cm)				5	15	10	Slope height (m)	8
Condition of discontinuities						Slope Stability		
Large scale roughness (RL)	Wavy		1,00	X			Stable	1
	Slightly wavy		0,95				Small problem	2
	Curved		0,85				Large problem*	3
	Slightly curved		0,80		X	X	Notes: 1) For infill "gouge>irregularities" and "flowing material" small scale roughness= 0,55 2) If roughness is anisotropic (e.g. Ripple marks, striation, etc.) roughness should be assessed perpendicular and parallel to the roughness and directions noted on this form 3) Non-fitting of discontinuities should be marked in roughness columns.	
	Straight		0,75					
Small scale roughness (RS)	Rough stepped		0,95	X				
	Smooth stepped		0,90		X	X		
	Polished stepped		0,85					
	Rough undulating		0,80					
	Smooth undulating		0,75					
	Polished undulating		0,70					
	Rough planar		0,65					
	Smooth planar		0,60					
Polished planar		0,55						
Infill material (IM)	Cemented / cemented infill		1,07					
	No infill - surface staining		1,00					
	Non-softening & sheared material	Coarse	0,95					
		Medium	0,90					
		Fine	0,85					
	Soft sheared material	Coarse	0,75					
		Medium	0,65					
		Fine	0,55	X	X	X		
	Gouge < irregularities		0,42					
	Gouge > irregularities		0,17					
Flowing material		0,05						
Karst (KA)	None		1,00	X	X	X		
	Karst		0,92					

STOP 1 FAILED ZONE - REFERENCE ROCK TABLE					
Intact Rock Strength (RIRS)					
RIRS = IRS / WE = 2 / 0,62					3,226
Discontinuity Spacing (SPA)					
Discontinuities	B	J1	J2	SPA = factor 1 x factor 2 x factor 3	
Dip direction (degrees)	138	236	320		
Dip (degrees)	74	38	27		
Spacing (m)	5	15	10		
The spacing parameter (SPA) is calculated based on the three discontinuity sets with the smallest spacings in following figure:				SPA = 0,50 x 0,50 x 0,48 = 0,120	0,255
				Corrected for weathering and method of excavation:	
				RSPA = SPA / (WE x ME)	
				RSPA = 0,120 / (0,62 x 0,76)	
Condition of discontinuities					
Discontinuities	B	J1	J2	RTC is the discontinuity condition of a single discontinuity (set) in the reference rock mass corrected for discontinuity weathering. $RTC = TC / \sqrt{1,452 - 1,220 * e^{(-WE)}}$	
Large scale roughness (Rl)	1,00	0,80	0,80		
Small scale roughness (Rs)	0,95	0,90	0,90		
Infill material (Im)	0,55	0,55	0,55		
Karst (Ka)	1,00	1,00	1,00		
TC = Rl x Rs x Im x Ka	0,523	0,396	0,396		
RTC	0,534	0,405	0,405		
Weighted by spacing: $CD = \frac{\frac{TC_1}{DS_1} + \frac{TC_2}{DS_2} + \frac{TC_3}{DS_3}}{\frac{1}{DS_1} + \frac{1}{DS_2} + \frac{1}{DS_3}} =$				0,465	
Corrected by weathering: RCD (with a maximum of 1.0165) = CD/WE =				0,465 / 0,62 =	0,750
Reference unit friction and cohesion (RFRI & FCOH)					
$\phi(RRM) = RIRS * 0,2417 + RSPA * 52,12 + RCD * 5,779 =$ (If RIRS > 132 MPa, then RIRS = 132)					18,40°
coh(RRM) = RIRS * 94,27 + RSPA * 28629 + RCD * 3593 = (If RIRS > 132 MPa, then RIRS = 132)					10,3 kPa

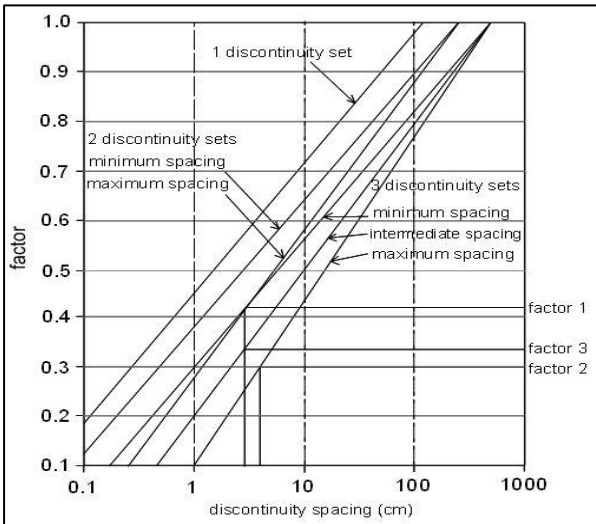
STOP 1 FAILED ZONE - STABILITY TABLE						
Method of Excavation (SME)			Weathering (SWE)			
Natural/hand-made		1,00	Unweathered		1,00	
Pneumatic hammer excavation*		0,76	Slightly		0,95	
Pre-splitting/smooth wall blasting		0,99	Moderately*		0,90	
Conventional blasting with result:			Highly		0,62	
Good		0,77	Completely		0,35	
Open discontinuities		0,75	Slope geometry features			
Dislodged blocks		0,72	Slope dip direction (degrees)		310	
Fractured intact rock		0,67	Slope dip (degrees)		40	
Crushed intact rock		0,62	Height (m)		8	
Orientation-independent stability						
Intact Rock Strength (SIRS)						
SIRS = RIRS (from reference rock mass) x SWE (weathering slope) =			3,226 x 0,62		2 MPa	
Discontinuity spacing (SSPA)						
SSPA = RSPA x SWE x SME			0,255x0,62x0,76		0,120	
Condition of discontinuity (SCD)						
SCD = RCD x SWE =			0,750 x 0,62		0,4653	
Slope unit friction and cohesion (SFRI & SCOH)						
SFRI = SIRS * 0,2417 + SSPA * 52,12 + SCD * 5,779 =					9,4°	
(If RIRS > 132 Mpa, then RIRS =132)						
SCOH = SIRS * 94,27 + SSPA * 28629 + SCD * 3593 =					5,3 kPa	
(If RIRS > 132 Mpa, then RIRS =132)						
If SFRI < slope dip, maximum possible height (Hmax):					3,9 m	
Hmax = (1,6x10 <sup>-4</sup> x SCOH) x sin(slopedip) x cos(SFRI) / (1 - cos(slopedip - SFRI)) =						
Ratios	SFRI / Slope dip				0,24	
	Hmax / Hslope				0,4875	
Stable probability: if SFRI > slope dip, probability = % 100, else use the figure for orientation-independent stability:					<5%	
Orientation-dependent stability						
Discontinuities		B	J1	J2		
Dip direction (degrees)		138	236	320		
Dip (degrees)		74	38	27		
With, Against, Vertical or Equal		A	W	W		
AP (degrees)		-73	12	27		
RTC		0,534	0,405	0,405		
STC = RTC x sqrt(1,452 - 1,220 x e <sup>(-SWE)</sup> )		0,523	0,396	0,396		
Stable probability:	Sliding	100%	>95%	>95%		
	Toppling	>95%	100%	100%		
Stable probability:		>95%				
Determine orientation stability:						
Calculate AP: β = discontinuity dip, σ = slope dip direction, τ= discontinuity dip direction, δ = σ - τ, AP= arctan(cosδ x tanβ)						
Stability		Sliding	Toppling	Stability	Sliding	Toppling
AP>84° or AP<-84°	Vertical	100%	100%	AP<0° and (-90-AP+slope dip)<0°	Against	100%
(slope dip + 5°) < AP < 84°	With	100%	100%	AP<0° and (-90-AP+slope dip)>0°	Against	100%
(slope dip - 5°) < AP < (slope dip + 5°)	Equal	100%	100%			
0° < AP < (slope dip - 5°)	With	Use graph sliding	100%			
Slope final stable probability		<5%				

STOP 2 - DATA COLLECTION TABLE								
Excavation Method (ME)			Intact Rock Strength (IRS)					
Natural/hand-made	1,00		<1.25 MPa		Crumbles in hand			
Pneumatic hammer excavation*	0,76		1.25-5 MPa		Thin slabs break easy in hand			
Pre-splitting/smooth wall blasting	0,99		5-12.5 MPa		Thin slabs broken by heavy hand pressure			
Conventional blasting with result:			12.5-50 MPa		Lumps broken by light hammer blows*			
Good	0,77		50-100 MPa		Lumps broken by heavy hammer blows			
Open discontinuities	0,75		100-200 MPa		Lumps only chip by heavy hammer blows			
Dislodged blocks	0,72		>200 MPa		Rocks ring on hammer blows			
Fractured intact rock	0,67		Weathering degree (WE)		Unweathered		1,00	
Crushed intact rock	0,62	Slightly			0,95			
Lithology		Moderately*			0,90			
Sandstone		Highly			0,62			
		Completely			0,35			
Discontinuities (B: Bedding; J: Joint)			B	J1	J2	Slope		
Dip direction (degrees)			270	100	15	Dip direction (degrees)	45	
Dip (degrees)			20	69	75	Dip (degrees)	70	
Spacing (DS) (cm)			30	40	20	Slope height (m)	9	
Condition of discontinuities						Slope Stability		
Large scale roughness (RL)	Wavy		1,00				Stable	1
	Slightly wavy		0,95				Small problem*	2
	Curved		0,85				Large problem	3
	Slightly curved		0,80	X	X	X	Notes: 1) For infill "gouge>irregularities" and "flowing material" small scale roughness= 0,55 2) If roughness is anisotropic (e.g. Ripple marks, striation, etc.) roughness should be assessed perpendicular and parallel to the roughness and directions noted on this form 3) Non-fitting of discontinuities should be marked in roughness columns.	
	Straight		0,75					
Small scale roughness (RS)	Rough stepped		0,95					
	Smooth stepped		0,90					
	Polished stepped		0,85					
	Rough undulating		0,80					
	Smooth undulating		0,75					
	Polished undulating		0,70					
	Rough planar		0,65					
	Smooth planar		0,60	X	X	X		
Polished planar		0,55						
Infill material (IM)	Cemented / cemented infill		1,07					
	No infill - surface staining		1,00					
	Non-softening & sheared material	Coarse	0,95					
		Medium	0,90					
		Fine	0,85					
	Soft sheared material	Coarse	0,75					
		Medium	0,65	X	X	X		
		Fine	0,55					
	Gouge < irregularities		0,42					
	Gouge > irregularities		0,17					
Flowing material		0,05						
Karst (KA)	None		1,00	X	X	X		
	Karst		0,92					

STOP 2 - REFERENCE ROCK TABLE					
Intact Rock Strength (RIRS)					
RIRS = IRS / WE = 16 / 0,90				17,778	
Discontinuity Spacing (SPA)					
Discontinuities	B	J1	J2	SPA = factor 1 x factor 2 x factor 3	0,371
Dip direction (degrees)	270	100	15		
Dip (degrees)	20	69	75		
Spacing (m)	30	40	20		
The spacing parameter (SPA) is calculated based on the three discontinuity sets with the smallest spacings in following figure:				SPA = 0,63 x 0,64 x 0,63 = 0,254	
				Corrected for weathering and method of excavation:	
				RSPA = SPA / (WE x ME)	
				RSPA = 0,254 / (0,90 x 0,76)	
Condition of discontinuities					
Discontinuities	B	J1	J2	RTC is the discontinuity condition of a single discontinuity (set) in the reference rock mass corrected for discontinuity weathering. RTC = TC /sqrt(1,452-1,220*e^(-WE))	
Large scale roughness (Rl)	0,80	0,80	0,80		
Small scale roughness (Rs)	0,60	0,60	0,60		
Infill material (Im)	0,65	0,65	0,65		
Karst (Ka)	1,00	1,00	1,00		
TC = Rl x Rs x Im x Ka	0,312	0,312	0,312		
RTC	0,319	0,319	0,319		
Weighted by spacing: CD = $\frac{\frac{TC_1}{DS_1} + \frac{TC_2}{DS_2} + \frac{TC_3}{DS_3}}{\frac{1}{DS_1} + \frac{1}{DS_2} + \frac{1}{DS_3}}$ =				0,312	
Corrected by weathering: RCD (with a maximum of 1.0165) = CD/WE=				0,312 / 0,90 =	0,347
Reference unit friction and cohesion (RFRI & FCOH)					
φ(RRM) = RIRS * 0,2417 + RSPA * 52,12 + RCD * 5,779 = (If RIRS > 132 MPa, then RIRS = 132)				25,64°	
coh(RRM) = RIRS * 94,27 + RSPA * 28629 + RCD * 3593 = (If RIRS > 132 MPa, then RIRS = 132)				13,5 kPa	

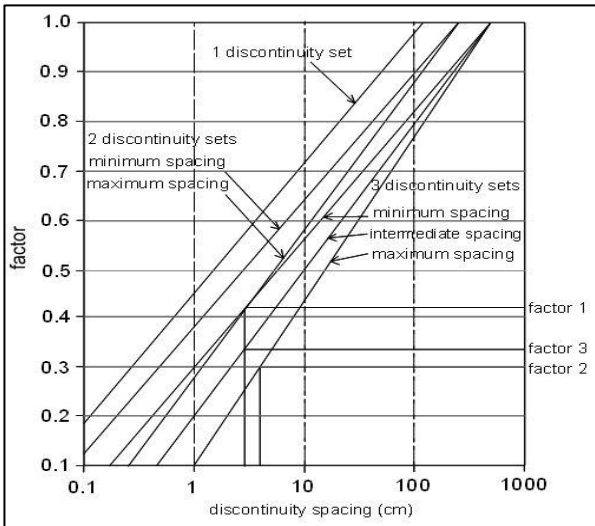
STOP 2 - STABILITY TABLE							
Method of Excavation (SME)			Weathering (SWE)				
Natural/hand-made		1,00	Unweathered		1,00		
Pneumatic hammer excavation*		0,76	Slightly		0,95		
Pre-splitting/smooth wall blasting		0,99	Moderately*		0,90		
Conventional blasting with result:			Highly		0,62		
Good		0,77	Completely		0,35		
Open discontinuities		0,75	Slope geometry features				
Dislodged blocks		0,72	Slope dip direction (degrees)		45		
Fractured intact rock		0,67	Slope dip (degrees)		70		
Crushed intact rock		0,62	Height (m)		9		
Orientation-independent stability							
Intact Rock Strength (SIRS)							
SIRS = RIRS (from reference rock mass) x SWE (weathering slope) =			17,778 x 0,90		16 MPa		
Discontinuity spacing (SSPA)							
SSPA = RSPA x SWE x SME			0,371x0,90x0,76		0,254		
Condition of discontinuity (SCD)							
SCD = RCD x SWE =			0,347 x 0,90		0,312		
Slope unit friction and cohesion (SFRI & SCOH)							
SFRI = SIRS * 0,2417 + SSPA * 52,12 + SCD * 5,779 =					18,91°		
(If RIRS > 132 Mpa, then RIRS =132)							
SCOH = SIRS * 94,27 + SSPA * 28629 + SCD * 3593 =					9,9 kPa		
(If RIRS > 132 Mpa, then RIRS =132)							
If SFRI < slope dip, maximum possible height (Hmax):							
Hmax = (1,6x10 <sup>-4</sup> x SCOH) x sin(slopedip) x cos(SFRI) / (1 - cos(slopedip - SFRI)) =					3,8		
Ratios	SFRI / Slope dip				0,270		
	Hmax / Hslope				0,422		
Stable probability: if SFRI > slope dip, probability = % 100, else use the figure for orientation-independent stability:					<5%		
Orientation-dependent stability							
Discontinuities		B	J1	J2			
Dip direction (degrees)		270	100	15			
Dip (degrees)		20	69	75			
With, Against, Vertical or Equal		A	W	W			
AP (degrees)		-14	56	72			
RTC		0,319	0,319	0,319			
STC = RTC x sqrt(1,452 - 1,220 x e <sup>(-SWE)</sup> )		0,312	0,312	0,312			
Stable probability:	Sliding	100%	100%	100%			
	Toppling	100%	100%	100%			
Stable probability:		100%					
Determine orientation stability:							
Calculate AP: β = discontinuity dip, σ = slope dip direction, τ= discontinuity dip direction, δ = σ - τ, AP= arctan(cosδ x tanβ)							
Stability		Sliding	Toppling	Stability		Sliding	Toppling
AP>84° or AP<-84°	Vertical	100%	100%	AP<0° and (-90-AP+slope dip)<0°	Against	100%	100%
(slope dip + 5°) < AP < 84°	With	100%	100%	AP<0° and (-90-AP+slope dip)>0°	Against	100%	Use graph toppling
(slope dip - 5°) < AP < (slope dip + 5°	Equal	100%	100%				
0°< AP < (slope dip - 5°	With	Use graph sliding	100%				
Slope final stable probability		<5%					

STOP 2 FAILED ZONE - DATA COLLECTION TABLE								
Excavation Method (ME)			Intact Rock Strength (IRS)					
Natural/hand-made	1,00	<1.25 MPa			Crumbles in hand			
Pneumatic hammer excavation*	0,76	1.25-5 MPa			Thin slabs break easy in hand			
Pre-splitting/smooth wall blasting	0,99	5-12.5 MPa			Thin slabs broken by heavy hand pressure			
Conventional blasting with result:		12.5-50 MPa			Lumps broken by light hammer blows*			
Good	0,77	50-100 MPa			Lumps broken by heavy hammer blows			
Open discontinuities	0,75	100-200 MPa			Lumps only chip by heavy hammer blows			
Dislodged blocks	0,72	>200 MPa			Rocks ring on hammer blows			
Fractured intact rock	0,67	Weathering degree (WE)			Unweathered		1,00	
Crushed intact rock	0,62				Slightly		0,95	
Lithology					Moderately*		0,90	
Sandstone					Highly		0,62	
					Completely		0,35	
Discontinuities (B: Bedding; J: Joint)				B	J1	J2	Slope	
Dip direction (degrees)				270	100	15	Dip direction (degrees)	45
Dip (degrees)				20	69	75	Dip (degrees)	70
Spacing (DS) (cm)				30	40	20	Slope height (m)	9
Condition of discontinuities							Slope Stability	
Large scale roughness (RL)	Wavy		1,00				Stable	1
	Slightly wavy		0,95				Small problem	2
	Curved		0,85				Large problem*	3
	Slightly curved		0,80	X	X	X	Notes: 1) For infill "gouge>irregularities" and "flowing material" small scale roughness= 0,55 2) If roughness is anisotropic (e.g. Ripple marks, striation, etc.) roughness should be assessed perpendicular and parallel to the roughness and directions noted on this form 3) Non-fitting of discontinuities should be marked in roughness columns.	
	Straight		0,75					
Small scale roughness (RS)	Rough stepped		0,95					
	Smooth stepped		0,90					
	Polished stepped		0,85					
	Rough undulating		0,80					
	Smooth undulating		0,75					
	Polished undulating		0,70					
	Rough planar		0,65					
	Smooth planar		0,60	X	X	X		
Polished planar		0,55						
Infill material (IM)	Cemented / cemented infill		1,07					
	No infill - surface staining		1,00					
	Non-softening & sheared material	Coarse	0,95					
		Medium	0,90					
		Fine	0,85					
	Soft sheared material	Coarse	0,75					
		Medium	0,65	X	X	X		
		Fine	0,55					
	Gouge < irregularities		0,42					
	Gouge > irregularities		0,17					
Flowing material		0,05						
Karst (KA)	None		1,00	X	X	X		
	Karst		0,92					

STOP 2 FAILED ZONE - REFERENCE ROCK TABLE					
Intact Rock Strength (RIRS)					
RIRS = IRS / WE = 5/ 0,62					8,065
Discontinuity Spacing (SPA)					
Discontinuities	B	J1	J2	SPA = factor 1 x factor 2 x factor 3	
Dip direction (degrees)	270	100	15		
Dip (degrees)	20	69	75		
Spacing (m)	30	40	20		
The spacing parameter (SPA) is calculated based on the three discontinuity sets with the smallest spacings in following figure:				SPA = 0,63 x 0,64 x 0,63 = 0,254	0,539
				Corrected for weathering and method of excavation:	
				RSPA = SPA / (WE x ME)	
				RSPA = 0,254 / (0,62 x 0,76)	
Condition of discontinuities					
Discontinuities	B	J1	J2	RTC is the discontinuity condition of a single discontinuity (set) in the reference rock mass corrected for discontinuity weathering. $RTC$ = $TC / \sqrt{1,452 - 1,220 * e^{(-WE)}}$	
Large scale roughness (Rl)	0,80	0,80	0,80		
Small scale roughness (Rs)	0,60	0,60	0,60		
Infill material (Im)	0,65	0,65	0,65		
Karst (Ka)	1,00	1,00	1,00		
TC = Rl x Rs x Im x Ka	0,312	0,312	0,312		
RTC	0,319	0,319	0,319		
Weighted by spacing: $CD = \frac{\frac{TC_1}{DS_1} + \frac{TC_2}{DS_2} + \frac{TC_3}{DS_3}}{\frac{1}{DS_1} + \frac{1}{DS_2} + \frac{1}{DS_3}} =$					0,312
Corrected by weathering: RCD (with a maximum of 1.0165) = CD/WE =				0,312 / 0,62 =	0,503
Reference unit friction and cohesion (RFRI & FCOH)					
$\phi(RRM) = RIRS * 0,2417 + RSPA * 52,12 + RCD * 5,779 =$ (If RIRS > 132 MPa, then RIRS = 132)					32,95°
coh(RRM) = RIRS * 94,27 + RSPA * 28629 + RCD * 3593 = (If RIRS > 132 MPa, then RIRS = 132)					18,0 kPa

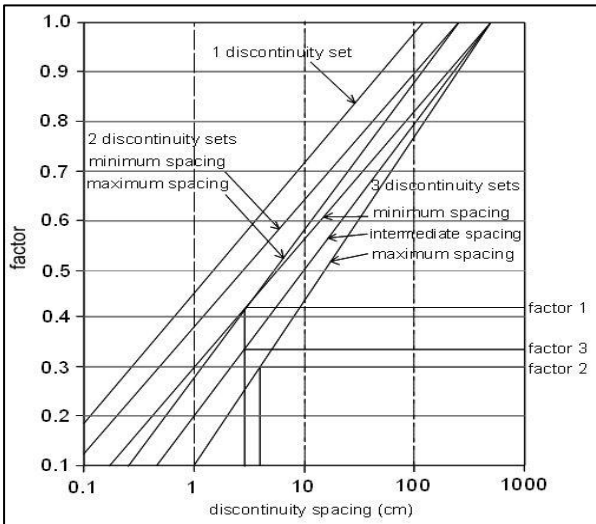
STOP 2 FAILED ZONE - STABILITY TABLE							
Method of Excavation (SME)		Weathering (SWE)					
Natural/hand-made	1,00	Unweathered	1,00				
Pneumatic hammer excavation*	0,76	Slightly	0,95				
Pre-splitting/smooth wall blasting	0,99	Moderately*	0,90				
Conventional blasting with result:		Highly	0,62				
Good	0,77	Completely	0,35				
Open discontinuities	0,75	Slope geometry features					
Dislodged blocks	0,72	Slope dip direction (degrees)	45				
Fractured intact rock	0,67	Slope dip (degrees)	70				
Crushed intact rock	0,62	Height (m)	9				
Orientation-independent stability							
Intact Rock Strength (SIRS)							
SIRS = RIRS (from reference rock mass) x SWE (weathering slope) =		8,065 x 0,62	5 MPa				
Discontinuity spacing (SSPA)							
SSPA = RSPA x SWE x SME		0,539x0,62x0,76	0,254				
Condition of discontinuity (SCD)							
SCD = RCD x SWE =		0,503 x 0,62	0,312				
Slope unit friction and cohesion (SFRI & SCOH)							
SFRI = SIRS * 0,2417 + SSPA * 52,12 + SCD * 5,779 =			16,25°				
(If RIRS > 132 Mpa, then RIRS =132)							
SCOH = SIRS * 94,27 + SSPA * 28629 + SCD * 3593 =			8,9 kPa				
(If RIRS > 132 Mpa, then RIRS =132)							
If SFRI < slope dip, maximum possible height (Hmax):							
Hmax = (1,6x10^-4 x SCOH) x sin(slopedip) x cos(SFRI) / (1 - cos(slopedip - SFRI)) =			3,1 m				
Ratios	SFRI / Slope dip			0,232			
	Hmax/ Hslope			0,344			
Stable probability: if SFRI > slope dip, probability = % 100, else use the figure for orientation-independent stability:			<5%				
Orientation-dependent stability							
Discontinuities		B	J1	J2			
Dip direction (degrees)		270	100	15			
Dip (degrees)		20	69	75			
With, Against, Vertical or Equal		A	W	W			
AP (degrees)		-14	56	72			
RTC		0,319	0,319	0,319			
STC = RTC x sqrt(1,452 - 1,220 x e^(-SWE))		0,312	0,312	0,312			
Stable probability:	Sliding	100%	100%	100%			
	Toppling	100%	100%	100%			
Stable probability:		100%					
Determine orientation stability:							
Calculate AP: β = discontinuity dip, σ = slope dip direction, τ= discontinuity dip direction, δ = σ - τ, AP= arctan(cosδ x tanβ)							
Stability		Sliding	Toppling	Stability	Sliding	Toppling	
AP>84°or AP<-84°	Vertical	100%	100%	AP<0° and (-90°<AP+slope dip)<0°	Against	100%	100%
(slope dip + 5°) < AP < 84°	With	100%	100%	AP<0° and (-90°<AP+slope dip)>0°	Against	100%	Use graph toppling
(slope dip - 5°) < AP < (slope dip + 5°	Equal	100%	100%				
0°< AP < (slope dip - 5°	With	Use graph sliding	100%				
Slope final stable probability		<5%					

STOP 3 - DATA COLLECTION TABLE							
Excavation Method (ME)			Intact Rock Strength (IRS)				
Natural/hand-made	1,00		<1.25 MPa		Crumbles in hand		
Pneumatic hammer excavation*	0,76		1.25-5 MPa		Thin slabs break easy in hand		
Pre-splitting/smooth wall blasting	0,99		5-12.5 MPa		Thin slabs broken by heavy hand pressure		
Conventional blasting with result:			12.5-50 MPa		Lumps broken by light hammer blows *		
Good	0,77		50-100 MPa		Lumps broken by heavy hammer blows		
Open discontinuities	0,75		100-200 MPa		Lumps only chip by heavy hammer blows		
Dislodged blocks	0,72		>200 MPa		Rocks ring on hammer blows		
Fractured intact rock	0,67		Weathering degree (WE)			Unweathered	1,00
Crushed intact rock	0,62					Slightly	0,95
Lithology						Moderately*	0,90
Sandstone						Highly	0,62
						Completely	0,35
Discontinuities (B: Bedding; J: Joint)			B	J1	J2	Slope	
Dip direction (degrees)			50	180	255	Dip direction (degrees)	245
Dip (degrees)			16	67	75	Dip (degrees)	60
Spacing (DS) (cm)			30	25	15	Slope height (m)	15
Condition of discontinuities					Slope Stability		
Large scale roughness (RL)	Wavy	1,00				Stable	1
	Slightly wavy	0,95				Small problem*	2
	Curved	0,85	X			Large problem	3
	Slightly curved	0,80		X	X	Notes: 1) For infill "gouge>irregularities" and "flowing material" small scale roughness= 0,55 2) If roughness is anisotropic (e.g. Ripple marks, striation, etc.) roughness should be assessed perpendicular and parallel to the roughness and directions noted on this form 3) Non-fitting of discontinuities should be marked in roughness columns.	
	Straight	0,75					
Small scale roughness (RS)	Rough stepped	0,95					
	Smooth stepped	0,90					
	Polished stepped	0,85					
	Rough undulating	0,80	X				
	Smooth undulating	0,75		X	X		
	Polished undulating	0,70					
	Rough planar	0,65					
	Smooth planar	0,60					
	Polished planar	0,55					
Infill material (IM)	Cemented / cemented infill		1,07				
	No infill - surface staining		1,00				
	Non-softening & sheared material	Coarse	0,95				
		Medium	0,90				
		Fine	0,85				
	Soft sheared material	Coarse	0,75				
		Medium	0,65	X	X		
		Fine	0,55				
	Gouge < irregularities		0,42				
	Gouge > irregularities		0,17				
	Flowing material		0,05				
Karst (KA)	None		1,00	X	X		
	Karst		0,92				

STOP 3 - REFERENCE ROCK TABLE				
Intact Rock Strength (RIRS)				
RIRS = IRS / WE = 8,5 / 0,90				9,444
Discontinuity Spacing (SPA)				
Discontinuities	B	J1	J2	SPA = factor 1 x factor 2 x factor 3
Dip direction (degrees)	50	180	255	
Dip (degrees)	16	67	75	
Spacing (m)	30	25	15	
The spacing parameter (SPA) is calculated based on the three discontinuity sets with the smallest spacings in following figure:				0,316
				
SPA = 0,59 x 0,62 x 0,59 = 0,216				
Corrected for weathering and method of excavation:				
RSPA = SPA / (WE x ME)				
RSPA = 0,216 / (0,90 x 0,76)				
Condition of discontinuities				
Discontinuities	B	J1	J2	RTC is the discontinuity condition of a single discontinuity (set) in the reference rock mass corrected for discontinuity weathering. $RTC = TC / \sqrt{1,452 - 1,220 * e^{(-WE)}}$
Large scale roughness (Rl)	0,85	0,80	0,80	
Small scale roughness (Rs)	0,80	0,75	0,75	
Infill material (Im)	0,65	0,65	0,65	
Karst (Ka)	1,00	1,00	1,00	
TC = Rl x Rs x Im x Ka	0,442	0,390	0,390	
RTC	0,452	0,399	0,399	
Weighted by spacing: $CD = \frac{\frac{TC_1}{DS_1} + \frac{TC_2}{DS_2} + \frac{TC_3}{DS_3}}{\frac{1}{DS_1} + \frac{1}{DS_2} + \frac{1}{DS_3}} =$				0,402
Corrected by weathering: RCD (with a maximum of 1.0165) = CD/WE =				0,402 / 0,90 = 0,447
Reference unit friction and cohesion (RFRI & FCOH)				
$\phi(RRM) = RIRS * 0,2417 + RSPA * 52,12 + RCD * 5,779 =$ (If RIRS > 132 MPa, then RIRS = 132)				21,33°
$coh(RRM) = RIRS * 94,27 + RSPA * 28629 + RCD * 3593 =$ (If RIRS > 132 MPa, then RIRS = 132)				11,5 kPa

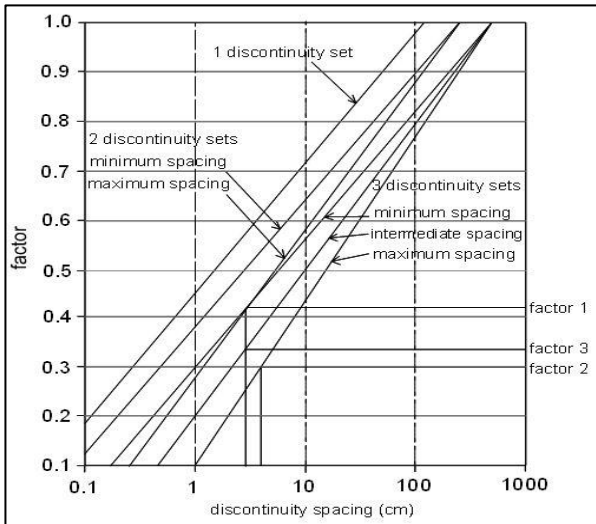
STOP 3 - STABILITY TABLE							
Method of Excavation (SME)			Weathering (SWE)				
Natural/hand-made	1,00	Unweathered	1,00				
Pneumatic hammer excavation*	0,76	Slightly	0,95				
Pre-splitting/smooth wall blasting	0,99	Moderately*	0,90				
Conventional blasting with result:		Highly	0,62				
Good	0,77	Completely	0,35				
Open discontinuities	0,75	Slope geometry features					
Dislodged blocks	0,72	Slope dip direction (degrees)	245				
Fractured intact rock	0,67	Slope dip (degrees)	60				
Crushed intact rock	0,62	Height (m)	15				
Orientation-independent stability							
Intact Rock Strength (SIRS)							
SIRS = RIRS (from reference rock mass) x SWE (weathering slope) =		9,444 x 0,90	8 MPa				
Discontinuity spacing (SSPA)							
SSPA = RSPA x SWE x SME		0,316x0,90x0,76	0,216				
Condition of discontinuity (SCD)							
SCD = RCD x SWE =		0,447 x 0,90	0,402				
Slope unit friction and cohesion (SFRI & SCOH)							
SFRI = SIRS * 0,2417 + SSPA * 52,12 + SCD * 5,779 =			15,51°				
(If RIRS > 132 Mpa, then RIRS =132)							
SCOH = SIRS * 94,27 + SSPA * 28629 + SCD * 3593 =			8,3 kPa				
(If RIRS > 132 Mpa, then RIRS =132)							
If SFRI < slope dip, maximum possible height (Hmax):				3,9 m			
Hmax = (1,6x10^-4 x SCOH) x sin(slopedip) x cos(SFRI) / (1 - cos(slopedip - SFRI)) =							
Ratios	SFRI / Slope dip			0,259			
	Hmax / Hslope			0,260			
Stable probability: if SFRI > slope dip, probability = % 100, else use the figure for orientation-independent stability:				<5%			
Orientation-dependent stability							
Discontinuities		B	J1	J2			
Dip direction (degrees)		50	180	255			
Dip (degrees)		16	67	75			
With, Against, Vertical or Equal		A	W	W			
AP (degrees)		-15	45	75			
RTC		0,452	0,399	0,390			
STC = RTC x sqrt(1,452 - 1,220 x e^(-SWE))		0,442	0,390	0,381			
Stable probability:	Sliding	100%	95%	100%			
	Toppling	100%	100%	100%			
Stable probability:		95%					
Determine orientation stability:							
Calculate AP: β = discontinuity dip, σ = slope dip direction, τ= discontinuity dip direction, δ = σ - τ, AP= arctan(cosδ x tanβ)							
Stability		Sliding	Toppling	Stability	Sliding	Toppling	
AP>84°or AP<-84°	Vertical	100%	100%	AP<0° and (-90-AP+slopedip)<0°	Against	100%	100%
(slopedip + 5°) < AP < 84°	With	100%	100%	AP<0° and (-90-AP+slopedip)>0°	Against	100%	Use graph toppling
(slopedip - 5°) < AP < (slopedip + 5°	Equal	100%	100%				
0°< AP < (slopedip - 5°	With	Use graph sliding	100%				
Slope final stable probability		<5%					

STOP 4 - DATA COLLECTION TABLE								
Excavation Method (ME)			Intact Rock Strength (IRS)					
Natural/hand-made	1,00	<1.25 MPa			Crumbles in hand			
Pneumatic hammer excavation*	0,76	1.25-5 MPa			Thin slabs break easy in hand			
Pre-splitting/smooth wall blasting	0,99	5-12.5 MPa			Thin slabs broken by heavy hand pressure			
Conventional blasting with result:		12.5-50 MPa			Lumps broken by light hammer blows*			
Good	0,77	50-100 MPa			Lumps broken by heavy hammer blows			
Open discontinuities	0,75	100-200 MPa			Lumps only chip by heavy hammer blows			
Dislodged blocks	0,72	>200 MPa			Rocks ring on hammer blows			
Fractured intact rock	0,67	Weathering degree (WE)			Unweathered		1,00	
Crushed intact rock	0,62				Slightly		0,95	
Lithology					Moderately*		0,90	
Granite					Highly		0,62	
					Completely		0,35	
Discontinuities (B: Bedding; J: Joint)				J1	J2	J3	Slope	
Dip direction (degrees)				90	250	340	Dip direction (degrees)	290
Dip (degrees)				5	65	64	Dip (degrees)	75
Spacing (DS) (cm)				20	10	15	Slope height (m)	8
Condition of discontinuities							Slope Stability	
Large scale roughness (RL)	Wavy		1,00				Stable	1
	Slightly wavy		0,95				Small problem*	2
	Curved		0,85				Large problem	3
	Slightly curved		0,80	X	X	X	Notes: 1) For infill "gouge>irregularities" and "flowing material" small scale roughness= 0,55 2) If roughness is anisotropic (e.g. Ripple marks, striation, etc.) roughness should be assessed perpendicular and parallel to the roughness and directions noted on this form 3) Non-fitting of discontinuities should be marked in roughness columns.	
	Straight		0,75					
Small scale roughness (RS)	Rough stepped		0,95					
	Smooth stepped		0,90	X	X	X		
	Polished stepped		0,85					
	Rough undulating		0,80					
	Smooth undulating		0,75					
	Polished undulating		0,70					
	Rough planar		0,65					
	Smooth planar		0,60					
Polished planar		0,55						
Infill material (IM)	Cemented / cemented infill		1,07					
	No infill - surface staining		1,00					
	Non-softening & sheared material	Coarse	0,95					
		Medium	0,90					
		Fine	0,85					
	Soft sheared material	Coarse	0,75					
		Medium	0,65	X	X	X		
		Fine	0,55					
	Gouge < irregularities		0,42					
	Gouge > irregularities		0,17					
Flowing material		0,05						
Karst (KA)	None		1,00	X	X	X		
	Karst		0,92					

STOP 4 - REFERENCE ROCK TABLE					
Intact Rock Strength (RIRS)					
RIRS = IRS / WE = 6 / 0,90					6,667
Discontinuity Spacing (SPA)					
Discontinuities	B	J1	J2	SPA = factor 1 x factor 2 x factor 3	
Dip direction (degrees)	90	250	340		
Dip (degrees)	5	65	64		
Spacing (m)	20	10	15		
The spacing parameter (SPA) is calculated based on the three discontinuity sets with the smallest spacings in following figure:				SPA = 0,56 x 0,55 x 0,53 = 0,163	0,238
				Corrected for weathering and method of excavation:	
				RSPA = SPA / (WE x ME)	
				RSPA = 0,163 / (0,90 x 0,76)	
Condition of discontinuities					
Discontinuities	B	J1	J2	RTC is the discontinuity condition of a single discontinuity (set) in the reference rock mass corrected for discontinuity weathering. $RTC = TC / \sqrt{1,452 - 1,220 * e^{(-WE)}}$	
Large scale roughness (Rl)	0,80	0,80	0,80		
Small scale roughness (Rs)	0,90	0,90	0,90		
Infill material (Im)	0,65	0,65	0,65		
Karst (Ka)	1,00	1,00	1,00		
TC = Rl x Rs x Im x Ka	0,468	0,468	0,468		
RTC	0,479	0,479	0,479		
Weighted by spacing: $CD = \frac{\frac{TC_1}{DS_1} + \frac{TC_2}{DS_2} + \frac{TC_3}{DS_3}}{\frac{1}{DS_1} + \frac{1}{DS_2} + \frac{1}{DS_3}} =$				0,468	
Corrected by weathering: RCD (with a maximum of 1.0165) = CD/WE =				0,468 / 0,90 = 0,520	
Reference unit friction and cohesion (RFRI & FCOH)					
$\phi(RRM) = RIRS * 0,2417 + RSPA * 52,12 + RCD * 5,779 =$ (If RIRS > 132 MPa, then RIRS = 132)					17,04°
coh(RRM) = RIRS * 94,27 + RSPA * 28629 + RCD * 3593 = (If RIRS > 132 MPa, then RIRS = 132)					9,3 kPa

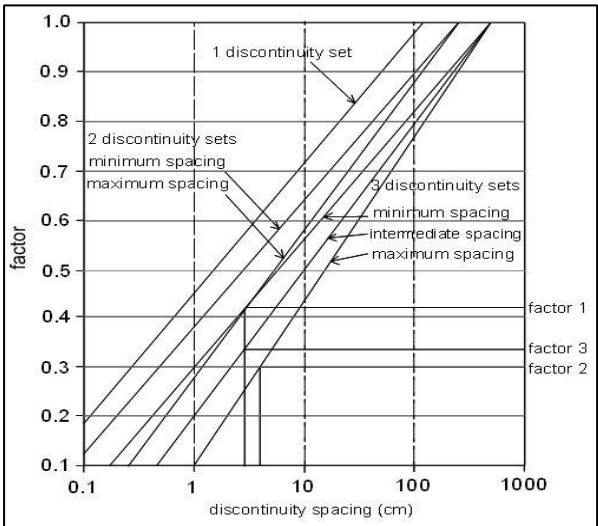
STOP 4 - STABILITY TABLE							
Method of Excavation (SME)				Weathering (SWE)			
Natural/hand-made		1,00		Unweathered		1,00	
Pneumatic hammer excavation*		0,76		Slightly		0,95	
Pre-splitting/smooth wall blasting		0,99		Moderately*		0,90	
Conventional blasting with result:				Highly		0,62	
Good		0,77		Completely		0,35	
Open discontinuities		0,75		Slope geometry features			
Dislodged blocks		0,72		Slope dip direction (degrees)		290	
Fractured intact rock		0,67		Slope dip (degrees)		75	
Crushed intact rock		0,62		Height (m)		8	
Orientation-independent stability							
Intact Rock Strength (SIRS)							
SIRS = RIRS (from reference rock mass) x SWE (weathering slope) =				6,667 x 0,9		6 MPa	
Discontinuity spacing (SSPA)							
SSPA = RSPA x SWE x SME				0,238x0,90x0,76		0,163	
Condition of discontinuity (SCD)							
SCD = RCD x SWE =				0,520 x 0,9		0,468	
Slope unit friction and cohesion (SFRI & SCOH)							
SFRI = SIRS * 0,2417 + SSPA * 52,12 + SCD * 5,779 =						12,65°	
(If RIRS > 132 Mpa, then RIRS =132)							
SCOH = SIRS * 94,27 + SSPA * 28629 + SCD * 3593 =						6,9 kPa	
(If RIRS > 132 Mpa, then RIRS =132)							
If SFRI < slope dip, maximum possible height (Hmax):						1,9 m	
Hmax = (1,6x10^-4 x SCOH) x sin(slopedip) x cos(SFRI) / ( 1 - cos(slopedip - SFRI)) =							
Ratios	SFRI / Slope dip					0,169	
	Hmax/ Hslope					0,2375	
Stable probability: if SFRI > slope dip, probability = % 100, else use the figure for orientation-independent stability:						<5%	
Orientation-dependent stability							
Discontinuities		B		J1	J2		
Dip direction (degrees)		90		250	340		
Dip (degrees)		5		65	64		
With, Against, Vertical or Equal		A		W	W		
AP (degrees)		-5		59	53		
RTC		0,479		0,479	0,479		
STC = RTC x sqrt(1,452 - 1,220 x e^(-SWE))		0,468		0,468	0,468		
Stable probability:	Sliding		100%	<5%	<5%		
	Toppling		100%	100%	100%		
Stable probability:		<5%					
Determine orientation stability:							
Calculate AP: β = discontinuity dip, σ = slope dip direction, τ= discontinuity dip direction, δ = σ - τ, AP= arctan(cosδ x tanβ)							
Stability		Sliding	Toppling	Stability		Sliding	Toppling
AP>84°or AP<-84°	Vertical	100%	100%	AP<0° and (-90 AP+slope dip)<0°	Against	100%	100%
(slope dip + 5°) < AP < 84°	With	100%	100%	AP<0° and (-90 AP+slope dip)>0°	Against	100%	Use graph toppling
(slope dip - 5°) < AP < (slope dip + 5°	Equal	100%	100%				
0°< AP < (slope dip - 5°	With	Use graph sliding	100%				
Slope final stable probability		<5%					

STOP 5 - DATA COLLECTION TABLE									
Excavation Method (ME)			Intact Rock Strength (IRS)						
Natural/hand-made		1,00	<1.25 MPa			Crumbles in hand			
Pneumatic hammer excavation*		0,76	1.25-5 MPa			Thin slabs break easy in hand			
Pre-splitting/smooth wall blasting		0,99	5-12.5 MPa			Thin slabs broken by heavy hand pressure			
Conventional blasting with result:			12.5-50 MPa			Lumps broken by light hammer blows *			
Good		0,77	50-100 MPa			Lumps broken by heavy hammer blows			
Open discontinuities		0,75	100-200 MPa			Lumps only chip by heavy hammer blows			
Dislodged blocks		0,72	>200 MPa			Rocks ring on hammer blows			
Fractured intact rock		0,67	Weathering degree (WE)			Unweathered		1,00	
Crushed intact rock		0,62				Slightly		0,95	
Lithology						Moderately*		0,90	
Basalt						Highly		0,62	
						Completely		0,35	
Discontinuities (B: Bedding; J: Joint)				J1	J2	J3	Slope		
Dip direction (degrees)				148	200	12	Dip direction (degrees)		295
Dip (degrees)				62	80	75	Dip (degrees)		75
Spacing (DS) (cm)				10	20	30	Slope height (m)		10
Condition of discontinuities						Slope Stability			
Large scale roughness (RL)	Wavy		1,00				Stable		1
	Slightly wavy		0,95				Small problem*		2
	Curved		0,85				Large problem		3
	Slightly curved		0,80	X	X	X	Notes: 1) For infill "gouge>irregularities" and "flowing material" small scale roughness= 0,55 2) If roughness is anisotropic (e.g. Ripple marks, striation, etc.) roughness should be assessed perpendicular and parallel to the roughness and directions noted on this form 3) Non-fitting of discontinuities should be marked in roughness columns.		
	Straight		0,75						
Small scale roughness (RS)	Rough stepped		0,95						
	Smooth stepped		0,90						
	Polished stepped		0,85						
	Rough undulating		0,80	X	X	X			
	Smooth undulating		0,75						
	Polished undulating		0,70						
	Rough planar		0,65						
	Smooth planar		0,60						
Polished planar		0,55							
Infill material (IM)	Cemented / cemented infill		1,07						
	No infill - surface staining		1,00						
	Non-softening & sheared material	Coarse	0,95						
		Medium	0,90						
		Fine	0,85						
	Soft sheared material	Coarse	0,75						
		Medium	0,65	X	X	X			
		Fine	0,55						
	Gouge < irregularities		0,42						
	Gouge > irregularities		0,17						
Flowing material		0,05							
Karst (KA)	None		1,00	X	X	X			
	Karst		0,92						

STOP 5 - REFERENCE ROCK TABLE					
Intact Rock Strength (RIRS)					
RIRS = IRS / WE = 4 / 0,90					4,444
Discontinuity Spacing (SPA)					
Discontinuities	B	J1	J2	SPA = factor 1 x factor 2 x factor 3	
Dip direction (degrees)	148	200	12		
Dip (degrees)	62	80	75		
Spacing (m)	10	20	30		
The spacing parameter (SPA) is calculated based on the three discontinuity sets with the smallest spacings in following figure:				SPA = 0,55 x 0,59 x 0,60 = 0,195	0,285
				Corrected for weathering and method of excavation:	
				RSPA = SPA / (WE x ME)	
				RSPA = 0,195 / (0,90 x 0,76)	
Condition of discontinuities					
Discontinuities	B	J1	J2	RTC is the discontinuity condition of a single discontinuity (set) in the reference rock mass corrected for discontinuity weathering. $RTC = TC / \sqrt{1,452 - 1,220 * e^{(-WE)}}$	
Large scale roughness (Rl)	0,80	0,80	0,80		
Small scale roughness (Rs)	0,80	0,80	0,80		
Infill material (Im)	0,65	0,65	0,65		
Karst (Ka)	1,00	1,00	1,00		
TC = Rl x Rs x Im x Ka	0,416	0,416	0,416		
RTC	0,425	0,425	0,425		
Weighted by spacing: $CD = \frac{\frac{TC_1}{DS_1} + \frac{TC_2}{DS_2} + \frac{TC_3}{DS_3}}{\frac{1}{DS_1} + \frac{1}{DS_2} + \frac{1}{DS_3}} =$				0,416	
Corrected by weathering: RCD (with a maximum of 1.0165) = CD/WE =				0,416 / 0,90 = 0,462	
Reference unit friction and cohesion (RFRI & FCOH)					
$\phi(RRM) = RIRS * 0,2417 + RSPA * 52,12 + RCD * 5,779 =$ (If RIRS > 132 MPa, then RIRS = 132)					18,60°
$coh(RRM) = RIRS * 94,27 + RSPA * 28629 + RCD * 3593 =$ (If RIRS > 132 MPa, then RIRS = 132)					10,2 kPa

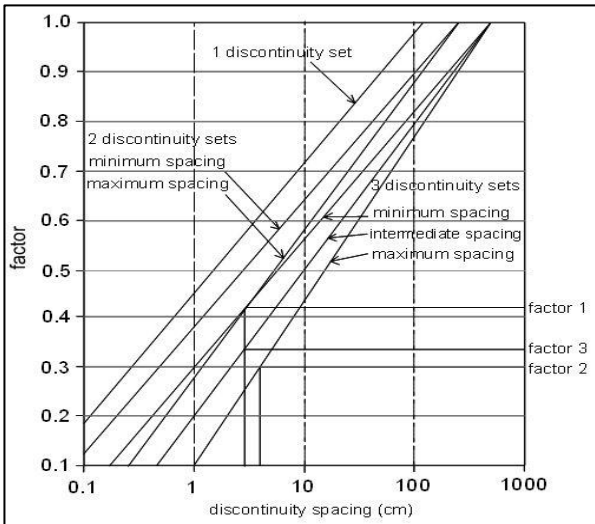
STOP 5 - STABILITY TABLE							
Method of Excavation (SME)			Weathering (SWE)				
Natural/hand-made		1,00	Unweathered		1,00		
Pneumatic hammer excavation*		0,76	Slightly		0,95		
Pre-splitting/smooth wall blasting		0,99	Moderately*		0,90		
Conventional blasting with result:			Highly		0,62		
Good		0,77	Completely		0,35		
Open discontinuities		0,75	Slope geometry features				
Dislodged blocks		0,72	Slope dip direction (degrees)		295		
Fractured intact rock		0,67	Slope dip (degrees)		75		
Crushed intact rock		0,62	Height (m)		10		
Orientation-independent stability							
Intact Rock Strength (SIRS)							
SIRS = RIRS (from reference rock mass) x SWE (weathering slope) =			4,444 x 0,9	4 MPa			
Discontinuity spacing (SSPA)							
SSPA = RSPA x SWE x SME			0,285x0,90x0,76	0,195			
Condition of discontinuity (SCD)							
SCD = RCD x SWE =			0,462 x 0,9	0,416			
Slope unit friction and cohesion (SFRI & SCOH)							
SFRI = SIRS * 0,2417 + SSPA * 52,12 + SCD * 5,779 = (If RIRS > 132 Mpa, then RIRS =132)					13,53°		
SCOH = SIRS * 94,27 + SSPA * 28629 + SCD * 3593 = (If RIRS > 132 Mpa, then RIRS =132)					7,5 kPa		
If SFRI < slope dip, maximum possible height (Hmax):							
Hmax = (1,6x10 <sup>-4</sup> x SCOH) x sin(slopedip) x cos(SFRI) / (1 - cos(slopedip - SFRI)) =					2,1 m		
Ratios	SFRI / Slope dip				0,1804		
	Hmax / Hslope				0,21		
Stable probability: if SFRI > slope dip, probability = % 100, else use the figure for orientation-independent stability:							
<5%							
Orientation-dependent stability							
Discontinuities		B	J1	J2			
Dip direction (degrees)		148	200	12			
Dip (degrees)		62	80	75			
With, Against, Vertical or Equal		A	A	W			
AP (degrees)		-58	-26	40			
RTC		0,425	0,425	0,425			
STC = RTC x sqrt(1,452 - 1,220 x e <sup>(-SWE)</sup> )		0,416	0,416	0,416			
Stable probability:	Sliding	100%	100%	60%			
	Toppling	50%	>95%	100%			
Stable probability:		50%					
Determine orientation stability:							
Calculate AP: β = discontinuity dip, σ = slope dip direction, τ= discontinuity dip direction, δ = σ - τ, AP= arctan(cosδ x tanβ)							
Stability		Sliding	Toppling	Stability		Sliding	Toppling
AP>84°or AP<-84°	Vertical	100%	100%	AP<0° and (-90°< AP+slope dip)<0°	Against	100%	100%
(slope dip + 5°) < AP < 84°	With	100%	100%	AP<0° and (-90°< AP+slope dip)>0°	Against	100%	Use graph toppling
(slope dip - 5°) < AP < (slope dip + 5°	Equal	100%	100%				
0°< AP < (slope dip - 5°	With	Use graph sliding	100%				
Slope final stable probability		<5%					

STOP 6 - DATA COLLECTION TABLE									
Excavation Method (ME)			Intact Rock Strength (IRS)						
Natural/hand-made	1,00	<1.25 MPa			Crumbles in hand				
Pneumatic hammer excavation*	0,76	1.25-5 MPa			Thin slabs break easy in hand				
Pre-splitting/smooth wall blasting	0,99	5-12.5 MPa			Thin slabs broken by heavy hand pressure				
Conventional blasting with result:		12.5-50 MPa			Lumps broken by light hammer blows*				
Good	0,77	50-100 MPa			Lumps broken by heavy hammer blows				
Open discontinuities	0,75	100-200 MPa			Lumps only chip by heavy hammer blows				
Dislodged blocks	0,72	>200 MPa			Rocks ring on hammer blows				
Fractured intact rock	0,67	Weathering degree (WE)			Unweathered		1,00		
Crushed intact rock	0,62				Slightly		0,95		
Lithology					Moderately		0,90		
Granite					Highly*		0,62		
					Completely		0,35		
Discontinuities (B: Bedding; J: Joint)				J1	J2	J3	Slope		
Dip direction (degrees)				125	25	245	Dip direction (degrees)	245	
Dip (degrees)				60	70	50	Dip (degrees)	65	
Spacing (DS) (cm)				10	30	20	Slope height (m)	10	
Condition of discontinuities							Slope Stability		
Large scale roughness (RL)	Wavy		1,00				Stable	1	
	Slightly wavy		0,95				Small problem*	2	
	Curved		0,85	X	X	X	Large problem	3	
	Slightly curved		0,80				Notes: 1) For infill "gouge>irregularities" and "flowing material" small scale roughness= 0,55 2) If roughness is anisotropic (e.g. Ripple marks, striation, etc.) roughness should be assessed perpendicular and parallel to the roughness and directions noted on this form 3) Non-fitting of discontinuities should be marked in roughness columns.		
	Straight		0,75						
Small scale roughness (RS)	Rough stepped		0,95						
	Smooth stepped		0,90						
	Polished stepped		0,85						
	Rough undulating		0,80						
	Smooth undulating		0,75	X	X	X			
	Polished undulating		0,70						
	Rough planar		0,65						
	Smooth planar		0,60						
	Polished planar		0,55						
Infill material (IM)	Cemented / cemented infill		1,07						
	No infill - surface staining		1,00						
	Non-softening & sheared material	Coarse	0,95						
		Medium	0,90						
		Fine	0,85						
	Soft sheared material	Coarse	0,75						
		Medium	0,65	X	X	X			
		Fine	0,55						
	Gouge < irregularities		0,42						
	Gouge > irregularities		0,17						
	Flowing material		0,05						
Karst (KA)	None		1,00	X	X	X			
	Karst		0,92						

STOP 6 - REFERENCE ROCK TABLE						
Intact Rock Strength (RIRS)						
RIRS = IRS / WE = 0,1 / 0,62					0,161	
Discontinuity Spacing (SPA)						
Discontinuities	B	J1	J2	SPA = factor 1 x factor 2 x factor 3	0,414	
Dip direction (degrees)	125	25	245			
Dip (degrees)	60	70	50			
Spacing (m)	10	30	20			
The spacing parameter (SPA) is calculated based on the three discontinuity sets with the smallest spacings in following figure:				SPA = 0,55 x 0,59 x 0,60 = 0,195		
				Corrected for weathering and method of excavation:		
				RSPA = SPA / (WE x ME)		
				RSPA = 0,195 / (0,62 x 0,76)		
Condition of discontinuities						
Discontinuities	B	J1	J2	RTC is the discontinuity condition of a single discontinuity (set) in the reference rock mass corrected for discontinuity weathering. $RTC = TC / \sqrt{1,452 - 1,220 * e^{(-WE)}}$		
Large scale roughness (Rl)	0,85	0,85	0,85			
Small scale roughness (Rs)	0,75	0,75	0,75			
Infill material (Im)	0,65	0,65	0,65			
Karst (Ka)	1,00	1,00	1,00			
TC = Rl x Rs x Im x Ka	0,414	0,414	0,414			
RTC	0,424	0,424	0,424			
Weighted by spacing: $CD = \frac{\frac{TC_1}{DS_1} + \frac{TC_2}{DS_2} + \frac{TC_3}{DS_3}}{\frac{1}{DS_1} + \frac{1}{DS_2} + \frac{1}{DS_3}} =$					0,414	
Corrected by weathering: RCD (with a maximum of 1.0165) = CD/WE =				0,414 / 0,62 =	0,668	
Reference unit friction and cohesion (RFRI & FCOH)						
$\phi(RRM) = RIRS * 0,2417 + RSPA * 52,12 + RCD * 5,779 =$ (If RIRS > 132 MPa, then RIRS = 132)					25,47°	
coh(RRM) = RIRS * 94,27 + RSPA * 28629 + RCD * 3593 = (If RIRS > 132 MPa, then RIRS = 132)					14,3 kPa	

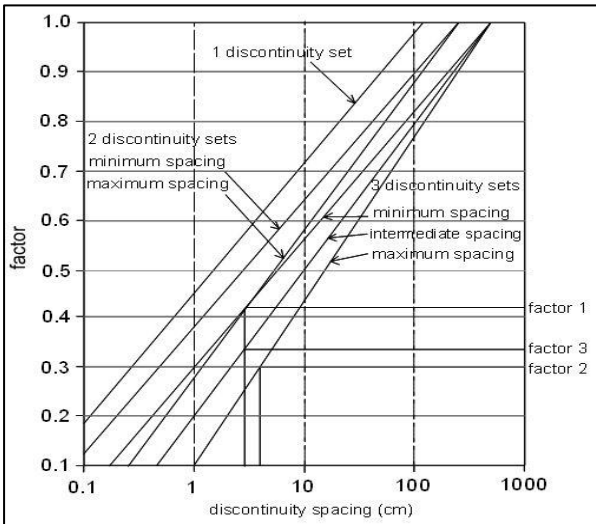
STOP 6 - STABILITY TABLE							
Method of Excavation (SME)				Weathering (SWE)			
Natural/hand-made		1,00		Unweathered		1,00	
Pneumatic hammer excavation*		0,76		Slightly		0,95	
Pre-splitting/smooth wall blasting		0,99		Moderately		0,90	
Conventional blasting with result:				Highly*		0,62	
Good		0,77		Completely		0,35	
Open discontinuities		0,75		Slope geometry features			
Dislodged blocks		0,72		Slope dip direction (degrees)		245	
Fractured intact rock		0,67		Slope dip (degrees)		65	
Crushed intact rock		0,62		Height (m)		10	
Orientation-independent stability							
Intact Rock Strength (SIRS)							
SIRS = RIRS (from reference rock mass) x SWE (weathering slope) =				0,161 x 0,62		0,1 MPa	
Discontinuity spacing (SSPA)							
SSPA = RSPA x SWE x SME				0,414x0,62x0,76		0,195	
Condition of discontinuity (SCD)							
SCD = RCD x SWE =				0,668 x 0,62		0,414	
Slope unit friction and cohesion (SFRI & SCOH)							
SFRI = SIRS * 0,2417 + SSPA * 52,12 + SCD * 5,779 =						12,58°	
(If RIRS > 132 Mpa, then RIRS =132)							
SCOH = SIRS * 94,27 + SSPA * 28629 + SCD * 3593 =						7,1 kPa	
(If RIRS > 132 Mpa, then RIRS =132)							
If SFRI < slope dip, maximum possible height (Hmax):						2,6 m	
Hmax = (1,6x10^-4 x SCOH) x sin(slopedip) x cos(SFRI) / (1 - cos(slopedip - SFRI)) =							
Ratios	SFRI / Slope dip					0,194	
	Hmax/ Hslope					0,260	
Stable probability: if SFRI > slope dip, probability = % 100, else use the figure for orientation-independent stability:						<5%	
Orientation-dependent stability							
Discontinuities		B		J1	J2		
Dip direction (degrees)		125		25	245		
Dip (degrees)		60		70	50		
With, Against, Vertical or Equal		A		A	W		
AP (degrees)		-40		-65	50		
RTC		0,424		0,424	0,424		
STC = RTC x sqrt(1,452 - 1,220 x e^(-SWE))		0,414		0,414	0,414		
Stable probability:	Sliding		100%	100%	<5%		
	Toppling		>95%	70%	100%		
Stable probability:		<5%					
Determine orientation stability:							
Calculate AP: β = discontinuity dip, σ = slope dip direction, τ= discontinuity dip direction, δ = σ - τ, AP= arctan(cosδ x tanβ)							
Stability		Sliding	Toppling	Stability		Sliding	Toppling
AP>84°or AP<-84°	Vertical	100%	100%	AP<0° and (-90° AP+slope dip)<0°	Against	100%	100%
(slope dip + 5°) < AP < 84°	With	100%	100%	AP<0° and (-90° AP+slope dip)>0°	Against	100%	Use graph toppling
(slope dip - 5°) < AP < (slope dip + 5°	Equal	100%	100%				
0°< AP < (slope dip - 5°	With	Use graph sliding	100%				
Slope final stable probability		<5%					

STOP 7 - DATA COLLECTION TABLE									
Excavation Method (ME)				Intact Rock Strength (IRS)					
Natural/hand-made		1,00	<1.25 MPa			Crumbles in hand			
Pneumatic hammer excavation*		0,76	1.25-5 MPa			Thin slabs break easy in hand			
Pre-splitting/smooth wall blasting		0,99	5-12.5 MPa			Thin slabs broken by heavy hand pressure			
Conventional blasting with result:			12.5-50 MPa			Lumps broken by light hammer blows			
Good		0,77	50-100 MPa			Lumps broken by heavy hammer blows*			
Open discontinuities		0,75	100-200 MPa			Lumps only chip by heavy hammer blows			
Dislodged blocks		0,72	>200 MPa			Rocks ring on hammer blows			
Fractured intact rock		0,67	Weathering degree (WE)			Unweathered		1,00	
Crushed intact rock		0,62				Slightly*		0,95	
Lithology						Moderately		0,90	
Granodiorite						Highly		0,62	
						Completely		0,35	
Discontinuities (B: Bedding; J: Joint)					J1	J2	J3	Slope	
Dip direction (degrees)					230	340	20	Dip direction (degrees)	180
Dip (degrees)					70	55	5	Dip (degrees)	75
Spacing (DS) (cm)					20	40	30	Slope height (m)	15
Condition of discontinuities							Slope Stability		
Large scale roughness (RL)	Wavy		1,00				Stable	1	
	Slightly wavy		0,95	X	X	X	Small problem*	2	
	Curved		0,85				Large problem	3	
	Slightly curved		0,80				Notes: 1) For infill "gouge">irregularities" and "flowing material" small scale roughness= 0,55 2) If roughness is anisotropic (e.g. Ripple marks, striation, etc.) roughness should be assessed perpendicular and parallel to the roughness and directions noted on this form 3) Non-fitting of discontinuities should be marked in roughness columns.		
	Straight		0,75						
Small scale roughness (RS)	Rough stepped		0,95						
	Smooth stepped		0,90						
	Polished stepped		0,85						
	Rough undulating		0,80	X	X	X			
	Smooth undulating		0,75						
	Polished undulating		0,70						
	Rough planar		0,65						
	Smooth planar		0,60						
	Polished planar		0,55						
Infill material (IM)	Cemented / cemented infill		1,07						
	No infill - surface staining		1,00	X	X	X			
	Non-softening & sheared material	Coarse	0,95						
		Medium	0,90						
		Fine	0,85						
	Soft sheared material	Coarse	0,75						
		Medium	0,65						
		Fine	0,55						
	Gouge < irregularities		0,42						
	Gouge > irregularities		0,17						
Flowing material		0,05							
Karst (KA)	None		1,00	X	X	X			
	Karst		0,92						

STOP 7 - REFERENCE ROCK TABLE					
Intact Rock Strength (RIRS)					
RIRS = IRS / WE = 13 / 0,95				13,684	
Discontinuity Spacing (SPA)					
Discontinuities	B	J1	J2	SPA = factor 1 x factor 2 x factor 3	
Dip direction (degrees)	230	340	20		
Dip (degrees)	70	55	5		
Spacing (m)	20	40	30		
The spacing parameter (SPA) is calculated based on the three discontinuity sets with the smallest spacings in following figure:				SPA = 0,63 x 0,63 x 0,63 = 0,250	0,346
				Corrected for weathering and method of excavation:	
				RSPA = SPA / (WE x ME)	
				RSPA = 0,250 / (0,95 x 0,76)	
Condition of discontinuities					
Discontinuities	B	J1	J2	RTC is the discontinuity condition of a single discontinuity (set) in the reference rock mass corrected for discontinuity weathering. $RTC = TC / \sqrt{1,452 - 1,220 * e^{(-WE)}}$	
Large scale roughness (Rl)	0,95	0,95	0,95		
Small scale roughness (Rs)	0,80	0,80	0,80		
Infill material (Im)	1,00	1,00	1,00		
Karst (Ka)	1,00	1,00	1,00		
TC = Rl x Rs x Im x Ka	0,760	0,760	0,760		
RTC	0,777	0,777	0,777		
Weighted by spacing: $CD = \frac{\frac{TC_1}{DS_1} + \frac{TC_2}{DS_2} + \frac{TC_3}{DS_3}}{\frac{1}{DS_1} + \frac{1}{DS_2} + \frac{1}{DS_3}} =$				0,760	
Corrected by weathering: RCD (with a maximum of 1.0165) = CD/WE =				0,760 / 0,95 = 0,800	
Reference unit friction and cohesion (RFRI & FCOH)					
$\phi(RRM) = RIRS * 0,2417 + RSPA * 52,12 + RCD * 5,779 =$ (If RIRS > 132 MPa, then RIRS = 132)				25,97°	
$coh(RRM) = RIRS * 94,27 + RSPA * 28629 + RCD * 3593 =$ (If RIRS > 132 MPa, then RIRS = 132)				14,1 kPa	

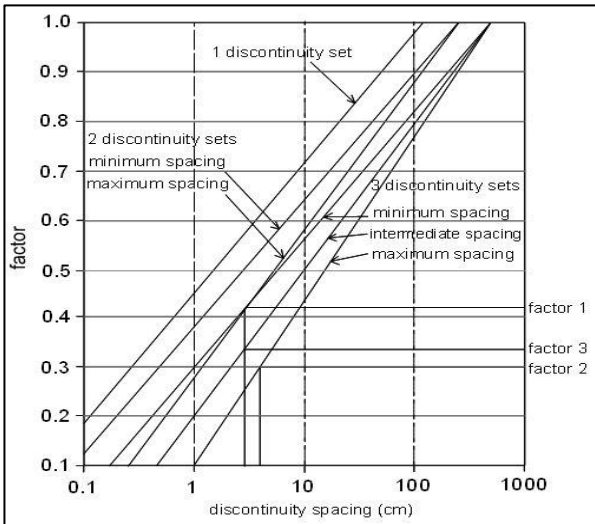
STOP 7 - STABILITY TABLE							
Method of Excavation (SME)		Weathering (SWE)					
Natural/hand-made	1,00	Unweathered	1,00				
Pneumatic hammer excavation*	0,76	Slightly*	0,95				
Pre-splitting/smooth wall blasting	0,99	Moderately	0,90				
Conventional blasting with result:		Highly	0,62				
Good	0,77	Completely	0,35				
Open discontinuities	0,75	Slope geometry features					
Dislodged blocks	0,72	Slope dip direction (degrees)	180				
Fractured intact rock	0,67	Slope dip (degrees)	75				
Crushed intact rock	0,62	Height (m)	15				
Orientation-independent stability							
Intact Rock Strength (SIRS)							
SIRS = RIRS (from reference rock mass) x SWE (weathering slope) =		13,684 x 0,95	13 MPa				
Discontinuity spacing (SSPA)							
SSPA = RSPA x SWE x SME		0,346x0,95x0,76	0,250				
Condition of discontinuity (SCD)							
SCD = RCD x SWE =		0,800 x 0,95	0,760				
Slope unit friction and cohesion (SFRI & SCOH)							
SFRI = SIRS * 0,2417 + SSPA * 52,12 + SCD * 5,779 =			20,56°				
(If RIRS > 132 Mpa, then RIRS =132)							
SCOH = SIRS * 94,27 + SSPA * 28629 + SCD * 3593 =			11,1 kPa				
(If RIRS > 132 Mpa, then RIRS =132)							
If SFRI < slope dip, maximum possible height (Hmax):							
Hmax = (1,6x10 <sup>-4</sup> x SCOH) x sin(slopedip) x cos(SFRI) / (1 - cos(slopedip - SFRI)) =			3,8 m				
Ratios	SFRI / Slope dip			0,274			
	Hmax / Hslope			0,2533333			
Stable probability: if SFRI > slope dip, probability = % 100, else use the figure for orientation-independent stability:							
<5%							
Orientation-dependent stability							
Discontinuities		B	J1	J2			
Dip direction (degrees)		230	340	20			
Dip (degrees)		70	55	5			
With, Against, Vertical or Equal		W	A	A			
AP (degrees)		60	-53	-5			
RTC		0,777	0,777	0,777			
STC = RTC x sqrt(1,452 - 1,220 x e <sup>(-SWE)</sup> )		0,760	0,760	0,760			
Stable probability:	Sliding	>95%	100%	100%			
	Toppling	100%	>95%	100%			
Stable probability:		>95%					
Determine orientation stability:							
Calculate AP: β = discontinuity dip, σ = slope dip direction, τ= discontinuity dip direction, δ = σ - τ, AP= arctan(cosδ x tanβ)							
Stability		Sliding	Toppling	Stability	Sliding	Toppling	
AP>84°or AP<-84°	Vertical	100%	100%	AP<0° and (-90-AP+slope dip)<0°	Against	100%	100%
(slope dip + 5°) < AP < 84°	With	100%	100%	AP<0° and (-90-AP+slope dip)>0°	Against	100%	Use graph toppling
(slope dip - 5°) < AP < (slope dip + 5°	Equal	100%	100%				
0°< AP < (slope dip - 5°	With	Use graph sliding	100%				
Slope final stable probability		<5%					

STOP 8 - DATA COLLECTION TABLE								
Excavation Method (ME)			Intact Rock Strength (IRS)					
Natural/hand-made	1,00	<1.25 MPa			Crumbles in hand			
Pneumatic hammer excavation*	0,76	1.25-5 MPa			Thin slabs break easy in hand			
Pre-splitting/smooth wall blasting	0,99	5-12.5 MPa			Thin slabs broken by heavy hand pressure			
Conventional blasting with result:		12.5-50 MPa			Lumps broken by light hammer blows*			
Good	0,77	50-100 MPa			Lumps broken by heavy hammer blows			
Open discontinuities	0,75	100-200 MPa			Lumps only chip by heavy hammer blows			
Dislodged blocks	0,72	>200 MPa			Rocks ring on hammer blows			
Fractured intact rock	0,67	Weathering degree (WE)			Unweathered		1,00	
Crushed intact rock	0,62				Slightly		0,95	
Lithology					Moderately*		0,90	
50% Sandstone / 50% Mudstone					Highly		0,62	
					Completely		0,35	
Discontinuities (B: Bedding; J: Joint)				B	J1	J2	Slope	
Dip direction (degrees)				310	170	70	Dip direction (degrees)	215
Dip (degrees)				30	70	70	Dip (degrees)	50
Spacing (DS) (cm)				50	80	40	Slope height (m)	15
Condition of discontinuities						Slope Stability		
Large scale roughness (RL)	Wavy		1,00				Stable	1
	Slightly wavy		0,95			X	Small problem*	2
	Curved		0,85	X	X		Large problem	3
	Slightly curved		0,80				Notes: 1) For infill "gouge">irregularities" and "flowing material" small scale roughness= 0,55 2) If roughness is anisotropic (e.g. Ripple marks, striation, etc.) roughness should be assessed perpendicular and parallel to the roughness and directions noted on this form 3) Non-fitting of discontinuities should be marked in roughness columns.	
	Straight		0,75					
Small scale roughness (RS)	Rough stepped		0,95					
	Smooth stepped		0,90	X	X	X		
	Polished stepped		0,85					
	Rough undulating		0,80					
	Smooth undulating		0,75					
	Polished undulating		0,70					
	Rough planar		0,65					
	Smooth planar		0,60					
Polished planar		0,55						
Infill material (IM)	Cemented / cemented infill		1,07					
	No infill - surface staining		1,00					
	Non-softening & sheared material	Coarse	0,95					
		Medium	0,90					
		Fine	0,85					
	Soft sheared material	Coarse	0,75					
		Medium	0,65	X	X	X		
		Fine	0,55					
	Gouge < irregularities		0,42					
	Gouge > irregularities		0,17					
Flowing material		0,05						
Karst (KA)	None		1,00	X	X	X		
	Karst		0,92					

STOP 8 - REFERENCE ROCK TABLE						
Intact Rock Strength (RIRS)						
RIRS = IRS / WE = 13 / 0,90					14,444	
Discontinuity Spacing (SPA)						
Discontinuities	B	J1	J2	SPA = factor 1 x factor 2 x factor 3	0,531	
Dip direction (degrees)	310	170	70			
Dip (degrees)	30	70	70			
Spacing (m)	50	80	40			
The spacing parameter (SPA) is calculated based on the three discontinuity sets with the smallest spacings in following figure:				SPA = 0,71 x 0,70 x 0,73 = 0,363		
				Corrected for weathering and method of excavation:		
				RSPA = SPA / (WE x ME)		
				RSPA = 0,363 / (0,90 x 0,76)		
Condition of discontinuities						
Discontinuities	B	J1	J2	RTC is the discontinuity condition of a single discontinuity (set) in the reference rock mass corrected for discontinuity weathering. $RTC = TC / \sqrt{1,452 - 1,220 * e^{(-WE)}}$		
Large scale roughness (Rl)	0,85	0,85	0,95			
Small scale roughness (Rs)	0,90	0,90	0,90			
Infill material (Im)	0,65	0,65	0,65			
Karst (Ka)	1,00	1,00	1,00			
TC = Rl x Rs x Im x Ka	0,497	0,497	0,556			
RTC	0,509	0,509	0,568			
Weighted by spacing: $CD = \frac{\frac{TC_1}{DS_1} + \frac{TC_2}{DS_2} + \frac{TC_3}{DS_3}}{\frac{1}{DS_1} + \frac{1}{DS_2} + \frac{1}{DS_3}} =$						0,523
Corrected by weathering: RCD (with a maximum of 1.0165) = CD/WE =				0,523 / 0,90 =	0,581	
Reference unit friction and cohesion (RFRI & FCOH)						
$\phi(RRM) = RIRS * 0,2417 + RSPA * 52,12 + RCD * 5,779 =$ (If RIRS > 132 MPa, then RIRS = 132)					34,53°	
coh(RRM) = RIRS * 94,27 + RSPA * 28629 + RCD * 3593 = (If RIRS > 132 MPa, then RIRS = 132)					18,7 kPa	

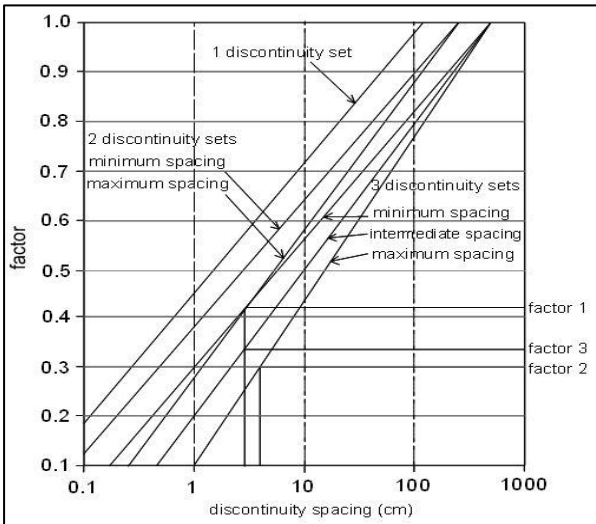
STOP 8 - STABILITY TABLE						
Method of Excavation (SME)			Weathering (SWE)			
Natural/hand-made		1,00	Unweathered		1,00	
Pneumatic hammer excavation*		0,76	Slightly		0,95	
Pre-splitting/smooth wall blasting		0,99	Moderately*		0,90	
Conventional blasting with result:			Highly		0,62	
Good		0,77	Completely		0,35	
Open discontinuities		0,75	Slope geometry features			
Dislodged blocks		0,72	Slope dip direction (degrees)		215	
Fractured intact rock		0,67	Slope dip (degrees)		50	
Crushed intact rock		0,62	Height (m)		15	
Orientation-independent stability						
Intact Rock Strength (SIRS)						
SIRS = RIRS (from reference rock mass) x SWE (weathering slope) =			14,444 x 0,90		13 MPa	
Discontinuity spacing (SSPA)						
SSPA = RSPA x SWE x SME			0,531x0,90x0,76		0,363	
Condition of discontinuity (SCD)						
SCD = RCD x SWE =			0,581 x 0,90		0,523	
Slope unit friction and cohesion (SFRI & SCOH)						
SFRI = SIRS * 0,2417 + SSPA * 52,12 + SCD * 5,779 =					25,08°	
(If RIRS > 132 Mpa, then RIRS =132)						
SCOH = SIRS * 94,27 + SSPA * 28629 + SCD * 3593 =					13,5 kPa	
(If RIRS > 132 Mpa, then RIRS =132)						
If SFRI < slope dip, maximum possible height (Hmax):					16,1 m	
Hmax = (1,6x10^-4 x SCOH) x sin(slopedip) x cos(SFRI) / (1 - cos(slopedip - SFRI)) =						
Ratios	SFRI / Slope dip				0,502	
	Hmax/ Hslope				1,073	
Stable probability: if SFRI > slope dip, probability = % 100, else use the figure for orientation-independent stability:					50%	
Orientation-dependent stability						
Discontinuities		B	J1	J2		
Dip direction (degrees)		310	170	70		
Dip (degrees)		30	70	70		
With, Against, Vertical or Equal		A	W	A		
AP (degrees)		-3	63	-66		
RTC		0,509	0,509	0,568		
STC = RTC x sqrt(1,452 - 1,220 x e^(-SWE))		0,497	0,497	0,556		
Stable probability:	Sliding	100%	100%	100%		
	Toppling	100%	100%	>95%		
Stable probability:		>95%				
Determine orientation stability:						
Calculate AP: β = discontinuity dip, σ = slope dip direction, τ= discontinuity dip direction, δ = σ - τ, AP= arctan(cosδ x tanβ)						
Stability		Sliding	Toppling	Stability	Sliding	Toppling
AP>84°or AP<-84°	Vertical	100%	100%	AP<0° and (-90°<AP+slope dip)<0°	Against	100%
(slope dip + 5°) < AP < 84°	With	100%	100%	AP<0° and (-90°<AP+slope dip)>0°	Against	Use graph toppling
(slope dip - 5°) < AP < (slope dip + 5°)	Equal	100%	100%			
0°< AP < (slope dip - 5°)	With	Use graph sliding	100%			
Slope final stable probability		50%				

STOP 9 - DATA COLLECTION TABLE							
Excavation Method (ME)			Intact Rock Strength (IRS)				
Natural/hand-made	1,00		<1.25 MPa		Crumbles in hand		
Pneumatic hammer excavation*	0,76		1.25-5 MPa		Thin slabs break easy in hand		
Pre-splitting/smooth wall blasting	0,99		5-12.5 MPa		Thin slabs broken by heavy hand pressure		
Conventional blasting with result:			12.5-50 MPa		Lumps broken by light hammer blows*		
Good	0,77		50-100 MPa		Lumps broken by heavy hammer blows		
Open discontinuities	0,75		100-200 MPa		Lumps only chip by heavy hammer blows		
Dislodged blocks	0,72		>200 MPa		Rocks ring on hammer blows		
Fractured intact rock	0,67		Weathering degree (WE)		Unweathered	1,00	
Crushed intact rock	0,62				Slightly	0,95	
Lithology					Moderately*	0,90	
50% Limestone / 50% Mudstone					Highly	0,62	
					Completely	0,35	
Discontinuities (B: Bedding; J: Joint)			B	J1	J2	Slope	
Dip direction (degrees)			145	235	290	Dip direction (degrees)	312
Dip (degrees)			48	66	30	Dip (degrees)	45
Spacing (DS) (cm)			40	30	20	Slope height (m)	8
Condition of discontinuities					Slope Stability		
Large scale roughness (RL)	Wavy	1,00	X			Stable	1
	Slightly wavy	0,95			X	Small problem*	2
	Curved	0,85		X		Large problem	3
	Slightly curved	0,80				Notes: 1) For infill "gouge">irregularities" and "flowing material" small scale roughness= 0,55 2) If roughness is anisotropic (e.g. Ripple marks, striation, etc.) roughness should be assessed perpendicular and parallel to the roughness and directions noted on this form 3) Non-fitting of discontinuities should be marked in roughness columns.	
	Straight	0,75					
Small scale roughness (RS)	Rough stepped	0,95					
	Smooth stepped	0,90					
	Polished stepped	0,85					
	Rough undulating	0,80	X				
	Smooth undulating	0,75		X	X		
	Polished undulating	0,70					
	Rough planar	0,65					
	Smooth planar	0,60					
	Polished planar	0,55					
Infill material (IM)	Cemented / cemented infill		1,07				
	No infill - surface staining		1,00				
	Non-softening & sheared material	Coarse	0,95				
		Medium	0,90				
		Fine	0,85				
	Soft sheared material	Coarse	0,75				
		Medium	0,65	X	X		
		Fine	0,55				
	Gouge < irregularities		0,42				
	Gouge > irregularities		0,17				
	Flowing material		0,05				
Karst (KA)	None		1,00	X	X	X	
	Karst		0,92				

STOP 9 - REFERENCE ROCK TABLE				
Intact Rock Strength (RIRS)				
RIRS = IRS / WE = 26 / 0,90				28,889
Discontinuity Spacing (SPA)				
Discontinuities	B	J1	J2	SPA = factor 1 x factor 2 x factor 3
Dip direction (degrees)	145	235	290	
Dip (degrees)	48	66	30	
Spacing (m)	40	30	20	
The spacing parameter (SPA) is calculated based on the three discontinuity sets with the smallest spacings in following figure:				SPA = 0,64 x 0,64 x 0,64 = 0,262  Corrected for weathering and method of excavation:  RSPA = SPA / (WE x ME)  RSPA = 0,262 / (0,90 x 0,76)
				
Condition of discontinuities				
Discontinuities	B	J1	J2	RTC is the discontinuity condition of a single discontinuity (set) in the reference rock mass corrected for discontinuity weathering. $RTC = TC / \sqrt{1,452 - 1,220 * e^{(-WE)}}$
Large scale roughness (Rl)	1,00	0,85	0,95	
Small scale roughness (Rs)	0,80	0,75	0,75	
Infill material (Im)	0,65	0,65	0,65	
Karst (Ka)	1,00	1,00	1,00	
TC = Rl x Rs x Im x Ka	0,520	0,414	0,463	
RTC	0,532	0,424	0,474	
Weighted by spacing: $CD = \frac{\frac{TC_1}{DS_1} + \frac{TC_2}{DS_2} + \frac{TC_3}{DS_3}}{\frac{1}{DS_1} + \frac{1}{DS_2} + \frac{1}{DS_3}} =$				0,461
Corrected by weathering: RCD (with a maximum of 1.0165) = CD/WE =				0,461 / 0,90 = 0,512
Reference unit friction and cohesion (RFRI & FCOH)				
$\phi(RRM) = RIRS * 0,2417 + RSPA * 52,12 + RCD * 5,779 =$ (If RIRS > 132 MPa, then RIRS = 132)				29,91°
$coh(RRM) = RIRS * 94,27 + RSPA * 28629 + RCD * 3593 =$ (If RIRS > 132 MPa, then RIRS = 132)				15,3 kPa

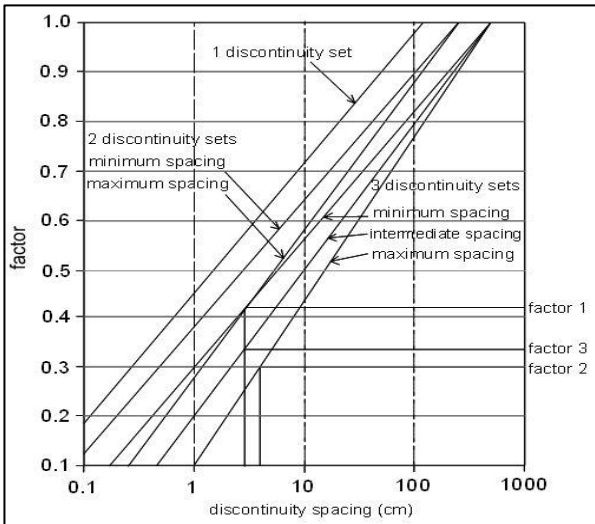
STOP 9 - STABILITY TABLE							
Method of Excavation (SME)			Weathering (SWE)				
Natural/hand-made		1,00	Unweathered		1,00		
Pneumatic hammer excavation*		0,76	Slightly		0,95		
Pre-splitting/smooth wall blasting		0,99	Moderately*		0,90		
Conventional blasting with result:			Highly		0,62		
Good		0,77	Completely		0,35		
Open discontinuities		0,75	Slope geometry features				
Dislodged blocks		0,72	Slope dip direction (degrees)		312		
Fractured intact rock		0,67	Slope dip (degrees)		45		
Crushed intact rock		0,62	Height (m)		8		
Orientation-independent stability							
Intact Rock Strength (SIRS)							
SIRS = RIRS (from reference rock mass) x SWE (weathering slope) =			28,889 x 0,90	26 MPa			
Discontinuity spacing (SSPA)							
SSPA = RSPA x SWE x SME			0,383x0,90x0,76	0,262			
Condition of discontinuity (SCD)							
SCD = RCD x SWE =			0,512 x 0,90	0,461			
Slope unit friction and cohesion (SFRI & SCOH)							
SFRI = SIRS * 0,2417 + SSPA * 52,12 + SCD * 5,779 =					22,60°		
(If RIRS > 132 Mpa, then RIRS =132)							
SCOH = SIRS * 94,27 + SSPA * 28629 + SCD * 3593 =					11,6 kPa		
(If RIRS > 132 Mpa, then RIRS =132)							
If SFRI < slope dip, maximum possible height (Hmax):					16,1 m		
Hmax = (1,6x10^-4 x SCOH) x sin(slopedip) x cos(SFRI) / (1 - cos(slopedip - SFRI)) =							
Ratios	SFRI / Slope dip				0,502		
	Hmax / Hslope				2,0125		
Stable probability: if SFRI > slope dip, probability = % 100, else use the figure for orientation-independent stability:					>95%		
Orientation-dependent stability							
Discontinuities		B	J1	J2			
Dip direction (degrees)		145	235	290			
Dip (degrees)		48	66	30			
With, Against, Vertical or Equal		A	W	W			
AP (degrees)		-47	27	28			
RTC		0,532	0,424	0,474			
STC = RTC x sqrt(1,452 - 1,220 x e^(-SWE))		0,520	0,414	0,463			
Stable probability:	Sliding	100%	>95%	>95%			
	Toppling	>95%	100%	100%			
Stable probability:		>95%					
Determine orientation stability:							
Calculate AP: β = discontinuity dip, σ = slope dip direction, τ= discontinuity dip direction, δ = σ - τ, AP= arctan(cosδ x tanβ)							
Stability		Sliding	Toppling	Stability	Sliding	Toppling	
AP>84°or AP<-84°	Vertical	100%	100%	AP<0° and (-90° AP+slope dip)<0°	Against	100%	100%
(slope dip + 5°) < AP < 84°	With	100%	100%	AP<0° and (-90° AP+slope dip)>0°	Against	100%	Use graph toppling
(slope dip - 5°) < AP < (slope dip + 5°)	Equal	100%	100%				
0°< AP < (slope dip - 5°)	With	Use graph sliding	100%				
Slope final stable probability		>95%					

STOP 10 - DATA COLLECTION TABLE									
Excavation Method (ME)			Intact Rock Strength (IRS)						
Natural/hand-made		1,00	<1.25 MPa			Crumbles in hand			
Pneumatic hammer excavation*		0,76	1.25-5 MPa			Thin slabs break easy in hand			
Pre-splitting/smooth wall blasting		0,99	5-12.5 MPa			Thin slabs broken by heavy hand pressure			
Conventional blasting with result:			12.5-50 MPa			Lumps broken by light hammer blows*			
Good		0,77	50-100 MPa			Lumps broken by heavy hammer blows			
Open discontinuities		0,75	100-200 MPa			Lumps only chip by heavy hammer blows			
Dislodged blocks		0,72	>200 MPa			Rocks ring on hammer blows			
Fractured intact rock		0,67	Weathering degree (WE)			Unweathered		1,00	
Crushed intact rock		0,62				Slightly		0,95	
Lithology						Moderately*		0,90	
80% Sandstone / 20% Mudstone						Highly		0,62	
						Completely		0,35	
Discontinuities (B: Bedding; J: Joint)				B	J1	J2	Slope		
Dip direction (degrees)				354	226	160	Dip direction (degrees)		200
Dip (degrees)				34	84	50	Dip (degrees)		50
Spacing (DS) (cm)				20	50	35	Slope height (m)		8
Condition of discontinuities						Slope Stability			
Large scale roughness (RL)	Wavy		1,00				Stable		1
	Slightly wavy		0,95				Small problem*		2
	Curved		0,85	X	X	X	Large problem		3
	Slightly curved		0,80				Notes: 1) For infill "gouge">irregularities" and "flowing material" small scale roughness= 0,55 2) If roughness is anisotropic (e.g. Ripple marks, striation, etc.) roughness should be assessed perpendicular and parallel to the roughness and directions noted on this form 3) Non-fitting of discontinuities should be marked in roughness columns.		
	Straight		0,75						
Small scale roughness (RS)	Rough stepped		0,95						
	Smooth stepped		0,90						
	Polished stepped		0,85						
	Rough undulating		0,80	X	X	X			
	Smooth undulating		0,75						
	Polished undulating		0,70						
	Rough planar		0,65						
	Smooth planar		0,60						
Polished planar		0,55							
Infill material (IM)	Cemented / cemented infill		1,07						
	No infill - surface staining		1,00						
	Non-softening & sheared material	Coarse	0,95						
		Medium	0,90						
		Fine	0,85						
	Soft sheared material	Coarse	0,75						
		Medium	0,65						
		Fine	0,55	X	X	X			
	Gouge < irregularities		0,42						
	Gouge > irregularities		0,17						
Flowing material		0,05							
Karst (KA)	None		1,00	X	X	X			
	Karst		0,92						

STOP 10 - REFERENCE ROCK TABLE					
Intact Rock Strength (RIRS)					
RIRS = IRS / WE = 7 / 0,90					7,778
Discontinuity Spacing (SPA)					
Discontinuities	B	J1	J2	SPA = factor 1 x factor 2 x factor 3	
Dip direction (degrees)	354	226	160		
Dip (degrees)	34	84	50		
Spacing (m)	20	50	35		
The spacing parameter (SPA) is calculated based on the three discontinuity sets with the smallest spacings in following figure:				SPA = 0,64 x 0,65 x 0,67 = 0,279	0,408
				Corrected for weathering and method of excavation:	
				RSPA = SPA / (WE x ME)	
				RSPA = 0,279 / (0,90 x 0,76)	
Condition of discontinuities					
Discontinuities	B	J1	J2	RTC is the discontinuity condition of a single discontinuity (set) in the reference rock mass corrected for discontinuity weathering. $RTC = TC / \sqrt{1,452 - 1,220 * e^{(-WE)}}$	
Large scale roughness (Rl)	0,85	0,85	0,85		
Small scale roughness (Rs)	0,80	0,80	0,80		
Infill material (Im)	0,55	0,55	0,55		
Karst (Ka)	1,00	1,00	1,00		
TC = Rl x Rs x Im x Ka	0,374	0,374	0,374		
RTC	0,383	0,383	0,383		
Weighted by spacing: $CD = \frac{\frac{TC_1}{DS_1} + \frac{TC_2}{DS_2} + \frac{TC_3}{DS_3}}{\frac{1}{DS_1} + \frac{1}{DS_2} + \frac{1}{DS_3}} =$					0,374
Corrected by weathering: RCD (with a maximum of 1.0165) = CD/WE =				0,374 / 0,90 =	0,416
Reference unit friction and cohesion (RFRI & FCOH)					
$\phi(RRM) = RIRS * 0,2417 + RSPA * 52,12 + RCD * 5,779 =$ (If RIRS > 132 MPa, then RIRS = 132)					25,54°
coh(RRM) = RIRS * 94,27 + RSPA * 28629 + RCD * 3593 = (If RIRS > 132 MPa, then RIRS = 132)					13,9 kPa

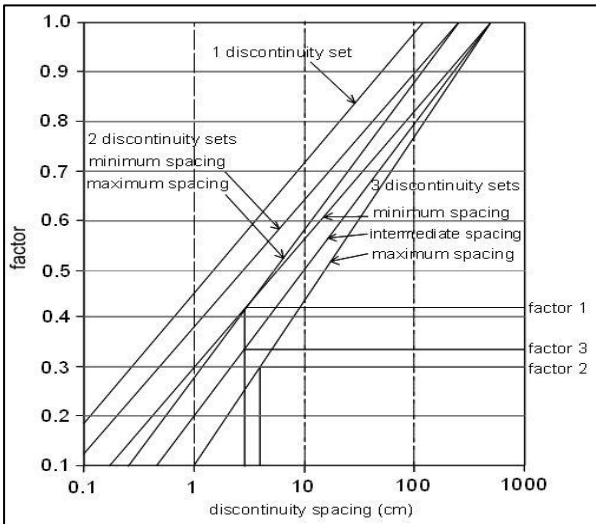
STOP 10 - STABILITY TABLE						
Method of Excavation (SME)			Weathering (SWE)			
Natural/hand-made		1,00	Unweathered	1,00		
Pneumatic hammer excavation*		0,76	Slightly	0,95		
Pre-splitting/smooth wall blasting		0,99	Moderately*	0,90		
Conventional blasting with result:			Highly	0,62		
Good		0,77	Completely	0,35		
Open discontinuities		0,75	Slope geometry features			
Dislodged blocks		0,72	Slope dip direction (degrees)	200		
Fractured intact rock		0,67	Slope dip (degrees)	50		
Crushed intact rock		0,62	Height (m)	8		
Orientation-independent stability						
Intact Rock Strength (SIRS)						
SIRS = RIRS (from reference rock mass) x SWE (weathering slope) =			7,778 x 0,9	7 MPa		
Discontinuity spacing (SSPA)						
SSPA = RSPA x SWE x SME			0,408x0,90x0,76	0,279		
Condition of discontinuity (SCD)						
SCD = RCD x SWE =			0,416 x 0,9	0,374		
Slope unit friction and cohesion (SFRI & SCOH)						
SFRI = SIRS * 0,2417 + SSPA * 52,12 + SCD * 5,779 =				18,39°		
(If RIRS > 132 Mpa, then RIRS =132)						
SCOH = SIRS * 94,27 + SSPA * 28629 + SCD * 3593 =				10,0 kPa		
(If RIRS > 132 Mpa, then RIRS =132)						
If SFRI < slope dip, maximum possible height (Hmax):				7,8 m		
Hmax = (1,6x10^-4 x SCOH) x sin(slopedip) x cos(SFRI) / (1 - cos(slopedip - SFRI)) =						
Ratios	SFRI / Slope dip			0,3678		
	Hmax / Hslope			0,975		
Stable probability: if SFRI > slope dip, probability = % 100, else use the figure for orientation-independent stability:				40%		
Orientation-dependent stability						
Discontinuities		B	J1	J2		
Dip direction (degrees)		354	226	160		
Dip (degrees)		34	84	50		
With, Against, Vertical or Equal		A	W	W		
AP (degrees)		-31	83	42		
RTC		0,383	0,383	0,383		
STC = RTC x sqrt(1,452 - 1,220 x e^(-SWE))		0,374	0,374	0,374		
Stable probability:	Sliding	100%	100%	<5%		
	Toppling	100%	100%	100%		
Stable probability:		<5%				
Determine orientation stability:						
Calculate AP: β = discontinuity dip, σ = slope dip direction, τ= discontinuity dip direction, δ = σ - τ, AP= arctan(cosδ x tanβ)						
Stability		Sliding	Toppling	Stability	Sliding	Toppling
AP>84°or AP<-84°	Vertical	100%	100%	AP<0° and (-90- AP+slope dip)<0°	Against	100%
(slope dip + 5°) < AP < 84°	With	100%	100%	AP<0° and (-90- AP+slope dip)>0°	Against	100%
(slope dip - 5°) < AP < (slope dip + 5°	Equal	100%	100%			
0° < AP < (slope dip - 5°	With	Use graph sliding	100%			
Slope final stable probability		<5%				

STOP 11 - DATA COLLECTION TABLE									
Excavation Method (ME)			Intact Rock Strength (IRS)						
Natural/hand-made		1,00	<1.25 MPa			Crumbles in hand			
Pneumatic hammer excavation*		0,76	1.25-5 MPa			Thin slabs break easy in hand			
Pre-splitting/smooth wall blasting		0,99	5-12.5 MPa			Thin slabs broken by heavy hand pressure			
Conventional blasting with result:			12.5-50 MPa			Lumps broken by light hammer blows*			
Good		0,77	50-100 MPa			Lumps broken by heavy hammer blows			
Open discontinuities		0,75	100-200 MPa			Lumps only chip by heavy hammer blows			
Dislodged blocks		0,72	>200 MPa			Rocks ring on hammer blows			
Fractured intact rock		0,67	Weathering degree (WE)			Unweathered		1,00	
Crushed intact rock		0,62				Slightly		0,95	
Lithology						Moderately*		0,90	
80% Sandstone / 20% Mudstone						Highly		0,62	
						Completely		0,35	
Discontinuities (B: Bedding; J: Joint)				B	J1	J2	Slope		
Dip direction (degrees)				336	150	215	Dip direction (degrees)	260	
Dip (degrees)				36	60	87	Dip (degrees)	60	
Spacing (DS) (cm)				20	15	25	Slope height (m)	6	
Condition of discontinuities							Slope Stability		
Large scale roughness (RL)	Wavy		1,00				Stable	1	
	Slightly wavy		0,95	X	X	X	Small problem*	2	
	Curved		0,85				Large problem	3	
	Slightly curved		0,80				Notes: 1) For infill "gouge>irregularities" and "flowing material" small scale roughness= 0,55 2) If roughness is anisotropic (e.g. Ripple marks, striation, etc.) roughness should be assessed perpendicular and parallel to the roughness and directions noted on this form 3) Non-fitting of discontinuities should be marked in roughness columns.		
	Straight		0,75						
Small scale roughness (RS)	Rough stepped		0,95						
	Smooth stepped		0,90						
	Polished stepped		0,85						
	Rough undulating		0,80	X	X	X			
	Smooth undulating		0,75						
	Polished undulating		0,70						
	Rough planar		0,65						
	Smooth planar		0,60						
Polished planar		0,55							
Infill material (IM)	Cemented / cemented infill		1,07						
	No infill - surface staining		1,00						
	Non-softening & sheared material	Coarse	0,95						
		Medium	0,90						
		Fine	0,85						
	Soft sheared material	Coarse	0,75						
		Medium	0,65	X	X	X			
		Fine	0,55						
	Gouge < irregularities		0,42						
	Gouge > irregularities		0,17						
Flowing material		0,05							
Karst (KA)	None		1,00	X	X	X			
	Karst		0,92						

STOP 11 - REFERENCE ROCK TABLE					
Intact Rock Strength (RIRS)					
RIRS = IRS / WE = 6 / 0,90					6,667
Discontinuity Spacing (SPA)					
Discontinuities	B	J1	J2	SPA = factor 1 x factor 2 x factor 3	
Dip direction (degrees)	336	150	215		
Dip (degrees)	36	60	87		
Spacing (m)	20	15	25		
The spacing parameter (SPA) is calculated based on the three discontinuity sets with the smallest spacings in following figure:				SPA = 0,60 x 0,59 x 0,58 = 0,205	0,300
				Corrected for weathering and method of excavation:	
				RSPA = SPA / (WE x ME)	
				RSPA = 0,205 / (0,90 x 0,76)	
Condition of discontinuities					
Discontinuities	B	J1	J2	RTC is the discontinuity condition of a single discontinuity (set) in the reference rock mass corrected for discontinuity weathering. $RTC$ $= TC / \sqrt{1,452 - 1,220 * e^{(-WE)}}$	
Large scale roughness (Rl)	0,95	0,95	0,95		
Small scale roughness (Rs)	0,80	0,80	0,80		
Infill material (Im)	0,65	0,65	0,65		
Karst (Ka)	1,00	1,00	1,00		
TC = Rl x Rs x Im x Ka	0,494	0,494	0,494		
RTC	0,505	0,505	0,505		
Weighted by spacing: $CD = \frac{\frac{TC_1}{DS_1} + \frac{TC_2}{DS_2} + \frac{TC_3}{DS_3}}{\frac{1}{DS_1} + \frac{1}{DS_2} + \frac{1}{DS_3}} =$				0,494	
Corrected by weathering: RCD (with a maximum of 1.0165) = CD/WE =				0,494 / 0,90 =	0,549
Reference unit friction and cohesion (RFRI & FCOH)					
$\phi(RRM) = RIRS * 0,2417 + RSPA * 52,12 + RCD * 5,779 =$ (If RIRS > 132 MPa, then RIRS = 132)					20,40°
$coh(RRM) = RIRS * 94,27 + RSPA * 28629 + RCD * 3593 =$ (If RIRS > 132 MPa, then RIRS = 132)					11,2 kPa

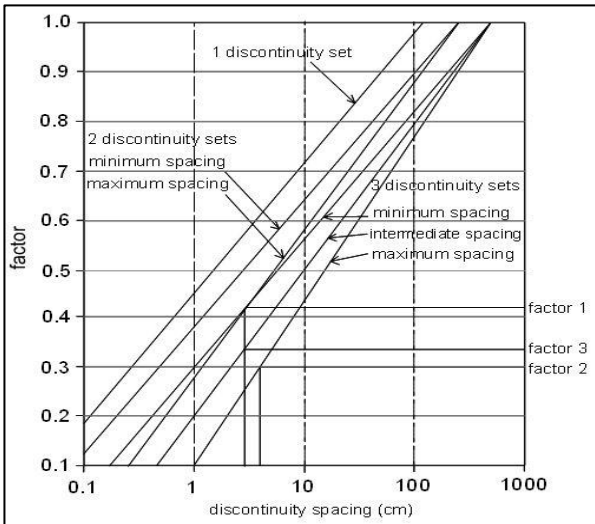
STOP 11 - STABILITY TABLE							
Method of Excavation (SME)			Weathering (SWE)				
Natural/hand-made		1,00	Unweathered		1,00		
Pneumatic hammer excavation*		0,76	Slightly		0,95		
Pre-splitting/smooth wall blasting		0,99	Moderately*		0,90		
Conventional blasting with result:			Highly		0,62		
Good		0,77	Completely		0,35		
Open discontinuities		0,75	Slope geometry features				
Dislodged blocks		0,72	Slope dip direction (degrees)		260		
Fractured intact rock		0,67	Slope dip (degrees)		60		
Crushed intact rock		0,62	Height (m)		6		
Orientation-independent stability							
Intact Rock Strength (SIRS)							
SIRS = RIRS (from reference rock mass) x SWE (weathering slope) =			6,667 x 0,90		6 MPa		
Discontinuity spacing (SSPA)							
SSPA = RSPA x SWE x SME			0,300x0,90x0,76		0,205		
Condition of discontinuity (SCD)							
SCD = RCD x SWE =			0,549 x 0,90		0,494		
Slope unit friction and cohesion (SFRI & SCOH)							
SFRI = SIRS * 0,2417 + SSPA * 52,12 + SCD * 5,779 =					15,00°		
(If RIRS > 132 Mpa, then RIRS =132)							
SCOH = SIRS * 94,27 + SSPA * 28629 + SCD * 3593 =					8,2 kPa		
(If RIRS > 132 Mpa, then RIRS =132)							
If SFRI < slope dip, maximum possible height (Hmax):					3,8 m		
Hmax = (1,6x10^-4 x SCOH) x sin(slopedip) x cos(SFRI) / (1 - cos(slopedip - SFRI)) =							
Ratios	SFRI / Slope dip				0,250		
	Hmax / Hslope				0,6333333		
Stable probability: if SFRI > slope dip, probability = % 100, else use the figure for orientation-independent stability:					<5%		
Orientation-dependent stability							
Discontinuities		B	J1	J2			
Dip direction (degrees)		336	150	215			
Dip (degrees)		36	60	87			
With, Against, Vertical or Equal		W	A	V			
AP (degrees)		10	-30	85			
RTC		0,505	0,505	0,505			
STC = RTC x sqrt(1,452 - 1,220 x e^(-SWE))		0,494	0,494	0,494			
Stable probability:	Sliding	>95%	100%	100%			
	Toppling	100%	100%	100%			
Stable probability:		>95%					
Determine orientation stability:							
Calculate AP: β = discontinuity dip, σ = slope dip direction, τ= discontinuity dip direction, δ = σ - τ, AP= arctan(cosδ x tanβ)							
Stability		Sliding	Toppling	Stability		Sliding	Toppling
AP>84° or AP<-84°	Vertical	100%	100%	AP<0° and (-90° < AP+slope dip)<0°	Against	100%	100%
(slope dip + 5°) < AP < 84°	With	100%	100%	AP<0° and (-90° < AP+slope dip)>0°	Against	100%	Use graph toppling
(slope dip - 5°) < AP < (slope dip + 5°)	Equal	100%	100%				
0°< AP < (slope dip - 5°)	With	Use graph sliding	100%				
Slope final stable probability		<5%					

STOP 12 - DATA COLLECTION TABLE									
Excavation Method (ME)			Intact Rock Strength (IRS)						
Natural/hand-made	1,00	<1.25 MPa			Crumbles in hand				
Pneumatic hammer excavation*	0,76	1.25-5 MPa			Thin slabs break easy in hand				
Pre-splitting/smooth wall blasting	0,99	5-12.5 MPa			Thin slabs broken by heavy hand pressure				
Conventional blasting with result:		12.5-50 MPa			Lumps broken by light hammer blows *				
Good	0,77	50-100 MPa			Lumps broken by heavy hammer blows				
Open discontinuities	0,75	100-200 MPa			Lumps only chip by heavy hammer blows				
Dislodged blocks	0,72	>200 MPa			Rocks ring on hammer blows				
Fractured intact rock	0,67	Weathering degree (WE)			Unweathered		1,00		
Crushed intact rock	0,62				Slightly		0,95		
Lithology					Moderately		0,90		
80% Sandstone / 20% Mudstone					Highly*		0,62		
					Completely		0,35		
Discontinuities (B: Bedding; J: Joint)				B	J1	J2	Slope		
Dip direction (degrees)				180	5	298	Dip direction (degrees)	240	
Dip (degrees)				35	55	66	Dip (degrees)	50	
Spacing (DS) (cm)				10	15	20	Slope height (m)	6	
Condition of discontinuities						Slope Stability			
Large scale roughness (RL)	Wavy		1,00				Stable	1	
	Slightly wavy		0,95				Small problem*	2	
	Curved		0,85		X		Large problem	3	
	Slightly curved		0,80	X		X	Notes: 1) For infill "gouge>irregularities" and "flowing material" small scale roughness= 0,55 2) If roughness is anisotropic (e.g. Ripple marks, striation, etc.) roughness should be assessed perpendicular and parallel to the roughness and directions noted on this form 3) Non-fitting of discontinuities should be marked in roughness columns.		
	Straight		0,75						
Small scale roughness (RS)	Rough stepped		0,95		X	X			
	Smooth stepped		0,90	X					
	Polished stepped		0,85						
	Rough undulating		0,80						
	Smooth undulating		0,75						
	Polished undulating		0,70						
	Rough planar		0,65						
	Smooth planar		0,60						
Infill material (IM)	Polished planar		0,55						
	Cemented / cemented infill		1,07						
	No infill - surface staining		1,00						
	Non-softening & sheared material	Coarse	0,95						
		Medium	0,90						
		Fine	0,85						
	Soft sheared material	Coarse	0,75						
		Medium	0,65	X	X	X			
		Fine	0,55						
	Gouge < irregularities		0,42						
Gouge > irregularities		0,17							
Flowing material		0,05							
Karst (KA)	None		1,00	X	X	X			
	Karst		0,92						

STOP 12 - REFERENCE ROCK TABLE						
Intact Rock Strength (RIRS)						
RIRS = IRS / WE = 6 / 0,62					9,677	
Discontinuity Spacing (SPA)						
Discontinuities	B	J1	J2	SPA = factor 1 x factor 2 x factor 3	0,346	
Dip direction (degrees)	180	5	298			
Dip (degrees)	35	55	66			
Spacing (m)	10	15	20			
The spacing parameter (SPA) is calculated based on the three discontinuity sets with the smallest spacings in following figure:				SPA = 0,56 x 0,55 x 0,53 = 0,163		
				Corrected for weathering and method of excavation:		
				RSPA = SPA / (WE x ME)		
				RSPA = 0,163 / (0,62 x 0,76)		
Condition of discontinuities						
Discontinuities	B	J1	J2	RTC is the discontinuity condition of a single discontinuity (set) in the reference rock mass corrected for discontinuity weathering. $RTC = TC / \sqrt{1,452 - 1,220 * e^{(-WE)}}$		
Large scale roughness (Rl)	0,80	0,85	0,80			
Small scale roughness (Rs)	0,90	0,95	0,95			
Infill material (Im)	0,65	0,65	0,65			
Karst (Ka)	1,00	1,00	1,00			
TC = Rl x Rs x Im x Ka	0,468	0,525	0,494			
RTC	0,479	0,537	0,505			
Weighted by spacing: $CD = \frac{\frac{TC_1}{DS_1} + \frac{TC_2}{DS_2} + \frac{TC_3}{DS_3}}{\frac{1}{DS_1} + \frac{1}{DS_2} + \frac{1}{DS_3}} =$					0,492	
Corrected by weathering: RCD (with a maximum of 1.0165) = CD/WE =				0,492 / 0,62 =	0,794	
Reference unit friction and cohesion (RFRI & FCOH)						
$\phi(RRM) = RIRS * 0,2417 + RSPA * 52,12 + RCD * 5,779 =$ (If RIRS > 132 MPa, then RIRS = 132)					24,95°	
coh(RRM) = RIRS * 94,27 + RSPA * 28629 + RCD * 3593 = (If RIRS > 132 MPa, then RIRS = 132)					13,7 kPa	

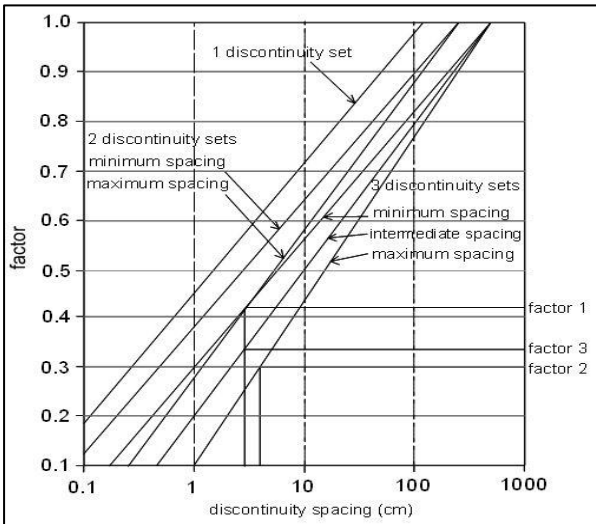
STOP 12 - STABILITY TABLE							
Method of Excavation (SME)			Weathering (SWE)				
Natural/hand-made		1,00	Unweathered		1,00		
Pneumatic hammer excavation*		0,76	Slightly		0,95		
Pre-splitting/smooth wall blasting		0,99	Moderately		0,90		
Conventional blasting with result:			Highly*		0,62		
Good		0,77	Completely		0,35		
Open discontinuities		0,75	Slope geometry features				
Dislodged blocks		0,72	Slope dip direction (degrees)		240		
Fractured intact rock		0,67	Slope dip (degrees)		50		
Crushed intact rock		0,62	Height (m)		6		
Orientation-independent stability							
Intact Rock Strength (SIRS)							
SIRS = RIRS (from reference rock mass) x SWE (weathering slope) =			9,677 x 0,62	6 MPa			
Discontinuity spacing (SSPA)							
SSPA = RSPA x SWE x SME			0,346x0,62x0,76	0,163			
Condition of discontinuity (SCD)							
SCD = RCD x SWE =			0,794 x 0,62	0,492			
Slope unit friction and cohesion (SFRI & SCOH)							
SFRI = SIRS * 0,2417 + SSPA * 52,12 + SCD * 5,779 =					12,79°		
(If RIRS > 132 Mpa, then RIRS =132)							
SCOH = SIRS * 94,27 + SSPA * 28629 + SCD * 3593 =					7,0 kPa		
(If RIRS > 132 Mpa, then RIRS =132)							
If SFRI < slope dip, maximum possible height (Hmax):					4,1 m		
Hmax = (1,6x10 <sup>-4</sup> x SCOH) x sin(slopedip) x cos(SFRI) / (1 - cos(slopedip - SFRI)) =							
Ratios	SFRI / Slope dip				0,256		
	Hmax / Hslope				0,683		
Stable probability: if SFRI > slope dip, probability = % 100, else use the figure for orientation-independent stability:					<5%		
Orientation-dependent stability							
Discontinuities		B	J1	J2			
Dip direction (degrees)		180	5	298			
Dip (degrees)		35	55	66			
With, Against, Vertical or Equal		W	A	E			
AP (degrees)		19	-39	50			
RTC		0,479	0,537	0,505			
STC = RTC x sqrt(1,452 - 1,220 x e <sup>(-SWE)</sup> )		0,468	0,525	0,494			
Stable probability:	Sliding	>95%	100%	100%			
	Toppling	100%	100%	100%			
Stable probability:		>95%					
Determine orientation stability:							
Calculate AP: β = discontinuity dip, σ = slope dip direction, τ= discontinuity dip direction, δ = σ - τ, AP= arctan(cosδ x tanβ)							
Stability		Sliding	Toppling	Stability		Sliding	Toppling
AP>84°or AP<-84°	Vertical	100%	100%	AP<0° and (-90°<AP+slope dip)<0°	Against	100%	100%
(slope dip + 5°) < AP < 84°	With	100%	100%	AP<0° and (-90°<AP+slope dip)>0°	Against	100%	Use graph toppling
(slope dip - 5°) < AP < (slope dip + 5°	Equal	100%	100%				
0°< AP < (slope dip - 5°	With	Use graph sliding	100%				
Slope final stable probability		<5%					

STOP 13 - DATA COLLECTION TABLE							
Excavation Method (ME)			Intact Rock Strength (IRS)				
Natural/hand-made	1,00		<1.25 MPa		Crumbles in hand		
Pneumatic hammer excavation*	0,76		1.25-5 MPa		Thin slabs break easy in hand		
Pre-splitting/smooth wall blasting	0,99		5-12.5 MPa		Thin slabs broken by heavy hand pressure		
Conventional blasting with result:			12.5-50 MPa		Lumps broken by light hammer blows*		
Good	0,77		50-100 MPa		Lumps broken by heavy hammer blows		
Open discontinuities	0,75		100-200 MPa		Lumps only chip by heavy hammer blows		
Dislodged blocks	0,72		>200 MPa		Rocks ring on hammer blows		
Fractured intact rock	0,67		Weathering degree (WE)		Unweathered		1,00
Crushed intact rock	0,62				Slightly		0,95
Lithology					Moderately*		0,90
70% Sandstone / 30% Mudstone					Highly		0,62
					Completely		0,35
Discontinuities (B: Bedding; J: Joint)			B	J2	J3	Slope	
Dip direction (degrees)			180	260	310	Dip direction (degrees)	225
Dip (degrees)			45	84	50	Dip (degrees)	70
Spacing (DS) (cm)			15	10	20	Slope height (m)	8
Condition of discontinuities					Slope Stability		
Large scale roughness (RL)	Wavy	1,00				Stable	1
	Slightly wavy	0,95		X	X	Small problem*	2
	Curved	0,85	X			Large problem	3
	Slightly curved	0,80				Notes: 1) For infill "gouge">irregularities" and "flowing material" small scale roughness= 0,55 2) If roughness is anisotropic (e.g. Ripple marks, striation, etc.) roughness should be assessed perpendicular and parallel to the roughness and directions noted on this form 3) Non-fitting of discontinuities should be marked in roughness columns.	
	Straight	0,75					
Small scale roughness (RS)	Rough stepped	0,95					
	Smooth stepped	0,90					
	Polished stepped	0,85					
	Rough undulating	0,80					
	Smooth undulating	0,75	X	X	X		
	Polished undulating	0,70					
	Rough planar	0,65					
	Smooth planar	0,60					
	Polished planar	0,55					
Infill material (IM)	Cemented / cemented infill		1,07				
	No infill - surface staining		1,00				
	Non-softening & sheared material	Coarse	0,95				
		Medium	0,90				
		Fine	0,85				
	Soft sheared material	Coarse	0,75				
		Medium	0,65	X	X		
		Fine	0,55				
	Gouge < irregularities		0,42				
	Gouge > irregularities		0,17				
	Flowing material		0,05				
Karst (KA)	None		1,00	X	X	X	
	Karst		0,92				

STOP 13 - REFERENCE ROCK TABLE					
Intact Rock Strength (RIRS)					
RIRS = IRS / WE = 7 / 0,90					7,778
Discontinuity Spacing (SPA)					
Discontinuities	B	J1	J2	SPA = factor 1 x factor 2 x factor 3	
Dip direction (degrees)	180	260	310		
Dip (degrees)	45	84	50		
Spacing (m)	15	10	20		
The spacing parameter (SPA) is calculated based on the three discontinuity sets with the smallest spacings in following figure:				SPA = 0,55 x 0,54 x 0,53 = 0,119	0,230
				Corrected for weathering and method of excavation:	
				RSPA = SPA / (WE x ME)	
				RSPA = 0,157 / (0,90 x 0,76)	
Condition of discontinuities					
Discontinuities	B	J1	J2	RTC is the discontinuity condition of a single discontinuity (set) in the reference rock mass corrected for discontinuity weathering. $RTC = TC / \sqrt{1,452 - 1,220 * e^{(-WE)}}$	
Large scale roughness (Rl)	0,85	0,95	0,95		
Small scale roughness (Rs)	0,75	0,75	0,75		
Infill material (Im)	0,65	0,65	0,65		
Karst (Ka)	1,00	1,00	1,00		
TC = Rl x Rs x Im x Ka	0,414	0,463	0,463		
RTC	0,424	0,474	0,474		
Weighted by spacing: $CD = \frac{\frac{TC_1}{DS_1} + \frac{TC_2}{DS_2} + \frac{TC_3}{DS_3}}{\frac{1}{DS_1} + \frac{1}{DS_2} + \frac{1}{DS_3}} =$				0,448	
Corrected by weathering: RCD (with a maximum of 1.0165) = CD/WE =				0,448 / 0,90 =	0,498
Reference unit friction and cohesion (RFRI & FCOH)					
$\phi(RRM) = RIRS * 0,2417 + RSPA * 52,12 + RCD * 5,779 =$ (If RIRS > 132 MPa, then RIRS = 132)					16,72°
$coh(RRM) = RIRS * 94,27 + RSPA * 28629 + RCD * 3593 =$ (If RIRS > 132 MPa, then RIRS = 132)					9,1 kPa

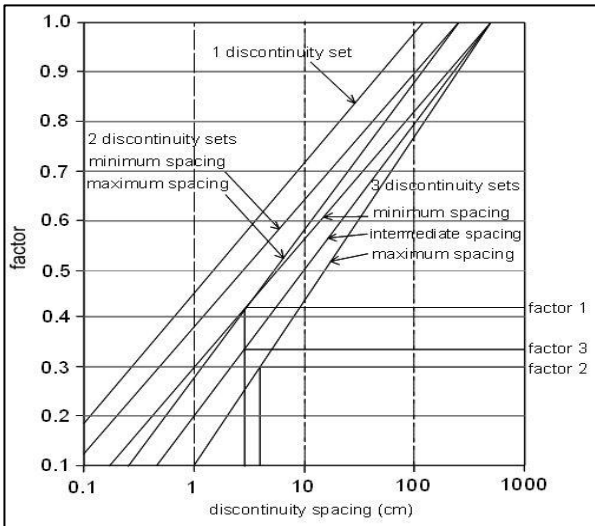
STOP 13 - STABILITY TABLE							
Method of Excavation (SME)			Weathering (SWE)				
Natural/hand-made		1,00	Unweathered		1,00		
Pneumatic hammer excavation*		0,76	Slightly		0,95		
Pre-splitting/smooth wall blasting		0,99	Moderately*		0,90		
Conventional blasting with result:			Highly		0,62		
Good		0,77	Completely		0,35		
Open discontinuities		0,75	Slope geometry features				
Dislodged blocks		0,72	Slope dip direction (degrees)		225		
Fractured intact rock		0,67	Slope dip (degrees)		70		
Crushed intact rock		0,62	Height (m)		8		
Orientation-independent stability							
Intact Rock Strength (SIRS)							
SIRS = RIRS (from reference rock mass) x SWE (weathering slope) =			7,778 x 0,90	7 MPa			
Discontinuity spacing (SSPA)							
SSPA = RSPA x SWE x SME			0,230x0,90x0,76	0,157			
Condition of discontinuity (SCD)							
SCD = RCD x SWE =			0,498 x 0,90	0,448			
Slope unit friction and cohesion (SFRI & SCOH)							
SFRI = SIRS * 0,2417 + SSPA * 52,12 + SCD * 5,779 =					12,46°		
(If RIRS > 132 Mpa, then RIRS =132)							
SCOH = SIRS * 94,27 + SSPA * 28629 + SCD * 3593 =					6,8 kPa		
(If RIRS > 132 Mpa, then RIRS =132)							
If SFRI < slope dip, maximum possible height (Hmax):							
Hmax = (1,6x10^-4 x SCOH) x sin(slopedip) x cos(SFRI) / (1 - cos(slopedip - SFRI)) =					2,2 m		
Ratios	SFRI / Slope dip				0,178		
	Hmax/ Hslope				0,275		
Stable probability: if SFRI > slope dip, probability = % 100, else use the figure for orientation-independent stability:					<5%		
Orientation-dependent stability							
Discontinuities		B	J1	J2			
Dip direction (degrees)		180	260	310			
Dip (degrees)		45	84	50			
With, Against, Vertical or Equal		W	W	W			
AP (degrees)		35	83	6			
RTC		0,424	0,474	0,474			
STC = RTC x sqrt(1,452 - 1,220 x e^(-SWE))		0,414	0,463	0,463			
Stable probability:	Sliding	80%	100%	>95%			
	Toppling	100%	100%	100%			
Stable probability:		80%					
Determine orientation stability:							
Calculate AP: β = discontinuity dip, σ = slope dip direction, τ= discontinuity dip direction, δ = σ - τ, AP= arctan(cosδ x tanβ)							
Stability		Sliding	Toppling	Stability		Sliding	Toppling
AP>84°or AP<-84°	Vertical	100%	100%	AP<0° and (-90° AP+slope dip)<0°	Against	100%	100%
(slope dip + 5°) < AP < 84°	With	100%	100%	AP<0° and (-90° AP+slope dip)>0°	Against	100%	Use graph toppling
(slope dip - 5°) < AP < (slope dip + 5°	Equal	100%	100%				
0°< AP < (slope dip - 5°	With	Use graph sliding	100%				
Slope final stable probability		<5%					

STOP 14 -DATA COLLECTION TABLE									
Excavation Method (ME)				Intact Rock Strength (IRS)					
Natural/hand-made		1,00		<1.25 MPa			Crumbles in hand		
Pneumatic hammer excavation*		0,76		1.25-5 MPa			Thin slabs break easy in hand		
Pre-splitting/smooth wall blasting		0,99		5-12.5 MPa			Thin slabs broken by heavy hand pressure		
Conventional blasting with result:				12.5-50 MPa			Lumps broken by light hammer blows*		
Good		0,77		50-100 MPa			Lumps broken by heavy hammer blows		
Open discontinuities		0,75		100-200 MPa			Lumps only chip by heavy hammer blows		
Dislodged blocks		0,72		>200 MPa			Rocks ring on hammer blows		
Fractured intact rock		0,67		Weathering degree (WE)			Unweathered		1,00
Crushed intact rock		0,62					Slightly		0,95
Lithology			Moderately*				0,90		
80% Sandstone / 20% Mudstone			Highly				0,62		
			Completely				0,35		
Discontinuities (B: Bedding; J: Joint)				B	J2	J3	Slope		
Dip direction (degrees)				130	35	215	Dip direction (degrees)	215	
Dip (degrees)				75	80	84	Dip (degrees)	50	
Spacing (DS) (cm)				20	15	10	Slope height (m)	10	
Condition of discontinuities							Slope Stability		
Large scale roughness (RL)	Wavy		1,00				Stable	1	
	Slightly wavy		0,95				Small problem*	2	
	Curved		0,85				Large problem	3	
	Slightly curved		0,80	X	X	X	Notes: 1) For infill "gouge>irregularities" and "flowing material" small scale roughness= 0,55 2) If roughness is anisotropic (e.g. Ripple marks, striation, etc.) roughness should be assessed perpendicular and parallel to the roughness and directions noted on this form 3) Non-fitting of discontinuities should be marked in roughness columns.		
	Straight		0,75						
Small scale roughness (RS)	Rough stepped		0,95						
	Smooth stepped		0,90						
	Polished stepped		0,85						
	Rough undulating		0,80						
	Smooth undulating		0,75						
	Polished undulating		0,70	X	X	X			
	Rough planar		0,65						
	Smooth planar		0,60						
	Polished planar		0,55						
Infill material (IM)	Cemented / cemented infill		1,07						
	No infill - surface staining		1,00						
	Non-softening & sheared material	Coarse	0,95						
		Medium	0,90						
		Fine	0,85						
	Soft sheared material	Coarse	0,75						
		Medium	0,65	X	X	X			
		Fine	0,55						
	Gouge < irregularities		0,42						
	Gouge > irregularities		0,17						
Flowing material		0,05							
Karst (KA)	None		1,00	X	X	X			
	Karst		0,92						

STOP 14 - REFERENCE ROCK TABLE					
Intact Rock Strength (RIRS)					
RIRS = IRS / WE = 12 / 0,90					13,333
Discontinuity Spacing (SPA)					
Discontinuities	B	J1	J2	SPA = factor 1 x factor 2 x factor 3	
Dip direction (degrees)	130	35	215		
Dip (degrees)	75	80	84		
Spacing (m)	20	15	10		
The spacing parameter (SPA) is calculated based on the three discontinuity sets with the smallest spacings in following figure:				SPA = 0,56 x 0,55 x 0,53 = 0,163	0,238
				Corrected for weathering and method of excavation:	
				RSPA = SPA / (WE x ME)	
				RSPA = 0,163 / (0,90 x 0,76)	
Condition of discontinuities					
Discontinuities	B	J1	J2	RTC is the discontinuity condition of a single discontinuity (set) in the reference rock mass corrected for discontinuity weathering. $RTC = TC / \sqrt{1,452 - 1,220 * e^{(-WE)}}$	
Large scale roughness (Rl)	0,80	0,80	0,80		
Small scale roughness (Rs)	0,70	0,70	0,70		
Infill material (Im)	0,65	0,65	0,65		
Karst (Ka)	1,00	1,00	1,00		
TC = Rl x Rs x Im x Ka	0,364	0,364	0,364		
RTC	0,372	0,372	0,372		
Weighted by spacing: $CD = \frac{\frac{TC_1}{DS_1} + \frac{TC_2}{DS_2} + \frac{TC_3}{DS_3}}{\frac{1}{DS_1} + \frac{1}{DS_2} + \frac{1}{DS_3}} =$					0,364
Corrected by weathering: RCD (with a maximum of 1.0165) = CD/WE =				0,364 / 0,90 =	0,404
Reference unit friction and cohesion (RFRI & FCOH)					
$\phi(RRM) = RIRS * 0,2417 + RSPA * 52,12 + RCD * 5,779 =$ (If RIRS > 132 MPa, then RIRS = 132)					17,98°
coh(RRM) = RIRS * 94,27 + RSPA * 28629 + RCD * 3593 = (If RIRS > 132 MPa, then RIRS = 132)					9,5 kPa

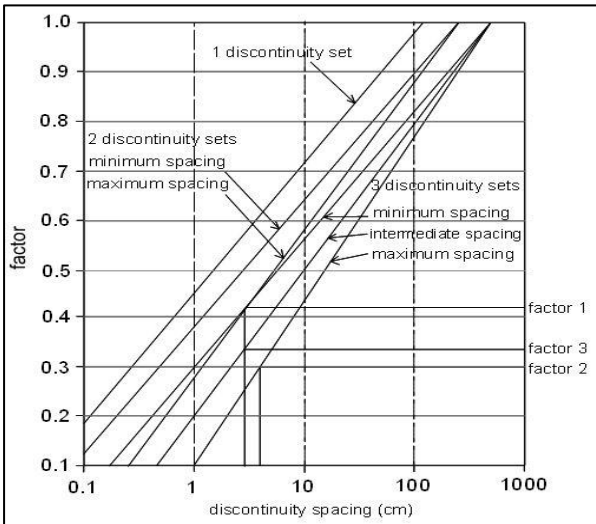
STOP 14 - STABILITY TABLE							
Method of Excavation (SME)			Weathering (SWE)				
Natural/hand-made		1,00	Unweathered		1,00		
Pneumatic hammer excavation*		0,76	Slightly		0,95		
Pre-splitting/smooth wall blasting		0,99	Moderately*		0,90		
Conventional blasting with result:			Highly		0,62		
Good		0,77	Completely		0,35		
Open discontinuities		0,75	Slope geometry features				
Dislodged blocks		0,72	Slope dip direction (degrees)		215		
Fractured intact rock		0,67	Slope dip (degrees)		50		
Crushed intact rock		0,62	Height (m)		10		
Orientation-independent stability							
Intact Rock Strength (SIRS)							
SIRS = RIRS (from reference rock mass) x SWE (weathering slope) =			13,333 x 0,90	12 MPa			
Discontinuity spacing (SSPA)							
SSPA = RSPA x SWE x SME			0,238x0,90x0,76	0,163			
Condition of discontinuity (SCD)							
SCD = RCD x SWE =			0,404 x 0,90	0,364			
Slope unit friction and cohesion (SFRI & SCOH)							
SFRI = SIRS * 0,2417 + SSPA * 52,12 + SCD * 5,779 = (If RIRS > 132 Mpa, then RIRS =132)					13,50°		
SCOH = SIRS * 94,27 + SSPA * 28629 + SCD * 3593 = (If RIRS > 132 Mpa, then RIRS =132)					7,1 kPa		
If SFRI < slope dip, maximum possible height (Hmax): Hmax = (1,6x10^-4 x SCOH) x sin(slopedip) x cos(SFRI) / (1 - cos(slopedip - SFRI)) =					4,3 m		
Ratios	SFRI / Slope dip				0,270		
	Hmax/ Hslope				0,43		
Stable probability: if SFRI > slope dip, probability = % 100, else use the figure for orientation-independent stability:					<5%		
Orientation-dependent stability							
Discontinuities		B	J1	J2			
Dip direction (degrees)		130	35	215			
Dip (degrees)		75	80	84			
With, Against, Vertical or Equal		W	A	V			
AP (degrees)		18	-6	85			
RTC		0,372	0,372	0,372			
STC = RTC x sqrt(1,452 - 1,220 x e^(-SWE))		0,364	0,364	0,364			
Stable probability:	Sliding	>95%	100%	100%			
	Toppling	100%	100%	100%			
Stable probability:		>95%					
Determine orientation stability:							
Calculate AP: β = discontinuity dip, σ = slope dip direction, τ= discontinuity dip direction, δ = σ - τ, AP= arctan(cosδ x tanβ)							
Stability		Sliding	Toppling	Stability		Sliding	Toppling
AP>84°or AP<-84°	Vertical	100%	100%	AP<0° and (-90° AP+slope dip)<0°	Against	100%	100%
(slope dip + 5°) < AP < 84°	With	100%	100%	AP<0° and (-90° AP+slope dip)>0°	Against	100%	Use graph toppling
(slope dip - 5°) < AP < (slope dip + 5°	Equal	100%	100%				
0° < AP < (slope dip - 5°	With	Use graph sliding	100%				
Slope final stable probability		<5%					

STOP 15 - DATA COLLECTION TABLE							
Excavation Method (ME)			Intact Rock Strength (IRS)				
Natural/hand-made	1,00		<1.25 MPa	Crumbles in hand			
Pneumatic hammer excavation*	0,76		1.25-5 MPa	Thin slabs break easy in hand			
Pre-splitting/smooth wall blasting	0,99		5-12.5 MPa	Thin slabs broken by heavy hand pressure			
Conventional blasting with result:			12.5-50 MPa	Lumps broken by light hammer blows*			
Good	0,77		50-100 MPa	Lumps broken by heavy hammer blows			
Open discontinuities	0,75		100-200 MPa	Lumps only chip by heavy hammer blows			
Dislodged blocks	0,72		>200 MPa	Rocks ring on hammer blows			
Fractured intact rock	0,67		Weathering degree (WE)	Unweathered		1,00	
Crushed intact rock	0,62			Slightly		0,95	
Lithology				Moderately*		0,90	
80% Sandstone / 20% Mudstone				Highly		0,62	
				Completely		0,35	
Discontinuities (B: Bedding; J: Joint)			B	J2	J3	Slope	
Dip direction (degrees)			330	145	255	Dip direction (degrees)	195
Dip (degrees)			55	49	78	Dip (degrees)	50
Spacing (DS) (cm)			30	50	40	Slope height (m)	15
Condition of discontinuities						Slope Stability	
Large scale roughness (RL)	Wavy	1,00				Stable	1
	Slightly wavy	0,95				Small problem*	2
	Curved	0,85				Large problem	3
	Slightly curved	0,80				Notes: 1) For infill "gouge">irregularities" and "flowing material" small scale roughness= 0,55 2) If roughness is anisotropic (e.g. Ripple marks, striation, etc.) roughness should be assessed perpendicular and parallel to the roughness and directions noted on this form 3) Non-fitting of discontinuities should be marked in roughness columns.	
	Straight	0,75	X	X	X		
Small scale roughness (RS)	Rough stepped	0,95					
	Smooth stepped	0,90					
	Polished stepped	0,85					
	Rough undulating	0,80					
	Smooth undulating	0,75					
	Polished undulating	0,70					
	Rough planar	0,65					
	Smooth planar	0,60	X	X	X		
	Polished planar	0,55					
Infill material (IM)	Cemented / cemented infill		1,07				
	No infill - surface staining		1,00				
	Non-softening & sheared material	Coarse	0,95				
		Medium	0,90				
		Fine	0,85				
	Soft sheared material	Coarse	0,75				
		Medium	0,65	X	X		
		Fine	0,55				
	Gouge < irregularities		0,42				
	Gouge > irregularities		0,17				
	Flowing material		0,05				
Karst (KA)	None		1,00	X	X	X	
	Karst		0,92				

STOP 15 - REFERENCE ROCK TABLE					
Intact Rock Strength (RIRS)					
RIRS = IRS / WE = 21 / 0,90					23,333
Discontinuity Spacing (SPA)					
Discontinuities	B	J1	J2	SPA = factor 1 x factor 2 x factor 3	
Dip direction (degrees)	330	145	255		
Dip (degrees)	55	49	78		
Spacing (m)	30	50	40		
The spacing parameter (SPA) is calculated based on the three discontinuity sets with the smallest spacings in following figure:				SPA = 0,69 x 0,68 x 0,67 = 0,314	0,453
				Corrected for weathering and method of excavation:	
				RSPA = SPA / (WE x ME)	
				RSPA = 0,314 / (0,90 x 0,76)	
Condition of discontinuities					
Discontinuities	B	J1	J2	RTC is the discontinuity condition of a single discontinuity (set) in the reference rock mass corrected for discontinuity weathering. $RTC = TC / \sqrt{1,452 - 1,220 * e^{(-WE)}}$	
Large scale roughness (Rl)	0,75	0,75	0,75		
Small scale roughness (Rs)	0,60	0,60	0,60		
Infill material (Im)	0,65	0,65	0,65		
Karst (Ka)	1,00	1,00	1,00		
TC = Rl x Rs x Im x Ka	0,293	0,293	0,293		
RTC	0,299	0,299	0,299		
Weighted by spacing: $CD = \frac{\frac{TC_1}{DS_1} + \frac{TC_2}{DS_2} + \frac{TC_3}{DS_3}}{\frac{1}{DS_1} + \frac{1}{DS_2} + \frac{1}{DS_3}} =$					0,293
Corrected by weathering: RCD (with a maximum of 1.0165) = CD/WE =				0,293 / 0,90 =	0,326
Reference unit friction and cohesion (RFRI & FCOH)					
$\phi(RRM) = RIRS * 0,2417 + RSPA * 52,12 + RCD * 5,779 =$ (If RIRS > 132 MPa, then RIRS = 132)					31,14°
$coh(RRM) = RIRS * 94,27 + RSPA * 28629 + RCD * 3593 =$ (If RIRS > 132 MPa, then RIRS = 132)					16,3 kPa

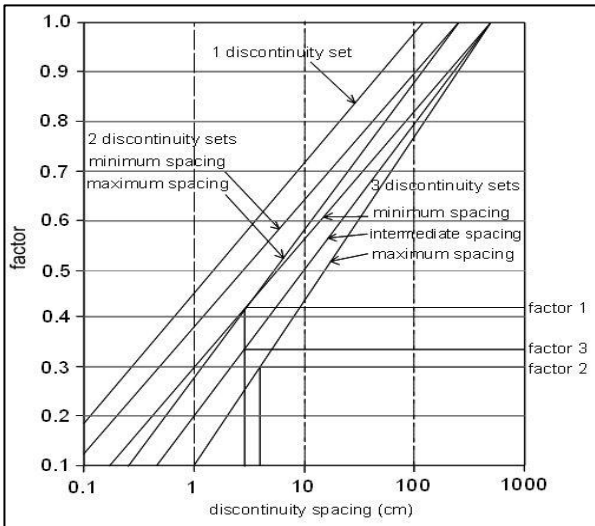
STOP 15 - STABILITY TABLE						
Method of Excavation (SME)			Weathering (SWE)			
Natural/hand-made		1,00	Unweathered		1,00	
Pneumatic hammer excavation*		0,76	Slightly		0,95	
Pre-splitting/smooth wall blasting		0,99	Moderately*		0,90	
Conventional blasting with result:			Highly		0,62	
Good		0,77	Completely		0,35	
Open discontinuities		0,75	Slope geometry features			
Dislodged blocks		0,72	Slope dip direction (degrees)		195	
Fractured intact rock		0,67	Slope dip (degrees)		50	
Crushed intact rock		0,62	Height (m)		15	
Orientation-independent stability						
Intact Rock Strength (SIRS)						
SIRS = RIRS (from reference rock mass) x SWE (weathering slope) =			23,333 x 0,90	21 MPa		
Discontinuity spacing (SSPA)						
SSPA = RSPA x SWE x SME			0,453x0,90x0,76	0,310		
Condition of discontinuity (SCD)						
SCD = RCD x SWE =			0,326 x 0,90	0,293		
Slope unit friction and cohesion (SFRI & SCOH)						
SFRI = SIRS * 0,2417 + SSPA * 52,12 + SCD * 5,779 =					22,93°	
(If RIRS > 132 Mpa, then RIRS =132)						
SCOH = SIRS * 94,27 + SSPA * 28629 + SCD * 3593 =					11,9 kPa	
(If RIRS > 132 Mpa, then RIRS =132)						
If SFRI < slope dip, maximum possible height (Hmax):						
Hmax = (1,6x10^-4 x SCOH) x sin(slopedip) x cos(SFRI) / (1 - cos(slopedip - SFRI)) =					12,3 m	
Ratios	SFRI / Slope dip				0,459	
	Hmax / Hslope				0,820	
Stable probability: if SFRI > slope dip, probability = % 100, else use the figure for orientation-independent stability:					20%	
Orientation-dependent stability						
Discontinuities		B	J1	J2		
Dip direction (degrees)		330	145	255		
Dip (degrees)		55	49	78		
With, Against, Vertical or Equal		A	W	W		
AP (degrees)		-45	36	67		
RTC		0,299	0,299	0,299		
STC = RTC x sqrt(1,452 - 1,220 x e^(-SWE))		0,293	0,293	0,293		
Stable probability:	Sliding	100%	15%	100%		
	Toppling	>95%	100%	100%		
Stable probability:		15%				
Determine orientation stability:						
Calculate AP: β = discontinuity dip, σ = slope dip direction, τ= discontinuity dip direction, δ = σ - τ, AP= arctan(cosδ x tanβ)						
Stability		Sliding	Toppling	Stability	Sliding	Toppling
AP>84°or AP<-84°	Vertical	100%	100%	AP<0° and (-90- AP+slope dip)<0°	Against	100%
(slope dip + 5°) < AP < 84°	With	100%	100%	AP<0° and (-90- AP+slope dip)>0°	Against	100%
(slope dip - 5°) < AP < (slope dip + 5°)	Equal	100%	100%			
0°< AP < (slope dip - 5°)	With	Use graph sliding	100%			
Slope final stable probability		15%				

STOP 16 - DATA COLLECTION TABLE								
Excavation Method (ME)			Intact Rock Strength (IRS)					
Natural/hand-made	1,00	<1.25 MPa			Crumbles in hand			
Pneumatic hammer excavation*	0,76	1.25-5 MPa			Thin slabs break easy in hand			
Pre-splitting/smooth wall blasting	0,99	5-12.5 MPa			Thin slabs broken by heavy hand pressure			
Conventional blasting with result:		12.5-50 MPa			Lumps broken by light hammer blows*			
Good	0,77	50-100 MPa			Lumps broken by heavy hammer blows			
Open discontinuities	0,75	100-200 MPa			Lumps only chip by heavy hammer blows			
Dislodged blocks	0,72	>200 MPa			Rocks ring on hammer blows			
Fractured intact rock	0,67	Weathering degree (WE)			Unweathered		1,00	
Crushed intact rock	0,62				Slightly		0,95	
Lithology					Moderately*		0,90	
Sandstone					Highly		0,62	
					Completely		0,35	
Discontinuities (B: Bedding; J: Joint)				B	J2	J3	Slope	
Dip direction (degrees)				350	80	165	Dip direction (degrees)	200
Dip (degrees)				65	60	50	Dip (degrees)	55
Spacing (DS) (cm)				20	40	15	Slope height (m)	6
Condition of discontinuities						Slope Stability		
Large scale roughness (RL)	Wavy		1,00				Stable	1
	Slightly wavy		0,95				Small problem*	2
	Curved		0,85				Large problem	3
	Slightly curved		0,80	X	X	X	Notes: 1) For infill "gouge>irregularities" and "flowing material" small scale roughness= 0,55 2) If roughness is anisotropic (e.g. Ripple marks, striation, etc.) roughness should be assessed perpendicular and parallel to the roughness and directions noted on this form 3) Non-fitting of discontinuities should be marked in roughness columns.	
	Straight		0,75					
Small scale roughness (RS)	Rough stepped		0,95					
	Smooth stepped		0,90					
	Polished stepped		0,85					
	Rough undulating		0,80					
	Smooth undulating		0,75	X	X	X		
	Polished undulating		0,70					
	Rough planar		0,65					
	Smooth planar		0,60					
	Polished planar		0,55					
Infill material (IM)	Cemented / cemented infill		1,07					
	No infill - surface staining		1,00					
	Non-softening & sheared material	Coarse	0,95					
		Medium	0,90					
		Fine	0,85					
	Soft sheared material	Coarse	0,75					
		Medium	0,65					
		Fine	0,55	X	X	X		
	Gouge < irregularities		0,42					
	Gouge > irregularities		0,17					
Flowing material		0,05						
Karst (KA)	None		1,00	X	X	X		
	Karst		0,92					

STOP 16 - REFERENCE ROCK TABLE					
Intact Rock Strength (RIRS)					
RIRS = IRS / WE = 12 / 0,90					13,333
Discontinuity Spacing (SPA)					
Discontinuities	B	J1	J2	SPA = factor 1 x factor 2 x factor 3	
Dip direction (degrees)	350	80	165		
Dip (degrees)	65	60	50		
Spacing (m)	20	40	15		
The spacing parameter (SPA) is calculated based on the three discontinuity sets with the smallest spacings in following figure:				SPA = 0,59 x 0,58 x 0,64 = 0,219	0,320
				Corrected for weathering and method of excavation:	
				RSPA = SPA / (WE x ME)	
				RSPA = 0,219 / (0,90 x 0,76)	
Condition of discontinuities					
Discontinuities	B	J1	J2	RTC is the discontinuity condition of a single discontinuity (set) in the reference rock mass corrected for discontinuity weathering. $RTC = TC / \sqrt{1,452 - 1,220 * e^{(-WE)}}$	
Large scale roughness (Rl)	0,80	0,80	0,80		
Small scale roughness (Rs)	0,75	0,75	0,75		
Infill material (Im)	0,55	0,55	0,55		
Karst (Ka)	1,00	1,00	1,00		
TC = Rl x Rs x Im x Ka	0,330	0,330	0,330		
RTC	0,338	0,338	0,338		
Weighted by spacing: $CD = \frac{\frac{TC_1}{DS_1} + \frac{TC_2}{DS_2} + \frac{TC_3}{DS_3}}{\frac{1}{DS_1} + \frac{1}{DS_2} + \frac{1}{DS_3}} =$					0,330
Corrected by weathering: RCD (with a maximum of 1.0165) = CD/WE =				0,330 / 0,90 =	0,367
Reference unit friction and cohesion (RFRI & FCOH)					
$\phi(RRM) = RIRS * 0,2417 + RSPA * 52,12 + RCD * 5,779 =$ (If RIRS > 132 MPa, then RIRS = 132)					22,03°
coh(RRM) = RIRS * 94,27 + RSPA * 28629 + RCD * 3593 = (If RIRS > 132 MPa, then RIRS = 132)					11,7 kPa

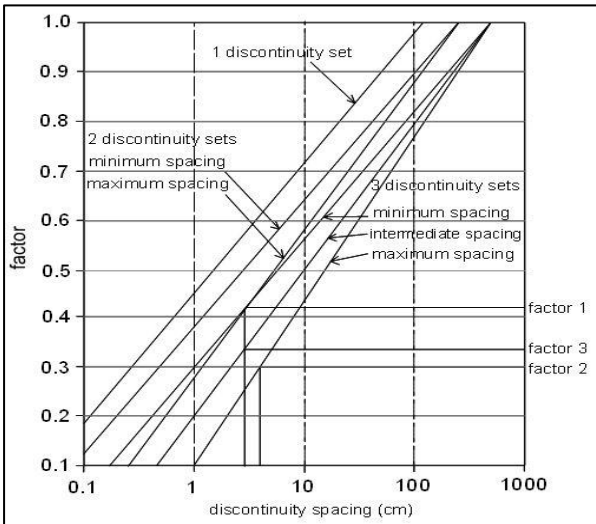
STOP 16 - STABILITY TABLE							
Method of Excavation (SME)			Weathering (SWE)				
Natural/hand-made		1,00	Unweathered		1,00		
Pneumatic hammer excavation*		0,76	Slightly		0,95		
Pre-splitting/smooth wall blasting		0,99	Moderately*		0,90		
Conventional blasting with result:			Highly		0,62		
Good		0,77	Completely		0,35		
Open discontinuities		0,75	Slope geometry features				
Dislodged blocks		0,72	Slope dip direction (degrees)		200		
Fractured intact rock		0,67	Slope dip (degrees)		55		
Crushed intact rock		0,62	Height (m)		6		
Orientation-independent stability							
Intact Rock Strength (SIRS)							
SIRS = RIRS (from reference rock mass) x SWE (weathering slope) =			13,333 x 0,90		12 MPa		
Discontinuity spacing (SSPA)							
SSPA = RSPA x SWE x SME			0,320x0,90x0,76		0,219		
Condition of discontinuity (SCD)							
SCD = RCD x SWE =			0,367 x 0,90		0,330		
Slope unit friction and cohesion (SFRI & SCOH)							
SFRI = SIRS * 0,2417 + SSPA * 52,12 + SCD * 5,779 =					16,22°		
(If RIRS > 132 Mpa, then RIRS =132)							
SCOH = SIRS * 94,27 + SSPA * 28629 + SCD * 3593 =					8,6 kPa		
(If RIRS > 132 Mpa, then RIRS =132)							
If SFRI < slope dip, maximum possible height (Hmax):					4,9 m		
Hmax = (1,6x10^-4 x SCOH) x sin(slopedip) x cos(SFRI) / (1 - cos(slopedip - SFRI)) =							
Ratios	SFRI / Slope dip				0,295		
	Hmax/ Hslope				0,8166667		
Stable probability: if SFRI > slope dip, probability = % 100, else use the figure for orientation-independent stability:					20%		
Orientation-dependent stability							
Discontinuities		B	J1	J2			
Dip direction (degrees)		350	80	165			
Dip (degrees)		65	60	50			
With, Against, Vertical or Equal		A	A	W			
AP (degrees)		-62	-40	44			
RTC		0,338	0,338	0,338			
STC = RTC x sqrt(1,452 - 1,220 x e^(-SWE))		0,330	0,330	0,330			
Stable probability:	Sliding	100%	100%	<5%			
	Toppling	>95%	80%	100%			
Stable probability:						<5%	
Determine orientation stability:							
Calculate AP: β = discontinuity dip, σ = slope dip direction, τ= discontinuity dip direction, δ = σ - τ, AP= arctan(cosδ x tanβ)							
Stability		Sliding	Toppling	Stability		Sliding	Toppling
AP>84° or AP<-84°	Vertical	100%	100%	AP<0° and (-90-AP+slope dip)<0°	Against	100%	100%
(slope dip + 5°) < AP < 84°	With	100%	100%	AP<0° and (-90-AP+slope dip)>0°	Against	100%	Use graph toppling
(slope dip - 5°) < AP < (slope dip + 5°	Equal	100%	100%				
0° < AP < (slope dip - 5°	With	Use graph sliding	100%				
Slope final stable probability		<5%					

STOP 17 - DATA COLLECTION TABLE										
Excavation Method (ME)			Intact Rock Strength (IRS)							
Natural/hand-made	1,00		<1.25 MPa			Crumbles in hand				
Pneumatic hammer excavation*	0,76		1.25-5 MPa			Thin slabs break easy in hand				
Pre-splitting/smooth wall blasting	0,99		5-12.5 MPa			Thin slabs broken by heavy hand pressure				
Conventional blasting with result:			12.5-50 MPa			Lumps broken by light hammer blows *				
Good	0,77		50-100 MPa			Lumps broken by heavy hammer blows				
Open discontinuities	0,75		100-200 MPa			Lumps only chip by heavy hammer blows				
Dislodged blocks	0,72		>200 MPa			Rocks ring on hammer blows				
Fractured intact rock	0,67		Weathering degree (WE)			Unweathered		1,00		
Crushed intact rock	0,62	Slightly				0,95				
Lithology		Moderately*				0,90				
Sandstone		Highly				0,62				
		Completely				0,35				
Discontinuities (B: Bedding; J: Joint)				B	J2	J3	Slope			
Dip direction (degrees)				350	60	195	Dip direction (degrees)		185	
Dip (degrees)				50	80	50	Dip (degrees)		45	
Spacing (DS) (cm)				15	30	10	Slope height (m)		6	
Condition of discontinuities						Slope Stability				
Large scale roughness (RL)	Wavy		1,00				Stable			1
	Slightly wavy		0,95				Small problem*			2
	Curved		0,85				Large problem			3
	Slightly curved		0,80	X	X	X	Notes: 1) For infill "gouge">irregularities" and "flowing material" small scale roughness= 0,55 2) If roughness is anisotropic (e.g. Ripple marks, striation, etc.) roughness should be assessed perpendicular and parallel to the roughness and directions noted on this form 3) Non-fitting of discontinuities should be marked in roughness columns.			
	Straight		0,75							
Small scale roughness (RS)	Rough stepped		0,95							
	Smooth stepped		0,90							
	Polished stepped		0,85							
	Rough undulating		0,80							
	Smooth undulating		0,75	X	X	X				
	Polished undulating		0,70							
	Rough planar		0,65							
	Smooth planar		0,60							
Polished planar		0,55								
Infill material (IM)	Cemented / cemented infill		1,07							
	No infill - surface staining		1,00							
	Non-softening & sheared material	Coarse	0,95							
		Medium	0,90							
		Fine	0,85							
	Soft sheared material	Coarse	0,75							
		Medium	0,65							
		Fine	0,55	X	X	X				
	Gouge < irregularities		0,42							
	Gouge > irregularities		0,17							
Flowing material		0,05								
Karst (KA)	None		1,00	X	X	X				
	Karst		0,92							

STOP 17 - REFERENCE ROCK TABLE					
Intact Rock Strength (RIRS)					
RIRS = IRS / WE = 8 / 0,90				8,889	
Discontinuity Spacing (SPA)					
Discontinuities	B	J1	J2	SPA = factor 1 x factor 2 x factor 3	0,266
Dip direction (degrees)	350	60	195		
Dip (degrees)	50	80	50		
Spacing (m)	15	30	10		
The spacing parameter (SPA) is calculated based on the three discontinuity sets with the smallest spacings in following figure:				SPA = 0,56 x 0,55 x 0,59 = 0,182	
				Corrected for weathering and method of excavation:	
				RSPA = SPA / (WE x ME)	
				RSPA = 0,182 / (0,90 x 0,76)	
Condition of discontinuities					
Discontinuities	B	J1	J2	RTC is the discontinuity condition of a single discontinuity (set) in the reference rock mass corrected for discontinuity weathering. $RTC = TC / \sqrt{1,452 - 1,220 * e^{(-WE)}}$	
Large scale roughness (Rl)	0,80	0,80	0,80		
Small scale roughness (Rs)	0,75	0,75	0,75		
Infill material (Im)	0,55	0,55	0,55		
Karst (Ka)	1,00	1,00	1,00		
TC = Rl x Rs x Im x Ka	0,330	0,330	0,330		
RTC	0,338	0,338	0,338		
Weighted by spacing: $CD = \frac{TC_1}{DS_1} + \frac{TC_2}{DS_2} + \frac{TC_3}{DS_3} = \frac{1}{\frac{1}{DS_1} + \frac{1}{DS_2} + \frac{1}{DS_3}}$				0,330	
Corrected by weathering: RCD (with a maximum of 1.0165) = CD/WE =				0,330 / 0,90 =	0,367
Reference unit friction and cohesion (RFRI & FCOH)					
$\phi(RRM) = RIRS * 0,2417 + RSPA * 52,12 + RCD * 5,779 =$ (If RIRS > 132 MPa, then RIRS = 132)				18,14°	
$coh(RRM) = RIRS * 94,27 + RSPA * 28629 + RCD * 3593 =$ (If RIRS > 132 MPa, then RIRS = 132)				9,8 kPa	

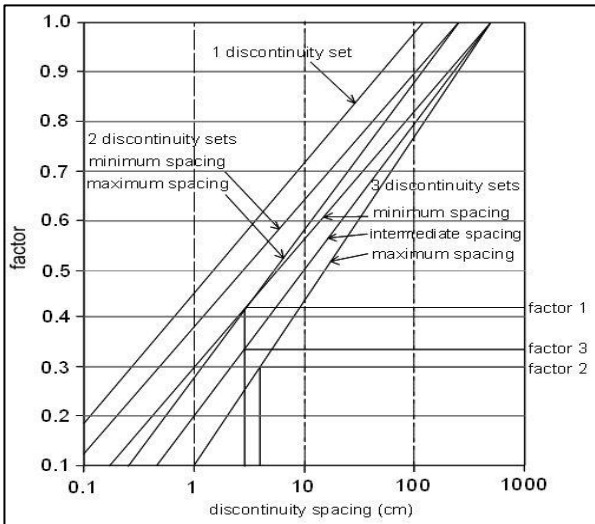
STOP 17 - STABILITY TABLE							
Method of Excavation (SME)			Weathering (SWE)				
Natural/hand-made		1,00	Unweathered	1,00			
Pneumatic hammer excavation*		0,76	Slightly	0,95			
Pre-splitting/smooth wall blasting		0,99	Moderately*	0,90			
Conventional blasting with result:			Highly	0,62			
Good		0,77	Completely	0,35			
Open discontinuities		0,75	Slope geometry features				
Dislodged blocks		0,72	Slope dip direction (degrees)	185			
Fractured intact rock		0,67	Slope dip (degrees)	45			
Crushed intact rock		0,62	Height (m)	6			
Orientation-independent stability							
Intact Rock Strength (SIRS)							
SIRS = RIRS (from reference rock mass) x SWE (weathering slope) =			8,889 x 0,90	8 MPa			
Discontinuity spacing (SSPA)							
SSPA = RSPA x SWE x SME			0,266x0,90x0,76	0,182			
Condition of discontinuity (SCD)							
SCD = RCD x SWE =			0,367 x 0,90	0,330			
Slope unit friction and cohesion (SFRI & SCOH)							
SFRI = SIRS * 0,2417 + SSPA * 52,12 + SCD * 5,779 = (If RIRS > 132 Mpa, then RIRS =132)				13,33°			
SCOH = SIRS * 94,27 + SSPA * 28629 + SCD * 3593 = (If RIRS > 132 Mpa, then RIRS =132)				7,2 kPa			
If SFRI < slope dip, maximum possible height (Hmax): Hmax = (1,6x10 <sup>-4</sup> x SCOH) x sin(slopedip) x cos(SFRI) / (1 - cos(slopedip - SFRI)) =				5,3 m			
Ratios	SFRI / Slope dip			0,296			
	Hmax/ Hslope			0,883			
Stable probability: if SFRI > slope dip, probability = % 100, else use the figure for orientation-independent stability:				30%			
Orientation-dependent stability							
Discontinuities		B	J1	J2			
Dip direction (degrees)		350	60	195			
Dip (degrees)		50	80	50			
With, Against, Vertical or Equal		A	A	E			
AP (degrees)		-49	-73	50			
RTC		0,338	0,338	0,338			
STC = RTC x sqrt(1,452 - 1,220 x e <sup>(-SWE)</sup> )		0,330	0,330	0,330			
Stable probability:	Sliding	100%	100%	100%			
	Toppling	>95%	80%	100%			
Stable probability:		80%					
Determine orientation stability:							
Calculate AP: β = discontinuity dip, σ = slope dip direction, τ= discontinuity dip direction, δ = σ - τ, AP= arctan(cosδ x tanβ)							
Stability		Sliding	Toppling	Stability	Sliding	Toppling	
AP>84°or AP<-84°	Vertical	100%	100%	AP<0° and (-90° AP+slope dip)<0°	Against	100%	100%
(slope dip + 5°) < AP < 84°	With	100%	100%	AP<0° and (-90° AP+slope dip)>0°	Against	100%	Use graph toppling
(slope dip - 5°) < AP < (slope dip + 5°	Equal	100%	100%				
0°< AP < (slope dip - 5°	With	Use graph sliding	100%				
Slope final stable probability		30%					

STOP 18 - DATA COLLECTION TABLE								
Excavation Method (ME)			Intact Rock Strength (IRS)					
Natural/hand-made		1,00	<1.25 MPa			Crumbles in hand		
Pneumatic hammer excavation*		0,76	1.25-5 MPa			Thin slabs break easy in hand		
Pre-splitting/smooth wall blasting		0,99	5-12.5 MPa			Thin slabs broken by heavy hand pressure		
Conventional blasting with result:			12.5-50 MPa			Lumps broken by light hammer blows*		
Good		0,77	50-100 MPa			Lumps broken by heavy hammer blows		
Open discontinuities		0,75	100-200 MPa			Lumps only chip by heavy hammer blows		
Dislodged blocks		0,72	>200 MPa			Rocks ring on hammer blows		
Fractured intact rock		0,67	Weathering degree (WE)			Unweathered		1,00
Crushed intact rock		0,62				Slightly		0,95
Lithology						Moderately*		0,90
70% Marl / 30% Mudstone						Highly		0,62
						Completely		0,35
Discontinuities (B: Bedding; J: Joint)				B	J2	J3	Slope	
Dip direction (degrees)				150	262	85	Dip direction (degrees)	240
Dip (degrees)				75	81	40	Dip (degrees)	45
Spacing (DS) (cm)				15	20	25	Slope height (m)	10
Condition of discontinuities						Slope Stability		
Large scale roughness (RL)	Wavy		1,00				Stable	1
	Slightly wavy		0,95		X	X	Small problem*	2
	Curved		0,85				Large problem	3
	Slightly curved		0,80	X			Notes: 1) For infill "gouge>irregularities" and "flowing material" small scale roughness= 0,55 2) If roughness is anisotropic (e.g. Ripple marks, striation, etc.) roughness should be assessed perpendicular and parallel to the roughness and directions noted on this form 3) Non-fitting of discontinuities should be marked in roughness columns.	
	Straight		0,75					
Small scale roughness (RS)	Rough stepped		0,95					
	Smooth stepped		0,90					
	Polished stepped		0,85					
	Rough undulating		0,80					
	Smooth undulating		0,75	X	X	X		
	Polished undulating		0,70					
	Rough planar		0,65					
	Smooth planar		0,60					
Polished planar		0,55						
Infill material (IM)	Cemented / cemented infill		1,07					
	No infill - surface staining		1,00					
	Non-softening & sheared material	Coarse	0,95					
		Medium	0,90					
		Fine	0,85					
	Soft sheared material	Coarse	0,75					
		Medium	0,65	X	X	X		
		Fine	0,55					
	Gouge < irregularities		0,42					
	Gouge > irregularities		0,17					
Flowing material		0,05						
Karst (KA)	None		1,00	X	X	X		
	Karst		0,92					

STOP 18 - REFERENCE ROCK TABLE					
Intact Rock Strength (RIRS)					
RIRS = IRS / WE = 27 / 0,90					30,000
Discontinuity Spacing (SPA)					
Discontinuities	B	J1	J2	SPA = factor 1 x factor 2 x factor 3	
Dip direction (degrees)	150	262	85		
Dip (degrees)	75	81	40		
Spacing (m)	15	20	25		
The spacing parameter (SPA) is calculated based on the three discontinuity sets with the smallest spacings in following figure:				SPA = 0,60 x 0,59 x 0,56 = 0,198	0,289
					
				Corrected for weathering and method of excavation:	
				RSPA = SPA / (WE x ME)	
				RSPA = 0,198 / (0,90 x 0,76)	
Condition of discontinuities					
Discontinuities	B	J1	J2	RTC is the discontinuity condition of a single discontinuity (set) in the reference rock mass corrected for discontinuity weathering. $RTC = TC / \sqrt{1,452 - 1,220 * e^{(-WE)}}$	
Large scale roughness (Rl)	0,80	0,95	0,95		
Small scale roughness (Rs)	0,75	0,75	0,75		
Infill material (Im)	0,65	0,65	0,65		
Karst (Ka)	1,00	1,00	1,00		
TC = Rl x Rs x Im x Ka	0,390	0,463	0,463		
RTC	0,399	0,474	0,474		
Weighted by spacing: $CD = \frac{\frac{TC_1}{DS_1} + \frac{TC_2}{DS_2} + \frac{TC_3}{DS_3}}{\frac{1}{DS_1} + \frac{1}{DS_2} + \frac{1}{DS_3}} =$				0,432	
Corrected by weathering: RCD (with a maximum of 1.0165) = CD/WE =				0,432 / 0,90 = 0,480	
Reference unit friction and cohesion (RFRI & FCOH)					
$\phi(RRM) = RIRS * 0,2417 + RSPA * 52,12 + RCD * 5,779 =$ (If RIRS > 132 MPa, then RIRS = 132)					25,11°
coh(RRM) = RIRS * 94,27 + RSPA * 28629 + RCD * 3593 = (If RIRS > 132 MPa, then RIRS = 132)					12,8 kPa

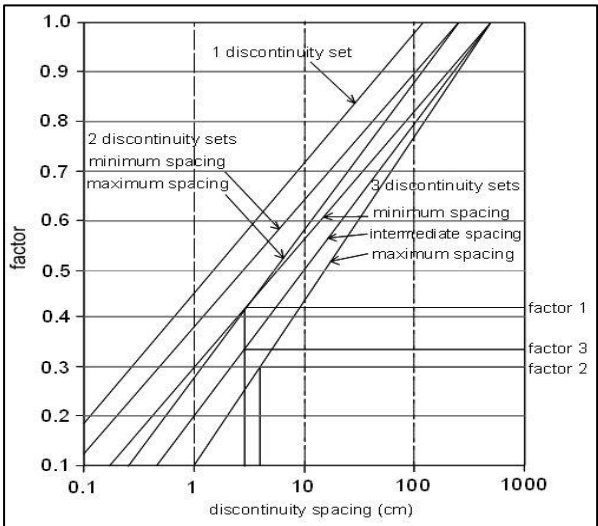
STOP 18 - STABILITY TABLE							
Method of Excavation (SME)			Weathering (SWE)				
Natural/hand-made		1,00	Unweathered		1,00		
Pneumatic hammer excavation*		0,76	Slightly		0,95		
Pre-splitting/smooth wall blasting		0,99	Moderately*		0,90		
Conventional blasting with result:			Highly		0,62		
Good		0,77	Completely		0,35		
Open discontinuities		0,75	Slope geometry features				
Dislodged blocks		0,72	Slope dip direction (degrees)		240		
Fractured intact rock		0,67	Slope dip (degrees)		45		
Crushed intact rock		0,62	Height (m)		10		
Orientation-independent stability							
Intact Rock Strength (SIRS)							
SIRS = RIRS (from reference rock mass) x SWE (weathering slope) =			30,000 x 0,90	27 MPa			
Discontinuity spacing (SSPA)							
SSPA = RSPA x SWE x SME			0,289x0,90x0,76	0,198			
Condition of discontinuity (SCD)							
SCD = RCD x SWE =			0,480 x 0,90	0,432			
Slope unit friction and cohesion (SFRI & SCOH)							
SFRI = SIRS * 0,2417 + SSPA * 52,12 + SCD * 5,779 = (If RIRS > 132 Mpa, then RIRS =132)					19,34°		
SCOH = SIRS * 94,27 + SSPA * 28629 + SCD * 3593 = (If RIRS > 132 Mpa, then RIRS =132)					9,8 kPa		
If SFRI < slope dip, maximum possible height (Hmax): Hmax = (1,6x10 <sup>-4</sup> x SCOH) x sin(slopedip) x cos(SFRI) / (1 - cos(slopedip - SFRI)) =					10,6 m		
Ratios	SFRI / Slope dip				0,430		
	Hmax / Hslope				1,06		
Stable probability: if SFRI > slope dip, probability = % 100, else use the figure for orientation-independent stability:					50%		
Orientation-dependent stability							
Discontinuities		B	J1	J2			
Dip direction (degrees)		150	262	85			
Dip (degrees)		75	81	40			
With, Against, Vertical or Equal		W	W	W			
AP (degrees)		0	80	31			
RTC		0,399	0,474	0,474			
STC = RTC x sqrt(1,452 - 1,220 x e <sup>^</sup> (-SWE))		0,390	0,463	0,463			
Stable probability:	Sliding	>95%	100%	>95%			
	Toppling	100%	100%	100%			
Stable probability:		>95%					
Determine orientation stability:							
Calculate AP: β = discontinuity dip, σ = slope dip direction, τ= discontinuity dip direction, δ = σ - τ, AP= arctan(cosδ x tanβ)							
Stability		Sliding	Toppling	Stability		Sliding	Toppling
AP>84° or AP<-84°	Vertical	100%	100%	AP<0° and (-90°<AP+slope dip)<0°	Against	100%	100%
(slope dip + 5°) < AP < 84°	With	100%	100%	AP<0° and (-90°<AP+slope dip)>0°	Against	100%	Use graph toppling
(slope dip - 5°) < AP < (slope dip + 5°	Equal	100%	100%				
0°< AP < (slope dip - 5°	With	Use graph sliding	100%				
Slope final stable probability		50%					

STOP 19 - DATA COLLECTION TABLE									
Excavation Method (ME)			Intact Rock Strength (IRS)						
Natural/hand-made		1,00	<1.25 MPa			Crumbles in hand			
Pneumatic hammer excavation*		0,76	1.25-5 MPa			Thin slabs break easy in hand			
Pre-splitting/smooth wall blasting		0,99	5-12.5 MPa			Thin slabs broken by heavy hand pressure			
Conventional blasting with result:			12.5-50 MPa			Lumps broken by light hammer blows *			
Good		0,77	50-100 MPa			Lumps broken by heavy hammer blows			
Open discontinuities		0,75	100-200 MPa			Lumps only chip by heavy hammer blows			
Dislodged blocks		0,72	>200 MPa			Rocks ring on hammer blows			
Fractured intact rock		0,67	Weathering degree (WE)			Unweathered		1,00	
Crushed intact rock		0,62				Slightly		0,95	
Lithology						Moderately*		0,90	
80% Marl / 20% Mudstone						Highly		0,62	
						Completely		0,35	
Discontinuities (B: Bedding; J: Joint)				B	J2	J3	Slope		
Dip direction (degrees)				130	60	235	Dip direction (degrees)		70
Dip (degrees)				75	30	80	Dip (degrees)		70
Spacing (DS) (cm)				25	20	15	Slope height (m)		8
Condition of discontinuities						Slope Stability			
Large scale roughness (RL)	Wavy		1,00				Stable		1
	Slightly wavy		0,95		X	X	Small problem*		2
	Curved		0,85				Large problem		3
	Slightly curved		0,80	X			Notes: 1) For infill "gouge">irregularities" and "flowing material" small scale roughness= 0,55 2) If roughness is anisotropic (e.g. Ripple marks, striation, etc.) roughness should be assessed perpendicular and parallel to the roughness and directions noted on this form 3) Non-fitting of discontinuities should be marked in roughness columns.		
	Straight		0,75						
Small scale roughness (RS)	Rough stepped		0,95						
	Smooth stepped		0,90						
	Polished stepped		0,85						
	Rough undulating		0,80						
	Smooth undulating		0,75	X	X	X			
	Polished undulating		0,70						
	Rough planar		0,65						
	Smooth planar		0,60						
	Polished planar		0,55						
Infill material (IM)	Cemented / cemented infill		1,07						
	No infill - surface staining		1,00						
	Non-softening & sheared material	Coarse	0,95						
		Medium	0,90						
		Fine	0,85						
	Soft sheared material	Coarse	0,75						
		Medium	0,65						
		Fine	0,55	X	X	X			
	Gouge < irregularities		0,42						
	Gouge > irregularities		0,17						
	Flowing material		0,05						
Karst (KA)	None		1,00	X	X	X			
	Karst		0,92						

STOP 19 - REFERENCE ROCK TABLE				
Intact Rock Strength (RIRS)				
RIRS = IRS / WE = 9,5 / 0,90				10,556
Discontinuity Spacing (SPA)				
Discontinuities	B	J1	J2	SPA = factor 1 x factor 2 x factor 3
Dip direction (degrees)	130	60	235	
Dip (degrees)	75	30	80	
Spacing (m)	25	20	15	
The spacing parameter (SPA) is calculated based on the three discontinuity sets with the smallest spacings in following figure:				SPA = 0,59 x 0,59 x 0,58 = 0,202
				Corrected for weathering and method of excavation:
				RSPA = SPA / (WE x ME)
				RSPA = 0,202 / (0,90 x 0,76)
				0,295
Condition of discontinuities				
Discontinuities	B	J1	J2	RTC is the discontinuity condition of a single discontinuity (set) in the reference rock mass corrected for discontinuity weathering. $RTC = TC / \sqrt{1,452 - 1,220 * e^{(-WE)}}$
Large scale roughness (Rl)	0,80	0,95	0,95	
Small scale roughness (Rs)	0,75	0,75	0,75	
Infill material (Im)	0,55	0,55	0,55	
Karst (Ka)	1,00	1,00	1,00	
TC = Rl x Rs x Im x Ka	0,330	0,392	0,392	
RTC	0,338	0,401	0,401	
Weighted by spacing: $CD = \frac{\frac{TC_1}{DS_1} + \frac{TC_2}{DS_2} + \frac{TC_3}{DS_3}}{\frac{1}{DS_1} + \frac{1}{DS_2} + \frac{1}{DS_3}} =$				0,376
Corrected by weathering: RCD (with a maximum of 1.0165) = CD/WE =				0,376 / 0,90 = 0,418
Reference unit friction and cohesion (RFRI & FCOH)				
$\phi(RRM) = RIRS * 0,2417 + RSPA * 52,12 + RCD * 5,779 =$ (If RIRS > 132 MPa, then RIRS = 132)				20,36°
$coh(RRM) = RIRS * 94,27 + RSPA * 28629 + RCD * 3593 =$ (If RIRS > 132 MPa, then RIRS = 132)				11,0 kPa

STOP 19 - STABILITY TABLE						
Method of Excavation (SME)			Weathering (SWE)			
Natural/hand-made		1,00	Unweathered	1,00		
Pneumatic hammer excavation*		0,76	Slightly	0,95		
Pre-splitting/smooth wall blasting		0,99	Moderately*	0,90		
Conventional blasting with result:			Highly	0,62		
Good		0,77	Completely	0,35		
Open discontinuities		0,75	Slope geometry features			
Dislodged blocks		0,72	Slope dip direction (degrees)	70		
Fractured intact rock		0,67	Slope dip (degrees)	70		
Crushed intact rock		0,62	Height (m)	8		
Orientation-independent stability						
Intact Rock Strength (SIRS)						
SIRS = RIRS (from reference rock mass) x SWE (weathering slope) =			10,556 x 0,90	9,5 MPa		
Discontinuity spacing (SSPA)						
SSPA = RSPA x SWE x SME			0,295x0,90x0,76	0,202		
Condition of discontinuity (SCD)						
SCD = RCD x SWE =			0,418 x 0,90	0,376		
Slope unit friction and cohesion (SFRI & SCOH)						
SFRI = SIRS * 0,2417 + SSPA * 52,12 + SCD * 5,779 = (If RIRS > 132 Mpa, then RIRS =132)				15,00°		
SCOH = SIRS * 94,27 + SSPA * 28629 + SCD * 3593 = (If RIRS > 132 Mpa, then RIRS =132)				8,0 kPa		
If SFRI < slope dip, maximum possible height (Hmax): Hmax = (1,6x10^-4 x SCOH) x sin(slopedip) x cos(SFRI) / (1 - cos(slopedip - SFRI)) =				2,7 m		
Ratios	SFRI / Slope dip			0,214		
	Hmax / Hslope			0,3375		
Stable probability: if SFRI > slope dip, probability = % 100, else use the figure for orientation-independent stability:				<5%		
Orientation-dependent stability						
Discontinuities		B	J1	J2		
Dip direction (degrees)		130	60	235		
Dip (degrees)		75	30	80		
With, Against, Vertical or Equal		W	W	A		
AP (degrees)		62	30	-80		
RTC		0,338	0,401	0,401		
STC = RTC x sqrt(1,452 - 1,220 x e^(-SWE))		0,330	0,392	0,392		
Stable probability:	Sliding	<5%	80%	100%		
	Toppling	100%	100%	<5%		
Stable probability:		<5%				
Determine orientation stability:						
Calculate AP: β = discontinuity dip, σ = slope dip direction, τ= discontinuity dip direction, δ = σ - τ, AP= arctan(cosδ x tanβ)						
Stability		Sliding	Toppling	Stability	Sliding	Toppling
AP>84°or AP<-84°	Vertical	100%	100%	AP<0° and (-90-AP+slope dip)<0°	Against	100%
(slope dip + 5°) < AP < 84°	With	100%	100%	AP<0° and (-90-AP+slope dip)>0°	Against	100%
(slope dip - 5°) < AP < (slope dip + 5°	Equal	100%	100%			
0°< AP < (slope dip - 5°	With	Use graph sliding	100%			
Slope final stable probability		<5%				

STOP 20 - DATA COLLECTION TABLE									
Excavation Method (ME)			Intact Rock Strength (IRS)						
Natural/hand-made	1,00	<1.25 MPa			Crumbles in hand				
Pneumatic hammer excavation*	0,76	1.25-5 MPa			Thin slabs break easy in hand				
Pre-splitting/smooth wall blasting	0,99	5-12.5 MPa			Thin slabs broken by heavy hand pressure				
Conventional blasting with result:		12.5-50 MPa			Lumps broken by light hammer blows*				
Good	0,77	50-100 MPa			Lumps broken by heavy hammer blows				
Open discontinuities	0,75	100-200 MPa			Lumps only chip by heavy hammer blows				
Dislodged blocks	0,72	>200 MPa			Rocks ring on hammer blows				
Fractured intact rock	0,67	Weathering degree (WE)			Unweathered		1,00		
Crushed intact rock	0,62				Slightly		0,95		
Lithology					Moderately*		0,90		
90% Marl / 10% Mudstone					Highly		0,62		
					Completely		0,35		
Discontinuities (B: Bedding; J: Joint)				B	J2	J3	Slope		
Dip direction (degrees)				130	50	220	Dip direction (degrees)		35
Dip (degrees)				70	15	70	Dip (degrees)		75
Spacing (DS) (cm)				10	20	15	Slope height (m)		10
Condition of discontinuities						Slope Stability			
Large scale roughness (RL)	Wavy		1,00				Stable		1
	Slightly wavy		0,95				Small problem*		2
	Curved		0,85	X	X	X	Large problem		3
	Slightly curved		0,80				Notes: 1) For infill "gouge">irregularities" and "flowing material" small scale roughness= 0,55 2) If roughness is anisotropic (e.g. Ripple marks, striation, etc.) roughness should be assessed perpendicular and parallel to the roughness and directions noted on this form 3) Non-fitting of discontinuities should be marked in roughness columns.		
	Straight		0,75						
Small scale roughness (RS)	Rough stepped		0,95						
	Smooth stepped		0,90						
	Polished stepped		0,85						
	Rough undulating		0,80	X	X	X			
	Smooth undulating		0,75						
	Polished undulating		0,70						
	Rough planar		0,65						
	Smooth planar		0,60						
Polished planar		0,55							
Infill material (IM)	Cemented / cemented infill		1,07						
	No infill - surface staining		1,00						
	Non-softening & sheared material	Coarse	0,95						
		Medium	0,90						
		Fine	0,85						
	Soft sheared material	Coarse	0,75						
		Medium	0,65						
		Fine	0,55	X	X	X			
	Gouge < irregularities		0,42						
	Gouge > irregularities		0,17						
Flowing material		0,05							
Karst (KA)	None		1,00	X	X	X			
	Karst		0,92						

STOP 20 - REFERENCE ROCK TABLE						
Intact Rock Strength (RIRS)						
RIRS = IRS / WE = 7 / 0,90					7,778	
Discontinuity Spacing (SPA)						
Discontinuities	B	J1	J2	SPA = factor 1 x factor 2 x factor 3	0,234	
Dip direction (degrees)	130	50	220			
Dip (degrees)	70	15	70			
Spacing (m)	10	20	15			
The spacing parameter (SPA) is calculated based on the three discontinuity sets with the smallest spacings in following figure:				SPA = 0,55 x 0,55 x 0,53 = 0,160		
				Corrected for weathering and method of excavation:		
				RSPA = SPA / (WE x ME)		
				RSPA = 0,160 / (0,90 x 0,76)		
Condition of discontinuities						
Discontinuities	B	J1	J2	RTC is the discontinuity condition of a single discontinuity (set) in the reference rock mass corrected for discontinuity weathering. $RTC = TC / \sqrt{1,452 - 1,220 * e^{-(WE)}}$		0,374
Large scale roughness (Rl)	0,85	0,85	0,85			
Small scale roughness (Rs)	0,80	0,80	0,80			
Infill material (Im)	0,55	0,55	0,55			
Karst (Ka)	1,00	1,00	1,00			
TC = Rl x Rs x Im x Ka	0,374	0,374	0,374			
RTC	0,383	0,383	0,383			
Weighted by spacing: $CD = \frac{\frac{TC_1}{DS_1} + \frac{TC_2}{DS_2} + \frac{TC_3}{DS_3}}{\frac{1}{DS_1} + \frac{1}{DS_2} + \frac{1}{DS_3}} =$					0,374	
Corrected by weathering: RCD (with a maximum of 1.0165) = CD/WE =				0,374 / 0,90 =	0,416	
Reference unit friction and cohesion (RFRI & FCOH)						
$\phi(RRM) = RIRS * 0,2417 + RSPA * 52,12 + RCD * 5,779 =$ (If RIRS > 132 MPa, then RIRS = 132)					16,47°	
coh(RRM) = RIRS * 94,27 + RSPA * 28629 + RCD * 3593 = (If RIRS > 132 MPa, then RIRS = 132)					8,9 kPa	

STOP 20 - STABILITY TABLE							
Method of Excavation (SME)			Weathering (SWE)				
Natural/hand-made		1,00	Unweathered		1,00		
Pneumatic hammer excavation*		0,76	Slightly		0,95		
Pre-splitting/smooth wall blasting		0,99	Moderately*		0,90		
Conventional blasting with result:			Highly		0,62		
Good		0,77	Completely		0,35		
Open discontinuities		0,75	Slope geometry features				
Dislodged blocks		0,72	Slope dip direction (degrees)		35		
Fractured intact rock		0,67	Slope dip (degrees)		75		
Crushed intact rock		0,62	Height (m)		10		
Orientation-independent stability							
Intact Rock Strength (SIRS)							
SIRS = RIRS (from reference rock mass) x SWE (weathering slope) =			7,778 x 0,90		7 MPa		
Discontinuity spacing (SSPA)							
SSPA = RSPA x SWE x SME			0,234x0,90x0,76		0,160		
Condition of discontinuity (SCD)							
SCD = RCD x SWE =			0,416 x 0,90		0,374		
Slope unit friction and cohesion (SFRI & SCOH)							
SFRI = SIRS * 0,2417 + SSPA * 52,12 + SCD * 5,779 =					12,19°		
(If RIRS > 132 Mpa, then RIRS =132)							
SCOH = SIRS * 94,27 + SSPA * 28629 + SCD * 3593 =					6,6 kPa		
(If RIRS > 132 Mpa, then RIRS =132)							
If SFRI < slope dip, maximum possible height (Hmax):							
Hmax = (1,6x10 <sup>-4</sup> x SCOH) x sin(slopedip) x cos(SFRI) / (1 - cos(slopedip - SFRI)) =					1,8 m		
Ratios	SFRI / Slope dip					0,174	
	Hmax/ Hslope					0,180	
Stable probability: if SFRI > slope dip, probability = % 100, else use the figure for orientation-independent stability:						<5%	
Orientation-dependent stability							
Discontinuities		B	J1	J2			
Dip direction (degrees)		130	50	220			
Dip (degrees)		70	15	70			
With, Against, Vertical or Equal		A	W	A			
AP (degrees)		-13	15	-70			
RTC		0,383	0,383	0,383			
STC = RTC x sqrt(1,452 - 1,220 x e <sup>(-SWE)</sup> )		0,374	0,374	0,374			
Stable probability:	Sliding	100%	>95%	100%			
	Toppling	100%	100%	<5%			
Stable probability:		<5%					
Determine orientation stability:							
Calculate AP: β = discontinuity dip, σ = slope dip direction, τ= discontinuity dip direction, δ = σ - τ, AP= arctan(cosδ x tanβ)							
Stability		Sliding	Toppling	Stability		Sliding	Toppling
AP>84° or AP<-84°	Vertical	100%	100%	AP<0° and (-90-AP+slope dip)<0°	Against	100%	100%
(slope dip + 5°) < AP < 84°	With	100%	100%	AP<0° and (-90-AP+slope dip)>0°	Against	100%	Use graph toppling
(slope dip - 5°) < AP < (slope dip + 5°	Equal	100%	100%				
0° < AP < (slope dip - 5°	With	Use graph sliding	100%				
Slope final stable probability		<5%					